

Lahaina Groundwater Tracer Study Lahaina, Maui, Hawai‘i

Final Report

Craig R. Glenn, Robert B. Whittier,
Meghan L. Dailer, Henrieta Dulaiova,
Aly I. El-Kadi, Joseph Fackrell,
Jacque L. Kelly, Christine A. Waters
and Jeff Sevadjan

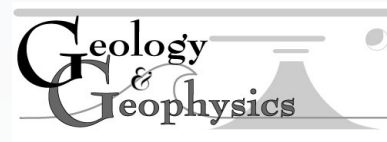
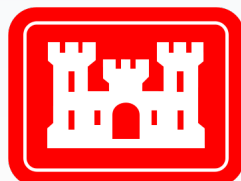
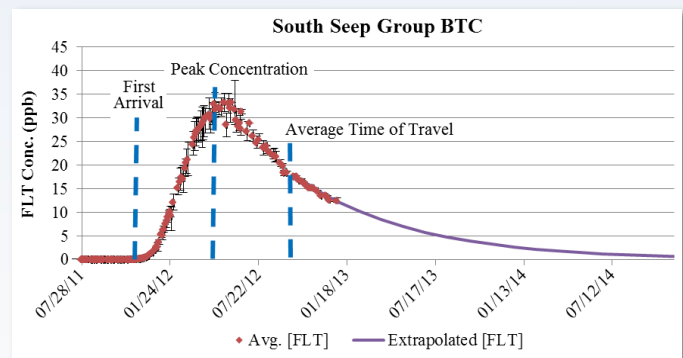
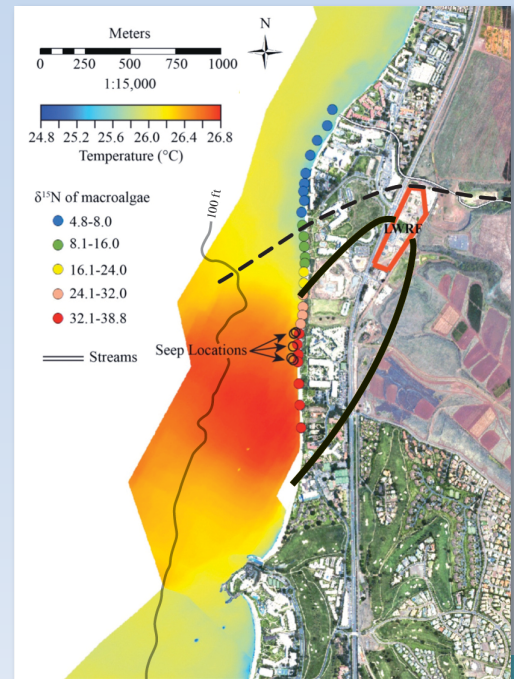
June 2013

Prepared For

State of Hawaii Department of Health
U.S. Environmental Protection Agency
U.S. Army Engineer Research and Development Center

Principal Investigator: Craig R. Glenn

School of Ocean and Earth Science and Technology
Department of Geology and Geophysics
University of Hawai‘i at Manoa
Honolulu, Hawai‘i 96822



LAHAINA GROUNDWATER TRACER STUDY – LAHAINA, MAUI, HAWAII

Final Report

**Craig R. Glenn, Robert B. Whittier, Meghan L. Dailer,
Henrieta Dulaiova, Aly I. El-Kadi, Joseph Fackrell,
Jacque L. Kelly, Christine A. Waters and Jeff Sevadjian**

June 2013

PREPARED FOR

State of Hawaii Department of Health
U.S. Environmental Protection Agency
U.S. Army Engineer Research and Development Center

Principal Investigator: Craig R. Glenn

School of Ocean and Earth Science and Technology
Department of Geology and Geophysics
University of Hawaii at Manoa
Honolulu, Hawaii 96822

Suggested Citation:

Suggested Citation:
Glenn, C.R., Whittier, R.B., Dailer, M.L., Dulaiova, H., El-Kadi, A.I., Fackrell, J., Kelly, J.L., Waters, C.A., and J. Sevadjian, 2013. Lahaina Groundwater Tracer Study – Lahaina, Maui, Hawaii, Final Report, prepared for the State of Hawaii Department of Health, the U.S. Environmental Protection Agency, and the U.S. Army Engineer Research and Development Center

This page is intentionally left blank.

TABLE OF CONTENTS

EXECUTIVE SUMMARY	ES-1
Overview	ES-1
Introduction	ES-4
Submarine Springs and Marine Control Locations of Sampling, Water Quality, and Fluorescence	ES-5
Aerial Infrared Sea Surface Temperature Mapping	ES-8
Submarine Groundwater Discharge	ES-9
Aqueous Geochemistry and Stable Isotopes	ES-12
Fluorescent Dye Groundwater Tracer Study	ES-15
Fluorescein Dye Tracer Test	ES-15
Sulpho-Rhodamine B Tracer Test	ES-17
Lahaina Groundwater Tracer Study Numerical Modeling	ES-18
SECTION 1: INTRODUCTION, BACKGROUND, AND PURPOSE	1-1
1.1 INTRODUCTION	1-1
1.1.1 Acknowledgements	1-2
1.2 GEOGRAPHIC SETTING	1-3
1.3 OVERVIEW OF THE LAHAINA WASTEWATER RECLAMATION FACILITY	1-3
1.4 HISTORY OF RELATED INVESTIGATIONS	1-5
1.5 STUDY AREA DESCRIPTIONS AND BACKGROUND	1-8
1.5.1 Climate	1-8
1.5.2 Land Use	1-9
1.5.3 Geology	1-10
1.5.4 Regional Groundwater Hydrology	1-11
1.5.4.1 Aquifer Properties	1-12
1.5.4.2 Submarine Groundwater Discharge	1-13
SECTION 2: SUBMARINE SPRING AND MARINE CONTROL LOCATION SAMPLING, WATER QUALITY, AND FLUORESCENCE	2-1

2.1 INTRODUCTION	2-1
2.2 METHODS	2-1
2.2.1 Submarine Spring Sampling	2-1
2.2.2 Submarine Spring Sampling Frequency and Placement	2-3
2.2.3 Sampling Control Locations	2-4
2.2.4 Field Measurements of Fluorescein and S-Rhodamine-B Fluorescence	2-4
2.2.5 Submarine Spring and Shoreline Surveys	2-5
2.3 RESULTS	2-6
2.3.1 Water Quality of Submarine Springs	2-6
2.3.2 Water Quality of Control Locations	2-6
2.3.3 Field Measurements of Fluorescein and S-Rhodamine-B Fluorescence	2-6
2.3.4 Submarine Spring Survey	2-8
2.4 SUMMARY	2-9
SECTION 3: SUBMARINE SPRING DISCHARGE MAGNITUDE AND DYNAMICS	3-1
3.1 INTRODUCTION	3-1
3.1.1 Seep Discharge Dynamics Measurements Using an Acoustic Doppler Current Profiler (ADCP)	3-1
3.2 METHODS	3-2
3.2.1 Study Area	3-2
3.2.2 HR Aquadopp Profiler Deployment	3-2
3.2.3 HR Aquadopp Data Processing	3-2
3.3 RESULTS	3-3
3.3.1 Vertical Fluxes	3-3
3.3.2 Determination of Seep Discharge Using ADCP	3-3
3.3.3 Groundwater-derived nutrient fluxes	3-4
3.4 SUMMARY	3-7
SECTION 4: FLUORESCENT DYE GROUNDWATER TRACER STUDY	4-1
4.1 INTRODUCTION	4-1
4.1.1 Tracer Dye Selection	4-2
4.1.2 Preliminary Planning	4-4

4.2 THE INJECTION WELLS 3 AND 4 TRACER TEST	4-5
4.2.1 Fluorescein Analysis	4-7
4.2.1.1 Fluorometer	4-7
4.2.1.2 Sample Handling	4-7
4.2.1.3 Laboratory Analysis	4-8
4.2.1.3.1 Fluorometer Calibration	4-8
4.2.1.3.2 Calibration Solutions – Deionized (DI) Water vs. Submarine Spring Water	4-8
4.2.1.3.3 FLT Method Detection Limit (MDL)	4-9
4.2.1.3.4 Laboratory Quality Assurance	4-11
4.2.1.3.5 FLT Synchronous Scans	4-12
4.2.2 Background Fluorescence Assessment and First Detection	4-12
4.2.3 The Breakthrough Curve - Fluorescein	4-14
4.2.3.1 North Seep Group	4-14
4.2.3.2 South Seep Group	4-14
4.2.3.3 Grab and Control Samples	4-15
4.2.3.4 The Relationship Between Dye Concentrations and Salinity	4-16
4.2.3.5 NSG and SSG Breakthrough Curves	4-17
4.2.4 Breakthrough Curve Analysis	4-18
4.2.4.1 Breakthrough Curve Extrapolation	4-18
4.2.4.2 QTracer2 Breakthrough Curve Analysis Model	4-18
4.2.4.2.1 QTracer2 Model Inputs and Outputs	4-19
4.2.4.2.2 QTracer2 Model Results	4-19
4.2.4.3 FLT Recovery and Treated Wastewater Fraction	4-20
4.2.5 Green Coloration in the South Seep Group Discharge	4-22
4.2.6 Area Survey Sampling and Results	4-25
4.2.6.1 Area Sampling Survey Description and Methods	4-25
4.2.6.2 Area Sampling Survey Results	4-27
4.3 INJECTION WELL 2 TRACER TEST	4-29
4.3.1 Sample Handling	4-30
4.3.2 SRB Analysis	4-31
4.3.2.1 SRB Laboratory Analysis	4-31

4.3.2.1.1 Spectrophotometer Calibration	4-32
4.3.2.1.2 SRB Method Detection Limit (MDL) Assessment.....	4-32
4.3.2.1.3 SRB Laboratory Quality Assurance.....	4-33
4.3.2.2 Measured Fluorescence in the SRB Wavelength.....	4-34
4.3.2.2.1 SRB Synchronous Scans.....	4-34
4.3.3 Possible Causes of the Lack of SRB Detection	4-37
4.4 STARWOOD VACATION OWNERSHIP RESORT (SVO) MONITORING WELL SAMPLING	4-39
4.4.1 SVO Well Sampling Procedures.....	4-39
4.4.2 SVO Well Sampling Results and Discussion	4-40
4.5 SUMMARY AND CONCLUSIONS	4-41
 SECTION 5: TRACER TEST NUMERICAL MODELING	 5-1
5.1 INTRODUCTION	5-1
5.2 MODELING OBJECTIVES.....	5-1
5.3 MODELING APPROACH.....	5-2
5.4 TRACER TEST DESIGN MODEL (TTDM)	5-3
5.4.1 Numerical Model	5-3
5.4.1.1 Model Grid.....	5-3
5.4.1.2 Boundary Conditions	5-3
5.4.1.3 Recharge	5-4
5.4.1.4 Hydrogeologic Parameters.....	5-4
5.4.1.5 Tracer Test Design Model – Transport Model	5-6
5.4.2 Tracer Test Design Model Results.....	5-7
5.5 LAHAINA GROUNDWATER TRACER TEST MODEL	5-7
5.5.1 Numerical Model	5-8
5.5.1.1 Model Grid.....	5-8
5.5.1.2 Boundary Conditions	5-8
5.5.1.3 Recharge	5-8
5.5.1.4 Hydrologic Parameters.....	5-8
5.5.1.5 Transport Model.....	5-9
5.5.2 Description of Scenarios	5-9

5.5.2.1 Effects of a Horizontal Flow Barrier	5-9
5.5.2.2 Effects of Bathymetry	5-10
5.5.2.3 Effects of a Preferential Flow Path	5-10
5.5.2.4 Effect of Porosity	5-10
5.5.2.5 Effect of Dispersivity	5-11
5.5.2.6 Effects of Sorption	5-11
5.5.2.7 Effects of Anisotropy	5-12
5.5.3 Model Results	5-13
5.5.3.1 Effects of a Horizontal Flow Barrier (HFB)	5-13
5.5.3.2 Effects of Bathymetry	5-13
5.5.3.3 Effects of a Preferential Flow Path	5-14
5.5.3.4 Effect of Dispersivity	5-14
5.5.3.5 Effect of Porosity	5-15
5.5.3.6 Effects of Sorption	5-15
5.5.3.7 Effects of Anisotropy	5-16
5.5.3.8 Best Fit Model	5-17
5.5.3.9 Fate of SRB	5-18
5.6 CONCEPTUAL MODEL OF THE KAA NAPALI GROUNDWATER FLOW AND TRANSPORT SYSTEM	5-19
5.7 THE BTC TRAILING EDGE	5-22
5.8 ASSUMPTIONS AND LIMITATIONS	5-24
5.9 CONCLUSIONS	5-25
SECTION 6: REFERENCES	6-1

APPENDICES

APPENDIX A: FIELD WATER QUALITY AND FLUORESCENCE MEASUREMENTS OF SUBMARINE SPRINGS AND CONTROL LOCATIONS	A-1
APPENDIX B: PROCEDURES FOR ESTABLISHING THE METHOD DETECTION LIMIT	B-1
APPENDIX C: DYE CONCENTRATIONS: LABORATORY RESULTS	C-1

APPENDIX D: STARWOOD VACATIONS OWNERSHIP RESORTS (SVO)
MONITORING WELL DATA..... D-1

APPENDIX E: FINAL REPORT REVIEW COMMENTS AND UNIVERSITY
OF HAWAII RESPONSES AND CORRECTIONS.....E-1

APPENDIX E-1: FINAL REPORT REVIEW COMMENTS FROM COUNTY OF
MAUIE-3

APPENDIX E-2: FINAL REPORT REVIEW COMMENTS FROM THE USEPA
REGION IXE-17

APPENDIX E-3: FINAL REPORT REVIEW COMMENTS FROM THE
HAWAII DEPARTMENT OF HEALTHE-36

LIST OF TABLES

Table ES-1. North and South Seep Group water quality parameters.	ES-22
Table ES-2. Summary of the June, 2011 Nutrient Data	ES-23
Table ES-3. Summary of the September, 2011 Nutrient Data	ES-24
Table ES-4. The progressive microbial decomposition of organic matter.	ES-25
Table ES-5. June, 2011 stable isotope data.....	ES-26
Table ES-6. September, 2011 stable isotope data.....	ES-27
Table ES-7. The output of the QTracer2 BTC Interpretation Model	ES-28
Table ES-8. Calculated percent of treated wastewater in the submarine spring discharge.	ES-29
Table 1-1. Construction Details of the LWRF Injection Wells	1-14
Table 1-2. Treated wastewater injections rates for April 2011 through March of 2013.....	1-15
Table 2-1. Submarine spring names and locations.	2-11
Table 2-2. North and South Seep Group water quality parameters.	2-12
Table 2-3. Control location water quality parameters.	2-14
Table 3-1. HR Aquadopp Profiler deployment configuration.	3-9
Table 3-2. Vertical velocities at Seep 4	3-9
Table 3-3. Calculated groundwater discharge	3-10
Table 3-4. Groundwater discharge characteristics at SSG and NSG determined using the time-series radon mass	3-10
Table 3-5. Radon mass-balance derived groundwater discharge at locations identified as groundwater discharge sites along the Kaanapali coastline	3-11
Table 3-6. Radon mass-balance derived groundwater fluxes and groundwater discharge per meter shoreline	3-13
Table 3-7. Nearshore coastal surface water (SW) nutrient concentration ranges in waters affected by groundwater discharge.....	3-15

Table 4-1. Mixing Schedule for the FLT Calibration Solutions.....	4-43
Table 4-2. The MDL Results for FLT Using the EPA Method.....	4-43
Table 4-3. The MDL Results for FLT Using the Hubaux and Vos Method.....	4-43
Table 4-4. The Turner 10AU calibration scalar, residual, coefficient of determination, and offset	4-44
Table 4-5. The results of the end of analysis zero baseline check of the fluorometer.....	4-45
Table 4-6. The results of the end of analysis upscale quality control check of the fluorometer.....	4-46
Table 4-7. The results of duplicate analyses ran at the end of each analysis run	4-47
Table 4-8. Table of replicate analyses to evaluate FLT sample degradation during storage.....	4-49
Table 4-9. Summary of Background Fluorescence for the NSG	4-50
Table 4-10. Summary of Background Fluorescence for the SSG.....	4-50
Table 4-11. Background Fluorescence for the Marine Waters.....	4-50
Table 4-12. Summary of salinity measured at the submarine springs	4-51
Table 4-13. The output of the QTracer2 BTC Interpretation Model	4-52
Table 4-14. Calculated percent of treated wastewater in the submarine spring discharge.	4-53
Table 4-15. The MDL Results for SRB Using the EPA Method.....	4-54
Table 4-16. The MDL Results for SRB Using the Hubaux and Vos Method	4-55
Table 4-17. Summary of the area survey sample results	4-55
Table 4-18. Hitachi F4500 Spectrophotometer calibration scalar, residual, and coefficient of determination.....	4-56
Table 4-19. The results of the end of analysis zero baseline check of the Hitachi F4500 Spectrophotometer.....	4-57
Table 4-20. The results of the end of analysis upscale quality control check of the Hitachi F4500 Spectrophotometer	4-58
Table 4-21. The results of synchronous scans done to evaluate samples for trace concentrations of SRB	4-59
Table 4-22. SVO Well construction details	4-62
Table 4-23. SVO Well measured pH, SEC, and FLT and SRB concentrations and water temperatures	4-62
Table 4-24. Nutrient results for the SVO Wells	4-63

Table 5-1. Hydraulic parameter values for the various geologic units used in the TTDM compared to that of other models	5-27
Table 5-2. A Comparison of the TTDM results and the measured NSG BTC	5-27
Table 5-3. Well injection and dye concentrations for the BTC Evaluation Model	5-28
Table 5-4. Coefficients from Sabatini (2000) used in the sorption simulation.....	5-28
Table 5-5. A summary of the simulated travel times and peak concentrations of the preferential flow simulations	5-28
Table 5-6. Results of Porosity and Dispersivity Sensitivity Simulations	5-29
Table A-1. Calibration of the handheld YSI for pH and specific conductivity	A-3
Table A-2. Calibration record of the hand held fluorometer	A-10
Table A-3. Water quality parameters collected from submarine spring samples in the South Seep Group (Seeps 3, 4, 5, and 11).....	A-14
Table A-4. North Seep Group (Seeps 1, 2, 6, 7, 8, 9, 10, 12, 13, 14, 15, 16, 17, 18, 19, 20, and 21) water quality parameters.....	A-31
Table A-5. Water quality parameters collected from control locations (Honokowai Beach Park, Wahikuli Wayside Beach Park, and Olowalu).	A-47
Table A-6. Submarine Spring, Shoreline Survey, and SVO Well Sampling Results.....	A-49
Table C-1. The fluorescent dye analytical results for the North Seep Group.....	C-3
Table C-2. The fluorescent dye analytical results for the South Seep Group.....	C-35
Table D-1. Field, water quality measurements, and tracer dye concentration for the 7/1/12 SVO well sampling.....	D-3
Table D-2. Field, water quality measurements, and tracer dye concentration for the 4/29/13 SVO well sampling.....	D-4
Table D-3. Field, water quality measurements, and tracer dye concentration for the 6/6/13 SVO well sampling.....	D-6

LIST OF FIGURES

Figure ES-1: Western Maui land-use map.....	ES-30
Figure ES-2: Detail of study area showing key locals along the coast.....	ES-31
Figure ES-3: Control and submarine spring sampling locations.....	ES-32
Figure ES-4: Aerial TIR sea surface temperature map thermal anomaly at North Kaanapali Beach.....	ES-33
Figure ES-5: Infrared SST pictured with $\delta^{15}N$ values of terrestrial and marine waters, and the intertidal macroalgae.....	ES-34
Figure ES-6: The FLT concentrations normalize to that at Seep 3 and shown in relation to the boundaries of the TIR plume.....	ES-35
Figure ES-7: Radon activities measured during coastal surveys in June and September, 2011.....	ES-36
Figure ES-8: Submarine spring component mix ternary diagram.....	ES-37
Figure ES-9: Submarine spring water FLT breakthrough curves for (a) the NSG and (b) the SSG.....	ES-38
Figure ES-10: The SRB wavelength fluorescence measured by this study at the NSG (a) and the SSG (b).....	ES-39
Figure ES-11: Synchronous scans of samples collected in February and March, 2012 compared to solutions spiked with SRB.....	ES-40
Figure ES-12: The conceptual model for the Lahaina Groundwater Study showing the extent of the submarine layers.....	ES-41
Figure ES-13: The probable downed stream valley shown in relation to the modeled horizontal flow barrier and the normalized FLT concentrations.....	ES-42
Figure ES-14: The FLT model results showing (a) the measured and simulated BTCs; and (b) simulated plume 620 days after dye addition.....	ES-43
Figure ES-15: The simulated SRB BTCs (a) and plume 620 days after dye addition (b).....	ES-44
Figure ES-16: The simulated SRB BTCs (a) and plume 620 days after dye addition (b).....	ES-45
Figure 1-1: Location and topography of the Island of Maui.....	1-18
Figure 1-2: Map showing the location of the LWRF in West Maui.....	1-19
Figure 1-3: Location of the LWRF in relation to the coast and the UIC line.....	1-20

Figure 1-4: Borehole stratigraphy for the LWRF injection wells developed from the driller’s logs.	1-21
Figure 1-5: Monthly average injection at the LWRF.....	1-21
Figure 1-6: Detail of study area showing key locals along the coast.....	1-22
Figure 1-7: Map of the LWRF, submarine springs, and Tetra Tech (1994) ocean sampling tracts	1-23
Figure 1-8: Western Maui land-use map.	1-24
Figure 1-9: West Maui geology and inferred high level/peripheral basal lens boundary. Geology from Sherrod et al. (2007).....	1-25
Figure 1-10: Geologic section of West Maui showing SGD and groundwater occurrence and movement.	1-26
Figure 1-11: Groundwater recharge distribution in West Maui.....	1-27
Figure 1-12: Calculated fresh submarine groundwater discharge to the ocean for the Island of Maui.	1-28
Figure 2-1: Schematics of submarine spring water sampling locations.	2-15
Figure 2-2: Control and submarine spring sampling locations.....	2-16
Figure 2-3: South Seep Group salinity and fluorescence (Seeps 3, 4, 5, and 11).....	2-17
Figure 2-4: North Seep Group salinity and fluorescence (Seeps 1, 2, 6, and 7).....	2-18
Figure 2-5: North Seep Group salinity and fluorescence (Seeps 8, 9, 10, and 12).....	2-19
Figure 2-6: North Seep Group salinity and fluorescence (Seeps 13, 14, 15, and 16).	2-20
Figure 2-7: North Seep Group salinity and fluorescence (Seeps 17, 18, 19, and 20).	2-21
Figure 2-8: North Seep Group salinity and fluorescence (Seep 21).	2-22
Figure 2-9: Control location salinity and fluorescence.....	2-23
Figure 2-10: Correlation between the Field and the Lab measured FLT.....	2-24
Figure 2-11: A time series showing the close correspondence between the field measured FLT concentration and the apparent SRB fluorescence.	2-24
Figure 2-12: The handheld fluorometer SRB channel response to FLT (only) calibration solutions.	2-25
Figure 2-13: Area covered at Honokowai Point during the submarine spring survey.....	2-26
Figure 2-14: Area covered at adjacent to the Honua Kai during the submarine spring survey.....	2-27

Figure 2-15: Area covered south of the Honua Kai and across Kahekili Reef during the submarine spring survey.	2-28
Figure 2-16: Area covered across Kahekili Reef during the submarine spring survey.	2-29
Figure 2-17: Area covered South of Kahekili Reef during the submarine spring survey.	2-30
Figure 2-18: Area covered North of Black Rock during the submarine spring survey.	2-31
Figure 2-19: The location of the flowing submarine springs showing an enveloping polygon for each seep group and the extent of the boxes used in the Radon flux calculations.	2-32
Figure 3-1: Mounting arrangement for the down looking HR Aquadopp profiler	3-16
Figure 3-2: ADCP vertical velocity spectral analysis graph.....	3-16
Figure 3-3: Tidal stage and ADCP measured vertical velocities averaged over tidal intervals	3-17
Figure 3-4: Tidal stage and ADCP measured vertical velocities averaged over demarcated interval.....	3-17
Figure 3-5: Tidal stage and ADCP measured vertical velocities averaged over period between higher tides	3-18
Figure 3-6: Groundwater and surface water nitrogen concentrations.....	3-19
Figure 4-1: Location and arrangement of monitoring points.....	4-64
Figure 4-2: The fluorescence in the FLT wavelength of water from various sources compared to solutions containing FLT.	4-65
Figure 4-3: Results of the Tracer Test Design Model.....	4-65
Figure 4-4: A line diagram of the LWRF showing the FLT dye addition points.	4-66
Figure 4-5: Mixing fluorescein in 55 gal. drums	4-67
Figure 4-6: Transferring fluorescein concentrate to 5 gal. buckets for delivery to wells.	4-67
Figure 4-7: Transfer of the dye concentrate into injection well 3.....	4-68
Figure 4-8: The residual dye was poured directly into the well.	4-68
Figure 4-9: The fluorescein concentrate mixing continued until midnight.	4-69
Figure 4-10: The fluorescein addition continued until about 02:00.	4-69

Figure 4-11: Effluent injection rates and resulting FLT concentrations for the first tracer test	4-70
Figure 4-12: Turner 10AU response to DI water based and submarine spring water based FLT solutions.....	4-70
Figure 4-13: The location of the background sampling points.	4-71
Figure 4-14: The FLT breakthrough curve measured at the NSG for each submarine spring.....	4-72
Figure 4-15: The FLT breakthrough curve measured at the SSG for each submarine spring.....	4-72
Figure 4-16: The South Seep Group grab samples FLT concentrations normalized to that of the submarine spring.....	4-73
Figure 4-17: The relationship between salinity and the FLT concentration.	4-73
Figure 4-18: The FLT concentration as measured and corrected for salinity at the SSG.	4-74
Figure 4-19: A comparison of NSG and SSG FLT breakthrough curves.	4-75
Figure 4-20: The NSG BTC extrapolated into the future until the FLT concentration drops below the MDL.	4-75
Figure 4-21: The SSG BTC extrapolated into the future until the FLT concentration drops below the MDL.	4-76
Figure 4-22: A laboratory sample with 35 ppb FLT in submarine spring water shows this dye is visible at concentrations much less than 100 ppb.....	4-76
Figure 4-23: Two-dimension synchronous scans of a submarine spring sample and a laboratory sample.	4-77
Figure 4-24: The light absorbance characteristics at the peak wavelength of 490 nm were nearly identical for calibration solutions and for samples collected at Seep 3.....	4-77
Figure 4-25: The location of points sampled during the area survey and the FLT concentration normalize to that at Seep 3.	4-78
Figure 4-26: The temperature measured in samples collected at the shoreline and at the SVO monitoring wells during the area surveys.	4-79
Figure 4-27: The specific electrical conductivity measured in samples collected at the shoreline and at the monitoring wells during the area surveys.	4-80
Figure 4-28: The results of macroalgae $\delta^{15}\text{N}$ values shown in relation to the normalized FLT concentrations of area survey.	4-81
Figure 4-29: The results of the nearshore radon survey shown in relation to the normalized FLT concentrations of area survey.	4-82
Figure 4-30: A line diagram of LWRF showing dye addition points for SRB.....	4-83

Figure 4-31: Effluent injection rates and the resulting SRB concentration.	4-84
Figure 4-32: Synchronous Scans of SRB calibration solutions.	4-84
Figure 4-33: Time series graphs showing fluorescence intensity measurements and emission wavelength synchronous scans of the 1 ppb SRB calibration solution.	4-85
Figure 4-34: Fluorescence in the SRB Wavelength Measured at the NSG.	4-86
Figure 4-35: Fluorescence in the SRB wavelength for the SSG.	4-86
Figure 4-36: Synchronous scans of samples collected in February and March, 2012 compared to solutions spiked with SRB.	4-87
Figure 4-37: Synchronous scans of samples collected in October and December, 2012 compared to solutions spiked with SRB.	4-88
Figure 4-38: Graphed are three synchronous scans to show the spectra of Fluorescein, SRB and fluorescein plus a hypothetical DA-SRB trace	4-89
Figure 4-39: The results of the particle tracking MODPATH model that shows the possible groundwater pathways injected wastewater	4-90
Figure 4-40: Temperature and specific electrical conductivity profiles for the SVO wells.	4-91
Figure 5-1: A plan view of the Tracer Test Design Model conceptual model and a cross section of the model grid.	5-30
Figure 5-2: The results of the MODPATH particle track simulation used adjust the conductance of the springs.	5-31
Figure 5-3: Results of the Tracer Test Design Model shown as the ratio of the submarine spring concentration to that at injection wells on the day of dye addition	5-32
Figure 5-4: The numeric grid used for the Lahaina Groundwater Tracer Study model.	5-33
Figure 5-5: The conceptual model for the Lahaina Groundwater Study showing the extent of the submarine layers	5-34
Figure 5-6: The Lahaina Groundwater Tracer Study conceptual model and the nearshore bathymetry.	5-35
Figure 5-7: Borehole stratigraphy for the LWRF injection wells developed from the drillers logs (County of Maui, 2004).	5-36
Figure 5-8: The conceptual model used in the PFP sensitivity simulations	5-37
Figure 5-9: The measured BTCs compare the model results when a horizontal flow barrier was included in the model.	5-38

Figure 5-10: The measured and simulated BTCs after the model marine boundaries were modified.	5-38
Figure 5-11: The modeled BTCs compared to that measured when a PFP was placed in Layer 2	5-39
Figure 5-12: The results of the dispersivity sensitivity simulations compared to the BTC for the NSG	5-39
Figure 5-13: The results of the porosity sensitivity simulations compared to the BTC at the NSG	5-40
Figure 5-14: Modeled BTC when sorption of FLT was simulated.....	5-41
Figure 5-15: The simulated and measured BTCs with differing anisotropy ellipse alignments	5-42
Figure 5-16: FLT plume simulated using and isotropic model (a) and an anisotropic model (b)	5-43
Figure 5-17: A map and modeled BTC when a PFP and anisotropy are simulated	5-44
Figure 5-18: Simulated SRB BTCs under two different treated wastewater injection scenarios.....	5-45
Figure 5-19: The SRB plume 1-year after dye addition under two different treated wastewater injection scenarios.....	5-46
Figure 5-20: The study area showing the location of a probable drowned stream valley relative to the FLT plume.....	5-47
Figure 5-21: A cross-section of a coastal aquifer comparing the dip of the lava bedding to the generalized groundwater flow path.....	5-48
Figure 5-22: The simulated FLT plume 620 days after the dye addition using an isotopic model (a) and using an anisotropic model (b).....	5-49
Figure 5-23: Simulated individual BTCs and composites showing a possible resulting BTC with multiple peaks and a plateau.	5-50

This page is intentionally left blank.

ACRONYMS

°C	degrees Celsius
°F	degrees Fahrenheit
µg	microgram
µm	micrometer
µM	micromoles
ADCP	Acoustic Doppler Current Profiler
asl	above sea level
BTC	breakthrough curve
C	Concentration
CFR	Code of Federal Regulations
cm	centimeter
cm ²	centimeters squared
d	day
DA-SRB	deaminoalkylated SRB
DI	deionized water
DIN	dissolved inorganic nitrogen
DON	dissolved organic nitrogen
DIP	dissolved inorganic phosphorus
DOP	dissolved organic phosphorus
dpm	decays per minute (units of radioactivity)
dpm/m ³	decays per minute per cubic meter
dpm/m ² /hour	decays per minute per square meter per hour
ex/em	excitation wavelength/emission wavelength
Ex ²²² Rn	excess radon isotope with atomic mass 222
FLT	Fluorescein
ft	feet
ft ²	square feet
ft/d	feet per day
ft bgs	feet below ground surface
ft msl	feet in reference to mean sea level
gal.	gallon
GPS	global positioning system
HDOH	State of Hawaii Department of Health
HDPE	high density polyethylene
HFB	horizontal flow barrier
HR ADCP	high resolution Acoustic Doppler Current Profiler
Hz	hertz
in	inch
in/yr	inches per year

km	kilometer
kmol/d	kilomoles per day
L	liter
LxDxW	Length multiplied by depth multiplied by width
L/min	liters per minute
lbs	pounds
LDPE	low density polyethylene
LWRF	Lahaina Wastewater Reclamation Facility
m	meter
m msl	meter reference to mean sea level
m/d	meter per day
m/s	meters per second
m ²	square meter
m ³	cubic meter
m ³ /d	cubic meter per day
m ³ /m ² /d	volume of cubic meter per area of square meter per day
MDL	Method Detection Limit
mg	milligram
mg/L	milligrams per liter
mgd	million gallons per day
MHz	mega hertz
mi	mile
ml	milliliter
ML & P	Maui Land and Pineapple
mm	millimeter
m msl	meters in reference to mean sea level
MODFLOW	Modular three-dimensional finite-difference ground-water flow model
MODPATH	A particle-tracking postprocessor model for MODFLOW
mmol/m/d	millimoles per meter per day
mol/d	moles per day
mrad	milliradian
MT3DMS	A modular 3-D multi-species transport model for simulation of advection, dispersion, and chemical reactions of contaminants in groundwater systems
n	number of samples in a statistical analysis
N	nitrogen
NA	not available
NAD-83	North American Datum of 1983
nm	nano-meters
NOAA	National Oceanic and Atmospheric Administration
NSG	North Seep Group
P	phosphorous
PFM	preferential flow path
ppb	parts per billion
ppm	parts per million

QTracer2	Program for tracer-breakthrough curve analysis for tracer tests in Karstic aquifers and other hydrologic systems
REV	Representative elementary volume
RWT	Rhodamine WT
s	period or second
sec	second
SGD	submarine groundwater discharge
SOEST	University of Hawaii School of Ocean and Earth Science and Technology
SRB	Sulpho-Rhodamine-B
SSG	South Seep Group
SST	sea surface temperature
TIR	thermal infrared
TTDM	Tracer Test Design Model
UNESCO	United Nations Educational, Scientific, and Cultural Organization
USACE	United States Army Corps of Engineers
USEPA	United States Environmental Protection Agency
USGS	United States Geological Survey
V	volume
WGS-84	World Geodetic Survey of 1984

This page is intentionally left blank.

EXECUTIVE SUMMARY

Overview

This project was completed by the University of Hawaii for the State of Hawaii Department of Health, the U.S. Environmental Protection Agency, and the U. S. Army Engineer Research and Development Center at Vicksburg, Mississippi. Its purpose has been to provide critical data about the possible existence of a hydraulic connection between the injection of treated wastewater effluent at the Lahaina Wastewater Reclamation Facility (LWRF), Maui County, Hawaii, and nearby coastal waters, confirm locations of emerging injected effluent discharge in these coastal waters, and determine a travel time from the LWRF injection wells to the coastal waters. The purpose of this Final Report is to detail final results of fluorescent dye tracer tests, associated groundwater modeling, and other results that have been made since the submission of the project's September 2012 Interim Report (Glenn et al., 2012). The purpose of this Executive Summary is to present an overview and synthesis of all principal project accomplishments, including both those presented in the Interim Report, and those of the new results presented in the Final Report Sections that follow here.

The principal findings of this project included the following key results:

- (1) Fluorescein tracer dye (FLT) added to LWRF injection Wells 3 and 4 arrived at coastal submarine spring sites with a time of first arrival of 84 days; a second dye, Sulpho-Rhodamine-B (SRB) was added to LWRF injection Well 2, with no confirmed detection of SRB.
- (2) Submarine springs releasing the fluorescein dye to the coastal ocean are located within two small and adjacent clusters termed the South Seep Group (SSG) and North Seep Group (NSG) at North Kaanapali Beach, approximately 0.85 km (0.5 miles) to the southwest of the LWRF, and within 3 to 25 meters of shore.
- (3) The peak concentration of the FLT tracer dye breakthrough curve occurred 9 and 10 months after the LWRF FLT addition at the south and north groups of submarine springs, respectively. The average travel time to both monitoring locations is in excess of one year (14 mo. for the SSG; 16 mo. for the NSG).
- (4) It is believed that the primary cause for the non-detection of SRB dye is the displacement of the injectate plume containing this dye away from a direct travel path from Injection Well 2 to the submarine springs by the greater injection volume into Wells 3 and 4. This interference further dilutes the SRB-containing plume prior to

reaching the submarine springs. In addition, secondary processes such as SRB dye degradation and sorption may also decrease the concentration to less than detectable levels.

(5) The oblique FLT travel path from the injection wells to the submarine springs are mainly attributed to the low hydraulic conductivity of the alluvium associated with the present and ancestral channel of the Honokowai Stream to the north and west, and the strong north-south hydraulic conductivity anisotropy caused by the steep west dipping lava flows relative to the near horizontal flow of the groundwater.

(6) Waters discharging the fluorescein dye from the submarine springs are warm and brackish, and have a temperature $>28^{\circ}\text{C}$, and an average salinity of 4.5 and a pH of 7.5.

(7) High-resolution airborne thermal infrared (TIR) mapping identified a large sea surface thermal anomaly associated with the warm water submarine springs. The nearshore surface area of this thermal anomaly is $\sim 674,000 \text{ m}^2$, or about 167 acres in size.

(8) The extent of shoreline where the FLT-tagged water is discharging is very close to that of the abnormally warm water identified in the airborne thermographic infrared mapping survey, and occurs to the southwest of a shortest (perpendicular) travel path from the point of injection to the coast.

(9) In total, all submarine springs mapped within the South Seep Group (106 seeps) were contained within an area of 500 m^2 , and all submarine springs mapped within the North Seep Group (183 seeps) were contained within an area of $1,800 \text{ m}^2$, located at the northeast corner of the large sea surface thermal anomaly. Ocean current flow likely rafts the thermal plume towards the southwest.

(10) Although numerous in number, individual submarine springs in the South and North Seep Groups are transitory in nature and small in size (5.4 cm^2 average). In combination with radon mass balance measurements, scaling the exit velocity of one vigorous and persistent spring to all springs mapped suggests that of the total output in the two spring groups, total groundwater discharge from the springs is ca. $<10\%$ of the total groundwater discharge, with diffuse groundwater discharge constituting the rest.

(11) As based on radon mass balance measurements, average total (fresh + marine) discharge from the submarine springs and the surrounding diffuse flow was about 2.19-3.33 million gallons per day (mgd) ($8,300\text{-}12,600 \text{ m}^3/\text{d}$). The freshwater component of that flow was about 1.61-2.88 mgd ($6,100\text{-}10,900 \text{ m}^3/\text{d}$), or about 73-87% of the total SGD.

(12) We have estimated that once the tracer dye break through curve has reached completion, that 64 percent of dye injected into Wells 3 and 4 will have been fully

discharged at the submarine spring areas. Thus, as viewed at steady state, it is also our conclusion based on these calculations that 64 percent of the treated wastewater injected into these wells currently discharges from the submarine spring areas.

(13) As based on geochemical/stable isotope source water partitioning analysis the estimated treated wastewater fractions in the submarine spring discharge ranged from 12 - 96 percent, with an average of 62 percent.

(14) Geochemical mixing analyses indicate that the submarine spring waters are predominately LWRF treated wastewater which while in transit to the submarine springs undergo oxic, suboxic and likely anoxic microbial degradation reactions that consume dissolved oxygen, dissolved nitrate, and organic matter.

(15) The N concentration of the submarine springs is reduced compared to LWRF treated wastewater, while the P concentration is enriched.

(16) The SSG and NSG seeps are distinct from other groundwater discharge sites studied in West Maui in the magnitude of DON, DOP and DIP fluxes per meter shoreline, and their low TN:TP and DIN:DIP ratios. The N:P ratios show that the seeps are enriched in P relative to N, when compared to other SGD sites

In sum, our results conclusively demonstrate that a hydrogeologic connection exists between LWRF Injection Wells 3 and 4 and the nearby coastal waters of West Maui. Eighty-four days following injection, FLT tracer dye introduced to these wells began to emerge from very nearshore seafloor along North Kaanapali Beach, approximately 0.85 km (0.5 miles) to the southwest of the LWRF. As proposed by Hunt and Rosa (2009), our results substantiate the conclusion that due to geologic controls that include a hydraulic barrier created by valley fills to the northwest, the main wastewater effluent plume from the LWRF travels obliquely towards the southwest. An estimated 64 percent of the Well 3&4 effluent follows this route and discharges at coast. The peak concentration of the FLT dye occurred 9 to 10 months following injection, with an average transit time of approximately 15 months. Since the treated wastewater plume is broad, the injectate travel time takes from about three months to arrive, to over an estimated four years for the draining trailing edge fully exit the coast. During this time, there is significant loss of nitrogen due to extensive denitrification and other suboxic to anoxic microbial degradation processes fueled by a sustained supply of organic matter transport within by effluent plume. The release of dissolved phosphorus, on the other hand, is relatively enriched. The treated wastewater discharges from the seafloor mixed with other marine and fresh waters predominantly as diffuse flow (>90%), but also through a patchwork of hundreds of very small (ca. 5 cm²) submarine springs. This central discharge area occurs as two adjacent clusters of diffuse flow and springs with a combined total seafloor area of 2,300 m². The emerging waters appear well mixed in the nearshore zone and, being relatively warm and brackish, spread over an area visible by thermal infrared imaging that covers an ocean surface area more than 167 acres in size. The lateral distribution of the FLT tracer dye agrees well with the lateral limits of the

anomalously warm ocean surface water plume detected by air. These conclusions drawn from both the Interim Report and this Final Report are summarized and discussed below.

Introduction

The study area is located in the Kaanapali District of West Maui, Hawaii. Current West Maui land use can be subdivided into (1) an urban center in the Lahaina area, (2) various diversified agriculture and pasture land on former pineapple and sugarcane fields on the lower slopes of the West Maui Mountains, (3) residential and resort development (including golf courses) along the shoreline, and (4) natural evergreen forest in the interior of the West Maui Mountains (Figure ES-1). Historical changes in agricultural land use within the western half of West Maui were documented by Engott and Vana (2007) for use in assessing the effects of rainfall and agricultural land-use changes on West and Central Maui's groundwater recharge. During the early 1900s until about 1979, land use was mostly unchanged except for some minor urbanization along the coasts. However, land-use changes became more significant as large-scale plantation agriculture declined after 1979. From 1979 to 2004, agricultural land use declined about 21 percent, mainly from the complete cessation of sugarcane agriculture. The Pioneer Mill Co. was the major sugarcane cultivator on the west side of the West Maui Mountains, operating during the late 1800s until 1999, when it ceased sugarcane production on approximately 6,000 acres and some of the land was subsequently converted to pineapple cultivation, including the area north of Honokowai Stream. The extent of pineapple agriculture in West Maui decreased extensively since the late 1990s, and stopped entirely in 2009 (Gingerich and Engott, 2012). Today, large portions of the former sugarcane and pineapple fields remain fallow, while other parcels have been converted to low-density housing and diversified agriculture.

The LWRF lies about 3 mi north of the town of Lahaina and serves the municipal wastewater needs for that community, including the major resorts along the coast. It receives approximately 4 million gallons per day (mgd) of sewage from a collection system serving approximately 40,000 people. The facility produces treated wastewater (tertiary treated with filtration and since October 2011 has been disinfected with chlorine to an R-2 standard), which is disposed of via four on-site injection wells. The tertiary treatment is biological nutrient removal, sand filtration, and the disinfection mentioned previously. All effluent undergoes this process. Tertiary treated wastewater that is disinfected with UV radiation to meet R-1 reuse water standards is also produced. Approximately 0.7 – 1.5 mgd of the facility's R-1 water is sold to customers, such as the Kaanapali Resort to be used for landscape and golf course irrigation. R-1 water that is not sold is discharged into the subsurface via the four on-site injection wells along with the tertiary treated effluent.

Multiple studies have investigated the nutrient flux to the West Maui waters and the role of the LWRF in contributing to the nutrient flux. A nutrient balance study of West Maui (Tetra Tech, 1993) identified the LWRF as one of the three primary nutrient release sources to Lahaina District coastal waters, in addition to sugarcane and pineapple

cultivation. That study ranked the LWRF second in annual nitrogen (N) contribution and first in phosphorous (P) contribution to these waters. Since that study was completed, the cultivation of both sugarcane and pineapple has been sharply curtailed, which implies that the LWRF may now be the primary contributor of nutrients to water in the study area. As an update, the West Maui Watershed Owner's Manual (West Maui Watershed Management Advisory Committee, 1997) concluded that the LWRF wastewater injection wells likely contributed about three times the amount of N, and at least an order of magnitude more P to the ocean than did any other source. Treatment process improvements in 1995 and the institution of wastewater reclamation since the release of the Tetra Tech (1993) study appears to have significantly facilitated an overall reduction of contributions of N and P to the LWRF injected effluent. However, both the concentrations and fluxes magnitude appears to remain significant both as a component of discharge from the submarine springs, as well as from other sources along the west Maui Coast (Interim Report Section 6; Final Report Section 3).

Over the past five years, researchers have repeatedly observed brackish, warmer-than-ambient-oceanic water emerging from the seafloor in the nearshore region (< 3 m depth) of Kahekili Beach Park. These submarine springs (termed freshwater seeps in other studies) were first found by scuba diving researchers in 2007. The observation that these submarine springs were noticeably warm, combined with the 2008 discovery of extremely elevated $\delta^{15}\text{N}$ values of macroalgae in the area (as high as 43.3‰; Dailer et al., 2010) heightened perceptions that this area might be affected by aquifer drainage from treated wastewater injection from the Lahaina Wastewater Reclamation Facility (LWRF). Hunt and Rosa (2009) investigated the use of multiple in situ tracers to identify the mechanisms controlling municipal wastewater effluent discharges to the nearshore marine environment and their point of release. These researchers sampled the LWRF effluent, submarine springs, nearshore marine waters, groundwater, and terrestrial surface water in vicinity of effluent injection sites in Lahaina and Kihei, Maui. In their work, the most conclusive tracers in the nearshore marine environment were the presence of pharmaceuticals, organic waste indicator compounds, and highly elevated $\delta^{15}\text{N}$ values in water samples and in coastal benthic macroalgal tissue. They identified the submarine springs as the coastal main exit locus of the LWRF injection plume. However, geochemical evidence from nearshore marine samples collected further south towards Kaanapali Golf Course showed effluent or effluent-derived irrigation water's influence. Based on this evidence, Hunt and Rosa (2009) delineated a probable extent of the LWRF effluent plume (Figure ES-2). The minimum extent of the plume is shown in Figure ES-2 as a red arc. Hunt and Rosa (2009) were less certain of their interpretation for the yellow arc shown Figure ES-2 that reaches further south because the elevated $\delta^{15}\text{N}$ values in water samples from dissolved NO_3^- could have been from irrigation recharge water that uses reclaimed water from the LWRF.

Submarine Springs and Marine Control Locations of Sampling, Water Quality, and Fluorescence

Section 2 of the Interim Report and Section 2 of this Final Report details:

- (1) techniques for sampling warm submarine springs at Kahekili for the injected tracer dye, radioisotope tracers, and geochemical and stable isotope tracers,
- (2) information on in-situ water quality parameters of the submarine springs and control locations,
- (3) field-determined fluorescence of samples collected from submarine springs, shore line points within the study area, control locations, and from a survey conducted in July 2012 to assess the quantity, size, and location of potential submarine springs from Honokowai Point to Black Rock and extending offshore to ~27 ft (~9 m) of depth.

This portion of the study included the installation of sampling infrastructure, collecting samples for the geochemical surveys, collecting more than 1,200 samples for field and tracer dye analysis, and deployment and collection of data from instruments for monitoring temperature and salinity.

The general clustering of the submarine springs were grouped into two groups termed the North Seep Group (NSG) and the South Seep Group (SSG), as noted above (Figure ES-3). Samples were collected from both groups and at three control locations. The submarine springs were sampled directly by drawing on SCUBA diver emplaced piezometers driven into springs, with the fluids extracted by peristaltic pump. Samples at other sites were collected as “grab samples.” The SSG is located approximately 25 m offshore and had three initial monitoring points (Seeps 3, 4, and 5). A fourth monitoring point, Seep 11, was added on November 24, 2011 due to high salinities being measured at Seeps 4 and 5. The Seep 4 piezometer was relocated in the NSG on April 24, 2012 to replace piezometers in that area that were covered by migrating sand. A total of 684 submarine spring samples were collected from the SSG from 7/5/2011 through 12/31/2012. The NSG is located approximately 3 to 5 m offshore with three initial monitoring points (Seep 1, 2, and 6). This location has proven extremely problematic to maintain throughout the duration of the project. The NSG’s close proximity to the shoreline subjected these piezometers to the persistent littoral migration of sand from the beach onto the seep group because of large north swells. As a piezometer was buried, it was replaced with a new one and all replacement piezometers were placed within 2 m of the original deployments. A total of 606 submarine spring samples were collected from the NSG from 7/5/2011 through 12/31/2012.

Submarine groundwater samples were also taken from 12/20/2012 through 1/8/2013 and on 4/29/13 and 5/1/13 at the shoreline adjacent to the North and South Seep Groups, south of Kahekili Beach Park, and adjacent to Honokowai Point. These samples were collected through piezometers outfitted with galvanized steel pipe extensions, allowing for the piezometer to be temporarily installed just offshore of the surge zone. In addition, on 12/29/2012, submarine springs in North and South Seep Groups and a substantial seep located between the two groups were sampled for the tracer dye.

Marine control locations for the dye tracer portion of the study were Honokowai Beach Park, Wahikuli Wayside Park, and Olowalu. Honokowai Beach Park, located ~1.8 km north of the study site, served as a site of possible dye emergence should the LWRF

effluent flow path proved to move to the north (Figure ES-3). Wahikuli Wayside Park, located ~4.3 km south of the main study, was targeted because of its proximity to the submarine spring locations. Olowalu is located ~13 km south of the main study area and was chosen to represent water with minimal anthropogenic impact due to lack of development and the termination of sugarcane operations in the late 1990's.

Water quality parameters of temperature, pH, specific conductivity, and salinity were measured on each seep sample (Table ES-1), the readings were taken at the discharge point of a peristaltic pump on the beach. In most locations, the salinity of the samples was less than 5, indicating that the captured seep waters were representative of submarine groundwater with little seawater influence. The pH of seeps in the NSG varied between 7.2 and 7.9 with an average of about 7.5. The pH of seeps in the SSG varied between 6.8 and 7.9 also with an average of about 7.5. The salinity of seeps in the NSG varied between 2.5 and 23 with an average of about 4.8. Seeps in the SSG had salinities that were slightly lower, varying between 3.8 and 22, with an average of about 4.1.

The seep water samples were also screened in the field for the presence of the project's two tracer dyes, Fluorescein (FLT), and Sulpho-Rhodamine-B (SRB). A pre-dye tracer injection monitoring period was conducted from July 5, 2011 through July 28, 2011, which was designed to measure the magnitude and variability of in situ fluorescence of the submarine spring water at the selected monitoring sites. Upon the addition of the dye, the sampling frequency was increased to two to three times per day. As the study progressed, the sampling frequency was decreased to one to two times per month when field sampling ended in December 2012. The SRB and FLT fluorescence measured in the field remained indistinguishable from background levels until late October, 2011. Subtle increases in field fluorometry measurements of FLT started to occur in samples from the NSG in late October, 2011, which provided the first indication that dye was emerging from the submarine springs. This was followed in mid-November by increasing FLT fluorescence of samples from the SSG. Beginning in January, 2012, the SRB wavelength fluorescence as read on the AquaFluor Handheld Fluorometer showed an increasing trend. Subsequent testing showed this was actually a response of the SRB channel the strong FLT fluorescence in the samples being analyzed and no SRB was in the samples being analyzed. As of May 13, 2013 there has been no confirmed detection of SRB.

A scuba diver survey was conducted in July, 2012 to document all visual submarine springs from Honokowai Point to Black Rock. The goal of this survey was to provide the project with information regarding the locations and dimensions (length and width) of additional submarine springs spanning study area. The survey was conducted by two scuba divers swimming together, and scanning the ocean floor for emerging submarine discharge. The locations of all submarine springs and any other areas that showed evidence of submarine groundwater discharge, such as by the presence of shimmering waters (a varying refraction of light as seen when fresh and salt or warm and cold water mix; sometimes referred to as "schlieren"), were mapped. Where encountered, the submarine springs were sampled directly using diver emplaced syringe sampling, and in other cases grab samples were collected in the shimmering water, normally near the

seafloor. When more than one submarine spring was found per square meter, all submarine springs were measured, one submarine spring was sampled with a syringe, and the location was marked with the GPS. Control samples for the North and South Seep Groups were taken over the main submarine spring areas. The surveys completed a total of 86 transects of various lengths from Honokowai Point to Black Rock, covering a combined distance of 20.8 km (12.9 miles).

In general, the divers were not able to find submarine springs other than those near or in the locations of already identified submarine springs in the North and South Seep Groups used in the tracer dye-monitoring portion of the project. In this nearshore region of Kahekili Reef, a total of 289 visible submarine springs were identified. The sum total of all visibly flowing areas of individually measured submarine springs in the North Seep Group was 2426.8 cm² or 0.243 m². The total of visibly flowing areas of measured submarine springs in the South Seep Group was 838.8 cm² or 0.0839 m². The combined total area of visibly flowing submarine springs was 3265.6 cm² or 0.336 m². In total, all submarine springs mapped within the North Seep Group were contained within an area of 1,800 m², and all submarine springs mapped within the South Seep Group were contained within an area of 500 m² (Figure ES-4). Most of the submarine spring samples collected through syringes revealed detectable FLT concentrations.

Aerial Infrared Sea Surface Temperature Mapping

The objective of thermal infrared (TIR) mapping portion of this investigation (Interim Report Section 4) was to determine the locations of both warm and cool emerging fluids to the coastal waters near the LWRF. For this work, we used high-resolution (2.3 m) aerial infrared remote sensing techniques to produce sea-surface temperature (SST) maps which revealed the existence of anomalously warm (~26.5°C), buoyant, emerging fluids relative to ambient coastal waters (25.5°C), as well as the presence of cooler, natural submarine groundwater discharge (20-22°C). These data were collected at night to eliminate the effects of solar surface water heating.

Our aerial thermal infrared methodology is highly accurate and sensitive to differentiating variations in both natural and anthropogenic surface water temperatures (Kelly et al., 2013), and we successfully identified a 673,900 m² (166.5 acre) thermal anomaly extending from the shoreline to at least 575 m (1886 ft) offshore (Figure ES-5). The thermal plumes from the springs themselves varied from 140 to 315 m² (1507 to 3391 ft²). Aside from the large thermal anomaly and the known warm submarine springs it resides over, no significant new warm water submarine spring locations were identifiable by the infrared thermography, nor by the regional scuba mapping surveys reported in Section 2 of this report.

Despite the fact that some thermal contributions from geothermal sources cannot be completely discounted (Glenn et al, 2012), the co-variance of the thermal anomaly and the warm effluent discharge from the submarine springs is clearly apparent (compare Figures ES-5, ES-6 and ES-7). The thermal anomaly is located southwest of the LWRF and occurs in direct association with the submarine springs (seeps) documented by our

tracer tests, groundwater modeling, and stable isotope studies to be hydraulically connected to the injected warm wastewater effluent from the LWRF. In addition, the anomaly lies well centered within the projected LWRF effluent plume trajectory predicted by Hunt and Rosa (2009), as well as that substantiated by our nearshore recovery of FLT tracer dye and the independently-determined tracer-based modeling results presented here (Figures ES-7 and ES-14). Furthermore, the spatial covariance between the TIR thermal anomaly and the $\delta^{15}\text{N}$ in macroalgae appears excellent (Figure ES-6). Approaching the locus of the submarine springs from the north, the thermal anomaly's surface water warming incrementally increases (~ 24.5 to 26.8°C) in agreement with the progressive increases in the $\delta^{15}\text{N}$ values of benthic macroalgae (+4.8 to +48.8 ‰) that reach a maxima centered at the submarine springs (Dailer et al., 2010). Dailer et al. (2012) found that the discharge from the submarine spring locations rises to the surface due to its positive buoyancy relative to the seawater column. Once at the surface, the anomalously warm waters flow in the summer is clearly towards the south-southwest, along with the most predominant bottom and surface water currents in the area (Storlazzi and Field, 2008; Swarzenski et al. 2012).

Submarine Groundwater Discharge

Our field observations revealed that visually obvious submarine groundwater discharge (SGD) within the study area occurs via seeps clustered into two groups, the SSG and NSG. FLT was identified in all seeps within SSG and NSG, but a proper mass balance of dye tracer recovery requires that the magnitude of seep discharge in these clusters be quantified. Thus, the objective of the SGD portions of the study was to quantify groundwater discharge via discrete seeps and evaluate the temporal variability of this discharge. In addition, groundwater discharge via diffuse seepage also occurs at these sites and may be responsible for some tracer fluxes. Our second objective was therefore to determine what fraction of total groundwater flux discharges via discrete seeps as opposed to diffuse seepage.

SGD to the nearshore waters in the study area (Interim Report Section 5; Final Report Section 3) was measured using two technologies. In the first, the groundwater radon signature was used in a coastal radon mass balance to measure SGD over the expanse of the study area. In the second, an Acoustic Doppler Current Profiler (ADCP) was used to measure point discharges of SGD. The ADCP technique measures water velocity profiles in 3 dimensions by transmitting short acoustic pulse pairs into the water, and calculating the phase shift between the two return signals.

Both the radon mass balance method and ADCP measurements provide total submarine groundwater discharge, i.e., freshwater plus recirculated marine water, but neither can detect or quantify the amount of wastewater effluent. It is, however, possible to calculate the fraction of fresh groundwater and, in combination with other geochemical information, also the fraction of the injected LWRF effluent. The relevance of these methods to the overall objectives of the project is to provide groundwater flux from the submarine springs to help determine the degree of dye recovery and the discharge of effluent through the submarine springs as the project progressed.

Radon and radium isotopes are highly enriched in groundwater and depleted in ocean water, and in the absence of other sources, their detection in coastal waters is an indication of SGD. A mass balance of these tracers can be used to estimate the amount of groundwater discharge required to supply the observed inventory of these tracers in the coastal zone. Owing to its short half-life (3.8 days) and the fact that ocean water has very low levels of radon, this gas has now almost universally become the routinely measured tracer for SGD flow rates, as the decay rate of ^{222}Rn is comparable to the time scales of many coastal circulation processes (Burnett et al., 2006). Thus, the dynamics of groundwater inputs as well as estimates of groundwater discharges may be examined via radon monitoring of coastal waters (Burnett and Dulaiova, 2003).

A radon mass balance model was constructed to estimate discharge from time series radon measurements in the surface water. The model accounted for radon evasion to the atmosphere, inputs by diffusion and from offshore ocean, in-situ production from dissolved ^{226}Ra , losses by coastal mixing and tidal exchange (Burnett and Dulaiova, 2003). It was found that groundwater discharge from the submarine springs is tidally modulated with minimal discharge at high tide and increased fluxes at low tide. Due to this variability, we expressed discharge as a 24-hour average. Figure ES-8 shows the area where the radon survey identified significant fluxes of groundwater discharge. The total (fresh + saline) groundwater discharge from the both NSG and SSG submarine spring groups including the direct discharge from the submarine springs and the surrounding diffuse flow was 8,300 m^3/d (2.19 mgd) and 12,600 m^3/d (3.33 mgd) in June and September of 2011, respectively. Out of this, fresh groundwater discharge amounted to 6,100 (1.61 mgd) and 10,900 m^3/d (2.88 mgd) in June and September 2011, respectively. Coastal radon surveys that apply a slightly different radon mass balance based on coastal flushing rates (Dulaiova et al., 2010) resulted in groundwater discharge of 8,800 m^3/d (2.32 mgd) total for NSG and SSG. This was derived from two combined surveys performed in June and September 2011. The surveys showed that there is significant groundwater discharge along the coastline north and south of the submarine springs. We found several sites with a total groundwater discharge ranging from 2,000 (0.53) to 28,000 m^3/d (7.4 mgd), the highest flux at 28,000 m^3/d (7.4 mgd) was at Hanakao'o Beach Park, the second largest at 15,000 m^3/d (3.96 mgd) was at Honokowai Beach Park. We also used the nearshore-marine radon survey to estimate the coastal SGD from North Honokowai to south of Hanakao'o Beach (Figure ES-8). This calculation did not represent the entire shoreline, but rather the areas of the highest discharge rates shown by the boxes in Figure ES-8. The summed total SGD for the areas of highest SGD was 54,000 m^3/d (14.3 mgd). This represents a total (freshwater + recirculated marine water) SGD of 7.45 $\text{m}^3/\text{m}/\text{d}$ (3.17 mgd/mi), as integrated over the 11.8 km of shoreline for this portion of the coast. As this value only represents the areas contained in the boxes in Figure ES-8, it represents a minimum estimate to total SGD. The large uncertainties in these estimates are discussed in Section 5 of the Interim Report.

Our initial ADCP vertical velocity measurement at selected seeps in September 2011 showed that water velocities are very close to the sensitivity of our instrument in an

upward looking deployment. In October and November 2012 we restricted our observations to only one seep, and used a downward-looking ADCP configuration to accurately measure seep discharge. To do this, the ADCP was mounted on an arm of a stand and centered above a seep at 1 m above the seafloor (Section 3). Due to the persistent problems of bottom instability due to sand migration at the NSG, we focused attention on measuring seep fluxes in the SSG, and selected Seep 4 within it as representative of all seeps within the two clusters to document discharge dynamics. Seep 4 had dimensions of 13 cm x 7 cm, which is 11% of the sum of the seep areas identified by the submarine spring survey in the SSG (838.8 cm²) and 3% of the sum of seep areas in the SSG and the NSG combined (3,265 cm²). We found that discharge varies throughout the tidal cycle and between tidal cycles. We observed a >100% variation in discharge between three deployment periods in October and November 2012. Using Seep 4 measurements to upscale to seep fluxes within SSG and NSG resulted in 21-86 m³/d (0.0056-0.023 mgd) and 83-336 m³/d (0.022-0.089 mgd) for SSG and SSG+NSG, respectively. When compared to total SGD determined in June and September 2011, the seep discharge as measured by the HR Aquadopp Profiler only represented <8% of total SGD determined by Rn methodologies at these two seep clusters, indicating that >90% of the discharge within the two seep groups is technically occurring as diffuse flow. Based on these findings we can conclude that the two seep groups consist of porous geology that allows groundwater to be discharged through discrete vents and other openings that may or may not be covered by sand or rock. We called the latter "diffuse seepage" because vents could not be identified. We also note, however, that the vents themselves are transient in nature and may disappear and reappear due sand migration. The major discharge areas are confined to two clusters of only a several meters width with very little discharge in between and around them.

We found that groundwater discharge is responsible for significant nutrient fluxes to the coastal ocean. Fluxes of dissolved inorganic and organic nitrogen (DIN and DON) are the largest at Hanakao'o Beach (DIN: 2.9 kmol/d or 41,440 g/d of N and DON: 1.7 kmol/d or 23,700 g/d of N). Second largest DIN flux along this coastline is from Honokowai (1.9 kmol/d or 27,500 g/d of N) and DON flux at SSG (up to 650 mol/d or 9,500 g/d of N). At Hanakao'o and Honokowai groundwater discharges along 1,200 m and 300 m length, while at the seep clusters the discharge locations are only 50-100 m long. SSG and NSG alone represent the largest sources of DON, dissolved inorganic and organic phosphorus (DIP and DOP) per meter coastline amongst all identified sources. The two seep groups are responsible for fluxes of 100-218 mol/d or 1,400-3,053 g/d of N as DIN, 120-910 mol/d or 1,670-12,750 g of N as DON, 99-116 mol/d or 3,070-3,600 g/d of P as DIP, and 16 mol/d or 480 g/d of P as DOP. These inputs impact coastal water quality and result in elevated nutrient concentrations. At SSG and NSG coastal seawater DIN ranges are 0.38-0.81 µM or 5.3-11.3 µg/L of N as opposed to offshore levels of <0.1 µM or <1.4 µg/L, DON ranges are 4.8-12.7 µM or 67-178 µg/L of N as opposed to 4.5-6 µM or 63-84 µg/L of N offshore, DIP ranges 0.16-0.44 µM or 5.0-13.6 µg/L of P in comparison to <0.1 µM or <3.0 µg/L of P offshore, and the DOP concentration range of 0.21-0.27 µM or 6.5-8.4 µg/L of P is comparable to offshore levels (Karl et al., 2001). SSG and NSG are not the only location with elevated nutrients, however. For comparison, Hanakao'o Beach coastal ocean DIN concentrations (7.7 µM or 108 µg/L of

N) are 10-times and DIP levels (0.84 μM or 26 $\mu\text{g/L}$ of P) are 2-times higher than at the seep clusters. In comparison to other studied locations along the coastline, SSG and NSG seep sites had the lowest observed TN:TP and DIN:DIP ratios in groundwater (2-8 and 1-2) and also in coastal ocean water (15-20 and 2).

The SSG and NSG seeps are distinct from other groundwater discharge sites studied in West Maui in the magnitude of DON, DOP and DIP fluxes per meter shoreline, and their low TN:TP and DIN:DIP ratios. The N:P ratios show that the seeps are enriched in P relative to N, when compared to other SGD sites and to ambient marine nutrient ratios.

We note that earlier studies identified surface runoff as an important coastal nutrient source (TetraTech, 1993). This current study did not quantify these inputs.

Aqueous Geochemistry and Stable Isotopes

This portion of the study (Interim Report Section 6) utilized a multi-tracer approach similar to, but broader in scope than that applied to this study area by Hunt and Rosa (2009). The purpose of our approach was to determine the proportion of different waters that exit the submarine springs, ascertain the origins of nutrients in the area's groundwater, evaluate the down-gradient geochemical evolution of the area's groundwater prior to its discharge to the ocean, and as possible identify the impact of land-derived nutrient fluxes on the geochemistry of coastal marine waters. Special emphasis was placed on determining the geochemical evolution and ultimate fate of the LWRP effluent after its injection. Data collection for this section was accomplished over two separate sampling intervals in 2011 (June 19-30 and September 19-25). Temperature, conductivity, salinity, pH, chloride (Cl^-) concentrations, nutrient concentrations, and stable isotope ratios of hydrogen (H) and oxygen (O) in water, and nitrogen (N) and O in dissolved nitrate (NO_3^-) were measured in order to characterize the geochemistry of the study area's groundwater, surface waters, treated wastewater, and coastal waters. Samples of gas bubbles emanating from the submarine springs and black precipitates that coat the rocks and coral rubble around submarine spring sites were also geochemically analyzed. Generally conservative tracers such as the isotopic ratios of H and O in water and Cl^- concentrations were used to evaluate mixing between potential end-members, while N loading was considered together with the isotopic ratios of N and O in dissolved NO_3^- to evaluate origin, evolution, and mixing of N species.

Figure ES-6 shows the distribution of $\delta^{15}\text{N}$ values in the samples collected from this study and compares this data with the intertidal macroalgal $\delta^{15}\text{N}$ values from Dailer et al. (2010), and the aerial TIR measured sea-surface temperatures obtained at night. Very highly enriched $\delta^{15}\text{N}$ values of dissolved nitrate from the submarine spring samples spatially correlates with the most highly enriched $\delta^{15}\text{N}$ values from the intertidal benthic macroalgae samples presented in Dailer et al. (2010). Tables ES-2 and ES-3 summarize the nutrient chemistry for the samples collected in June and September, 2011, respectively.

Although a thorough regional quantitative evaluation of nutrient sources was not accomplished in this study, this work identified several potential nutrient sources to the coastal zone based on the spatial distribution of nutrient species with respect to current and former land-use practices. These potential sources are:

- (1) Fertilizer applied in support of former agriculture appears to still be contributing to N and P loading of basal groundwater (though to a lesser extent than in the past, when these agricultural practices were ongoing). The production wells upgradient of the past and present agricultural influence had N and P concentrations of about 30 and 60 $\mu\text{g/L}$, respectively. The production wells most impacted by agriculture had N and P concentrations of about 2,500 and 180 – 300 $\mu\text{g/L}$, respectively.
- (2) Injected LWRF effluent appears to contribute significant amounts of N and P to groundwater (although the concentrations are much less than prior to wastewater treatment upgrades in 1995), but the temporally variable and non-conservative behavior of these species complicates the overall assessment of the magnitude of the source. The N and P concentrations in the LWRF effluent were ca. 7,200 and 700 $\mu\text{g/L}$, respectively for June, 2011, and ca. 6,200 and 170 $\mu\text{g/L}$, respectively for September, 2011. The N concentration of the submarine springs appears to be reduced compared to the LWRF wastewater effluent, while the P concentration appears to be enriched. The average N and P concentrations in samples collected from the submarine springs were ca. 600 and 400 $\mu\text{g/L}$, respectively, for June, 2011, and ca. 1,600 and 450 $\mu\text{g/L}$, respectively, for September, 2011.
- (3) R1 irrigation water and possibly fertilizer appear to contribute to N and P loading in groundwater supplying Black Rock lagoon. During the June, 2011 sampling event the N and P concentrations in the Black Rock Lagoon were 3,400 and 190 $\mu\text{g/L}$, respectively.

All biological compounds can undergo various forms of alteration and decomposition. As a result of this decomposition, organic matter is degraded into simpler molecules and inorganic species, including nutrients. Whether it be in soils, fresh water or marine conditions, the most important and fundamental of these processes is the microbial decomposition of organic matter, which generally follows a succession of steps that depend largely on the nature and availability of the oxidizing agent, as shown in Table ES-4 (e.g. Froelich et al, 1979; Berner, 1980; Appelo and Potsma, 1993; Berner and Berner, 1996; Stumm and Morgan, 1996). Thus, as shown in Table ES-4, when provided with an ample supply of labile organic matter (shown for simplicity as CH_2O), such as the injected wastewater effluent at the LWRF, O_2 is first used as the oxidizing agent until it becomes sufficiently to completely depleted by aerobes. After aerobic O_2 depletion, further decomposition occurs in steps as nitrate reduction, manganese oxide reduction, iron reduction, and so on. In combining geochemical approaches, we have found evidence for significant down-gradient oxygen depletion and geochemical evolution of the groundwaters within the study area including:

- (1) Mixing analysis using conservative tracers suggests that the submarine spring water is primarily injected LWRF wastewater effluent (Table ES-8, Figure ES-9).
- (2) Although likely subject to temporal variation, the majority of the NO_3^- present in the LWRF wastewater effluent has been acutely attenuated via suboxic denitrification (nitrate reduction) prior to its emergence at the submarine springs at the time of this study (cf. Table ES-4). A bi-product of these reactions is the ubiquitous presence of highly N_2 -enriched gas bubbles that conspicuously vent from both the submarine springs and nearby unconsolidated sands into the ocean in this area.
- (3) As manganese must be in the reduced state (Mn^{2+}) in order to be aqueous and mobile, the presence of solid phase Mn-oxide and/or Mn-oxyhydroxide impregnations and coating rocks and coral rubble surrounding the submarine springs indicates that the exiting waters have additionally undergone suboxic to anoxic manganese reduction.
- (4) The injected LWRF wastewater effluent is augmented in PO_4^{3-} in the subsurface prior to its emergence at the submarine spring sites. We believe this is likely due to aquifer conditions promoting the release or dissolution of previously particle-adsorbed and/or mineral-bound PO_4^{3-} .
- (5) Groundwater at, and down gradient of locations subjected to significant artificial recharge is augmented in SiO_4^{4-} , likely mobilized via accelerated rock weathering.

By analyzing the spatial distribution of various water parameters in the marine environment, including nutrient concentrations and stable isotope values (Tables ES-5 and ES-6; Figure ES-6), we have located several coastal ocean areas with terrestrial nutrient contribution. These are:

- (1) The marine environment immediately surrounding the submarine springs, which shows a dissolved NO_3^- isotopic signature consistent with the heavily ^{15}N -enriched (very positive $\delta^{15}\text{N}$) values characteristic of nitrate reduction measured in the submarine spring water.
- (2) The area near the mouth of Black Rock lagoon, which shows generally elevated nutrient concentrations relative to nearby waters and a dissolved NO_3^- isotopic signature consistent with values measured in Black Rock lagoon itself.
- (3) The area near Wahikuli Wayside Park, which also shows generally elevated nutrient concentrations relative to nearby waters, and shows a dissolved NO_3^- isotopic signature suggestive of denitrification from fertilizer or natural sources and/or sewage/manure content. Sugarcane was grown in the Wahikuli area until 1999, and the current community is unsewered with many cesspools and septic systems.

Fluorescent Dye Groundwater Tracer Study

Two tracer dye tests were conducted at the LWRF (Interim Report Section 3, Final Report Section 4). These tests were aimed at providing critical data about potential hydrological connections between the injected treated wastewater effluent and the coastal waters, confirming the locations where injected treated wastewater effluent discharges into the coastal waters, and determining a travel time from the injection wells to the coastal waters. In the first tracer test, Fluorescein (FLT) was added to LWRF Injection Wells 3 and 4 on July 28, 2011. This was followed two weeks later by an addition of Sulpho-Rhodamine-B (SRB) into Injection Well 2 on August 11, 2011, which has a significantly higher injection capacity than the other three wells. The second tracer test was conducted to investigate whether the effluent from this well discharges into the marine environment at the same locations as Wells 3 and 4.

Fluorescein Dye Tracer Test

The FLT dye from this tracer test started discharging at the nearshore submarine springs of the NSG in late October, 2011, about 84 days after addition to Wells 3 and 4 (Figure ES-10). At the NSG, the FLT concentration increased to about 21 ppb then plateaued in late February 2012 at the NSG. The peak concentration of 22.5 ppb occurred at this seep group about 306 days after the FLT addition. The BTC at the NSG plateaued from late February, 2012 to mid-May, 2012. At the SSG, the initial detection of FLT occurred 109 days after the FLT addition. The FLT concentration then increased to a peak of 34 ppb about 271 days following the FLT addition. Both BTCs exhibit a long trailing edge with the slope of the descending limb being much flatter than the ascending limb. The field sampling ended prior the tracer concentrations dropping below the MDL. To compute the mean time of travel and the percent recovery of the FLT, the remainder of the BTCs was estimated using an exponential curve fit based on the last three months of measured data.

Our analysis of the BTC was completed using the EPA's tracer test model Qtracer2 of Field (2002). This program uses the BTC to analyze the tracer test results providing critical information, such as the time to first arrival and to the peak concentration, mean transit time, average tracer velocity, dispersivity, and the percent of the injected dye mass recovered. The latter calculations require groundwater flux data. Qtracer2 was run at two discharge points, (1) the NSG and (2) the SSG. This approach was acceptable because the submarine spring survey showed that these locations were the primary discharge points for the FLT. The submarine spring survey (Sections 2.3.4 and 4.2.6.2) showed that the FLT concentrations measured during the long term monitoring were representative of that from the submarine springs surrounding the monitored submarine springs. Table ES-7 details the output of the QTracer2 calculations for the NSG and SSG. Based on the QTracer2 analysis, the first detection of FLT at the NSG occurred on October 22, 2011, 86 days after FLT addition. At the SSG, the first detection occurred on November 14, 2011, 109 days after the FLT addition. The time of peak concentration occurred 306 and 271 days after the FLT addition for the NSG and SSG, respectively.

The average time of travel occurred 487 and 435 days after the FLT addition at the NSG and SSG, respectively.

The percent of dye mass recovery was used to estimate the percent of treated wastewater in the SGD at the submarine springs (Table ES-8). QTracer2 estimated that 64 percent of the FLT dye added to Injection Wells 3 and 4 is accounted for by the BTC analysis at the NSG and the SSG, which represents the fraction of treated wastewater reaching these areas. The average injection rate into Wells 3 and 4 for the period from April, 2011 through March 2012 (data from Table 1-2 in the interim project report) was 2.47 mgd (9,340 m³/d). Thus, at the combined average Well 3 and 4 injection rate of 2.47 mgd and a QTracer2 tracer dye recovery rate of 64%, the average delivery rate of treated wastewater to the ocean at the north and south seep groups for this period of time was 1.58 mgd (5,978 m³/d). In addition, the fraction of treated wastewater as a component of total SGD at the submarine springs can also be calculated using the FLT percent recovery. That is, since the volume of treated wastewater discharge at the submarine springs was 1.58 mgd (5,978 m³/d), the treated wastewater fraction of the 2.32 mgd (8,800 m³/d) total SGD from the submarine springs is 68 percent.

The fraction of the treated wastewater in the submarine spring discharge was also estimated by geochemical/stable isotope methods (Figure ES-9). These data and their critical uncertainties can be found in Table 6-14 and Section 6 in the project Interim Report (Glenn et al., 2012). Those results are summarized here (Table ES-8) and compared to the percent of dye mass recovery method. As shown, three sets of mixing end members were used in geochemical/stable isotope source water partitioning analysis: (1) $\delta^{18}\text{O}$ and $\delta^2\text{H}$, (2) $\delta^{18}\text{O}$ and Cl, and (3) $\delta^2\text{H}$ and Cl, and listed for each are the minimum, average, and maximum percent of treated wastewater in the submarine springs. Collectively, the estimated treated wastewater fractions in the submarine spring discharge as determined in this manner ranged from 12 percent to 96 percent with an average of 62 percent. The tracer dye percent recovery analysis described above falls well within the bounds of the isotopic mixing analysis, and is reasonably close to this average value.

To better define the spatial extent of FLT plume, three rounds of sampling were conducted throughout the entire nearshore region between Honokowai Point to the north, and Black Rock to the south (Figures ES-2 and ES-7). In this effort, the seafloor was surveyed in detail by scuba, submarine spring samples were collected by syringe, grab sampling where collected from diffuse seepage, and porewater samples were collected through a piezometer just offshore of the surge zone. Shallow monitoring wells were also sampled on the Starwood Vacation Ownership Resorts (SVO) property fronting the area where FLT is discharging. Figures ES-4 and ES-7 shows the location of all samples collected. Specific electrical conductivity (SEC) measurements were used to correct the measured FLT concentration for elevated salinity. To reference the results of these different surveys to a single diagnostic parameter, the FLT concentrations were normalized to the concentration at Seep 3, this seep being chosen as the point of maximum FLT concentration. The actual normalization was computed using the ratio

C_i/C_{\max} , where C_i is the concentration at sample location “i,” and where C_{\max} is the maximum concentration of the plume (i.e., the concentration at Seep 3).

Area survey sampling showed that the FLT plume was quite extensive with the northern and southern extents closely matching that of the TIR plume boundaries (Figure ES-7). The area survey results also demonstrated that the FLT concentrations in the samples collected of the long term monitoring program were representative of the concentrations in the water discharging from the surrounding springs. A sample collected 125 m north of the NSG had an FLT concentration that was 11 percent of the concentration measured as Seep 3. The shoreline sampling survey continued 980 m to the north of the location of that sample, but none tested positive for FLT. Eighteen samples were collected south of the SSG. Five of these samples had FLT fluorescence that exceeded that of the background and were evaluated as containing FLT. All of the samples south of the SSG that tested positive for FLT were at or were north of southern TIR plume boundary.

Sulpho-Rhodamine B Tracer Test

The second dye tracer test was conducted using SRB dye to evaluate whether the effluent from Injection Well 2 discharges at the same locations as that from Injection Wells 3 and 4. Well 2 has a significantly higher injection capacity than the other wells, indicating that it may have a hydraulic connection to a preferential flow path. For this second test, SRB was added to the LWRP effluent on August 11, 2011. To date, there has been no confirmed detection of the SRB dye in the nearshore marine waters, but there were a limited number of samples that had a fluorescence spectrum consistent with trace concentrations of SRB. Figure ES-11 shows a 15 month time series of the SRB analysis for the NSG and SSG. Plotted are the average SRB wavelength fluorescence and error bars showing the magnitude of maximum and minimum measured values for each sample day. The fluorescence measured is that of background plus that of any dye that may be present. There were no confirmed detections of SRB and the samples with elevated SRB wavelength were generally isolated occurrences with the sample prior and following exhibiting baseline SRB fluorescence.

At the time of this writing, in excess of 1.5y have elapsed since SRB was added to the treated wastewater stream at the LWRP Well 2. Although there were no confirmed detections of SRB, several samples had fluorescence characteristics indicative of trace concentrations of this dye, and possible deaminoalkylation shifts of the SRB emission spectrum to shorter wavelengths (in the direction of the FLT peak) were detected. Eighty-eight samples were evaluated for DA-SRB and for trace concentrations of SRB using synchronous scans. Three samples collected from Seeps 3 and 12 during February and March, 2012 showed elevated fluorescence peaks at 580 nm, the peak emission fluorescence of SRB. Three samples collected from Seeps 3 and 5 in October and December, 2012 also exhibited fluorescence peaks at 580 nm. Finally, a sample collected from SRV Well 2 on July 31, 2012 fronting the study area had a fluorescence peak at 570 nm indicating possible DA-SRB. Figure ES-12 compares: (1) synchronous scans of the samples collected from Seep 3 and Seep 12, (2) a sample from SVO Well 2, (3) a sample from Seep 3 on June 14, 2012 and (4) a laboratory solution prepared for this study. The

laboratory solution was prepared with a FLT concentration of 35 ppb, similar to that of the submarine spring samples, and a SRB concentration of 0.05 ppb. This figure illustrates the similarity between the Seep 3 sample and the sample spiked with 35 ppb FLT and 0.05 ppb SRB. Still, we consider this as only a "possible" SRB detection, however, since there have been no subsequent samples collected with similar fluorescence characteristics. The samples collected from Seep 3 on February 10, 2012 and from Seep 12 on March 14, 2012 displayed only slightly elevated fluorescence in the SRB emission wavelengths. An additional sample collected from Seep 3 on June 14, 2012 (shown in violet) had no elevated fluorescence in the SRB emission wavelengths and is presented for reference. The sample collected from SVO Well 2 had emission wavelength fluorescence similar to that of the laboratory standard, except that its peak fluorescence occurred at 570 nm rather than 580 nm. This could indicate that SRB altered by deaminalkylation was present in the SVO Well 2 sample. Due to the failure to positively detect SRB, and interference with the SRB plume due to the injection in Wells 3 and 4, no conclusions can be made regarding the hydraulic connection between Well 2 and the nearshore waters at Kaanapali.

Lahaina Groundwater Tracer Study Numerical Modeling

Groundwater modeling was used by this study to aid in the design of the tracer test, interpret the dye tracer breakthrough curve (BTC), and assess processes that affect the fate and transport of the injected treated wastewater (Interim Report Section 7, Final Report Section 5). The specific modeling objectives were to (1) provide critical data needed to design the tracer test; (2) investigate the role of hydrologic features such as barriers or preferential flow paths on the dye transport; and (3) assess the impacts of processes such as sorption and dispersion on the temporal and spatial distribution of the tracer dye.

Our modeling approach was three fold. First, a basic model was developed to aid in the design of the tracer test, which was termed the Tracer Test Design Model (TTDM). The primary purpose of this model was to estimate the tracer dye dilution that would occur as it traveled from the injection wells to the submarine springs. Second, to aid the sampling plan, we estimated the time of the first dye arrival and the duration of the BTC. Once the dye started emerging from the submarine springs, the developing BTC was compared to the output of the TTDM. As differences were noted, the TTDM was modified to improve the agreement between the model output and the actual tracer data. Finally, after the BTC was sufficiently developed, the model output was compared against the actual tracer data and a comprehensive revision of the model was undertaken. Under data limitations, the final model was modified to obtain a reasonable match between the main features of BTC compared to field data. Different hydrogeological processes were then tested to determine which process may be affecting the tracer dye transport.

The models used in this study neglected density-dependent flow by only considering freshwater movement. The saltwater interface used to specify the bottom boundary of the model was based on the density-dependent model developed by Gingerich (2008). Using this approach was deemed reasonable since models by Hunt (2006), Burnham et al.

(1977) and Wheatcraft et al. (1976) indicated that shortly after being injected, the buoyancy of the wastewater causes it to rise relative the surrounding saline water, placing it in the freshwater zone. Hence, the majority of the flow is restricted to the fresh water lens.

The Modular Finite Difference Groundwater Flow Model MODFLOW (Harbaugh et al., 2000) was used for simulating groundwater systems. The flow solution computed by MODFLOW was used by transport models MODPATH and MT3D-MS to simulate the movement of dissolved constituents. The MODPATH (Pollock, 1994) model uses the groundwater flow solution from MODFLOW to track the movement of virtual particles from cell to cell in the finite difference grid, by only considering advection, and with the output as a visual track representing the path the virtual particles take from a point of origin to a point of termination. The point of termination can either be defined by an elapsed time designated by the modeler, or a boundary or sink in the modeled area. The model is very useful for evaluation of groundwater flow paths. The solute transport code Multi-Species Transport Model in Three Dimensions (MT3DMS) (Zheng and Wang, 1999; Zheng, 2006) was used to simulate the fate in transport of both FLT and SRB. The code simulates the effect of advection, hydrodynamic dispersion retardation (slowing of the plume transport due to the dissolved species sorbing onto the aquifer matrix), and the role that hydraulic conductivity anisotropy play in the transport of the dissolved tracer dye.

Figure ES-13 shows the final model's area coverage and the submarine boundaries. These boundaries accurately follow the nearshore bathymetry, while those of the planning model (Tracer Test Design Model = TTDM) were more general. With the exception of this noted difference, the coverage, geologic distribution, and other boundaries remained same throughout the modeling process. Initial model runs were used to plan the amount of the dyes needed, and to estimate the expected arrival time of the dyes at the submarine springs. With very minimal calibration, the TTDM was successfully able to estimate the first arrival, time of peak concentration, and, of critical importance, the expected dye dilution.

After the initial detection of the FLT dye, the results of the developing BTC were compared to those simulated by the TTDM, and the model was modified to improve agreement. The TTDM conceptual model was modified to (1) accurately reflect the addition of two dyes (FLT and SRB), (2) include the average injection rates into each well rather than injection into a single well, and (3) complete limited sensitivity analyses to identify the geologic configurations, features, and boundary conditions that produce the best agreement between the simulated and actual BTCs. Following the model modifications, the effect of the streambed alluvium to the north and possibly west of the LWRF was tested on the simulated BTC. Also tested, were the effects of varying the nearshore bathymetry, porosity, hydraulic conductivity, anisotropy, and sorption. These tests were performed to identify which factors were most important in controlling the transport of the dyes (primarily FLT), the primary goal being to explain the oblique travel path taken by FLT from the injection wells to the submarine springs. A secondary goal was to identify which processes and factors that might account for the major features of

the BTC (i.e., the time of first arrival, time and magnitude of peak concentration, and the slope of the descending limb).

The groundwater flow and transport modeling completed in this study identified four major controls on the pathway the injectate takes. These are: (1) the density difference between saltwater and the non-saline treated wastewater; (2) the low hydraulic conductivity alluvium and weathered basalt associated with the current and past channels of the Honokowai Stream; (3) the nearshore bathymetric gradient; and (4) the dominant north-south hydraulic conductivity of the basalt aquifer.

The low hydraulic conductivity alluvium and weathered basalt associated with current and past channels of the Honokowai Stream pose a barrier to the transport of the injectate to the north and probably to the west. Valley fill associated with stream channels are a well-recognized barrier to groundwater flow (Mink and Lau, 1992a, 1992b, 1993a, 1993b; Nichols et al., 1996; Oki, 2005). The proximity of the submarine valley shown by the bathymetry in Figure ES-14 to the current Honokowai Stream strengthens the hypothesis of Hunt and Rosa (2009) and of this study that stream valley fill and weathered basalt pose a barrier to flow of the LWRF injectate to the north and west.

Modifying model boundaries to more precisely follow actual bathymetry changed the peak FLT concentration simulated at the SSG from less than 1 ppb to about 15 ppb. Even though the simulated SSG FLT concentration was about half of that measured, the improvement over the previous model version was substantial. Modifying the model to accurately reflect the nearshore bathymetry resulted in a bathymetric gradient that was steeper near the submarine springs than it was north of the submarine springs. This placed the specified head boundaries of the submarine layers closer to the shoreline specified head boundary of layer 1 decreasing the width of the low permeable sediments which the FLT plume has to transverse to the submarine springs.

The above controls on the FLT plume were instrumental in obtaining a reasonable match between the simulated and measured BTCs. However, the spatial distribution of FLT simulated by the model fell well short of the southern extent indicated by tracer sampling program, the $\delta^{15}\text{N}$ survey, and the TIR survey. To arrive at reasonable agreement between modeled and measured plume extent, an anisotropy factor of 3 had to be used with the direction of dominant hydraulic conductivity aligned north-south. This direction is perpendicular to the dip of the lava flows and contradicts the prevailing assumption that the direction of dominant hydraulic conductivity is parallel to lava flow dip. However, there is a difference between the plane of the dip of the lava flows and the near horizontal to slightly vertical direction of groundwater flow. In West Maui, the lava flows dip from 5 to 20 degrees with thicknesses ranging from 1 to 100 ft (Stearns and MacDonald, 1942). By contrast, the water table in the study area is nearly horizontal relative to the dip of the lava beds. In addition, near the coast, the thinning of the freshwater zone adds an upward vertical component to the groundwater flow. Figure ES-15(a) compares the BTC simulated by the model using a dominant north-south hydraulic conductivity to the measured BTCs. There is good agreement between simulated NSG BTC ascending limb and initial curve peak and that which was measured. The simulated

peak concentration for FLT at the SSG was only about one-third of that measured; however this model revision produced the intended result. The primary reason to implement the dominant north-south hydraulic conductivity was to extend the simulated plume southward to the southern TIR plume boundary and to the location most southerly that test positive for FLT. Figure ES-15(b) shows the simulated plume 620 days after the FLT addition extends southward nearly to the southern TIR plume boundary, which is very close to the southern extent of the FLT detection.

The reason for the lack of SRB detection was also investigated by modeling. Our conclusion is that the primary injection wells (Wells 3 and 4) displaced the SRB injected into Well 2 away from the submarine springs monitored by this study. Wells 3 and 4 lie directly between Well 2 and the identified submarine springs southwest of the LWRF. Wells 3 and 4 are the primary injection wells, receiving more than 80 percent of the treated wastewater. Figure ES-16(a) shows that this interference reduces the SRB concentration at the submarine springs more than an order of magnitude to concentration values just above the MDL for this dye. Figure ES-16(b) indicates that the core of the SRB plume is diverted to southeast before it can make its way to the submarine discharge points. The displacement significantly lengthens the travel path this dye takes and increases its dispersion. Other processes such as sorption and degradation have a greater chance to further reduce the concentration due to the increased pathway length and travel time. To test the true hydraulic connectivity between Well 2 and the nearby coastal environment, a second tracer test would need to be conducted, with Well 2 as the primary injection well.

Table ES-1. North and South Seep Group water quality parameters. Data (means \pm SD and range) were collected from 7/19/2011 through 5/2/2012 with a handheld YSI Model 63.

South Seeps	Temp. (°C)	pH	Spec. Cond. (mS/cm)	Salinity
Seep 3	28.7 \pm 2.0	7.52 \pm 0.12	6.43 \pm 2.57	3.25 \pm 1.5
	24.9 to 34.9	7.22 to 7.94	5.20 to 28.18	2.50 to 16.1
Seep 4	28.6 \pm 2.0	7.50 \pm 0.12	8.98 \pm 6.57	4.77 \pm 4.0
	24.5 to 34.6	7.20 to 7.90	5.63 to 37.70	2.80 to 22.5
Seep 5	28.4 \pm 2.0	7.53 \pm 0.20	9.24 \pm 6.59	4.94 \pm 4.0
	24.9 to 34.9	7.32 to 7.90	5.29 to 34.75	2.90 to 21.8
Seep 11	26.8 \pm 2.5	7.61 \pm 0.20	6.48 \pm 0.62	3.39 \pm 0.3
	25.2 to 29.0	7.37 to 7.68	5.00 to 8.32	3.10 to 4.5
North Seeps				
Seep 1	29.1 \pm 2.0	7.45 \pm 0.09	8.33 \pm 1.04	4.25 \pm 0.5
	24.8 to 34.4	7.18 to 7.76	7.32 to 14.80	3.90 to 7.3
Seep 2	28.9 \pm 2.3	7.46 \pm 0.11	8.47 \pm 1.41	4.35 \pm 0.7
	24.0 to 34.9	7.13 to 7.75	7.04 to 17.36	3.80 to 9.9
Seep 6	29.3 \pm 2.2	7.41 \pm 0.14	8.33 \pm 0.90	4.25 \pm 0.4
	23.8 to 35.9	6.90 to 7.94	7.00 to 13.54	3.80 to 7.0
Seep 7	27.5 \pm 1.7	7.51 \pm 0.19	8.19 \pm 1.32	4.31 \pm 0.8
	22.4 to 30.3	7.26 to 7.81	7.24 to 15.08	3.90 to 8.2
Seep 8	27.4 \pm 1.7	7.35 \pm 0.18	9.36 \pm 5.98	5.01 \pm 3.6
	24.7 to 31.0	7.09 to 7.90	7.47 to 37.88	4.00 to 22.0
Seep 9	27.4 \pm 1.7	7.43 \pm 0.21	13.65 \pm 11.35	7.58 \pm 6.7
	23.3 to 30.5	6.75 to 7.80	7.21 to 42.91	3.90 to 25.3
Seep 10	28.2 \pm 1.0	7.60 \pm 0.15	9.02 \pm 1.17	4.70 \pm 0.6
	26.5 to 29.5	7.26 to 7.76	7.99 to 11.85	4.10 to 6.2
Seep 12	28.2 \pm 1.1	7.60 \pm 0.11	8.37 \pm 0.50	4.35 \pm 0.2
	26.6 to 29.6	7.36 to 7.78	7.88 to 9.55	4.10 to 4.9
Seep 13	28.0 \pm 1.9	7.69 \pm 0.02	8.18 \pm 0.53	4.27 \pm 0.1
	26.0 to 29.7	7.67 to 7.71	7.69 to 8.74	4.20 to 4.4
Seep 14	27.1 \pm 2.1	7.67 \pm 0.05	7.91 \pm 0.21	4.17 \pm 0.1
	24.7 to 28.7	7.66 to 7.72	7.67 to 8.02	4.10 to 4.2
Seep 15	28.4 \pm 2.4	7.58 \pm 0.10	9.99 \pm 3.28	5.31 \pm 2.1
	24.6 to 30.6	7.45 to 7.72	7.86 to 16.54	4.20 to 9.3
Seep 16	30.1 \pm 0.6	7.63 \pm 0.12	8.85 \pm 0.09	4.47 \pm 0.1
	29.4 to 30.6	7.50 to 7.71	8.79 to 8.95	4.40 to 4.5

Table ES-2. Summary of the June, 2011 Nutrient Data

Sample Type	No. of Samples		TP	TN	PO ₄ ³⁻	SiO ₄ ⁴⁻	NO ₃ ⁻	NO ₂ ⁻	NH ₄ ⁺
			(µg/L as P)	(µg/L as N)	(µg/L as P)	(µg/L as Si)	(µg/L as N)	(µg/L as N)	(µg/L as N)
Terrestrial Surface	6	Min.	21	88	18	4,852	1	0.8	0.6
		Avg.	161	2,121	75	17,427	1,189	9.0	51
		Max.	255	4,043	159	25,679	3,166	31	129
		Std. Dev.	91	1,566	50	8,431	1,540	11	49
Production Wells	7	Min.	60	292	48	17,944	205	0.7	0.8
		Avg.	100	1,330	72	19,283	968	1.1	1.4
		Max.	184	2,429	105	21,958	1,916	2.0	2.9
		Std. Dev.	52	778	25	1,611	731	0.5	0.8
Monitoring Well	1		91	2,342	52	16,206	1,608	6.2	0.0
Treated Wastewater	1		206	7,245	102	17,231	2,641	530	1,307
Submarine Springs	4	Min.	350	326	279	11,984	142	14	4
		Avg.	396	486	340	16,948	278	23	6
		Max.	421	651	365	20,624	366	31	7
		Std. Dev.	32	146	41	4,069	108	9	1
Marine Surface	25	Min.	11	64	3	134	3	0.3	0.0
		Avg.	14	100	6	356	22	0.3	1
		Max.	34	306	26	1,249	146	1	10
		Std. Dev.	5	57	5	303	34	0.1	2

Table ES-3. Summary of the September, 2011 Nutrient Data

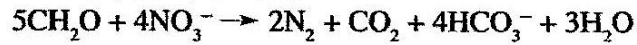
Sample Type	No. of Samples		TP	TN	PO ₄ ³⁻	SiO ₄ ⁴⁻	NO ₃ ⁻	NO ₂ ⁻	NH ₄ ⁺
			(µg/L as P)	(µg/L as N)	(µg/L as P)	(µg/L as Si)	(µg/L as N)	(µg/L as N)	(µg/L as N)
Terrestrial Surface	3	Min.	123	2,146	42	8,237	1,083	6	24
		Avg.	201	4,551	86	16,373	2,923	86	59
		Max.	261	6,751	155	24,160	4,239	237	103
		Std. Dev.	70	2,309	60	7,967	1,642	131	40
Production Wells	7	Min.	66	277	50	17,948	226	0.7	2.2
		Avg.	136	1,463	112	20,115	1,142	1.0	5.9
		Max.	309	2,559	254	23,792	2,487	1.5	7.1
		Std. Dev.	88	874	76	2,400	817	0.2	1.7
Monitoring Well	1		73	2,759	55	18,085	1,210	2.8	17
Treated Wastewater	2	Min.	164	6,061	70	16,462	3,172	423	156
		Avg.	177	6,238	88	16,678	3,313	466	211
		Max.	191	6,415	106	16,893	3,454	509	267
		Std. Dev.	19	250	25	304	199	61	79
Submarine Springs	2	Min.	451	1,573	393	19,693	96	10	6.4
		Avg.	459	1,598	404	20,426	121	18	6.8
		Max.	468	1,624	415	21,159	145	27	7.1
		Std. Dev.	12	36	16	1,037	35	12	0.5
Marine Surface	23	Min.	11	127	2.8	98	0.0	0.3	0.1
		Avg.	13	173	4.5	202	5.7	0.5	1.4
		Max.	20	225	14	607	41	1.1	2.9
		Std. Dev.	1.9	19.8	2.3	136	8.6	0.2	0.9

Table ES-4. The progressive microbial decomposition of organic matter. Reactions succeed each one another in the order written as each oxidant is completely consumed. From Berner and Berner, 1996.

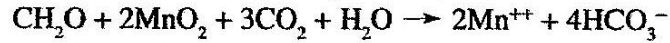
Oxygenation (oxic)



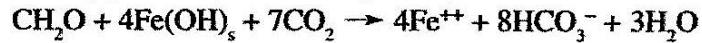
Nitrate reduction (mainly anoxic)



Manganese oxide reduction (mainly anoxic)



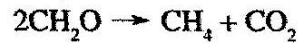
Ferric oxide (hydroxide) reduction (anoxic)



Sulfate reduction (anoxic)



Methane formation (anoxic)



Note: Organic matter schematically represented as CH₂O.

Table ES-5. June, 2011 stable isotope data

TS = Terrestrial Surface, PW = Production Well, SS = Submarine Spring, MS = Marine Surface water; - denotes measurement not performed.

Sample Name (Type)	$\delta^{18}\text{O}$ of H_2O (‰) ¹	$\delta^2\text{H}$ of H_2O (‰) ¹	$\delta^{15}\text{N}$ of NO_3^- (‰) ²	$\delta^{15}\text{N}$ σ (‰) ³	$\delta^{18}\text{O}$ of NO_3^- (‰) ¹	$\delta^{18}\text{O}$ σ (‰) ³
Kaanapali 1 (TS)	-	-	12.63	2.26	2.84	4.3
Kaanapali 2 (TS)	-	-	14.99	2.26	-1.82	4.3
Kaanapali GC-1 (TS)	-	-	4.96	1.67	-1.62	1.45
Hahakea 2 (PW)	-3.77	-15.33	0.65	1.15	0.7	1.17
Honokowai B (PW)	-3.79	-15.05	3.15	1.67	-3.5	1.45
Kaanapali P-1 (PW)	-3.8	-14.94	1.31	1.67	-1.74	1.45
Kaanapali P-2 (PW)	-3.75	-15.3	1.07	1.67	-0.16	1.45
Kaanapali P-4 (PW)	-3.57	-14.51	0.92	0.52	4.3	1.78
Kaanapali P-5 (PW)	-3.45	-14.46	4.19	1.67	3	1.45
Kaanapali P-6 (PW)	-3.39	-13.85	3.29	1.67	3.3	1.45
Lahaina Deep Monitor Well	-3.55	-13.75	1.8	1.67	-0.22	1.45
LWRF Treated Effluent	-	-	29.25	0.52	19.82	1.78
Seep 1 Piez-1 (SS)	-3.21	-11.01	86.47	1.15	21.56	1.17
Seep 1 Piez-2 (SS)	-	-	77.82	0.56	22.86	0.19
Seep 2 Piez-1 (SS)	-1.52	-5.19	-	-	-	-
Seep 3 Piez-1 (SS)	-3.03	-10.91	83.89	0.56	22.07	0.19
Seep 4 Piez-1 (SS)	-2.26	-7.64	-	-	-	-
Maui 10 (MS)	-	-	52.46	1	16.35	0.82
Maui 12 (MS)	-	-	57.73	1	21.55	0.82
Maui 14 (MS)	-	-	55.5	1	15.52	0.82
Maui 15 (MS)	-	-	54.43	1	15.67	0.82
Maui 2 (MS)	-	-	12.71	2.26	6.55	4.3
Maui 5 (MS)	-	-	19.71	1	9.24	0.82
Maui 6 (MS)	-	-	18.04	0.56	9.69	0.19
Wahikuli (MS)	-	-	11.86	0.56	3.53	0.19

¹Measured relative to VSMOW

²Measured relative to AIR

³Average standard deviation of standards and duplicate samples

Table ES-6. September, 2011 stable isotope data
 TS = Terrestrial Surface, PW = Production Well, SS = Submarine Spring, MS = Marine
 Surface water; - denotes measurement not performed.

Sample Name (Type)	$\delta^{18}\text{O}$ of H_2O (‰) ¹	$\delta^2\text{H}$ of H_2O (‰) ¹	$\delta^{15}\text{N}$ of NO_3^- (‰) ²	$\delta^{15}\text{N}$ σ (‰) ³	$\delta^{18}\text{O}$ of NO_3^- (‰) ¹	$\delta^{18}\text{O}$ σ (‰) ³
Black Rock 1 (TS)	-	-	10.12	0.23	2.29	0.49
Black Rock 2 (TS)	-	-	8.84	1	2.41	0.82
Kaanapali GC-R1 Pond (TS)	-3.09	-11.34	30.78	0.23	11.72	0.49
Hahakea 2 (PW)	-3.63	-14.69	0.91	0.23	-0.91	0.49
Kaanapali P-1 (PW)	-3.67	-14.64	2.32	0.23	-1.87	0.49
Kaanapali P-2 (PW)	-3.73	-15.11	2.21	0.23	-2.16	0.49
Kaanapali P-4 (PW)	-3.59	-14.65	2	0.39	-0.27	1.54
Kaanapali P-5 (PW)	-3.46	-14.03	2.41	0.39	0.5	1.54
Kaanapali P-6 (PW)	-3.42	-13.93	3.49	0.39	0.33	1.54
Honokowai B (PW)	-3.68	-14.69	2.03	0.39	-1.18	1.54
Lahaina Deep Monitor Well	-3.65	-15.7	1.98	0.39	0.79	1.54
LWRF Treated Effluent	-3.06	-11.37	30.85	0.23	15.92	0.49
LWRF-R1 Treated Effluent	-3.12	-11.39	31.54	0.23	15.03	0.49
Seep 1-2 Piez (SS)	-3.1	-11.45	83.03	0.23	24.46	0.49
Seep 3-2 Piez (SS)	-2.85	-10.54	93.14	0.23	22.45	0.49
Maui 19 (MS)	-	-	22.8	1	1.76	0.82
Maui 22 (MS)	-	-	29.22	1	8.77	0.82
Maui 23 (MS)	0.37	2.32	17.72	1	4.87	0.82
Maui 25 (MS)	0.44	2.82	-	-	-	-
Maui 28 (MS)	0.39	2.24	-	-	-	-
Maui 32 (MS)	0.47	2.64	-	-	-	-

¹Measured relative to VSMOW

²Measured relative to AIR

³Average standard deviation of standards and duplicate samples

Table ES-7. The output of the QTracer2 BTC Interpretation Model

Parameter	Units	North Seep Group	South Seep Group	Comments
Duration of BTC	d	2,435	2,001	Length of time from injection until FLT concentration drops below the MDL
Distance from input to outflow point	m	821	932	
Seep Group Discharge	m ³ /d	1,752	5,439	Combined discharge = 7,162
Time to First Arrival	d	86	109	
Time to Peak Concentration	d	306	271	
Peak Tracer Concentration	ppb	22.5	35	
Mean Transit Time	d	487	435	
Mean Tracer Velocity	m/d	1.7	2.1	
Maximum Tracer Velocity	m/d	9.5	8.6	-
Mass of Tracer Inject	kg	119	119	
Mass of Tracer Recovered	kg	16.8	59.9	
Percent of Tracer Mass Recovered	%	14.1	50.3	Total Percent Recovery = 64%
Dispersion coefficient	m ² /s	1.37E-03	1.15E-03	
Longitudinal dispersivity	m	70	46	
Peclet Number	Unitless	12	20	Advection > Diffusion

Note: Seep group discharge is taken from Table 5-5 in the Lahaina Groundwater Tracer Study Interim Report (Glenn et al., 2012)

Table ES-8. Calculated percent of treated wastewater in the submarine spring discharge.

FLT Tracer Dye Estimates of Percent Recovery and of Percent Effluent				
	Units	North Seep Group	South Seep Group	Total
Total SGD (saline+fresh) ¹	(m ³ /d)	2,500	6,300	8,800
SGD – FLT plume fraction	(m ³ /d)	1,752	5,439	7,162
Mass of Tracer Dye Added	(kg)	----	----	119
Mass of Tracer Dye Recovered	(kg)	16.8	59.9	76.7
Percent Tracer Dye Mass Recovery at the Submarine Spring Groups	(%)	14.1	50.3	64.0
Average Injection Rate into LWRF Wastewater Injection Wells 3 and 4	(m ³ /d)	----	----	9,340
Effluent Discharge at Submarine Springs ²	(m ³ /d)	----	----	5,978
Percent Effluent in the Submarine Spring Discharge (Effluent Discharge/Total SGD)	(%)	----	----	68
Geochemical Parameters Used in % Effluent		Percent Effluent in the Submarine Spring Discharge		
Mixing Endmember Calculations³		Low	Avg	High
$\delta^{18}\text{O} / \delta^2\text{H}$ End Member Mixing Calculations		53%	77%	96%
$\delta^{18}\text{O} / [\text{Cl}^-]$ End Member Mixing Calculations		12%	41%	60%
$\delta^2\text{H} / [\text{Cl}^-]$ End Member Mixing Calculations		67%	69%	71%
Average		----	62%	----

¹Radon Mass Balance Model of Glenn et al. (2012, Section 5).

²64% of Average Injection Rate into Wells 3 and 4.

³See Section 6.4.2.3 of Glenn et al. (2012) for a discussion of end member mixing analysis techniques.

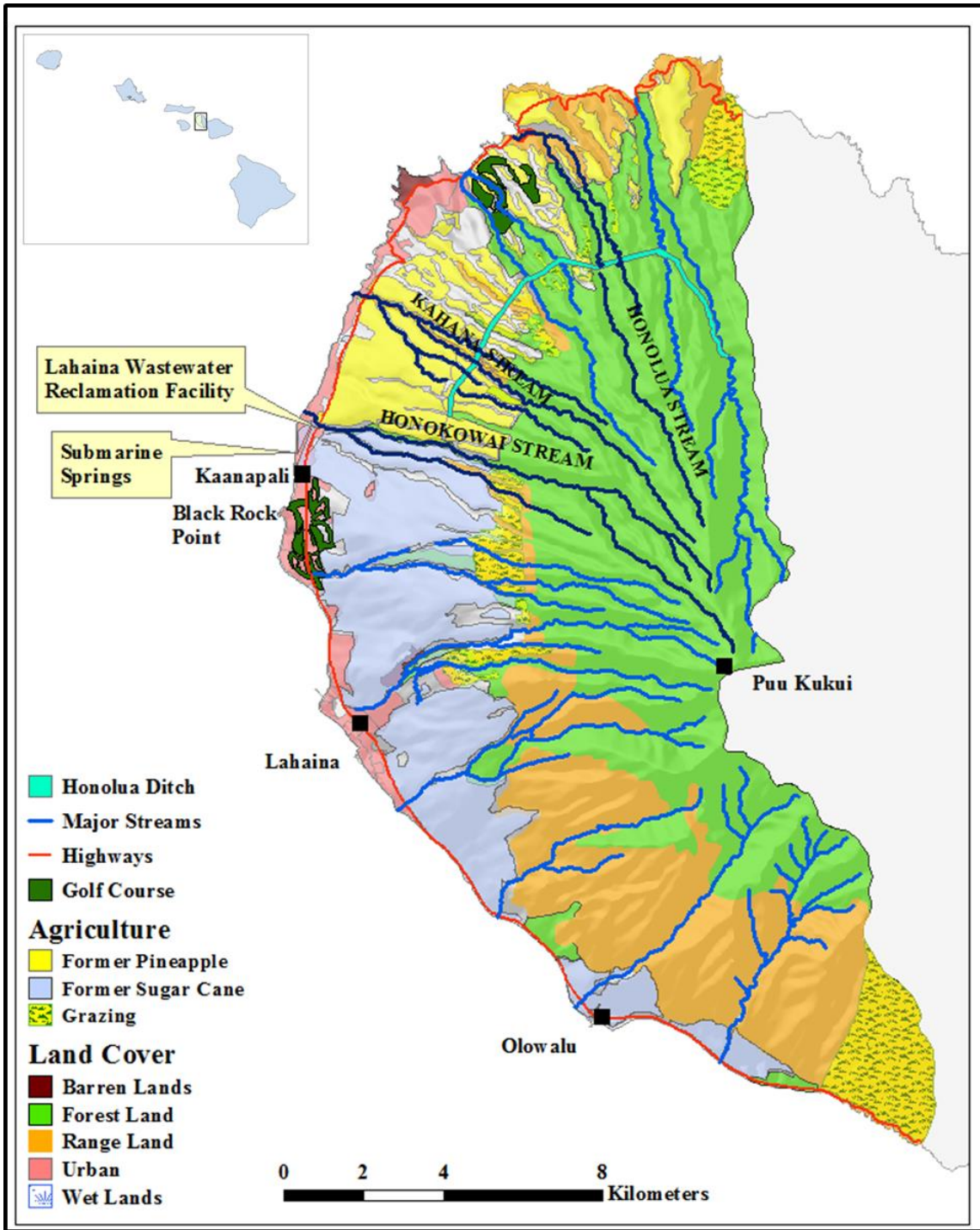


Figure ES-1: Western Maui land-use map.

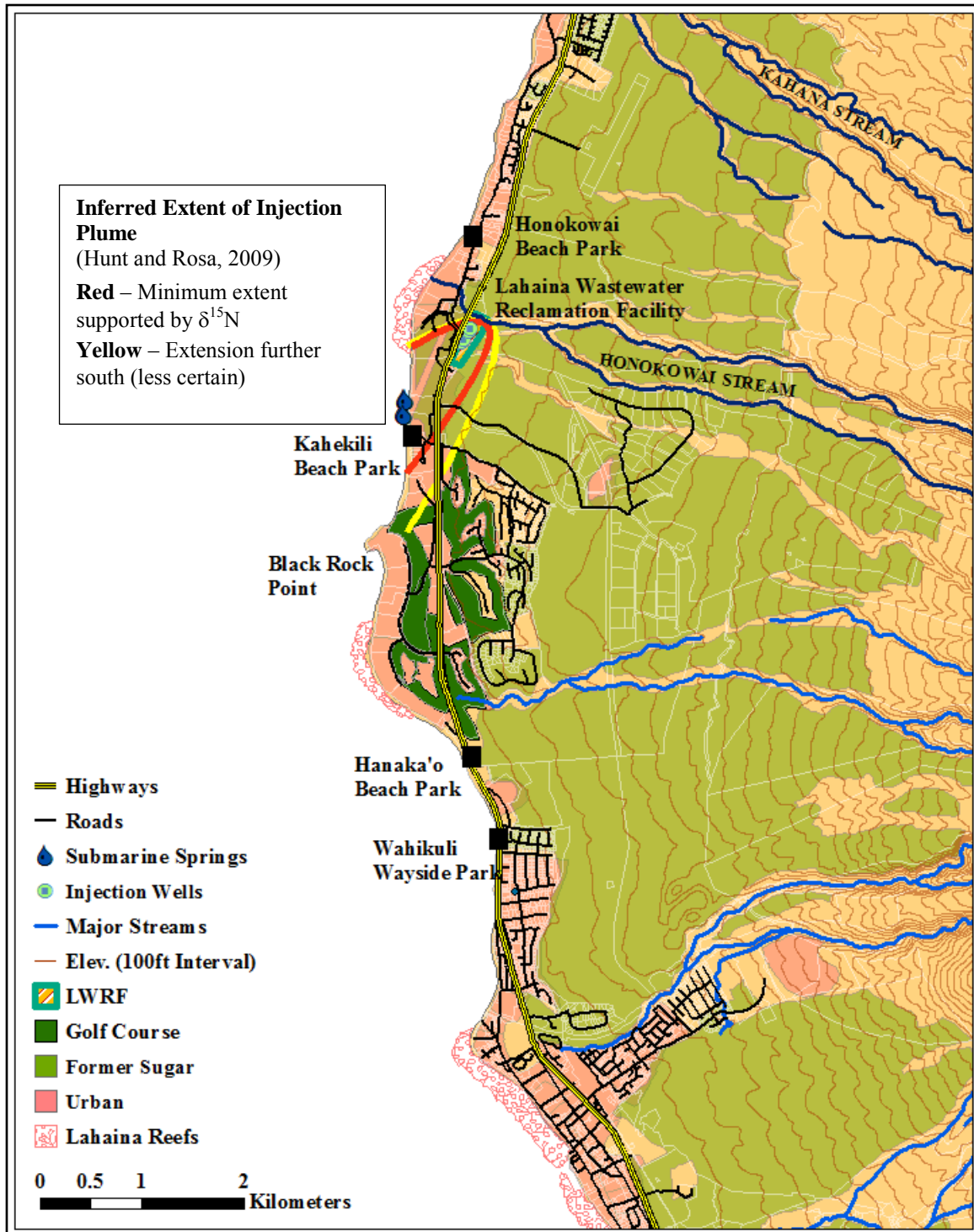


Figure ES-2: Detail of study area showing key locals along the coast. LWRF injection wells and inferred subsurface minimum and maximum spatial extent of LWRF injection plume from Hunt and Rosa (2009) is also shown.

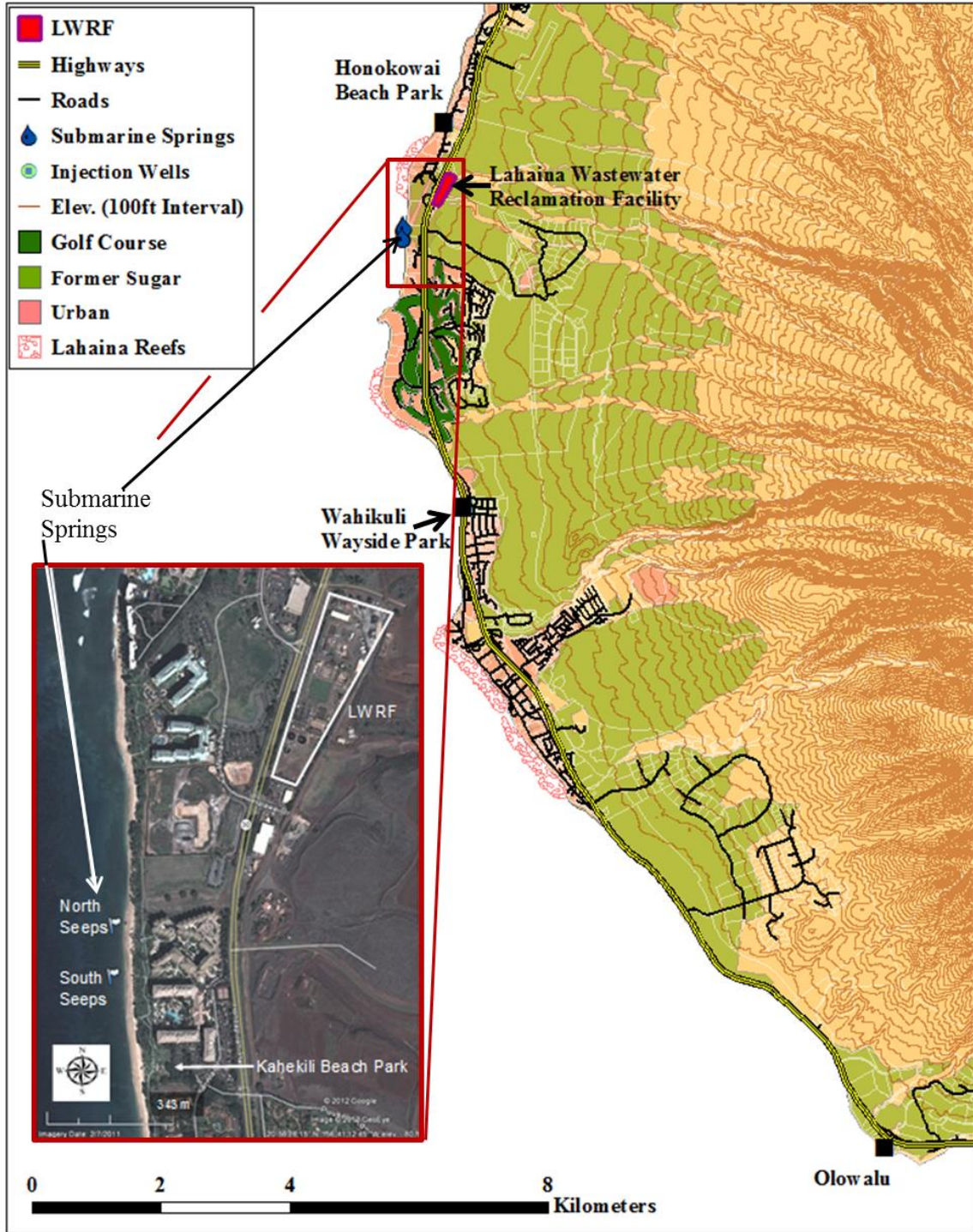


Figure ES-3: Control and submarine spring sampling locations. Control locations include: Honokowai Beach Park, Wahikuli Wayside Park, and Olowalu. Also shown are the North and South Seep Groups.

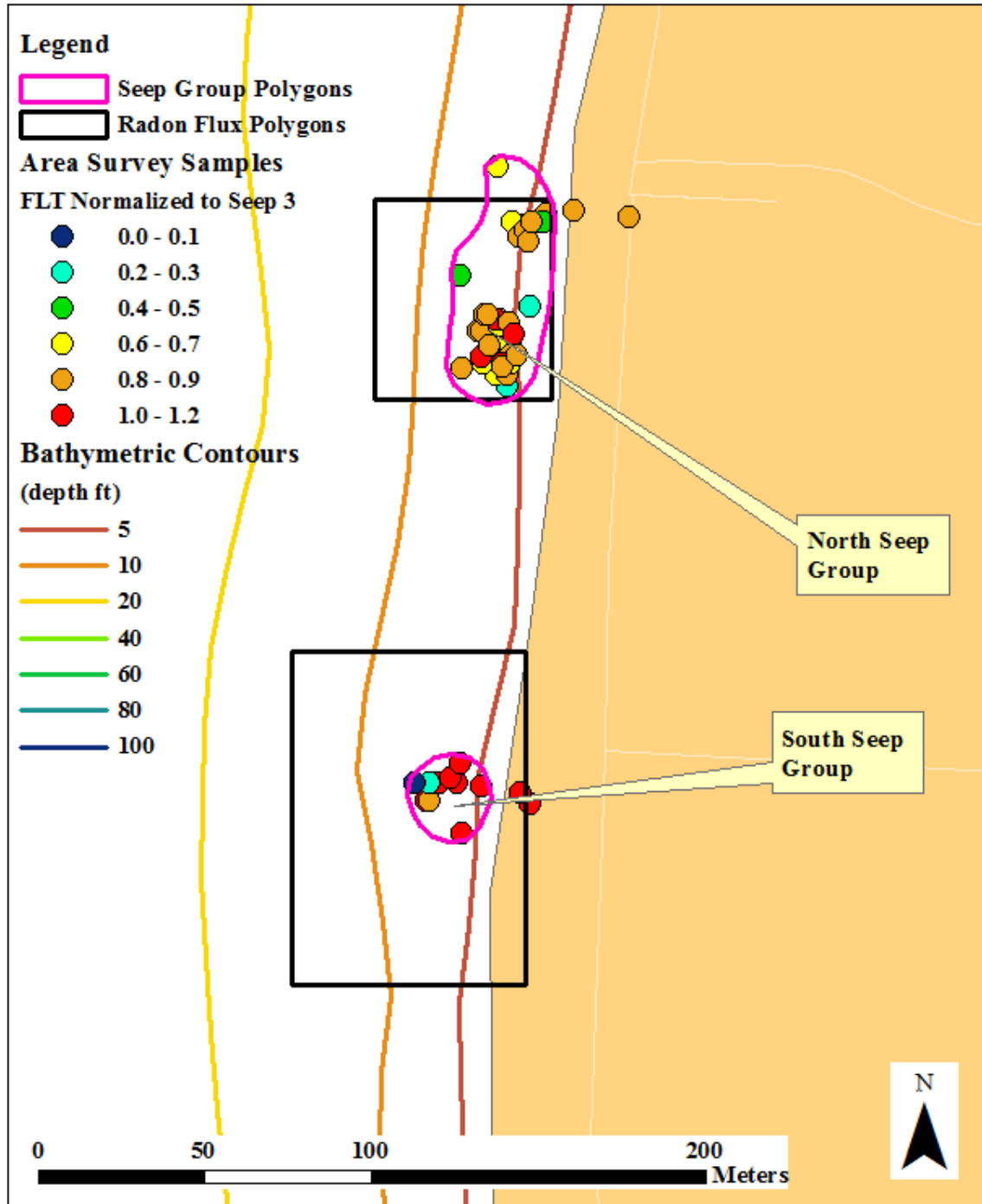


Figure ES-4: The location of the flowing submarine springs showing an enveloping polygon for each seep group and the extent of the boxes used in the Radon flux calculations (compare with Figure ES-8).

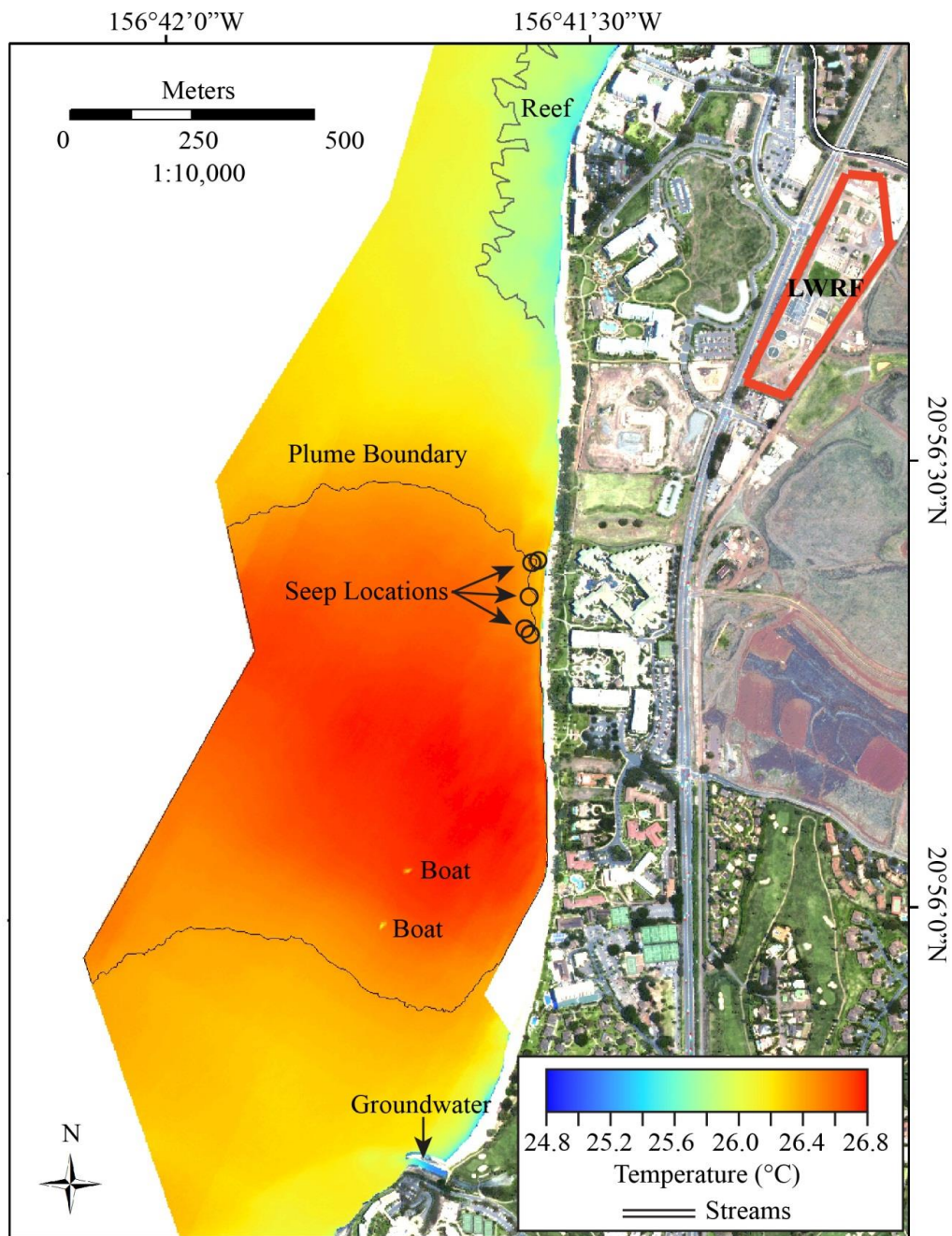


Figure ES-5: Aerial TIR sea surface temperature map thermal anomaly at North Kaanapali Beach.

The TIR plume is > 575 m (1886 ft) in width (from the shoreline to the edge of the flight line). There is less than 0.6°C temperature variation within the plume area. The lagoon emptying into the ocean at the southern end of the figure is fed by cold groundwater. Submarine spring (seep) locations are shown on the map correspond to small-scale and semi-isolated thermal anomalies.

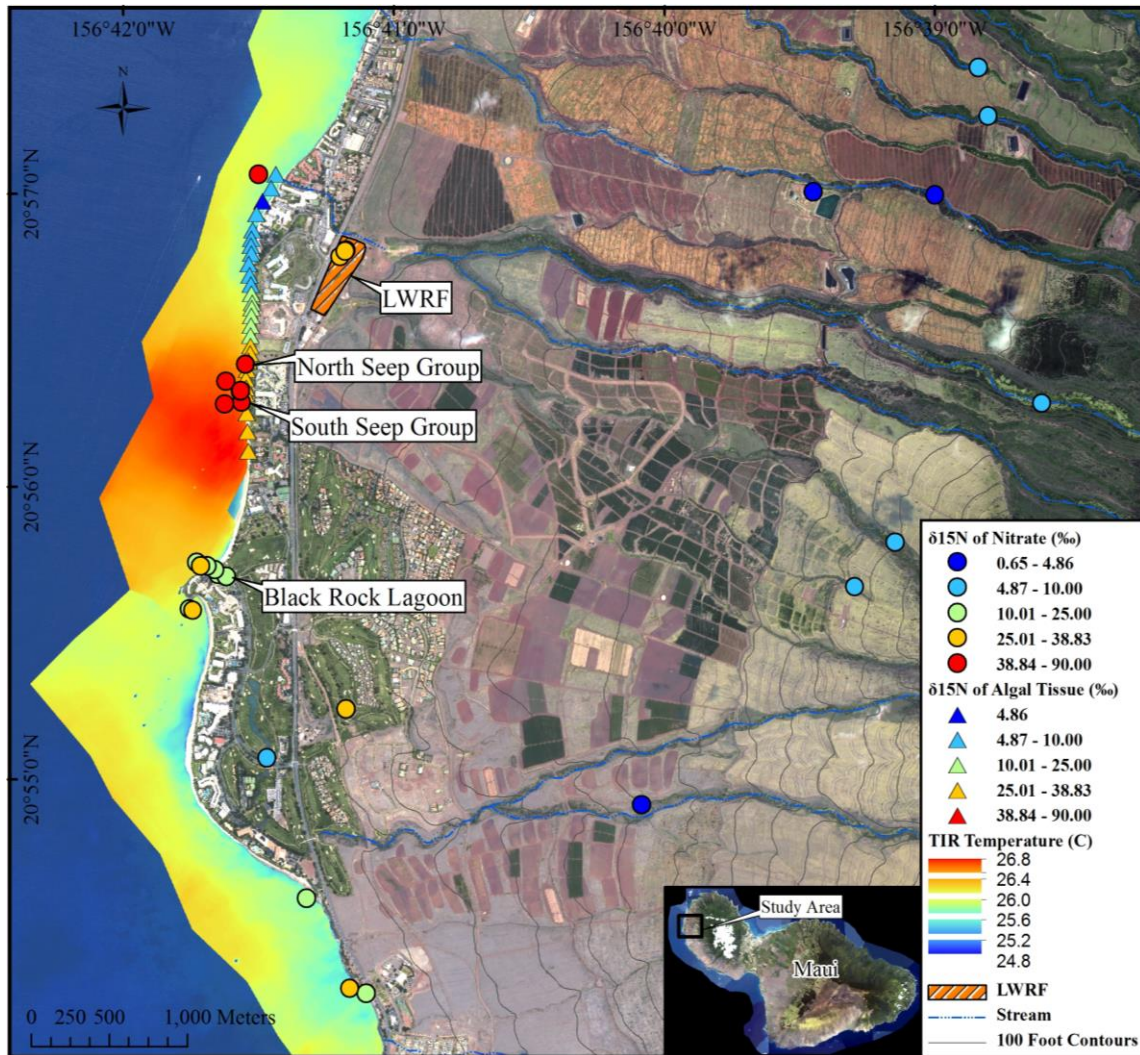


Figure ES-6: Infrared SST pictured with $\delta^{15}\text{N}$ values of terrestrial and marine waters, and the intertidal macroalgae. Shown are the $\delta^{15}\text{N}$ values of intertidal macroalgae (triangles) reported by Dailer et al. (2010) and $\delta^{15}\text{N}$ values of NO_3^- dissolved in water (circles) reported in this study. The region of elevated SST offshore of Kahekili Beach Park corresponds with elevated $\delta^{15}\text{N}$ values of macroalgal tissue and dissolved NO_3^- . Note that the majority of marine samples collected had dissolved NO_3^- concentrations below $0.9 \mu\text{M}$, the minimum concentration required to perform the dissolved NO_3^- $\delta^{15}\text{N}$ analysis used in this study. The marine samples pictured here are the few that were above this analytical threshold and thus provide a good spatial representation of above-background dissolved NO_3^- .

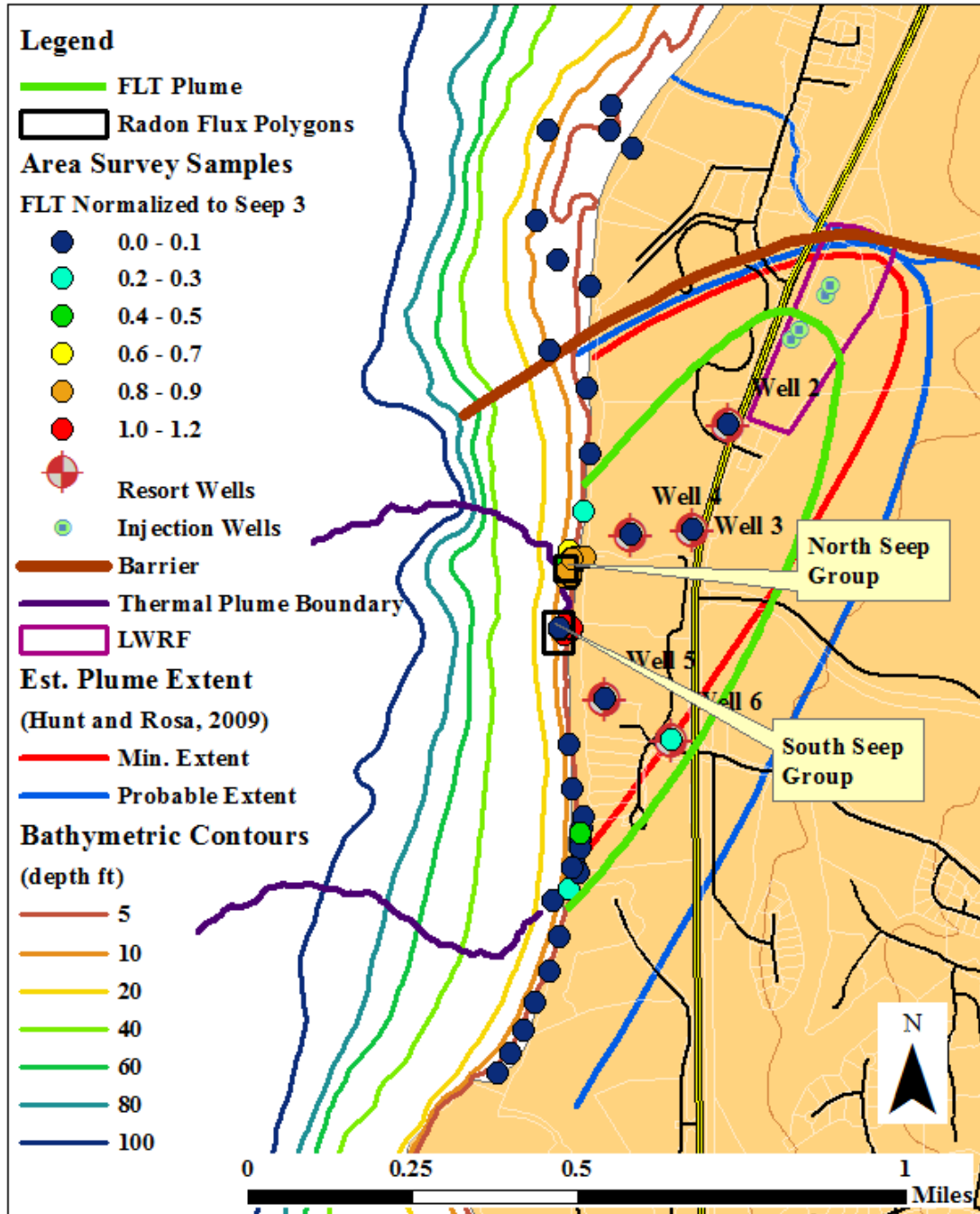


Figure ES-7: The FLT concentrations normalize to that at Seep 3 and shown in relation to the boundaries of the TIR plume.

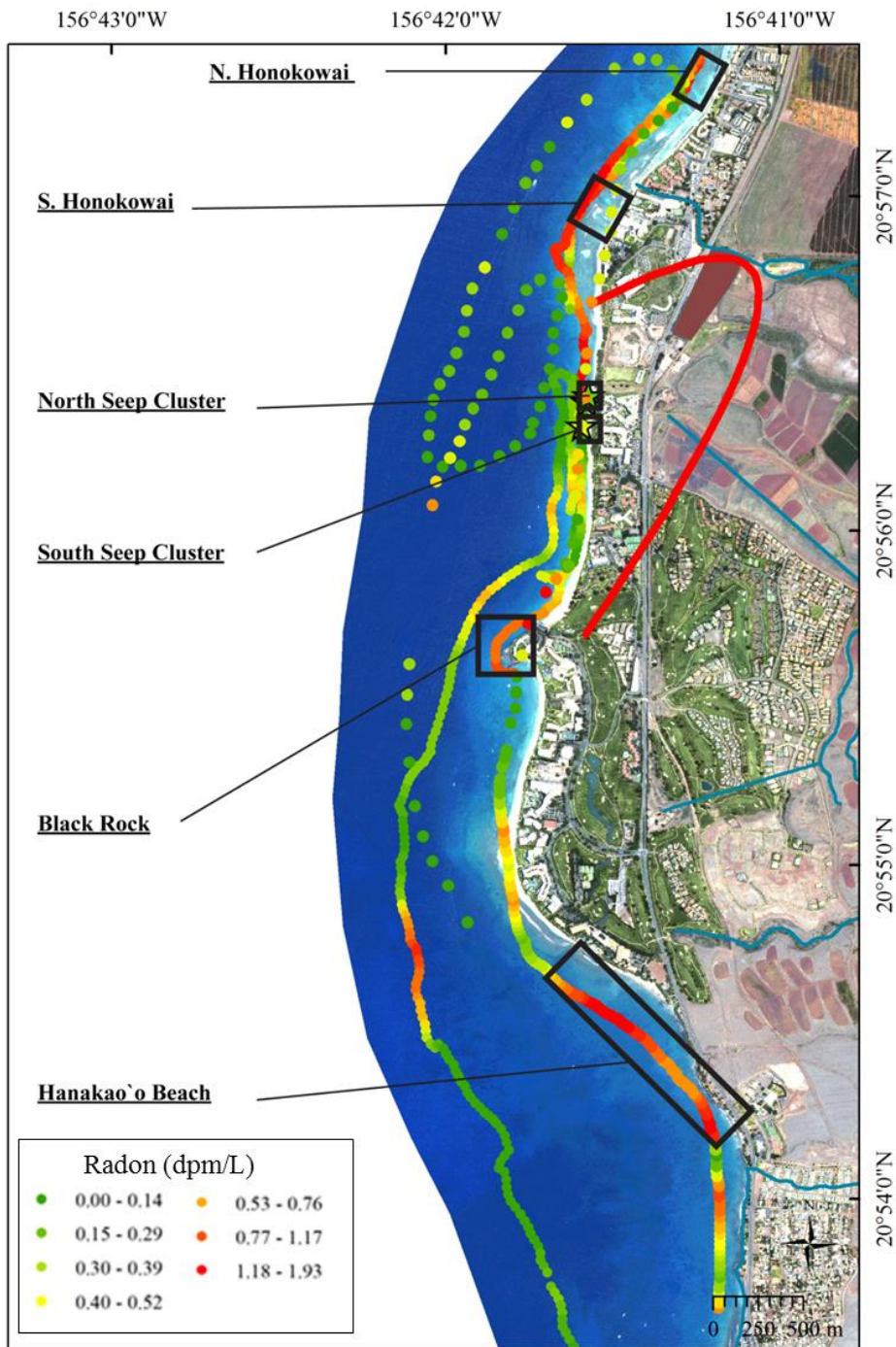


Figure ES-8: Radon activities measured during coastal surveys in June and September, 2011.

Sites with elevated surface radon activities are outlined with a black box. The lengths of the boxes are the approximate lengths of coastline that was within 100 dpm/m³ of the mean radon concentration for each site and the widths are the distance of the radon survey from the coastline. The latter assumes that groundwater emanates at the coastline. Coastal groundwater fluxes were estimated from these areas. FLT plume boundary is also shown,

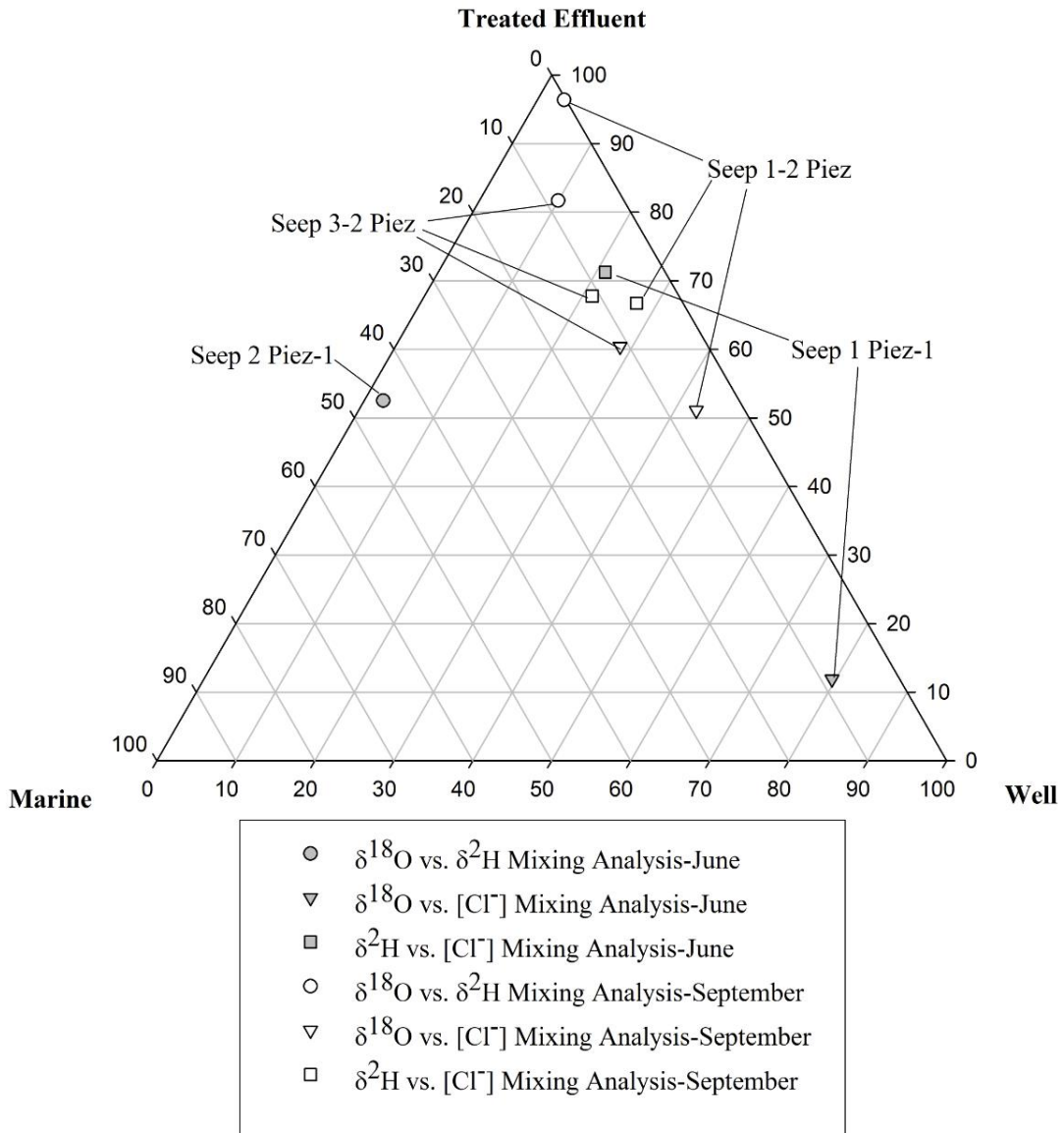
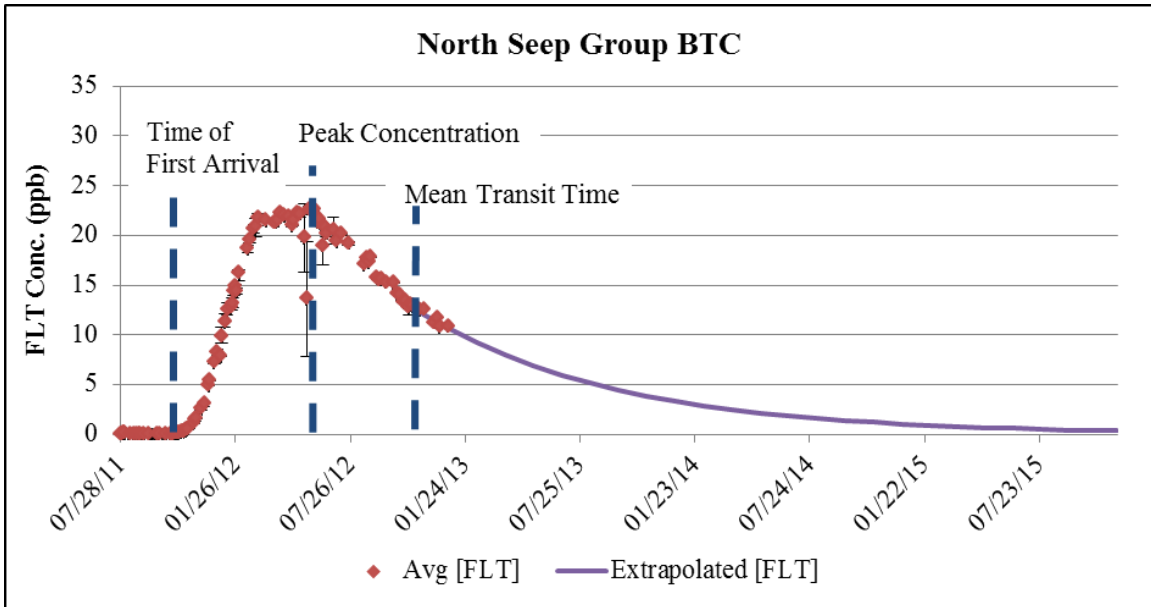
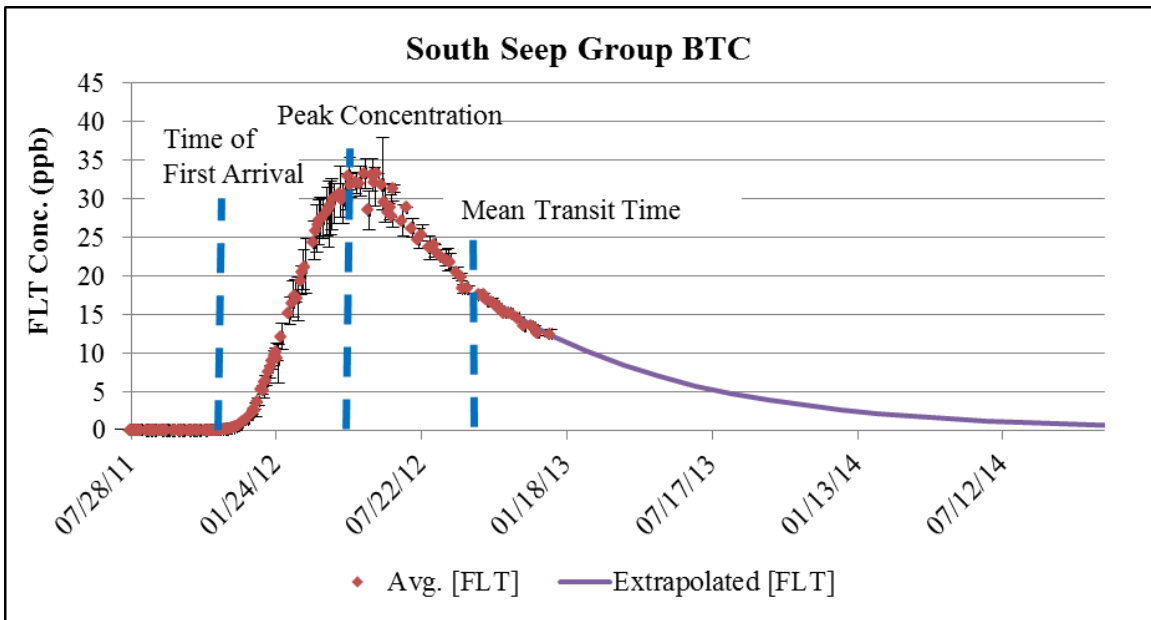


Figure ES-9: Submarine spring component mix ternary diagram. Submarine spring component percentages for samples plotting within the mixing triangles shown in Figures 6-14, 6-15, and 6-16 of Project Interim Report (Glenn et al., 2012).



(a) North Seep Group



(b) South Seep Group

Figure ES-10: Submarine spring water FLT breakthrough curves for (a) the NSG and (b) the SSG.

The first arrival of dye occurred in late October, 2011 at the NSG and early November, 2011 at the SSG. Both BTCs appear have reached maximum concentrations by May, 2012 with the FLT concentration at the SSG being about 1.5 times that at the NSG. The maximum concentration at the NSG occurred in late May, 2012 after a three month plateau. The peak concentration at the SSG occurred in mid-May, 2012 with no plateau. Both BTCs exhibit a long trailing edge on their declining limbs. The limbs extending past January 2012 are synthetic projections.

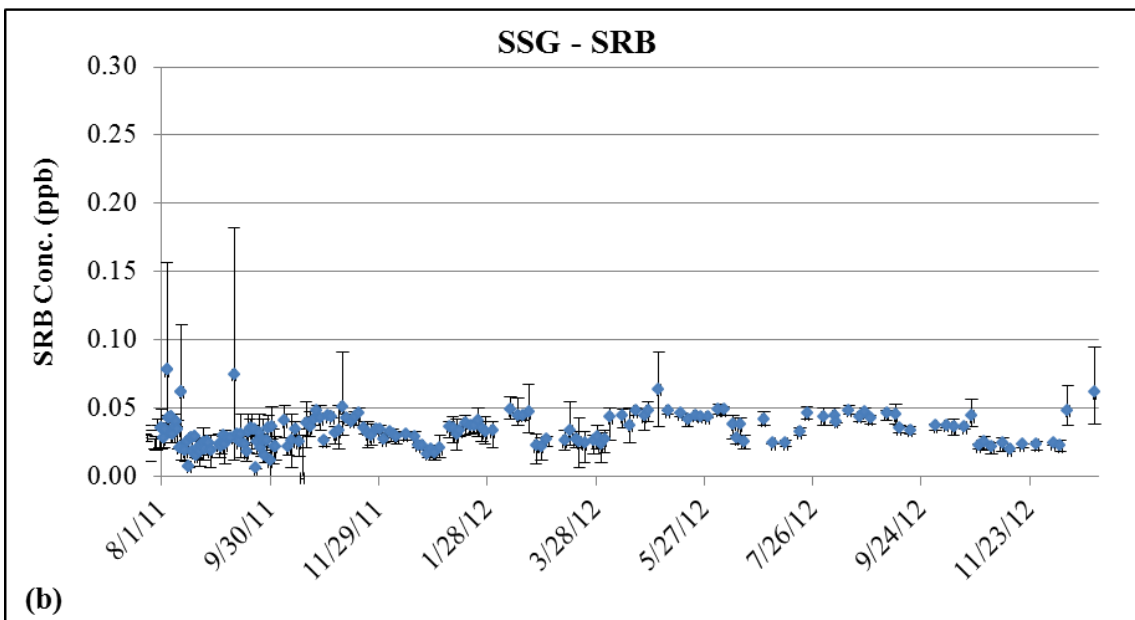
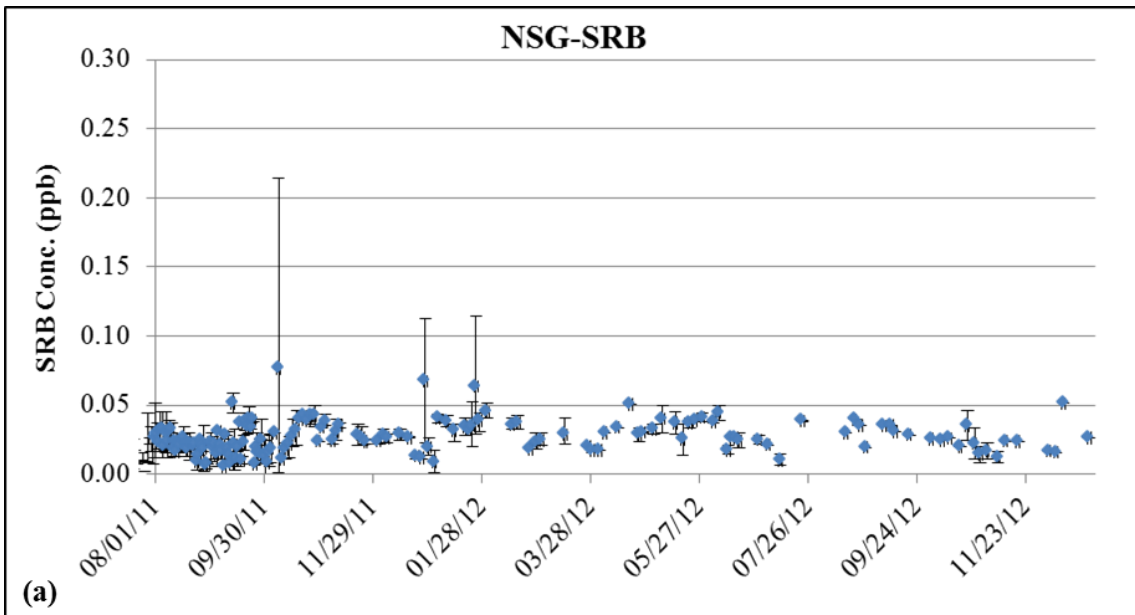


Figure ES-11: The SRB wavelength fluorescence measured by this study at the NSG (a) and the SSG (b).

There no confirmed detections of SRB and the samples with elevated SRB wavelength were generally isolated occurrences with the sample prior and following exhibiting baseline SRB fluorescence.

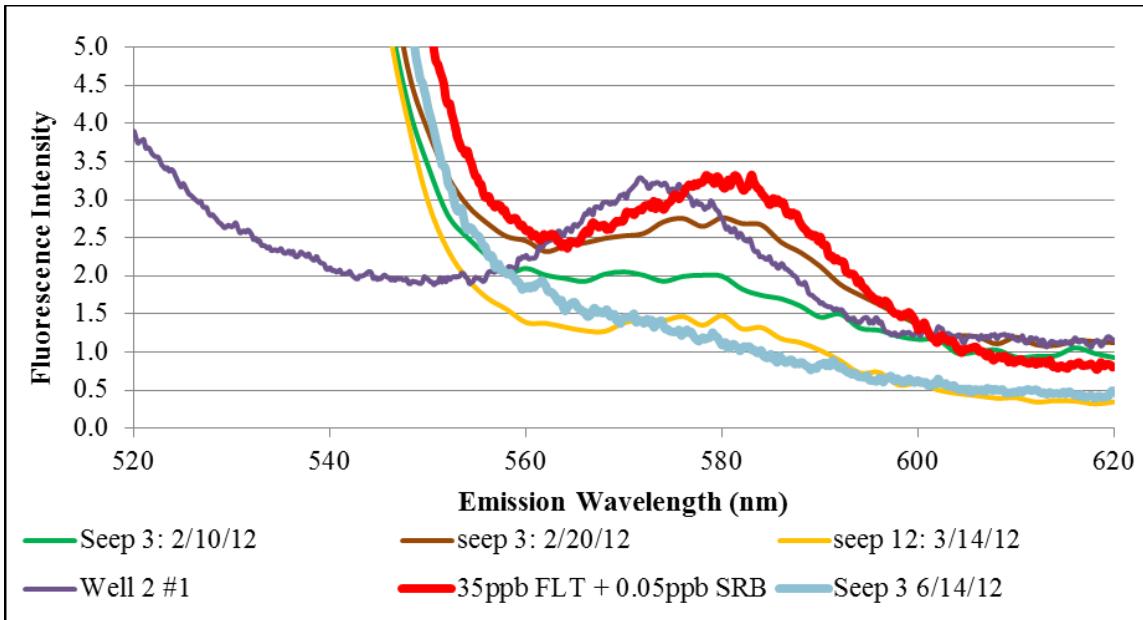


Figure ES-12: Synchronous scans of samples collected in February and March, 2012 compared to solutions spiked with SRB.

The laboratory prepared sample (35 ppb FLT + 0.05ppb SRB) is a reference to which the field samples can be compared. The declining limb of the FLT peak is evident from about 550 to 560 nm. The SRB is shown as curve with a peak center at 580 nm. The sample “Seep 3 6/14/12” is shown as an example of a sample with no indication of SRB.

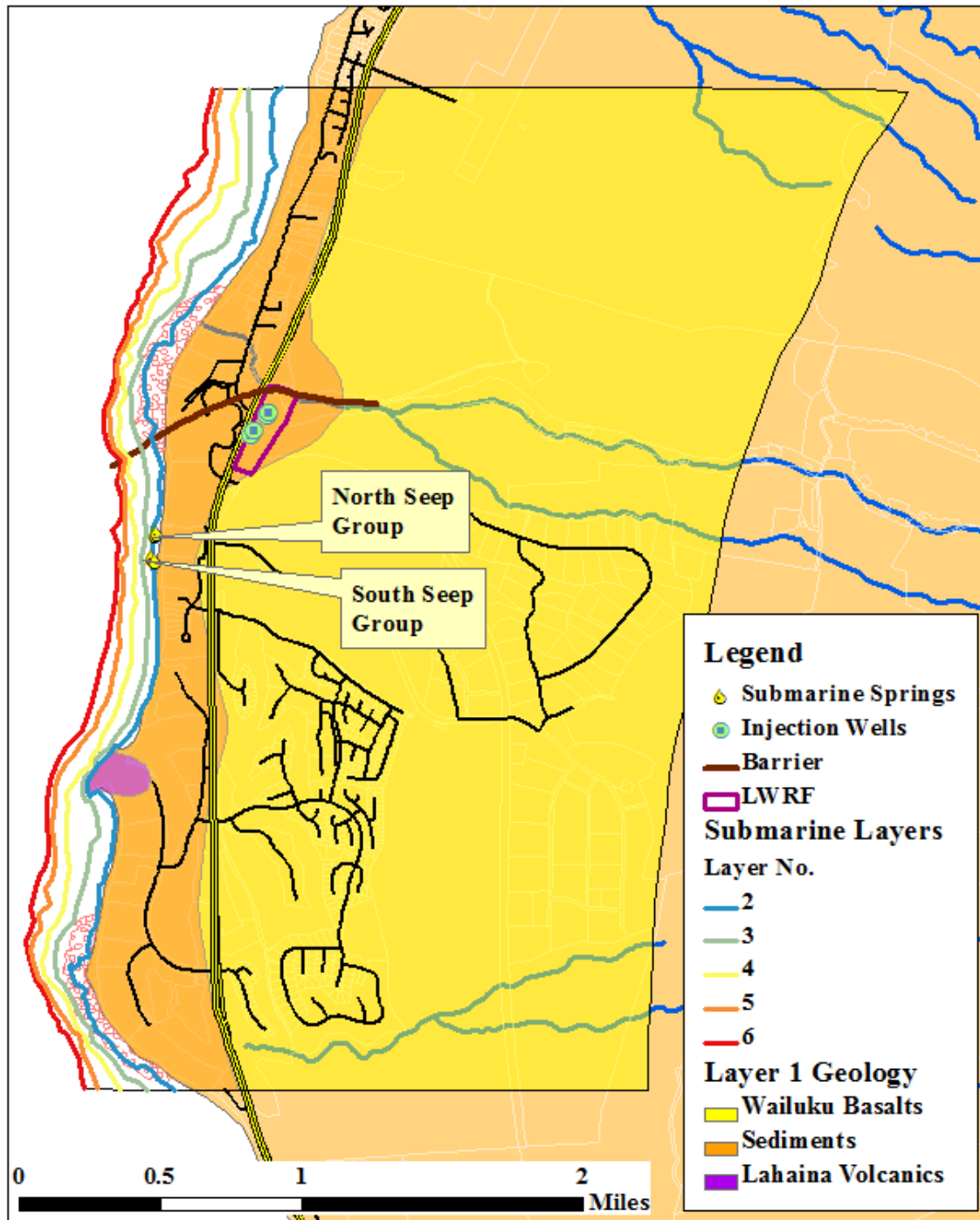


Figure ES-13: The conceptual model for the Lahaina Groundwater Study showing the extent of the submarine layers. Western boundaries of layers 2 through 6 followed the 6.6, 18, 29.5, 41, and 54 ft depth contours respectively.

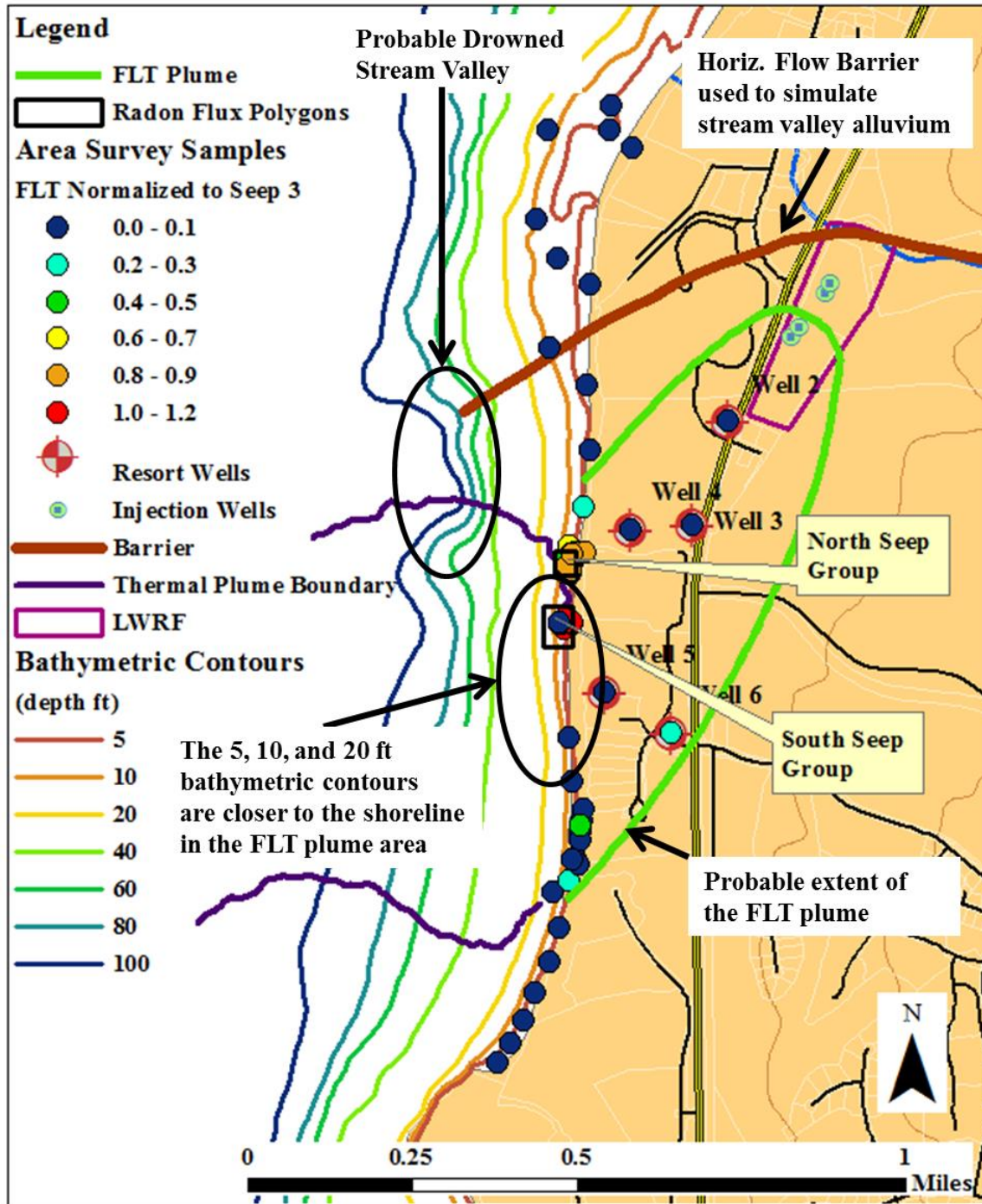


Figure ES-14: The probable drowned stream valley shown in relation to the modeled horizontal flow barrier and the normalized FLT concentrations

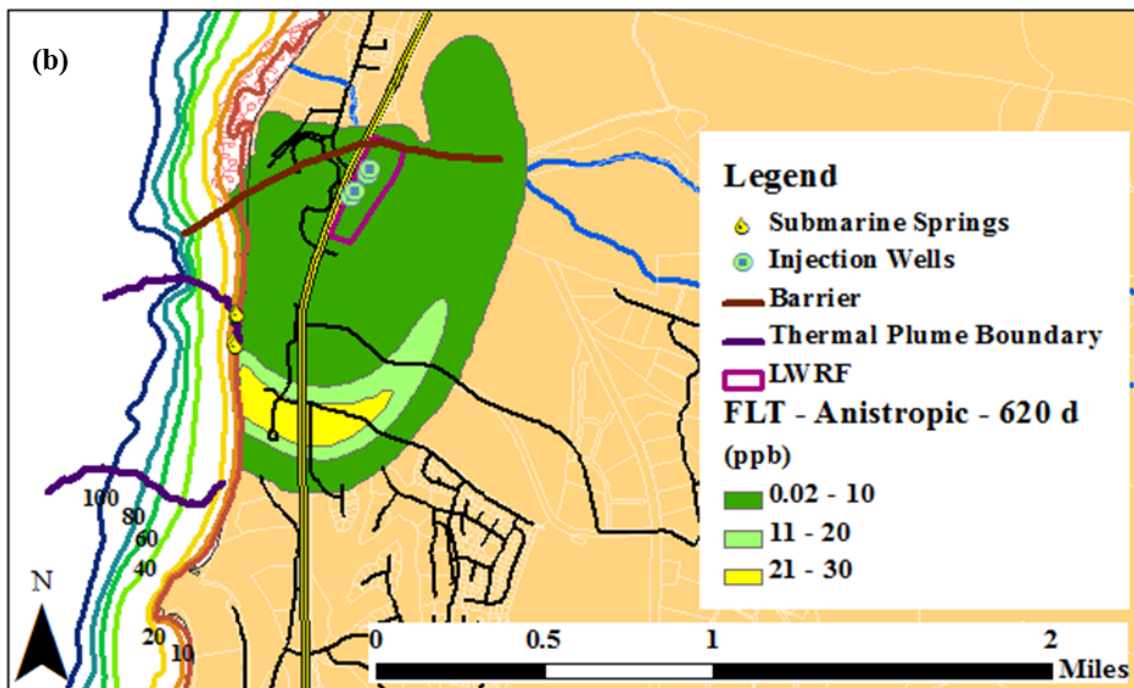
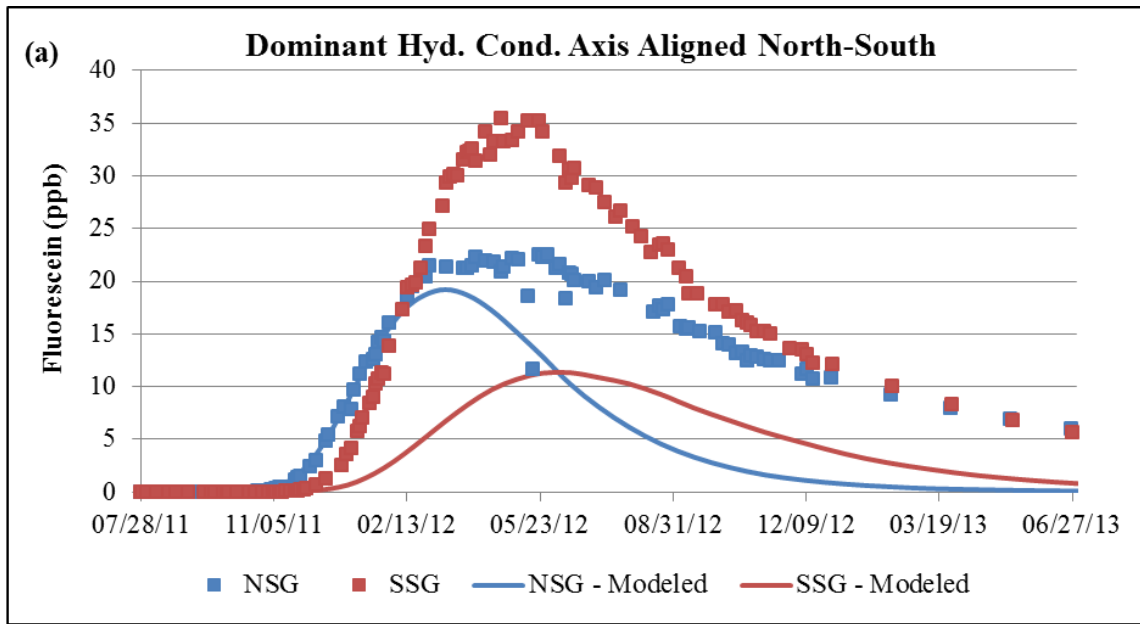


Figure ES-15: The FLT model results showing (a) the measured and simulated BTCs; and (b) simulated plume 620 days after dye addition. The model results show reasonable agreement between the simulated and measured BTC ascending limb and initial peak for the NSG. The simulated peak concentration for the SSG as about one-third of that measured. When the dominant hydraulic conductivity axis is aligned north-south, the plume reaches the southern TIR boundary.

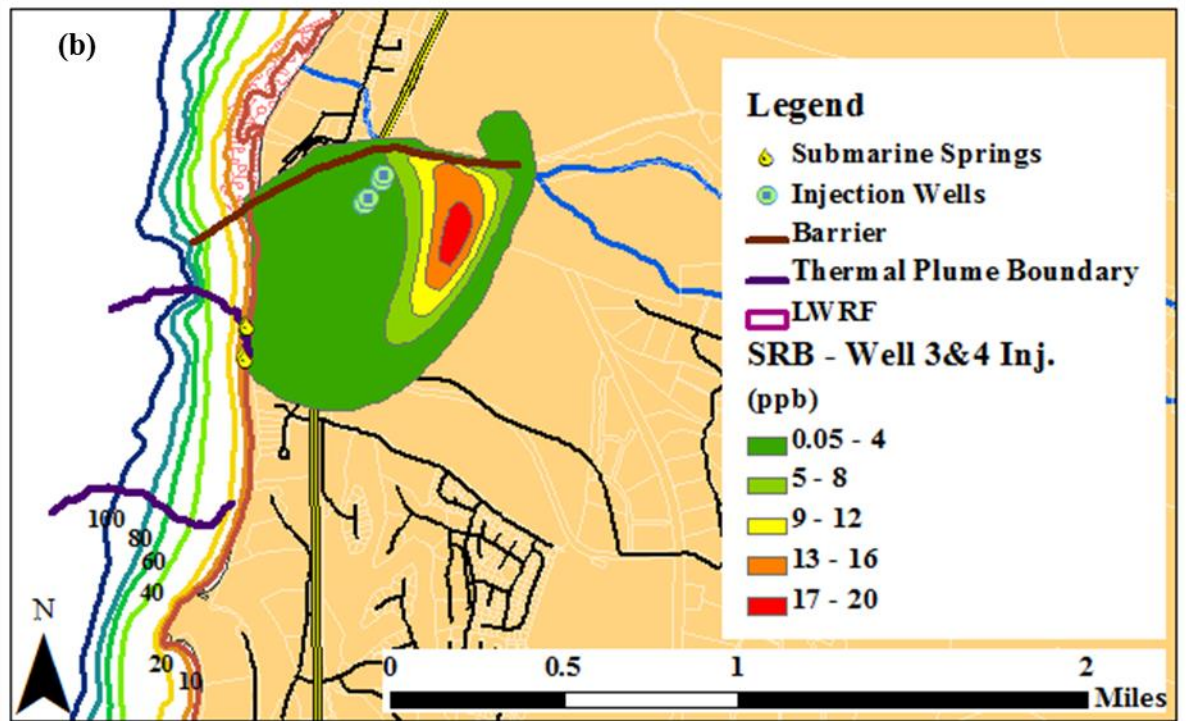
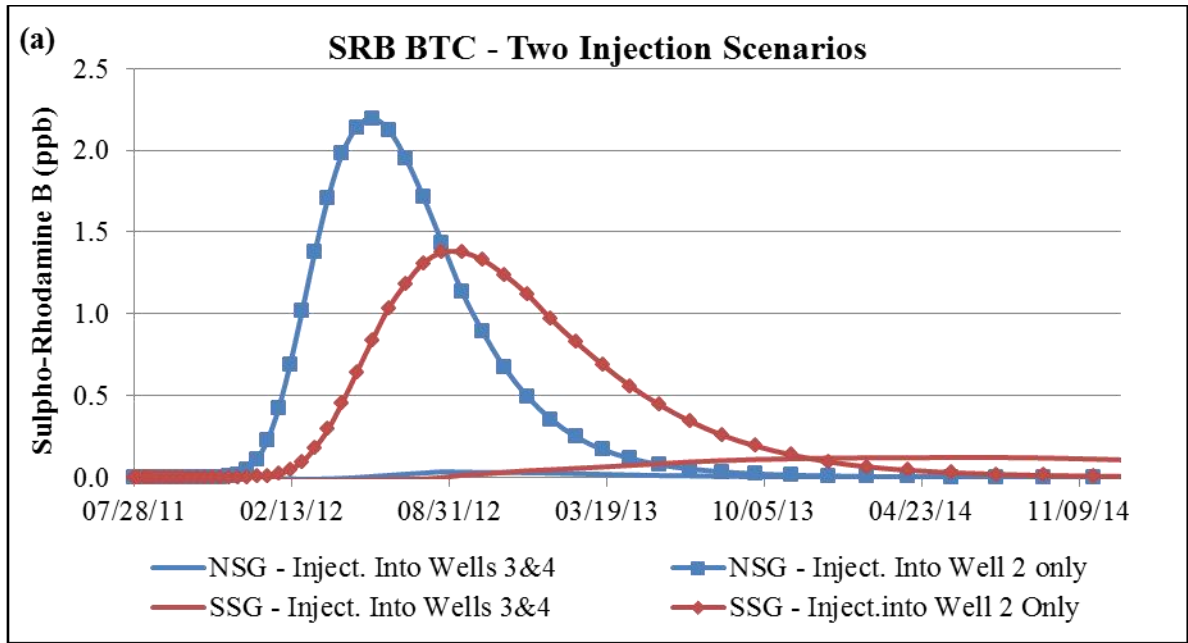


Figure ES-16: The simulated SRB BTCs (a) and plume 620 days after dye addition (b). The first injection scenario (lines only) simulates treated wastewater injection continuing into Wells 3 and 4 after the addition of SRB. The second scenario (lines and symbols) shows the simulated BTCs if treated wastewater was injected into Well 2 only after the addition of SRB. Continuing injection into Wells 3 and 4 after the addition of SRB displaces the core of the plume to the southeast. The valley fill barrier to the north and west prevent plume from moving in those directions.

This page is intentionally left blank

SECTION 1: INTRODUCTION, BACKGROUND, AND PURPOSE

1.1 INTRODUCTION

This Final Report was prepared by the University of Hawaii (UH) for the State of Hawaii, Department of Health Agreement Number 11-047 with funding provided by a grant from the U.S. Environmental Protection Agency. The purpose of this Final Report is to provide the final details and results from the project that have resulted since completion of the project's Final Interim Report, submitted in November 2012 (Glenn et al., 2012). The goals of the project have been to provide critical data about the geohydrological connection between the injected treated wastewater from the Maui County, Hawaii, Lahaina Wastewater Reclamation Facility (LWRF) and the nearby coastal waters, confirm the locations of emerging injected treated wastewater discharge in these coastal waters, and determine a travel time from the LWRF injection wells to the coastal waters. The sections that follow provide the final results of findings that stem from the study's principal objectives: (1) implement a tracer dye study from the LWRF (Section 4); (2) locate and conduct continuous monitoring for the emergence of the injected tracer dyes at the most probable points of emergence at nearshore sites within the coastal reaches of the LWRF (Section 2); (3) measure the SGD flux from the submarine springs (Section 3); (4) combine SGD fluxes with complete dye emergence breakthrough curves to estimate the treated wastewater flux in the nearshore waters (Section 4); and (5) develop groundwater flow and transport models to understand the flow paths of the treated wastewater to the coastal zone (Section 5). Each of these sections contains their own set of methodologies, results, and conclusions, and each has its own appendices, grouped together at the end of the report.

A very important part of the study has been the completion of a fluorescent dye tracer test to investigate any linkage that may exist between the underground injection of treated municipal wastewater effluent into the sub-surface waters north of the town of Lahaina, Maui, Hawaii, and the discharge of that treated wastewater to the nearshore coastal waters close to the treatment facility. As detailed in Section 4 (Fluorescent Dye Groundwater Tracer Study), we completed two tracer dye injections at the LWRF. In the first, fluorescein (FLT) was added to two wells (Injection Wells 3 and 4). In the second, sulpho-rhodamine-B (SRB) was added two weeks later into Injection Well 2, which has a significantly higher injection capacity than Wells 3 and 4. The SRB injection was conducted to investigate whether the treated wastewater from this well discharges into the marine environment at the same location as Wells 3 and 4. The FLT tracer dye injected at the LWRF has been detected in the coastal waters with the FLT breakthrough sufficiently established to calculate travel times and estimate the percent of dye recovery. The travel times are estimates and this part of the study has been combined with

continued coastal water flux measurements to estimate the total flux of treated wastewater and nutrient load being discharged into the nearshore waters. Groundwater and transport modeling were used to interpret the tracer breakthrough curve. Despite the broad area covered by our sampling program, SRB was not conclusively detected in the nearby coastal waters. The possible reasons for the failure to detect this dye were investigated by groundwater modeling.

1.1.1 Acknowledgements

We would like to acknowledge the contributions that many people and organizations have made to this project. The assistance of Hailey Ramey was important to the success of the field sampling, particularly the hours of scuba diving that were required for the submarine spring survey. We are very grateful to Russell Sparks, Skippy Hau, Kristy Stone, Linda Castro, Darla White, and Edward Kekoa of the Department of Aquatic Resources (DAR), State of Hawaii Department of Land and Natural Resources. These personnel from the Maui DAR were critical in supporting the on the ground portion of the aerial TIR survey, assisting in marine operations, and allowing us to store equipment at their facility. Dan Chang of the Hawaii Department of Health, Safe Drinking Water Branch was instrumental in the outreach to the Maui County Department of Environmental Services, assisted in the setup for the tracer tests, spent two sleepless nights adding dye to injection stream, and assisted in the well sampling. The assistance of the Maui County Department of Environmental Management was absolutely critical to the success of this project. They made facilities at the LWRF available, assisted in the design of the tracer test, and provided whatever assistance was requested during the addition of the dye. In particular, we would like to recognize Scott Rollins, Ken Knapp, and Kathleen Lawson. We also are very grateful for the help and assistance of Erin Vander Zee, James Watts, and Gary Byrd of Hawaii Rural Water who aided in the tracer dye portion of the project. Critical aid during the high frequency submarine spring sampling was made possible with the assistance of the project's University of Hawaii undergraduate trainees Jonathan Molina, Tatiana Martinez, Michelle Del Rosario, Jezelyn Gonsolves, and Ignacio Roger. These students worked hard to ensure that the tracer dye would not be missed if the travel time had been short. We extend our thanks to Hawaii Water Service Company (Kaanapali Water Corp.) for helping us with sampling the region's drinking water and irrigation wells, and Carlos Rivera and Starwood Vacation Ownership Resorts for allowing us to sample their monitoring wells. Critical assistance was provided by Jeff Sevadjan in the design and data interpretation of the Acoustic Doppler Current Profiler used to measure the discharge flux from the submarine springs. We are indebted to Joseph Kennedy and Jeff Skrotzki who helped in the field and in the writing of the project's Interim Report. We would like to acknowledge the Honolulu Office of the U.S. Geological Survey for making their facilities available to us for a conference briefing and for the feedback provided by Charles Hunt and Steve Anthony. Finally, we would like to acknowledge Dr. Benjamin Hagedorn for assisting in the groundwater sampling, performing important chemical analysis, and doing background research for the report. We realize that this list is incomplete would like to thank all of those that made this important research possible.

1.2 GEOGRAPHIC SETTING

Located between 155° 57' and 156° 42' west longitude, and 20° 34' and 20° 59' north latitude, the Island of Maui lies near the middle of the Pacific Ocean, far from any continental land mass. Maui is part of an island chain that was formed as the Pacific Tectonic Plate passed over a mid-ocean hotspot. The primary shield volcanoes forming this island chain generally occur in parallel trending pairs (Langenheim and Clague, 1987). Maui is no exception, consisting of the East Maui Volcano, Haleakala, and the West Maui Volcano. The older volcano, the West Maui Volcano (also referred to as the West Maui Mountain), rises to an altitude of 5,788 ft above sea level (asl) and the younger volcano, the East Maui Volcano (commonly referred to as Haleakala), rises to an altitude of 10,023 ft asl (Figure 1-1). The two volcanoes are separated by the central Maui isthmus, generally at an altitude less than 300 ft asl, that is covered with terrestrial and marine sedimentary deposits (Stearns and MacDonald, 1942).

The site of this study is located on the western extent of the West Maui Volcano, near the towns of Lahaina and Kaanapali. Steep mountain slopes and narrow stream channels in the uplands and gently dipping plains towards the coast characterize the area. According to the 2010 United States Census Bureau (Department of Business, Economic Development, and Tourism, 2010), there were 14,110 people, 4593 households, and 2875 families residing from the town of Lahaina to just north of the study area. The population density in this area is 445 people per square mile. The LWRF is located about three miles north of the town of Lahaina.

1.3 OVERVIEW OF THE LAHAINA WASTEWATER RECLAMATION FACILITY

The study area (Figure 1-2) is located in the Kaanapali District of West Maui, Hawaii. The LWRF is about three miles north of the town of Lahaina and serves the municipal wastewater needs for that community, including the major resorts along the coast. The LWRF receives approximately 4 million gallons per day (mgd) of sewage from a collection system serving approximately 40,000 people. The facility produces tertiary treated wastewater, which is disposed of via four on-site injection wells, and tertiary treated wastewater that is disinfected with UV radiation to meet R-1 reuse water standards. This R-1 water is sold to customers such as Kaanapali Resort to be used for landscape and golf course irrigation. The R-1 water that is not sold is also discharged into the subsurface via the injection wells.

The LWRF consists of two separate plants capable of operating in parallel. The first plant, constructed in 1976 (and currently not in operation), has an average flow capacity of 3.2 mgd. The other plant, constructed in 1985 (and modified in 1995), has an average flow capacity of 6.7 mgd. After primary settling to remove the majority of the suspended solids, the LWRF effluent undergoes secondary treatment. This treatment reduces the biodegradable dissolved solids by microbial action that metabolizes the organic matter.

The LWRF also incorporates biological nutrient removal to promote nitrogen removal. The effluent is sand filtered to remove solids before injection or further treatment. The effluent that undergoes disinfection using ultraviolet radiation is sold as R-1 grade reuse water for irrigation and other approved uses (e.g., construction dust control, etc.). This grade of reuse water can be used for irrigation with very few restrictions (Limtiaco Consulting Group, 2005; and County of Maui, 2012-2013). Prior to October 28, 2011, the effluent discharged into the LWRF injection wells was only partially disinfected with chlorine.

Limtiaco Consulting Group (2005) summarized the history of the reuse water production at the LWRF. Up to the late 1980s, the LWRF provided R-2 water (reclaimed wastewater with restrictions placed on its use) to the Pioneer Mill for sugarcane irrigation. However, with the phase-out of sugarcane this disposal option disappeared. In the mid-1990s Maui County upgraded the plant to produce R-1 water to be used as a resource and in part to address concerns about seasonal benthic algal blooms that were proliferating along the coast. The distribution system was extended to make R-1 water available to the Maui Land and Pineapple Company for pineapple irrigation in 2003. This water was to be blended with non-potable water from the Honolua Ditch. However, due to ample rain and the phase-out of pineapple, little use has been made of this option. This infrastructure may be beneficial to the expansion of reuse in the Kaanapali area and the emerging diversified agriculture in West Maui.

The LWRF injects the secondary treated effluent into four injection wells (Figures 1-3 and 1-4). Under the Safe Drinking Water Act an Underground Injection Control (UIC) permit is required from the U.S. Environmental Protection Agency (USEPA) for the injection of subsurface wastewater effluents that might affect potential sources of drinking water. The LWRF's UIC permit expired on June 6, 2005 but per the USEPA's approval, the facility is operating under the expired permit until a renewal is approved. Sections 1421 through 1445 and Section 1450 of the Safe Drinking Water Act require that each state establish an UIC program to protect drinking water sources from contamination due to sub-surface fluid injection. Title 40 of the Code of Federal Regulations, Parts 144 through 148 details the UIC permit regulations. Part 144 lays out the minimum permitting and program requirements. Part 145 details the elements and permitting procedures for a state program, while Part 146 spells out the technical requirements. Part 147 sets forth the UIC program for each state including Hawaii. Much of the oversight of UIC activities is delegated to the states. However, the UIC program for the State of Hawaii is administered by the USEPA. The Hawaii UIC program requirements are codified in the Hawaii Revised Statutes (HAR) Title 11, Chapters 23 and 23a.

The State of Hawaii UIC restrictions are less stringent if an aquifer is not a potential source of drinking water due to high concentrations of total dissolved solids (TDS). The area of an aquifer that is seaward of an UIC Line is classified as an exempted aquifer. Class V injection wells are allowed in exempted aquifers and this class includes the injection of sewage derived wastewater. The LWRF is located seaward of the UIC line (Figure 1-3) and injects treated effluent to depths between 180 and 255 feet below ground

surface (or -55 and -229 feet above mean sea level). The screen length or open interval of the wells varies from 95 to 150 feet below ground surface. Table 1-1 gives the construction details for the injection wells while Figure 1-4 shows geology of the boreholes drilled to install these wells and the screened or open interval of the wells. The average flow rate into the plant is currently about 4.0 mgd. After reuse, the injection volume averages about 3.2 mgd. During warmer, dryer months no more than 3.0 mgd is expected to be injected underground as current reuse has typically reached 1.8 mgd in these periods (County of Maui, pers. communication). The permitted daily maximum rate is 19.8 mgd and the maximum weekly average injection was 9.0 mgd for 2010 (County of Maui, 2010). Table 1-2 and Figure 1-5 show the average daily injection by well for the months from April, 2011 through March, 2013. As mentioned above, Maui County is in the process of renewing the UIC permit for these wells, operating under Permit No. UM-1357, which expired 3/28/2009 but operating under an extension to that permit through 8/28/2013. Concerns about the potential impact of the injection well operations on the coastal environment has prompted research into the amount, distribution, and discharge points of nutrients and other chemicals into the marine environment.

Scientific evidence (e.g., Hunt and Rosa, 2009; Dailer et al., 2010, 2012) supports the hypothesis that treated wastewater injectate from the LWRF is discharging into the nearshore waters southwest of the treatment facility. However, at the time that the present study was started, the extent of that link had not been irrefutably established. One of the goals of this project has therefore been to tag the treated wastewater with fluorescent dyes prior to injection and monitor the nearshore coastal waters for the emergence of the dyes at nearby submarine springs, particularly those identified by Hunt and Rosa (2009) and Dailer et al. (2010, 2012). Figures 1-6 and 1-7 show the location of the submarine springs relative to the LWRF.

1.4 HISTORY OF RELATED INVESTIGATIONS

Examples of relevant previous studies include nutrient characterizations and loading estimates for this area (Souza, 1981; Tetra Tech, 1993; Soicher and Peterson, 1997), a dye tracer test (e.g., Tetra Tech, 1994), and those concerning the potential linkages land-derived nutrients and algae blooms (e.g., Dollar and Andrews, 1997; Borke, 1996; Smith et al., 2005; Smith and Smith, 2007). More recent scientific investigations on Maui include Hunt and Rosa's (2009) geochemical approach to detect treated wastewater discharges in Lahaina and Kihei, Dailer et al.'s (2010, 2012) work using stable isotope data from intertidal and nearshore cultivated algae, and recent groundwater investigations for West Maui modeling by the USGS (Gingerich, 2008; Gingerich and Engott, 2012).

In response to concerns prompted by seasonal algae blooms in West Maui, the USEPA sponsored a nutrient balance study of West Maui (Tetra Tech, 1993). That report identified the LWRF as one of the three primary nutrient release sources to Lahaina District coastal waters, with sugarcane and pineapple cultivation being the other two. That study also ranked the LWRF second in annual nitrogen contribution and first in phosphorous contribution to these waters. Since that study was completed, the

cultivation of both sugarcane and pineapple has been sharply curtailed. This implies that the LWRF may now be the primary contributor of nutrients to water in the study area. The West Maui Watershed Owner's Manual (West Maui Watershed Management Advisory Committee, 1997) reevaluated N and P loadings in the watershed and concluded that as of 1996, wastewater injection wells contributed ca. 94% of land-derived phosphorus-loading and ca. 57% of land-derived nitrogen-loading to the ocean, relative to the other sources evaluated (cesspools and inputs from pineapple-, sugarcane- and golf course-developed lands). As discussed in Section 6 of our Project Interim Report (Glenn et al., 2012), however, it must be noted that since the release of the Tetra Tech (1993) report, all nutrient species concentrations in the LWRF treated wastewater appear to have been significantly reduced, likely in association with the inception of treatment process improvements such as biological nutrient removal in 1995.

Tetra Tech (1994) also estimated the travel time of treated wastewater from the point of injection to the coast using a two-dimensional numerical flow model. Based on that model, the travel time could be as short as ten days. In the absence of any injection, travel time would increase to 50 days based on the average groundwater-flow velocity. The model assumed an aquifer thickness of 20 ft. Using the Ghyben-Hertzberg principle, the freshwater lens thickness is 41 times the groundwater elevation above sea level (Fetter, 1988), which yields a more accurate aquifer thickness of 80 to 100 ft near the LWRF. This is based on a water table elevation of 2-2.5 ft msl (Gingerich, 2008). The thinner modeled aquifer thickness would result in a shorter travel time. Also, the distance between the LWRF injection wells and the nearest identified submarine spring is approximately 0.49 mi, which is greater than the direct path distance to the shoreline. The eastern boundary of the Tetra Tech (1994) model was the interface between the high level water at the interior of the island and the basal groundwater. This was assigned as a no-flow boundary condition. In actuality, however, there is significant groundwater flow from the high-level water body to the basal groundwater (Gingerich, 2008; Gingerich and Engott, 2012).

Because the LWRF was identified as a major contributor of nutrients to the marine environment in the 1993 study, an effluent fate and transport study was commissioned by the USEPA. Tetra Tech (1994) conducted a dye tracer test to identify the submarine locations where the treated wastewater was discharging into the marine environment. They added Rhodamine WT (RWT), a fluorescent tracer dye, into the treated wastewater stream prior to underground injection at a concentration of approximately 100 parts per billion (ppb). This injection lasted for 58 days. To monitor for the emergence of the treated wastewater tagged with RWT, they completed a series of monitoring transects offshore north-northeast transects. Every 200 yards, a pump-suction line was let drift to the ocean bottom. The suction line was connected to a pump on the survey boat with the discharge from the pump ported through a constant monitoring fluorometer. In that study, only two occurrences of elevated fluorescence were detected at adjacent sampling locations, in the southeast corner of their sampling grid (Figure 1-7). The fluorescence value was low, about three times that of background. The first detection occurred 55 days after the start of injection and the second detection occurred 61 days after the start of injection. The location of the Tetra Tech elevated fluorescence detections was very near

the submarine springs identified by Hunt and Rosa (2009) and Dailer et al. (2010, 2012) as probable, and as confirmed by this study, discharge points for the LWRF treated wastewater. Due to the fluorescence values being only slightly above background, it is uncertain whether the source was the RWT dye, or another fluorophore such as dissolved organic matter. Figure 1-7 illustrates the location where Tetra Tech (1994) detected RWT fluorescence, the submarine springs suspected of discharging treated wastewater, and the plume area proposed by Hunt and Rosa (2009).

Hunt and Rosa (2009) investigated the use of multiple in-situ geochemical tracers to identify where and how municipal wastewater treated wastewater discharges to the nearshore marine environment. These researchers sampled the LWRF treated wastewater, submarine springs, nearshore marine waters, groundwater, and terrestrial surface water in vicinity of treated wastewater injection sites in Lahaina and Kihei, Maui. They sampled the entire nearshore region including the submarine springs in 2008 for a suite of parameters including: (1) $\delta^{15}\text{N}$ values of macroalgae and water column samples; (2) temperature; (3) salinity; (4) turbidity; (5) dissolved oxygen; (6) pH; (7) chlorophyll a; (8) fluorescence; (9) conductivity; (10) nutrient concentrations of water column samples; (11) waste indicator compounds of water column samples; and (12) pharmaceuticals. They concluded that the most conclusive tracers were the presence of pharmaceuticals, organic waste indicator compounds, and a highly elevated $\delta^{15}\text{N}$ values in water samples and coastal benthic macroalgal tissue. These researchers identified the submarine springs as the coastal locus of the LWRF injection plume, although they also cited nearshore marine samples collected further south towards the Kaanapali Golf Course as showing geochemical evidence of treated wastewater or effluent-derived irrigation water influence. They also noted elevated nutrient concentrations and potential treated wastewater or effluent-derived irrigation water influence in Black Rock lagoon, an apparently groundwater fed, ocean-connected drainage feature located on the Kaanapali Golf Course at the southern end of North Kaanapali beach. Particularly pertinent to the current study, they investigated background fluorescence along the shoreline near the LWRF, where they measured fluorescence with a handheld fluorometer with an optical brightener and a Rhodamine WT channel. They detected optical brightener fluorescence in samples collected at the submarine springs that was 15 times that in the water column near the submarine springs. There was no difference in Rhodamine WT fluorescence between the submarine spring and the water column samples. This indicates that non-dye fluorophores in LWRF treated wastewater were probably not responsible for the elevated Rhodamine WT fluorescence detected by Tetra Tech (1994). This further indicates that the elevated fluorescence in the Rhodamine WT wavelength detected by Tetra Tech (1994) was likely from the dye they added to the treated wastewater.

Dailer et al. (2010, 2012) used the stable isotopic composition of macroalgae ($\delta^{15}\text{N}$) to map the anthropogenic input of nitrogen to the nearshore waters of Maui. Atmospheric and fertilizer $\delta^{15}\text{N}$ values generally fall in the range of -4‰ to +4‰. Input from sewage can generally be identified by its higher $\delta^{15}\text{N}$ values that range from 7‰ to 38‰ (e.g., Kendall, 1998; Gartner et al., 2002), although isotope effects associated with various biogeochemical N transformations must be carefully considered when attempting to

identify original N sources using this methodology. The two highest $\delta^{15}\text{N}$ values (33.2 and 43.3‰) measured by Dailer et al. (2010) were found at sites near the submarine springs. These researchers also observed that the submarine spring discharge was warmer than ambient seawater and that the discharge points were surrounded by rocks coated with a distinctive black precipitate thought to consist of iron oxides.

Significant work has been done on the wastewater injection and the fate of this injectate in Hawaii. Oberdorfer and Peterson (Oberdorfer and Peterson, 1982; Oberdorfer, 1983) studied the processes that lead to injection well clogging and the fate of nutrients in the injected treated wastewater. They found that a significant amount of denitrification (nitrate reduction) occurs in the subsurface after injection. Petty and Peterson (1979) investigated sewage injection practices in West Maui including resorts and condominiums. The fate of wastewater injection plumes was modeled by Hunt (2007), Burnham et al. (1977), Wheatcraft et al. (1976), Tetra Tech (1993), and Hunt and Rosa (2009) and all studies showed that once the treated wastewater is injected, the plume tends to rise due to its positive buoyancy relative to the surrounding saline groundwater.

There have been several geochemical surveys (including nutrients, isotopes, and general water quality parameters) and studies of anthropogenic inputs into the coastal waters of West Maui in addition to those already cited. Laws et al. (2004) showed that coastal nutrient concentrations exceeded State water-quality standards for marine waters. Street et al. (2008) investigated submarine groundwater discharge (SGD) using multiple tracers such as the radon/radium pair, silica, and salinity. They estimated that the SGD near the study site was 0.07 to 0.12 meters cubed (m^3) per meters squared (m^2) per day (d), delivering a dissolved inorganic nitrogen load of 13.3 to 36.8 mM per m^2/d . Dollar et al. (1999) and Atkinson et al. (2003) monitored for estrogen as indicator of discharge of cesspool effluent to the waters of west and south-central Maui. Soicher and Peterson (1997) studied the nutrient input to West Maui coastal waters and concluded that stream discharges were an acute nitrogen source, but chronic SGD was the major contributor.

1.5 STUDY AREA DESCRIPTIONS AND BACKGROUND

1.5.1 Climate

Maui's climate is characterized by mild and uniform temperatures, seasonal variation in rainfall, and great geographic variation in rainfall (Lau and Mink, 2006). The average temperature in Lahaina, on the leeward coast of the West Maui Volcano, is 75.7° F, whereas the average at Haleakala summit is 47° F (WRCC, 2011). During the warmer dry season (May-September), the stability of the north Pacific anticyclone produces persistent northeasterly trade winds, which blow 80-95 % of the time (Gingerich, 2008). During the cooler rainy season (October through April), migratory weather systems often travel past the Hawaiian Islands, resulting in less persistent trade winds that blow 50-80% of the time (Gingerich, 2008). Low-pressure systems and associated southerly (Kona) winds can bring heavy rains to the island, and the dry coastal areas can receive most of their rainfall from these systems.

The variation in mean annual rainfall with altitude is extreme on Maui, with differences of more than 130 inches within one mile of the summit of West Maui Volcano where average annual rainfall exceeds 340 inches per year (in/yr) (Giambelluca et al., 2011). Mean annual rainfall at the Kaanapali coast in the dry leeward areas south of Lahaina is less than 15 in/yr (Giambelluca et al., 2011). At higher altitudes, precipitation is a combination of rainfall and fog drip where the montane forest canopy intercepts cloud water. Engott and Vana (2007) and Scholl et al. (2004) estimated that fog drip contributes to an additional 20% of rainfall along the windward flanks of West Maui above an elevation of 2000 ft asl.

Annual pan evaporation of West Maui has been reported by Ekern and Chang (1985) and Engott and Vana (2007) to range between 90 and 100 in/yr near the Kaanapali coast and from 50 to 60 in/yr near the summit of the West Maui Volcano. The streams in the Lahaina area are typically perennial above 1,000 ft asl, but diversions and loss to groundwater at lower altitudes result in intermittent flow as the streams approach the ocean. Honokohau Stream (Figures 1-6 and 1-8) is the only true perennial stream in the immediate study area; however, stream flow is flashy due to intense rainfall and the steep topography (Tetra Tech, 1993).

1.5.2 Land Use

Current West Maui land use can be subdivided into several sectors: (1) an urban center in the Lahaina area; (2) various diversified agriculture and pasture land on former pineapple and sugarcane fields on the lower slopes of the West Maui Mountain; (3) residential and resort development (including golf courses) along the shoreline; and (4) natural evergreen forest in the interior of the West Maui Mountain (Figure 1-8). Historical changes in agricultural land use within the western half of West Maui were estimated by Engott and Vana (2007) in order to estimate the effects of rainfall and agricultural land use changes on West and Central Maui groundwater recharge, and the following sections on land use are summarized from their work, and as summarized by Gingerich (2008) and Gingerich and Engott (2012). During the early 1900s until about 1979, land use was mostly unchanged except for some minor urbanization along the coasts. However, as large-scale plantation agriculture declined after 1979, land-use changes were more significant. From 1979 to 2004, agricultural land use declined about 21 percent, mainly from the complete cessation of sugarcane agriculture.

The Pioneer Mill Co. was the major sugarcane cultivator on the west side of the West Maui Mountain, operating during the late 1800s until 1999, when it ceased sugarcane production and the land was subsequently bought by Maui Land and Pineapple (ML & P) and other private investors. ML & P had a long history of cultivating pineapple on the northwest slope of West Maui Mountain generally on land located to the north of the former sugarcane fields. More recently, they grew pineapple on former Pioneer Mill Co. sugarcane lands located north of Honokowai Stream. The extent of pineapple agriculture in West Maui decreased extensively since the late 1990s and was stopped entirely in 2009 (Gingerich and Engott, 2012). Large portions of the former sugarcane and pineapple

fields remain fallow while other parcels have been converted to low-density housing and diversified agriculture.

1.5.3 Geology

The study site is located on the northwestern extent of the West Maui Volcano. This is the older of the two Maui shield volcanoes. Figure 1-9 shows the geology of West Maui, which consists of a central caldera and two main rift zones that trend north-northwest and south-southeast from the caldera (Stearns and MacDonald, 1942; Sherrod et al., 2007). Numerous dikes occur as thin, near-vertical sheets of massive, low-permeability rock that are present within the rift zones and increase in abundance toward the caldera and with depth. Other dikes also exist outside the two major rift zone trends (Figure 1-9), creating a radial pattern of dikes emanating from the caldera (MacDonald et al., 1983). The volcanic rocks that originated from vents in and near the caldera and rift zones comprise (1) the mostly shield-stage Wailuku Basalt, (2) the postshield-stage Honolua Volcanics, and (3) the rejuvenated-stage Lahaina Volcanics, a minor unit of the West Maui Volcano. All these rocks are Pleistocene in age and are mainly comprised of tholeiitic/picritic basalt, trachyte, and basanite layers ranging in thickness from 1 to 500 ft (Stearns and MacDonald, 1942; Langenheim and Clague, 1987; Sherrod et al., 2007). These layers in the Wailuku Basalt show numerous interflow structures within a series of lava flows and associated pyroclastic and sedimentary formations. The Wailuku Basalts in the area are characterized by high permeability and storage capacity and comprise the main aquifers for groundwater withdrawal (Gingerich, 2008). The Honolua Volcanics were produced by late eruptions, and overlie the Wailuku basalts. They are more massive and tend toward andesitic compositions. Due to their increased thickness and denser nature, their permeability is much lower than those of the Wailuku Basalts. They are more prevalent in the northeast and northwest slopes of the West Maui Volcano (Gingerich, 2008; Sherrod et al., 2007) and do not intersect the groundwater in the study area. The Lahaina Volcanics resulted from rejuvenation stage eruptions that took place 610,000–385,000 years ago. As with the Honolua Volcanics, they are more massive in nature. However, their small areal extent and proximity to the coast makes this unit less important when assessing groundwater flow than the other volcanic units. An outcrop of the Lahaina Volcanic series known as Puu Kekaa, or Black Rock, is located in the southwest portion of the study area (Figure 1-9).

Gingerich and Engott's (2012) work projected the top of the West Maui Wailuku Basalts to reach depths of about 600 meters below sea level (m bsl) at a distance of about 10 km from the shore. Wedge-shaped consolidated Quaternary alluvium forms a sedimentary surface veneer that drapes and overlies the Wailuku Basalt along the coast, infills the deep canyons in the West Maui Volcano, and very likely into the offshore (Stearns and MacDonald, 1942; see Figures 1-9, 1-10). These alluvial deposits formed as a result of the extensive erosion that carved deep valleys into the eastern flanks of the West Maui Volcano, and formed West Maui's low-permeability caprock. It is probable that some of these sediments also contain relict marine carbonates deposited in relation to former stands of the sea. This formation, like elsewhere in Hawaii, is of great hydraulic importance as it overlies high-permeability dike-free volcanic rocks below and, due to its

relatively low conductivity, generally impedes fresh groundwater discharge towards the coast (cf. Lau and Mink, 2006; Rotzoll et al., 2007; Gingerich and Engott, 2012, and discussion and references therein).

After the shield building stage of the Wailuku Basalts ended, stream channels eroded into the flanks of West Maui (Stearns and MacDonald, 1942). Thus, the current stream channels, including the Honokowai stream, could have started forming as early as the early to mid-Pleistocene (0.13 to 1.8 million years ago). No later stage lava flows (Honolua or Lahaina Volcanics) are present in the Kaanapali area inland or in the vicinity of the LWRF or Honokowai Stream (Figure 1-9) that would have filled the stream valleys incised into the Wailuku basalts. Since that time, Maui has experienced emergence and submergence. During periods of emergence, stream channels could be cut to beneath the current sea level then filled with alluvium of low hydraulic conductivity as submergence occurred (e.g. this Report, Section 5). Stearns and Macdonald (1942) estimated that there had been at least three cycles of submergence and re-emergence since the cessation of major volcanic activity on West Maui. The submergence could have resulted in a shoreline 2,500 ft above the current shoreline. The emergence could have resulted in a shoreline 950 ft below the current sea level. This process occurred over a period of 1.8 million years providing ample time for deep cut stream valleys to develop during the period of emergence.

1.5.4 Regional Groundwater Hydrology

The precipitation that falls on West Maui is partitioned between surface runoff, evapotranspiration, soil moisture storage, and groundwater recharge. Recharge, the fraction of groundwater that reaches the water table, flows radially out from the central highlands to discharge areas along the coast. Figure 1-11 shows the groundwater recharge distribution for West Maui and the extent of the high-level water body (Engott and Vana, 2007; Gingerich, 2008). Recharge rates range from 350 inches per year (in/yr) at the high elevations to less than 10 in/yr along the coast. The high recharge and low hydraulic conductivity of the dike zones in the interior regions of the West Maui Volcano result in a water table with elevations up to 3,000 feet above mean sea level (ft msl) (Gingerich, 2008). Figure 1-9 shows the approximate interface between the high level and basal aquifers (Mink and Lau, 1990b). The dike impoundment of the groundwater is breached in areas where erosion has cut deep valleys and subterranean water provides baseflow for the streams.

In the subsurface, once the groundwater flows out of the high-level water body, it becomes a lens of freshwater floating on the underlying saltwater with a water table elevation of less than a few tens of feet above sea level. This Ghyben-Herzberg principle states the thickness of the freshwater lens is 41 times the elevation of the water table above sea level. This is only an estimation based on simplifying assumptions, however, and the actual thickness of the freshwater lens can deviate from this value due to factors such as non-horizontal flow and heterogeneous geology (Izuka and Gingerich, 1998). The mixing of the two waters in the basal lens along the groundwater flow path results in a sloping transition rather than a sharp interface between fresh and saltwater.

As the groundwater approaches the shoreline, it may encounter the sedimentary caprock described above, which retards the groundwater's seaward flow (Figure 1-10). The effective hydraulic conductivity of the caprock is significantly lower than that of thin-bedded lavas, causing a thicker freshwater lens due to the higher potentiometric (or hydraulic head) surface and the barrier that reduces saltwater intrusion into the aquifer. As shown in the highly generalized Figure 1-10, the condition in the basalt aquifer changes from an unconfined condition to a confined condition where the water table meets the bottom of the caprock, which can be considered itself as an unconfined aquifer. The height of the water table within this aquifer should be lower than the potentiometric surface. Drilling logs from the injection wells at the LWRF indicate that sedimentary deposits extend below the potentiometric surface caused by that overlying confining layer for a portion of the aquifer between the facility and the coast (County of Maui, 2004). Preferential flow paths in the aquifer can result in well-defined submarine springs, as is the case in this study area. In addition to preferential-flow point discharges, a more diffuse discharge may also be present over a larger area.

1.5.4.1 Aquifer Properties

Total porosity estimates for basaltic rocks on Hawaii and elsewhere ranges from less than 0.05 to more than 0.5 (Hunt, 1996; Kwon et al., 1993; Nichols et al., 1996). Low porosity values may be associated with massive features, including dense flows, a'a cores, dikes, and thick lava flows; high values may be associated with fractures and a'a clinker zones. Estimates of effective porosity (which includes only the hydraulically interconnected pore spaces) derived from modeling studies range between 0.04 and 0.10 for volcanic-rock aquifers (Gingerich and Voss, 2005; Oki, 2005). Souza and Voss (1987) and Gingerich (2008) estimated an average effective porosity of the volcanic rocks on Hawaii of 0.15. Rotzoll and El-Kadi (2007) analyzed aquifer-test data from wells in central Maui and estimated specific storage and specific yield from one test to be 2.0×10^{-6} and 0.07, respectively. Hydraulic conductivities (K) of the igneous and sedimentary rocks on West Maui are highly variable and are distributed heterogeneously around the area. Regional K values have been estimated from specific capacity values of aquifers to range between 250 ft/d to 4,100 ft/d (Rotzoll and El-Kadi, 2007).

Though high and low conductivity volcanic aquifers may alternate over several feet in depth (Stearns and MacDonald, 1942), the volcanic aquifers on Maui are generally regarded as one unconfined system (Gingerich, 2008). This is because highly permeable structures, such as clinkers and vertical fractures, have been commonly observed in all lava flows, both in outcrops and rock cores (Langenheim and Clague, 1987). Additionally, numerical groundwater flow models yielded a relatively good agreement between modeled and measured water levels on Maui when uniform conductivity, porosity and specific yield values had been assigned (Gingerich, 2008).

The water transport characteristics of the various aquifer materials vary greatly along the flow path. The hydraulic conductivity of the dike-intruded lavas in Hawaii is estimated to range from 1 to 500 ft/d (Hunt, 1996). The low end of this estimate would be more

representative of the West Maui Volcano due to the high density of dikes in the inland high water body. In a groundwater model of the Lahaina District, Gingerich and Engott (2012) assigned a longitudinal horizontal hydraulic conductivity of 1,800 ft/d, a transverse hydraulic conductivity of 590 ft/d, and a vertical hydraulic conductivity of 17.0 ft/d for the Wailuku Basalts in the Lahaina area. For the sedimentary deposits Gingerich and Engott (2012) used values of 190 and 3.8 ft/d for the horizontal and vertical hydraulic conductivity, respectively.

1.5.4.2 Submarine Groundwater Discharge

The ultimate natural and final release of most groundwater in the Hawaiian Islands is to the ocean as submarine groundwater discharge (SGD). Nearly all groundwaters undergo chemical modifications and additions due to natural leaching of nutrients along their flow paths. Infiltration from agricultural, urban and metropolitan lands, and wastewater injections near the coast can also contribute to the dissolved load of the SGD subterranean flow. These waters thus exit as chemically-modified mixtures of freshwater and recirculated seawater that flow seaward throughout each island's peripheral aquifers. Geohydrological budgets (Shade, 1996, 1997, 1999) indicate that the majority of groundwater that enters and recharges Maui's uplands is eventually discharged as SGD (Figure 1-12). In most settings in Hawaii, SGD exits along the coast as relatively cool, brackish waters. The most strikingly anomalous expression of SGD within the present study area, however, is the seepage of localized and anomalously *warm* and brackish SGD, particularly in the area described as submarine springs (or "seeps") along the Kaanapali coast near Kahekili Beach Park, about 0.5 miles southwest of the LWRF. The warm and brackish SGD issuing from these warm water submarine springs entrain gas bubbles and discharge from cracks and small vents in the semi-consolidated hard bottoms, as well as from unconsolidated patches of surficial sands on the seafloor. During this study, we grouped these warm water submarine springs into two groups, termed the North Seep Group (NSG), which occurs within 3 to 5 m of shore, and the South Seep Group (SSG), which occurs within 25 m of shore (Figure 1-7). Over 18 months of study, the salinity of the seeps in the NSG varied between 3.8 and 25.3, with an average of about 4.7. Seeps in the SSG had salinities that were slightly lower, varying between 2.5 to 22.5, with an average of about 3.2. The detection, mapping, and investigation of the dye tagged SGD emerging from these submarine springs is a major focal point addressed throughout this report.

Table 1-1. Construction Details of the LWRF Injection Wells

Injection Well No.	1	2	3	4
Construction Date	1979	1979	1985	1985
Elevation (ft msl)	33	33	28	29
Total Depth of Well (ft bgs)	200	180	225	255
Solid Casing Length (ft)	88	88	108	108
Bottom of Well (ft msl)	-168	-150	-200	-229
Screen/open hole length (ft)	115	95	120	150
Top of Screen/Open Hole elevation (ft msl)	-55	-55	-80	-79
Bottom of Screen/Open Hole Elevation (ft msl)	-170	-150	-200	-229

Data from Maui County Department of Environmental Management

Table 1-2. Treated wastewater injections rates for April of 2011 through March of 2013

	Well 1	Well 2	Well 3	Well 4	Total Injection
	(mgd)	(mgd)	(mgd)	(mgd)	(mgd)
April, 2011					
Minimum	0.17	0.99	0.66	0.58	2.86
Average	0.22	1.63	0.88	0.82	3.55
Maximum	0.27	2.75	1.05	1.06	4.86
May, 2011					
Minimum	0.15	0.31	0.74	0.67	2.41
Average	0.21	1.04	1.05	0.83	3.14
Maximum	0.29	2.10	1.36	0.94	4.23
June, 2011					
Minimum	0.10	0.14	0.31	0.86	2.00
Average	0.20	0.70	1.18	1.03	3.11
Maximum	0.28	1.52	1.62	1.27	4.03
July, 2011					
Minimum	0.07	0.02	1.19	1.03	2.56
Average	0.19	0.41	1.36	1.15	3.11
Maximum	0.27	1.14	1.74	1.32	3.80
August, 2011					
Minimum	0.00	0.21	1.10	1.04	2.57
Average	0.20	0.62	1.22	1.13	3.17
Maximum	0.27	2.12	1.47	1.46	5.05
September, 2011					
Minimum	0.02	0.01	1.02	0.93	2.36
Average	0.13	0.25	1.23	1.07	2.69
Maximum	0.23	0.72	1.56	1.41	3.73
October, 2011					
Minimum	0.12	0.07	1.11	1.00	2.61
Average	0.17	0.50	1.25	1.12	3.04
Maximum	0.29	0.97	1.43	1.36	3.75
November, 2011					
Minimum	0.06	0.07	1.16	1.14	2.59
Average	0.16	0.63	1.32	1.37	3.48
Maximum	0.22	1.06	1.48	1.67	4.30
December, 2011					
Minimum	0.00	0.00	0.00	0.00	0.00
Average	0.13	0.67	1.13	1.30	3.24
Maximum	0.19	2.19	1.41	1.67	4.89

Table 1-2. Treated wastewater injections rates for April of 2011 through March of 2013 (Continued)

	Well 1	Well 2	Well 3	Well 4	Total Injection
	(mgd)	(mgd)	(mgd)	(mgd)	(mgd)
January 2012					
Minimum	0.04	0.18	1.04	1.18	3.17
Average	0.13	0.75	1.25	1.51	3.64
Maximum	0.19	1.65	1.54	2.08	4.76
February 2012					
Minimum	0.01	0.00	0.58	1.21	2.06
Average	0.08	0.18	1.59	1.53	3.38
Maximum	0.13	0.56	2.53	1.81	4.03
March 2012					
Minimum	0.00	0.00	1.57	1.07	2.72
Average	0.07	0.06	1.90	1.39	3.42
Maximum	0.19	0.20	2.41	1.87	4.65
April 2012					
Minimum	0.00	0.00	1.56	0.84	2.40
Average	0.04	0.01	1.81	1.16	3.03
Maximum	0.16	0.15	2.14	1.49	3.79
May 2012					
Minimum	0.00	0.00	1.46	0.79	2.32
Average	0.03	0.01	1.80	1.19	3.03
Maximum	0.16	0.06	2.25	1.74	4.07
June 2012					
Minimum	0.00	0.00	1.53	0.96	2.52
Average	0.08	0.02	1.94	1.33	3.36
Maximum	0.22	0.12	2.35	1.84	4.48
July 2012					
Minimum	0.00	0.00	1.61	0.93	2.75
Average	0.03	0.03	2.00	1.16	3.22
Maximum	0.11	0.38	2.33	1.46	3.98
August 2012					
Minimum	0.00	0.00	1.61	0.18	2.46
Average	0.02	0.00	1.93	1.12	3.07
Maximum	0.08	0.01	2.41	1.46	3.64

Table 1-2. Treated wastewater injections rates for April of 2011 through March of 2013 (Continued)

	Well 1	Well 2	Well 3	Well 4	Total Injection
	(mgd)	(mgd)	(mgd)	(mgd)	(mgd)
September 2012					
Minimum	0.00	0.00	0.00	0.18	0.82
Average	0.07	0.11	1.65	1.19	3.02
Maximum	0.26	1.65	2.53	2.08	4.76
October 2012					
Minimum	0.00	0.00	1.75	0.69	2.55
Average	0.05	0.03	1.93	0.93	2.93
Maximum	0.16	0.12	2.21	1.18	3.57
November 2012					
Minimum	0.00	0.00	1.70	0.57	2.46
Average	0.07	0.06	1.99	0.86	2.97
Maximum	0.22	0.14	2.36	1.23	3.95
December 2012					
Minimum	0.03	0.01	1.67	0.66	2.63
Average	0.13	0.11	1.89	1.10	3.23
Maximum	0.26	0.21	2.02	1.72	3.98
January, 2013					
Minimum	0.02	0.00	1.90	1.23	3.24
Average	0.18	0.11	1.90	1.49	3.68
Maximum	0.33	0.57	1.90	1.79	4.19
February, 2013					
Minimum	0.01	0.00	1.90	1.25	3.16
Average	0.20	0.20	1.90	1.81	4.11
Maximum	0.34	0.89	1.90	3.13	6.03
March, 2013					
Minimum	0.03	0.00	0.11	0.62	2.09
Average	0.18	0.13	1.83	1.27	3.41
Maximum	0.33	0.69	2.26	2.35	5.15
Summary					
Minimum	0.00	0.00	0.00	0.00	0.00
Average	0.12	0.34	1.50	1.19	3.16
Maximum	0.34	2.75	2.53	3.13	6.03

Data from Maui County Department of Environmental Management

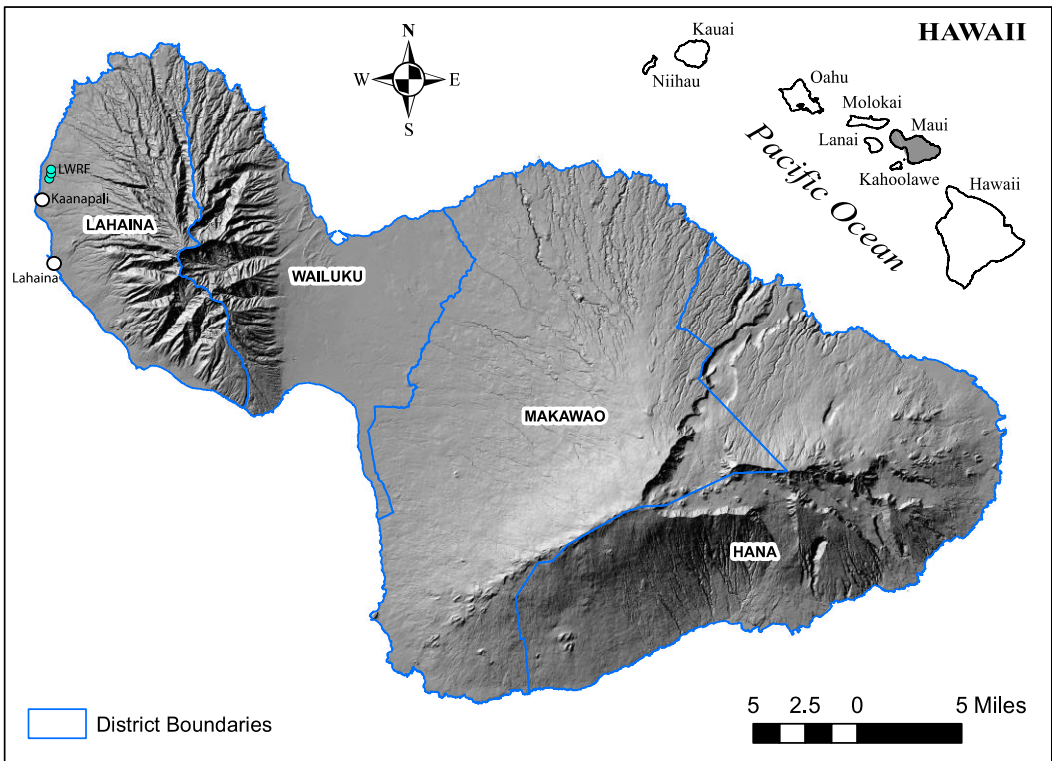


Figure 1-1: Location and topography of the Island of Maui

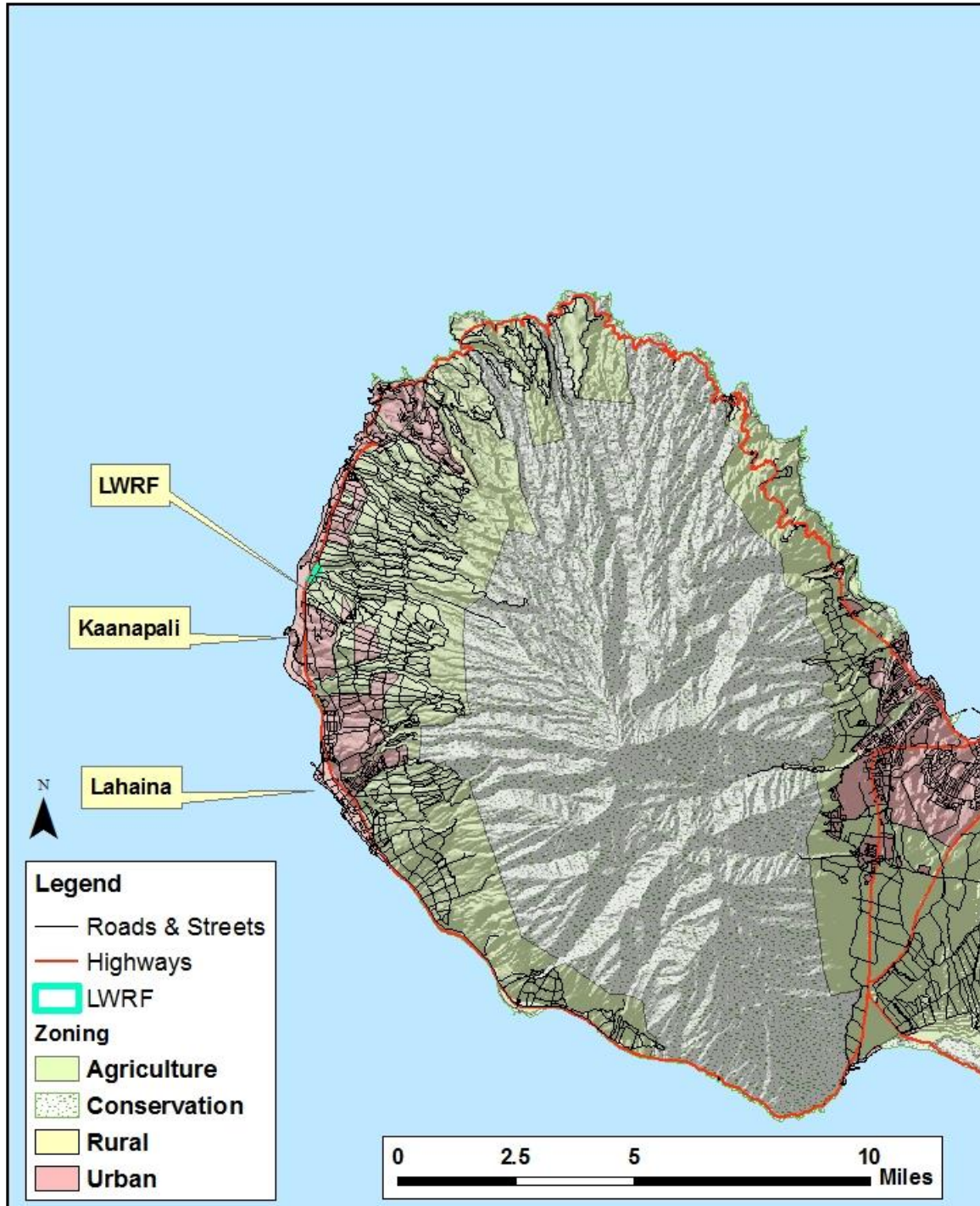


Figure 1-2: Map showing the location of the LWRF in West Maui.

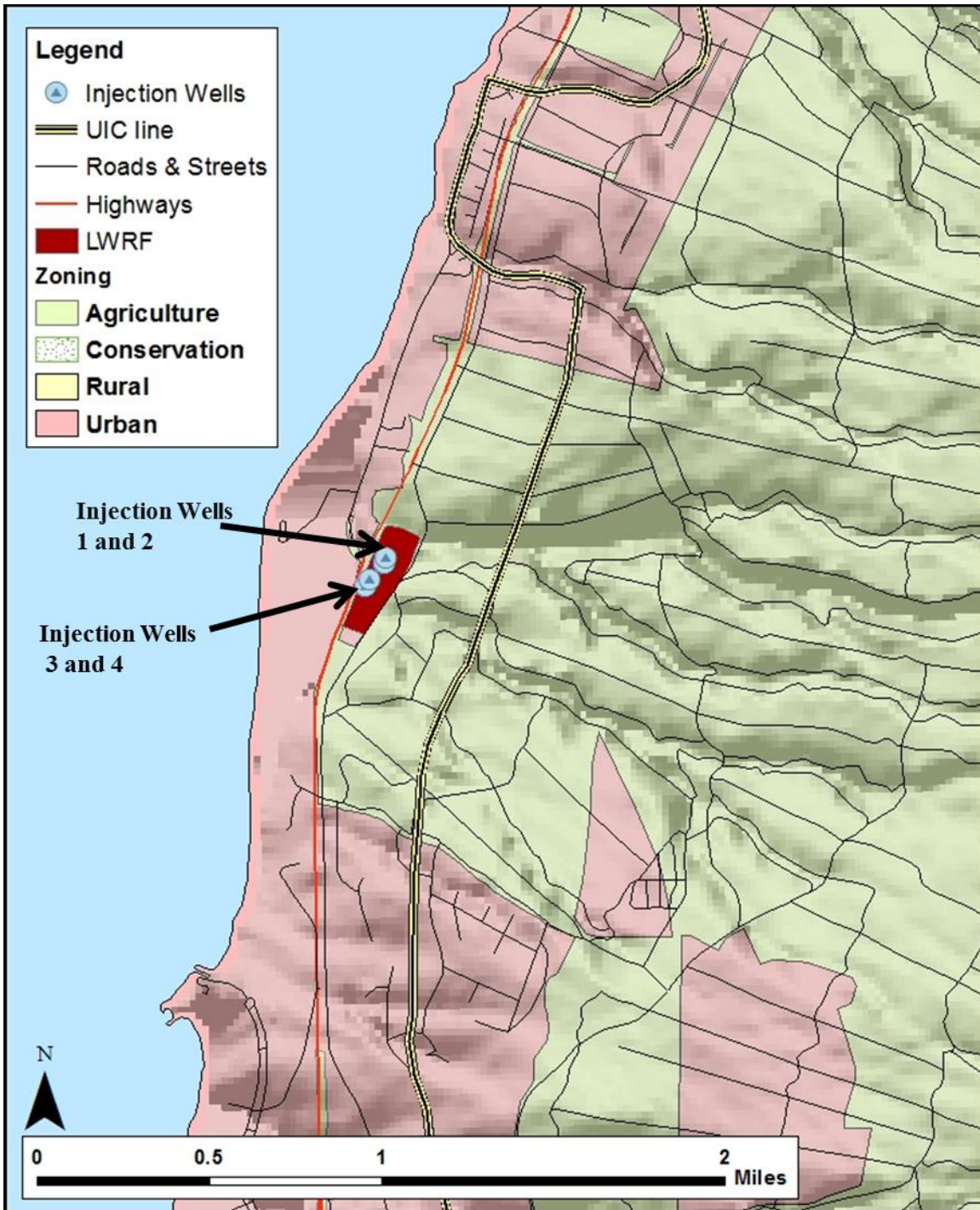


Figure 1-3: Location of the LWRF in relation to the coast and the UIC line. LWRF Injection Wells 1 and 2, which receive the majority of treated wastewater effluent, lie to the northeast of Wells 3 and 4.

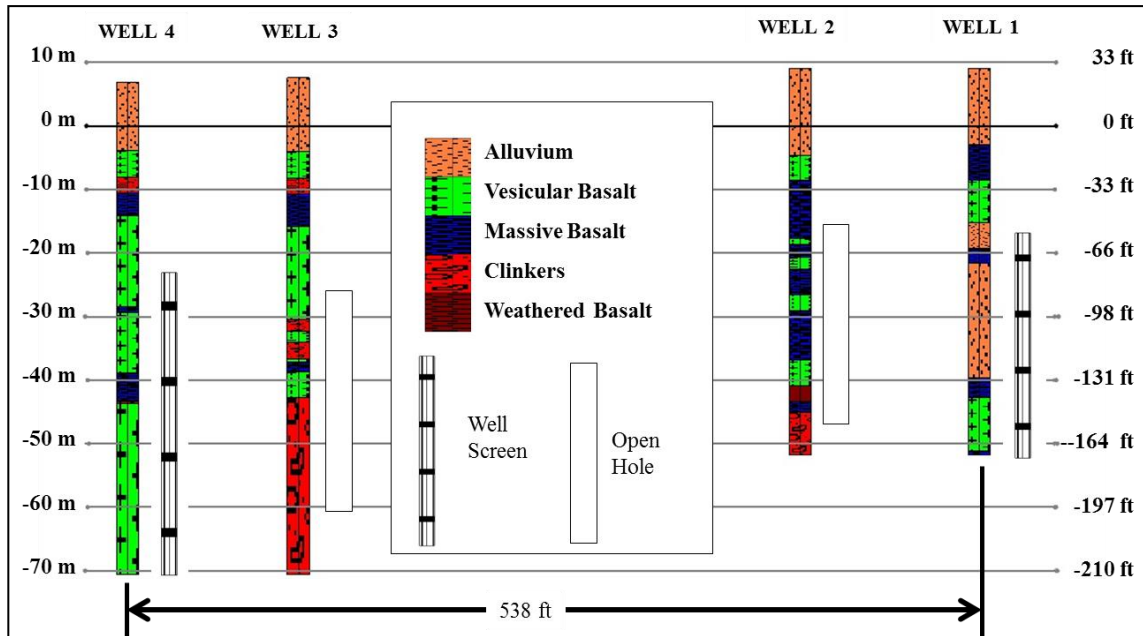


Figure 1-4: Borehole stratigraphy for the LWRF injection wells developed from the drillers' logs. (County of Maui, 2004)

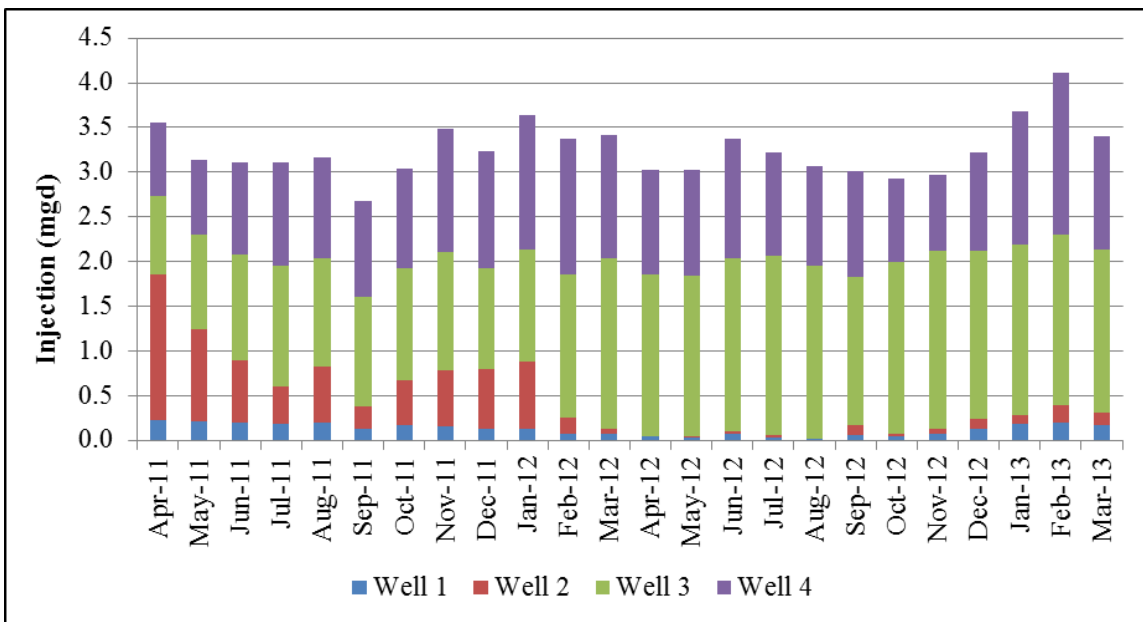


Figure 1-5: Monthly average injection at the LWRF. (County of Maui, 2011; and County of Maui, 2012-2013)

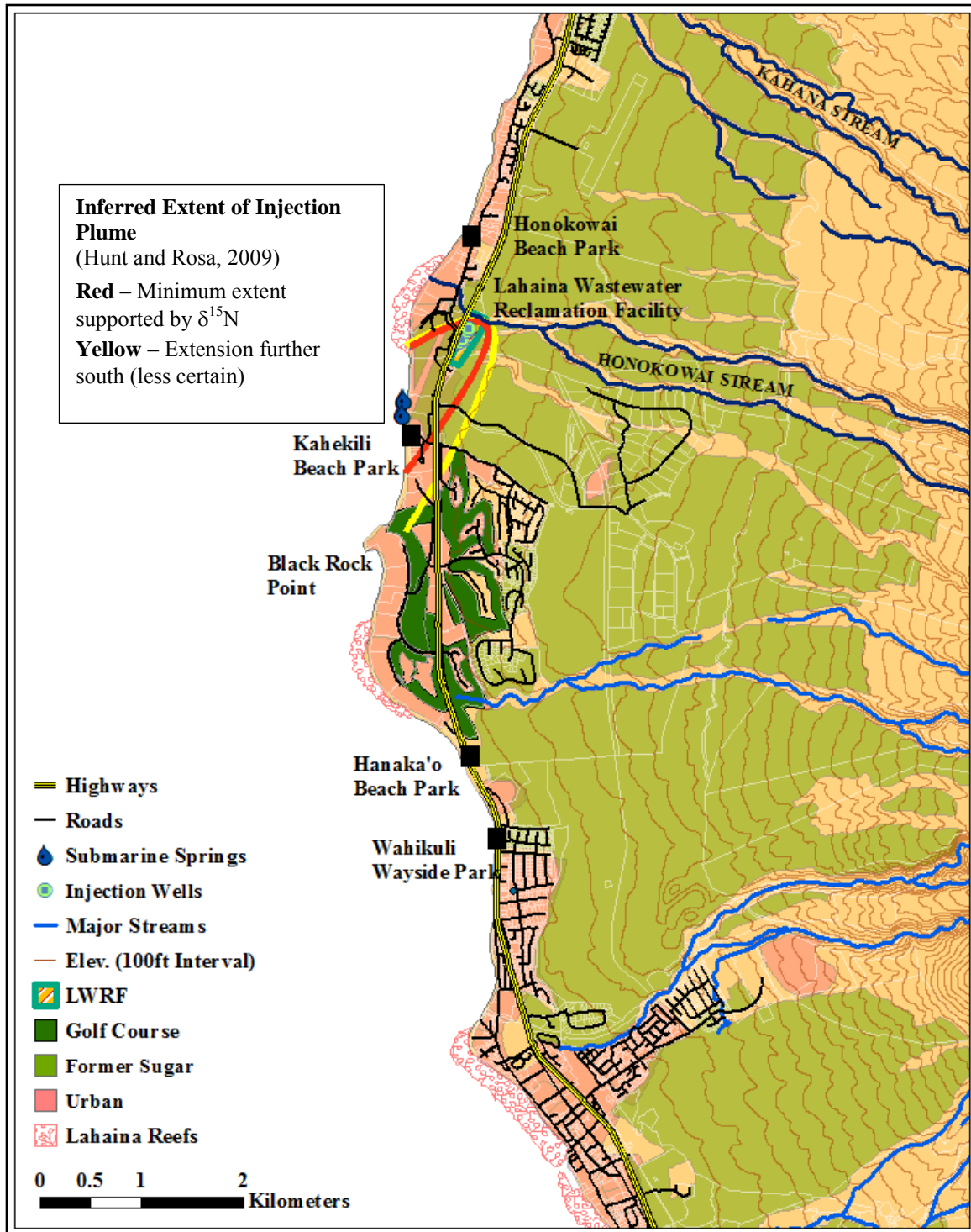


Figure 1-6: Detail of study area showing key locals along the coast. LWRF injection wells and inferred subsurface minimum and maximum spatial extent of LWRF injection plume from Hunt and Rosa (2009) is also shown.

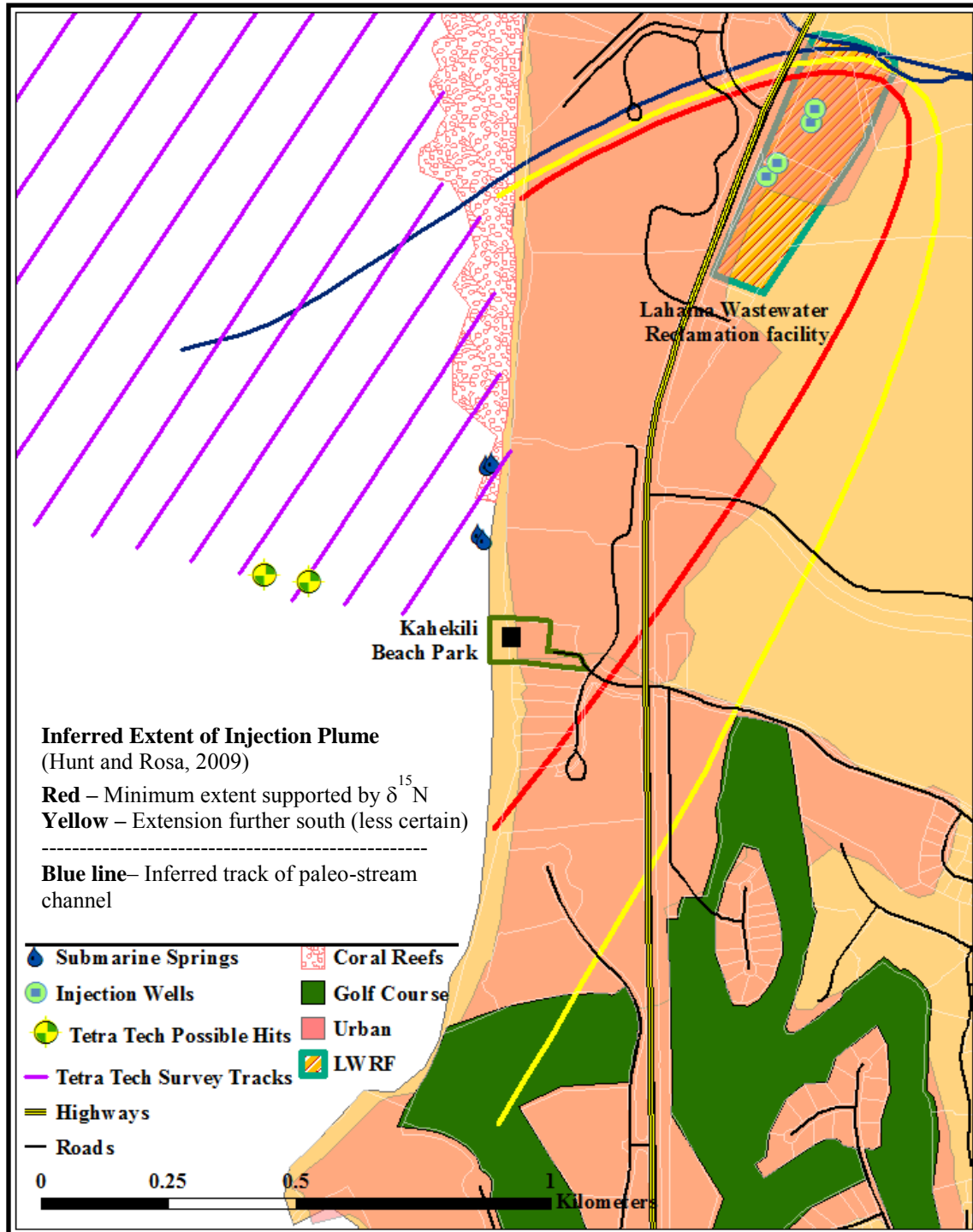


Figure 1-7: Map of the LWRF, submarine springs, and Tetra Tech (1994) ocean sampling tracts.

The location of the two occurrences of elevated fluorescence (“hits”) measured by Tetra Tech (1994) are shown. Also shown (as concluded by Hunt and Rosa, 2009) are the likely minimum (red) and less certain maximum (yellow) spatial extents of the LWRF injectate plume, and inferred subsurface paleo-stream alluvium hydraulic barrier (blue).

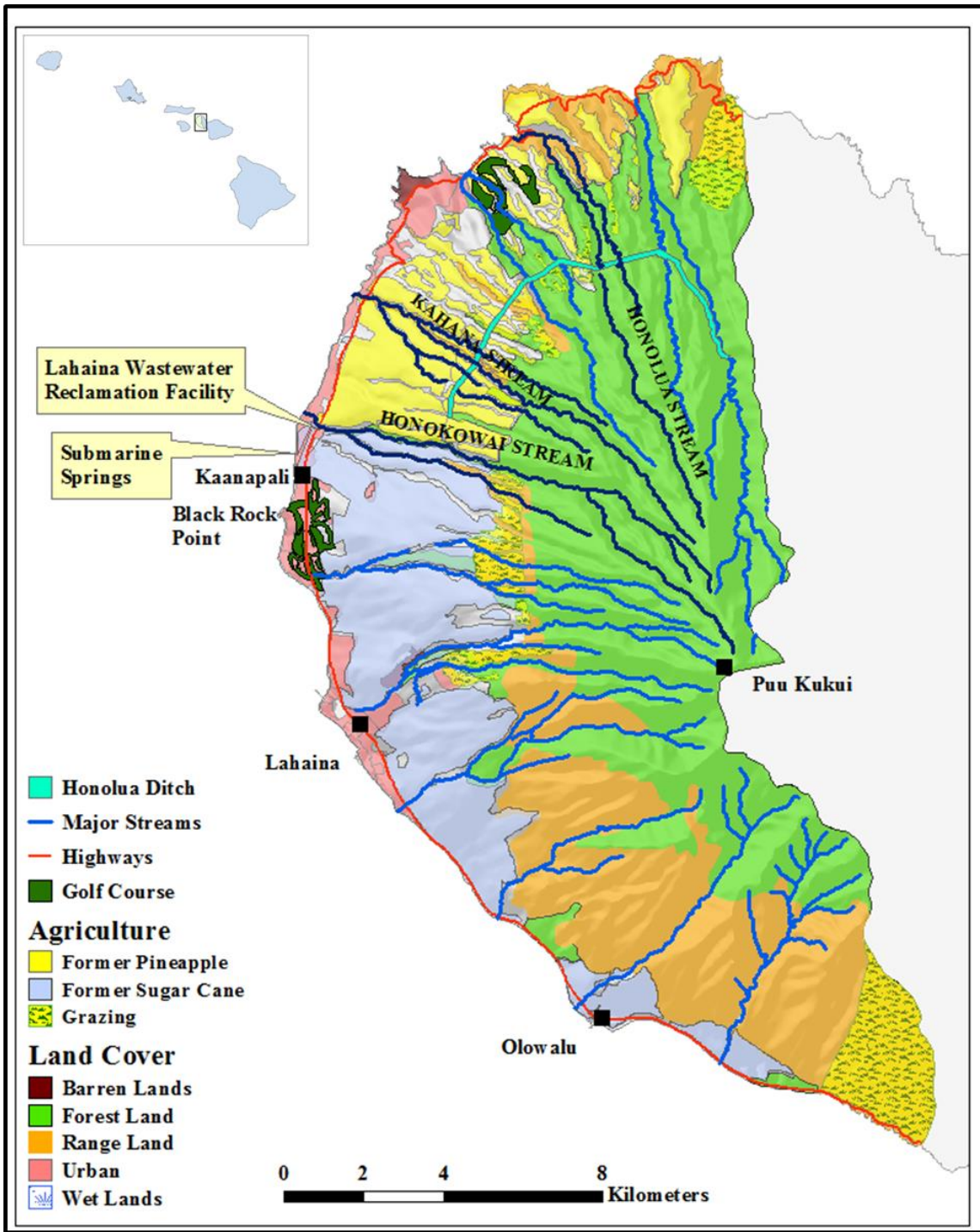


Figure 1-8: Western Maui land-use map.

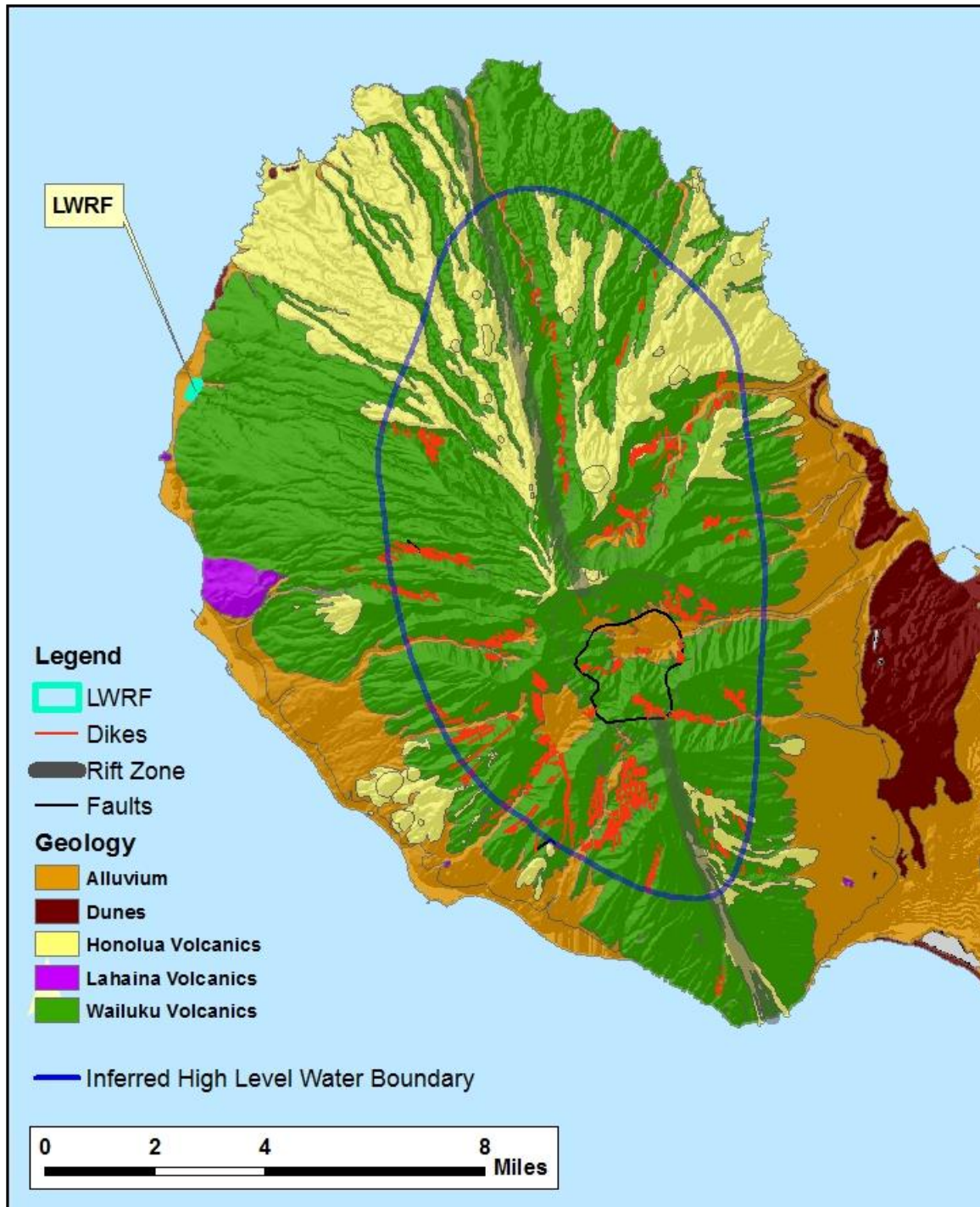


Figure 1-9: West Maui geology and inferred high level/peripheral basal lens boundary. Geology from Sherrod et al. (2007).

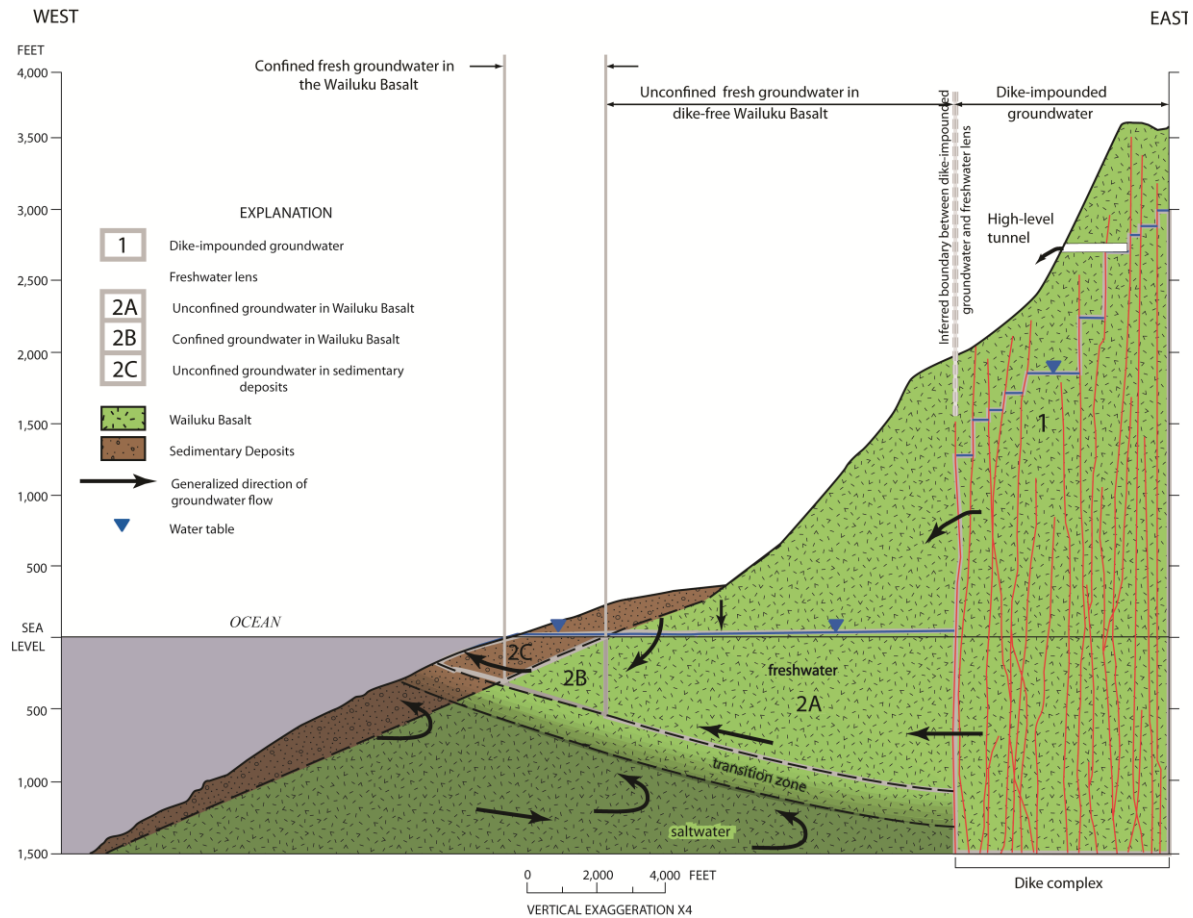


Figure 1-10: Geologic section of West Maui showing SGD and groundwater occurrence and movement.

The figure (from Gingerich and Engott, 2012) is diagrammatic and generalized. Within the study area the actual lateral distribution and thickness of caprock and subterranean freshwater-marine mixing (transition zone) is not well known, but the upper boundary of the transition zone (freshwater-seawater mixing zone) in the present study area at North Kaanapali Beach is assuredly higher than that shown here and resides at or slightly above present sea level.

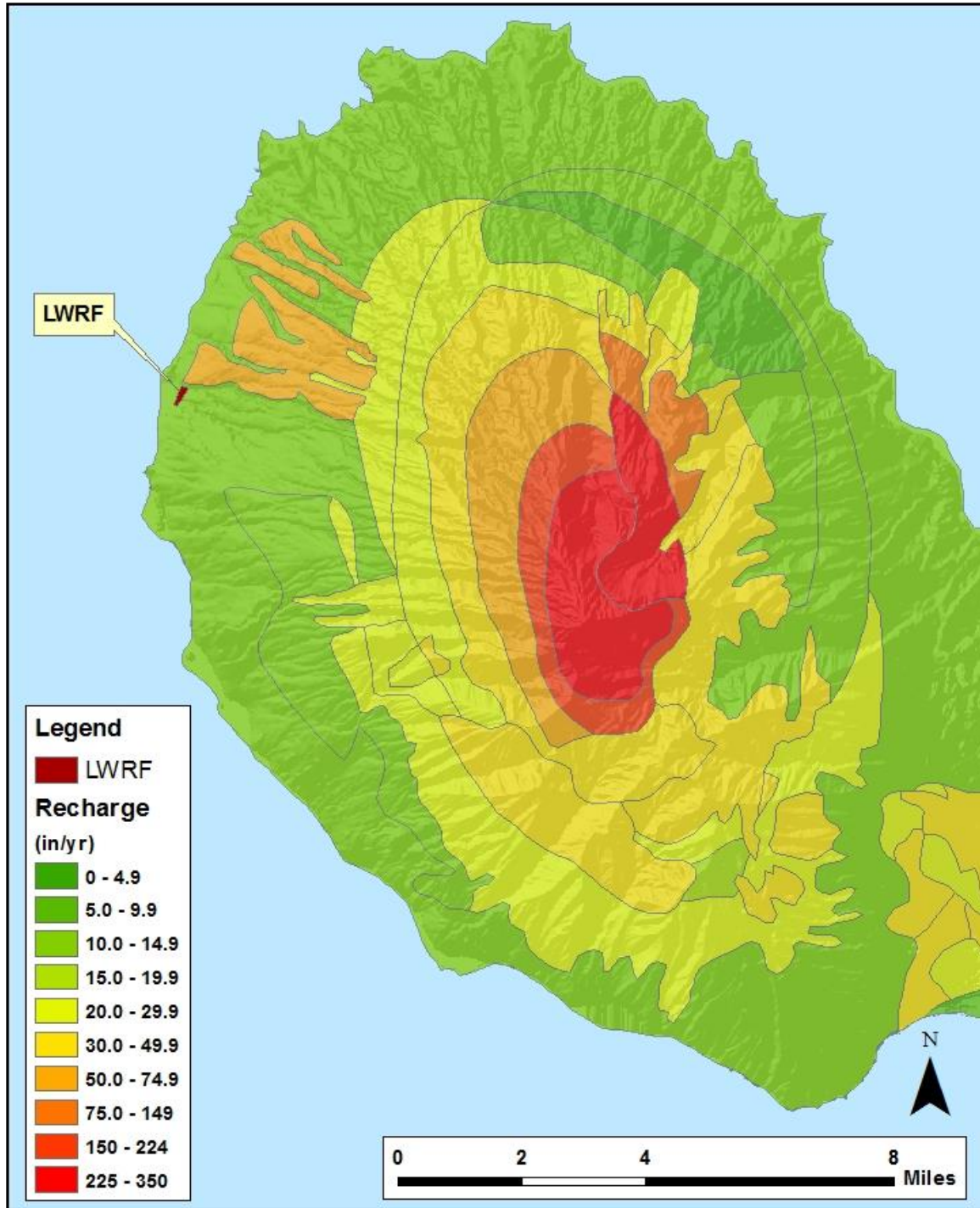


Figure 1-11: Groundwater recharge distribution in West Maui. From Engott and Vana (2007) and Gingerich (2008).

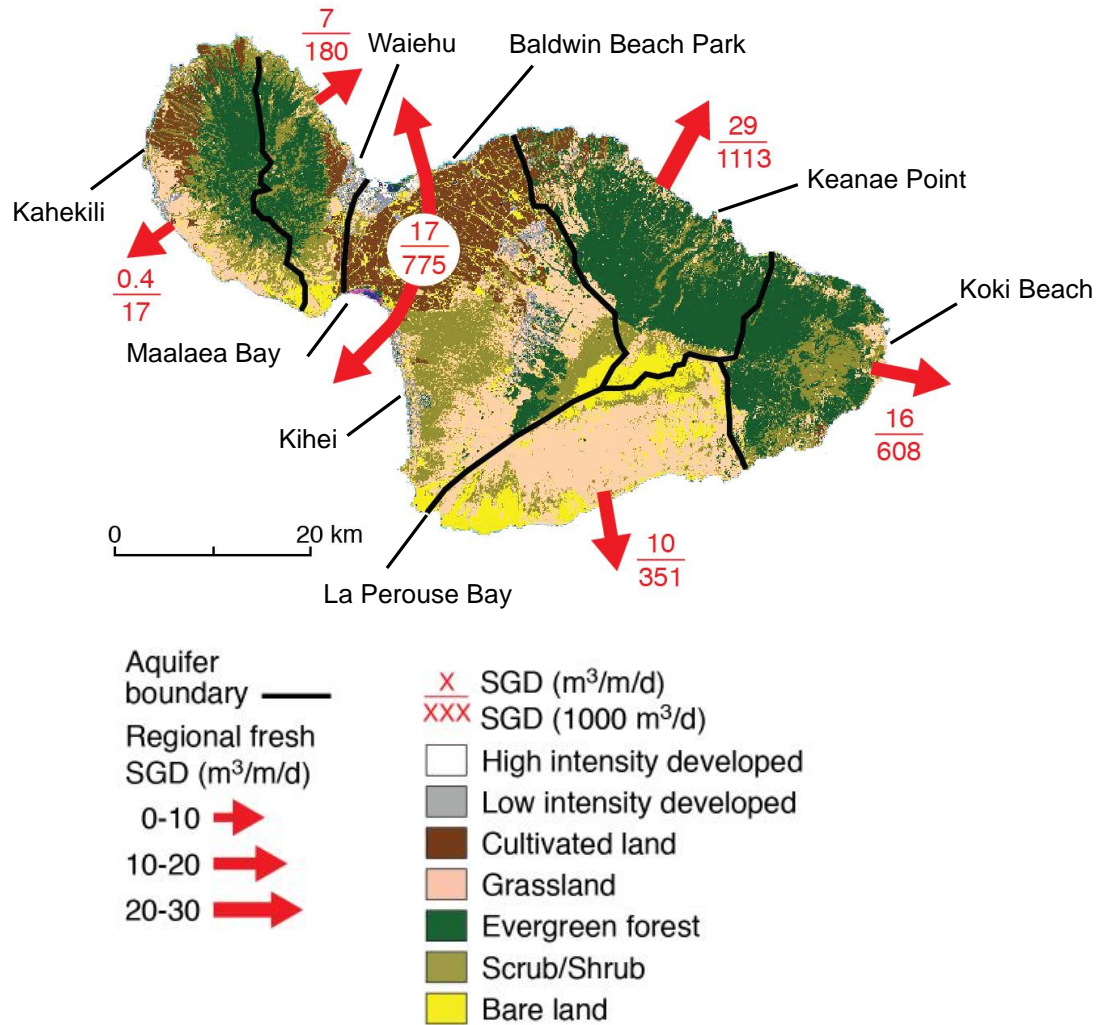


Figure 1-12: Calculated fresh submarine groundwater discharge to the ocean for the Island of Maui.

Satellite derived land-use map of the island of Maui from NOAA's Coastal Change Analysis Program. Maui's principal aquifer divides are shown in black lines. Fresh groundwater discharge estimates (red arrows) are based on regional-scale hydrologic budgets calculated by Shade (1996, 1997, and 1998). The magnitude of fresh discharge for each aquifer sector per meter of coastline (top number) is indicated in $m^3 m^{-1} d^{-1}$ and regional fresh SGD (bottom number) is shown in $1000 m^3 d^{-1}$.

SECTION 2: SUBMARINE SPRING AND MARINE CONTROL LOCATION SAMPLING, WATER QUALITY, AND FLUORESCENCE

2.1 INTRODUCTION

This section of the Final Report summarizes the continual monitoring of the submarine springs presented in the Interim Report with additional information collected from May 6th, 2012 through December 31st, 2012 and presents additional information concerning additional areas of submarine groundwater discharge within the study area. More specifically, this section provides: (1) details of how the submarine springs at Kahekili were sampled for radioisotope tracers (Section 3) and the injected tracer dye (Section 4); (2) water quality parameters of the submarine springs and control locations from July 2011 through December 2012; (3) field-determined fluorescence of samples collected from submarine springs, shore line points within the study area, and control locations from July 2011 through December 2012; and (4) results from a survey conducted in July 2012 to assess the quantity, size, and location of submarine springs from Honokowai Point to Black Rock and extending offshore to ~27 ft (~9 m) of depth (as far as 250 m offshore in some areas).

2.2 METHODS

2.2.1 Submarine Spring Sampling

Hunt and Rosa (2009) employed an inverted funnel to sample the submarine springs off of Kahekili Beach Park, which undesirably allowed for oceanic water to mix with the submarine spring water. To provide the best submarine spring samples for this study we sampled the submarine springs through steel-shaft piezometers (Model 615 6" Drive-point piezometers, Solinst Canada Limited, Georgetown, Ontario, Canada, part number 103160) that were installed while scuba diving. In the nearshore region of the study area, the seafloor consists of limestone, dead coral, and basalt. Therefore, the piezometers were driven into fissures at submarine spring discharge points with a mallet and a 0.5 m connective pipe temporarily attached to the top of the piezometer. A short (15 to 20 cm) piece of polyethylene tubing equipped with a quick-connect fitting was permanently attached to each piezometer with a steel compression fitting. Submarine spring sample collection was accomplished using a variable speed DC-battery-powered peristaltic pump (Geotech Environmental Inc., Series II, Denver, Colorado) fitted to a 50 m section of polyethylene tubing that was temporarily attached to each piezometer with a quick-connect fitting. During the collection of the samples, the peristaltic pump was stationed on shore. The peristaltic pump flow rate ranged from 0.33 to 0.5 L/min. The tubing used for sample collection was purged for four minutes prior to acquiring each sample to ensure adequate and complete flushing of the piezometer-to-pump-station tubing. This

same installation and configuration was used to sample the submarine springs for radiochemical tracers (Section 3) and the injected dye tracers (Section 4).

Submarine spring samples collected for dye tracer analysis were collected in 125 mL high-density polyethylene (HDPE) amber plastic bottles to prevent photo-degradation of dye tracers. Prior to sample collection, sample bottles were thoroughly cleaned with Fisherbrand Sparkleen laboratory detergent (5 mL to 1.0 L). Sample bottles were rinsed twice with the submarine spring water, filled, and labeled with the submarine spring (seep) number, date and time of collection. An additional 250 or 500 mL submarine spring water samples were collected approximately every 20 samples for quality assurance and quality control purposes (see Section 4). Submarine spring samples were immediately placed in a dry, lightproof cooler in the field, transported in that cooler from the field to the location of analytical procedures, and stored at room temperature in a larger dry cooler until field fluorescence measurements of fluorescein (FLT) and s-rhodamine-B (SRB) (see Section 2.2.4 below) were performed. The calibration solutions were also stored at room temperature in a dry, lightproof cooler. After analyses were performed, the samples were stored at room temperature in a large, dry, lightproof cooler until shipment to Oahu for further analyses of FLT using a Turner Designs 10AU Fluorometer (Turner Designs, 1999) (Section 4) and a Hitachi F-4500 Fluorescence Spectrophotometer (Hitachi High-Technologies Corporation) for SRB measurements (Section 4).

Following the review of the project's Interim Report, our sample handling and storage methods were revised because the EPA expressed concerns about sample stability in non-chilled environments. To ensure such stability, the adapted procedure used on Maui since early September 2012 has been as follows. Submarine spring samples are collected into 125 mL HDPE amber plastic bottles and immediately placed into the cooler with blue ice. The samples are then transported to a facility for analytical procedures. They are then transferred to and stored in a refrigerator until analyses can be performed. The calibration standards were also stored in the same refrigerator as the submarine spring samples. When the analytical procedures were performed on Maui, the calibration standards and the samples to be analyzed were removed from the refrigerator and placed in a plastic bin with a lid over night to keep the samples in a dark space and allow for room temperature equilibration prior to analyses for the tracer dye. After analyses were performed, the samples were stored in the same refrigerator until shipment to Oahu for further analyses. The samples were shipped in lightproof coolers with blue ice to maintain a chilled environment during the transfer.

Immediately following every submarine spring sample collection, an additional clear 750 mL container was rinsed two times with the submarine spring water and then filled for water quality measurement of temperature, pH, specific conductivity, and salinity. These parameters were measured with an YSI Model 63 (YSI Inc., Yellow Springs, OH), recorded, and then the submarine spring water was discarded. The YSI was calibrated with YSI standards of pH 7.00 and 10.00 and Equipco specific conductivity standards of 1,000 and 58,700 μS ; calibrations are provided in Appendix Table A-1. Once all the

submarine spring water sampling was completed, the long tubing was disconnected from the piezometer and returned to the beach.

2.2.2 Submarine Spring Sampling Frequency and Placement

In July, 2011, three piezometers installed in the North and South Seep Groups (six total) were selected for the most high frequency monitoring for the dye tracer emergence (Figure 2-1; Table 2-1). A pre-dye tracer injection-monitoring period that occurred from 7/5/2011 to 7/28/2011 was designed to measure the magnitude and variability of in situ fluorescence of the submarine spring water at these sites. Following the dye tracer injection of FLT on 7/28/2011 into injection wells 3 and 4, the submarine spring water sampling occurred two times per day from 7/28/2011 to 9/6/2011. From 7/30/2011 to 8/18/2011, one of the submarine springs in the North Seep Group was sampled at midnight in order not to miss the dye tracers if the arrival time of the treated wastewater was faster than expected. As time increased after the injection of the dye tracers, the frequency of submarine spring sampling decreased. Submarine spring sampling occurred thereafter once per day from 9/7/2011 to 10/6/2011, every two days from 10/8/2011 to 1/31/2012, two to three times per week from 2/5/2012 to 5/29/2012, one to two times per week from 6/2/2012 to 12/31/2012. Currently, the submarine spring water is sampled once or twice per month.

The South Seep Group is located approximately 25 m offshore. The submarine spring piezometer locations within this group (Seeps 3, 4, and 5) remained unchanged through the duration of the high frequency sampling portion of the project, and have been sampled from 7/5/2011 to the present time. Seep 11 was installed in the South Seep Group on 1/19/2012 (Figure 2-1) because Seeps 4 and 5 began to have high salinity values (> 5), although the piezometers and associated tubing appeared structurally intact. Seep 4 consistently displayed salinity values > 15 , so the piezometer at this seep was removed and redeployed in the North Seep Group on 4/24/2012. A total of 684 submarine spring samples were collected from the South Seep Group from 7/5/2011 through 12/31/2012.

The North Seep Group is located approximately 3 to 5 m offshore, and it has been extremely problematic to maintain sampling locations at this location throughout the duration of the project. This is because the close proximity of the North Seep Group to the shoreline subjects the piezometers at this location to the persistent littoral migration of sand from the beach as a result of large north swells, as well as the removal of seafloor sands as a result of large south swells. Every time that a piezometer had to be reinstalled within this site, it was given a new seep number designation. The history of submarine spring sampling within the North Seep Group therefore occurred in the following way throughout the duration of project. Seeps 1, 2, and 6 were installed on 7/19/2011. Seeps 1 and 2 were lost and replaced with Seeps 7 and 8 on 11/14/2011. Seep 6 was lost and replaced with Seep 9 on 11/24/2011. Seep 8 was lost and replaced with Seep 10 on 1/19/2012. Seep 9 was lost and replaced with Seep 12 on 1/24/2012. Seeps 7 and 10 were lost and replaced with Seeps 13 and 14 on 3/10/2012. Seeps 12, 13, and 14 were lost and replaced with Seep 15 on 3/24/2012. This left only one sampling point in the north

(due to the amount of lost piezometers) until Seep16 was installed on 4/24/2012. Seeps 9, 13, 14, and 15, were recovered and removed. Seep 17 was installed with Seep 16's piezometer (due to increased exposure of the piezometer and consequently increased salinity) and Seep 10 was found fully intact on 6/25/2012; sampling points became Seeps 10 and 17. Seep 10 was lost and Seep 18 was installed on 7/10/2012. Seeps 17 and 18 were lost on 8/7/2012. Seep 18 was recovered and removed and Seep 19 was installed on 8/8/2012. The Seep 19 piezometer was stolen and Seep 19 was re-installed with a new piezometer on 8/15/2012. Seep 19 was lost and Seep 20 was installed on 9/18/2012. Seep 19 was recovered and removed on 10/2/2012. Seep 6 was recovered and removed on 10/18/2012. Seep 21 was installed on 10/19/2012. Seep 10 was recovered and removed on 10/22/2012. Seep 7 was recovered and removed on 11/2/2012. Currently, submarine spring sampling occurs at Seeps 20 and 21 within the North Seep Group. It is important to note that despite this apparent "hop-scotch" of submarine spring sampling locations, the re-installation of piezometers in the North Seep Group has always occurred within 2 m of the original piezometer locations (Seeps 1, 2, and 6) and generally occurred within 0.25 m of each other (Figure 2-1). A total of 606 submarine spring samples were collected from the North Seep Group from 7/5/2011 through 12/31/2012.

2.2.3 Sampling Control Locations

Control locations for the dye tracer portion of this study were Honokowai Beach Park (20°57'16.80"N, 156°41'13.60"W), Wahikuli Wayside Park (20°54'9.64"N, 156°41'7.50"W) and Olowalu (20°48'26.24"N, 156°36'9.06"W; Figure 2-2). Honokowai Beach Park, located ~ 2 km to the north of the main study area, served as a site of possible dye emergence if the LWRF treated wastewater flow path was to the north. Wahikuli Wayside Park is ~ 4 km south of the main study area and therefore served as a southern control site with the possibility of detecting the dye tracers. In terms of the nutrient studies for this project, it is important to note that the Wahikuli area has many unconnected cesspools. Olowalu is located ~ 13 km south of the main study area and currently has no major land-based pollution impacts due to the lack of major development and the termination of sugarcane operations in the late 1990's. At all three locations, samples were taken from the nearshore surface water (1.0 m offshore and 0.5 m depth). The water quality parameters (temperature, pH, salinity, and specific conductivity) were also recorded with a handheld YSI Model 63. The locations were sampled weekly from 8/5/2011 to 5/29/2012 for Honokowai and Wahikuli Wayside Parks, and 12/2/2011 to 5/19/2012 for Olowalu. Samples from these sites were collected in clean 125 mL HDPE amber plastic bottles (as described above), which were rinsed twice prior to nearshore sample collection.

2.2.4 Field Measurements of Fluorescein and S-Rhodamine-B Fluorescence

All samples collected for the tracer dye monitoring portion of the project were analyzed in the field for fluorescein and s-rhodamine-B fluorescence using a handheld Aquafluor fluorometer model 8000-010 (Turner Designs, Sunnyvale, California). Sample cuvettes were cleaned with Fisherbrand Sparkleen laboratory detergent (5 mL to 1.0 L) and

thoroughly rinsed with steamed distilled water prior to use. Prior to analyzing samples, the fluorometer was calibrated with 100 ppb standards of fluorescein and s-rhodamine-B prepared as described in Section 4 (calibrations are provided in Appendix Table A-2). Samples from the submarine springs and control locations were analyzed in the following way. Clean cuvettes were rinsed three times with the sample water then completely filled and placed in the fluorometer. Once the sample was analyzed, the fluorescence values were recorded, and the bottle cap was secured to the bottle with electrical tape to ensure that it wouldn't open during shipment to Oahu for additional fluorescence measurements (see Section 4).

2.2.5 Submarine Spring and Shoreline Surveys

A scuba diver survey was conducted in July 2012 to document all visual submarine springs from Honokowai Point to Black Rock. The goal of this survey was to provide the project with information regarding the locations and dimensions (length and width) of additional submarine springs spanning study area. The survey was conducted by two scuba divers swimming together and scanning the ocean floor. The survey extended from the shoreline to a water depth of 9 m (27 ft), and as far as 250 m offshore in some areas. Once a submarine spring was located, a 100 ml syringe was rinsed three times with the surface water, closed, and brought down to the submarine spring. The scuba divers then attempted to obtain optimum spring water samples by putting the syringe directly into the point of spring water emergence. Once the syringe was full, it was brought to the surface to rinse twice and was then fully emptied into a clean 125 mL HDPE amber plastic bottle (as used for submarine spring monitoring). This process was repeated until the 125 mL HDPE sample bottle was completely filled. The submarine spring's dimensions were then measured (length and width) and its location was marked with a handheld 76CS Plus Garmin GPS. When more than one submarine spring was found per square meter, all submarine springs were measured, one submarine spring was sampled with a syringe, and the location was marked with the GPS. Control samples for the North and South Seep Groups were taken over the main submarine spring areas by rinsing the syringe three times with surface water and filling the syringe with surface water then rinsing the sample bottle twice with the syringe water. Then the sample bottle was filled with the syringe collected surface water. Submarine spring and control samples were handled as described above in Section 2.2.1.

Submarine groundwater samples were taken from 12/20/2012 through 1/8/2012 at the shoreline adjacent to the North and South Seep Groups, south of Kahekili Beach Park, and adjacent to Honokowai Point. These samples were collected through the same abovementioned piezometers outfitted with a three foot galvanized steel pipe extension allowing for the piezometer to be temporarily installed in the sand just offshore of the surge zone. In addition, on 12/29/2012, submarine springs in North and South Seep Groups and a substantial seep located between the two groups were sampled for the tracer dye with clean 100 ml syringes. The syringes were brought to the surface and decanted to clean 125 mL HDPE amber plastic bottles. This was repeated until the bottle was completely filled. The results of these surveys are discussed in Section 4.

2.3 RESULTS

2.3.1 Water Quality of Submarine Springs

The submarine spring water sampled through piezometers generally had lower pH, salinity, and specific conductivity compared to that of coastal water throughout the project. Water quality parameters for samples taken from 7/19/2011 through 12/29/2012 are provided in Appendix Table A-3 for the South Seep Group and Appendix Table A-4 for the North Seep Group. Measured analytical means, standard deviations, and ranges for each of the submarine springs are provided in Table 2-2. Seep 3 consistently had the lowest salinity, averaging at 3.32 ± 1.4 and ranging from 2.50 to 16.1 (Table 2-2).

2.3.2 Water Quality of Control Locations

All control locations generally showed little to no freshwater influence with salinities, specific conductivity, and pH values close to that of coastal water. All water quality parameters for the control locations are provided in Appendix Table A-5. Measured analytical means, standard deviations, and ranges for each control location are provided in Table 2-3.

2.3.3 Field Measurements of Fluorescein and S-Rhodamine-B Fluorescence

The fluorescence of FLT and SRB measured in the field of samples collected from 7/19/2011 through 12/29/2012 are provided in Appendix Table A-3 for the South Seep Group (684 samples total) and Appendix Table A-4 for the North Seep Group (606 samples total). The fluorescence of FLT and SRB measured in the field of the control locations for samples collected from 8/5/2011 to 5/29/2012 (66 samples total) is provided in Appendix Table A-5.

A notable increasing trend in FLT fluorescence was found in all submarine spring water samples beginning on January 4th 2012 (Figures 2-3 to 2-8; Appendix Tables A-3 and A-4), while no change in fluorescence was observed in the samples obtained from the control locations (Figure 2-9). Although the obvious increase in FLT fluorescence occurred on January 4th 2012, subtle increases in field fluorometry that started at the North Seep Group in late October 2011 provided the first indication that the FLT dye was emerging from the submarine springs. A follow-up laboratory analysis that confirmed the presence of dye was prompted by a review of the field data. The field fluorescence of FLT and SRB and salinity of submarine spring water samples is graphed in Figure 2-3 for Seeps 3, 4, 5, and 11; Figure 2-4 for Seeps 1, 2, 6, and 7; Figure 2-5 for Seeps 8, 9, 10, and 12; Figure 2-6 for Seeps 13 to 16; Figure 2-7 for Seeps 17 to 20; and Figure 2-8 for Seep 21. The fluorescence of FLT and SRB and salinity values of samples from control locations are provided in Figure 2-9. The covariance of the salinity and the fluorescence values of FLT in the submarine spring water is quite substantial, as can be seen in the data for Seep 4, for example, where increased salinity (spikes) coincides with decreases

in the dye fluorescence (Figure 2-3). Increased salinity of the submarine spring water is indicative of ocean water mixing with the submarine spring water, which therefore dilutes the concentration of the dye tracer. The fluorescence data collected in the field has not been adjusted for the salinity to account for the dilution by seawater. Additional details on the relationship between the variations in dye concentration and salinity can be found in Section 4.

The FLT fluorescence values from the field fluorometer were higher than those measured using the laboratory fluorometer from 1/7/2012 to 6/29/2012. This was due to a problem with the calibration standards. As is often common practice in tracer dye studies, early laboratory and field calibration standards were mixed using deionized (DI) water. During our method of detection limit study (Section 4), however, we found that the fluorescence intensities of standards mixed with the submarine spring water from these study sites were significantly greater than those mixed with DI water. When this problem with the DI-based calibration solution was discovered, the research team was awaiting the arrival of SRB, and an uninterrupted analytical history for the handheld fluorometer was desired. Thus, the original calibration standards were left in the field during this interval so that continuity could be maintained with earlier measurements made with the handheld fluorometer. The field fluorometry was used to screen the submarine spring water samples for changes in fluorescence that would indicate the arrival of a dye or, in the case of FLT, a peaking of the breakthrough curve. Simultaneously, the field and laboratory FLT results were compared to correct the readings of the handheld fluorometer; this comparison indicated that the field values could be corrected to the approximate laboratory values by using the following equation: $FLT_{corrected} = 0.33 * FLT_{field} - 0.65$ (Figure 2-10). The field FLT fluorescence data presented in the figures and appendices have thus been corrected for the period from 1/7/2012 to 6/29/2012 to provide the correct dye concentration measurements recovered during this time interval.

A second instrumentation complication arose during this study with the discovery that the strong fluorescence of FLT can produce a false indication of SRB dye detection when read by the field fluorometer. Figure 2-11, for example, shows an apparent increase of fluorescence in the SRB wavelength that tracks the true increase in FLT. Although initially it was believed that SRB fluorescence was being detected, subsequent laboratory analysis found no SRB in the samples. The correlation, illustrated in Figure 2-11, was investigated whereby the response of the SRB channel to the FLT calibration solutions was measured with a handheld fluorometer. These solutions were prepared using submarine spring water collected prior to the FLT and SRB dye addition into the treated wastewater stream. Therefore, the FLT that was added in the laboratory during these experiments was assured to be the only dye present in these solutions. These tests confirmed that the very strong FLT fluorescence was being carried over into the wavelength monitored by the rhodamine channel, giving a false positive indication of SRB fluorescence. Figure 2-12 shows the results of this test and the linear response ($r^2 = 1.00$) of the SRB channel to solutions containing only FLT. In the absence of the high FLT dye concentration, however, our laboratory calibrations do indicate that when SRB calibration solutions are used the field fluorometer responds faithfully to the detection of SRB, and is thus suitable for tracer studies using rhodamine dyes. However, this

instrument is not appropriate to measure the fluorescence of rhodamine dyes when FLT is also used in tracer test.

2.3.4 Submarine Spring Survey

In order to locate and measure all visible submarine springs within the study area a survey team consisting of two scuba divers completed a total of 86 transects of various lengths (from the shortest 47 m or 153 ft to the longest 536 m or 1760 ft) from Honokowai Point to Black Rock, covering a total of 20.8 km (12.9 miles) in July 2012. The survey was only conducted when conditions permitted at least 5 ft visibility per diver. Figures 2-13 through 2-18 show the area covered by the 86 transects. The width of each transect in the figures is directly proportional to the visibility of the divers at the time of the survey, for example if an offshore transect had visibility of 20 feet per diver then the total width of the transect is shown as 40 feet to reflect the total field of view. On Honokowai Point, the divers were able to locate “shimmery water” (a varying refraction of light seen when fresh water and salt water mix, or when warm and cold water mix; sometimes referred to as “schlieren”), but this may have only been mixing warm nearshore water with colder offshore water as no visible submarine springs were found. North of Black Rock offshore, the divers located very diffuse flow emerging from the sand, but this was not a strong flowing submarine spring.

In general, the divers were not able to find submarine springs other than those near or in the locations of already identified submarine springs in the North and South Seep Groups used in the tracer dye-monitoring portion of the project. In this nearshore region of Kahekili Reef, a total of 289 visible submarine springs were identified; the furthest location offshore was 109 feet (33 m) from the shoreline. The submarine springs ranged in length from 0.2 cm to 24 cm, width from 0.2 cm to 13 cm, and area from 0.04 cm² to 216.0 cm². The average length and width of the submarine springs were 3.2 and 1.7 cm, respectively, giving an average area of 5.4 cm². The total area of measured submarine springs in the North Seep Group was 2426.8 cm² or 0.243 m². The total area of measured submarine springs in the South Seep Group was 838.8 cm² or 0.0839 m². The combined total area of measured discrete submarine springs found to be issuing groundwater was 3265.6 cm² or 0.336 m². In total, all submarine springs mapped within the North Seep Group were contained within an area of 1,800 m³, and all submarine springs mapped within the South Seep Group were contained with an area of 500 m² (Figure 2-19). Most of the submarine spring samples collected through syringes revealed detectable FLT concentrations (provided in Appendix Table A-6). The specific conductivity of the samples was measured in the laboratory with an YSI ProPlus Water Quality Analyzer when the samples were filtered. For samples where FLT was detected the concentration was adjusted to a pre-seawater mixing dye concentration in the nearshore groundwater by correcting the measured dye concentration for the fraction of seawater in the water sample. A description of the fluorescence and specific conductivity measurements, and the corrections made are provided in Section 4.2.6.

2.4 SUMMARY

The field portion of this study installed the sampling infrastructure, collected samples for the geochemical survey, collected nearly 1,200 samples for field and tracer dye analysis, and deployed and collected data from instruments for monitoring temperature and salinity.

Submarine springs were sampled with a variable speed DC-battery-powered peristaltic pump (Geotech Environmental Inc., Series II, Denver, Colorado) fitted to a 50 m section of polyethylene tubing that was temporarily attached to the piezometer with a quick-connect fitting. This method of sampling the submarine springs was found to be a very effective method of sampling the springs. In most locations the salinity of the samples collected was less than 5, indicating that the water captured was representative of submarine groundwater with little seawater influence. Water quality parameters of temperature, pH, specific conductivity, and salinity were measured with an YSI Model 63. The sample water was screened for the presence of the two tracer dyes, FLT and SRB, using a Turner Designs 10AU Fluorometer.

Samples were collected from submarine springs in the North and South Seep Groups, and from three control locations. The South Seep Group is located approximately 25 m offshore and had three initial monitoring points (Seeps 3, 4, and 5). A fourth, Seep 11, was added on November 24th, 2011 due to high salinities being measured at Seeps 4 and 5. The Seep 4 piezometer was relocated to the North Seep Group on April 24th, 2012 to replace piezometers in that area that were covered by migrating sand. A total of 684 submarine spring samples were collected from the South Seep Group from 7/5/2011 through 12/31/2012. The North Seep Group is located approximately 3 to 5 m offshore with three initial monitoring points (Seep 1, 2, and 6). This location was extremely problematic to maintain throughout the duration of the project. The North Seep Groups' close proximity to the shoreline subjected these piezometers to the persistent littoral migration of sand from the beach onto the seep group as a result of large north swells. By November 24th, 2011 all of the original piezometers were buried by migrating sand. As a piezometer was buried it was replaced with a new one. All replacement piezometers were located within 2 m of the original locations. A total of 606 submarine spring samples were collected from the North Seep Group from 7/5/2011 through 12/31/2012.

Control locations for the dye tracer portion of this study were Honokowai Beach Park, Wahikuli Wayside Park, and Olowalu. Honokowai Beach Park served as a site of possible dye emergence if the LWRF treated wastewater flow path was to the north. Wahikuli Wayside Park is south of the main study, but specifically targeted because of its proximity to the submarine spring locations, and therefore served as a southern control site with the possibility to detect the dye tracers. Olowalu is located ~13 km south of the main study area and currently has no known major land-based pollution impacts due to the minimal development and the termination of sugarcane operations in the late 1990's.

A pre-dye tracer injection monitoring period that occurred from July 5th through July 28th, 2011 was designed to measure the magnitude and variability of in situ fluorescence of the

submarine spring water at the selected monitoring sites. Following the dye tracer injection of FLT into Injection Wells 3 and 4, the submarine spring water sampling occurred two times per day, with one spring being sampled three times per day, for ~ 40 days following the FLT addition to ensure that the dye transported by preferential flow paths would not be missed. As time progressed, the sampling frequency was decreased to one or two times per week.

The SRB and FLT fluorescence measured in the field remained indistinguishable from background levels until late October, 2011. Subtle increases in field fluorometry measurements of FLT started to occur in samples from the North Seep Group in late October 2011 and provided the first indication that dye was emerging from the submarine springs. This was followed in mid-November by increasing FLT fluorescence of samples from the South Seep Group. However, no pronounced FLT fluorescence increase was noted in the field data until January 2012. An inverse correlation was noted between the FLT fluorescence and the salinity measured at the monitoring points. An increase in the salinity of the submarine spring water is indicative of ocean water mixing with the submarine spring water, which dilutes the concentration of the dye tracer.

Beginning in January 2012, the SRB wavelength fluorescence as read on the AquaFlour Handheld Fluorometer showed an increasing trend. Subsequent testing showed this was actually a response of the SRB channel to the strong FLT fluorescence in the samples being analyzed and no SRB was in the samples being analyzed. As of May 13, 2013 there has been no confirmed detection of SRB.

The July 2012 submarine spring survey covered 20.8 km (12.9 miles) of the seafloor in 86 transects that extended from Honokowai Point to Black Rock (linear distance of 2.9 km). The survey located and measured 289 submarine springs all of which were near the known locations of already identified submarine springs used in the tracer-dye monitoring portion of the project. The total seafloor area populated by submarine springs in the NSG was 1,800 m², and the total area of seafloor populated by submarine springs in the SSG was 500 m². The individual submarine springs ranged in length from 0.2 cm to 24 cm, width from 0.2 cm to 13 cm, and covered areas from 0.04 cm² to 216.0 cm². The average length and width of the individual submarine springs were 3.2 and 1.7 cm, respectively, giving an average area of 5.4 cm². The summed area of individual submarine springs in the NSG was 2426.8 cm² or 0.243 m². The summed area of individual submarine springs in the SSG was 838.8 cm² or 0.0839 m². The combined total area of measured individual submarine springs was 3265.6 cm² or 0.336 m². Most of the submarine spring samples collected through syringes revealed detectable FLT concentrations.

Table 2-1. Submarine spring names and locations. Locations were recorded with a handheld 76CS Plus Garmin GPS.

It is important to note that Seeps 4, 5, and 11 in the south and 1, 2, 6, 7, 9, 10, 12, 13, 14, 15, 16, 17, 18, 19, 20, and 21 in the north are all within 1 m of each other and therefore can only be represented by a single point within the spatial resolution obtainable with a GPS.

	Seep Number	Latitude	Longitude
South Seep Group	Seep 3	20°56'19.61"N	156°41'35.19"W
	Seep 4	20°56'19.36"N	156°41'35.14"W
	Seep 5	20°56'19.36"N	156°41'35.14"W
	Seep 11	20°56'19.36"N	156°41'35.14"W
North Seep Group	Seep 1	20°56'24.69"N	156°41'34.08"W
	Seep 2	20°56'24.69"N	156°41'34.08"W
	Seep 6	20°56'24.69"N	156°41'34.08"W
	Seep 7	20°56'24.69"N	156°41'34.08"W
	Seep 8	20°56'24.69"N	156°41'34.18"W
	Seep 9	20°56'24.69"N	156°41'34.08"W
	Seep 10	20°56'24.69"N	156°41'34.08"W
	Seep 12	20°56'24.69"N	156°41'34.08"W
	Seep 13	20°56'24.69"N	156°41'34.08"W
	Seep 14	20°56'24.69"N	156°41'34.08"W
	Seep 15	20°56'24.69"N	156°41'34.08"W
	Seep 16	20°56'24.69"N	156°41'34.08"W
	Seep 17	20°56'24.69"N	156°41'34.08"W
	Seep 18	20°56'24.69"N	156°41'34.08"W
	Seep 19	20°56'24.69"N	156°41'34.08"W
	Seep 20	20°56'24.69"N	156°41'34.08"W
	Seep 21	20°56'24.69"N	156°41'34.08"W

Table 2-2. North and South Seep Group water quality parameters. Data (means \pm SD and range) were collected from 7/19/2011 through 12/29/2012 with a handheld YSI Model 63.

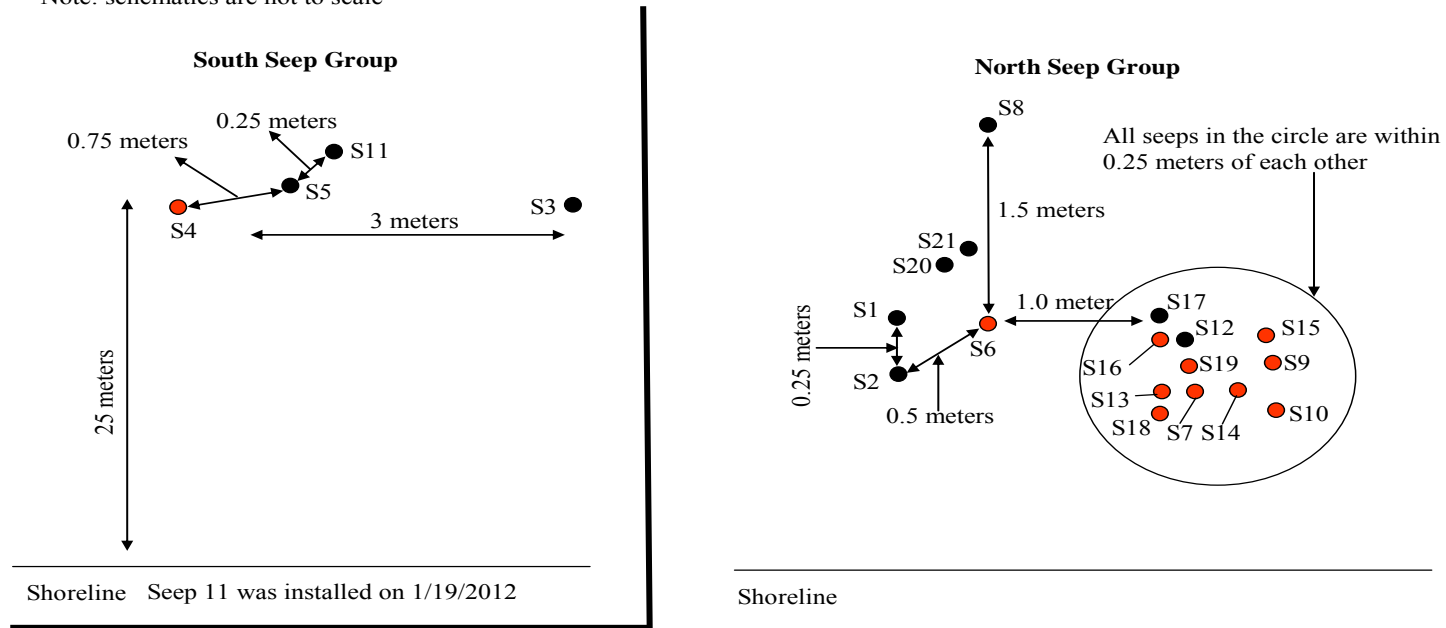
South Seep Group	Temp. (°C)	pH	Spec. Cond. (mS/cm)	Salinity
Seep 3	29.0 \pm 2.1	7.52 \pm 0.11	6.59 \pm 2.52	3.32 \pm 1.4
	24.2 to 35.1	7.22 to 7.94	5.20 to 28.2	2.50 to 16.1
Seep 4	28.6 \pm 2.0	7.50 \pm 0.12	8.98 \pm 6.57	4.77 \pm 4.0
	24.5 to 34.6	7.20 to 7.90	5.63 to 37.70	2.80 to 22.5
Seep 5	28.7 \pm 2.1	7.52 \pm 0.11	9.27 \pm 6.23	4.92 \pm 3.8
	24.9 to 34.9	7.30 to 7.90	5.29 to 34.8	2.90 to 21.8
Seep 11	29.1 \pm 2.3	7.54 \pm 0.07	7.40 \pm 0.37	3.75 \pm 1.46
	25.2 to 34.6	7.37 to 7.78	5.00 to 25.89	3.10 to 14.3
North Seep Group				
Seep 1	29.1 \pm 2.0	7.45 \pm 0.09	8.33 \pm 1.04	4.25 \pm 0.5
	24.8 to 34.4	7.18 to 7.76	7.32 to 14.8	3.90 to 7.30
Seep 2	28.9 \pm 2.3	7.46 \pm 0.11	8.47 \pm 1.41	4.35 \pm 0.7
	24.0 to 34.9	7.13 to 7.75	7.04 to 17.4	3.80 to 9.90
Seep 6	29.3 \pm 2.2	7.41 \pm 0.14	8.33 \pm 0.90	4.25 \pm 0.4
	23.8 to 35.9	6.90 to 7.94	7.00 to 13.5	3.80 to 7.0
Seep 7	27.5 \pm 1.7	7.51 \pm 0.19	8.19 \pm 1.32	4.31 \pm 0.8
	22.4 to 30.3	7.26 to 7.81	7.24 to 15.1	3.90 to 8.20
Seep 8	27.4 \pm 1.7	7.35 \pm 0.18	9.36 \pm 5.98	5.01 \pm 3.6
	24.7 to 31.0	7.09 to 7.90	7.47 to 37.9	4.00 to 22.0
Seep 9	27.4 \pm 1.8	7.43 \pm 0.21	13.7 \pm 11.4	7.58 \pm 6.7
	23.3 to 30.5	6.75 to 7.80	7.21 to 42.9	3.90 to 25.3
Seep 10	28.9 \pm 2.1	7.58 \pm 0.16	9.01 \pm 1.10	4.69 \pm 0.57
	26.5 to 34.6	7.26 to 7.76	7.99 to 11.9	4.10 to 6.20
Seep 12	28.2 \pm 1.1	7.60 \pm 0.11	8.37 \pm 0.50	4.35 \pm 0.24
	26.6 to 29.6	7.36 to 7.78	7.88 to 9.55	4.10 to 4.90
Seep 13	28.0 \pm 1.9	7.69 \pm 0.02	8.18 \pm 0.53	4.27 \pm 0.12
	26.0 to 29.7	7.67 to 7.71	7.69 to 8.74	4.20 to 4.40
Seep 14	27.1 \pm 2.1	7.67 \pm 0.05	7.91 \pm 0.21	4.17 \pm 0.06
	24.7 to 28.7	7.66 to 7.72	7.67 to 8.02	4.10 to 4.20
Seep 15	30.4 \pm 2.9	7.58 \pm 0.10	9.63 \pm 2.20	4.87 \pm 1.44
	24.6 to 34.9	7.40 to 7.75	7.86 to 16.5	4.20 to 9.30

North Seep Group Cont.	Temp. (°C)	pH	Spec. Cond. (mS/cm)	Salinity
Seep 16	31.5 ± 2.5 27.1 to 34.8	7.58 ± 0.12 7.38 to 7.80	10.1 ± 3.21 8.57 to 21.6	5.05 ± 1.93 4.40 to 12.0
Seep 17	32.9 ± 3.4 29.0 to 35.0	7.66 ± 0.15 7.53 to 7.83	22.5 ± 8.86 12.3 to 28.6	11.4 ± 4.31 6.50 to 14.5
Seep 18	31.1 ± 2.3 28.9 to 33.4	7.59 ± 0.07 7.52 to 7.65	9.48 ± 0.36 9.79 to 9.08	4.67 ± 0.06 4.60 to 4.70
Seep 19	30.8 ± 3.5 25.4 to 34.9	7.65 ± 0.07 7.49 to 7.73	9.25 ± 0.72 8.33 to 10.5	4.59 ± 0.20 4.50 to 4.90
Seep 20	30.0 ± 1.67 25.7 to 32.3	7.70 ± 0.07 7.59 to 7.82	18.06 ± 0.36 9.08 to 29.8	9.66 ± 4.08 4.50 to 15.9
Seep 21	29.8 ± 1.4 27.3 to 30.6	7.62 ± 0.06 7.55 to 7.70	11.3 ± 2.19 9.27 to 13.7	5.84 ± 1.35 4.70 to 4.5

Table 2-3. Control location water quality parameters.
 Data (means \pm SD and range) were collected from 8/5/2011 to 5/29/2012 with a handheld YSI Model 63 from Honokowai Beach Park, Wahikuli Wayside Park, and Olowalu.

Location	Temp. (°C)	pH	Spec. Cond. (mS/cm)	Salinity
Honokowai	27.4 \pm 1.3	8.06 \pm 0.09	54.0 \pm 2.7	33.8 \pm 1.7
Beach Park	25.1 to 30.3	7.90 to 8.27	47.3 to 58.0	29.9 to 35.7
Wahikuli	26.5 \pm 1.2	8.05 \pm 0.07	54.5 \pm 1.9	34.9 \pm 0.9
Wayside Park	24.9 to 29.7	7.89 to 8.16	50.4 to 57.7	32.7 to 36.4
Olowalu	28.2 \pm 2.0	8.03 \pm 0.07	55.5 \pm 2.5	34.2 \pm 1.7
	24.8 to 31.5	7.92 to 8.13	48.1 to 58.3	29.5 to 36.3

Note: schematics are not to scale



North Seep Group history in brief:

- | | |
|--|--|
| Seeps 1, 2 & 6 installed on 7/19/2011 | Seep 17 lost on 8/1/2012 |
| Seeps 1 & 2 lost on 11/14/2011, Seeps 7 & 8 installed | Seep 18 recovered on 8/8/2012, Seep 19 installed |
| Seep 6 lost on 11/24/2011, Seep 9 installed | Seep 19 lost on 8/15/2012, Seep 19 re-installed |
| Seep 8 lost on 1/19/2012, Seep 10 installed | Seep 19 lost on 9/18/2012, Seep 20 installed |
| Seep 9 lost on 1/24/1012, Seep 12 installed | Seep 19 recovered & removed on 10/2/2012 |
| Seeps 7 & 10 lost on 3/10/2012, Seeps 13 & 14 installed | Seep 6 recovered & removed on 10/18/2012 |
| Seeps 12, 13, & 14 lost on 3/24/2012, Seep 15 installed | Seep 21 installed on 10/19/2012 |
| Seep 16 installed on 4/24/2012 | Seep 10 recovered & removed on 10/22/2012 |
| Seeps 9, 13, 14, & 15, recovered on 6/25/2012, Seep 17 installed | Seep 7 recovered & removed on 11/2/2012 |
| Seep 18 installed on 7/10/2012 | |

Figure 2-1: Schematics of submarine spring water sampling locations. As specified in the North and South Seep Groups: Black circles represent Seep locations, red circles represent recovered and removed piezometer from seep location.

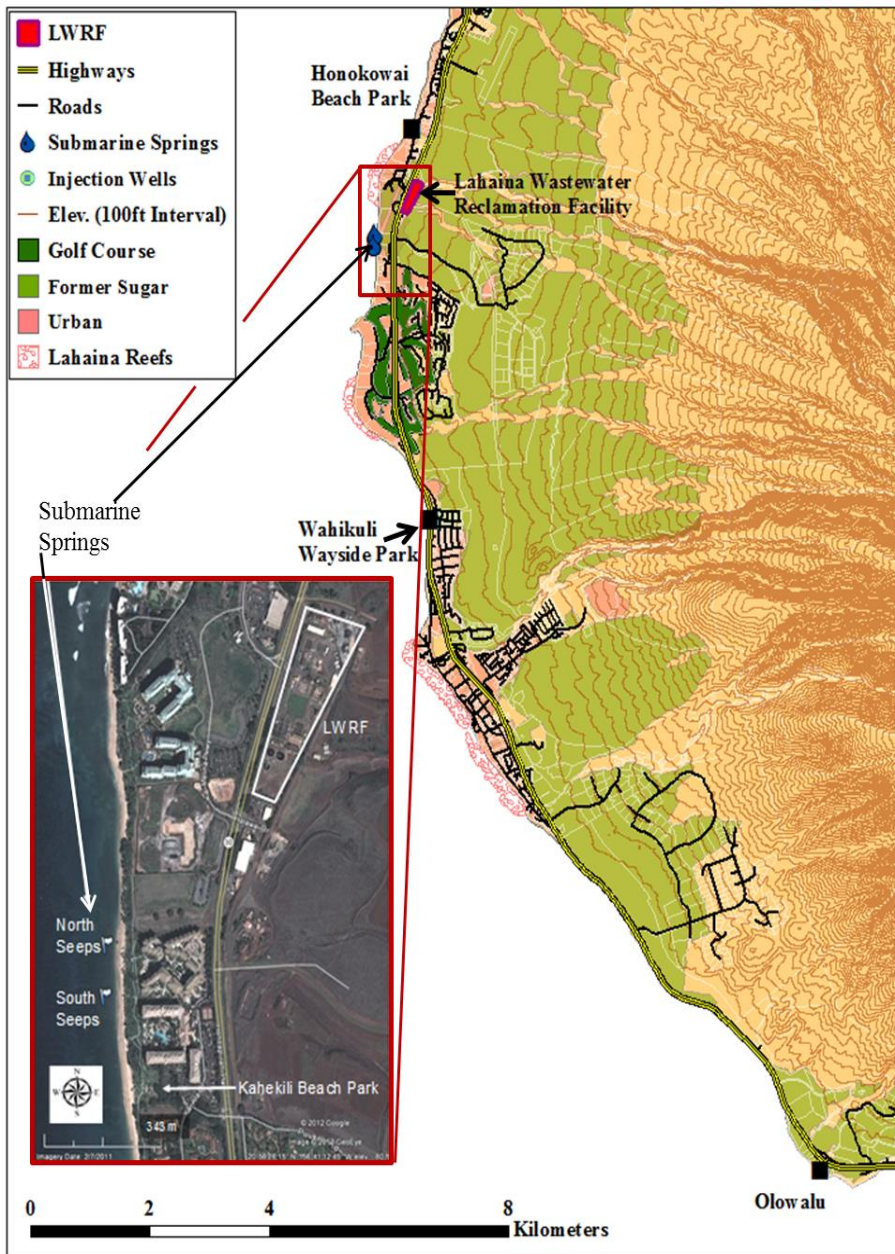


Figure 2-2: Control and submarine spring sampling locations. Control locations include: Honokowai Beach Park, Wahikuli Wayside Park, and Olowalu. Also shown are the locations of the North and South Seep Groups.

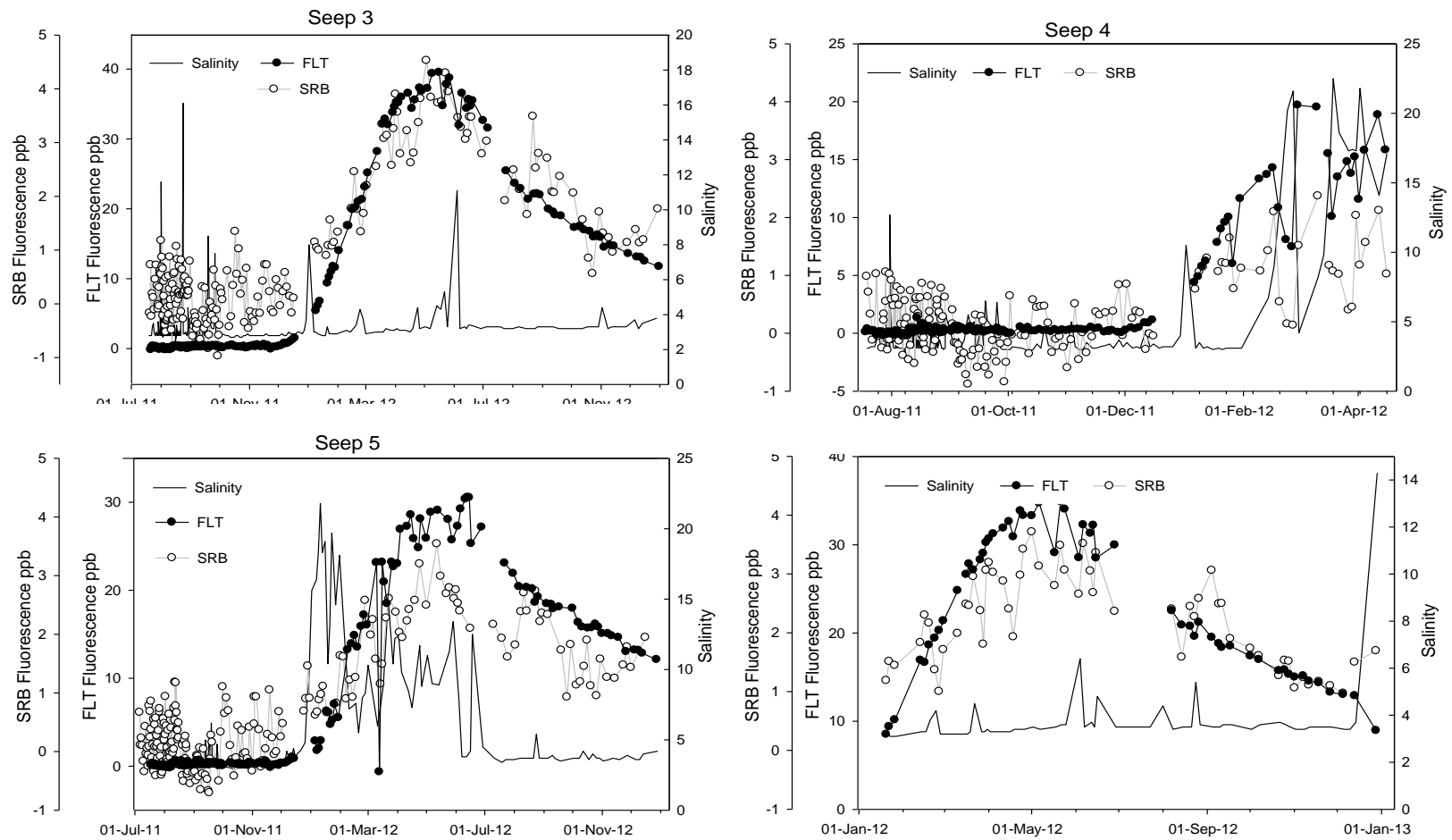


Figure 2-3: South Seep Group salinity and fluorescence (Seeps 3, 4, 5, and 11).

Field salinity (solid line) and fluorescence of SRB (open circles) and FLT (solid circles) of samples collected from Seeps 3, 4, 5, and 11 over time. FLT and SRB additions at the LWRF were performed on 7/28/11 and 8/11/11, respectively. Note the change in scale of the FLT fluorescence and salinity per seep.

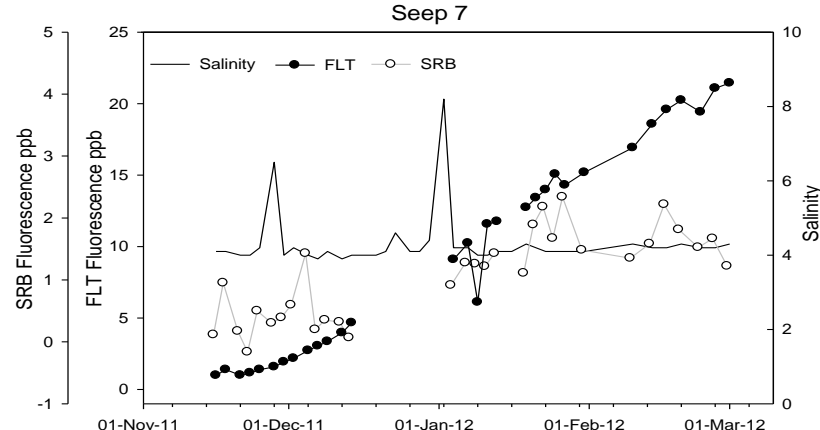
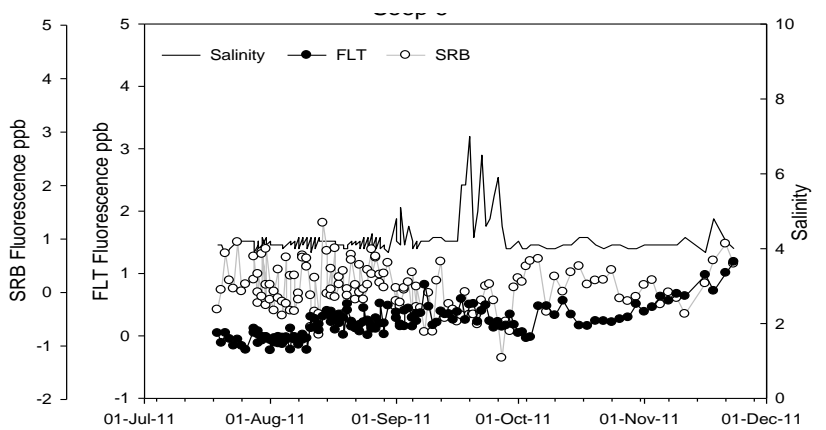
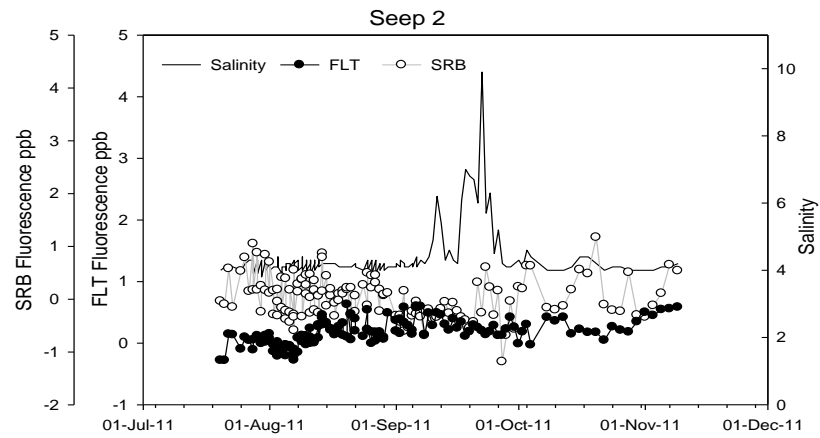
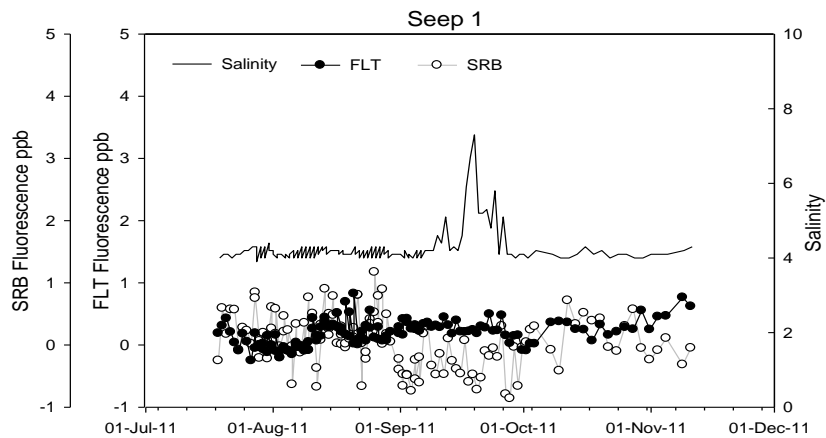


Figure 2-4: North Seep Group salinity and fluorescence (Seeps 1, 2, 6, and 7).

Field salinity (solid line) and fluorescence of SRB (open circles) and FLT (solid circles) of samples collected from Seeps 1, 2, 6, and 7 over time. FLT and SRB additions were performed at the LWRF on 7/28/11 and 8/11/11, respectively. Note the change in scale of the FLT fluorescence axis for Seep 7.

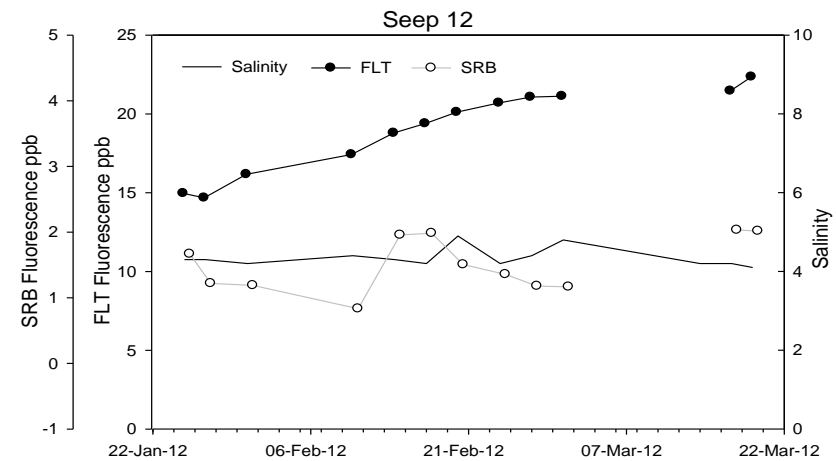
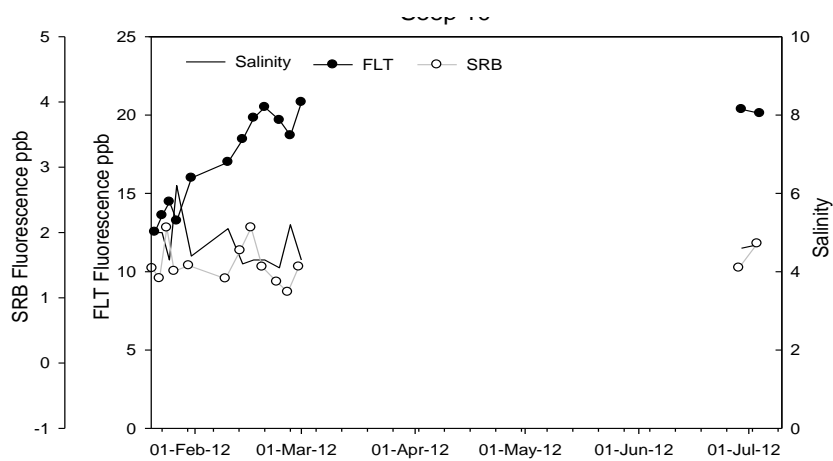
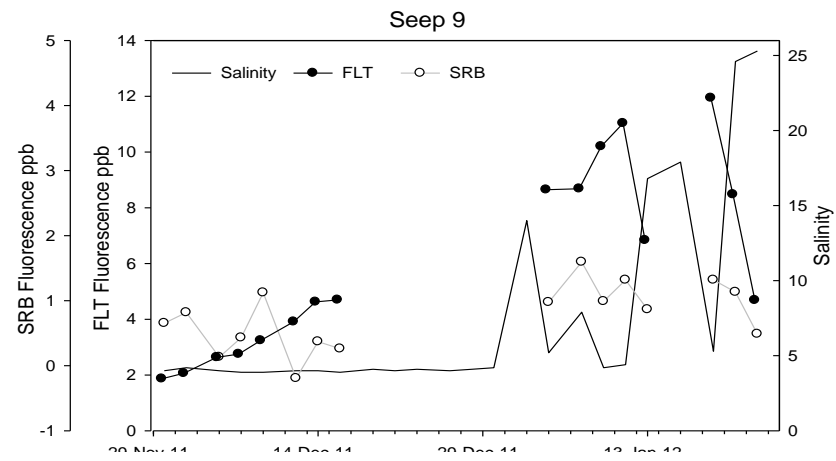
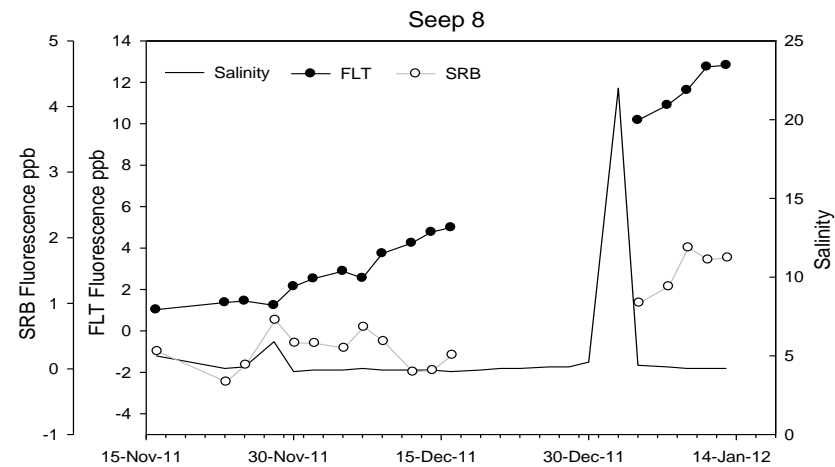


Figure 2-5: North Seep Group salinity and fluorescence (Seeps 8, 9, 10, and 12).

Field salinity (solid line) and fluorescence of SRB (open circles) and FLT (solid circles) of samples collected from Seeps 8, 9, 10, and 12 over time. FLT and SRB additions at the LWRF were performed on 7/28/11 and 8/11/11, respectively. Note the change in scale of the FLT fluorescence and salinity axis per seep.

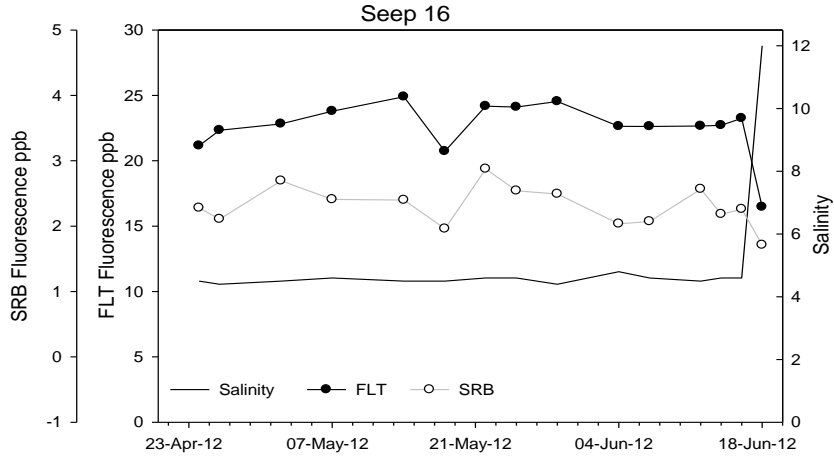
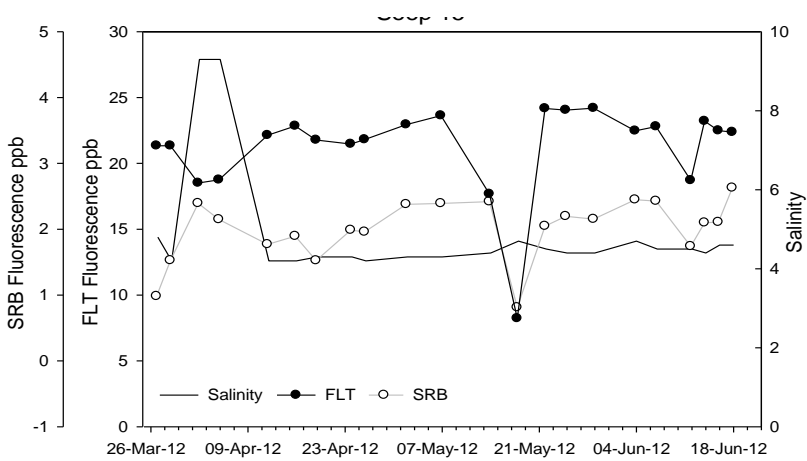
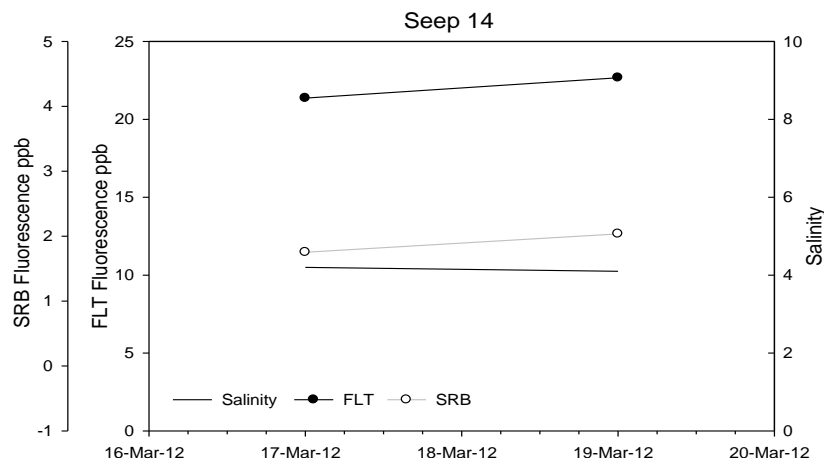
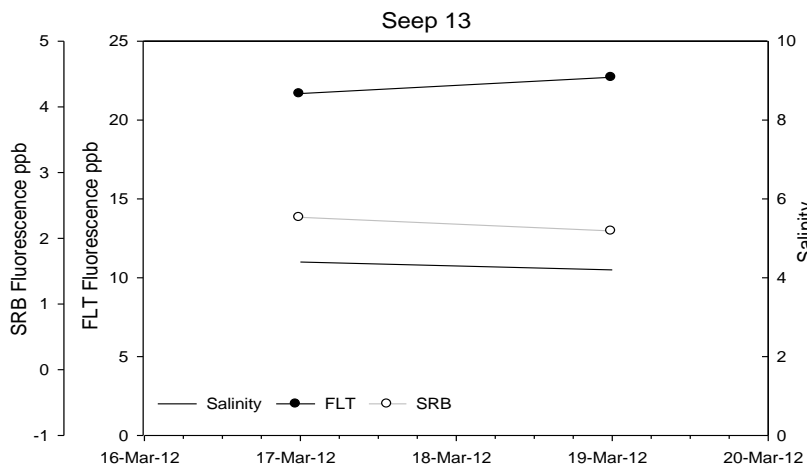


Figure 2-6: North Seep Group salinity and fluorescence (Seeps 13, 14, 15, and 16). Field salinity (solid line) and fluorescence of SRB (open circles) and FLT (solid circles) of samples collected from Seeps 13, 14, 15, and 16 over time. FLT and SRB additions at the LWRF were performed on 7/28/11 and 8/11/11, respectively.

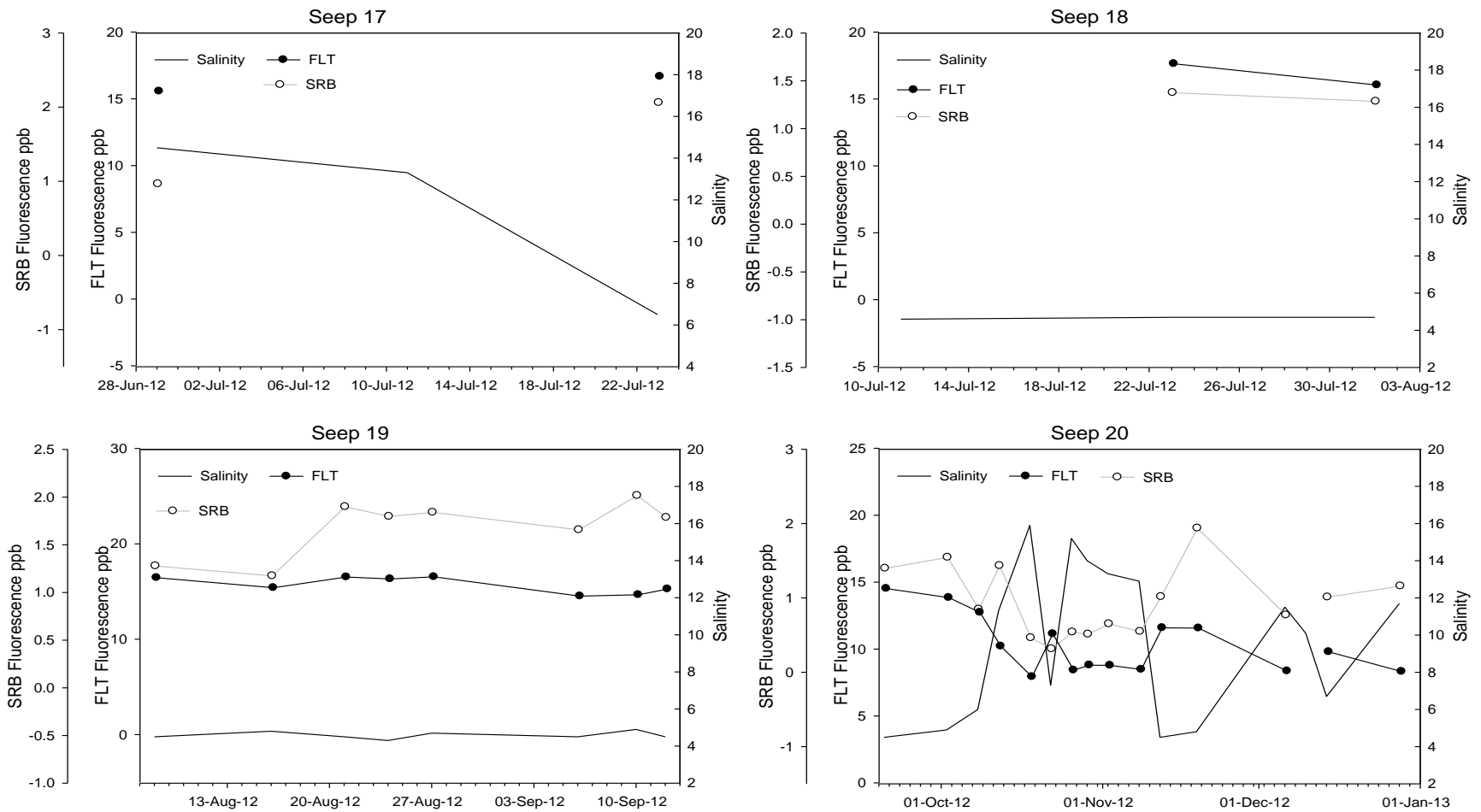


Figure 2-7: North Seep Group salinity and fluorescence (Seeps 17, 18, 19, and 20). Field salinity (solid line) and fluorescence of SRB (open circles) and FLT (solid circles) of samples collected from Seeps 17, 18, 19, and 20 over time. FLT and SRB additions at the LWRF were performed on 7/28/11 and 8/11/11, respectively.

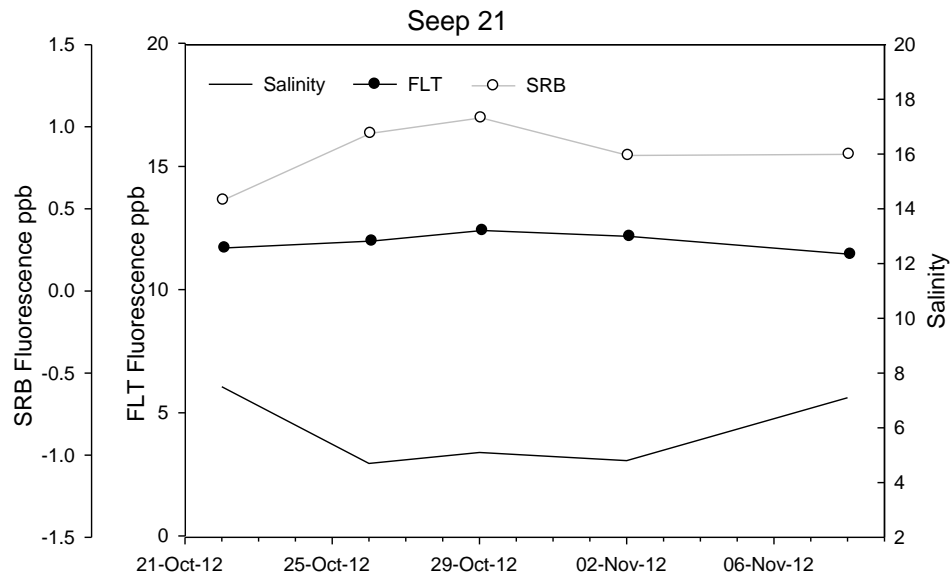


Figure 2-8: North Seep Group salinity and fluorescence (Seep 21). Field salinity (solid line) and fluorescence of SRB (open circles) and FLT (solid circles) of samples collected from Seep 21 over time. FLT and SRB additions at the LWRF were performed on 7/28/11 and 8/11/11, respectively.

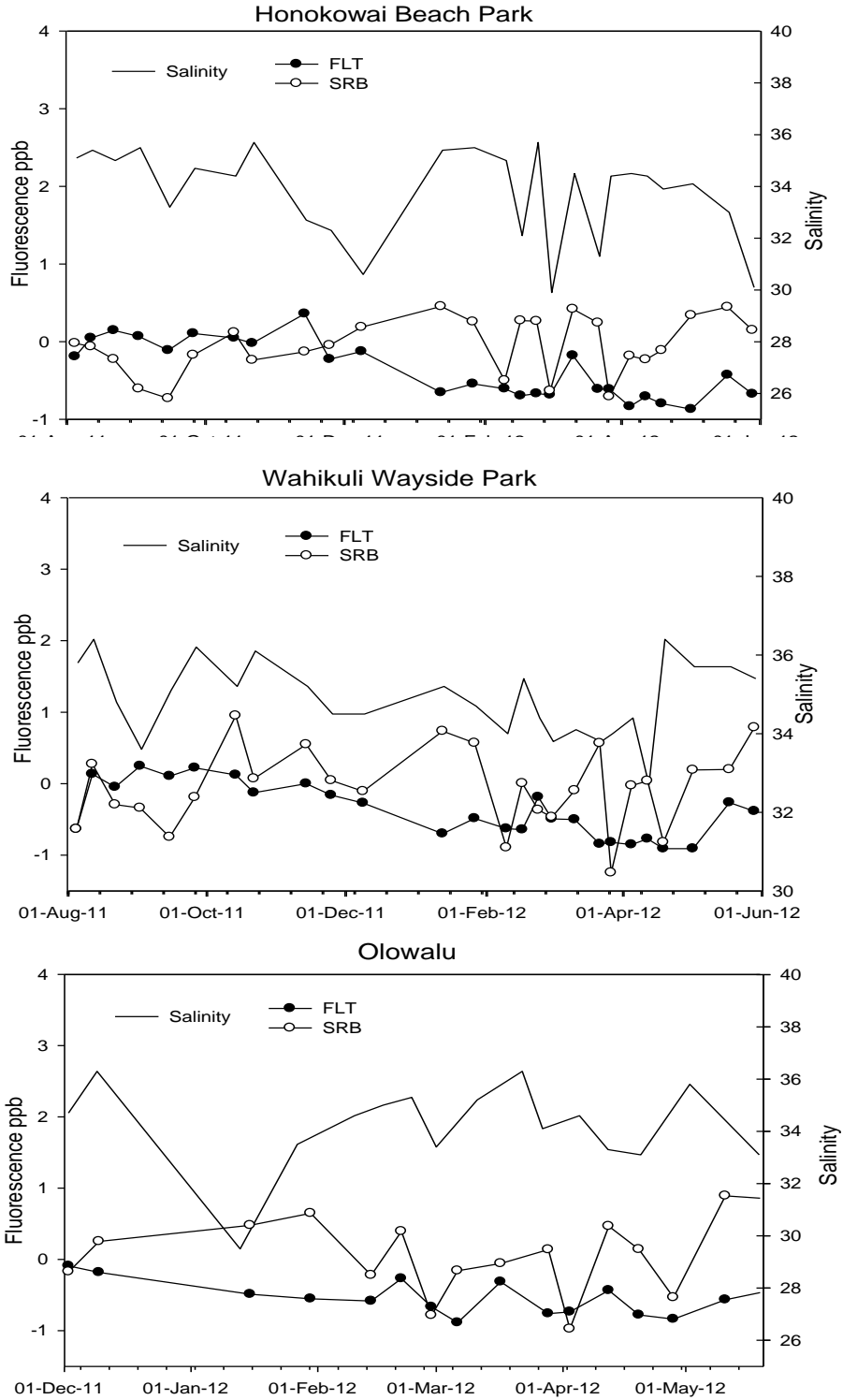


Figure 2-9: Control location salinity and fluorescence. Field salinity (solid line) and fluorescence of SRB (open circles) and FLT (solid circles) of samples collected at the control locations Honokowai Beach Park, Wahikuli Wayside Park, and Olowalu over time.

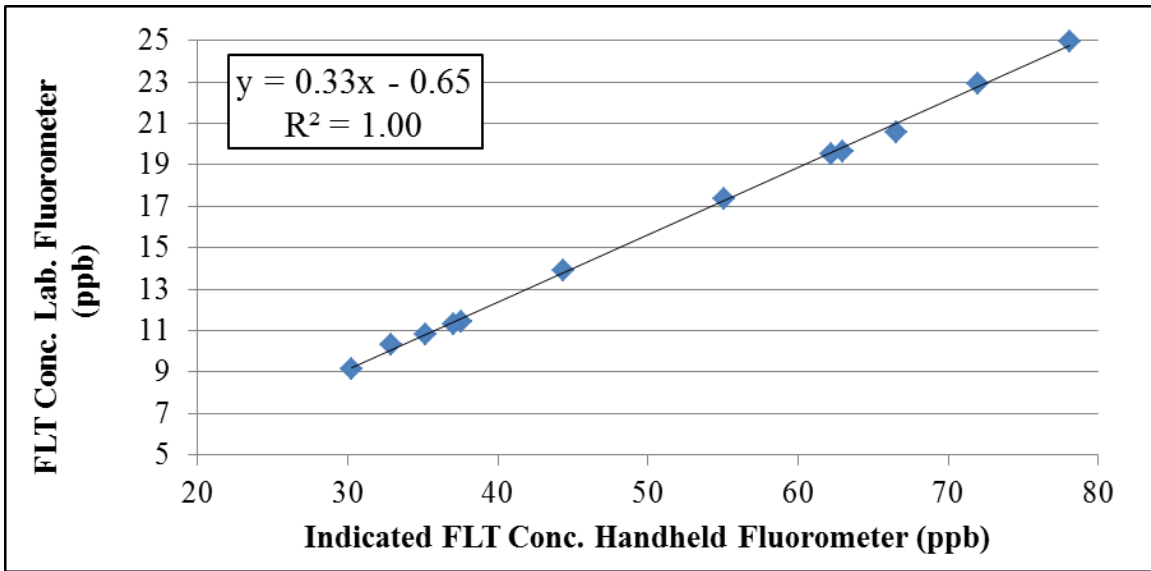


Figure 2-10: Correlation between the Field and the Lab measured FLT. A best-fit trend line shows that the actual FLT concentration is 0.33 times that of the field measured FLT concentration.

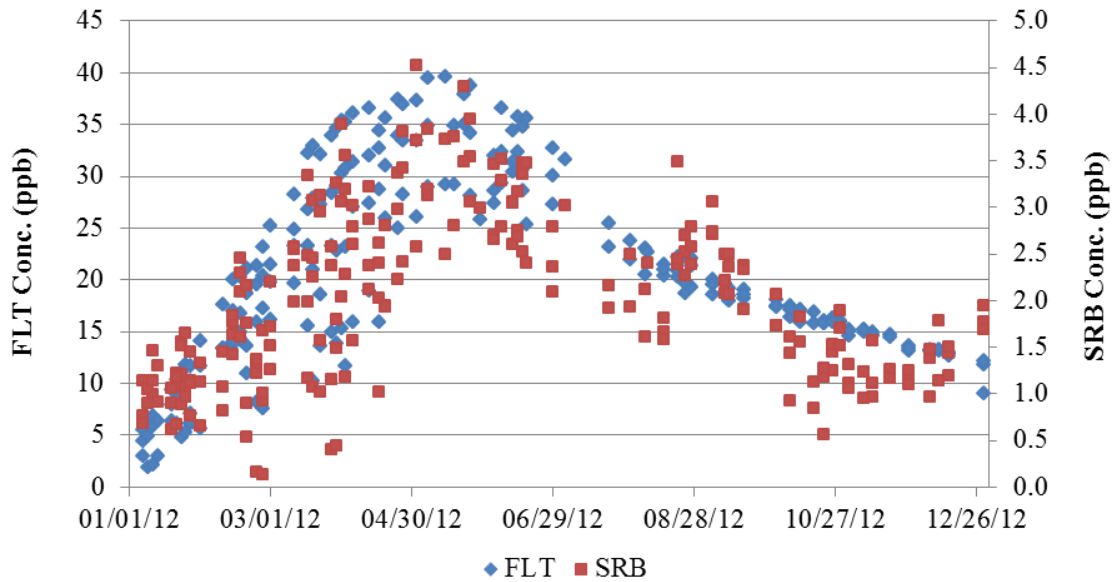


Figure 2-11: A time series showing the close correspondence between the field measured FLT concentration and the apparent SRB fluorescence.

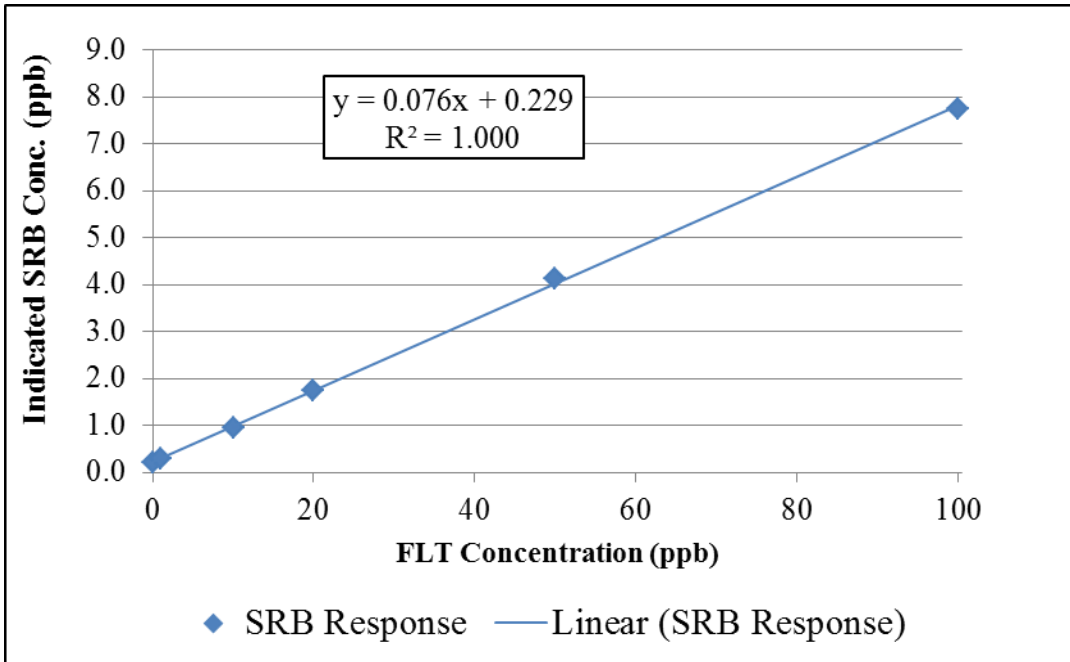


Figure 2-12: The handheld fluorometer SRB channel response to FLT (only) calibration solutions.

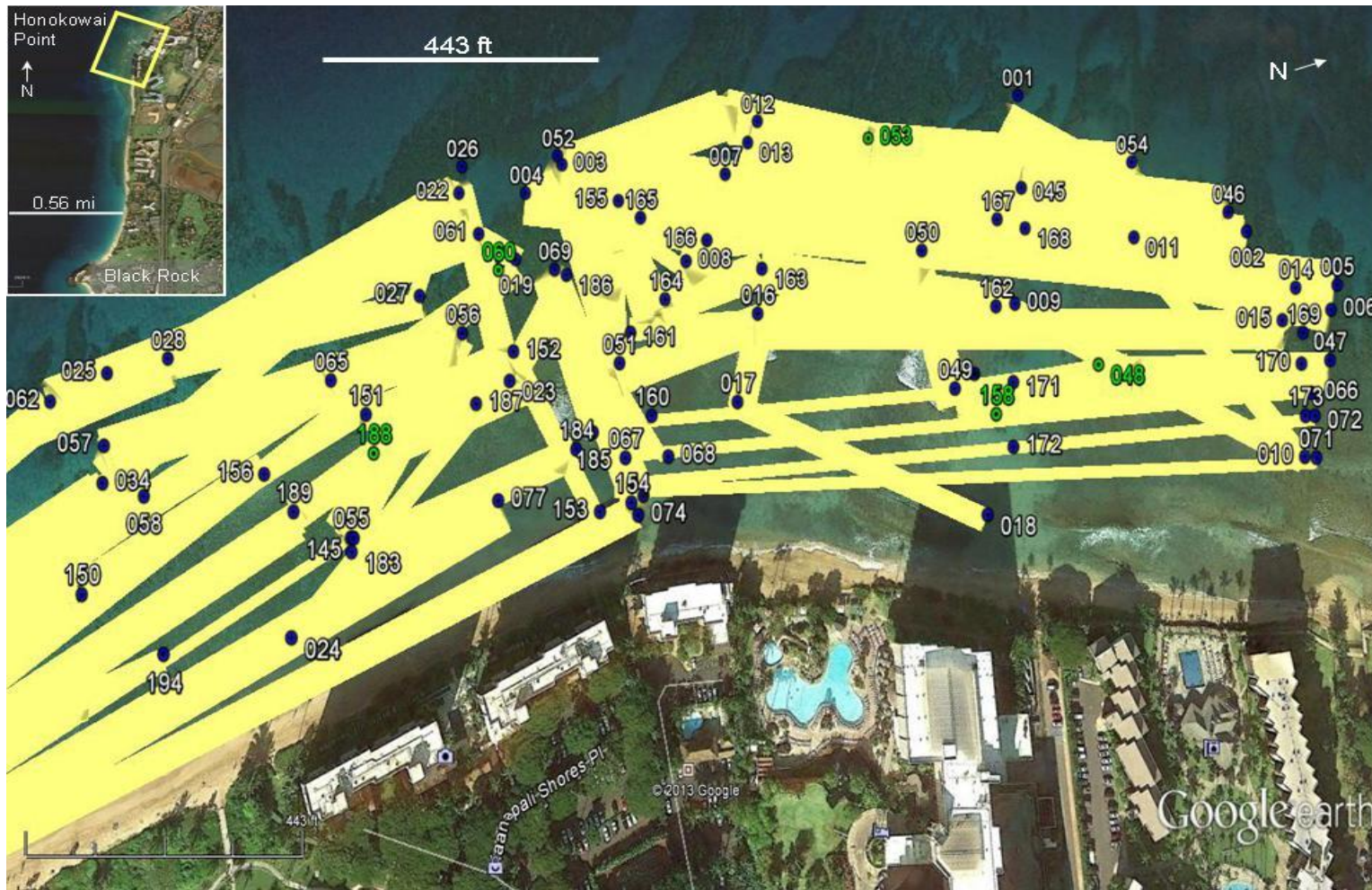


Figure 2-13: Area covered at Honokowai Point during the submarine spring survey. The area surveyed is shown in the yellow box of the map insert. Blue dots with white numbers represent the start and end of the transects; the transect widths (in yellow) are directly proportional to the visibility of the scuba divers at the time of the survey. Green dots with numbers represent samples collected from shimmery water (Appendix Table A-6).



Figure 2-14: Area covered at adjacent to the Honua Kai during the submarine spring survey. The area surveyed is shown in the yellow box of the map insert. Blue dots with white numbers represent the start and end of the transects; the transect widths (in yellow) are directly proportional to the visibility of the scuba divers at the time of the survey. Green dots with numbers represent samples collected from shimmery water (Appendix Table A-6).



Figure 2-15: Area covered south of the Honua Kai and across Kahekili Reef during the submarine spring survey. The area surveyed is shown in the yellow box of the map insert. Blue dots with white numbers represent the start and end of the transects; the transect widths (in yellow) are directly proportional to the visibility of the scuba divers at the time of the survey. Green dots with numbers represent samples collected from submarine springs (Appendix Table A-6).

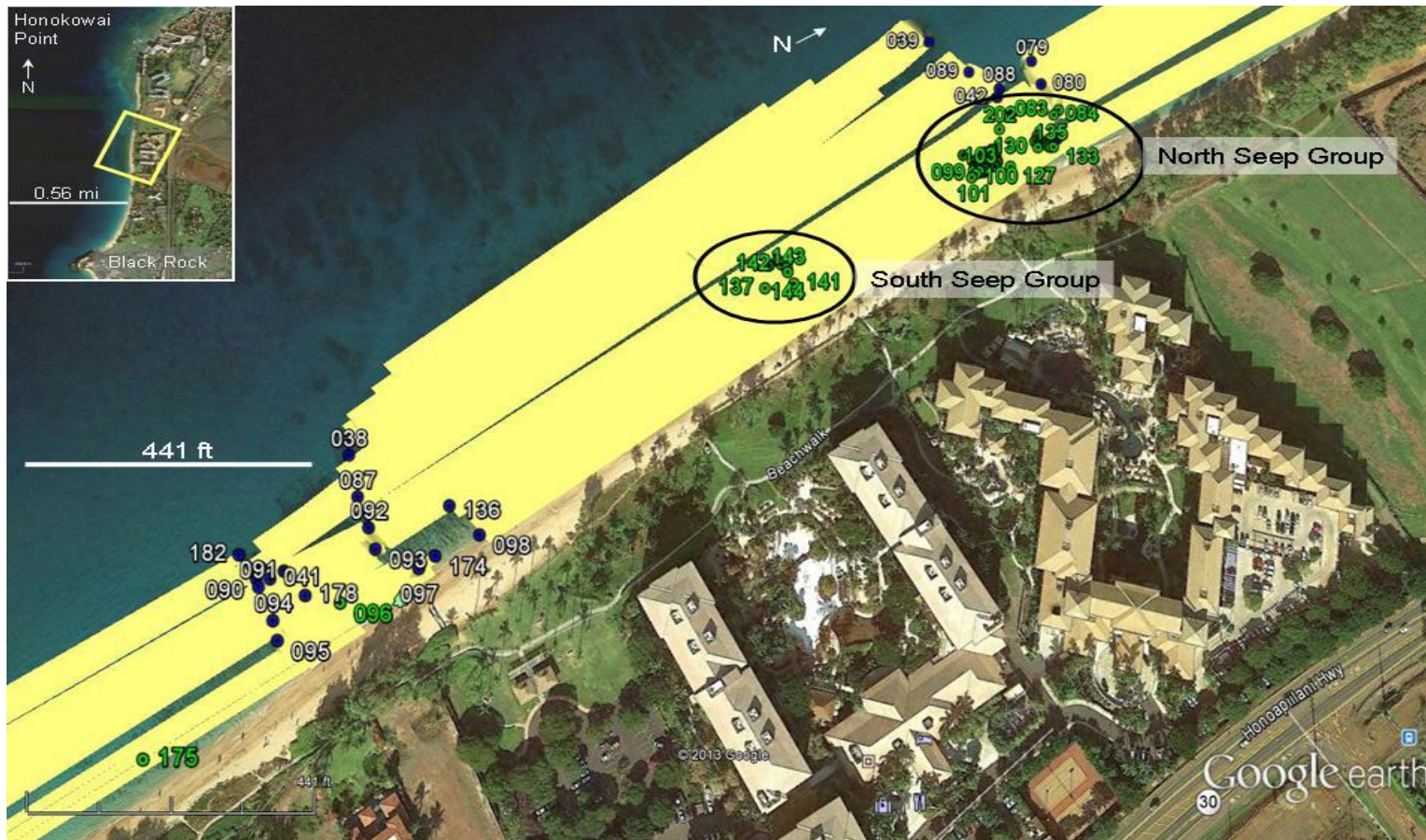


Figure 2-16: Area covered across Kahekili Reef during the submarine spring survey. The area surveyed is shown in the yellow box of the map insert. Blue dots with white numbers represent the start and end of the transects; the transect widths (in yellow) are directly proportional to the visibility of the scuba divers at the time of the survey. Green dots with numbers represent samples collected from submarine springs, with the exception of 096 and 175, which were from diffuse discharge (Appendix Table A-6).



Figure 2-17: Area covered South of Kahekili Reef during the submarine spring survey. The area surveyed is shown in the yellow box of the map insert. Blue dots with white numbers represent the start and end of the transects; the transect widths (in yellow) are directly proportional to the visibility of the scuba divers at the time of the survey. Green dots with numbers represent samples collected from diffuse discharge (Appendix Table A-6).

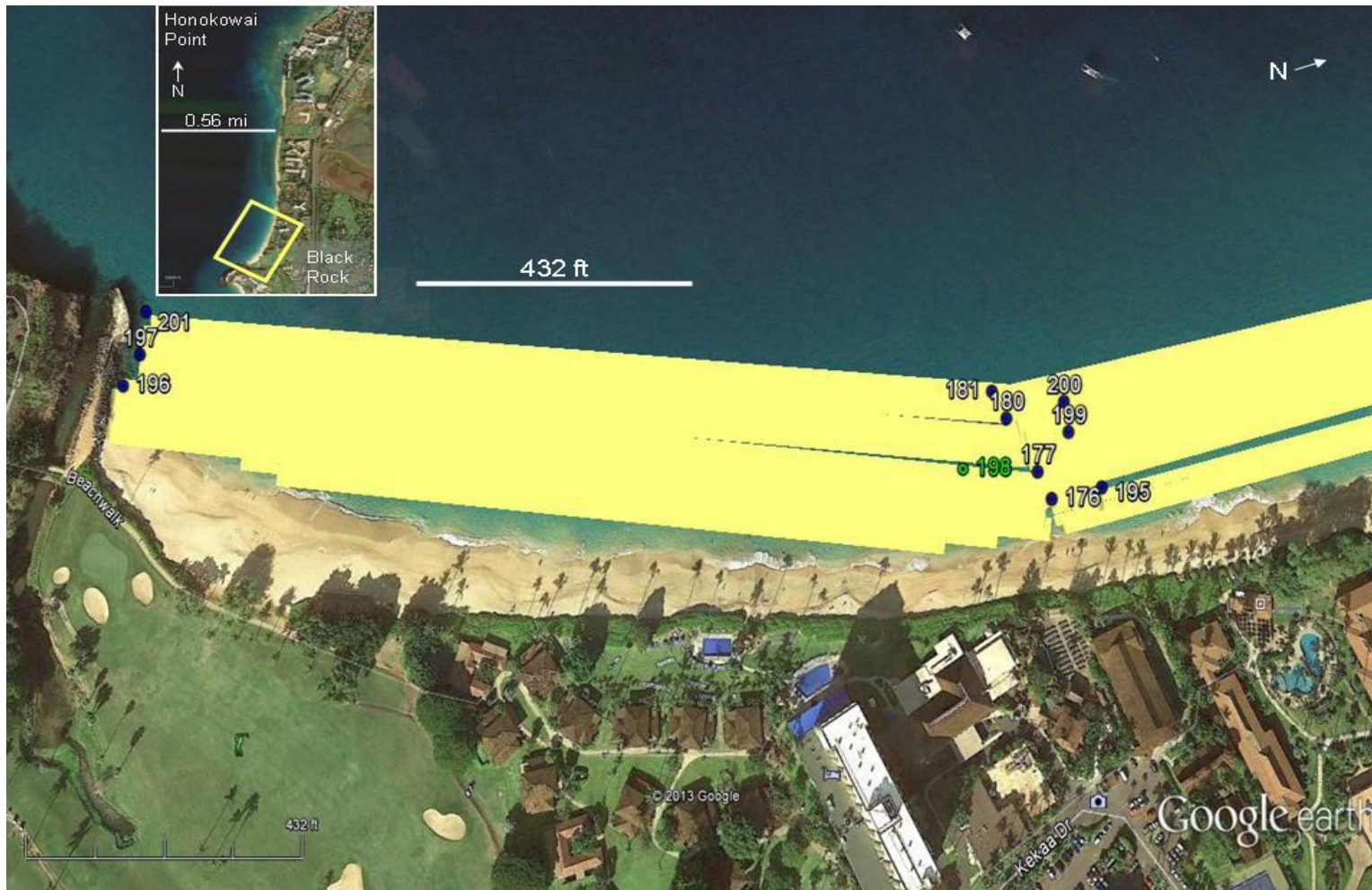


Figure 2-18: Area covered North of Black Rock during the submarine spring survey. The area surveyed is shown in the yellow box of the map insert. Blue dots with white numbers represent the start and end of the transects: the transect widths (in yellow) are directly proportional to the visibility of the scuba divers at the time of the survey. The green dots and numbers represent a sample collected from diffuse discharge (Appendix Table A-6).

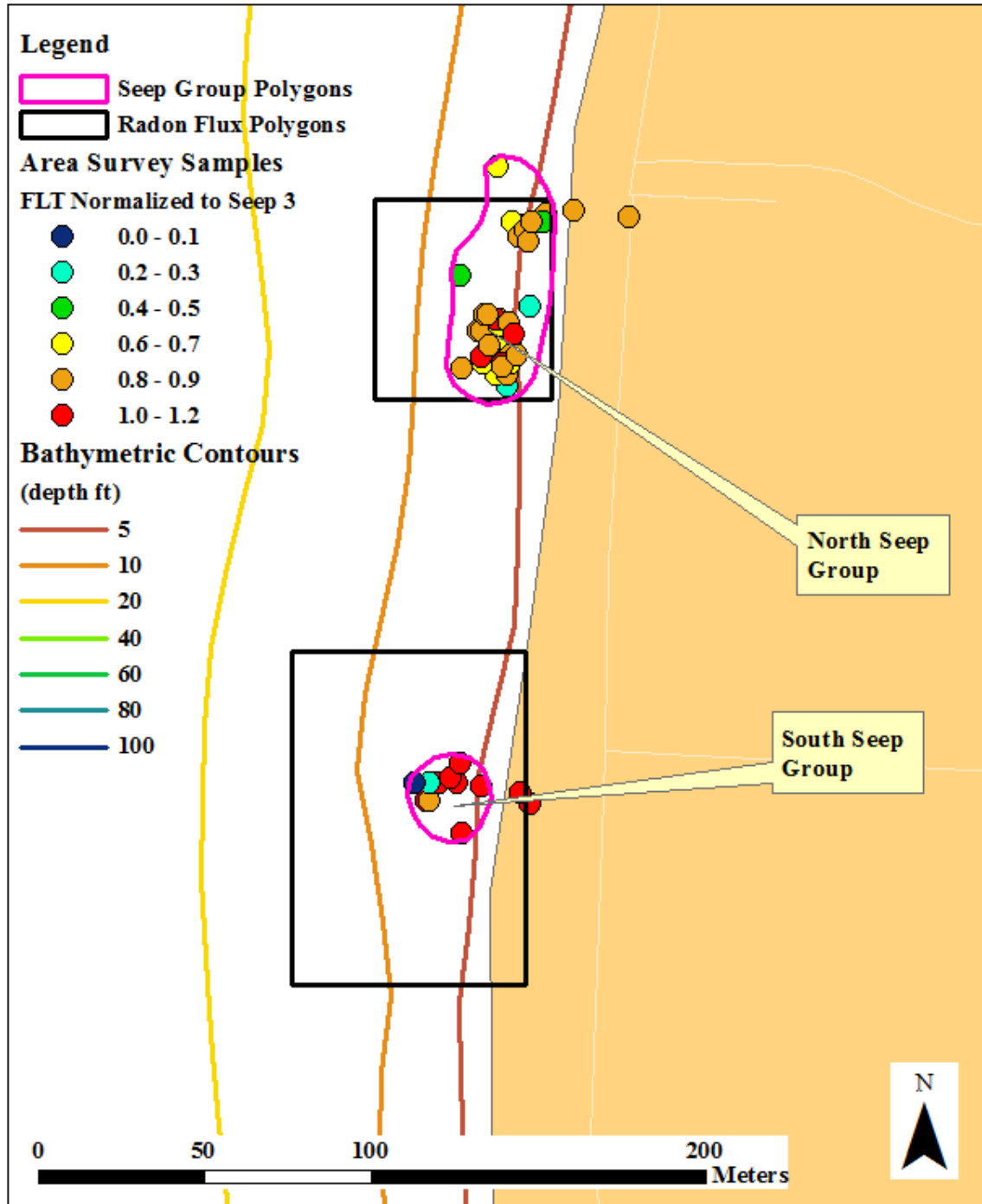


Figure 2-19: The location of the flowing submarine springs showing an enveloping polygon for each seep group and the extent of the boxes used in the Radon flux calculations

SECTION 3: SUBMARINE SPRING DISCHARGE MAGNITUDE AND DYNAMICS

3.1 INTRODUCTION

Field observations described in Section 2 revealed that visually obvious submarine groundwater discharge (SGD) within the study area occurs via seeps clustered into two groups, SSG and NSG (Figures 2-1 and 2-15). FLT was identified in all seeps within SSG and NSG (Section 2), but a proper mass balance of dye tracer recovery requires that the magnitude of seep discharge in these clusters be quantified. Thus, the objective of this section was to quantify groundwater discharge via discrete seeps and evaluate the temporal variability of this discharge. In addition, groundwater discharge via diffuse seepage also occurs at these sites and may be responsible for some tracer fluxes. Our second objective was therefore to determine what fraction of total groundwater flux discharges via discrete seeps as opposed to diffuse seepage. The estimated total (discrete seep and diffuse seepage) groundwater flux was previously quantified by this project using geochemical tracers (Glenn et al., 2012). In this section, we use those estimates and the newly acquired measured seep fluxes to determine the fraction of discharge via discrete seeps as opposed to diffuse seepage.

Only one ADCP was available for this project, so we had to restrict our observations to only one seep. Due to the persistent problem of bottom instability as a result of persistent sand migration at the NSG, we focused our attention on measuring seep fluxes in the SSG and selected Seep 4 within it as a representative of all seeps within the two clusters to document discharge dynamics. Seep 4 had dimensions of 13 cm x 7 cm, which is 11% of the sum of seep areas in SSG (838.8 cm²) and 3% of the sum of seep areas in SSG and NSG together (3,265 cm²) (see Section 2).

3.1.1 Seep Discharge Dynamics Measurements Using an Acoustic Doppler Current Profiler (ADCP)

In the first phase of the project, in September 2011, vertical velocities of water discharging from NSG Seep 6 and SSG Seep 4 were quantified using a 1 MHz High Resolution Aquadopp Profiler (Acoustic Doppler Velocimeter, or ADCP). This instrumentation allows the quantification of vertical water velocities at high frequency, and provides a profile of velocities in cells of pre-set dimensions across the water column. The HR Aquadopp Profiler was positioned on the seafloor next to the seeps in an upward-looking configuration. Because of its blanking distance, a distance between the ADCP head and the first measurement cell (across which the instrument is unable to measure velocities), it was unable to adequately resolve vertical water velocities at the discharge point of the seeps. The measured average upward velocities were 0.004 m/s and 0.02 m/s at Seep 6 and 4, respectively. The magnitude of upward fluxes was tidally dependent with lower upward velocities occurring at high tide and higher velocities at

low tide. Therefore, it is essential to compare upward velocities with respect to measured water level, which is recorded by the instrument as water pressure, and that a tidal averaged velocity is used as a representative seep velocity per day. In September 2011, at Seep 4 the instrument was only deployed for six hours so the flux does not represent the whole tidal cycle. Because the September 2011 vertical velocities were just at, or barely above, the resolution of the sensor in this configuration we selected a down-looking instrument configuration for all consequent deployments when the HR Aquadopp was installed at a set distance away from the bottom of the seafloor with the ADCP head centered over the seep (Figure 4-1). This allowed a better resolution of velocities closer to the ocean floor.

3.2 METHODS

3.2.1 Study Area

As noted, the focus site for the ADCP time-series measurements was Seep 4 within the SSG (Figure 2-1) as this is one site where FLT has been detected throughout the monitoring period. Although Seep 4 began to have high salinity values (>5) and decreasing FLT in January 19, 2012, discharge from this seep seemed to be dominant within SSG. The ocean bottom in the area is rocky with dead coral and sand patches. The water at this seep discharges via a vent with dimensions of 7 x 13 cm.

3.2.2 HR Aquadopp Profiler Deployment

Seep 4 vertical velocities were measured between October and November 2012. We performed three deployments: October 1-2, 2012; October 17-19, 2012; and November 2-3, 2012. Later deployments were not possible due to unfavorable sea conditions. We built an aluminum stand (Figure 3-1) that was fixed to a block on the ocean bottom. The HR Aquadopp Profiler was mounted on the arm of the stand in a down-looking configuration at 1 m distance from the ocean bottom. The head of the instrument was centered above the seep. The instrument was configured to have a blanking distance of 40 cm and create a water velocity profile in 22 3-cm sized cells at the ocean bottom with measurement intervals of 1 s. Other details of the deployment configuration are listed in Table 3-1.

3.2.3 HR Aquadopp Data Processing

Raw velocity and pressure data were truncated to times when the sensor was underwater and stationary. Velocity data with amplitude < 120 counts and correlation $< 40\%$ were removed prior to analysis. Abrupt changes in the mean amplitude and correlation profiles were used in corroboration with diver measurements to identify the cell closest to the seep. Data quality control was performed with the velocity data in beam coordinates, which were then converted to earth-referenced coordinates using the instrument's heading and tilt sensor measurements. Local high and low tide times were calculated using 2-hr low-pass filtered pressure data. These demarcated times were checked against

predicted tides for the NOAA Kahului tide station and were typically within 20 min of the predicted tides.

3.3 RESULTS

3.3.1 Vertical Fluxes

The HR Aquadopp Profiler sampling frequency was set to 1 s, which allowed the registration of high frequency events, such as results from swell and wave action. To resolve these, power spectra were computed from the de-trended pressure and vertical velocity data using a Hanning window with four ensembles. During the 17-19 October deployment, which was the longest of the three, two peaks in vertical velocity spectra were apparent at periods $T \sim 10-13$ s and 18-21 s. These corresponded to peaks in the power spectrum of pressure that were likely due to a combination of shorter- and longer-period surface swell (Figure 3-2). The majority of energy in the vertical velocity fluctuations resolved here was at periods shorter than 21 s, indicating that surface swell is a dominant driver of variability over periods $< \sim 20$ min. The longer-term (tidal-scale) averaged velocities indicate that the tidal component, although not resolved in our spectral analysis due to the short deployment period, is significant. Similar findings were observed during the other two deployments.

Average vertical velocities were calculated for different tide periods for the three deployments so that full tidal period average flux comparison could be made to assess changes in discharge. Low/high tide times were demarcated using the filtered pressure data on which we found the mid-point between tidal stages and averaged velocities within those periods. Figure 3-3 shows low- and high-tide periods in colors that illustrate the demarcated times used for average velocity calculations. The figure shows the tidal stage with calculated average and sum of fluxes over the respective time periods. During the two lower low tides, vertical upward velocities averaged 0.0065 and 0.0103 m/s. During high tides the velocities averaged -0.0019, 0.0015 and 0.0062 m/s. For best comparison we have to consider averages over the full tidal period. The October 17-19 record was long enough to compare variability over full tidal periods at different times and the data show that averages vary significantly depending on the tidal period selected. Average vertical velocity doubles between higher-low to higher-low (Figure 3-4) and higher-high to higher-high tides (Figure 3-5), other combinations are listed in Table 3-2.

3.3.2 Determination of Seep Discharge Using ADCP

By deploying the Aquadopp in a downward-looking configuration at a known distance to a solid boundary (e.g., the sea floor), ambiguities in velocity measurements were reduced. The majority (70%) of individual vertical velocity measurements were greater than the quoted uncertainty of the instrument of 1 cm s^{-1} . In addition, two findings suggest that the measured velocities were greater than instrument noise: (1) coherence between pressure and vertical velocity was significant at the 95% C.I. level ($\gamma^2 > 0.8$) at periods typical of surface swell ($2 \text{ s} < T < 21 \text{ s}$); and (2) there was a consistent pattern of

increased vertical velocities averaged over falling and low tide compared to that of high tide.

Tidal average vertical water velocities from all three deployments were multiplied by the seep area to derive groundwater discharge from vents. Seep 4 area was 13 x 7 cm² and assumed to be constant over the study period. The calculated discharges are indicated in Table 3-2. The data show some variation in discharge rates over time, at times as much as >100% change between the three deployments. Such changes in discharge rates are not surprising given the changes in injection rates and hydrological conditions and are supported by our findings of discharges derived from a radon mass balance reported in this project's Interim Report (Glenn et al., 2012).

Based on seep vent area measurements, Seep 4 represents 11% of the sum of seep areas in SSG (838.8 cm²) and 3% of the sum of seep areas in SSG and NSG together (3,265 cm²) as shown in Figures 2-1 and 2-15. The two seep groups represent 289 identified seeps (submarine springs) along the coastline. In addition to their identification by divers, we delineate the two seep clusters based on the radon plume identified during the radon survey performed in June and September 2011. SSG consists of 106 seeps plus any diffuse seepage in a 70 x 100 m² area identified as an isolated radon plume in the surface water, and NSG consists of 183 seeps plus any diffuse seepage contributing to the 53x60 m² large surface radon plume. For a rough estimate of total discharge from the vents, we assume that all seeps within SSG and NSG discharge water at the same vertical velocity as Seep 4. This neglects the fact that vents may have higher or lower vertical water velocities depending on their size or location with respect to the groundwater plume. The uncertainty introduced by this assumption cannot be quantified as no other seep discharge was investigated in a systematic manner. By multiplying total seep areas with the above-derived vertical fluxes, we arrive at a total vent discharge of 21-76 m³/d and 83-296 m³/d for SSG (106 seeps) and SSG+NSG (289 seeps), respectively (Table 3-3). Average (June and September 2011) radon mass-balance derived total groundwater fluxes were 7,550 m³/d at SSG (106 seeps plus any diffuse seepage in a 70 x 100 m² area identified as an isolated radon plume in the surface water) and 2,950 m³/d at NSG (183 seeps plus any diffuse seepage in a 53x60 m² area). These results indicate that total SGD via seeps is only 0.5-1% at the SSG and 2-8% at the NSG of total water discharge and that >90% of groundwater discharge is via diffuse seepage within the 70 x 100 m² area of SSG and 53 x 60 m² area of NSG (Table 3-4). This result may be biased because only documented seeps were used and others may exist in the area. Sand may cover cracks and other leakage points that were not identified as discrete seeps. At NSG we observed that some of the vents are transient in that they are buried and then uncovered due to shifting sands. Our estimates may also be conservative because vertical water velocities were only slightly above instrument resolution and due to sea bottom roughness we could not use a cell closest to the ocean bottom.

3.3.3 Groundwater-derived nutrient fluxes

Groundwater discharge estimated based on a coastal radon mass-balance and ADCP were used to estimate groundwater-derived nutrient fluxes to the coastal ocean. We

determined that a significant amount of groundwater discharges not just at the SSG and NSG but also at other locations along the coastline. Among these Black Rock, Honokowai, and Hanakao‘o Beaches had significant discharge (Table 3-5). We measured groundwater nutrient composition at SSG and NSG in seeps and at a spring at Black Rock that was located in the lagoon. For these locations, nutrient concentrations were multiplied by groundwater discharge to derive nutrient fluxes to the coastline (Table 3-6). For Honokowai and Hanakao‘o, however, groundwater discharge occurs as diffuse seepage or from an individual spring that could not be located, and so the best estimate of groundwater nutrient composition was derived from that of higher elevation wells. We sampled three wells upstream of Honokowai, which were located 4 km from the coastline (Kaanapali P-4, P-5, P-6; see Tables 6-3 and 6-4 and Figure 6-2 in Glenn et al., 2012) and one well (Hahakea 2) 2 km upstream of Hanakao‘o Beach. These wells captured nutrient signatures from agricultural activities from pineapple (Kaanapali P-4, P-5, P-6) and sugarcane (Hahakea 2) cultivation and had relatively elevated nutrient levels (see Figure 6-1, Tables 6-3 and 6-4 in Glenn et al., 2012).

As a simple approach, we consider conservative behavior for nitrogen and phosphorus species within the aquifer and assume that groundwater composition doesn't change along its flow path to the coastal zone. For nitrogen, this would be supported by findings of Green and Young (1970) who found rapid movement of nitrate in soil water and assumed great mobility of nitrates, the dominant chemical species of nitrogen in groundwater in the sampled wells. Conservative nitrogen behavior was assumed in other groundwater discharge studies in West Maui (Street et al., 2008) and Hawaii (Knee et al., 2008).

Depending on land-use, organic matter content, geology, etc. nutrients may be removed (dilution and geochemical cycling) and/or added (fertilizer use, cesspools or septic systems) along the groundwater flow path. Our study (Glenn et al., 2012) showed significant denitrification in groundwaters exiting SSG and NSG seeps based on a very heavy $\delta^{15}\text{N}$ signature (see Figure 6-22 in Glenn et al., 2012). But denitrification was only evaluated at these two locations and these findings cannot be expanded to Honokowai and Hanakao‘o. Coastal $\delta^{15}\text{N}$ values in the Hanakao‘o area were high enough to suggest that denitrification (possibly fueled by input of organic C and NO_3^- from irrigation with recycled waste water) is occurring in groundwater entering the ocean as SGD (see Table 6-12 in Glenn et al., 2012). In an earlier study, Tetra Tech (1993) estimated a 4-time dilution of the nitrate signature in the Honokowai and Hanakao‘o area between upstream agricultural and coastal locations. This estimate was based on a hydrological model and only assumed dilution of the nutrient content by ambient groundwater. Any additions of nutrients near the coastal areas were neglected. This same study assumed that soluble reactive phosphorus (SRP) is immobile and estimated negligible phosphorus flux to the coastal zone via groundwater discharge. Our measurements at the seeps and Black Rock spring, as well as other locations around Hawaii (Johnson et al., 2008) indicate significant SRP discharges that require that phosphorus be at least partially mobile in these aquifers.

Table 3-6 therefore represents nutrient fluxes that assume conservative nutrient behavior in Honokowai and Hanakao‘o aquifers in the absence of better understanding of N and P

cycling in the aquifers of West Maui. As a result of large volumetric groundwater discharge and elevated nutrient levels in wells, dissolved inorganic and organic nitrogen (DIN and DON) fluxes are largest at Hanakao‘o Beach (2.9 kmol/d or 41,440 g/d of N as DIN, and 1.7 kmol/d or 23,700 g/d of N as DON). The second largest DIN flux along this coastline is from Honokowai (1.9 kmol/d or 27,500 g/d of N) and DON flux at SSG (up to 650 mol/d or 9,500 g/d of N). At Hanakao‘o and Honokowai groundwater discharges are 1,200 and 300 m in length, while at the seep clusters the discharge locations are only 50 and 100 m long. When discharge per meter shoreline is considered, SSG and NSG DON fluxes in September 2011 are far above fluxes at any other discharge location with 6.5 and 4.9 mol/m/d or 91 and 69 g/m/d of N as DON, respectively (Table 3-6). Dissolved inorganic phosphorus (DIP) fluxes are the largest at Hanakao‘o and SSG (201 and 73-84 mol/d or 6,225 and 2,260-2,600 g/d of P as DIP). NSG and SSG DIP and DOP fluxes are largest when discharge per meter coastline is considered (485-598 and 735-844 mmol/m/d or 15.0-18.5 and 22.7-26 g/m/d of P as DIP, and 90 and 110 mmol/m/d or 2.8-3.4 g/m/d of P as DOP). For a lower-limit estimate, nutrient fluxes for Honokowai and Hanakao‘o reported in Table 3-6 can be divided by four (Tetra Tech, 1993). This estimate is based on a hydrological model and only assumes dilution of the nutrient content by ambient groundwater. No biogeochemical transformations and additions of nutrients near the coastal areas were assumed. Under the lower-limit scenario of 4-fold nutrient dilution at Hanakao‘o and Honokowai Beaches, DIN flux at SSG and NSG is comparable to other locations and DIP fluxes are significantly higher than at any other location.

Groundwater discharge and seep nutrient fluxes derived here compare well with previous findings of Swarzenski et al. (2012) who found an average groundwater discharge for the seep site (NSG+SSG) of 55 m³/m/d or 0.015 mgd/m and nutrient fluxes of 2,200 mmol/m/d or 31 g/m/d of N as DIN, 540 mmol/m/d or 7.6 g/m/d of N as DON and 700 mmol/m/d or 22 m/g/d of P as DIP in July 2010.

The seeps at SSG and NSG have 100 times higher SRP concentration than ambient ocean levels and represent a significant phosphorus source to the coastline (Table 3-6). Indeed, nutrient concentrations in coastal nearshore marine samples in all these regions affected by groundwater discharge are above offshore oligotrophic surface central Pacific Ocean concentrations (Table 3-7 and Figure 3-6). While coastal DON and DOP levels are comparable or only slightly elevated above offshore values, DIN is as much as 10 times higher and DIP is 8 times higher in coastal surface water.

Another groundwater signature that may have a potential effect on coastal ecosystems is the N:P ratio of nutrients in discharging groundwater. These range from the low 1-2 in the seep groups to as high as 63 at Honokowai for the inorganic nutrient species and 2-3 in seeps and 75 at Honokowai for organic nutrient species (Table 3-5). Coastal surface water nutrient ratios are comparable to values observed in offshore waters except at Black Point where DIN:DIP is 17, and at SSG and NSG where this ratio is only 2 (Table 3-7).

3.4 SUMMARY

We used a HR Aquadopp Profiler to measure vertical velocities of water discharging from Seep 4 within SSG. Our objective was to quantify groundwater discharge and evaluate its temporal variability. We found that discharge varies throughout the tidal cycle and between tidal cycles. We observed a >100% variation in discharge between three deployment periods in October and November 2012. We used Seep 4 measurements to upscale to seep fluxes within SSG and NSG, which resulted in 21-86 m³/d and 83-336 m³/d for SSG and SSG+NSG, respectively. These measured seep fluxes were then compared to total SGD determined in June and September 2011. Seep discharge as measured by the HR Aquadopp Profiler only represented <8% of total SGD determined by Rn methodologies at these two seep clusters. Based on these findings we can conclude that the two seep groups consist of porous geology that allows groundwater to be discharged through discrete vents and other openings that may or may not be covered by sand or rock. We called the latter diffuse seepage as vents could not be identified, but we also note that the vents themselves are transient in nature and may disappear and reappear due to sand migration. The major discharge areas are confined to two clusters, only several meters wide, with very little discharge in between and around them.

We found that groundwater discharge is responsible for significant nutrient fluxes to the coastal ocean. Fluxes of dissolved inorganic and organic nitrogen (DIN and DON) are the largest at Hanakao‘o Beach (DIN: 2.9 kmol/d or 41,440 g/d of N and DON: 1.7 kmol/d or 23,700 g/d of N). The second largest DIN flux along this coastline is from Honokowai (1.9 kmol/d or 27,500 g/d of N) and DON flux at SSG (up to 650 mol/d or 9,100 g/d of N). At Hanakao‘o and Honokowai groundwater discharges are 1,200 m and 300 m long, while at the seep clusters the discharge locations are only 50-100 m long. SSG and NSG alone represent the largest sources of DON, dissolved inorganic and organic phosphorus (DIP and DOP) per meter coastline amongst all identified sources. The two seep groups are responsible for fluxes of 100-218 mol/d or 1,400-3,053 g/d of N as DIN, 120-910 mol/d or 1,670-12,750 g of N as DON, 99-116 mol/d or 3,070-3,600 g/d of P as DIP, and 16 mol/d or 485 g/d of P as DOP. These inputs impact coastal water quality and result in elevated nutrient concentrations. At SSG and NSG coastal seawater DIN ranges are 0.38-0.81 μM or 5.3-11.3 μg/L of N as opposed to offshore levels (ambient oligotrophic surface central Pacific Ocean at Station Aloha, data from Karl et al., 2001) of <0.1 μM or <1.4 μg/L of N. DON ranges are 4.8-12.7 μM or 67-178 μg/L of N as opposed to 4.5-6 μM or 63-84 μg/L of N offshore. DIP ranges from 0.16-0.44 μM or 5.0-13.6 μg/L of P in comparison to <0.1 μM or <3.0 μg/L of P offshore. The DOP concentration range of 0.21-0.27 μM or 6.5-8.4 μg/L of P is comparable to offshore levels (Karl et al., 2001). SSG and NSG are not the only location with elevated nutrients, however. For comparison, Hanakao‘o Beach coastal ocean DIN concentrations (7.7 μM or 108 μg/L of N) are 10-times and DIP levels (0.84 μM or 26 μg/L of P) are 2-times higher than at the seep clusters. These elevated nutrient levels may be a result of less intense coastal mixing, lower biotic nutrient uptake, and/or larger nutrient fluxes. In comparison to other studied locations along the coastline, SSG and NSG seep sites had

the lowest observed TN:TP and DIN:DIP ratios in groundwater (2-8 and 1-2) and also in coastal ocean water (15-20 and 2).

The SSG and NSG seeps are distinct from other groundwater discharge sites studied in West Maui in the magnitude of DON, DOP and DIP fluxes per meter shoreline, and their low TN:TP and DIN:DIP ratios. The N:P ratios show that the seeps are enriched in P relative to N when compared to other SGD sites (and to the Redfield ratio of 16:1).

We note that earlier studies identified surface runoff as an important coastal nutrient source (TetraTech, 1993). Our study did not quantify these inputs.

Table 3-1. HR Aquadopp Profiler deployment configuration.

Measurement/burst interval	1 sec
Cell size	30 mm
Orientation	DOWNLOOKING
Distance to bottom	1.00 m
Extended velocity range	OFF
Profile range	0.66 m
Horizontal velocity range	0.55 m/s
Vertical velocity range	0.23 m/s
Number of cells	22
Average interval	1 sec
Blanking distance	0.396 m

Table 3-2. Vertical velocities at Seep 4.

Vertical water velocities per tidal periods at Seep 4 covering the October 1-2, and 17-19, and November 1-3, 2012 HR Aquadopp deployments. Assuming a 13 x 7 cm opening for Seep 4 the velocities are converted to seep discharge (m³/d).

Tidal period	Sum of velocities (m/tidal period)	Average velocity (m/s)	Duration of tidal period (d)	Velocity (m/d)	Discharge (m³/d)
10/1 13:03–10/2 13:06	754	0.0092	1.00*	753	6.9
10/17 11:34–10/18 13:33	271	0.0031	1.08	256	2.3
10/17 15:53–10/18 17:05	363	0.0042	1.05	346	3.1
10/17 22:19–10/18 22:51	502	0.0057	1.02	492	4.5
10/18 05:59–10/19 06:38	557	0.0063	1.03	543	4.9
11/2 12:14–11/3 12:05	901	0.0113	0.99*	907	8.3

*Denote velocities that represent only 24 hours and not an entire 24.8-h tidal cycle

Table 3-3. Calculated groundwater discharge.

Calculated groundwater discharge for Seep 4, SSG, NSG, and all seeps at SSG+NSG. These were derived based on vent areas within each vent cluster. Also expressed are % seep discharge of total submarine groundwater discharge (SGD) at SSG and NSG, respectively. These were derived based on radon mass-balance derived total SGD reported in Glenn et al. (2012).

Tidal period	Discharge Seep 4 (m³/d)	Discharge SSG (m³/d)	Discharge NSG (m³/d)	Discharge All seeps (m³/d)	% total SGD at SSG	% total SGD at NSG
10/1 13:03–10/2 13:06	6.9	63	183	246	0.8	6.2
10/17 11:34–10/18 13:33	2.3	21	62	83	0.3	2.1
10/17 15:53–10/18 17:05	3.1	29	84	113	0.4	2.8
10/17 22:19–10/18 22:51	4.5	41	119	161	0.5	4.0
10/18 05:59–10/19 06:38	4.9	46	132	177	0.6	4.5
11/2 12:14–11/3 12:05	8.3	76	220	296	1.0	7.5

Table 3-4. Groundwater discharge characteristics at SSG and NSG determined using the time-series radon mass balance in June and September 2011 and as based on ADCP measurements at Seep 4 within SSG in October and November 2012.

	Rn time-series model derived		ADCP derived discharge (m³/d)	
	Discharge (m³/d)		Seep vents only	
	Total	Fresh	Total seep	Fresh seep
NSG	2,500 ¹ -3,400 ²	1,500 ¹ -3,100 ²	62-220 ³	55-194 ⁴
SSG	5,900 ¹ -9,200 ²	4,600 ¹ -7,800 ²	21-76 ³	19-69 ⁴

¹Measured in June 2011.

²Measured in September 2011.

³Measured Oct 11-12, 17-19, Nov 2-3, 2012.

⁴SSG salinity = 3 at Seeps 3, 4, 5, 11; NSG salinity = 4 at Seeps 1, 2, 6, 7, 8, 9, 10, 12, 13, 14, 15, 16, 17, 18, 19, 20, and 21.

Table 3-5a. Radon mass-balance derived groundwater discharge at locations identified as groundwater discharge sites along the Kaanapali coastline.

Radon mass-balance derived groundwater discharge at locations identified as groundwater discharge sites along the Kaanapali coastline during the radon survey in June and September 2011. Corresponding groundwater (GW) nutrient concentrations and N:P ratios in seeps, springs, and groundwater wells are indicated in units of $\mu\text{mol/L}$. For springs and wells we list averages from June and September 2011 samplings, which resulted in reproducible nutrient concentrations with standard deviation of the averages between 5 and 35%. For NSG and SSG June and September averages are listed separately as an observed range due to large changes in dissolved inorganic nitrogen (DIN) and dissolved organic nitrogen (DON) concentrations. DIN is a sum of nitrate, nitrite, and ammonium. DON is calculated as total dissolved nitrogen less DIN. Dissolved inorganic phosphorus (DIP) is orthophosphate. Dissolved organic phosphorus (DOP) is calculated as total soluble phosphorus minus DIP.

Site Name	Total GW Discharge (m ³ /d)	Fresh GW Discharge (m ³ /d)	Salinity of GW	DIN of GW ($\mu\text{mol/L}$)	DON of GW ($\mu\text{mol/L}$)	DIP of GW ($\mu\text{mol/L}$)	DOP of GW ($\mu\text{mol/L}$)	TN:TP	DIN:DIP	DON:DOP
Black Rock ¹	2,250	2,130	1.87	234.2	64.4	4.5	3.1	39	52	20
SSG	6,300	4,950	7.46	12.8-28.6	14.6-103	11.7-13.4	1.7	3-8	1-2	8-60
NSG	2,500	1,600	12.64	8.1-15.1	11.1-104	10.3-12.7	1.9	2-8	1	6-55
S. Honokowai ²	7,100		0.44	131	23	2.1	0.3	65	63	75
N. Honokowai ²	7,900		0.44	131	23	2.1	0.3	65	63	75
Hanakao‘o Beach ³	28,000		0.37	106	60	7.2	1.9	18	15	32

¹Nutrient concentrations given as an average of three measured values in Kaanapali 1 and Kaanapali 2 springs in June and September 2011, standard deviation for all averages are 6-20%.

²Nutrient concentrations given as an average of four measured values in Kaanapali P5 and Kaanapali P6 wells in June and September 2011, standard deviation for all averages are 20-35%.

³Nutrient concentrations given as an average of two measured values in Hahakea 2 well in June and September 2011, standard deviation for all averages are 5-20%.

For well and spring locations refer to Glenn et al., 2012: Figure 6-2 and 6-3.

Table 3-5b. Groundwater discharge in million gallons per day (mgd) and nutrient concentrations expressed as micrograms per liter ($\mu\text{g/L}$).

Site Name	Total GW Discharge (mgd)	Fresh GW Discharge (mgd)	Salinity of GW	DIN of GW ($\mu\text{g/L N}$)	DON of GW ($\mu\text{g/L N}$)	DIP of GW ($\mu\text{g/L P}$)	DOP of GW ($\mu\text{g/L P}$)	TN:TP	DIN:DIP	DON:DOP
Black Rock ¹	0.59	0.56	1.87	3,281	902	141	97	39	52	20
SSG	1.66	1.31	7.46	179-401	204-1,445	361-415	53-54	3-8	1-2	8-60
NSG	0.66	0.42	12.64	113-211	156-1,460	319-393	58	2-8	1	6-55
S. Honokowai ²	1.88		0.44	1,841	323	64	10	65	63	75
N. Honokowai ²	2.09		0.44	1,841	323	64	10	65	63	75
Hanakao‘o Beach ³	7.40		0.37	1,480	846	222	58	18	15	32

Table 3-6a. Radon mass-balance derived groundwater fluxes and groundwater discharge per meter shoreline.

Radon mass-balance derived groundwater fluxes and groundwater discharge per meter shoreline at locations identified as groundwater discharge sites during the radon survey in June and September 2011. Nutrient fluxes estimated from the seeps (SSG and NSG) and coastal springs (Black Rock) represent best estimates, as we were able to measure the nutrient enrichment in groundwater at the point of discharge. At other sites (Honokowai and Hanakao‘o) where discharge occurs as diffuse seepage or from an individual spring that cannot be located. Because it is impossible to sample groundwater at the sediment-water interface, we sampled upstream of these coastal locations in wells used as a groundwater end-member. This is done with the assumption that the groundwater nutrient signature is preserved over its flow path to the coastal zone. Depending on land-use, organic matter content, geology, etc. this assumption may not be correct.

Site Name	Total GW Discharge (m ³ /d)	Total GW Discharge (m ³ /m/d)	DIN Flux (mol/d)	DON Flux (mol/d)	DIP Flux (mol/d)	DOP Flux (mol/d)	DIN Flux (mmol/m/d)	DON Flux (mmol/m/d)	DIP Flux (mmol/m/d)	DOP Flux (mmol/m/d)
Black Rock ¹	2,250	6	527	145	10	7.0	1,424	392	28	12
SSG	6,300	63	80-180	92-650	73-84	11	804-1,802	917-6,498	735-844	110
NSG	2,500	47	20-38	28-260	26-32	5.0	380-711	524-4,914	485-598	90
SSG+NSG*		55					2,200	540	700	
S. Honokowai ²	7,100	65	933	164	15	2.2	8,481	1,487	134	20
N. Honokowai ²	7,900	46	1,038	182	16	2.4	6,106	1,071	97	14
Hanakao‘o Beach ³	28,000	23	2,958	1,692	201	52	2,465	1,410	168	44

¹Fluxes calculated based on an average of three measured nutrient values in Kaanapali 1 and Kaanapali 2 springs in June and September 2011, standard deviation for all nutrient averages are 6-20%.

²Fluxes calculated based on an average of four measured nutrient values in Kaanapali P5 and Kaanapali P6 wells in June and September 2011, standard deviation for all nutrient averages are 20-35%.

³Fluxes calculated based on an average of two measured nutrient values measured in Hahakea 2 well in June and September 2011, standard deviation for all nutrient averages are 5-20%.

For well and spring locations refer to Figure 6-2 and 6-3 in Glenn et al., 2012.

*Estimate from Swarzenski et al., 2012 as combined SSG+NSG nutrient loading per meter coastline.

Table 3-6b: Groundwater discharge in million gallons per day per meter shoreline (mgd/m) and nutrient concentrations expressed as gram per meter per day (g/m/d).

Site Name	Total GW Discharge (mgd/m)	Total GW Discharge (mgd/m)	DIN Flux (g/d N)	DON Flux (g/d N)	DIP Flux (g/d P)	DOP Flux (g/d P)	DIN Flux (g/m/d N)	DON Flux (g/m/d N)	DIP Flux (g/m/d P)	DOP Flux (g/m/d P)
Black Rock ¹	0.59	0.0016	7,381	2,030	316	219	19.9	0.39	1.4	0.59
SSG	1.66	0.017	1,126-2,524	1,285-9,104	2,276-2,613	340	11.3-25.2	0.9-6.5	22.7-26.1	3.3-3.4
NSG	0.66	0.012	282-528	389-3,649	797-982	145	5.3-9.9	7.3-69	15-19	2.7
SSG+NSG*		0.015					31	7.6	22	
S. Honokowai ²	1.88	0.017	13,070	2,292	457	68	119	21	4.2	0.62
N. Honokowai ²	2.09	0.012	14,543	2,550	508	76	86	15	3.0	0.45
Hanakao‘o Beach ³	7.40	0.006	41,437	23,701	6,229	1,617	35	20	5.2	1.3

*Estimate from Swarzenski et al., 2012 as combined SSG+NSG nutrient loading per meter coastline.

Table 3-7a. Nearshore coastal surface water (SW) nutrient concentration ranges in waters affected by groundwater discharge.

Site Name	Total GW Discharge (m ³ /d)	DIN of SW (µmol/L)	DON of SW (µmol/L)	DIP of SW (µmol/L)	DOP of SW (µmol/L)	TN:TP	DIN:DIP	DON:DOP
Black Rock	2,250	0.6-11	5.3-13	0.1-0.3	0.26-0.32	27	17	30
SSG	6,300	0.46-0.81	5.6-10.8	0.20-0.44	0.21-0.27	15	2	36
NSG	2,500	0.38-0.57	4.8-12.7	0.16-0.28	0.24-0.27	20	2	33
S. Honokowai	7,100	0.5-1.2	4-9.3	0.12-0.15	0.23-0.27	19	6	26
N. Honokowai	7,900	0.35-0.7	5.3-12.3	0.08-0.13	0.26-0.33	23	4	32
Hanakao‘o Beach	28,000	1.1-7.7	4.5-17.6	0.12-0.84	0.24-0.28	23	9	40
Offshore surface Pacific (Karl et al., 2001)		0.001-0.1	4.5-6	0.01-0.1	0.15-0.25	15-25	<5	15-30

Table 3-7b. Groundwater discharge in million gallons per day (mgd) and nutrient concentrations expressed as micrograms per liter (µg/L).

Site Name	Total GW Discharge (mgd)	DIN of SW (µg/L)	DON of SW (µg/L)	DIP of SW (µg/L)	DOP of SW (µg/L)	TN:TP	DIN:DIP	DON:DOP
Black Rock	0.59	8.4-154	74-182	3.0-9.3	8.1-9.9	27	17	30
SSG	1.66	6.4-11	78-151	6.2-14	6.5-8.4	15	2	36
NSG	0.66	5.3-8.0	67-178	5.0-8.7	7.4-8.4	20	2	33
S. Honokowai	1.88	7.0-17	56-130	3.7-4.6	7.1-8.4	19	6	26
N. Honokowai	2.09	4.9-9.8	74-172	2.5-4.0	8.1-10	23	4	32
Hanakao‘o Beach	7.40	15-108	63-247	3.7-26	7.4-8.7	23	9	40
Offshore surface Pacific (Karl et al., 2001)		0.014-1.4	63-84	0.31-3.1	4.6-7.7	15-25	<5	15-30

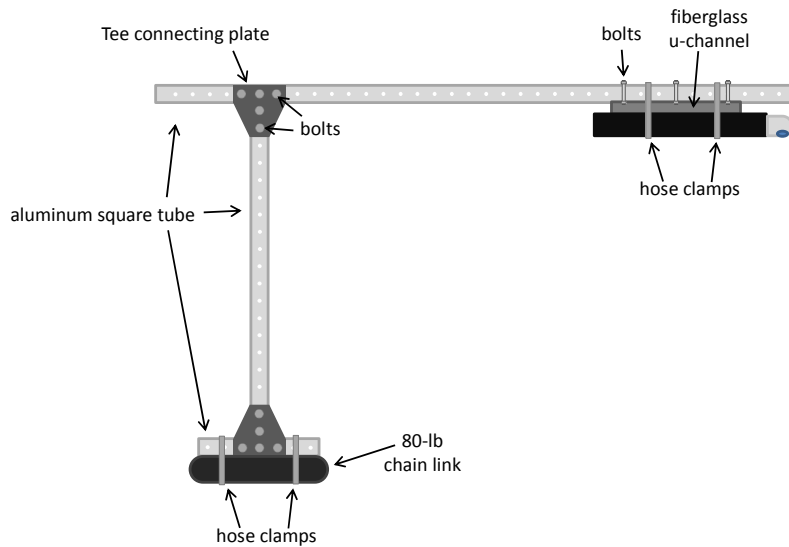


Figure 3-1: Mounting arrangement for the down looking HR Aquadopp profiler. Down-looking HR Aquadopp profiler deployment for seep vertical velocity measurements (sketch by J. Sevadjan).

The profiler is mounted on the horizontal arm head downward at 1 m above the sea floor.

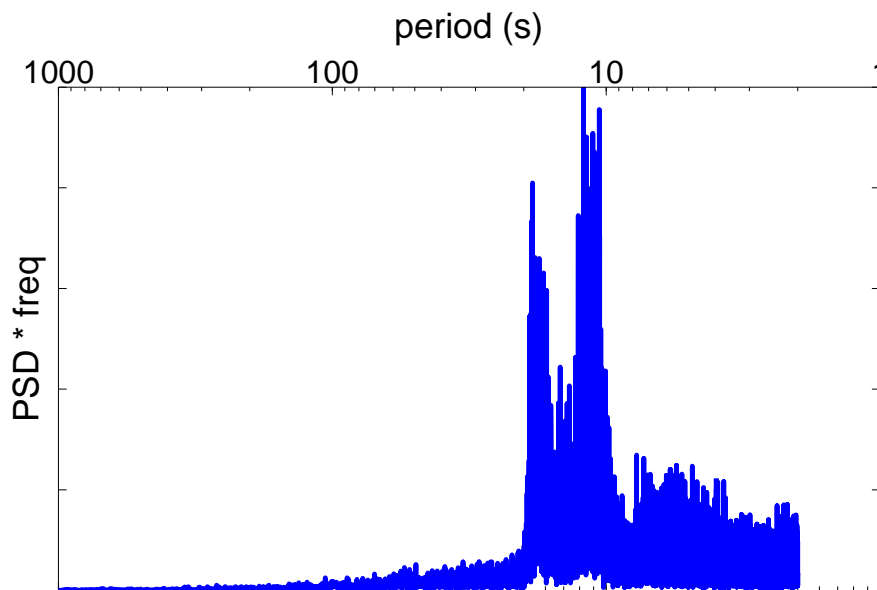


Figure 3-2: ADCP vertical velocity spectral analysis graph. Spectral analysis of vertical velocities from the Oct. 17-19, 2012 deployment.

The two peaks in the vertical velocity spectra are at periods $T \sim 10-13$ s and $18-21$ s, likely due to a combination of shorter- and longer-period surface swell.

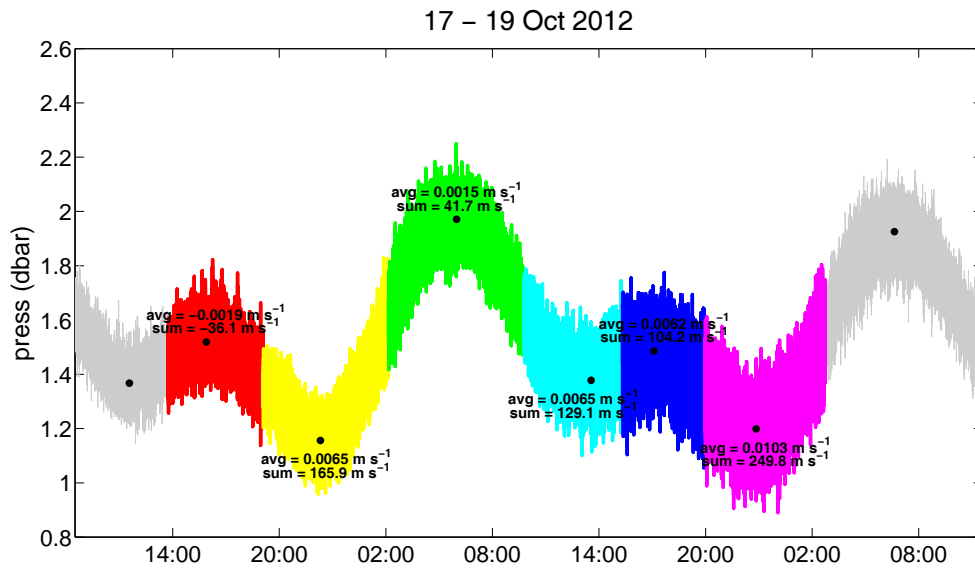


Figure 3-3: Tidal stage and ADCP measured vertical velocities averaged over tidal intervals. Tidal stage measured by the HR Aquadopp Profiler with demarcated low and high tide periods. Calculated averages and sums of vertical water velocities over the respective time periods are indicated at each interval.

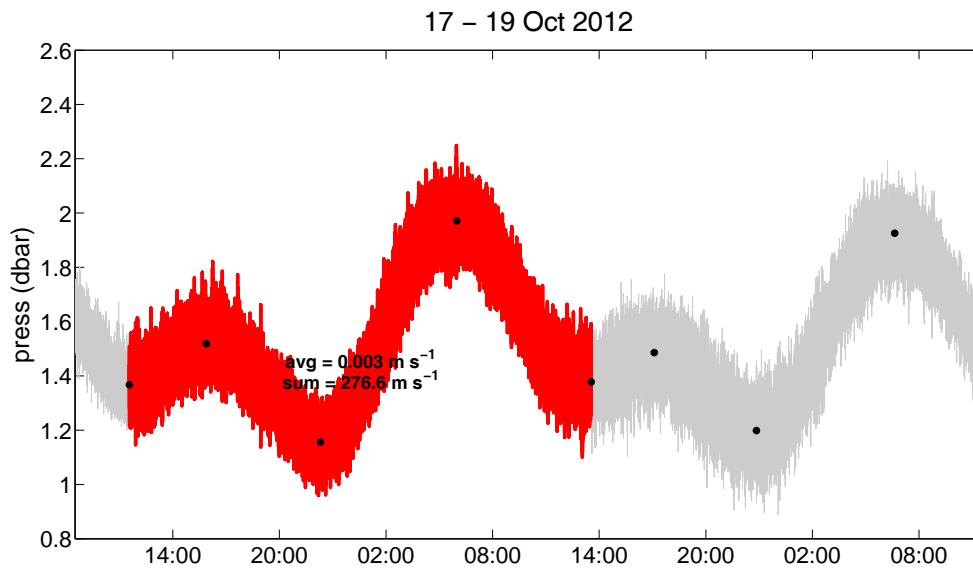


Figure 3-4: Tidal stage and ADCP measured vertical velocities averaged over demarcated interval. Tidal stage measured by the HR Aquadopp Profiler with demarcated full tidal period between two higher-low tides. Calculated average and sum of vertical water velocities represent the whole demarcated interval.

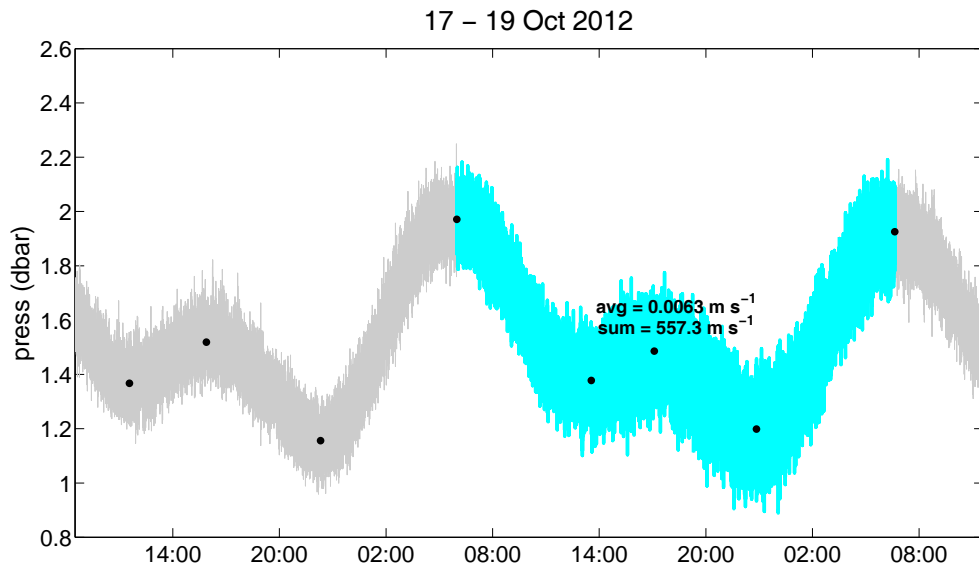


Figure 3-5: Tidal stage and ADCP measured vertical velocities averaged over period between higher tides.

Tidal stage measured by the HR Aquadopp Profiler with demarcated full tidal period between two higher-high tides. Calculated average and sum of vertical water velocities represent the whole demarcated interval.

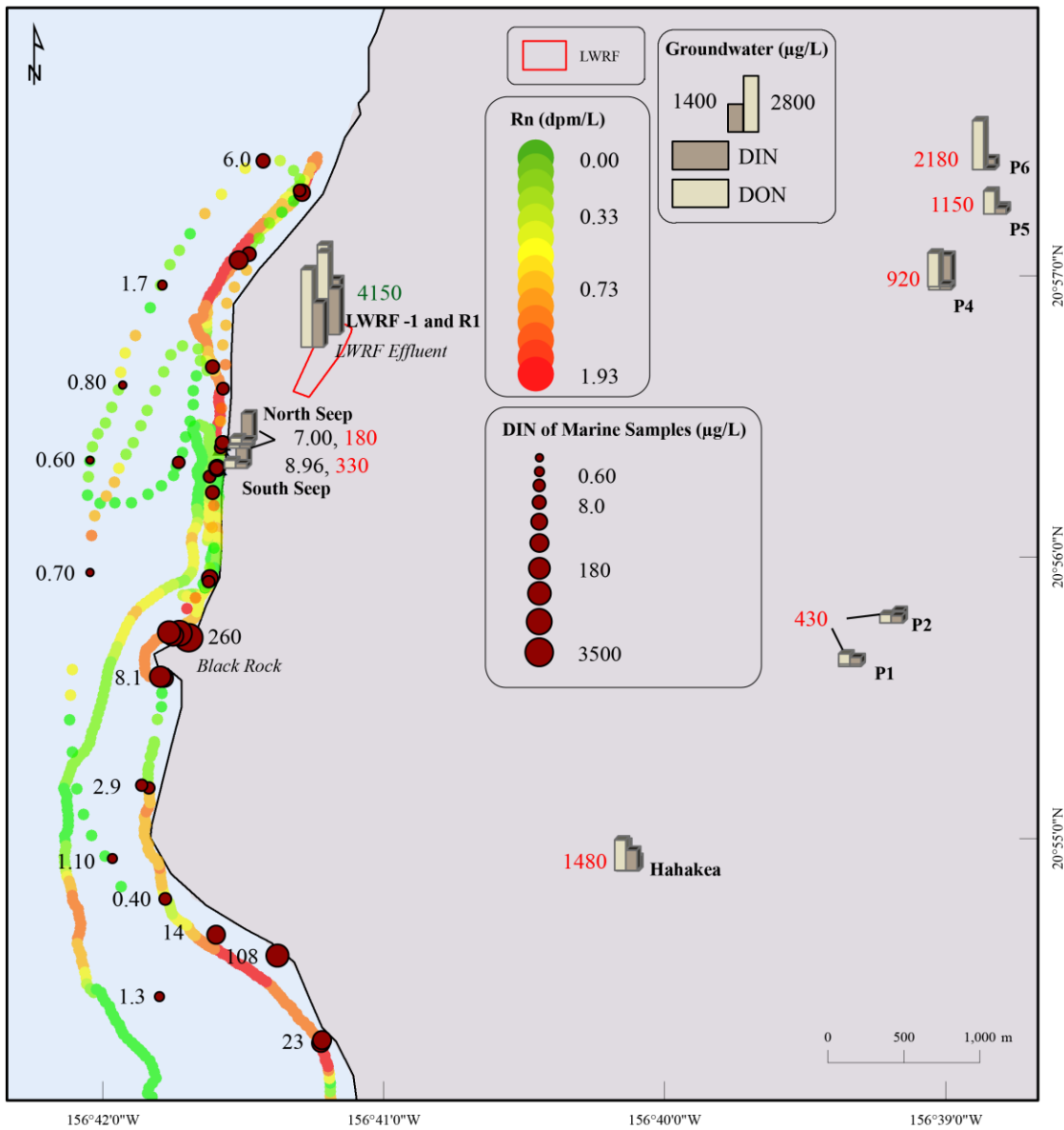


Figure 3-6: Groundwater and surface water nitrogen concentrations (µg/L). Groundwater (averages from June and September 2011) and surface sea water nitrogen concentrations in the Kaanapali coastal region.

The bars indicate groundwater dissolved inorganic and organic nitrogen (DIN and DON) concentrations and red numbers stand for average DIN values. The injected water at LWRF has its average DIN value in green. Coastal surface water samples are indicated by filled circles with DIN concentrations in black letters. Also plotted is coastal radon where red circles indicate elevated radon and large groundwater discharge (see Table 3-5). The figure suggests that coastal nitrogen is elevated where higher radon values indicate groundwater inputs to the coastal ocean.

This page is intentionally left blank

SECTION 4: FLUORESCENT DYE GROUNDWATER TRACER STUDY

4.1 Introduction

This section describes the results of this project's fluorescent dye tracer test at the site of the underground injection of treated wastewater at the Lahaina Wastewater Reclamation Facility (LWRF), north of the town of Lahaina, Maui, Hawaii (Figure 4-1). At the LWRF, the treated wastewater is injected into four wells, designated Injection Wells 1 through Well 4. The fluorescent dye tracer test provided critical data about the hydrological connection between the treated wastewater effluent injected and coastal waters, confirming the locations where the injected treated wastewater effluent discharges into the coastal waters, and determining a transit time of the treated wastewater from the injection wells to the coastal waters. Fluorescent dye was added to the effluent prior to injection followed by a robust surveillance program to monitor the dye arrival to the nearshore marine environment. Figure 4-1 shows the location of the LWRF, the injection wells, and the submarine springs (seeps) where the dye was monitored. Two tracer tests were conducted using fluorescent dyes. In the first tracer test, fluorescein (FLT) was added to Injection Wells 3 and 4. This was followed two weeks later by an addition of sulpho-rhodamine-B (SRB) into Injection Well 2, which has a significantly higher injection capacity than the other three wells. The second tracer test was designed to investigate whether the effluent from Well 2 discharged into the marine environment at the same location as that of Wells 3 and 4.

The only confirmed detection by the tracer dye-monitoring program has been FLT. This dye's first arrival occurred about three months following its addition to the LWRF's effluent stream. The concentration of this dye at the submarine springs peaked 9 to 10 months following the initiation of the tracer test. There was no confirmed detection of SRB, although low-level elevated fluorescence in the SRB wavelength range was observed in four samples collected in February 2012 and December 2012. These samples showed SRB fluorescence slightly above the method detection limit (MDL) of 0.05 ppb and wavelength spectra consistent with SRB. The reason for the lack of definitive detection of SRB at the submarine springs remains inconclusive. As discussed below, factors such as dye degradation, sorption onto the aquifer matrix, or plume displacement by the discharge from Well 3 and Well 4 could account for the failure of this dye to reach the monitored submarine springs. One process of SRB degradation is deaminoalkylation (Käss, 1988) that causes the original SRB fluorescence to shift to a shorter wavelength. Evaluating samples for deaminoalkylated SRB (DA-SRB) was done in this study by performing fluorescent wavelength scans of nearly 100 samples. No samples had characteristics consistent with the deaminoalkylation of SRB.

4.1.1 Tracer Dye Selection

Many techniques exist for tracking the movement of groundwater using introduced or natural tracers. As specified by Stanley et al. (1980), an ideal tracer should be non-toxic, chemically stable over the duration of the tracer test, and detectable at very low concentrations. In addition, the tracer should move with the flow of groundwater and not be removed by natural filtration. Finally, and most importantly, it should not be naturally present in concentrations that would make it difficult to discriminate the added dye from the natural occurrence of the tracer.

There is no ideal tracer, but suitable candidates include ionic salts (Wood and Dykes, 2002; Levy and Chamber, 1987; Olsen and Tenbus, 2004), fluorescent dyes (Smart and Laidlaw, 1977; Chua et al., 2007; Flury and Wai, 2003; Sabatini, 2000), dissolved gases (Malcolm et al., 1980; Wilson and McKay, 1993), radionuclides (Section 3 of this report), and spores and bacteria (Davis et al., 1980; Harvey, 1997). Ionic salts are attractive because they can be detected in low concentrations with ion specific probes. The most widely used are chloride and bromide salts. In this study, interference from marine salts was a problem due to the existence of seawater chloride. The bromide ion is present in Hawaii groundwaters at concentrations of 0.06 milligrams per liter (mg/L) to 0.8 mg/L (Hunt, 2004) making this an attractive secondary tracer. However, in this study, the tracer was monitored at submarine springs where a mixture of freshwater and re-circulated seawater was discharging. The seawater dissolved bromide-concentration measured by this study in September, 2011 varied from 9.1 to 14 mg/L and that measured at the submarine springs varied from 0.83 to 1.4 mg/L. The high tracer concentration required to overcome the interference from seawater bromide made this option too expensive. The presences of dissolved gas tracers can be monitored on-site and in low concentrations (Davis et al., 1980), but the equipment is bulky and expensive. Radionuclides have safety and regulatory issues, while the special techniques needed to analyze for spores and bacteria are not field friendly.

The tracer of choice for many studies is fluorescent dyes. They are non-toxic (Field et al., 1995), detectable at parts per trillion concentrations with a fluorometer, many are stable, and tend to remain in solution rather than sorbing to the aquifer matrix or onto suspended particulate matter. For these reasons the yellow-green dye FLT and the orange-red dye rhodamine WT (RWT) are the most widely used of this class of tracers. The tracer dyes considered for this study were FLT, RWT, and SRB. FLT was selected as for this study because it has strong fluorescence, is economical, is stable in groundwater with little sorption or decay, and is compatible with existing equipment at UH. A second dye was needed that could be distinguished from FLT if the two dyes were in the same sample. The rhodamine dyes have an excitation/emission wavelength couple that is significantly longer than that of FLT reducing or eliminating analytical interference. SRB was chosen over RWT for this study because RWT occurs as two isomers with differing sorption characteristics (Sutton et al., 2001). As the transit time of RWT increases the two isomers would tend to separate in the flow path resulting in confusion when analyzing the breakthrough curve. Both FLT and SRB can be analyzed with existing equipment at the Hawaii Department of Health laboratory.

FLT was chosen as the primary tracer dye for tracing the primary wastewater effluent injections in Wells 3 and 4. FLT is a yellow-green dye that has been used in tracer studies since the end of the 19th century (Smart and Laidlaw, 1977). FLT is non-toxic to humans and the environment at concentration ranges used in tracer tests (1 to 2 mg/L) (Field et al., 1995). This dye has the advantage of being relatively economical and widely available. A disadvantage for this study is that some constituents in wastewater have fluorescence characteristics that may be similar to that of the tracer.

During fluorescence analysis, a dye is bombarded with light energy of a specific wavelength (the excitation wavelength – “ex”), and the energy state of the dye molecule is elevated. The dye then emits light of another wavelength (the emission wavelength – “em”) (Brown, 2009; Guilbault, 1990). Literature reviews showed that the most common values for ex/em couples for fluorescein were 490/520 nm (Smart and Laidlaw, 1977; Kasnavia et al., 1999; Sabatini, 2000). In water, Käss (1998) lists the ex/em wavelength couple for FLT as 491/512. Other constituents in water, and particularly wastewater, emit light energy at similar wavelengths. Galapate et al. (1998) found fluorescence peaks at 524 nm for gray water and 531 nm for sewage effluent close to that of FLT. These findings necessitated a thorough background fluorescence investigation and resulted in this study using tracer dyes at concentrations high enough to overcome such interference problems. In addition, FLT is unstable when exposed to artificial or natural light; a process that alleviates problems with dye coloring the nearshore waters, but necessitates the collection of samples in dark colored or opaque bottles. Because the travel path for the tracer test is underground, no photodegradation occurred prior to sample collection. Fluorescence of FLT also decreases at pH values less than 6.5 (Smart and Laidlaw, 1977). The pH of the effluent sampled in this study varied from 6.5 to 7.1, while the pH of the samples collected at the submarine springs varied from 7.2 to 7.9 (see Section 2). Hence, for this study, the pH of the water sampled does not adversely affect the fluorescence of FLT.

SRB is a red dye that is commonly used in wastewater investigations. Literature lists various ex/em couples for SRB. For example, Smart and Laidlaw (1977) list values 565/590, Nikon (<http://www.microscopyu.com/articles/fluorescence/filtercubes/green/greenhome.html>) and Käss (1998) list values of 565/586 and 560/584 nm, respectively. These are significantly longer than that of wastewater effluent reducing interference. It is stable in waters with a pH higher than 5 (Smart and Laidlaw, 1977). SRB was selected over RWT because RWT occurs in two isomers with differing sorption characteristics (Sutton et al., 2001). As the transit time of the tracer dye increases, there would be a separation of the two isomers resulting in double-peaked breakthrough curves with added difficulties for interpretation. Due to the good separation in the wavelength spectrum between FLT and SRB, SRB is recommended as a secondary tracer when FLT is used as primary tracer (Käss 1998).

4.1.2 Preliminary Planning

The preliminary planning for the tracer test sought to accomplish four goals: (1) estimate a minimum dye concentration that could be reliably detected at the submarine springs; (2) estimate the amount of dilution of the tracer that would be expected between the point of addition at the injection wells and the point of sampling at the submarine springs; (3) estimate the time of first arrival at the submarine springs; and (4) develop a dye addition schedule to ensure that the dye plume is of sufficient temporal length, thereby not missing the tracer if the time to first arrival is short. The first goal was accomplished by testing the natural fluorescence in the FLT wavelength of different waters. This was only done for FLT because the literature search indicated that the fluorescence interference between this dye and wastewater was much greater than that for SRB. The second and third goals were accomplished using a groundwater flow and transport model.

The potential interference between FLT and the effluent raised significant concern during the development of the project's Work Plan. To investigate this possible problem, the fluorescence of treated wastewater, natural groundwater, municipal tap water, and coastal seawater was measured using a Turner Designs 10AU Fluorometer with the FLT optics package installed. The treated wastewater was collected from the LWRF, while natural groundwater was collected from the Waipahu III Wells in Waipio, Oahu, Hawaii. Seawater was collected from an exposed section of the coastline located on southwest Oahu, Hawaii. The treated wastewater was filtered with a coffee filter to remove the majority of the suspended solids, and then its fluorescence was measured. As shown in Figure 4-2, the fluorescence (in raw fluorescence values) of tap water, groundwater, and seawater were very low and nearly identical. The treated wastewater fluorescence was nearly identical to that of a 1 ppb FLT standard. The fluorescence of the 10 ppb FLT standard, however, was an order of magnitude greater than the treated wastewater.

The minimum concentration of a dye that can reliably be detected by a fluorometer depends on the fluorescence of the dye, the background fluorescence of the water in which the dye is added, and the variability of the background fluorescence. Our initial background fluorescence assessment (Figure 4-2) did not account for the variability of the background fluorescence because only a single wastewater sample was evaluated. Thus, for the tracer test planning, a worst-case detection limit equal to the natural 1 ppb fluorescence of the LWRF treated wastewater was assumed. If there was no fluorescence loss in the wastewater from the time of injection to the time of submarine spring discharge, samples collected at the submarine springs could possess FLT range fluorescence equivalent to 1 ppb of this dye. Mixing with natural groundwater could reduce the fluorescence and result in significant variability. This means that if the natural FLT wavelength fluorescence measured at the submarine springs varied significantly around the 1 ppb fluorescence of the wastewater and, based on the evidence available during the planning phase, it could take up to 1 ppb of fluorescence from FLT to be reliably detected.

A groundwater flow and transport model was used to evaluate the dilution of the tracer dye due to dispersion as it traveled from the injection wells to the submarine springs as

well as to estimate the time to first arrival. This section provides a description of the model and the results that pertain to the planning of the tracer test. Details of the application of this model can be found in Section 5. Figure 4-3 shows the Tracer Test Design Model (TTDM) breakthrough curves for the North Seep Group (NSG) and the South Seep Group (SSG) depicted in Figure 4-1. The results from this model indicated that by the time the tracer plume reached the NSG monitoring point, the dye concentration will have decreased by about three orders of magnitude. It further showed that approximately 108 days would elapse before the dye concentration would be high enough to be discernible from the background fluorescence (based on a detection limit of 1 ppb). This model indicated that only a small concentration of dye would be detected at the SSG, a result that proved to be inaccurate. However, the TTDM did meet the primary goals the tracer test preliminary design by estimating that a three order of magnitude dye dilution needed to be accounted for, that it would take about three months for the dye to emerge at the submarine springs, and the breakthrough curve (BTC) would take years to fully develop.

Although the TTDM predicted a time to first arrival of about three months, much shorter times to first arrival were not discounted during the tracer test planning. Tetra Tech (1993) developed a groundwater model that indicated the transit time of the effluent to the shoreline as short as ten days if there were a preferential pathway such as a lava tube. Thus, a broad range of times to first arrival were accounted for by using a front-end loaded monitoring program. Daily sampling began three weeks prior to the first dye addition to characterize the background fluorescence at the study site. Upon addition of the first dye into Injection Wells 3 and 4, the frequency to sample all locations was increased to twice a day, and this pace continued for four weeks after the second dye addition. An additional sample was collected from one of the submarine springs each night until a week after the second dye addition. Daily sampling occurred at the submarine springs between five and eight weeks after the second dye addition. The frequency was decreased with the increase of time following the dye addition. During the final month of the field sampling (December 2012), samples were only collected twice a month from the submarine springs. Section 2.2.2 details the field-sampling program. It is important to point out that this front-end loading sampling approach ensured that any dye discharge resulting from fast-preferential flow path would not be missed by this study.

4.2 The Injection Wells 3 and 4 Tracer Test

The first dye addition was into the south well group (Injection Wells 3 and 4) using FLT (see Figure 4-4 for a line diagram of the LWRF system) on July 28, 2011. The target dye concentration in the effluent was approximately 12,500 ppb based on an assumed injection rate of 2.5 million gallons per day (mgd) into this well group. The dye was received from the vendor in a powder form that was 77% active ingredient by weight. The dye was mixed on site in a utility shed by using ten pounds (lbs) of powder (one-half of a 20 lb bucket) and a sufficient amount of water to make 50 gallons (gal.) of dye solution. The strength of this concentrate was 1.8% active ingredient by weight. The powder was dissolved into the water using a heavy-duty paint/mortar mixer with a helical

mixing paddle (Figure 4-5). The shaft length was extended from 15 inches to 36 inches for use in the 55-gallon plastic drum. The mixing was done into two drums at a time so the entire contents of one powder bucket could be used during a single mixing iteration. Once mixed, the concentrate was transferred to 5 gal. pails using a small utility pump (Figure 4-6). The pails had screw-on lids with a sealing gasket to prevent spillage. The pails were then delivered from the mixing site to the injection wells via pickup truck. The dye was added to the injection wells through a port on the top flange of the well casing using a small submersible fountain pump (Figure 4-7). When the level in the bucket got below the suction of the fountain pump, the remaining dye concentrate was directly poured into the well port (Figure 4-8). A dose of dye was added every 15 minutes at an appropriate rate to sustain the target concentration of 12,500 ppb. Dye addition started at 07:00 on July 28th 2011 and continued uninterrupted until 02:00 on July 29th 2011 (Figures 4-9 and 4-10).

Two hundred and sixty-two lbs of active ingredient, or 340 lbs of total FLT powder weight, were procured for this event. The actual weight of dye added was slightly less than this amount due to minor spillage. At the planned mixing rate, this weight of powder should produce 1,700 gal. concentrate, which represents 34 drums and 340 buckets of liquid, with expected measurement error. Based on records kept at the wells, a total of 1,670 gal. concentrate was added to the wells. The dye addition was terminated one hour early because the dye was expended. It was determined upon review of the mixing volumes and the rate at which the dye powder buckets used that one drum was mixed to a concentration twice as much as the target value. When this mixing error was taken into account, the planned volume added would be 1,650 gal. This leads to a difference of a little over 1%, well within the certainty of measurement methods.

Figure 4-11 compares actual FLT concentration in the effluent to the rate of effluent injection. The tracer addition started at the onset of the 07:00 morning increase in effluent discharge. The initial pulse addition of FLT was small giving a starting dye concentration of about 4,400 ppb. However, by 08:00, the dye addition rate had been increased to match the rise in effluent injection, resulting in a dye concentration of about 12,500 ppb. There was slight variation in both the injection rate into these wells and dye concentration during the hours from 09:00 on July 28th 2011 through hour 00:00 on July 29th 2011. The injection rate was 3.2 +/- 0.25 mgd. The average dye concentration was 13,700, varying between 12,500 and 14,300 ppb. Just after midnight, the effluent injection rate started to decrease resulting in a dye concentration of 17,400 ppb during the final hour of dye addition. The average FLT concentration in Wells 3 and 4 during dye addition was 13,140 ppb. When injection into all of the wells is considered, the average addition concentration was 10,010 ppb.

4.2.1 Fluorescein Analysis

4.2.1.1 Fluorometer

In fluorescence analysis, the sample is subjected to a beam of light with a wavelength (excitation wavelength) specific to the species being analyzed. This excites the atoms of the analyte, which emits light at another wavelength (the emission wavelength). The FLT concentration was measured in the laboratory using a Turner Designs 10-AU Fluorometer (Turner Designs, 1999), which is capable of detecting FLT concentrations as low as 0.01 ppb. This instrument is equipped with a 10-086R optical kit that includes a blue mercury vapor lamp, a 486 nm excitation filter, a 510-700 nm emission filter, and 485 nm and higher reference filter.

4.2.1.2 Sample Handling

Once received at UH, the samples were stored in an air-conditioned room until they were filtered and analyzed. The fluorescein analyses were completed at UH in an air-conditioned room, separate from the building where the filtering was done. When filtering, a sample aliquot was discharged into an opaque brown HPDE Nalgene bottle to prevent photodegradation. After filtering, the samples were taken to another building for analysis. Because the temperature of analysis room is much colder (16–19°C) than the filtering room, the samples were stored in the analysis room overnight to allow the samples and calibration solutions to become temperature equilibrated prior to analysis.

Upon completion of all analyses the samples were refrigerated. The time between sample collection and completion of analysis was up to 1.5 months. Delay in sample refrigeration could result in faster biological degradation of the dye in the samples and in the calibration solutions. To evaluate the stability of the dyes, we stored the calibration solutions on the shelf, and not in the refrigerator. As part of the calibration process, we read the raw fluorescence of the standards (10 ppb only for fluorescein and all solutions for SRB) to document any change in fluorescence intensity with time. Thus, if degradation during storage were a factor, it would be detected by a decrease in the raw fluorescence intensity of the unrefrigerated calibration solutions. We also routinely completed synchronous scans of selected solutions to document any change in the wavelength spectrum of the solutions. No signs of degradation were found.

In consultation with the EPA, we revised our sampling handling procedures to minimize the time that samples were not refrigerated. Upon receipt of the samples at the UH, they were immediately filtered or placed in a refrigerator until they could be filtered. Once the samples were filtered, they were delivered to the laboratory room where the analysis was done. They were again stored overnight in the room where the temperature varies between 16 to 19°C, and were then analyzed the next day. The samples were also stored in this laboratory room until taken to the HDOH laboratory for SRB analyses. This typically occurred within a few days after the FLT analyses.

4.2.1.3 Laboratory Analysis

4.2.1.3.1 Fluorometer Calibration

FLT calibration solutions were mixed to establish a basis for converting the measured fluorescence to a concentration of FLT. These calibration solutions were prepared by diluting a 100,000 ppb stock solution with water. Initially, deionized (DI) water was used, but this produced unstable solutions, due to the low pH of DI water (See Section 4.2.1.3.2 below). Subsequent solutions were prepared using submarine spring water that collected prior to the dye addition. The submarine spring water was filtered with 0.45-micron paper prior to mixing the solutions.

An initial FLT stock solution with a concentration of 100,000 ppb was made by adding 133 mg of 75% active-ingredient FLT powder to a small glass beaker. The dye powder was weighed using a precision scale. 1 L of distilled water was measured in a volumetric flask that was filled to the 1 L mark. The majority of the water in the volumetric flask was decanted into a 1 L amber bottle. The dye powder was then added to the bottle. The water remaining in the volumetric flask was then used to rinse the remaining powder from the small beaker into the solution added to the amber bottle. This stock solution was then used to prepare the calibration solutions. This was accomplished by completing a series of dilutions of the 100,000 ppb stock solution. These serial dilutions were limited to two to minimize propagation error. A 100 ppb calibration solution was made by diluting 1 milliliter (ml) the stock solution with 999 ml of water using a precision pipette and volumetric flask. The remaining dye calibration solutions were mixed using the 100 ppb calibration solution as shown in Table 4-1.

All samples, including the submarine spring water used for preparing the calibration solutions for FLT and SRB, were filtered using a 0.45 micron paper pre-filter prior to analysis. To hold the samples and calibration solutions during analysis, 13-mm glass cuvettes were used. Following a half-hour warm-up period, the system baseline was set using a distilled water blank. The fluorometer span was then set using a 10 ppb FLT calibration solution. Linearity of the instrument response was verified with 0, 1, 10, 20, 50, and 100 ppb FLT solutions.

4.2.1.3.2 Calibration Solutions – Deionized (DI) Water vs. Submarine Spring Water

When mixing solutions for the Method Detection Limit (MDL) study (described in Section 4.2.1.3.3 below) it was found that the measured fluorescence was four times the expected value. The increased fluorescence was confirmed by mixing two FLT solutions using the same mass of dye in each. One solution was mixed using DI water, while the other was mixed using dye-free submarine spring water (collected prior the addition of FLT to effluent stream). The fluorescence of the submarine spring water was read with the fluorometer prior to adding dye to ensure that its natural fluorescence was consistent with background values measured by this study. FLT was added to DI water and submarine spring water solutions to produce concentrations of 1, 10, 20, 50, and 100 ppb. The fluorometer span was set using the 10 ppb submarine spring water based solution and

the linearity was verified with the remaining submarine spring water based solutions. The fluorescence of both sets of solutions was then read with the fluorometer. Figure 4-12 shows that the fluorescence of the submarine spring water solutions was indeed about four times greater than that of the DI water based solutions. All subsequent calibration solutions were mixed using submarine spring water collected prior to the FLT addition. New SRB calibration solutions were also mixed using submarine spring water to maintain consistency between the methods used to analyze the two dyes. However, comparison of the DI and submarine spring water based SRB solutions showed no difference. Using the submarine spring water as a base for the calibration solutions aided when comparing the emission wavelength scans of field collected samples to that of calibration solutions and other laboratory prepared standards.

A literature search confirmed problems related to the use of DI water to mix the calibration solutions. Brown (2009), for example, found that the indicated fluorescence of a FLT solution mixed using distilled water was about one-third of the measured FLT fluorescence when natural spring water was used. This quenching of the FLT fluorescence by DI was due to the lower pH of water with negligible dissolved ion content (i.e., the DI water used in the original calibration solutions). The pH of a DI water based FLT solution was less than 4.0 when measured at the WRRC laboratory at the University of Hawaii. Smart and Laidlaw (1977) show a nearly complete quenching of FLT fluorescence at a pH of 3.0. Dever (1997) calculated the pH of pure water in equilibrium with the atmosphere to be 3.1. Taken together, these references show the problem encountered with the DI-based calibration solutions was due to the low pH of pure water, a problem that was simply resolved by using submarine spring water to mix the calibration solutions

4.2.1.3.3 FLT Method Detection Limit (MDL)

The Method Detection Limit (MDL) is defined as “the minimum concentration of a substance that can be measured and reported with 99% confidence that the analyte concentration is greater than zero, and is determined from analysis of a sample in a given matrix containing the analyte” (Wisconsin Dept. of Natural Resources, 1996). For this study, two methods were used to assess the MDL. The first was that used by the U.S. EPA and is codified in the U.S. Code of Federal Regulations (CFR), 40 CFR Appendix B to Part 136 (USEPA, 2011). This approach is based on a single concentration design, which assumes that variability at a certain concentration is equal to the variability at the true MDL. When using this method, the following conditions are recommended by the USEPA (2011):

- The candidate MDL sample have an analyte concentration one to five times that of the estimated MDL.
- The analyte concentration in the MDL sample should not exceed ten times the actual MDL.
- At least seven aliquots at the candidate MDL concentration need to be analyzed to document the analytical variance.

- The concentration of the MDL candidate should be at least three times solution deviation of the replicate analyses.
- The signal to noise ratio should fall in the range between 2.5 to 5.

Details of this method are provided in Appendix B.

The second MDL assessment method was developed by Hubaux and Vos (1970) who were the first to apply the theory of statistical prediction to estimating the MDL. They defined the limit of detection as the point at which we can have 99% confidence that the response signal is not the critical level, which was defined as the value of the prediction limit for zero concentration (i.e., that no analyte is present in the sample). This method involves the use of a calibration design and assumes that the variability is constant throughout the range of concentrations used in the calibration design. Hubaux and Vos (1970) suggest that the limit of detection can be obtained graphically by locating the abscissa corresponding to the critical level on the lower prediction limit. In order to determine the MDL, a series of samples is spiked at known concentrations in the range of the hypothesized MDL. From these samples, the variability is determined by examining the deviations of the actual response signal on known concentrations. In this case, it is assumed that the distribution of these deviations from the fitted regression line is normal with a constant variance across the range of concentrations used in the study. The details of this method are elucidated in Appendix B.

To accommodate both MDL analysis methods, four sets of solutions were mixed. For FLT, these included concentrations of 0.0, 0.1, 0.2, and 0.5 ppb. The dye, in the appropriate volume, was added to 1 L of unfiltered submarine spring water. Each MDL solution batch was processed in the same way the tracer samples were, including filtering the sample with a 0.45-micron paper pre-filter into a 125 ml brown plastic bottle. This resulted in eight aliquots at each concentration for the MDL analysis. The individual aliquots were then analyzed in the same manner as the tracer samples and the results were entered into an MDL calculator spreadsheet that was downloaded from http://www.chemiasoft.com/mdl_calc.html. The fluorescence values entered were the total fluorescence as read on the fluorometer minus the average no-dye fluorescence. Tables 4-2 and 4-3 summarize the results of the MDL calculations using the methods by EPA and by Hubaux and Vos (1970), respectively. The MDL calculated by the EPA method for the lowest concentration solution (0.1 ppb) was 0.011 ppb. However, this concentration was about one-tenth of the concentration of the lowest solution tested. This resulted in a signal to noise of ratio of 28.6, which was greater than the recommended range of 2.5 to 10.

The MDL calculated by the Hubaux and Vos (1970) method depends on the linearity of multiple concentrations rather than on that of a single concentration and resulted in a slightly higher MDL. For this method, the MDL calculator only allowed three samples per concentration, so the lowest, the highest, and the average concentrations for MDL solution set was entered into the MDL calculator. The resulting MDL was 0.02 ppb above background, slightly higher than that of the EPA method, and was used as the fluorescein MDL for this study. The critical response concentration is the instrument

response (fluorescein plus background) at which the analyte (fluorescein) can be distinguished from background and is considered detected. As described in the next section, the background concentration of FLT was 0.11 ppb, making the MDL 0.13 ppb as read on the fluorometer. The critical concentration is the actual analyte concentration when it is first detected. The MDL differs from the critical concentration in that the former provides concentration values of the analyte detected with 95% certainty.

4.2.1.3.4 Laboratory Quality Assurance

To ensure the accuracy and integrity of the tracer dye analysis program, five quality assurance tests were done: (1) calibrating the fluorometer as described in Section 4.2.1.3.1; (2) challenging the fluorometer with a six calibration solutions that varied in concentration from 0.0 to 100 ppb to check the instrument linearity; (3) completing duplicate analysis of three samples at the end of each analysis run; (4) challenging the fluorometer with calibration standards with a concentration of 0.0 and 10 or 20 ppb at the end of each analysis run; and (5) periodically re-analyzing an archived sample for comparison with the initial analysis. Table 4-4 shows the results of linearity test and the offset calculated for establishing the zero baseline (i.e., no FLT present) of the fluorometer. The linearity of the fluorometer was excellent with coefficient of determination being greater than 0.99 in all cases. The coefficient of the line of best fit varied between 1.00 and 1.03 indicating that a slight adjustment was needed to make to the value that was read on the fluorometer reflect the actual FLT concentration. The baseline offset was that value that needed to be subtracted from the fluorometer reading to set the reference fluorescence of deionized water blank to zero. This value varied from -0.07 to 0.27 ppb. The variation was caused primarily by changes in room temperature where the analysis was done. Table 4-5 shows the results when the fluorometer was challenged with deionized water blank at the end of an analysis run. The expected concentration was 0.00 ppb, while all measured values were within 0.01 ppb of that value. Table 4-6 shows the results when the fluorometer was challenged with 10 or 20 ppb FLT solutions at the end of an analysis run. All differences, with the exception of two cases, were within 5% of that expected value. The maximum difference was 6% at the end of the analytical run on October 3, 2012. In addition, at the end of each analytical run, three samples were selected for duplicate analysis. Table 4-7 shows that the duplicate analysis agreed was within 5% (or 0.1 ppb for primary results less than 1 ppb) of the primary analysis, except for one sample analyzed on October 12, 2012. The difference for that duplicate analysis was 6.5%. The end of the analytical run tests showed that the instrument accuracy did not drift during each analytical run. Finally, Table 4-8 shows the results of the analysis of replicate or archived samples. This test was done to evaluate any change in FLT concentration in a sample over time. Differences for all but three samples were less than 5%. There was a very significant difference in analytical results of two samples collected from Seep 3 on August 1, 2012. The samples were collected within 20 minutes of each other. The cause of this difference is not known. Excluding these, the average difference in the duplicate analyses was -0.2% with a standard deviation of 2.9%. This indicates very little change in sample fluorescence occurred while the samples were in storage.

4.2.1.3.5 FLT Synchronous Scans

FLT spectrum analyses were completed using a Hitachi F4500 Fluorescence Spectrophotometer, which is used to measure the fluorescence, phosphorescence and luminescence in the ultraviolet and visible regions of the spectrum. This instrument is programmable, so that the fluorescence intensity of the wavelengths from 200 to 730 nm can be measured. The Hitachi F4500 was used to evaluate the wavelength spectrum of samples using a process known as synchronous scan.

A synchronous scan is a sequential series of fluorescence measurements performed on a sample. This is done by defining a starting and ending excitation wavelength, and designating an increment by which to increase the excitation wavelength for each step. Also defined when programming a synchronous scan is the emission wavelength monitored as a function of the excitation wavelength. Unless otherwise noted, the instrument was programmed to scan from 400 to 600 nm for the FLT synchronous scans. The spectrophotometer produces a spectra graph and printout (the printout is excitation wavelength versus fluorescence intensity in user-defined increments, usually 2 nm) and an electronic file of fluorescent intensity at 0.2 nm increments of excitation or emission wavelengths. The fluorescence intensity of the emission wavelength monitored was the excitation wavelength plus 20 nm. The FLT synchronous scans were done to evaluate any degradation of calibration solutions and to investigate the presences of fluorophores other than FLT and SRB in the submarine spring samples.

4.2.2 Background Fluorescence Assessment and First Detection

The fluorometer used in this study has a manufacturer specified detection limit of 0.01 ppb for FLT. But fluorescence variability in tracer samples collected in the field may mask very low concentrations of dye. Quantifying the natural fluorescence of the study area and the concentration at which the fluorometer can reliably discriminate between natural and tracer fluorescence is critical in establishing the first arrival time of the dye.

Natural and anthropogenic compounds in the water mixture emerging from the submarine springs have fluorescence characteristics that may mimic that of the dyes selected for this study (Meus et al., 2006; Smart and Karunaratne, 2002). For example, these interferences can be caused by fabric brightener agents that fluoresce in the blue wavelengths (Poiger et al., 1998). Although these agents are expected in the LWRF wastewater effluent, the blue wavelengths are well below that of the dyes used in this study. Other in situ sources of fluorescence, such as fluvic acids, also fall in wavelengths significantly shorter than that of FLT (Baker et al., 2003). More problematic are fluorescent peaks at about 520 nm that have been identified in a number of studies such as that by Smart and Karunaratne (2002), who attributed this peak to antifreeze containing FLT. In a study of the fluorescence of domestic wastes in the Kurose River in Japan, Galapate et al. (1998) showed there was a 531 nm peak in sewage effluent; when effluent was mixed with river water, this peak shifted to a wavelength of 524 nm, which is very close to that of FLT.

Since organic matter may fluoresce in a manner similar to the tracer dyes (Meus et al., 2006; Smart and Karunaratne, 2002), this interference needed to be evaluated. This process consisted of directly measuring the fluorescence of submarine spring water tagged with the tracer dye at various concentrations (see Method Detection Limit, Section 4.2.1.3.3 for details) and measuring the fluorescence of the submarine spring samples collected for a period before the dye arrival.

Our background assessment served two purposes. First, it characterized the background or natural fluorescence in the FLT wavelength. The natural fluorescence values were subtracted from the measured values to quantify that attributable to the dye only. The second purpose is that knowing the background fluorescence is important in estimating the time for a dye's first arrival. Collection of samples from the submarine springs began on July 5th, 2011, more than three weeks prior to the first dye release to the LWRP injection wells. Since dye was not detected in the marine submarine springs (seeps) until mid-October 2011, the samples collected prior to October 1, 2011 were included in the background fluorescence assessment.

Tables 4-9 and 4-10 provide a summary of the fluorescence in the FLT wavelength measured during the background evaluation period. The average background fluorescence for both the NSG and the SSG was equivalent to that 0.11 ppb FLT. There was minor variability except for Seep 4, where the lowest background concentration measured was equivalent to 0.01 ppb of FLT. The small number of samples included in the background analysis was due to problems with the calibration solutions prepared using DI water (previously described). After the fluorometer was calibrated with the submarine spring water calibration solutions, a minimum of twelve background samples from each of the original submarine spring locations were chosen at random and re-analyzed.

The background fluorescence in the FLT wavelength was much less than expected and very small compared to the FLT concentrations measured except those at the very beginning of the tracer breakthrough curve. A value of 0.11 ppb was subtracted from the laboratory measured FLT fluorescence as a background correction for the final FLT concentration. For this study, the time of first dye arrival was defined as when the first measured concentration that equaled or exceeded 0.13 ppb (the computed MDL of 0.02 ppb plus a background fluorescence of 0.11 ppb) and marked the start of an increasing trend in dye concentration. Using a MDL of 0.13 ppb, the first detection of FLT occurred at the NSG on October 20, 2011. This date was the same for all sampling points in this group, giving an elapsed time between the dye addition and the first detection at this location of about 84 days. The first detection of FLT at the SSG occurred at Seep 3 on November 5, 2011. The last submarine spring in this group to reveal a detectable concentration was Seep 4 on November 11, 2011. With an average first detection date of November 8, 2011 at the SSG, the elapsed time between the dye addition and this seep group was about 103 days. FLT was detected at the SSG 19 days after it was detected at the NSG.

Grab samples were also collected to assess the marine water fluorescence just above a submarine spring in each seep group, and also from “control” locations not expected to be affected by the discharged LWRF effluent (Section 2). These control locations included Honokowai Beach Park, Wahikuli Wayside Park, and the beach fronting Olowalu (Figure 4-13). Table 4-11 summarizes the fluorescence of the marine samples collected prior to October 1, 2011. The average fluorescence in the FLT wavelength at these locations was negligible and equivalent to about 0.01 ppb of FLT.

4.2.3 The Breakthrough Curve - Fluorescein

A breakthrough curve (BTC) is a graph illustrating tracer concentration versus time at a certain location. It is used to evaluate the time of first dye arrival, dispersion characteristics of the aquifer, average time of travel, and when combined with water flux, the mass of the tracer that can be accounted for. Relative to the total mass injected, this mass can be used to estimate the percent of tracer recovery.

4.2.3.1 North Seep Group

The North Seep Group (NSG) was the location of the initial FLT detection. Sampling at this location proved to be problematic due to sand moving offshore (and likely along-shore) covering the sampling piezometers (see Section 2.2.2 for details about this problem). Figure 4-14 shows the FLT range fluorescence at the NSG measured by this study from July 5, 2011 through December 28, 2012. Heavy surf in early to mid-November, 2011 buried all of the original piezometers (Seeps 1, 2, and 6) in the NSG. This problem continued to plague the project. As a piezometer was buried, a replacement was installed to maintain three sampling points in this group. At times, only one piezometer was in place (for example, Seep 15 was the only piezometer in service from March 27, 2012 through April 19, 2012). In spite of frequently replacing piezometers due their loss, however, the data shows good fluorescence continuity between sampling points as the buried piezometers were replaced by newly installed units, all of which were located within 1.5 m of the original sampling points. There were also periods of significant variability at Seep 9, Seep 17, and Seep 21. As will be discussed in Section 4.2.3.4, salinity measurements indicate this reduction in FLT concentration was due to capturing dye-free seawater in the piezometer during sampling. This capture of dye-free seawater may have been caused by ocean turbulence mixing seawater with the non-saline groundwater in the subsurface, or by tidal affects increasing the salinity of the shallow submarine groundwater.

Despite the difficulties, the monitoring results at the NSG identified the most significant features of the BTC, including the first arrival, and peak concentration, in addition to a major portion of the declining limb (Figure 4-14). The FLT concentration first became detectable above the background fluorescence in late October, 2011. Once the leading edge of the BTC was established, the dye concentration increased at a rate of about 0.2 ppb/d until February 27th, 2012. On this date, there was an abrupt flattening of the BTC, following which the dye concentration remained steady at about 21 ppb. The peak concentration of 22.3 ppb occurred at Seep 16 on May 14, 2012. In early June 2012, the

declining limb of the BTC became evident and continued a near linear decrease of 0.05 ppb/d until the cessation of sampling December 28, 2012. A complete history of the FLT data for the NSG can be found in Table C-1, Appendix C.

4.2.3.2 South Seep Group

The South Seep Group was the location that recorded the highest measured concentrations of FLT and, since it was farther offshore, sand movement was not problematic. For the duration of sampling, all of the piezometers installed at this site at the beginning of the project remained in service, except for the Seep 4 piezometer that was relocated on April 24, 2012 to provide a second sampling point for the NSG. A piezometer was installed at Seep 11 on January 21, 2012 to augment the data collected at this site since the dye concentrations at Seep 4 and Seep 5 had significant variability. Figure 4-15 illustrates the BTC for this seep group. From the start of background sampling on July 5, 2011 through the last sampling event on December 29, 2012, this seep group displayed much greater variability among the sampling points than there was at the NSG. This was due to the greater distance between sampling points and the higher incidence of capturing seawater in the piezometer.

The FLT concentrations measured at this location had a greater rate of increase, higher peak concentration, and steeper declining limb than the NSG. The FLT concentration increased above background levels at this location in early November, 2011. Seep 3 consistently had the highest concentration and showed a near linear increase of about 0.5 ppb per day (ppb/d) during the majority of the rising limb of the BTC. Seep 4 had the lowest and most variable dye concentration. Discussed below, this sampling point also has the greatest variability in salinity. Seep 5 also had significant variability in the salinity and in the dye concentration. Seep 11, although installed after the arrival of the dye, produced a consistent BTC that was very close to that of Seep 3. The FLT concentration at the SSG plateaued at about 33 ppb starting in early April, which was not as distinct as at the NSG, and continued until late May when the declining limb of the BTC became evident. The delay between the plateau at the NSG and the SSG was about a month, which was slightly longer than the delay between first detections noted above. The rate of decline was about 0.1 ppb/d, much faster than that at the NSG. A complete history of the FLT data for the SSG can be found in Table C-2, Appendix C.

4.2.3.3 Grab and Control Samples

In addition to collecting samples by drawing water from piezometers driven into the seafloor, grab samples were collected. At each seep group, a grab sample was collected by uncapping a submerged bottle just above a submarine spring discharge. Figure 4-16 shows that, with few exceptions, the FLT concentration in the grab samples were less than 20% of that collected from the piezometer at the SSG on that same day. This signifies strong mixing between the submarine spring and ocean water immediately adjacent to the submarine springs. As described in Section 2.2.3, the control samples collected at Honokowai Beach Park, Wahikuli Wayside Park, and Olowalu showed no indication of FLT.

4.2.3.4 The Relationship Between Dye Concentrations and Salinity

Many of the sampling locations, particularly in the SSG, showed a significant variability in the BTC. As will be detailed below, the sampling locations that showed the greatest variability in FLT dye concentration also had the greatest variability in the salinity measured at the time of sampling. Table 4-12 provides a summary of the salinities measured at each submarine spring from January 1 through December 29, 2012. Also included in this table for the SSG, is the standard deviation of the difference between the FLT concentration measured at a submarine spring and the average FLT concentration measured on that day. The points with the greatest variability in salinity and their respective FLT concentration were Seeps 4 and 5. Seep 3, with the lowest variability in salinity, also had the lowest FLT variability. It is important to note that Seep 4 and Seep 11 were not in service for the entire duration of the BTC and hence their respective FLT variability would be biased. In spite of this limitation, Seep 4 with the highest variability in salinity also had the highest variability in FLT. Variability of FLT analysis was not done for the NSG since there were no sampling locations in service for the entire duration of the sampling period. Inspection of Figure 4-14 shows that Seep 9 in the NSG had the highest FLT variability. This corresponds with high salinity variability for this sampling location. Seeps 15 and 16 also showed significant salinity and FLT concentration variability.

The relationship between the variability in FLT concentration and salinity variability was tested graphically and statistically. Figure 4-17 shows the relationship between salinity and dye concentration at Seeps 4 and 5 compared to that measured at Seep 3. Since the dye concentration varies with time, the data presented actually compares ratios. The ratio on the x-axis is that for the salinity measured at Seeps 4 and 5 to that measured at Seep 3, while the ratio on the y-axis is that for the respective dye concentration measured at the two submarine springs compared to Seep 3. The low variability in salinity at Seep 3 and in the dye concentration at this sampling location made this data set a good reference for these computations. The regression coefficient and the coefficient of determination (r -squared linear value) for the Seep 4 to Seep 3 comparison data were -0.084 and 0.87, respectively. The linear regression coefficient and the coefficient of determination for the Seep 5 comparison (shown in red) were -0.088 and 0.87, respectively. This shows a strong and inverse relationship between salinity and FLT concentration.

The inverse relationship between the dye concentration and salinity was caused by mixing of dye-tagged non-saline treated wastewater with seawater that was nearly void of dye. This is a volumetric dilution effect for which the dilution by seawater can be corrected as based on the measured salinity of a sample (cf. Hunt and Rosa, 2009). In the present case, we wish to normalize the salinities of all seeps to make them comparable to that of Seep 3. The pre-mixing dye concentration in the submarine spring water can be estimated by correcting the measured dye concentration for the fraction of seawater in the submarine spring water sample.

This was done using the following formula:

$$FLT_{adj} = FLT_{meas} \div \left(1 - \frac{Sal_{meas} - Sal_{seep\ 3-avg}}{Sal_{SW} - Sal_{seep\ 3-avg}}\right) \quad \text{Equation (4-1)}$$

Where:

FLT_{adj} = the dye concentration at Seep 4 or 5 adjusted for salinity (ppb)

FLT_{meas} = the dye concentration measured at Seep 4 or 5

Sal_{meas} = the salinity measured at Seep 4 or 5

$Sal_{seep\ 3-avg}$ = the average salinity measured at Seep 3 (salinity is 3.1)

Sal_{SW} = the average salinity of seawater (salinity assumed to be 35).

Thus, employing the above equation, Figure 4-18 provides a graph of FLT concentrations at Seeps 4, 5, and 11 that would be expected at the sampling locations if the salinities were the same as the average salinity at Seep 3. Even when the dye concentration in Seeps 4 and 5 are adjusted to remove the effect of the higher salinity, the dye concentrations at these locations are still lower than that measured at Seep 3. The relative difference increases as the magnitude of the dye concentration increases.

4.2.3.5 NSG and SSG Breakthrough Curves

To compare the BTCs of the NSG and SSG, a BTC for each submarine spring group was graphed in Figure 4-19 using the FLT concentrations corrected for salinity by Equation 4-1. The symbols represent the average FLT concentration for each sampling day with the error bars represent the minimum and maximum FLT concentration for each sampling day. The standard deviation was also computed for days when more than one piezometer was sampled in a seep group (this was the case for the majority of sampling days). Once adjusted by salinity, there was a small daily variability (as shown by the error bars) in the FLT concentrations, except for a limited number of data points near the peaks of each curve. The average FLT concentration was then graphed on Figure 4-19 with error bars showing the minimum and maximum adjusted FLT concentration for each sampling day.

Although similar in appearance, there are significant differences between the BTC of the NSG and of the SSG, indicating different characteristics in their respective travel paths. FLT was first detected at the NSG followed by the SSG about 23 days later. However, the rate of rise in the concentration at the NSG was less than that at the SSG, resulting in the concentration at the SSG overtaking the NSG in late February 2012. At this time, the FLT concentration at the NSG plateaued, while that at the SSG continued to increase. The peak average concentration of 22.5 ppb occurred at the NSG on May 22, 2012, while the peak average concentration of 33.1 ppb occurred at SSG a week earlier on May 14, 2012. As with the rising limb, the receding limb the NSG was less steep than that of the SSG. During mid-May 2012 when the BTCs for both submarine spring groups were near their peak, the concentration at the SSG was 147% higher than at the NSG. By the time field sampling ended in late December 2012 the FLT concentration at the SSG was only

115% higher than that at the NSG. Based on the extrapolated BTCs the FLT concentration at the SSG will drop below that at the NSG in late December 2013.

4.2.4 Breakthrough Curve Analysis

4.2.4.1 Breakthrough Curve Extrapolation

The field sampling ended prior the tracer concentrations dropping below the MDL. However, it is important to have a complete BTC to compute the mean time of travel and the percent recovery of the FLT. To develop a complete BTC, the remainder of the BTC was estimated using an exponential curve fit based on the last three months of measured data. Equation 4-2 below gives the curve fit equation used to extrapolate the remainder of the BTC.

$$C(t) = C_i * e^{-b(t-t_i)} \quad \text{Equation 4-2}$$

Where:

$C(t)$ = the FLT concentration at time t (ppb)

C_i = the FLT concentration on October 10, 2012 (ppb)

b = the regression exponent

for the NSG $b = 0.0054$

for the SSG $b = 0.0043$

t = the elapsed time since October 10, 2012 (d)

The curve fit coefficients of determination for the predicted extrapolations for the NSG (Figure 4-20) and the SSG (Figure 4-21) were 0.97 and 0.98, respectively. Measured data are shown as points of averaged measured FLT concentration with error bars indicating the minimum and maximum concentrations measured on a given day. Major points of the BTC are annotated and indicated by the red squares. The BTC extrapolation predicts that the FLT concentrations will remain above the MDL 3 to 5 more years.

4.2.4.2 QTracer2 Breakthrough Curve Analysis Model

Our analysis of the BTC was completed using the EPA tracer test model Qtracer2 (Field, 2002). This program uses the BTC to quantify the tracer test results providing critical information, such as the time for first arrival and to the peak concentration, mean transit time, average tracer velocity, dispersivity, and percent of the injected dye mass recovered (when integrated with groundwater flux). First arrival time and time of peak concentration can easily be determined by inspection of the BTC. However, mean transit time, associated average particle velocity, and percent recovery are best done by a program that can accurately integrate the BTC over time. The mean transit time requires finding the centroid of mass of the BTC. Since the declining limb of the BTC was elongated compared to the ascending limb, the average time of travel will be biased toward the right (toward a longer time). Thus, estimating the mean transit time cannot be done simply by inspection of the BTC. The percent of mass recovery requires estimating the total tracer mass discharged by accurately integrating the concentration and flux at the

submarine springs. The cumulative mass is then divided by the mass of tracer injected. As with estimating the average time of travel, this is best done using a specialized computer program such as QTracer2.

4.2.4.2.1 QTracer2 Model Inputs and Outputs

The extended BTC was imported into a QTracer2 breakthrough curve analysis model (Field, 2002). Inputs to this model include: Mass and duration of dye addition, volumetric water discharge at the sample collection point, distance between the point of dye addition and point of sample collection, nature of the medium through which the tracer plume travels (i.e., porous, fractured, channel type flow paths) and the BTC data. Critical to computing the percent of tracer mass that can be accounted for by the BTC is the groundwater flux at the sampling points. The values used for this analysis were those calculated for each seep group by the coastal radon survey (refer to the project's Interim Report [Glenn et al., 2012], Section 5.4.2 for a detailed description of methods and results). A uniform FLT concentration was assumed for the area for which the groundwater fluxes were computed. Average concentrations relative to that measured at Seep 3 for samples collected during the area survey were 0.72 and 0.96 for the NSG and the SSG respectively. The ratio of the peak concentration at the NSG to that at the SSG was 0.65. Based on these data, a uniform concentration based on the measured BTC at each seep group is a reasonable assumption.

The output of the QTracer2 includes: time to first tracer arrival, peak concentration, mean transit time, percent of the tracer mass that can be account for by the BTC, dispersion characteristics, and relative contributions of molecular diffusion and hydrodynamic dispersion to spreading of the tracer plume. Table 4-13 tabulates the critical parameters of the BTC as calculated by QTracer2.

4.2.4.2.2 QTracer2 Model Results

Qtracer2 was run at two discharge points: (1) the North Seep Group, and (2) the South Seep Group. These locations were the focus of the monitoring where sufficient temporal data for the Qtracer analysis. This approach was acceptable because the submarine spring survey showed that these locations were the primary discharge points for the FLT. The submarine spring survey (Sections 2.3.4 and 4.2.6.2) showed that the FLT concentrations measured during the long term monitoring were representative of concentrations from the submarine springs surrounding the monitored submarine springs. Based on the QTracer2 analysis, the first detection of FLT at the NSG occurred on October 22, 2011, 86 days after FLT addition. At the SSG, first detection occurred on November 14, 2011, 109 days after the FLT addition. The time of peak concentration occurred 306 and 271 days after the FLT addition for the NSG and SSG, respectively. The average time of travel occurred 487 and 435 days after the FLT addition at the NSG and SSG, respectively. It may be noteworthy that both the time of the peak concentration and the mean transit occurred at the SSG before they occurred at the NSG, while the time of first arrival occurred first at the NSG.

4.2.4.3 FLT Recovery and Treated Wastewater Fraction

For the purposes of this study, a critical parameter is the percent of dye mass that can be accounted for at the discharge of the monitored submarine springs. The estimated percent of dye mass recovered can also be used to make estimates of the fraction of treated wastewater in the submarine spring discharge, although it must be stressed that there are significant uncertainties associated with these calculations. The accuracy of this estimate is dependent on the accuracies, both temporally and spatially, of the submarine groundwater discharge (SGD) and the FLT concentration. The SGD estimate was based on two nearshore radon activities surveys, one conducted in June, 2011, and the other conducted in September, 2011. The methodology and results can be found in Section 5 of the Interim Report (Glenn, et al., 2012). The values used for this analysis were 0.65 mgd (2,500 m³/d) for the NSG and 1.6 mgd (6,300 m³/d) for the SSG. The salinity basis for these fluxes (12.6 for the NSG and 7.46 for the SSG, refer to Table 4-4) was significantly greater than the average salinity of 3.1 to which the FLT BTC concentrations were adjusted. The fraction of FLT plume water in the SGD discharge was calculated using salinity by Equation 4-3.

$$f_{FLT} = \frac{Sal_{SW} - Sal_{Rn}}{Sal_{SW} - Sal_{seep\ 3-avg}} \quad \text{Equation 4-3}$$

Where:

f_{FLT} = the fraction of FLT plume water in the SGD

Sal_{SW} = the salinity of seawater (35)

Sal_{Rn} = the salinity of SGD discharge

$Sal_{seep\ 3-avg}$ = the average salinity of the samples collected from the piezometer at Seep 3

The fractions of FLT plume water in the SGD was 70 and 86% for the NSG and the SSG respectively. The resulting FLT plume water in the SGD was 0.51 mgd (1,752 m³/d) and 1.4 mgd (5,439 m³/d) for the NSG and SSG respectively.

The FLT concentration was measured by the submarine spring sampling program and two area-sampling surveys that occurred in July and December 2012 (see Section 2.2.2 and 2.2.5). Within the area surrounding the submarine springs, the broad-area sampling surveys indicated little variability in the dye concentration. The average FLT concentration in samples at points of visible SGD within the seep group radon activity survey zones delineated by the rectangles surrounding the seep groups in Figure 4-25 (cf. Section 3) were approximately equal to that of the submarine spring samples when adjustments for salinity were made. The Qtracer2 BTC interpretation runs for the NSG and SSG computed percent recovery estimates of 14.1 and 50.3%, respectively, for the seep groups. The total percent recovery was 64% or 76.7 kg out of 119 kg of FLT added to Wells 3 and 4 (Table 4-14).

The percent of dye mass recovery can be used to estimate the percent of treated wastewater in the SGD at the submarine springs. Refer to Table 4-14 for the specific

values used in these calculations. As described above, QTracer2 estimated that 64% FLT dye added to Injection Wells 3 and 4 was accounted for by the BTC analysis. If correct, this means that 64% of treated wastewater injected into these wells would be discharged from the monitored submarine springs. The average injection rate into Wells 3 and 4 for the period from April 2011 through March 2012 (data from Table 1-2 in the interim project report) was 2.74 mgd (9,340 m³/d). At the time of dye Break Through Curve completion, 64% of the FLT dye-traced-effluent will have been recovered at the spring areas, so at steady state, 64% of the total LWRP Wells 3 and 4 injection rate of 9340 m³/d is released within the spring area, which is 5978 m³/d (Table 4-14). Thus, 1.93 mgd (5,978 m³/d) or 64% of the treated wastewater injected into these wells discharges into nearshore waters. There is significant uncertainty associated with the effluent percentage estimated by this method due to the assumption of a uniform FLT concentration over the entire area that the radon SGD estimates were based on, the variability of SGD flux with time, and variability of the fraction of FLT plume water over the area used in these computations. The seep groups have been identified as the areas of nearshore point discharge. However, as the area survey, TIR imaging, $\delta^{15}\text{N}$ data, and modeling indicate (Section 5) the FLT plume is quite extensive and more diffuse discharge through the sea bottom sediments will occur. Also, as described in Section 3.3.3, the tracer test conducted by Tetra Tech (1994) may have detected tracer discharge deeper and further from shore than this study had the capability to monitor.

To determine the proportion of FLT dye-traced-effluent discharge that is a component of the Total SGD rate, we divide 5,978 m³/d (FLT dye-traced-effluent discharge) by 8,800 m³/d (total SGD) to estimate that 68% of the SGD at submarine springs and surrounding areas is Wells 3 and 4 injectate. One point of doing this calculation (with respect to total SGD) is to compare the tracer-dye result with that made on the basis of the stable isotope/geochemical ternary component analysis (Table 4-14), which was calculated quite independently (with its own uncertainties), and yielded a mean submarine spring effluent discharge proportion of 62%, which we conclude is very reasonable agreement.

The fraction of the treated wastewater in the submarine spring discharge was also estimated by geochemical/stable isotope methods. These data can be found in Table 6-14 in the Interim Report (Glenn et al., 2012). Those results are summarized here (Table 4-14) and compared to the percent of dye mass recovery method. As shown, the following three sets of mixing end members were used in geochemical/stable isotope source water partitioning analysis: (1) $\delta^{18}\text{O}$ and $\delta^2\text{H}$, (2) $\delta^{18}\text{O}$ and Cl, and (3) $\delta^2\text{H}$ and Cl, and listed for each are the minimum, average, and maximum percent of treated wastewater in the submarine spring. Excluded from the summary are those analyses that resulted in negative fractions or those greater than one. Collectively, the estimated treated wastewater fractions in the submarine spring discharge as determined in this manner ranged from 12% to 96% with an average of 62%. The tracer dye % recovery analysis described above falls well within the bounds of the isotopic mixing analysis, and is reasonably close to overall average value.

4.2.5 Green Coloration in the South Seep Group Discharge

Following the tracer dye additions, and starting in late February 2012, a green coloration was noted in the waters discharging from the submarine springs in the SSG. The FLT concentration at the SSG was about 23 ppb when the green coloration was first observed. This phenomenon was not observed prior to this, and was not observed at the NSG where the maximum measured FLT concentration was 23.2 ppb. The green coloration was visible at the SSG until about mid-October 2012 when the FLT concentration dropped to about 17 ppb. The source of the green coloration has not been conclusively resolved, but the available evidence strongly supports the conclusion that the FLT added to the injection wells was the source. While it might be assumed that this coloration was due to the FLT itself, the measured FLT concentration from the SSG of 23 ppb in late February and the maximum of 34 ppb in mid-April were below the generally accepted visual threshold for FLT, which is 100 ppb (Kingscote Chemical, 2010; Stuart et al., 2008). Explanations of the green coloring include the possibility that FLT exists in visible concentrations far less than 100 ppb. It can also be due to the existence of iron containing minerals, such as iron (II) hydroxides, or other green minerals. Finally, it could be the result of reactions between chlorine and other dissolved constituents. Efforts to identify the source of this coloration included:

- Performing a broad spectrum fluorescence scan to determine if any fluorophores other than FLT were present;
- Analyzing these samples for dissolved iron and other metal content; and
- Performing a light adsorption analysis on these samples to determine if the intensity of the green coloration correlated with the FLT fluorescence intensity.

The 100 ppb visual threshold for FLT solutions appears to be a general but not universally accepted value. A laboratory solution prepared by mixing optically clear submarine spring water with a 35 ppb FLT concentration showed a distinct green coloration when placed in a 2 liter beaker (Figure 4-22). This demonstrates that FLT is visible at concentrations less than 100 ppb. This observation is consistent with those of Aley (2002), and Stokes and Griffiths (2000). Although the FLT concentration at the NSG did reach the 23 ppb threshold where the green became visible at the SSG, the discharge is dispersed by sand prior to being discharged into the ocean. Thus, the absence of the green coloration at the NSG where FLT was also discharging does not preclude this dye from being the source of the green coloration at the SSG.

If the samples drawn from the piezometers captured marine water rather than SGD, for example as due to poor installation or clogged screens, the dye concentration measured by the fluorometry would be lower than that discharging from the submarine springs. Our data, however, shows that samples collected at the submarine springs are representative of a non-saline SGD, and not marine water. The samples were analyzed for pH, specific conductivity, and salinity. The salinity in the vast majority of the samples was < 5 , indicating that the samples were non-saline groundwater. This shows that the piezometer screens were not clogged and were properly installed in the openings

where groundwater was discharging, and were thus truly capturing the SGD prior to emergence and mixing with marine bottom waters.

It is important to affirmatively state that although the cause of the green coloration is not fully determined nor understood, its presence does not weaken our finding that FLT injected at the LWRF was being discharged from the submarine springs. Figure 4-23 for example shows the results of synchronous scans completed for two samples. The excitation spectrum of the scan extended from 250 to 600 nm at increments of 0.2 nm. The fluorescence intensity of the emission wavelength monitored was the excitation wavelength plus 20 nm. The first sample was prepared in the laboratory, and contains 35 ppb of FLT and 0.1 ppb SRB. The second sample was collected from Seep 3 on June 7, 2012, and contains 33 ppb of FLT. The traces are identical, except for a small peak at 580 nm, which is the fluorescence of the SRB in the laboratory prepared solution. This test strongly indicates that the FLT is the only fluorophore in the samples collected at the submarine springs.

Since the green coloration was a visual phenomenon, light absorbance wavelength scans were done using a Hach DR4000 Spectrophotometer. During these tests a beam of light of known intensity and wavelength is directed at the sample. A photosensitive cell on the opposite side of the sample measures the intensity of the incident light after it passes through the sample. The difference in intensity indicates the amount of light of that is absorbed by the sample in the wavelength range of the source light. The light absorbance spectrum of samples collected from Seep 3 when the green coloration was visible was compared to that of FLT calibration solutions. The Seep 3 samples were selected from those collected during the period from February 27, 2012 through July 11, 2012 when the green coloration was the most prevalent. The FLT concentration in the calibration solutions ranged from 0 to 100 ppb. In the calibration solutions, with the exception of the 0 ppb solution, the maximum absorbance occurred at 490 nm. This was also true for all of the Seep 3 samples except those acidified to a pH <2 with nitric acid. With the acidified sample, the maximum light absorbance occurred at 700 nm with a secondary peak at 520 nm. The light absorbance at 490 nm was -0.032 ABS, which is much less than that of any other samples. The acidification alters the molecular structure of FLT eliminating its fluorescence, and thus alters its light absorbance properties (Smart and Laidlaw, 1977). Figure 4-24 shows a graph of FLT concentration versus absorbance (ABS is the arbitrary unit of absorbance used by the spectrophotometer) for the full range of FLT concentrations tested. The lines of best fit through the calibration solutions and the Seep 3 samples are nearly identical, indicating very similar light absorbance properties. If a substance other than FLT was causing the green color then the submarine spring samples should have shown a different light absorption spectrum than that of the calibration solutions.

We have also completed some preliminary chemical experiments to investigate the potential role of reduced iron as a cause of green coloration. We used samples collected from Seep 3 and Seep 11 in the SSG, and from Seep 16 in the NSG on 6/18/12. The samples were filtered through a 0.45 micron filter and acidified to pH 2 using nitric acid. The samples were then analyzed for metals at the HDOH lab on Oahu. Dissolved iron was not detected above the MDL in these samples. These analytical results did not rule

out presence of reduce iron in the samples since they were subjected to a 50 times dilution as part of the analytical process. To further investigate whether or not dissolved iron was in the submarine spring discharge water a second set of analysis was done. On 8/1/12 samples were collected from Seep 3, Seep 5, and Seep 11 in the SSG, and from Seep 18 in the NSG. These samples were also filtered with 0.45 micron filter. They were analyzed in the field for dissolved iron (II) using method 8146-Phenanthroline chelation, and a Hach DR820 colorimeter. This method has a detection limit of 0.03 mg/L. The results of these analyses were:

- Seep 3, <0.03mg/L
- Seep 5, <0.03 mg/L
- Seep 11, 0.11 mg/L
- Seep 18, <0.03 mg/L.

These results indicate that only a slight amount of iron reduction is occurring. Thus, it is unlikely that a complex containing iron is the source of the green coloration.

Overlapping with our work, Swarzenkski et al. (2012) also studied the trace metal concentrations of samples collected from submarine springs and from the water column above them and came to a similar conclusion. Their analysis showed iron concentrations that ranged from 0.0002 to 0.40 mg/L, and that the iron concentrations in the water column directly above the seeps were very close to that in the groundwater extracted from the seeps themselves. These values are exceptional high relative to both open seawater and other coastal waters (e.g., Bienfang et al., 2009). However, due to the high oxidation potential of the waters immediately surrounding the vents, we would expect any solubilized Fe^{+2} to be immediately oxidized or complexed as iron oxyhydroxides and to precipitated, **yet iron precipitates were found in the black crusts surrounding the vents** (Interim Report Section 6; Glenn et al., 2012).

Although our tests do not entirely exclude some other substance being the source of the green coloration, the spectral and chemical tests and the disappearance of the green coloration that occurred with decreasing FLT concentrations strongly indicates that FLT was the source of this anomaly. Regardless, the source of the green tint other than FLT does not affect the results of this study. Spectrophometry confirmed that the fluorescence spectrum of the samples measured by this study was consistent in wavelength characteristics and intensity with that of FLT calibration solutions (see Section 4.3.2.1.1). Thus the accuracy of the FLT analysis that the conclusions of this study are based on was not affected by a green substance that may be in the sample aliquots. In summary, the hypothesis that the green coloration observed in the SSG was due to the FLT content in the discharging water is strengthened by several factors. These factors include: (1) a strong correlation between the light absorbance characteristics of the submarine spring samples compared to that of the FLT calibration solutions, (2) the demonstrated visibility of FLT at concentrations comparable to those found emerging from the submarine springs, and (3) the temporal agreement between the visibility of the green tint and the measured FLT concentration.

4.2.6 Area Survey Sampling and Results

The percent recovery calculations when merged with the SGD flux estimated by radon indicate that a majority of the treated wastewater injected into Wells 3 and 4 is discharged in the vicinity of the monitored submarine springs. This does not preclude diffuse seepage from a much larger area, however. In fact, the lateral extent of the elevated nitrogen-15 ($\delta^{15}\text{N}$) ratios measured in the Kaanapali area (Dailer et al, 2010) as well as our aerial TIR imaging survey, indicate a plume of large spatial extent. In addition, both the elevated $\delta^{15}\text{N}$ values and the abnormally warm water could be carried from the identified submarine springs by currents resulting in an apparent footprint that is larger in extent than the area where the treated wastewater is actively being discharge.

4.2.6.1 Area Sampling Survey Description and Methods

To better define the spatial extent of FLT plume, three rounds of sampling were conducted throughout the entire nearshore region between Honokowai Point to the north, and Black Rock Point to the south (Figure 4-13). In this effort, the seafloor was surveyed in detail by scuba, and samples were collected from the seafloor using a syringe when springs were observed, and by grab sampling where diffuse seepage was visible. These operations are detailed in Section 2.2.2 and 2.2.5 and were performed during July 2012. Samples were also collected from shallow monitoring wells on the Starwood Vacation Resorts (SVO) property fronting the area where FLT is discharging on July, 31, 2012 and April 29, 2013. Porewater samples were collected just offshore in the surge zone during December 2012, and April and May 2013, by driving a piezometer into the seafloor and extracting these using a peristaltic pump. Figure 4-25 shows the location of all samples collected. During these operations, the grab, syringe, and piezometer samples captured a significant amount of saline groundwater during collection, and this necessitated making adjustments for salinity similar to as described for the submarine spring samples in Section 4.2.3.4. Water quality instruments that measure salinity actually compute this parameter from a direct measurement of the waters electrical conductivity (YSI, Inc, no date). When the measured electrical conductivity is corrected to a temperature of 25°C this is referred to as specific electrical conductivity (SEC). The USGS recommends reading the SEC directly then computing the salinity from this measurement if necessary (Wagner et al., 2006). For this reason, SEC rather than salinity was used to correct the measured FLT concentration for elevated salinity. SEC was read in the laboratory with an YSI ProPlus Water Quality Analyzer when the samples were filtered. For samples where FLT was detected, the concentration was adjusted to the pre-mixing dye concentration in the nearshore groundwater by correcting the measured dye concentration for the fraction of seawater in the water sample. This was computed using the following formula.

$$FLT = (FLT_{meas} - Background) \div \left[1 - \frac{(SEC_{sample} - SEC_{seep\ 3-avg})}{(SEC_{SW} - SEC_{seep\ 3-avg})} \right]$$

(Equation 4-4)

Where:

FLT_{adj} = the dye concentration in the sample adjusted for salinity (ppb)

FLT_{meas} = the dye concentration measured sample (ppb)

Background = a baseline correction to prevent artificial estimates of FLT (ppb)

SEC_{sample} = the salinity measured sample ($\mu\text{s}/\text{cm}$)

$SEC_{seep\ 3-avg}$ = the average specific measured at Seep 3 (specific conductivity was 6,600 $\mu\text{s}/\text{cm}$)

SEC_{SW} = the average specific electrical conductivity of seawater (salinity assumed to be 53,100 $\mu\text{s}/\text{cm}$)

A significant length of time elapsed between the first area survey in July 2012 and the subsequent area surveys in December 2012, and April and May 2013. To reference the results of these different surveys to a single diagnostic parameter, the FLT concentrations were normalized to the concentration at Seep 3. Seep 3 FLT fluorescence was chosen as the normalization point because Seep 3 is assumed to be the point of maximum FLT concentration. The actual normalization was computed using the ratio C_i/C_{max} , where C_i is the concentration at sample location “i,” and where C_{max} is the maximum concentration of the plume (i.e., the concentration at Seep 3). Appendix Table A-6 details the data associated with area survey including both the pre-adjustment and adjusted normalized FLT concentrations, as well as the specific electrical conductivity of each sample.

Five monitoring wells on the Starwood Vacations Resort property were sampled on July 31, 2012. Two samples were collected from each well. The first was collected by carefully lowering a bailer to just below the water’s surface to prevent mixing of the water in the well bore. This first sample thus represents collection from the top of the water table prior to mixing of the well water by purging. The well was then purged a minimum of three well volumes prior to collecting the second sample. SVO Well 6 was purged with a SP400 Fultz submersible low volume pump. The remaining wells were purged with a 1.5 in. disposable PVC bailer. Water quality parameters that included pH, specific electrical conductivity, and temperature were measured with an YSI XLM 6000 Water Quality Analyzer. The tracer samples were collected in a 125 ml brown opaque HPDE plastic bottle. The samples were immediately stored in an ice filled cooler.

4.2.6.2 Area Sampling Survey Results

Figure 4-25 shows the FLT distribution of the area survey samples. Our results indicate that all major locations of submarine spring discharge occur in close proximity to the two seep group locations that have been sampled over the course of this study. This is shown in Figure 4-25 by the close grouping of samples that in most cases have a C_i/C_{max} ratio of 0.9 or greater. To the south, FLT concentrations greater than background were found along the lower limb of the Hunt and Rosa (2009) delineation of the probable extent of treated wastewater plume. This was evidenced by C_i/C_{max} ratios of greater than 0.1 in three of the samples in that area. Two of the samples were collected from the shoreline with a piezometer. The concentrations in these samples prior to adjusting for the elevated SEC were 0.9 and 0.06 ppb, above the background fluorescence of 0.11 ppb. These concentrations were then adjusted to a value of a SEC equaling that at Seep 3. The results were FLT concentrations of 5.8 and 2.4 ppb based on SECs of 46,000 and 52,400 $\mu\text{s}/\text{cm}$, respectively. No samples collected south of the TIR plume southern boundary tested positive for FLT. A third location nearby with elevated an FLT concentration was SVO Well 6. The second sample (collected after purging the well) had a FLT concentration of 4.6 ppb. There were no adjustments for SEC for this sample since it was collected directly from the groundwater and mixing with seawater was not an issue. To the north of NSG only one sample tested positive for FLT, although sampling in this northern sector was difficult due to a hard substrate just beneath the sand. Table 4-15 summarizes the FLT concentrations normalized to the concentration at Seep 3 on the day area-survey sample was collected. The average values of 0.72 and 0.96 at the NSG and SSG respectively show that the FLT concentrations measured at the monitored submarine springs are reflective of the concentrations in the radon flux computation boxes used to compute SGD flux at each seep group.

An important finding of the area survey was the establishment of the presence of FLT adjacent to the two seep groups as well as at a significant distance to the south of these groups. The southernmost sample that tested positive for FLT confirms that the dye plume exists at least as far south as the southern TIR plume boundary, and likely to the southern limb of the possible extent of the treated wastewater plume postulated by Hunt and Rosa (2009). The shoreline sampling also showed that the FLT plume only extends a short distance north of the NSG. Based on the results of the area sampling survey the extent of plume from Injection Wells 3 and 4 was delineated. In summary, Figure 4-25 shows our finding for plume extent to be very similar to that of Hunt and Rosa (2009), except that northern limb of the delineation is much closer to the northern TIR plume boundary.

When evaluating the FLT tracer plume, temperature should also be considered. Elevated temperature is a characteristic of this plume as described in Section 4 of the Interim Report (Glenn et al., 2012). Injected LWTF treated wastewater ranged from 26-31°C, the lower temperature of which was consistent with the nighttime surface water temperatures imaged in the TIR plume. In contrast, normal (far field) SGD temperatures range from 20°-22°C (Mink, 1964). Figure 4-26 shows the temperatures measured in the SVO monitoring wells. All of the wells showed elevated temperatures, with SVO Well 2 and SVO Well 6 having temperatures greater than 28°C. Elevated temperatures in the wells

could result from directly capturing the plume water in the sample or by heating of the overlying water through thermal conduction. There is not enough data to discriminate between the two processes except that the elevated FLT concentration at SVO Well 6 shows a direct connection to the FLT plume. SVO Well 2 showed an elevated temperature, which would be expected since it is the monitoring well closest to the LWRF. However, an only slightly elevated FLT concentration (0.15 ppb) was measured at this well. This was in the initial sample collected from this well. SVO Well 3 showed a slightly elevated temperature and SVO Well 4 showed a moderately elevated temperature. The thickness of the overlying alluvium may constrain the tracer plume to the basalt portion of the aquifer placing it below the bottom of the monitoring well screens. Conduction could be warming SVO Wells 3 and 4 indicating the presence of a tracer plume beneath but not in contact with well screens.

Figure 4-27 shows the spatial distribution of the specific electrical conductivity (SEC) values of the area survey samples. An analysis of these SEC values provides an assessment of the quality of the FLT concentration SEC adjustments described above. The reliability of the adjustment for SEC decreases as the value of SEC approaches that of seawater. Any elevated FLT calculated by the SEC adjustment method was considered suspect by this study for values of SEC greater than 50,000 $\mu\text{s}/\text{cm}$. Since the difference between the measured and seawater SEC is in the denominator of Equation 4-1, as this difference becomes small the estimated FLT concentration very quickly amplifies any measurement errors. Thus, the corrected FLT concentration of the most southerly sample is not reliable because the measured SEC was 52,400 $\mu\text{s}/\text{cm}$. However, immediately north of that sample, another sample with elevated FLT concentration had a SEC value of 45,970 $\mu\text{s}/\text{cm}$, indicating 14% non-saline water. The fraction of non-saline water is high enough for a reliable adjustment for SEC. Two samples collected south of the southern TIR plume boundary had SECs less than 50,000 but no detectable FLT. If FLT were present at these locations it would have been easily detectable by the fluorometer. Samples collected within the delineated FLT plume extent had SECs low enough for proper FLT analysis, but showed no indication of this dye. For example a shoreline sample collected just north of a group of closely spaced samples on the southern limb of the Hunt and Rosa (2009) probable plume extent line had a SEC of 48,400 $\mu\text{s}/\text{cm}$. A SEC of this value indicates the non-saline water fraction was high enough for reliable FLT quantification. This sample only had a trace concentration of FLT. Such a low value indicated that the southern lobe of the tracer and thus the treated wastewater plume may be narrow with an edge that falls just north of the southern limb that Hunt and Rosa (2009) delineated as the probable extent of treated wastewater plume. This could indicate a fingering of the plume rather than a single large plume.

The area sampling survey was conducted to better characterize the extent of the tracer plume. The survey showed that FLT was present as far south as the southern extent estimated by Hunt and Rosa (2009) and within the southern boundary of the TIR plume. The northern extent of the plume appears to be at least slightly north of that estimated by the TIR survey based on the position of the NSG and the lone positive FLT detection to the north. The findings of this survey are consistent with others.

Figure 4-28 compares normalized FLT with the distribution of the $\delta^{15}\text{N}$ values of algal samples from Dailer et al., (2010) from the survey area. North of the NSG the algal $\delta^{15}\text{N}$ values start decreasing, reaching baseline values at Honokowai Point. Figure 4-28 indicates the $\delta^{15}\text{N}$ enrichments starts declining just north of the NSG and have decreased significantly just north of the FLT plume northern limb.

Figure 4-29 compares normalized FLT with the results of the radon coastal survey (for details, see the interim project report Section 5) for the area survey. Areas of significant SGD flux as indicated by the moderate radon activity 0.40 to 0.52 disintegrations per minute per liter) occur at the southern end of the area survey where elevated FLT concentrations were found. Elevated radon activity also indicates significant SGD flux in the area of the submarine springs and the area of elevated, but decreasing, algal $\delta^{15}\text{N}$ values north of the NSG.

Our area survey sampling showed that the FLT plume was quite extensive with the northern and southern extents closely matching that of the TIR plume boundaries. The sampling took place three times. The first was in July 2012 and included a nearshore scuba survey where samples were collected from active submarine springs and from five monitoring wells located on the property of the Starwood Vacation Ownership (SVO) resort property. The second was in December 2012 when samples were collected in the surf zone by installing a piezometer in the sand and drawing a sample with a peristaltic pump. The third was in April and May, 2013, and included shoreline piezometer and SVO-resort monitoring well sampling. The FLT concentrations of samples were adjusted to a SEC equal to the average SEC measured in the samples collected from the Seep 3 piezometer. The concentrations were then normalized to that of the sample collected from the Seep 3 piezometer on the day the area survey sample was collected. The area survey results show the FLT was present in SGD discharging north and south of the two monitored groups of submarine springs. To the north, 125 m north of the NSG, FLT concentration was 11% of the concentration measured at Seep 3. The shoreline sampling survey continued 980 m to the north of the location of that sample, and none of the samples tested positive for FLT. Eighteen samples were collected south of the SSG, and five of which had FLT fluorescence that exceeded that of the background confirming the existence of FLT. All of the samples south of the SSG that tested positive for FLT were at or were north of southern TIR plume boundary.

4.3 Injection Well 2 Tracer Test

A second tracer test was performed at the LWRF Injection Well 2 to investigate whether effluent from Well 2 discharges into the ocean at the same locations identified in the first tracer test in Wells 3 and 4. The injection capacity of Well 2 is significantly greater than that of the other wells, implying that it may have a hydraulic connection to the ocean with a preferential flow path. So that the two tracer test could be readily distinguished, the second dye addition, SRB, was added on August 11, 2011, two weeks after the first FLT dye additions at Wells 3 and 4.

Despite its higher injection capacity, the effluent flow into LWRF Injection Well 2 is significantly less than that into Wells 3 and 4 because the wellhead elevation is higher, resulting in less gravity flow to this well. The average injection rate into Well 2 during the period of August 3 - 10, 2011 was 0.76 mgd, in contrast to that of Well 3 and Well 4 that were 1.3 and 1.1 mgd, respectively. The flow into Well 2 generally occurred between the hours of 10:00 to 20:00. Our assessment indicated that the flow rate and duration into Well 2 were not sufficient to adequately assess the hydraulic connectivity between the well and the nearshore waters. Therefore, the plant operations were modified to sustain an injection rate greater than 1 mgd on the day of SRB addition. This was accomplished by diverting all R1 water to injection and throttling down on the wellhead valves for Well 3 and Well 4 at the start of dye injection.

The dye mixing process for this test was the same as described above for FLT, with a mixing rate of 10 lbs per 50 gal. The active ingredient fraction of the SRB powder is approximately 25%, which resulted in a solution that is 0.60% active ingredient by weight. A total of 180 lbs of dye powder was used to provide a total of 900 gal. of SRB dye solution. The planned concentration of SRB mixed with the effluent in Well 2 was 2,600 ppb. The dye was added at the Effluent Splitter Box (Figure 4-30) at 15-minute intervals starting at 07:00 and continuing through 00:45.

Figure 4-31 shows the well injection rates and the resulting dye concentration in Well 2 for this test. When the dye addition started at 07:15 on August 11, 2011, the flow into Well 2 had not reached the desired magnitude, which produced a very high concentration for the first hour at about 38,000 ppb. Throttling down of the valves at the wellhead of Wells 3 and 4 resulted in increased flow to Well 2, which decreased the injection concentration to about 1,500 ppb. For the period from 09:00 until 22:00, the flow into Well 2 was less variable and the dye injection concentration varied from about 2,100 ppb to about 3,500 ppb. At about 22:15, the flow into Well 2 started to decrease and less amount of dye was added to keep the dye concentration range in the range between 2,000 to 2,500 ppb until about midnight. At that point, due to the falling effluent injection into Well 2, the remaining dye concentrate (about 22.5 gal.) was added to the splitter box between 00:00 and 00:45. This increased the dye injection concentration for the final hour of dye addition to about 12,000 ppb. Dye addition was terminated at 00:45 on August 12th. For the 24-hour period from 07:00 August 11 until 07:00 on August 12, 2011, the flow into Well 2 was 2.1 million gal. and total flow to all wells was 5.1 million gal. The average SRB concentration in the Well 2 and all injected effluent was 2,500 and 1,000 ppb, respectively.

4.3.1 Sample Handling

To ensure the integrity of the SRB sample analysis, the aliquots need to be properly handled from the point of collection, during the shipment to and storage at UH Manoa, and during the transport from the University to the laboratory in Pearl City, where the samples were analyzed. Temperature can affect the dye fluorescence, so for these analyses the samples and calibration solutions were stored overnight at ambient temperature. Hawaii nighttime temperatures are similar to that of an air-conditioned

room. Early the next morning (prior to 7:30 am), the samples were delivered to the HDOH laboratory for analysis. The warm-up time for the spectrophotometer was about 30 minutes, so calibration solutions, samples, and instrument were all located in the same room for approximately one hour during the equipment warm-up time and set up procedure for analyses. An hour does not ensure complete temperature equilibration with the instrument, but since the calibration solutions and the samples were stored and transported together, they were temperature equilibrated.

The temperature effect on a dye's fluorescence varies depending on the dye analyzed. The variation in the fluorescence intensity of a dye with a change in temperature is an exponential coefficient. The exponent for SRB is -0.029, so that for every 1°C increase in the temperature, the fluorescence of SRB decreases the equivalent of approximately 0.7 ppb (Smart and Laidlaw, 1977). For comparison the temperature coefficient for FLT is -0.0036/°C (Smart and Laidlaw, 1977). Following SRB analysis, the samples were placed in a refrigerator for archival storage for the duration of the project.

4.3.2 SRB Analysis

4.3.2.1 SRB Laboratory Analysis

SRB analyses were completed using a Hitachi F4500 Fluorescence Spectrophotometer, which is used to measure the fluorescence, phosphorescence, and luminescence in the ultraviolet and in the visible regions of the spectrum. This instrument is programmable, so that the fluorescence intensity of the wavelengths from 200 to 730 nm can be measured. When analyzing a specific dye, an excitation/emission couple is programmed into the instrument. For SRB, an excitation wavelength of 565 nm and an emission wavelength of 586 nm were used based on spectrophotometry guidance from Nikon Instruments

(<http://www.microscopyu.com/articles/fluorescence/filtercubes/green/greenhome.html>).

The bandwidth slit, which sets the bandwidth of the wavelengths, was set to 5 nm for both excitation and emission.

This instrument is also used for performing synchronous scans, where a sequential series of fluorescence measurements are performed on a sample. Synchronous scans were thus also completed to verify that any elevated fluorescence in the SRB wavelength couple was consistent with that of SRB and, further, to investigate any change in fluorescence characteristics of the low concentration SRB solutions with time. For the synchronous scans, the instrument was programmed to scan from 500 to 600 nm when evaluating the SRB spectrum and 400 to 600 nm when evaluating samples for FLT and deaminoalkylated SRB (DA-SRB). The spectrophotometer produces a spectra graph and printout (the printout is excitation wavelength versus fluorescence intensity in user-defined increments, usually 2 nm) and an electronic file of fluorescent intensity at 0.2 nm increments of excitation or emission wavelengths. The fluorescence intensity of the emission wavelength monitored was the excitation wavelength plus 20 nm.

4.3.2.1.1 Spectrophotometer Calibration

The fluorescence spectrophotometer was calibrated using 0.0, 1.0, 10, 20, 50, and 100 ppb calibration solutions. These were mixed in the same manner as the FLT calibration solutions except for the 100,000 ppb stock solution. For formulating the SRB dye concentrated stock solution, 400 mg of 25% active ingredient powder were added to a small glass beaker. The dye powder was weighed using an analytical balance. Prior to analysis each calibration solution aliquot was scanned three times and the fluorescence recorded. The resultant calibration consisted of a linear best curve fit between the indicated fluorescence intensity and the actual dye concentration.

4.3.2.1.2 SRB Method Detection Limit (MDL) Assessment

As with FLT, both the EPA and Hubaux and Vos (1970) methods were used to assess the MDL for SRB. Solutions were prepared using submarine spring water spiked to concentrations of 0.01, 0.02, and 0.05 ppb. In addition, a solution with no SRB was analyzed in the same manner as the MDL samples to establish background fluorescence for this assessment. The MDL samples were prepared in 1 L volumes that were then filtered and otherwise processed in the same manner as the field samples. Tables 4-16 and 4-17 list the results of the two MDL assessment methods.

For the EPA method, the average no-dye fluorescence of 0.046 ppb was subtracted from the fluorescence measured in the MDL samples. This was done so the percent recovery could be computed correctly. The sample spiked to a concentration of 0.02 ppb was the only sample that met all of the requirements for MDL analysis. The associated computations gave a MDL of 0.013 ppb and a limit of quantification of 0.044 ppb. For sample analysis, the instrument response is the sum of the dye and background fluorescence. The average background fluorescence of samples collected in August and September, 2011 was 0.03 ppb. This gives a MDL and limit of quantification of 0.043 and 0.071 ppb, respectively, as read directly from the spectrophotometer.

The Hubaux and Vos (1970) method gave a much lower MDL of 0.005 ppb. The aliquot spiked to 0.01 ppb was excluded because the percent error was greater than the recommended value of 20%. To more definitively evaluate the MDL, a synchronous scan was run on dye free and MDL aliquots spiked to 0.01 and 0.02 ppb. Figure 4-32 shows the results of the synchronous scan, which indicate that the sample spiked to a SRB concentration of 0.01 was not discernible from a sample with no dye. However, the sample spiked to a SRB concentration of 0.02 ppb had a marked increase in fluorescence at about 580 nm. Based on this analysis, the MDL for SRB was estimated to be 0.02 ppb. This is consistent with the MDL estimate from the EPA method. Rounding the background fluorescence to the nearest tenth of a ppb, the MDL as read directly from the spectrophotometer is 0.05 ppb and the limit of quantification is 0.08 ppb.

4.3.2.1.3 SRB Laboratory Quality Assurance

To ensure the accuracy and integrity of the SRB tracer-dye analysis program, three quality assurance tests were done: (1) calibrating the spectrophotometer as described in Section 4.3.2.1.1; (2) challenging the spectrophotometer with 0.0 and 1.0 or 10 ppb SRB calibration standards at the end of an analysis run; and (3) evaluating the calibration solutions for stability. Table 4-18 shows the results of linearity test and the offset calculated for establishing the zero baseline (i.e., no SRB present) of the spectrophotometer. The calibrations for the sets of analyses done from August 2011 through February 2012 had coefficients of determination less than 0.999 and baseline offsets greater than 0.5 ppb. As proficiency was gained in the mixing of calibration standards and the use of the spectrophotometer, calibration statistics improved significantly. The coefficient of determination was greater than 0.999 in all cases after February 2012. The coefficient of the line of best fit varied between 0.055 and 0.065 with an average of 0.060. Unlike the FLT calibrations where the best fit line was used to refine the fit between indicated fluorescence in unit of ppb FLT to the calibration solution concentration, this best fit line was used to convert the arbitrary units of raw fluorescence value to units of ppb SRB. Physical factors such as variations in the temperature of the laboratory or in the calibration solutions could cause slight variation in the slope of the best-fit line. Tables 4-19 and 4-20 show the results of the analysis tests for zero baseline and upscale check, respectively. The zero baseline check concentrations ranged from 0.00 to 0.02 ppb, values less than the MDL, showing the zero point of the spectrophotometer did not drift during any analysis set. As with the calibration statistics, the end of analysis upscale tests were very good after proficiency was gained with the instrument and mixing the calibration solutions. From March 2012 through January 2013, the greatest difference was 0.06 ppb for the 1 ppb calibration solution and 0.16 ppb for the 10 ppb calibration solution. The upscale tests done from August 2011 through December 2011 showed differences of greater than 1 ppb for the 1 ppb solution and 3 ppb for the 10 ppb calibration solution. These problems were resolved when a new set of calibration solutions mixed in March 2012. The early problems with the laboratory QA had no effect on the conclusions of the study because SRB was not detected during the affected time periods. Had SRB been present it would result in an upscale reading on the spectrophotometer, however, there would have been small inaccuracies. Synchronous scans of samples collected during this time period also showed no indication of SRB.

A concern of this study was the long-term stability of SRB. The fluorescence of this dye could decrease with time or the fluorescence wavelength characteristics could change. Degradation of SRB was evaluated by recording the raw fluorescence of the 1 ppb standard during each analysis. The stability of the wavelength characteristics was evaluated by periodically performing a synchronous scan on the 1 ppb calibration solution. Figure 4-33a compares the fluorescence of the 1 ppb calibration solution mixed on March 5, 2012 to the average fluorescence measured during calendar year 2012. This graph shows no decrease in fluorescence with time until nearly a year after the solution was mixed. The last two fluorescence measurements, taken on April 3, 2013 and May 7, 2013, do show a slight decrease in fluorescence that could be due to SRB degradation. Figure 4-33b shows the results of periodic synchronous scans done on this same solution

to evaluate any shift in emission wavelength spectrum. The scans occurred over a nine month period (the date of each scan is given in the legend). The peak fluorescence intensity of SRB emission spectrum occurred at 582 nm for the early scans (April 2012 and May 2012) but shifted to a slightly shorter wavelength of 579 nm for the remaining scans. There was no significant shift to shorter wavelengths, which would be consistent with deaminoalkylation. Peak SRB emission fluorescence at or near the expected of value of 584 nm is consistent with the possible detection of SRB at Seep 3 on December 28, 2012. The peak fluorescence intensity of the SRB emission spectrum of the December 28 sample occurred at 575.6 nm. The closeness of the peak emission wavelength values to 584 nm indicate that if deaminoalkylation was occurring the effect on the emission spectrum was not significant (see Section 4.3.2.2.1 for details on the synchronous scans).

4.3.2.2 Measured Fluorescence in the SRB Wavelength

There have been no positive detections greater than the MDL of SRB from the submarine springs. However, there were a limited number of samples that had a fluorescence spectrum consistent with trace concentrations of SRB. Figures 4-34 and 4-35 show a time series of the SRB analysis for the NSG and SSG, respectively. Plotted on these graphs are the average SRB wavelength fluorescence and error bars showing the magnitude of maximum and minimum measured values for each sample day. The fluorescence measured is that of background plus that of any dye that may be present. The average concentration for all submarine springs for the period from August 1st, 2011 through September 30th, 2011 was 0.03 ppb. This was also the long-term average for the duration of the submarine spring sampling for this project. The July, 2011 samples were excluded from background analysis due to the large number of outliers in the SSG, attributed to laboratory errors, such as, improperly seating the sample in the spectrophotometer carousel. As proficiency developed in the use of the instrument, errors such as these decreased. Also plotted on this graph is the MDL of 0.05 ppb. Only 39 samples collected after the SRB addition on August 11th, 2011 had fluorescence greater than the MDL of 0.05 ppb. Most of these were collected from the SSG (31 out 39) and were sporadic in nature, in that, the sample collected prior to and just after the anomalously high SRB sample had baseline SRB fluorescence. Due to the isolated occurrence of the elevated fluorescence, it seems that these rises were, in most cases, due to factors other than the presence of SRB. However, some samples were evaluated as possible detections of SRB. The history of the SRB fluorescence measured from samples from the NSG and SSG is provided in Appendix C Tables C-1 and C-2.

4.3.2.2.1 SRB Synchronous Scans

Synchronous scans were done to evaluate samples with slightly elevated fluorescence in the SRB wavelength for the presence of this dye and to evaluate samples for the presence of DA-SRB. Samples collected in February, March, October, and December had elevated fluorescence in the SRB wavelengths. These samples were evaluated for the presence of SRB by synchronous scans. A sample collected from Seep 12 on February 20th, 2012 showed slightly elevated fluorescence at 580 nm, consistent with SRB when

evaluated by a synchronous scan. However, samples collected from that location after that date showed no elevated fluorescence in the SRB wavelengths. Two samples collected from Seep 3, one on February 12th, 2012 and the other on February 20th, 2012 also showed elevated fluorescence at 580 nm when evaluated by a synchronous scan. Figure 4-36 compares: (1) the synchronous scan of those samples collected from Seep 3 and Seep 12; (2) a sample collected from the SVO Well 2; and (3) a laboratory solution prepared for this study. The laboratory solution had an FLT concentration of 35 ppb, similar to that of the submarine spring samples, and a SRB concentration of 0.05 ppb. An additional sample collected from Seep 3 on June 14, 2012 (shown in violet) had no elevated fluorescence in the SRB emission wavelengths and is presented for reference. This graph shows that the sample collected from Seep 3 on February 20, 2012 had fluorescence characteristics very similar to the sample spiked with 35 ppb FLT and 0.05 ppb SRB. However, this was only considered as a “possible” SRB detection, because there have been no subsequent samples collected with similar fluorescence characteristics. The samples collected from Seep 3 on February 10, 2012 and from Seep 12 on March 14, 2012 displayed only slightly elevated fluorescence in the SRB emission wavelengths.

The synchronous scans shown in Figure 4-36 also show that a possible detection of DA-SRB and low level interference between the strong FLT fluorescence and the weak tracer concentration fluorescence of SRB. The sample collected from SVO Well 2 (Figure 4-36) had emission wavelength fluorescence similar to that of the laboratory standard except that peak fluorescence occurred at 570 nm rather than 580 nm. This shift to a shorter wavelength could be the result of SRB deaminoalkylation. Figure 4-36 further shows that the trailing edge of the FLT tracer slightly elevates the fluorescence in the SRB wavelength at about 580 nm, and that this trailing edge needs to be considered when evaluating very low concentrations of SRB.

Two other samples collected near the end of field monitoring program also showed elevated fluorescence in the SRB emission wavelengths. Both samples were collected from Seep 3 on October 26, 2012 and December 28, 2012. Figure 4-37 is a synchronous scan of these two samples. Shown for comparison is a laboratory prepared aliquot with 8.9 ppb FLT and 0.05 ppb SRB, and a sample with no elevated fluorescence in the SRB emission wavelength collected from Seep 11 on December 14, 2012.

SRB degradation could also shift the emission spectrum to shorter wavelengths (in the direction of the FLT peak). The degradation of SRB through the process known as deaminoalkylation could lead to the failure of the primary SRB analysis methods (described above) to detect this dye. Deaminoalkylated SRB (DA-SRB) should fluoresce at wavelengths of 535 to 540 nm, which is shorter than that of unaltered SRB (Käss, 1998). If the fluorescence intensity of DA-SRB relative to the concentration is similar to that of SRB, the fluorescence of either SRB or DA-SRB as indicated by the Rhodamine channel of the AquaFluor Handheld Fluorometer would show up clearly in synchronous scans. Figure 4-38, for example, compares synchronous scans of a laboratory-prepared aliquot containing 35 ppb of FLT and 0.1 ppb of SRB (shown as a red line) with a sample collected at Seep 3 on June 7, 2012 (shown as a green line). Both FLT traces show

symmetrical curves that extend from about 470 to 560 nm. The 0.1 ppb SRB added to the laboratory-prepared sample clearly shows up as the elevated fluorescence from about 562 to 605 nm. The Seep 3 apparent SRB concentration as read in the field on the AquaFluor Handheld Fluorometer was 3.3 ppb, a concentration that should result in a prominent fluorescence peak centered at 580 nm. If the DA-SRB rather than SRB was the cause of the elevated SRB channel reading of the AquaFluor Handheld Fluorometer, this should also be easily detectable in a synchronous scan trace. The reason for this is that fluorescence from fluorophores tends to be additive (Meus et al., 2006). Because the fluorescence of fluorescein extends beyond the 535 to 540 nm wavelengths identified by Käss (1998) as the zone of peak fluorescence for DA-SRB, then DA-SRB should be manifest as an asymmetrical fluorescein trace with the descending limb showing a bulge. The third trace on Figure 4-38 (shown as a blue line) is a hypothetical computer-generated sample containing both fluorescein and DA-SRB. This trace was generated by multiplying fluorescence of the portion of the 0.1 ppb SRB trace that extends above background by 33 to upscale it to 3.3 ppb. This trace was then shifted to the shorter wavelengths so the peak was centered over 538 nm, the approximate peak fluorescence of DA-SRB. Finally, the fluorescence of this hypothetical DA-SRB trace was added to the fluorescence of the Seep 3 sample to superimpose the DA-SRB fluorescence on the fluorescein curve. The result is an easily observable bulge on the descending limb of the fluorescein curve from about 535 to 555 nm.

Eighty-eight samples were evaluated for DA-SRB and for trace concentrations of SRB using synchronous scans. These scans were evaluated for fluorescence spectrum anomalies that could indicate the presence of DA-SRB and elevated for fluorescence in the SRB wavelength spectrum. Table 4-21 summarizes the results of these scans. Early scans (16 scans) were done with an excitation wavelength range from 520 to 620 nm. Although this range does not cover the entire FLT wavelength spectrum it does cover the range of 535 - 540 nm where DA-SRB is likely to occur (Käss, 1998). The scanned emission wavelength spectrum was then expanded to the range from 420 to 620 nm to capture the entire FLT emission spectrum. No scans showed any indication of DA-SRB. Figure 4-23 is a typical example of the synchronous scans, the wavelength traces of three samples are compared to a laboratory prepared sample with 35 ppb FLT and 0.1 ppb SRB. No anomalies similar to what would be expected from DA-SRB (refer to Figure 4-37) were present. Very trace concentrations of DA-SRB could be masked by the FLT fluorescence, however, SRB concentrations consistent with those measured by the AquaFluor hand held fluorometer (1.0 to 1.8 for the samples in Figure 4-38) would be clearly visible on the emission spectrum, whether unaltered or deaminoalkylated. No evidence of DA-SRB was found and only four samples were evaluated as possibly containing SRB. The trace concentrations present in the samples discussed above indicated that relying only on the direct readout of the spectrophotometer to evaluate samples was insufficient. Synchronous scans proved to be a valuable tool to evaluate samples for trace concentrations of SRB and to investigate whether or not dye degradation was occurring.

4.3.3 Possible Causes of the Lack of SRB Detection

If the transport processes and pathway taken by SRB were similar to that of FLT, the detection of SRB should have occurred due to its sub-ppb detection limit, the significant amount of time that has elapsed since the dye addition, and the large amount of SRB added to Well 2. The possible causes for the lack SRB detection are: (1) the injectate is displaced to other discharge locations by the injection into Wells 3 and 4, but would discharge at the monitored submarine springs if Well 2 were the only injection well used; (2) the injectate into Well 2 is discharging at a location other than those monitored regardless of the injection into other wells; (3) SRB sorbing onto the aquifer matrix slows its arrival time and decreases the concentration to below detectable limits; and/or (4) due to the long transit time, SRB degrades by deaminoalkylation or some other process that prevents its detection.

The spacing between LWRF injection wells is such that there is a significant interference between the injection flow fields. Injection Wells 3 and 4 inject the majority of effluent and are located between Injection Well 2 and the submarine springs where the FLT emergence was monitored. The dominant flow from Wells 3 and 4 may thus likely displace the injected wastewater effluent from Well 2 around the Well 3 and 4 flow fields. If so, the probable result is that the flow from Well 2 would take a different path other than directly towards the submarine springs. Figure 4-39 shows the results of computer simulations using the USGS groundwater flow model MODFLOW (Harbaugh et al., 2000) and the particle tracking model MODPATH (Pollock, 1994). MODPATH uses the groundwater flow solution from MODFLOW to trace the track that simulated particles will take as they are moved by the advection of groundwater. The model does not account for dispersion or diffusion. The model output is a set of arcs that represent the particle track path lines. Figure 4-39a shows the model output of particle tracks created by injection into Wells 3 and 4 (shown in red) and created by the injection into Well 2 (shown in green). This shows that with simultaneous injection into these three wells, which currently occurs, the injectate from Well 2 is displaced from a pathway to the submarine springs. This model shows that the injectate from Well 2 is diverted to the east around the simulated barrier before taking a northwesterly path to the ocean. Figure 4-39b shows that with only injection into Well 2, the majority of the underground discharge from Well 2 travels to the known submarine springs. A detailed description of the modeling for this project can be found in Section 5. Again, due to the non-detection of SRB the model results cannot be validated, but it does show a probable result of conducting the Well 2 SRB tracer test while continuing the injection into Wells 3 and 4. This does not, however, preclude the possibility that the injected effluent into Well 2 would assume the same underground flow path as that of Wells 3 and 4 if it were to become the primary injection well.

One of the goals of the area survey described in Section 4.2.6 was to investigate other discharge locations for SRB. No discharge locations were confirmed during that survey, although a degradation product of this dye may have been detected at a trace concentration level in SVO Well 2. Obviously, the potential of the discharge of the Well 2 injectate at a location other than those monitored cannot adequately be evaluated.

However, it may be beneficial to re-evaluate a past tracer study done at the LWRF in light of the new findings of the current study. In 1993, the dye Rhodamine WT was added to Injection Well 2 at a concentration of approximately 100 parts per billion for 58 days (Tetra Tech, 1994). In that study, a marine survey was conducted from a boat in an attempt to identify areas where the LWRF wastewater effluent might be discharging into the ocean. They used a pump with a hose attached that was lowered to the seafloor for each sample collection. The discharge of the pump was connected to a fluorometer with a flow cell. The background fluorescence in the Tetra Tech (1994) study varied between 0.04 and 0.06, similar to that of this study. Elevated levels of fluorescence of about 0.18 ppb were detected 55 and 61 days after the start of injection at survey points adjacent to each other. Although scant, the location of the elevated fluorescence detections was very close to the area monitored by this study, but deeper (about 30 m) and farther offshore (about 300 m) than the submarine springs monitored by this study. According to Tetra Tech (1994), the dye emergence was not expected at this location and the elevated fluorescence was evaluated as being from another fluorophore such as dissolved organic matter. It is not possible to confirm whether the Tetra Tech study actually detected the dye, but our study indicates the effluent from Well 2 may not be discharging into the nearshore waters and a discharge point deeper and further from shore needs to be considered.

The lack of detection of SRB may additionally be related to matrix sorption within the aquifer. Sorption of SRB onto the solid media of the aquifer would slow the transport velocity and decrease the SRB concentration at points of emergence. Sorption could decrease the concentration to values less than the MDL, resulting in non-detection even though the fluids injected into Well 2 are discharging at the monitored locations. Sabatini (2000) assessed FLT and SRB sorption. Sabatini found that significant SRB sorption occurred when the aquifer matrix was limestone. Sediments consisting of alluvium, unconsolidated and consolidated carbonate sands, and reef limestone form the coastal and nearshore sedimentary structure commonly referred to as caprock. The caprock (shown as the alluvium along the coast in Figure 1-9) is present in varying thicknesses in the study area. Because the NSG and SSG are located near the shoreline, calcareous sands, reef limestone, and sandstone in the caprock would be present sorption sites in the SRB plume travel path. As will be discussed in Section 5, the sorption of SRB could reduce the concentration of this dye to below the MDL.

At the time of this writing, in excess 1.5y have elapsed since SRB was added to the treated wastewater stream at the LWRF Well 2. During that time, this dye could degrade to a non-fluorescent species or, more likely, undergo transformation that would result in different fluorescent characteristics (i.e., deaminoalkylation). The longer the transit time for SRB, the more likely it is that such a process has occurred. If DA-SRB were present, the synchronous scans performed by this study would have detected this altered SRB if it were present above trace concentrations. This study did not test for or evaluate other degradation/transformation processes and cannot rule them out. We conclude that primary cause for the non-detection of SRB is displacement of the SRB plume away from the submarine springs by injection into Wells 3 and 4. Also, due to the failure to positively detect SRB and inference with the SRB plume resulting from the injection into

Wells 3 and 4, no conclusions can be made regarding the hydraulic connection between Well 2 and the nearshore waters at Kaanapali.

4.4 Starwood Vacation Ownership (SVO) Monitoring Well Sampling

Five monitoring wells on the property of Starwood Vacation Ownership Resorts (SVO) were sampled as part of this study. These wells were located within the boundaries of the FLT plume (Figure 4-25). Table 4-22 lists the well construction data available for these wells.

4.4.1 SVO Well Sampling Procedures

Prior to purging and sampling the wells, a temperature and specific conductivity profile was taken to document any stratification that may be present. The measurements were done using an YSI EC300 Conductivity/Temperature Meter with a 10 m cable. The probe of the YSI EC300 was lowered in one foot intervals until the bottom of the well was reached. A temperature and SEC reading was taken at each interval..

Sampling was done with 1.5 inch disposable PVC bailers. A dedicated bailer was used for each well to prevent cross contamination between wells. Prior to purging a well, an initial sample was collected for fluorescent dye analysis (FLT and SRB). Thus, this initial pre-purge sample was intended to capture any dye that may have been present at the top of water table. With purging, samples would be diluted by water deeper in the well bore and by water flowing into the well from the surrounding formation, which could decrease the concentrations below the detection limit. The pre-purge sampling was done by carefully lowering a disposable bailer to just below the water surface.

Once the initial sample was collected, the wells were purged until a quantity of water equal to three well volumes was extracted from the well. The water quality parameters were measured during the well purging included water temperature, pH, and specific conductivity. The water quality parameters were stabilized so that no more than a 10% change would occur during the last three consecutive measurements. The purged water was containerized in a 3 gal. bucket marked in 1 gal. increments to facilitate measurements of the purge volumes.

A set of nutrient samples and a second tracer sample was collected after three well volumes of water had been purged. No further samples were collected during the first and second round of sampling. During the third round of sampling, purging was resumed after the initial three well volume purge. A small submersible pump, rather than disposable bailers, was used to collect a third tracer sample. The pump was lowered to a depth just above of the bottom of the well. The pump was then turned on and a volume of water equal to three well volumes was purged from the well. A set of tracer dye samples and a set of nutrient samples to be analyzed by UH were then collected. This was done to investigate whether or not selectively pumping from the bottom of the well could obtain a sample more representative of the treated wastewater plume. An increase

in the FLT concentration in the pumped sample would indicate the sample was more representative of the treated wastewater plume.

Samples collected at the SVO wells were analyzed for: (1) FLT content by using a Turner 10AU Filter Fluorometer at the University of Hawaii; (2) SRB content by using a Hitachi F4500 Spectrophotometer at the Hawaii Department of Health Environmental Laboratory at Pearl City, Hawaii; (3) and nitrate/nitrite, total nitrogen, and phosphorous content at the same laboratory. During each sampling round, a duplicate sample was collected from one well. The duplicate sample was labeled Well 7 with a sample time of 12:05.

4.4.2. SVO Well Sampling Results and Discussion

The vertical temperature/SEC profile measured during the initial round of sampling showed that some stratification exists. Figure 4-40 shows the vertical profile for temperature (a) and SEC (b). All wells showed elevated temperatures at water surface. Wells 3 and 4 showed some increase in temperature starting at a water depth of six ft. The SEC profile was uniform for Wells 3 and 4, while SVO Well 2 showed a small increase in SEC starting at a water depth of nine ft. Wells 5 and 6 showed significant stratification with sharp increases in SEC starting at a water depth of one foot. Table 4-23 provides temperature, pH, SEC, and dye fluorescence measured at the monitoring wells. Water quality parameter values were those measured when the final tracer dye sample was collected.

The initial tracer samples collected from these wells confirmed the detection of FLT and a possible detection of trace concentrations of degraded SRB. As Table 4-23 shows, four of the ten samples collected had FLT fluorescence greater than the method detection limit of 0.11 ppb. Sample 2 from Well 6 showed strong fluorescence in the FLT wavelength. Two wells, Well 2 (Sample 1) and Well 6 (Sample 1) had sulpho-rhodamine B (SRB) fluorescence greater than the method detection limit of 0.05 ppb. A synchronous scan done on these two samples showed that Well 2, Sample 1, had an emission wavelength spectrum that showed elevated fluorescence at 570 nm, slightly shorter than that expected for SRB. Elevated fluorescence at 570 could indicate deaminoalkylated SRB or the presences of some other fluorophore. The elevated fluorescence was too small to discriminate between the two possibilities. Tables D-1 through D-3 in Appendix D list the water quality and tracer dye results for each sampling round. Tables D-2 and D-3 also detail the water quality parameters measured during the purging of SVO Wells.

During the April 29, 2013 and June 6, 2013 rounds of sampling, the FLT concentrations were low in all wells (0.2 - 0.5 ppb) and there was possibly a trace concentration of SRB in Well 2 (similar to the results of the July 31, 2012 round of sampling). If the wells had a direct hydraulic connection to the basalt aquifer, the FLT concentrations should have been much higher. The FLT transport model indicates that during the July 31, 2012 round of sampling, FLT concentrations would range from 1.7 at SVO Well 6 to 21 ppb at SVO Well 4. The modeled FLT concentrations at the SVO Wells during the April 29 and June 6, 2013 rounds of sampling ranged from 0.34 at Well 2 to 25.4 at Well 6. By April and June, 2013, the simulated plume had migrated past all of the wells except Well 6,

leaving only residual concentrations at the other wells. The FLT concentrations currently measured at the submarine springs are about 6 to 8 ppb, much higher than that measured at the SVO Wells.

The nutrient sampling showed that the nitrogen and phosphorus concentrations in these wells were generally very low. Table 4-24 includes the nutrient chemistry results that were available at the time that this report is written. Nutrient chemistry done by UH and HDOH are available for the July 31, 2012 sampling round. The University of Hawaii has completed the nutrient analysis for the April 29, 2013 sampling round and the June 6, 2013 nutrient chemistry analysis has not yet been completed by UH. Results are still pending from HDOH for the April 29 and June 6, 2013 sampling rounds. The nutrient chemistry results will be forwarded when they become available. Based on the nutrient chemistry that is currently available, the only well that had any nitrogen species concentration greater than 1 mg/L was Well 5. Concentrations from this well are not representative of those in the groundwater that discharges to the ocean since the water column is very short (less than two ft) and would only reflect the chemistry at the surface of the water table. This zone would be heavily influenced by landscape fertilizers and not reflect the bulk chemistry of the non-saline groundwater. In addition, the recovery after water was purged from Well 5 was very slow indicating potential well installation problems. For these reasons, Well 5 was not sampled during subsequent two rounds of sampling.

Temperature data indicate that the wastewater plume is likely passing beneath the wells, which are completed in the alluvium and do not penetrate to the basal aquifer, as confirmed by the low FLT concentrations. The water collected from these wells is probably a combination of landscaping irrigation recharge and some upwelling from the confined basal aquifer.

4.5 Summary and Conclusions

Two tracer tests were conducted during this study to assess the hydraulic connectivity between the effluent injection wells at the LWRF and the coastal nearshore waters. During the first, FLT was added to Wells 3 and 4 on July 28, 2011. The dye from this tracer test began discharging at the nearshore submarine springs in late October, 2011, after about 84 days. The FLT concentration increased to about 21 ppb then plateaued in late February 2012 at the North Seep Group (NSG). The peak concentration of 22.5 ppb occurred at this seep group about 306 days after the FLT addition. At the South Seep Group (SSG), the initial detection of FLT occurred 109 days after the FLT addition. The FLT concentration then increased to a peak of 34 parts per billion (ppb) about 271 days following the FLT addition. The natural background fluorescence at the monitoring sites was assessed by analyzing the samples taken prior to the arrival of the dye. It was found that background fluorescence was very small, at about 0.11 ppb relative to the magnitude of the FLT fluorescence detected. The dye concentrations were higher at the SSG than at the NSG for most of the BTC. This could be due to spatial variability, or because the SSG may be closer to the center of the groundwater plume than the NSG. If it is the latter case, then there is an indication of effluent discharging points existing to the south

of the SSG, which has been confirmed by area sampling during a survey of additional possible dye discharge points.

Mass balance calculations done using the BTC in the QTracer2 BTC analysis program indicated that 64% of the FLT that was added into Wells 3 and 4 will have been fully discharged at the submarine spring areas. Thus, as viewed at steady state, it is also our conclusion based on these calculations that 64% of the treated wastewater injected into these wells currently discharges from the submarine spring areas. As discussed in Section 4.2.4.3, 68% of the SGD at the submarine springs and surrounding areas is Wells 3 and 4 injectate. This is very reasonable agreement with the average submarine spring discharge proportion of 62% estimated by the stable isotope/geochemical ternary component analysis (Table 4-14).

The FLT Tracer test data shows a definite hydraulic connection between Injection Wells 3 and 4 and the nearshore waters near Kahekili Beach Park. The average time of travel between the wells and the submarine springs is well in excess of a year. This proven hydraulic connection does not preclude other discharge points, however, including in areas at deeper water depths and further from shore.

The second tracer test was conducted to evaluate whether the effluent from Injection Well 2 discharges at the same locations as that from Injection Wells 3 and 4. Well 2 has a significantly higher injection capacity than the other wells indicating that it may have a hydraulic connection to a preferential flow path. For this tracer test, SRB was added to the effluent on August 11th, 2011. There has been no confirmed detection of this dye, but sporadic cases of elevated fluorescence in the SRB wavelengths did occur in February and December 2012. Synchronous scans showed that these samples may contain very low concentrations of SRB. No other samples were analyzed with similar fluorescent characteristics; these are only evaluated as possible detections.

During the course of this project, there has been no confirmed detection of SRB at the submarine springs monitored by this study or in the area survey samples collected, and the ultimate fate of the effluent injected into Well 2 remains unresolved. The possible causes of the failure to positively detect SRB include: (1) injectate from Wells 3 and 4 displacing the SRB plume away from the submarine springs; (2) SRB plume is discharging at a location other than those monitored; (3) SRB sorbing onto the aquifer matrix; and (4) SRB degradation. We suggest that the most likely conclusion is that the SRB plume has been diverted from the submarine springs by the continued injection into Wells 3 and 4. This will increase the transit time by greatly increasing the distance this dye must travel to the submarine discharge. Sorption and degradation then occur as secondary causes for the lack of SRB detection within the defined study area.

Table 4-1. Mixing schedule for the FLT calibration solutions.

Desired Concentration (ppb)	Volume of 100 ppb Calibration Solution (ml)	Volume of Submarine spring Water (ml)	Comments
1	2.5	247.5	Note 1
10	50	450	
20	50	200	
50	125	125	

Note 1. An extra volume of the 10 ppb solution was mixed since it was used to calibrate the instrument and verify accuracy at the end of each analysis session

Table 4-2. The MDL results for FLT using the EPA method.

Spiked Conc. (ppb)	Mean (ppb)	Solution Deviation (ppb)	MDL (ppb)	Average Recovery (%)	Signal to Noise Ratio	Limit of Quantification (ppb)	Remarks
0	0.001	0.004	NA	NA	NA	NA	
0.1	0.101	0.004	0.011	101.25	28.6	0.035	Signal to noise ratio > 10
0.2	0.192	0.005	0.014	96.24	41.6	0.046	Signal to noise ratio > 10
0.5	0.479	0.006	0.019	95.7	74.7	0.064	Signal to noise ratio > 10

Red indicates a value outside of acceptable limits

Table 4-3. The MDL results for FLT using the Hubaux and Vos method

Conc. (ppb)	Mean (ppb)	Calculated Concentration (ppb)	Percent Error	Included in Analysis
0.00	0.12	-0.006	NA	Yes
0.10	0.22	0.10	4.5	Yes
0.20	0.31	0.20	2.1	Yes
0.50	0.57	0.50	0.5	Yes
MDL (ppb)				0.02
Critical Response (ppb)				0.13
Critical Concentration (ppb)				0.008
r ²				0.9994

Table 4-4. The Turner 10AU calibration scalar, residual, coefficient of determination, and offset

Analysis Date	Scalar	Residual	Coefficient of Determination	Baseline Offset (ppb)
1/27/12	1.01	-0.26	0.9998	0.21
1/30/12	1.01	-0.21	0.9999	0.16
2/7/12	1.01	-0.25	0.9998	0.20
2/8/12	1.02	-0.23	0.9999	0.18
2/9/11	1.01	-0.03	1.0000	-0.02
2/10/11	1.01	-0.24	0.9998	0.18
2/20/12	1.02	-0.25	0.9999	0.20
3/5/12	1.03	-0.15	1.0000	0.10
3/18/12	1.02	-0.21	1.0000	0.04
3/24/12	1.02	-0.33	0.9998	0.27
4/11/12	1.00	-0.04	1.0000	-0.02
5/11/12	1.02	-0.27	1.0000	0.22
6/14/12	1.01	-0.25	0.9999	0.19
6/15/12	1.01	-0.20	1.0000	0.14
6/29/12	1.01	-0.26	1.0000	0.20
7/20/12	1.00	-0.19	1.0000	0.14
7/23/12	1.03	-0.25	1.0000	0.19
7/25/12	1.03	-0.19	1.0000	0.13
8/3/12	1.03	-0.19	1.0000	0.14
8/24/12	1.02	-0.01	0.9999	-0.05
9/28/12	1.02	-0.13	0.9999	0.07
10/3/12	1.01	-0.05	1.0000	-0.01
10/12/12	1.01	-0.05	0.9999	0.00
11/2/12	1.01	-0.16	1.0000	0.10
11/17/12	1.01	-0.20	1.0000	0.14
12/14/12	1.02	-0.11	1.0000	0.06
1/12/13	1.03	-0.19	1.0000	0.13
2/14/13	1.01	-0.13	1.0000	0.07
2/26/13	1.02	-0.06	1.0000	0.01

Table 4-5. The results of the end of analysis zero baseline check of the fluorometer.

FLT Conc. (ppb)	Date Solution Prepared	Date Analyzed	Corrected Conc. (ppb)	Difference (ppb)
0.0	12/21/11	2/20/12	0.00	0.00
0.0	12/21/11	2/9/12	0.00	0.00
0.0	12/21/11	2/10/12	0.00	0.00
0.0	12/21/11	1/27/12	0.00	0.00
0.0	12/21/11	1/30/12	0.00	0.00
0.0	12/21/11	2/7/12	0.00	0.00
0.0	12/21/11	3/5/12	0.00	0.00
0.0	12/21/11	2/8/12	0.00	0.00
0.0	12/21/11	3/18/12	-0.01	-0.01
0.0	12/21/11	3/24/12	-0.01	-0.01
0.0	12/21/11	4/11/12	0.00	0.00
0.0	12/21/11	5/11/12	0.00	0.00
0.0	4/11/12	6/14/12	-0.01	-0.01
0.0	4/11/12	6/15/12	0.00	0.00
0.0	4/11/12	6/29/12	0.00	0.00
0.0	4/11/12	7/25/12	0.00	0.00
0.0	4/11/12	8/3/12	0.00	0.00
0.0	4/11/12	8/24/12	0.00	0.00
0.0	4/11/12	10/3/12	0.00	0.00
0.0	4/11/12	11/2/12	0.00	0.00
0.0	4/11/12	11/17/12	0.00	0.00
0.0	4/11/12	12/14/12	0.00	0.00
0.0	4/11/12	1/12/13	0.00	0.00
0.0	4/11/12	2/26/13	0.00	0.00

Table 4-6. The results of the end of analysis upscale quality control check of the fluorometer

FLT Conc. (ppb)	Date Solution Prepared	Analysis Date	Measured Conc. (ppb)	Difference
10	1/27/12	2/9/11	9.94	-0.6%
10	1/27/12	2/10/11	9.97	-0.3%
10	1/27/12	2/7/12	9.97	-0.3%
10	1/27/12	2/8/12	9.96	-0.4%
10	1/27/12	2/20/12	9.91	-0.9%
10	1/27/12	3/5/12	10.00	0.0%
10	1/27/12	3/18/12	9.90	-1.0%
10	1/27/12	3/24/12	9.95	-0.5%
10	4/10/12	4/11/12	9.95	-0.5%
10	4/16/12	5/11/12	9.92	-0.8%
10	4/16/12	6/14/12	9.91	-0.9%
10	4/16/12	6/15/12	10.0	0.0%
10	4/16/12	6/29/12	10.10	1.0%
10	4/11/12	7/25/12	9.89	-1.1%
10	7/20/12	8/3/12	9.99	-0.1%
20	7/20/12	8/24/12	19.50	-2.5%
10	10/3/12	10/3/12	10.60	6.0%
10	7/20/12	10/3/12	10.10	1.0%
20	10/3/12	10/3/12	21.00	5.0%
10	10/3/12	11/2/12	9.93	-0.7%
20	10/3/12	11/17/12	19.90	-0.5%
20	10/3/12	12/14/12	19.60	-2.0%
20	10/3/12	1/12/13	19.30	-3.5%
10	10/3/12	2/26/13	9.84	-1.6%

Table 4-7. The results of duplicate analyses ran at the end of each analysis run

Location	Date	Time	Analysis Date	FLT Conc. (ppb)	Duplicate Conc. (ppb)	Difference	Difference Units
seep 3	1/19/12	10:52	2/10/11	9.13	9.49	3.9	percent
seep 3	1/19/12	10:52	2/10/11	9.13	9.49	3.9	percent
seep 3	1/31/12	12:25	2/10/11	13.92	13.92	0.0	percent
seep 7	11/25/11	10:08	1/27/12	1.54	1.56	1.6	percent
seep 8	1/7/12	15:08	1/27/12	11.40	11.24	-1.3	percent
Honokowai Beach Park	12/9/11	12:05	1/30/12	0.01	0.01	0.00	ppb
seep 4	11/23/11	10:37	1/30/12	0.21	0.21	0.00	ppb
seep 4	12/28/11	10:53	2/7/12	2.71	2.74	1.1	percent
seep 5	1/23/12	13:36	2/10/12	4.57	4.62	1.1	percent
seep 3	1/21/12	14:37	2/20/12	10.30	10.09	-2.0	percent
seep 7	1/25/12	9:43	2/20/12	14.66	14.56	-0.7	percent
north grab	2/10/12	11:35	3/5/12	0.49	0.49	0.00	ppb
seep 11	2/20/12	15:27	3/5/12	18.40	18.40	0.0	percent
seep 4	2/20/12	15:00	3/5/12	10.81	10.81	0.0	percent
north grab	3/14/12	10:05	3/18/12	1.15	1.15	0.2	percent
seep 3	3/14/12	11:05	3/18/12	29.37	29.37	0.0	percent
seep 3	3/11/12	11:59	3/24/12	27.21	27.21	0.0	percent
seep 4	2/27/12	12:13	3/24/12	7.76	7.65	-1.3	percent
south grab	3/11/12	12:30	3/24/12	1.18	1.16	-1.6	percent
seep 11	3/27/12	11:46	4/11/12	26.93	27.34	1.5	percent
seep 3	3/29/12	11:19	4/11/12	32.35	32.55	0.6	percent
south grab	3/27/12	11:15	4/11/12	1.10	1.10	0.1	percent
seep 3	4/16/12	10:44	5/11/12	32.02	32.23	0.6	percent
seep 4	4/5/12	9:40	5/11/12	14.96	15.06	0.7	percent
south grab	3/29/12	11:30	5/11/12	2.10	2.10	0.1	percent
Seep 15	5/14/12	9:22	6/14/12	15.72	15.82	0.6	percent
Seep 15	5/18/12	13:29	6/14/12	7.54	7.57	0.4	percent
Seep 3	6/7/12	13:20	6/14/12	31.90	32.00	0.3	percent
Olowalu	5/19/12	11:46	6/15/12	0.01	0.01	0.00	ppb
Seep 11	6/4/12	15:12	6/15/12	25.74	25.94	0.8	percent
South Grab	5/7/12	11:30	6/15/12	5.78	5.74	-0.7	percent
North Grab	6/12/12	11:40	7/20/12	0.29	0.29	0.00	ppb
Seep 15	6/12/12	11:27	7/20/12	16.40	16.40	0.0	percent
Seep 3	6/14/12	15:37	7/20/12	30.55	30.55	0.0	percent
north grab	7/11/12	13:05	7/25/12	1.07	1.07	0.0	percent
seep 3	7/19/12	11:40	7/25/12	26.02	26.44	1.6	percent

Table 4-7 (Continued). The results of duplicate analyses ran at the end of each analysis run.

Location	Date	Time	Analysis Date	FLT Conc. (ppb)	Duplicate Conc. (ppb)	Difference	Difference Units
seep 3	8/1/12	10:15	8/3/12	14.91	15.02	0.7	percent
seep 3	8/1/12	10:15	8/3/12	14.91	15.02	0.7	percent
North grab	8/1/12	9:30	10/3/12	2.74	2.74	-0.1	percent
seep 5	8/7/12	10:40	10/3/12	22.09	21.88	-0.9	percent
north grab	9/12/12	9:30	10/12/12	3.42	3.45	0.9	percent
seep 20	10/2/12	11:30	10/12/12	13.95	14.86	6.5	percent
seep 5	9/18/12	13:20	10/12/12	17.68	17.79	0.6	percent
seep 20	10/12/12	11:05	11/2/12	10.47	10.37	-1.0	percent
seep 20	10/18/12	11:19	11/2/12	8.00	7.91	-1.1	percent
seep 3	10/18/12	12:42	11/2/12	17.16	16.75	-2.4	percent
north grab	10/26/12	10:46	11/17/12	0.50	0.50	0.00	ppb
north grab	10/26/12	10:46	11/17/12	0.50	0.50	0.00	ppb
seep 11	10/29/12	12:25	11/17/12	15.35	15.66	2.0	percent
seep 3	11/2/12	15:40	11/17/12	14.75	14.85	0.7	percent
north grab	12/6/12	11:05	12/14/12	0.08	0.08	0.00	ppb
seep 3	12/6/12	11:47	12/14/12	13.35	13.35	0.0	percent
seep 5	11/19/12	12:15	12/14/12	14.48	14.68	1.4	percent
seep 5	12/14/12	13:15	1/12/13	12.64	12.64	0.0	percent

Red indicates a difference >5%

Table 4-8. Table of replicate analyses to evaluate FLT sample degradation during storage.

Location	Date	Time	Initial Analysis Date	Replicate Analysis Date	Initial Results (ppb)	Replicate Results (ppb)	Difference
seep 1	11/9/11	10:11	1/27/12	6/29/12	0.5	0.5	1.8%
seep 11	3/14/12	11:42	3/18/12	11/2/12	25.4	25.3	-0.5%
seep 11	3/27/12	11:46	4/11/12	6/29/12	26.9	27.2	1.2%
seep 11	8/1/12	11:35	8/3/12	8/24/12	23.7	24.2	1.9%
seep 11	11/2/12	16:10	11/17/12	11/17/12	15.2	15.0	-0.7%
seep 13	3/14/12	9:53	3/18/12	11/17/12	20.9	20.5	-1.7%
seep 14	3/17/12	9:23	4/11/12	1/21/13	20.4	19.9	-2.4%
seep 15	3/29/12	10:28	4/11/12	1/12/13	20.6	20.0	-2.9%
seep 15	4/16/12	9:09	5/11/12	9/2/12	21.8	22.4	2.7%
seep 17	7/11/12	13:53	7/25/12	12/14/12	13.7	13.0	-4.8%
seep 18	8/1/12	9:15	8/3/12	8/24/12	17.1	16.8	-1.3%
seep 19	9/10/12	12:51	10/3/12	12/14/12	14.7	13.9	-5.7%
seep 3	11/23/11	10:25	1/27/12	6/29/12	0.3	0.3	0.3%
seep 3	11/28/11	10:35	1/27/12	6/29/12	0.4	0.4	-0.3%
seep 3	1/7/12	15:51	1/27/12	6/29/12	5.9	5.9	0.5%
seep 3	1/19/12	10:52	2/10/11	6/29/12	9.1	9.4	2.6%
seep 3	3/1/12	12:34	3/18/12	11/2/12	25.0	24.6	-1.7%
seep 3	8/1/12	10:15	8/3/12	8/24/12	14.9	15.0	0.7%
Seep 3	8/1/12	10:35	10/3/12	8/3/12	25.2	14.9	-40.9%
seep 4	10/28/11	10:30	2/7/12	12/14/12	0.1	0.1	4.6%
seep 4	11/11/11	10:55	1/27/12	2/20/12	0.1	0.1	5.0%
seep 4	11/14/11	9:58	1/30/12	6/29/12	0.1	0.1	-1.4%
seep 4	12/14/11	10:22	2/7/12	6/29/12	1.0	1.0	3.4%
Seep 4	1/25/12	13:39	2/20/12	11/17/12	10.1	10.0	-1.1%
seep 4	3/22/12	11:08	4/11/12	6/29/12	12.9	13.2	2.8%
seep 5	1/23/12	13:36	2/10/12	6/29/12	4.6	4.7	2.2%
seep 5	4/2/12	11:44	4/11/12	1/12/13	21.2	20.7	-2.2%
Seep 5	5/25/12	13:57	6/14/12	11/2/12	24.9	24.7	-0.9%
seep 5	10/18/12	12:43	11/2/12	11/2/12	15.8	15.7	-0.6%
seep 6	11/21/11	9:37	1/27/12	1/27/12	1.2	1.2	-0.9%
seep 7	11/25/11	10:08	1/27/12	6/29/12	1.5	1.4	-8.1%
seep 7	1/21/12	16:00	2/10/11	6/29/12	13.3	13.6	2.5%
seep 7	2/20/12	13:46	3/5/12	11/2/12	19.9	19.5	-2.2%

Red indicates a value outside of acceptable limits

Table 4-9. Summary of background fluorescence for the NSG.

	Seep 1	Seep 2	Seep 6	Average
Number of Samples	15	15	13	14
Minimum	0.09	0.08	0.11	0.09
Average	0.11	0.11	0.11	0.11
Maximum	0.13	0.12	0.12	0.12
Standard Deviation	0.01	0.01	0.00	0.01
First Detection	10/20/11	10/20/11	10/20/11	10/20/11

Table 4-10. Summary of background fluorescence for the SSG.

	Seep 3	Seep 4	Seep 5	Average
Number of Samples	13	18	13	15
Minimum	0.09	0.01	0.08	0.06
Average	0.12	0.10	0.11	0.11
Maximum	0.13	0.14	0.12	0.13
Standard Deviation	0.01	0.03	0.01	0.02
First Detection	11/05/11	11/11/11	11/07/11	11/08/11

Table 4-11. Background fluorescence for the marine waters.

	North Seep Grab	South Seep Grab	Other Locations
Number of Samples	27	27	26
Minimum	-0.01	-0.01	0.001
Average	0.01	0.01	0.01
Maximum	0.04	0.06	0.05
Standard Deviation	0.02	0.02	0.02

Table 4-12. Summary of salinity measured at the submarine springs

Location	No. of Samples	Salinity			FLT - Avg. FLT	
		Minimum	Average	Maximum	Standard Deviation	Standard Deviation
Seep 3	85	2.8	3.4	11.1	1.1	2.0
Seep 4	35	3.0	10.0	22.5	7.1	6.6
Seep 5	76	3.4	8.3	21.8	4.9	2.8
Seep 11	74	3.1	3.7	14.3	1.4	1.1
Seep 7	13	4.0	4.2	4.3	0.1	****
Seep 8	3	4.2	4.3	4.4	0.1	****
Seep 9	7	4.2	12.3	25.3	7.8	****
Seep 10	13	4.1	4.7	6.2	0.6	****
Seep 12	10	4.2	4.3	4.8	0.2	****
Seep 15	22	4.2	4.9	9.3	1.5	****
Seep 16	16	4.4	5.0	12.0	1.9	****

**** Insufficient sample history computing standard deviation for the difference between the monitoring point FLT concentration and the average of the seep group.

Table 4-13. The output of the QTracer2 BTC interpretation model.

Parameter	Units	North Seep Group	South Seep Group	Comments
Duration of BTC	d	2,435	2,001	Length of time from injection until FLT concentration drops below the MDL
Distance from input to outflow point	m	821	932	
Seep Group Discharge	m ³ /d	1,752	5,439	Combined discharge = 7,162
Time to First Arrival	d	86	109	
Time to Peak Concentration	d	306	271	
Peak Tracer Concentration	ppb	22.5	35	
Mean Transit Time	d	487	435	
Mean Tracer Velocity	m/d	1.7	2.1	
Maximum Tracer Velocity	m/d	9.5	8.6	-
Mass of Tracer Inject	kg	119	119	
Mass of Tracer Recovered	kg	16.8	59.9	
Percent of Tracer Mass Recovered	%	14.1	50.3	Total percent Recovery = 64%
Dispersion coefficient	m ² /s	1.37E-03	1.15E-03	
Longitudinal dispersivity	m	70	46	
Peclet number	Unitless	12	20	Advection > Diffusion

Note: Seep group discharge is taken from Table 5-5 in the Lahaina Groundwater Tracer Study Interim Report (Glenn et al., 2012)

Table 4-14. Calculated percent of treated wastewater in the submarine spring discharge.

FLT Tracer Dye Estimates of Percent Recovery and of Percent Effluent				
	Units	North Seep Group	South Seep Group	Total
Total SGD (saline+fresh) ¹	(m ³ /d)	2,500	6,300	8,800
SGD – FLT plume fraction	(m ³ /d)	1,752	5,439	7,162
Mass of Tracer Dye Added	(kg)	----	----	119
Mass of Tracer Dye Recovered	(kg)	16.8	59.9	76.7
Percent Tracer Dye Mass Recovery at Submarine Spring Groups	(%)	14.1%	50.3%	64.0%
Average Injection Rate into LWRF Wastewater Injection Wells 3 and 4	(m ³ /d)	----	----	9,340
Effluent Discharge at Submarine Springs ²	(m ³ /d)	----	----	5,978
Percent Effluent in the Submarine Spring Discharge (Effluent Discharge/Total SGD)	(%)	----	----	68%
Geochemical Parameters Used in % Effluent		Percent Effluent in the Submarine Spring Discharge		
Mixing Endmember Calculations³		Low	Avg	High
$\delta^{18}\text{O} / \delta^2\text{H}$ End Member Mixing Calculations		53%	77%	96%
$\delta^{18}\text{O} / [\text{Cl}^-]$ End Member Mixing Calculations		12%	41%	60%
$\delta^2\text{H} / [\text{Cl}^-]$ End Member Mixing Calculations		67%	69%	71%
Average		----	62%	----

¹Radon Mass Balance Model of Glenn et al. (2012, Section 5).

²64% of Average Injection Rate into Wells 3 and 4.

³See Section 6.4.2.3 of Glenn et al. (2012) for a discussion of end member mixing analysis techniques.

Table 4-15. Summary of the area survey sample results.

Area	Minimum	Average	Maximum	Standard Deviation	Number of Samples
North Seep Group	0.09	0.72	0.95	0.19	83
South Seep Group	0.87	0.96	1.19	0.08	28
North of the NSG	0.00	0.03	0.11	0.03	11
South of the SSG but north of the southern TIR Boundary	0.00	0.07	0.48	0.13	13
South of the southern TIR Boundary	0.00	0.00	0.00	0.00	6
SVO Wells	0.00	0.04	0.20	0.07	5
All Area Survey Samples	0.00	0.60	1.19	0.37	149

Units are $C_i/C_{\text{seep } 3}$ where:

C_i = the FLT concentration of sample "i" adjusted to Seep 3 SEC

$C_{\text{seep } 3}$ = the FLT concentration at Seep 3 on the sample "i" was collected

Table 4-16. The MDL results for SRB using the EPA method.

Spiked Conc.	Mean	Standard Deviation	MDL	Average Recovery	Signal to Noise Ratio	Limit of Quantification	Remarks
(ppb)	(ppb)	(ppb)	(ppb)	(%)		(ppb)	
0.00	0.005	0.006	NA	NA	NA	NA	Note 1
0.01	0.004	0.003	0.01	45	1.4	0.03	Average recovery and SNR not acceptable
0.02	0.017	0.004	0.013	85	3.9	0.044	Met all requirements
0.05	0.054	0.018	0.058	108	2.4	0.18	SNR not acceptable

Note 1. The mean dye-free aliquot concentration 0.03ppb was subtracted from the fluorescence for the MDL samples

Red indicates a value outside of acceptable limits

Table 4-17. The MDL Results for SRB Using the Hubaux and Vos Method

Spiked Conc.	Mean Conc. _{Note 1}	Calculated Concentration _{Note 2}	Percent Error	Included in Analysis
(ppb)	(ppb)	(ppb)		
0.00	0.043	0.0015	NA	Yes
0.01	0.050	0.007	26.8	No _{Note 3}
0.02	0.062	0.017	12.8	Yes
0.05	0.10	0.051	2.0	Yes
MDL (ppb)				0.005
Critical Response (ppb)				0.044
Critical Concentration (ppb)				0.0025
r^2				0.9922

Note 1: Mean concentration is the background (about 0.03 ppb) plus the dye fluorescence.

Note 2: Calculated concentration is based on best fit line through the MDL data.

Note 3: The 0.01 ppb aliquot excluded from the analysis due to the high percent error.

Allowable error is 20% or less

Table 4-18. Hitachi F4500 Spectrophotometer calibration scalar, residual, and coefficient of determination.

Date Analyzed	Scalar	Residual	Coefficient of Determination	Baseline Offset
8/24/11	0.063	2.36	0.9998	2.37
8/31/11	0.062	0.65	0.9996	0.65
9/9/11	0.062	1.32	0.9890	1.32
9/23/11	0.058	0.19	0.9940	0.20
10/4/11	0.065	-0.31	0.9980	-0.29
10/14/11	0.060	-0.08	0.9985	-0.07
11/4/11	0.064	-0.14	0.9991	-0.11
11/23/11	0.061	-0.17	0.9920	-0.15
12/5/11	0.062	-0.47	0.9979	-0.45
12/14/11	0.065	-0.20	0.9979	-0.18
12/30/11	0.056	-0.03	0.9999	-0.01
1/11/12	0.060	-0.34	0.9992	-0.32
1/20/12	0.059	-0.72	0.9983	-0.70
2/14/12	0.062	-1.19	0.9970	-1.17
3/7/12	0.056	-0.05	0.9992	-0.04
3/21/12	0.056	0.47	1.0000	0.48
4/12/12	0.061	0.08	0.9998	0.10
5/17/12	0.061	-0.34	0.9994	-0.32
6/22/12	0.061	-0.48	0.9992	-0.46
7/26/12	0.062	-0.23	0.9997	-0.21
8/2/12	0.062	-0.28	0.9996	-0.26
9/7/12	0.057	-0.13	0.9995	-0.11
10/9/12	0.060	-0.18	0.9995	-0.16
10/19/12	0.057	-0.01	0.9999	0.01
11/2/12	0.059	-0.03	0.9992	-0.15
11/19/12	0.056	0.01	0.9992	0.03
12/19/12	0.060	-0.04	0.9991	-0.03
1/16/13	0.055	0.17	0.9999	0.18

Table 4-19. The results of the end of analysis zero baseline check of the Hitachi F4500 Spectrophotometer.

SRB Conc. (ppb)	Analysis Date	Indicated Conc. (ppb)	Difference (ppb)
0.00	11/23/11	0.02	0.02
0.00	12/5/11	0.01	0.01
0.00	12/14/11	0.01	0.01
0.00	1/11/12	0.00	0.00
0.00	1/20/12	0.01	0.01
0.00	3/7/12	0.02	0.02
0.00	3/21/12	0.00	0.00
0.00	4/12/12	0.00	0.00
0.00	5/17/12	0.01	0.01
0.00	7/26/12	0.00	0.00
0.00	8/2/12	0.00	0.00
0.00	9/7/12	0.01	0.01
0.00	10/9/12	0.00	0.00
0.00	11/19/12	0.01	0.01
0.00	12/19/12	0.00	0.00
0.00	1/16/13	0.00	0.00

Table 4-20. The results of the end of analysis upscale quality control check of the Hitachi F4500 Spectrophotometer.

SRB Conc.	Date Solution Prepared	Analysis Date	Measured Conc. (ppb)	Difference (ppb)
1	8/24/11	8/24/11	0.86	-0.14
1	8/24/11	2/14/12	2.17	1.17
1	3/5/12	3/7/12	1.05	0.05
1	3/5/12	3/21/12	1.05	0.05
1	3/5/12	4/12/12	1.02	0.02
1	3/5/12	4/12/12	1.04	0.04
1	3/5/12	5/17/12	1.06	0.06
1	3/5/12	7/26/12	1.05	0.04
1	3/5/12	7/26/12	1.06	0.06
1	3/5/12	8/2/12	1.04	0.04
1	3/5/12	9/7/12	1.09	0.09
1	3/5/12	10/9/12	0.99	-0.01
1	3/5/12	11/2/12	1.02	0.02
1	3/5/12	11/19/12	1.01	0.01
1	3/5/12	1/16/13	1.05	0.05
10	8/24/11	8/24/11	7.03	-2.97
10	8/24/11	11/23/11	8.16	-1.84
10	10/11/11	12/5/11	8.33	-1.67
10	10/11/11	12/14/11	8.77	-1.23
10	10/11/11	1/11/12	10.02	0.02
10	10/11/11	1/20/12	10.16	0.16
10	8/24/11	2/14/12	10.00	0.00

Table 4-21. The results of synchronous scans done to evaluate samples for trace concentrations of SRB.

Location	Date	Date Scanned	Start Ex	End Ex	Comments
Sand Sample 2 (area survey)	12/20/12	02/26/13	420	620	Negative
Sand Sample 4 (area survey)	12/20/12	02/26/13	420	620	Negative
Sand Sample 5 (area survey)	12/20/12	02/26/13	420	620	Negative
Sand Sample 6 (area survey)	12/21/12	02/26/13	420	620	Negative
Sand Sample 8 (area survey)	12/21/12	02/26/13	420	620	Negative
Sand Sample 9 (area survey)	12/21/12	02/26/13	420	620	Negative
Sand Sample NSG (area survey)	02/25/13	02/26/13	420	620	Negative
Seep 1	10/02/11	03/13/13	420	620	Negative
Seep 11	11/27/11	12/19/12	420	620	Negative
Seep 11	03/19/12	04/12/12	520	620	Negative
Seep 11	06/14/12	03/13/13	420	620	Negative
Seep 11	09/12/12	10/09/12	420	620	Negative
Seep 11	10/02/12	10/09/12	420	620	Negative
Seep 11	11/02/12	03/13/13	420	620	Negative
Seep 11	11/12/12	11/19/12	420	620	Negative
Seep 11	12/14/12	03/13/13	420	620	Negative
Seep 12	03/14/12	04/12/12	520	620	Slightly Elevated SRB Spectrum
Seep 13	03/14/12	11/19/12	420	620	Negative
Seep 14	03/17/12	01/13/13	420	620	Negative
Seep 15	03/29/12	01/13/13	420	620	Negative
Seep 15	04/05/12	02/15/13	420	620	Negative
Seep 15	04/16/12	03/13/13	420	620	Negative
Seep 15	05/02/12	02/15/13	420	620	Negative
Seep 15	06/14/12	03/13/13	420	620	Negative
Seep 17	07/11/12	12/19/12	420	620	Negative
Seep 19	08/16/12	02/15/13	420	620	Negative
Seep 19	09/10/12	12/19/12	420	620	Negative
Seep 2	11/09/11	03/13/13	420	620	Negative

Table 4-21 (Continued). The results of synchronous scans done to evaluate samples for trace concentrations of SRB.

Location	Date	Date Scanned	Start Ex	End Ex	Comments
Seep 20	09/20/12	11/19/12	420	620	Negative
Seep 20	10/02/12	03/13/13	420	620	Negative
Seep 20	10/02/12	03/13/13	420	620	Negative
Seep 20	11/08/12	03/13/13	420	620	Negative
Seep 20	11/08/12	03/13/13	420	620	Negative
Seep 20	11/12/12	02/15/13	420	620	Negative
Seep 20	12/14/12	01/13/13	420	620	Negative
Seep 20	02/25/13	02/26/13	420	620	Negative
Seep 21	10/26/12	11/19/12	420	620	Negative
Seep 21	10/29/12	03/13/13	420	620	Negative
Seep 3	11/28/11	03/13/13	420	620	Negative
Seep 3	02/10/12	04/12/12	520	620	Slightly Elevated SRB Spectrum
Seep 3	02/20/12	04/12/12	520	620	Possible Trace SRB
Seep 3	02/27/12	03/07/12	520	620	Negative
Seep 3	03/01/12	03/07/12	520	620	Negative
Seep 3	03/01/12	12/19/12	420	620	Negative
Seep 3	03/11/12	03/07/12	520	620	Negative
Seep 3	03/14/12	03/07/12	520	620	Negative
Seep 3	03/17/12	04/12/12	520	620	Negative
Seep 3	03/19/12	04/12/12	520	620	Negative
Seep 3	03/24/12	03/07/12	520	620	Negative
Seep 3	06/14/12	11/19/12	420	620	Negative
Seep 3	10/02/12	03/13/13	420	620	Negative
Seep 3	10/18/12	03/13/13	420	620	Negative
Seep 3	10/26/12	02/15/13	420	620	Slightly Elevated SRB Spectrum
Seep 3	11/27/12	03/13/13	420	620	Negative
Seep 3	12/28/12	01/13/13	420	620	Possible Trace SRB
Seep 3	02/11/13	02/15/13	420	620	Negative
Seep 3	02/25/13	02/26/13	420	620	Negative
Seep 3 Acidified	06/18/12	03/13/13	420	620	Negative
Seep 3 Acidified then Neutralized	06/18/12	03/13/13	420	620	Negative

Table 4-21 (Continued). The results of synchronous scans done to evaluate samples for trace concentrations of SRB.

Location	Date	Date Scanned	Start Ex	End Ex	Comments
Seep 4	10/28/11	12/19/12	420	620	Negative
Seep 4	12/02/11	03/13/13	420	620	Negative
Seep 4	01/16/12	01/20/12	420	620	Negative
Seep 4	01/25/12	11/19/12	420	620	Negative
Seep 4	02/17/12	03/07/12	520	620	Negative
Seep 4	02/24/12	03/13/13	420	620	Negative
Seep 4	03/22/12	12/19/12	420	620	Negative
Seep 5	12/10/11	12/19/12	420	620	Negative
Seep 5	01/25/12	11/19/12	420	620	Negative
Seep 5	01/31/12	03/13/13	420	620	Negative
Seep 5	02/20/12	03/07/12	520	620	Negative
Seep 5	03/29/12	04/12/12	520	620	Negative
Seep 5	04/02/12	01/13/13	420	620	Negative
Seep 5	04/16/12	03/13/13	420	620	Negative
Seep 5	08/21/12	02/15/13	420	620	Negative
Seep 5	10/18/12	03/13/13	420	620	Negative
Seep 5	11/08/12	11/19/12	420	620	Negative
Seep 5	12/14/12	01/13/13	420	620	Possible Trace SRB
Seep 5	02/11/13	02/15/13	420	620	Negative
Seep 5	02/25/13	02/26/13	420	620	Negative
Seep 7	01/16/12	03/13/13	420	620	Negative
Seep 7	01/25/12	03/07/12	520	620	Negative
Seep 7	02/20/12	01/13/13	420	620	Negative
Seep 7	02/27/12	03/07/12	520	620	Negative
Seep 7	11/25/12	01/13/13	420	620	Negative
SSG Sand Sample 2	12/20/12	02/26/13	420	620	Negative
SVO Well 2#1	07/31/12	08/02/12	420	620	Possible Trace SRB with Wavelength shifted downward 10 nm
SVO Well 6#1	07/31/12	08/02/12	420	620	Negative
SVO Well 6#2	07/31/12	08/02/12	420	620	Negative

Table 4-22. SVO Well construction details.

Well	Total Depth (ft btoc)	Depth to Water (ft btoc)			Latitude	Longitude
		7/1/12	4/29/13	6/6/13		
Well 2	22.83	16.31	16.43	16.22	20.94303	-156.68915
Well 3	21.00	9.97	10.31	10.36	20.94076	-156.69003
Well 4	21.30	7.71	8.03	7.53	20.94068	-156.69149
Well 5	17.20	13.94	NT	NT	20.93710	-156.69215
Well 6	32.00	23.65	23.88	23.56	20.93618	-156.69061

ft btoc - feet below top of casing

NT - not taken

Table 4-23. SVO Well measured pH, SEC, and FLT and SRB concentrations and water temperatures.

Well	Temp. (°C)	pH	SEC (µs/cm)	FLT 1 (ppb)	FLT 1 (ppb)	FLT 3 (ppb)	SRB 1 (ppb)	SRB 2 (ppb)	SRB 3 (ppb)
Sample Date: 7/31/12									
Well 2	31.1	7.52	2,527	0.15	0.04	NT	0.09	0.06	NT
Well 3	27.0	7.54	970	0.07	0.09	NT	0.02	0.01	NT
Well 4	27.0	7.81	2,892	0.09	0.09	NT	0.03	0.03	NT
Well 6	28.3	6.85	2,841	0.46	4.59	NT	0.07	0.03	NT
Sample Date: 4/29/13									
Well 2	28.6	7.53	2,391	0.33	0.25	NT	0.06	0.04	NT
Well 3	26.6	7.45	902	0.87	0.03	NT	0.01	0.01	NT
Well 4	27.2	7.69	2,926	0.34	0.58	NT	0.02	0.03	NT
Well 6	27.9	6.98	2,690	0.52	0.24	NT	0.02	0.02	NT
Sample Date: 6/6/13									
Well 2	29.1	7.49	2,435	0.37	0.27	0.25	0.05	0.06	0.09
Well 3	27.0	7.43	904	0.03	0.04	0.04	0.01	0.05	0.02
Well 4	27.2	7.71	2,936	0.11	0.56	0.46	0.03	-0.03	0.00
Well 6	28.3	6.87	2,780	0.30	0.18	0.16	0.06	0.07	0.03

NT – Not Taken

Table 4-24. Nutrient results for the SVO Wells.

NAME	DATE	TIME	University of Hawaii				Hawaii Dept. of Health Laboratory			
			NH ₃ -N	NO ₃ +NO ₂	Total N	Total P	NH ₃ -N	NO ₃ +NO ₂	Total N	Total P
			(mg/L)	(mg/L)	(mg/L)	(mg/L)	(mg/L)	(mg/L)	(mg/L)	(mg/L)
Well 2	7/31/12	14:20	0.01	0.00	0.16	0.11	0.01	0.04	0.16	0.14
Well 2	4/29/13	15:15	0.01	0.02	0.14	0.04				
Well 3	7/31/12	15:22	0.00	0.00	0.20	0.22	0.00	0.21	0.28	0.16
Well 3	4/29/13	13:30	0.00	0.13	0.16	0.17				
Well 4	7/31/12	16:14	0.14	0.00	0.18	0.20	0.12	0.01	0.28	0.13
Well 4	4/29/13	14:15	0.15	0.03	0.21	0.06				
Well 5	7/31/12	12:14	0.02	1.56	1.44	0.12	0.00	1.56	2.21	0.14
Well 6	7/31/12	13:03	0.00	0.37	0.45	0.54	0.00	0.64	0.78	0.57
Well 6	4/29/13	16:15	0.00	0.44	0.51	0.52				
Well 7	4/29/13	12:05	0.00	0.45	0.60	0.54				

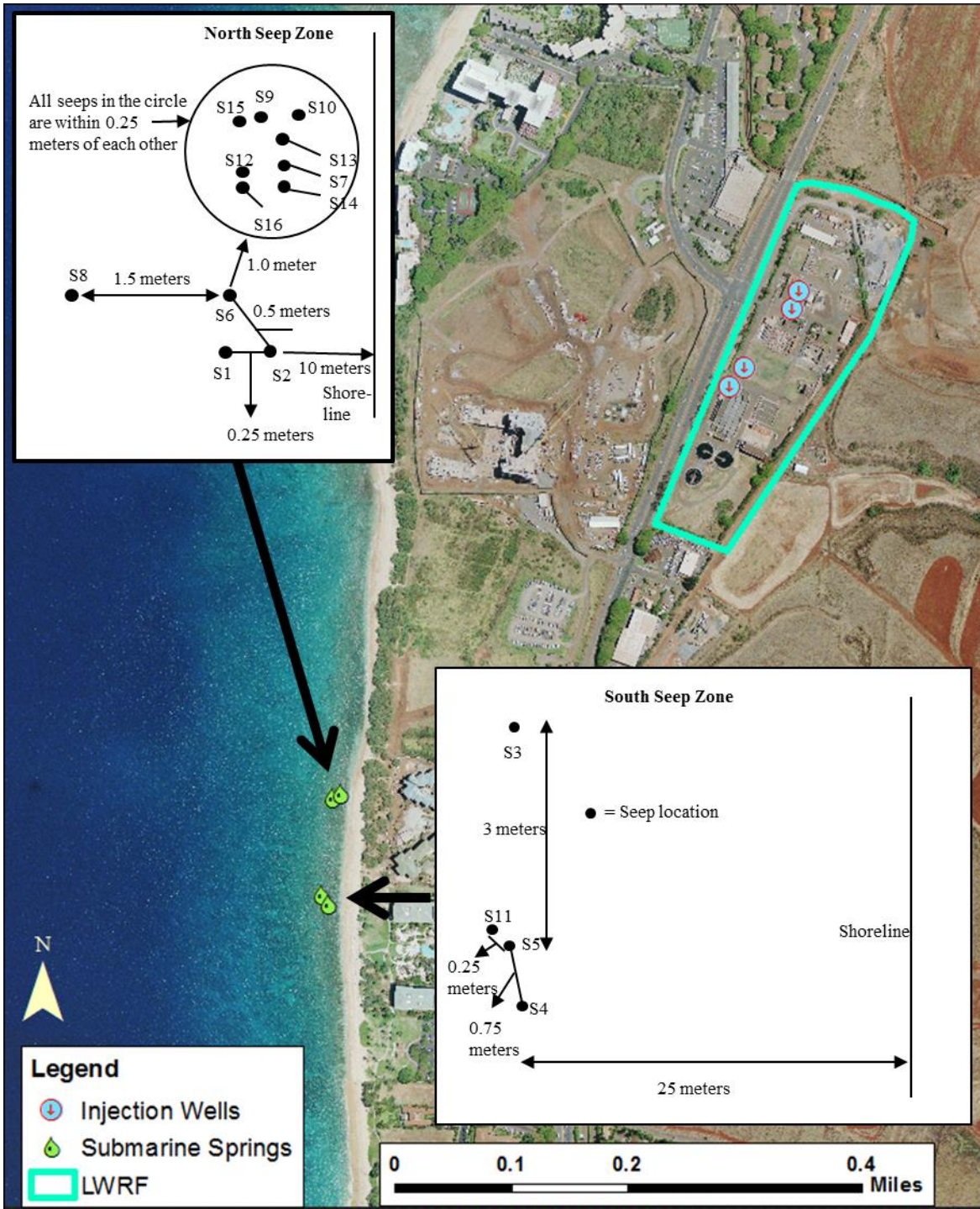


Figure 4-1: Location and arrangement of monitoring points.

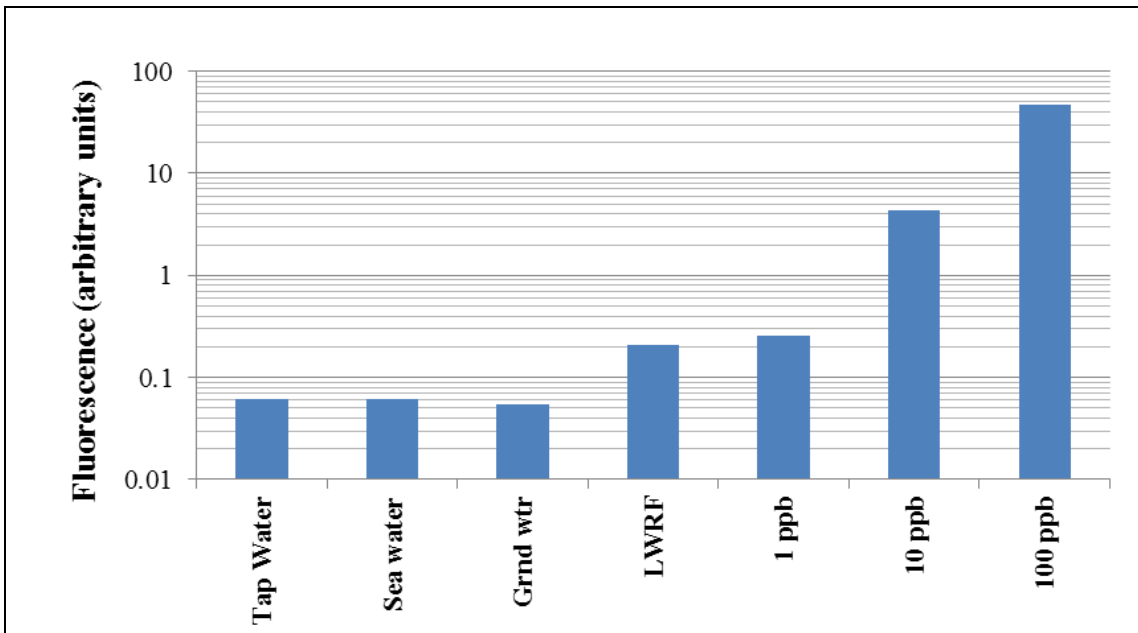


Figure 4-2: The fluorescence in the FLT wavelength of water from various sources compared to solutions containing FLT.

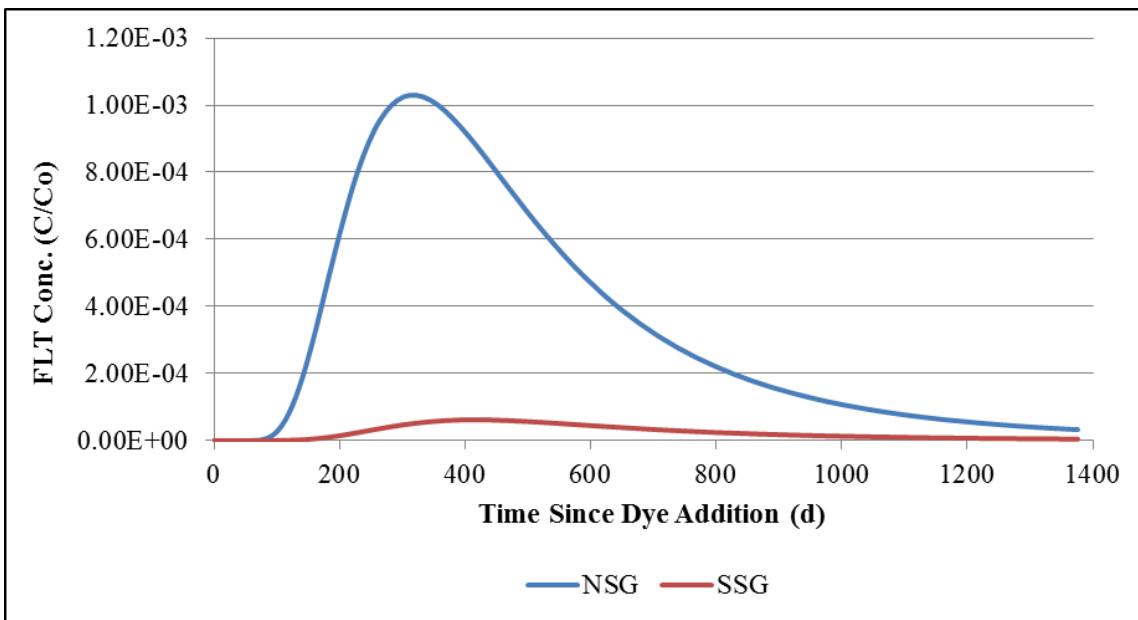


Figure 4-3: Results of the Tracer Test Design Model.

The Tracer Test Design Model simulation predicted that the tracer would reach the NSG (blue) about 90 days after addition, would be diluted by about 1000 times at the peak of the break through curve (BTC) after about one year, and that the full BTC would take several years to fully develop.

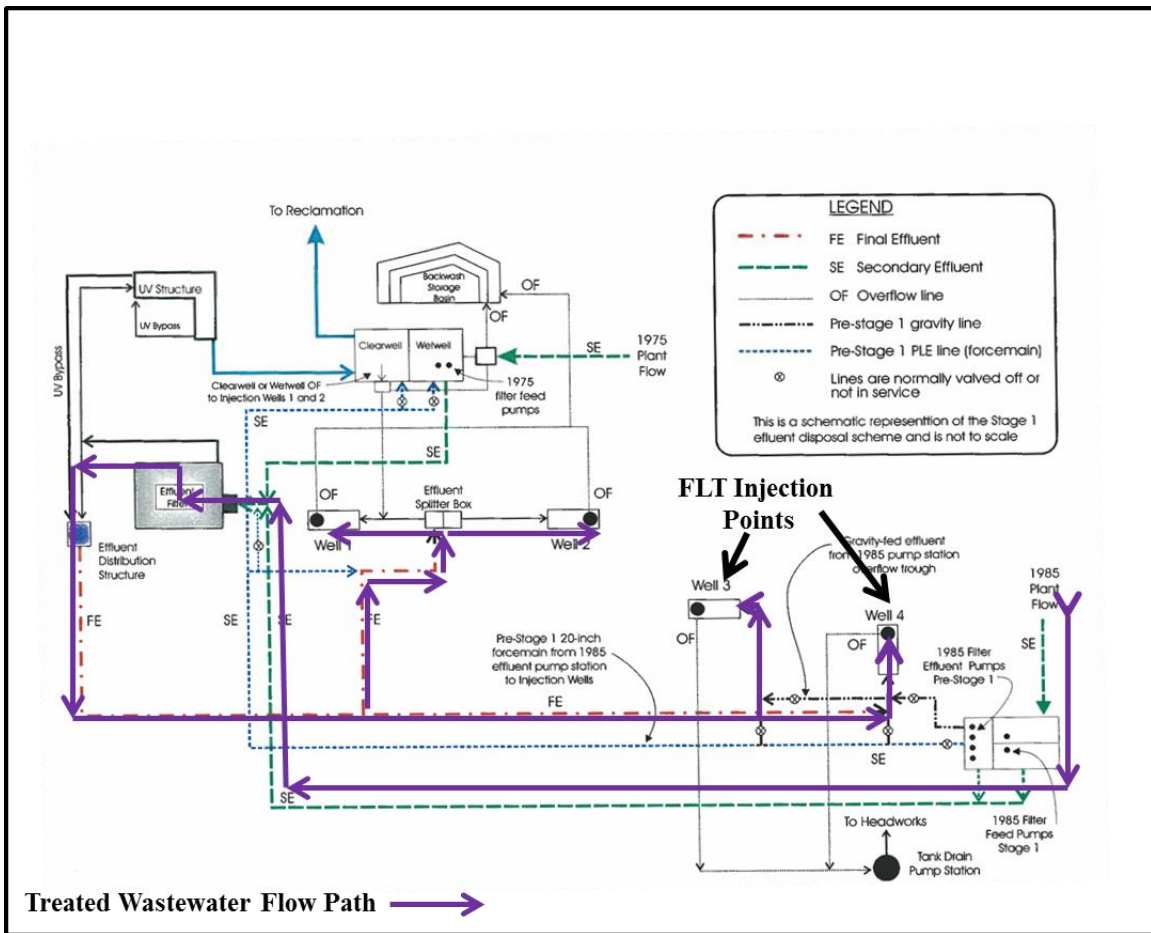


Figure 4-4: A line diagram of the LWRF showing the FLT dye addition points (diagram from County of Maui, 2010).

Violet lines represent the flow path through the LWRF taken by the treated wastewater. The FLT was added directly to Well 3 and Well 4 (diagram courtesy County of Maui, 2010).



Figure 4-5: Mixing fluorescein in 55 gal. drums.



Figure 4-6: Transferring fluorescein concentrate to 5 gal. buckets for delivery to wells.



Figure 4-7: Transfer of the dye concentrate into injection Well 3.



Figure 4-8: The residual dye was poured directly into the well.



Figure 4-9: The fluorescein concentrate mixing continued until midnight.



Figure 4-10: The fluorescein addition continued until about 02:00.

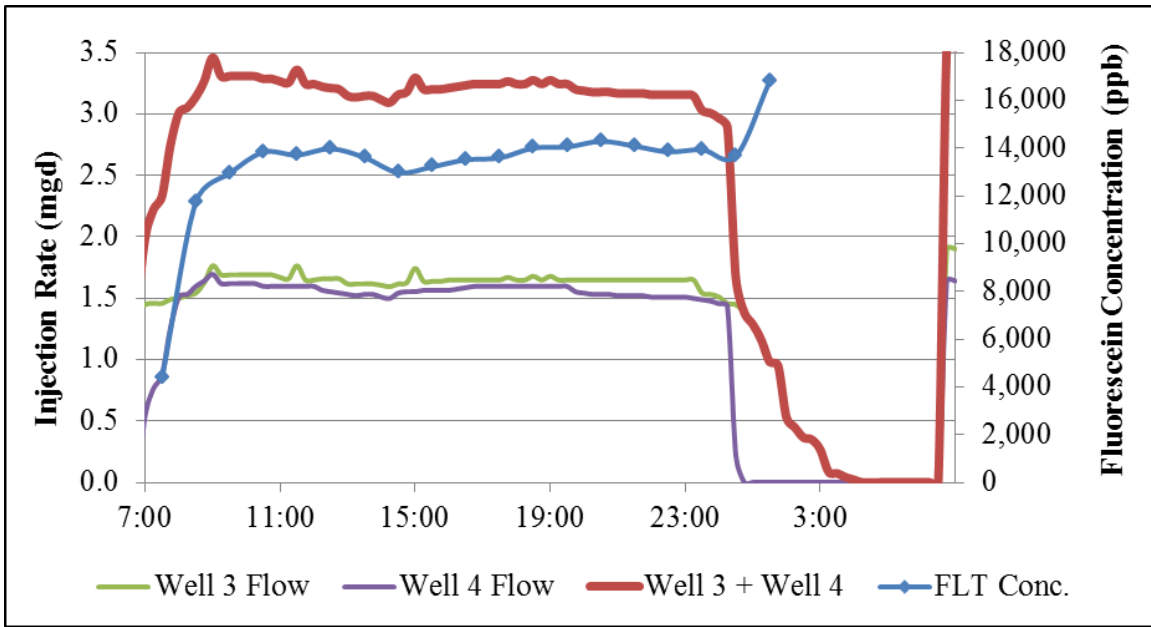


Figure 4-11: Effluent injection rates and resulting FLT concentrations for the first tracer test.

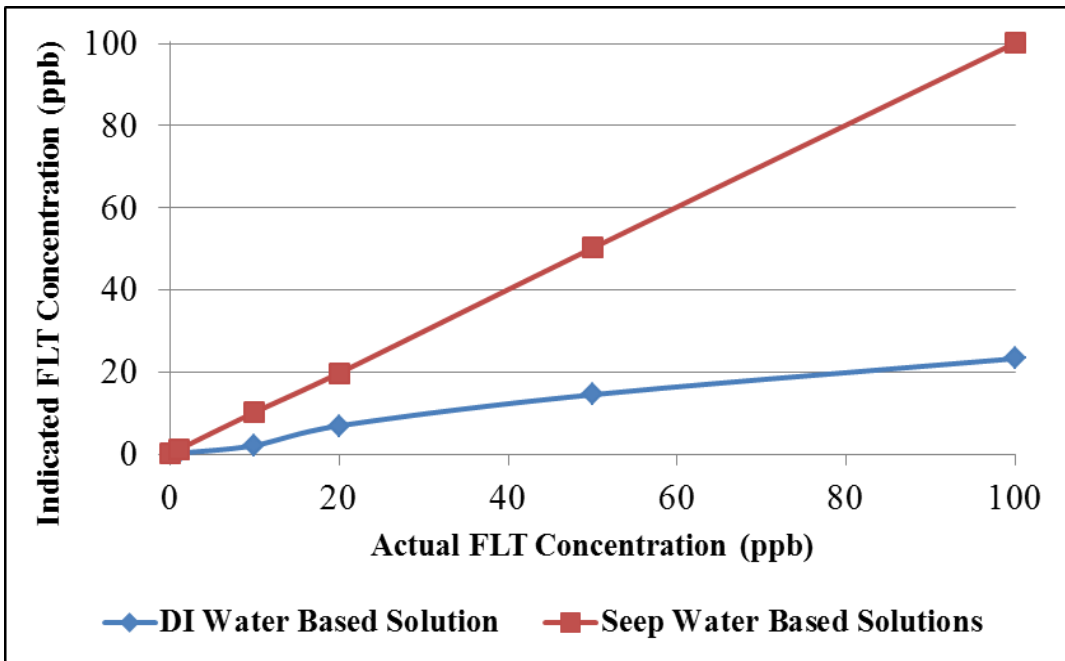


Figure 4-12: Turner 10AU response to DI water based and submarine spring water based FLT solutions.

The fluorometer was calibrated using the submarine spring water based FLT solutions.

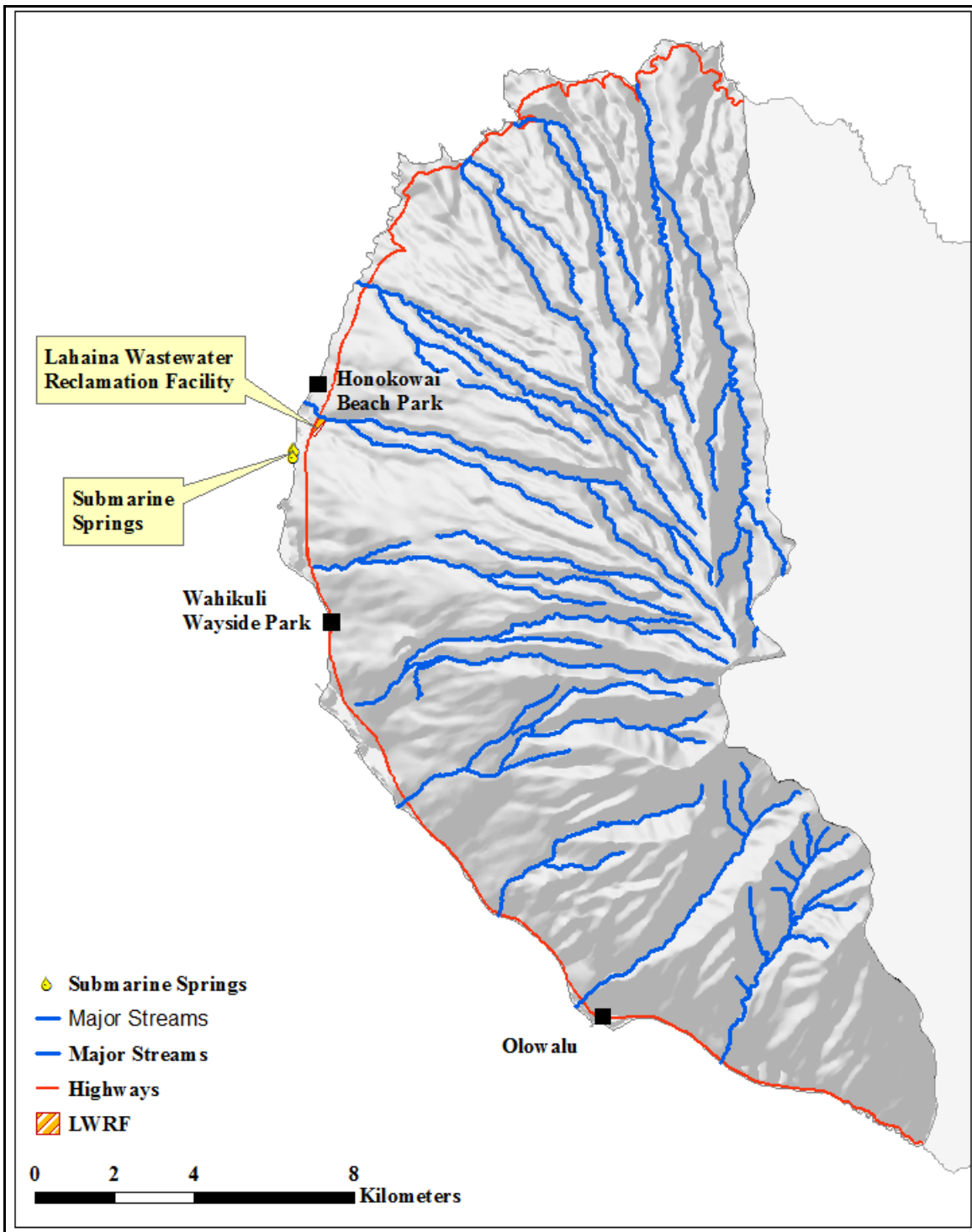


Figure 4-13: The location of the background sampling points.

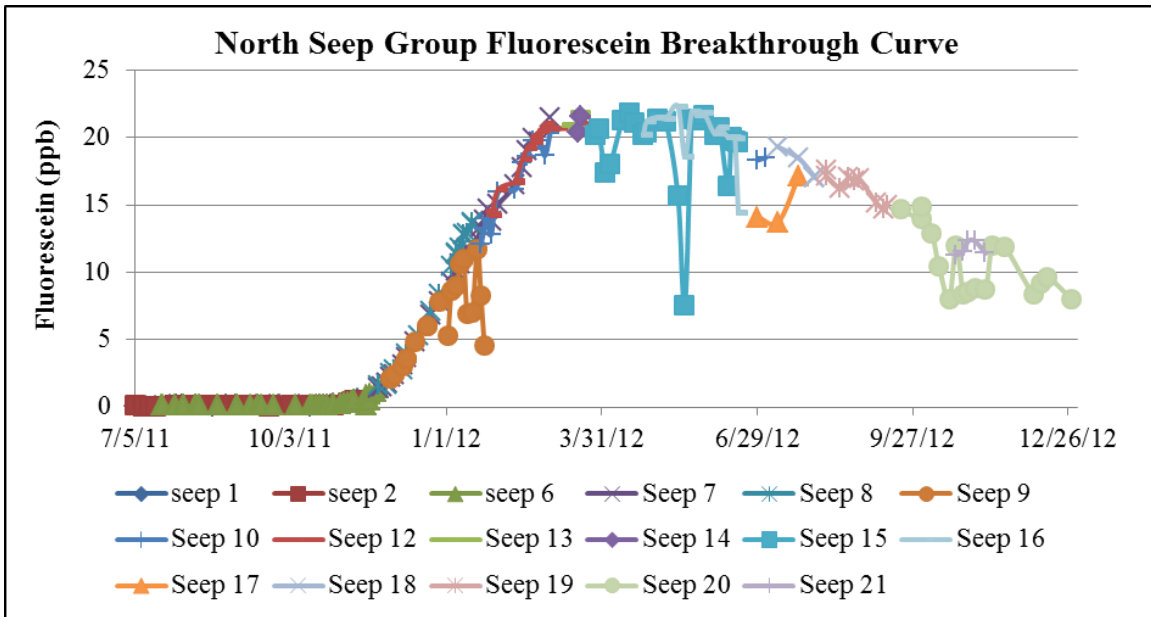


Figure 4-14: The FLT breakthrough curve measured at the NSG for each submarine spring.

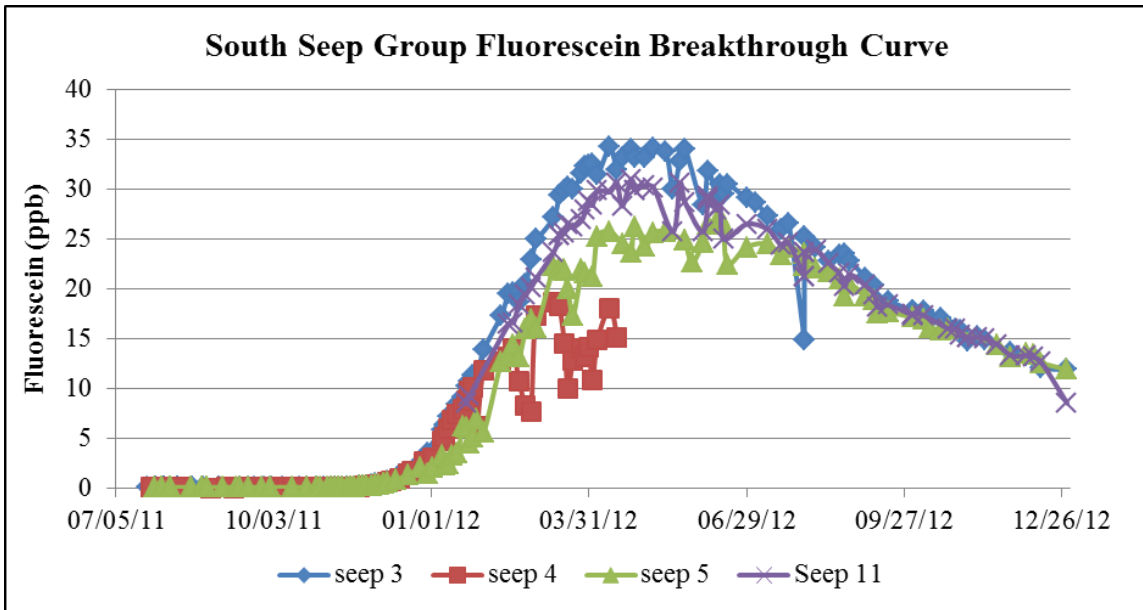


Figure 4-15: The FLT breakthrough curve measured at the SSG for each submarine spring.

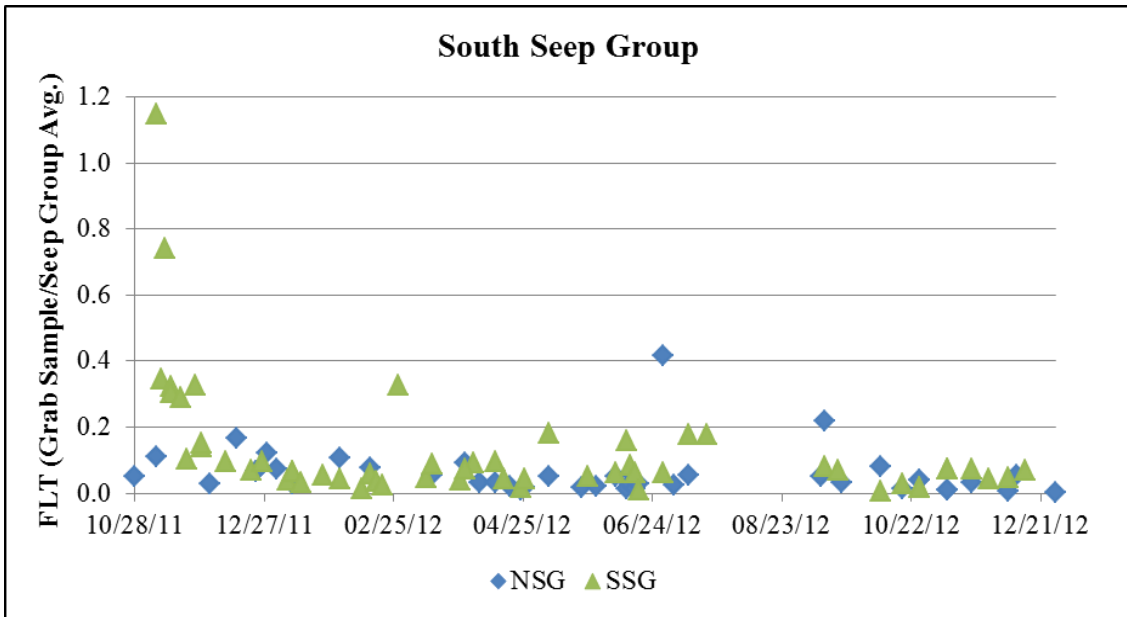


Figure 4-16: The South Seep Group grab samples FLT concentrations normalized to that of the submarine spring.

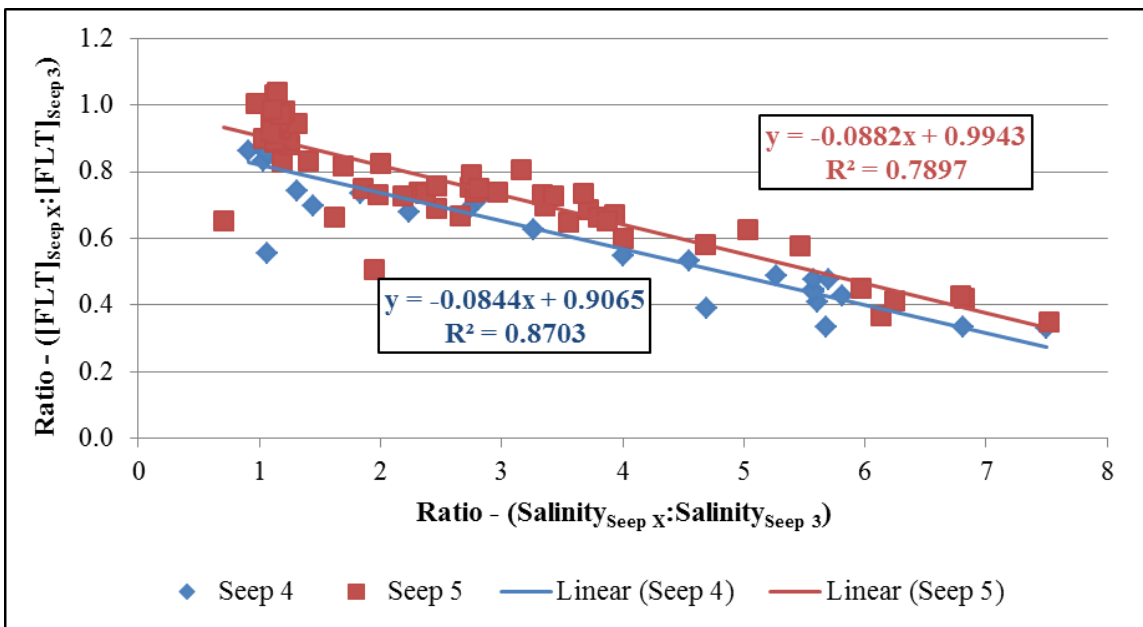


Figure 4-17: The relationship between salinity and the FLT concentration.

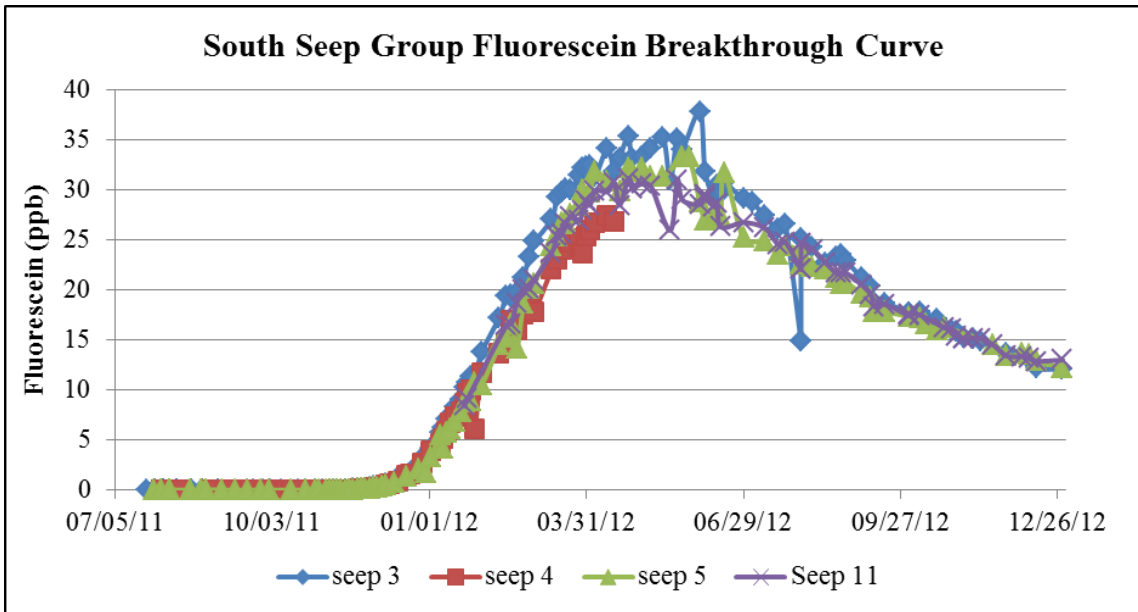


Figure 4-18: The FLT concentration as measured and corrected for salinity at the SSG.

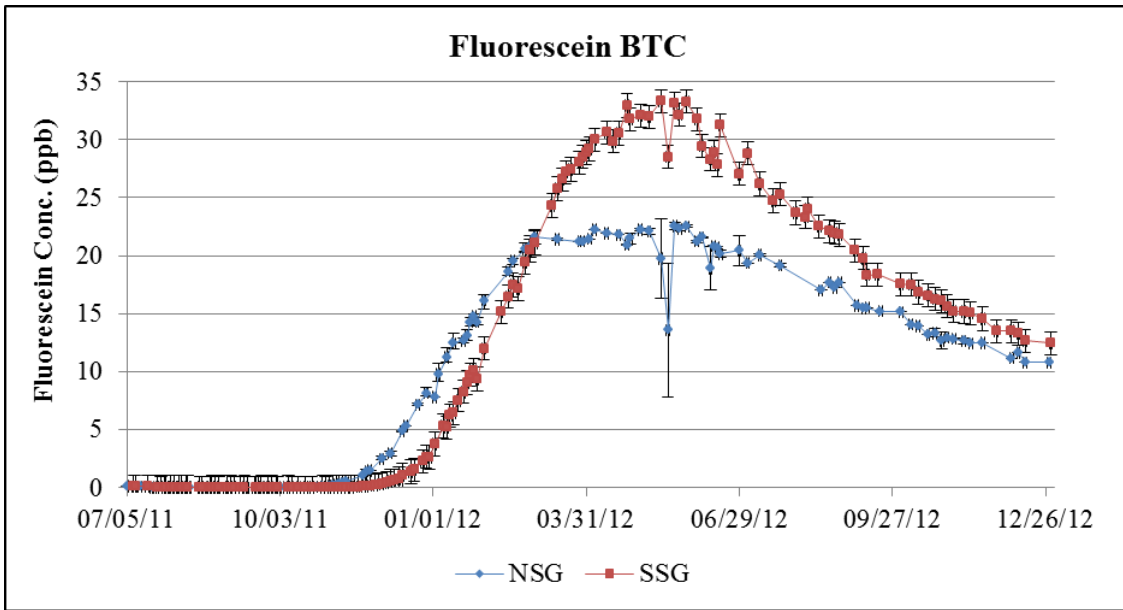


Figure 4-19: A comparison of NSG and SSG FLT breakthrough curves.

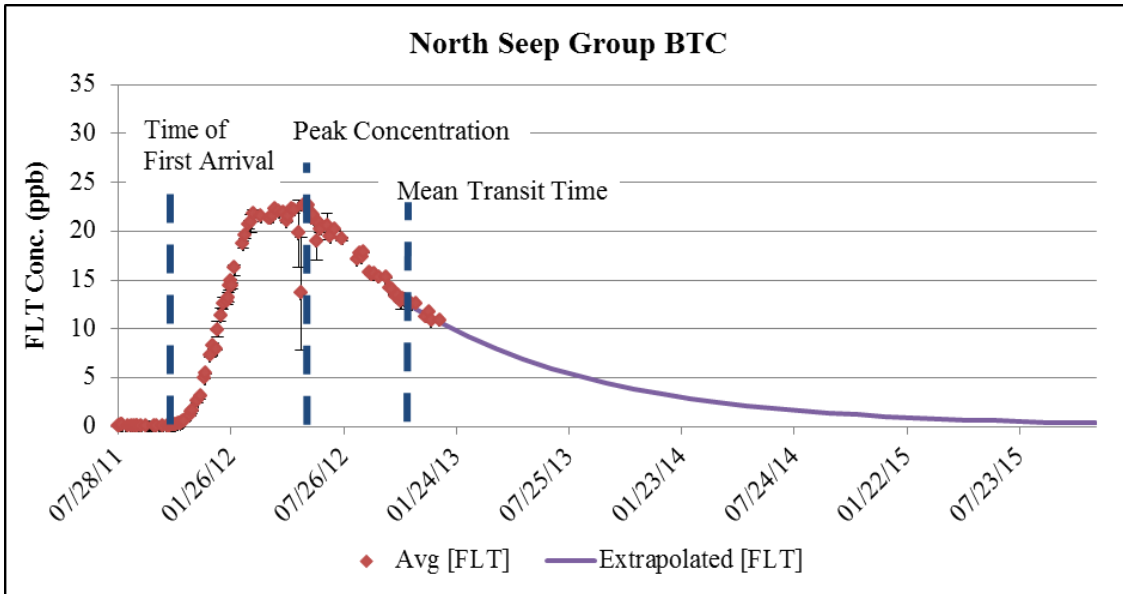


Figure 4-20: The NSG BTC extrapolated into the future until the FLT concentration drops below the MDL.

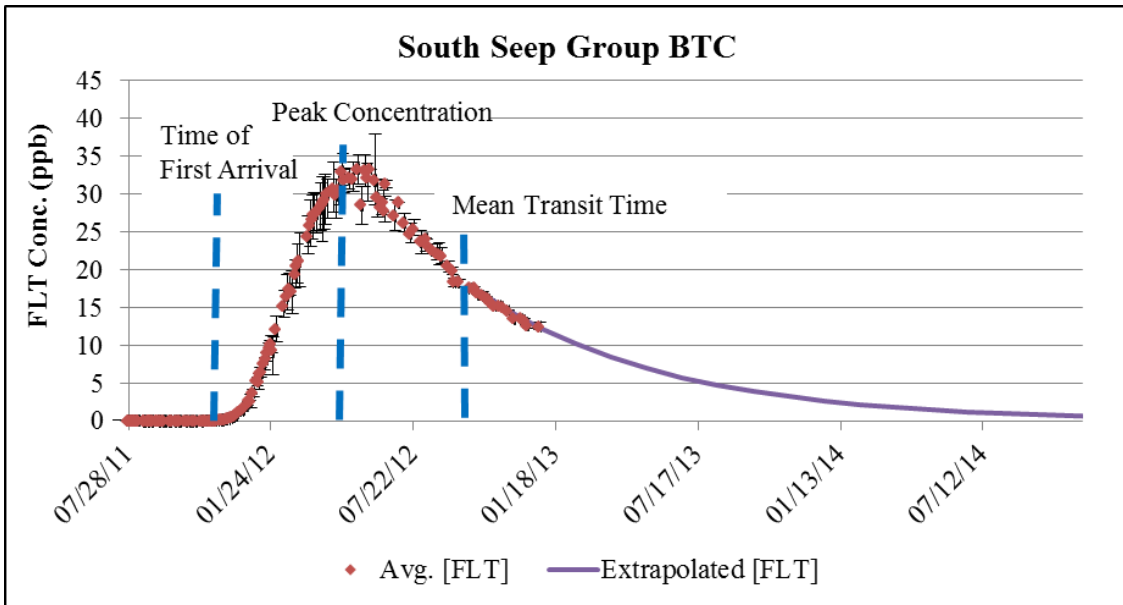


Figure 4-21: The SSG BTC extrapolated into the future until the FLT concentration drops below the MDL.

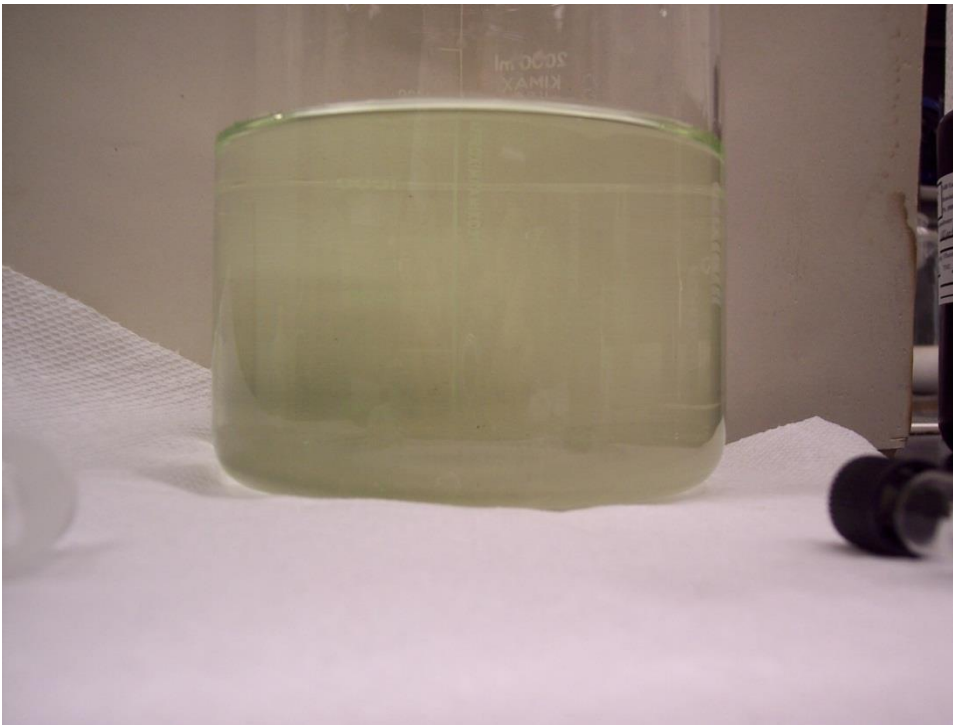


Figure 4-22: A laboratory sample with 35 ppb FLT in submarine spring water shows this dye is visible at concentrations much less than 100 ppb.

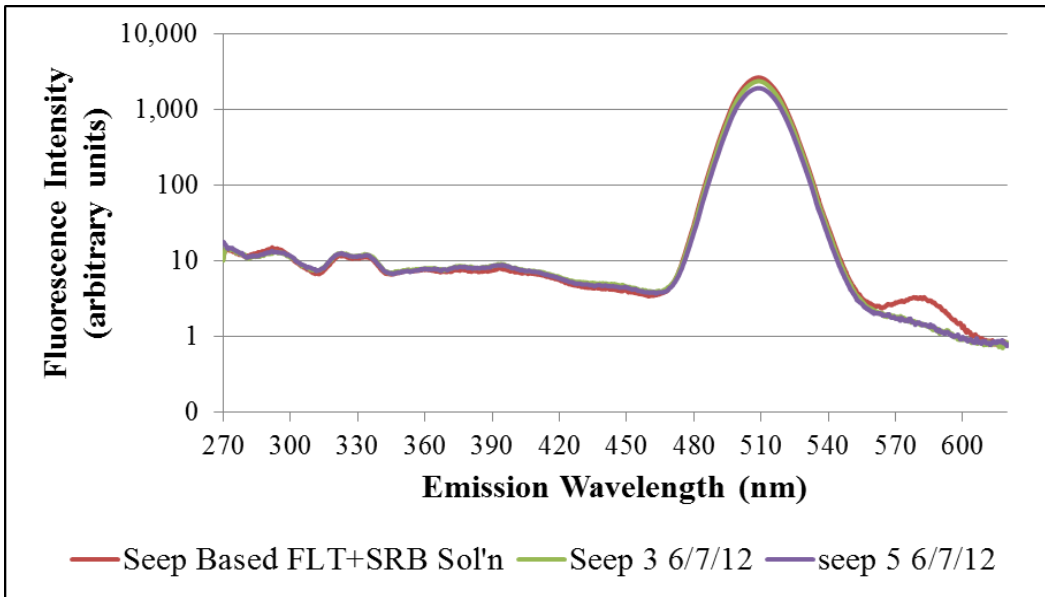


Figure 4-23: Two-dimension synchronous scans of a submarine spring sample and a laboratory sample.

The laboratory sample prepared with submarine spring water (Lab. FLT + SRB Sol'n) contains 35 ppb of FLT and 0.1 ppb of SRB. The submarine spring sample (Seep 3 6/7/12) has a fluorescence intensity spectrum nearly identical to that of the laboratory sample with the exception of the SRB peak at 580 nm.

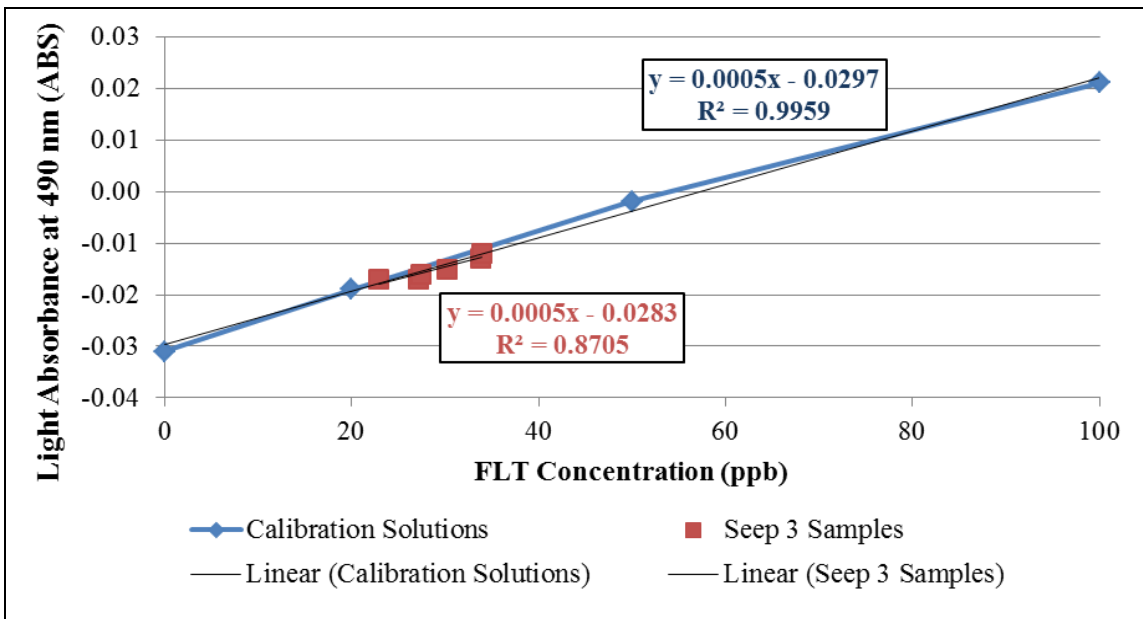


Figure 4-24: The light absorbance characteristics at the peak wavelength of 490 nm were nearly identical for calibration solutions and for samples collected at Seep 3.

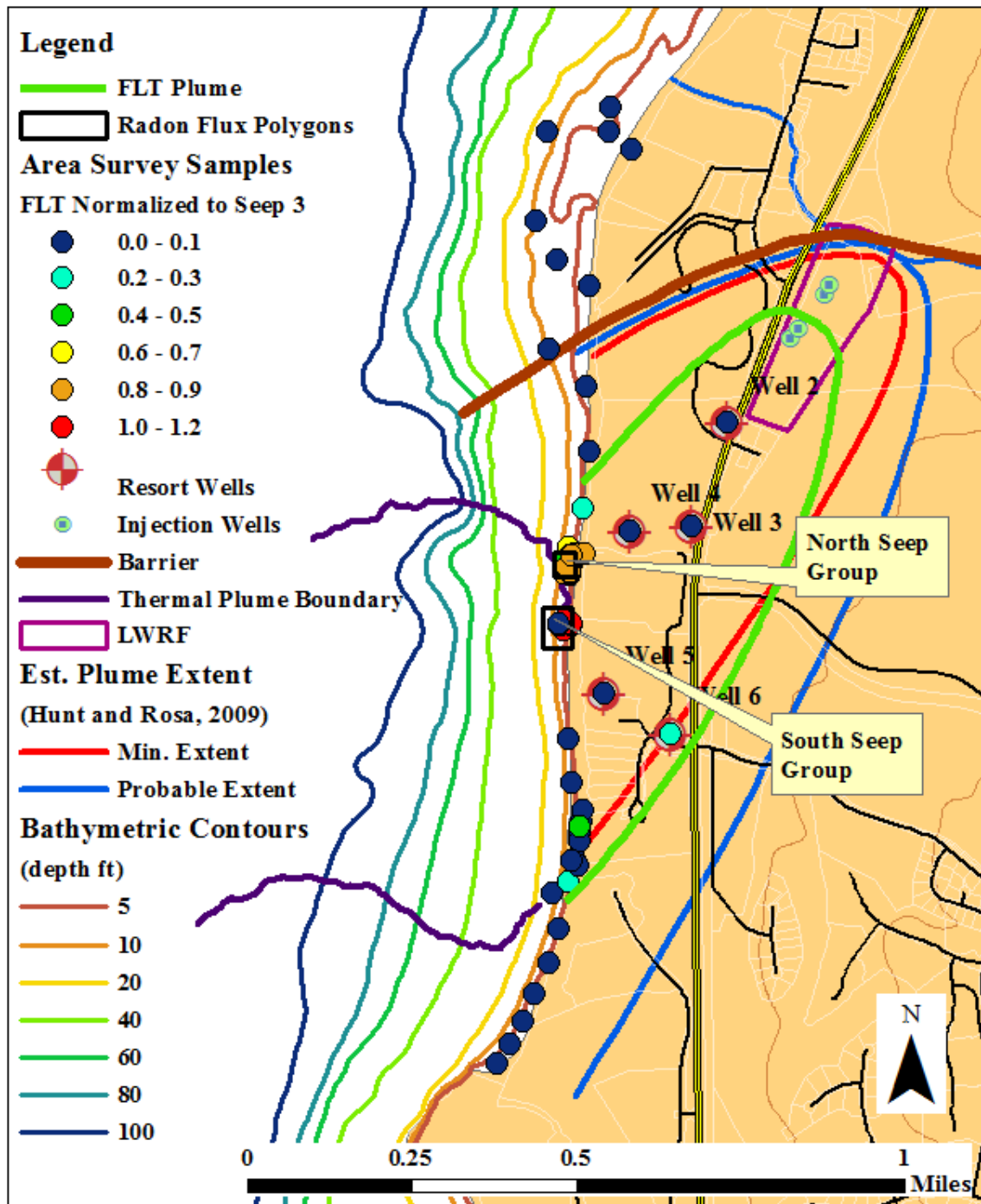


Figure 4-25: The location of points sampled during the area survey and the FLT concentration normalize to that at Seep 3.

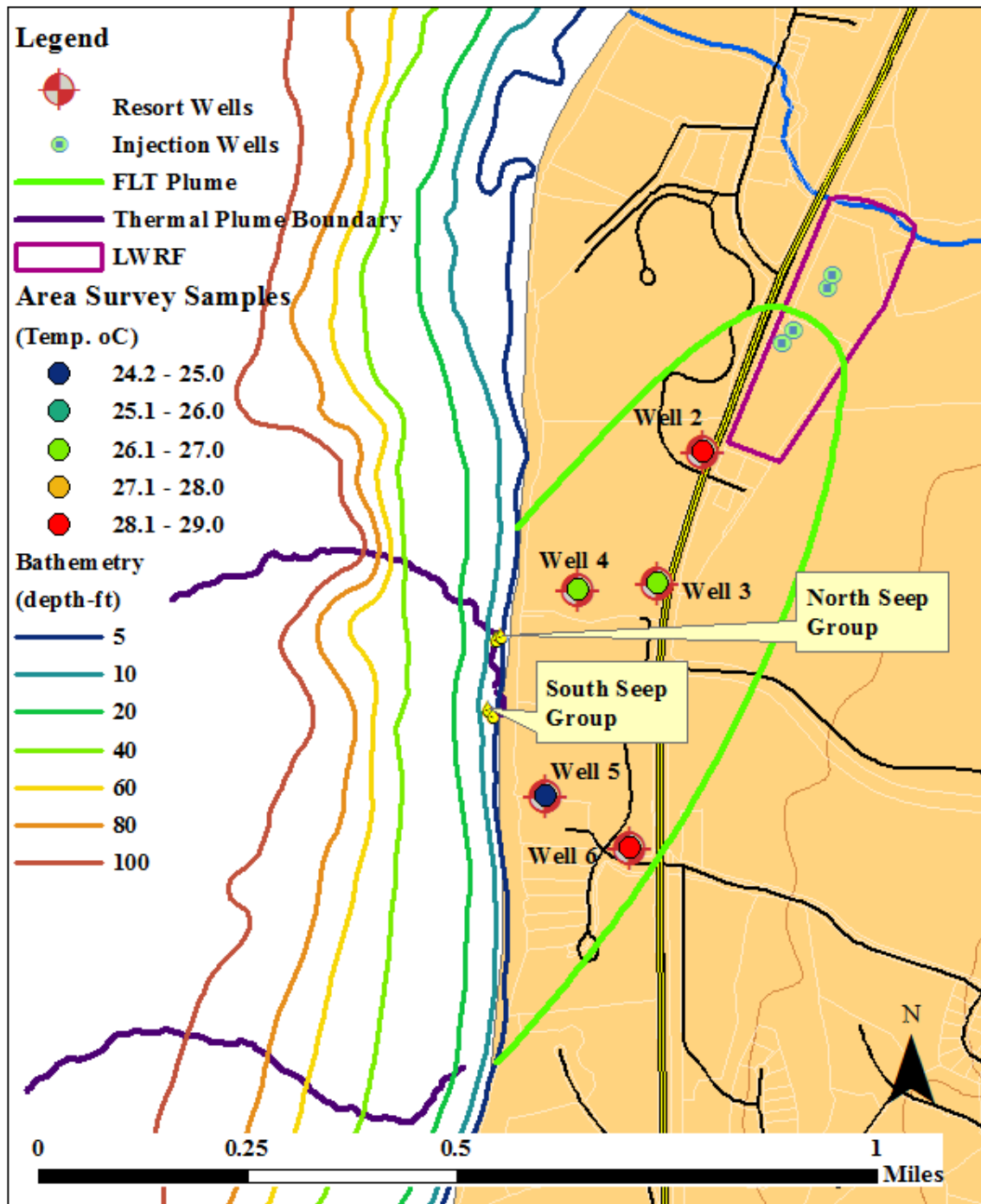


Figure 4-26: The temperature measured in samples collected at the shoreline and at the SVO monitoring wells during the area surveys.

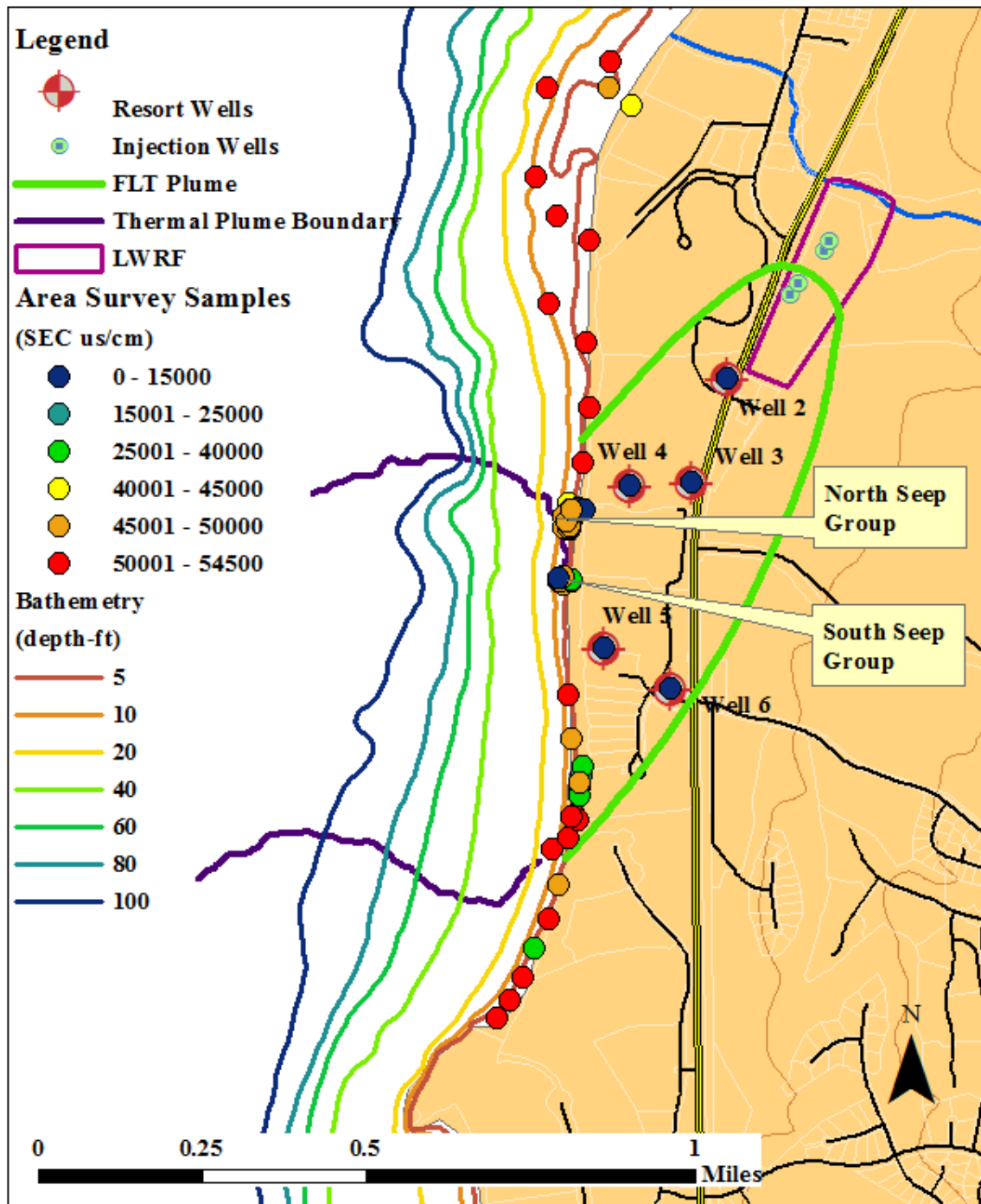


Figure 4-27: The specific electrical conductivity measured in samples collected at the shoreline and at the monitoring wells during the area surveys.

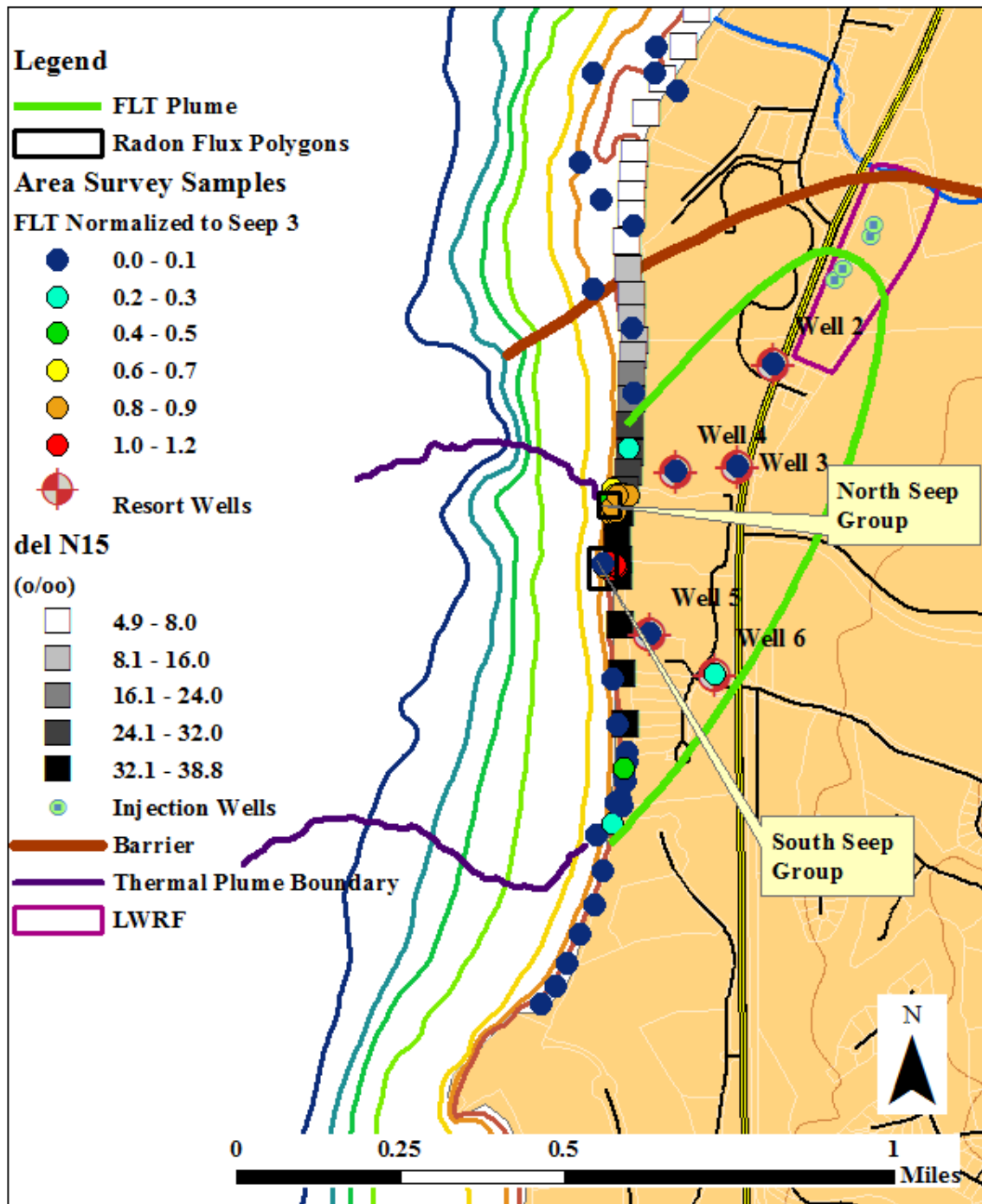


Figure 4-28: The results of macroalgae $\delta^{15}\text{N}$ values shown in relation to the normalized FLT concentrations of area survey.

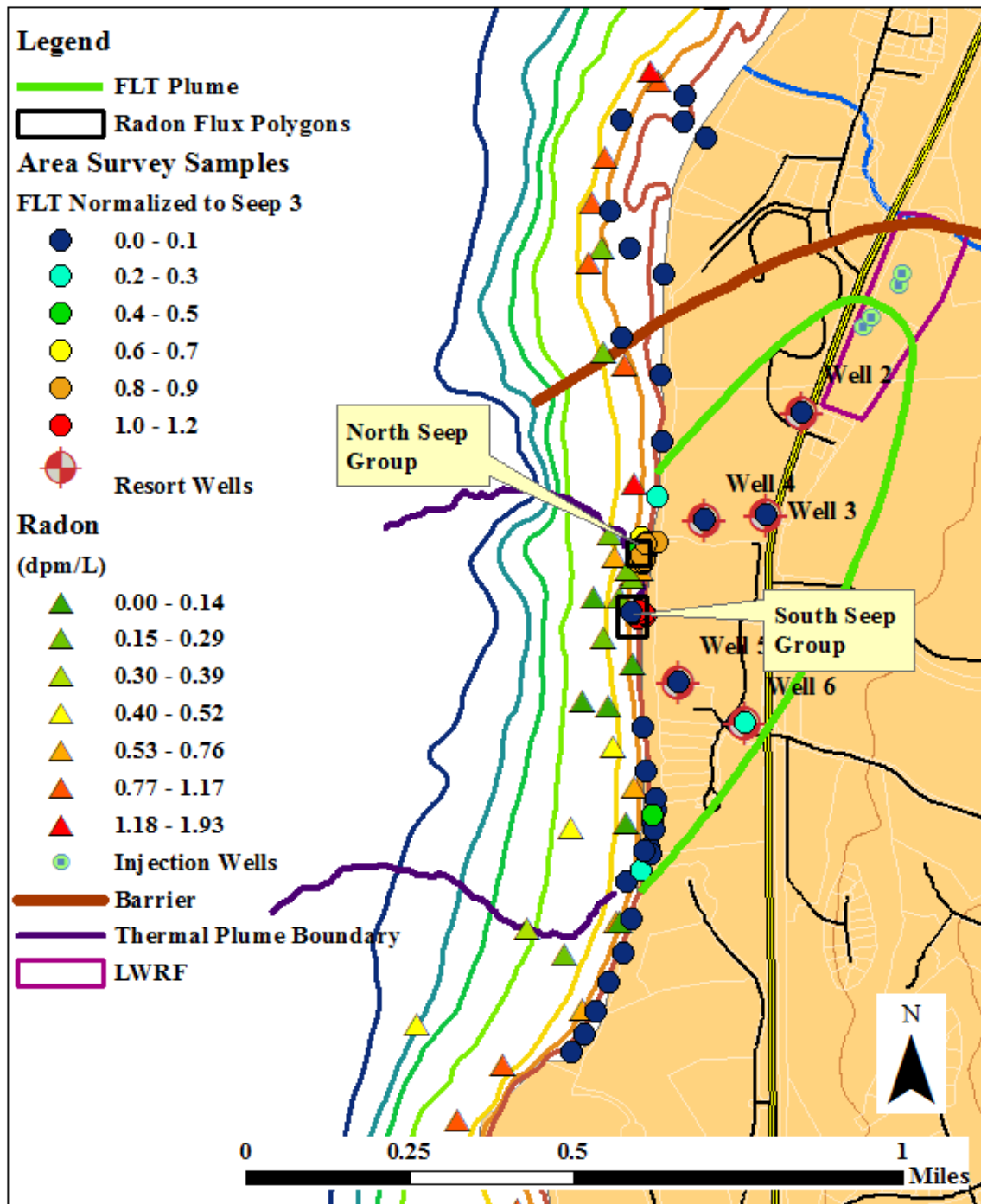


Figure 4-29: The results of the nearshore radon survey shown in relation to the normalized FLT concentrations of area survey.

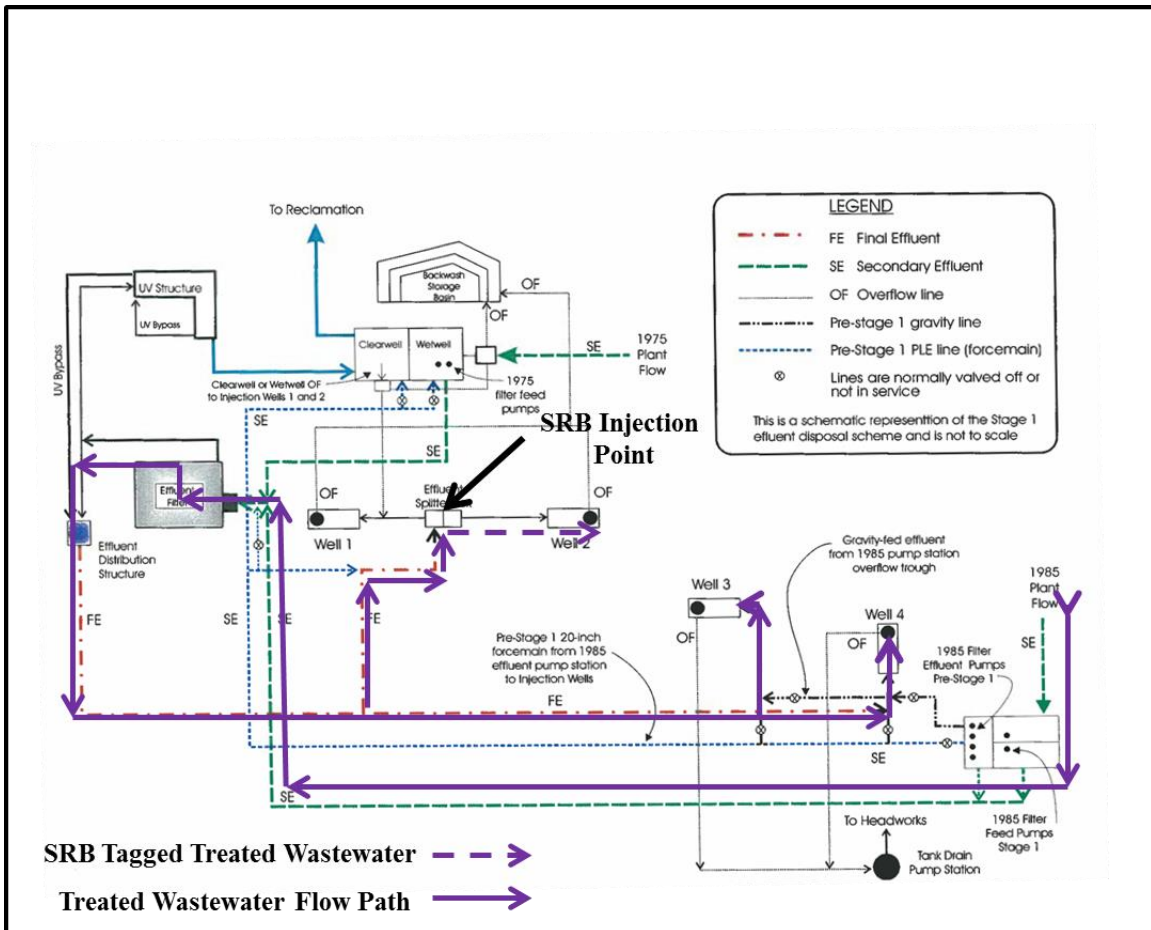


Figure 4-30: A line diagram of LWRF showing dye addition points for SRB. Violet lines represent the flow path of the treated wastewater through LWRF. The SRB was added to the splitter box between Well 1 and Well 2. Well 1 was shut off during the dye addition (diagram courtesy County of Maui, 2010).

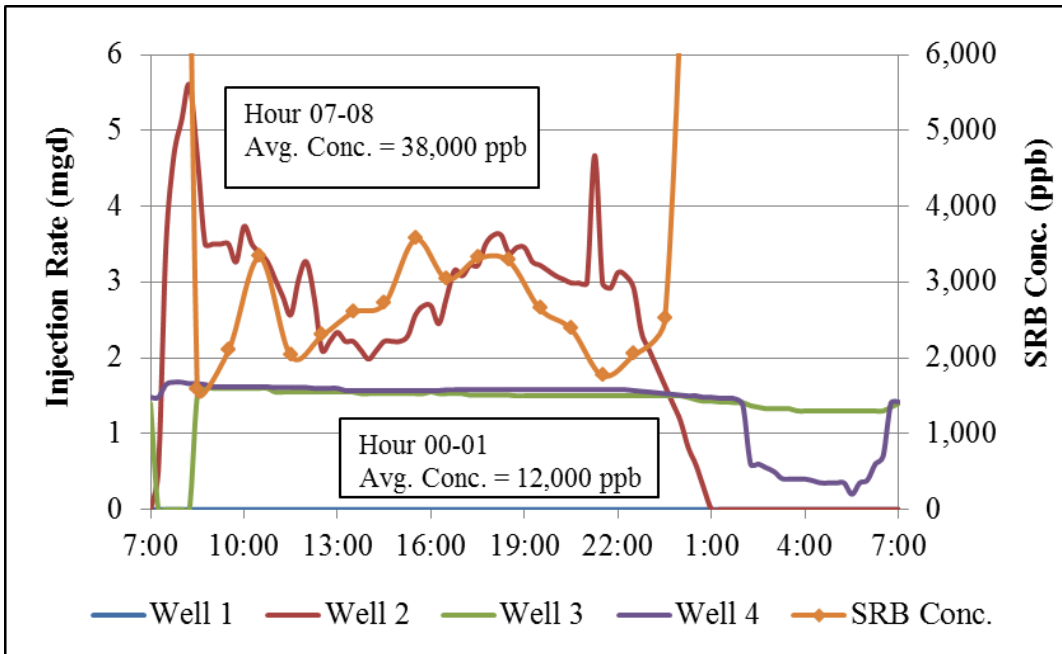


Figure 4-31: Effluent injection rates and the resulting SRB concentration.

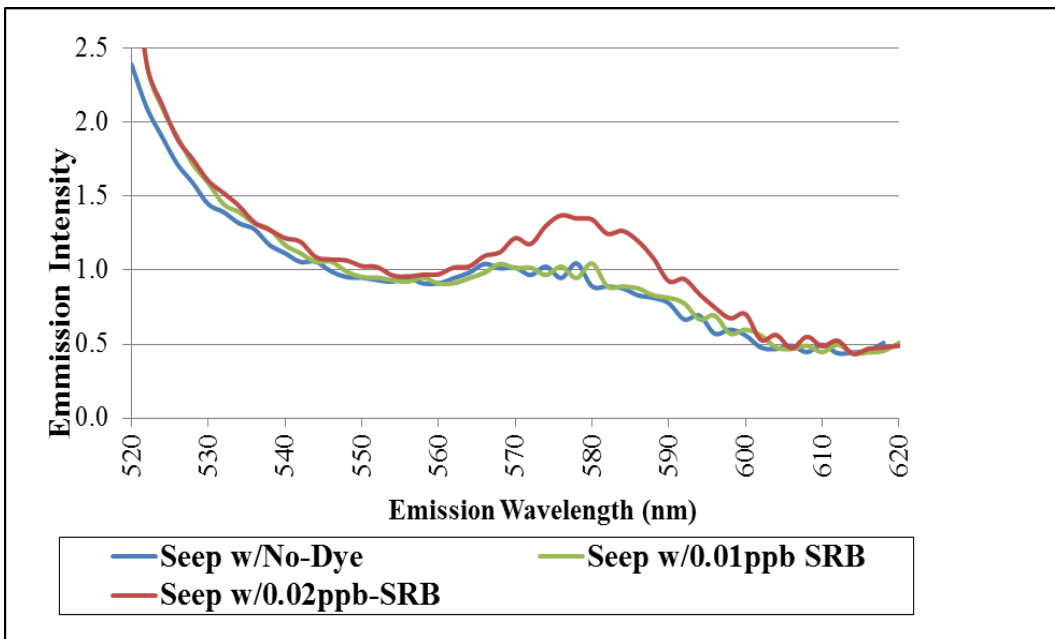


Figure 4-32: Synchronous scans of SRB calibration solutions.

Solutions were mixed using submarine spring water containing no dye (blue), and spiked to 0.01(ppb) (green) and 0.02 ppb (red) with SRB. There is no discernible difference between emission intensity of the no-SRB and 0.01 ppb SRB solutions.

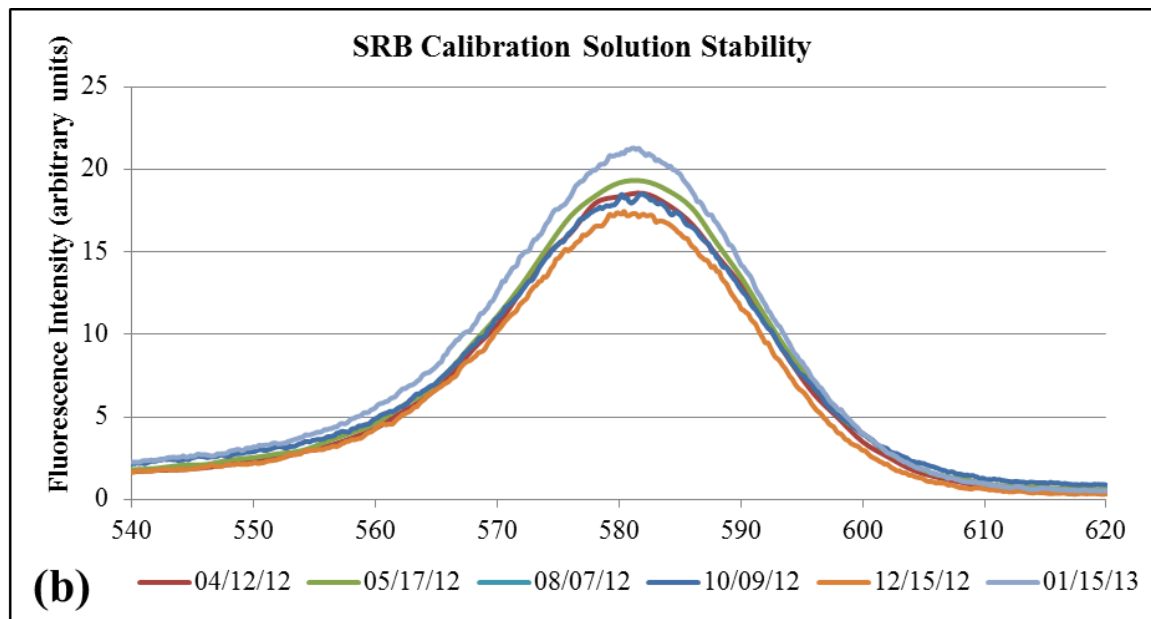
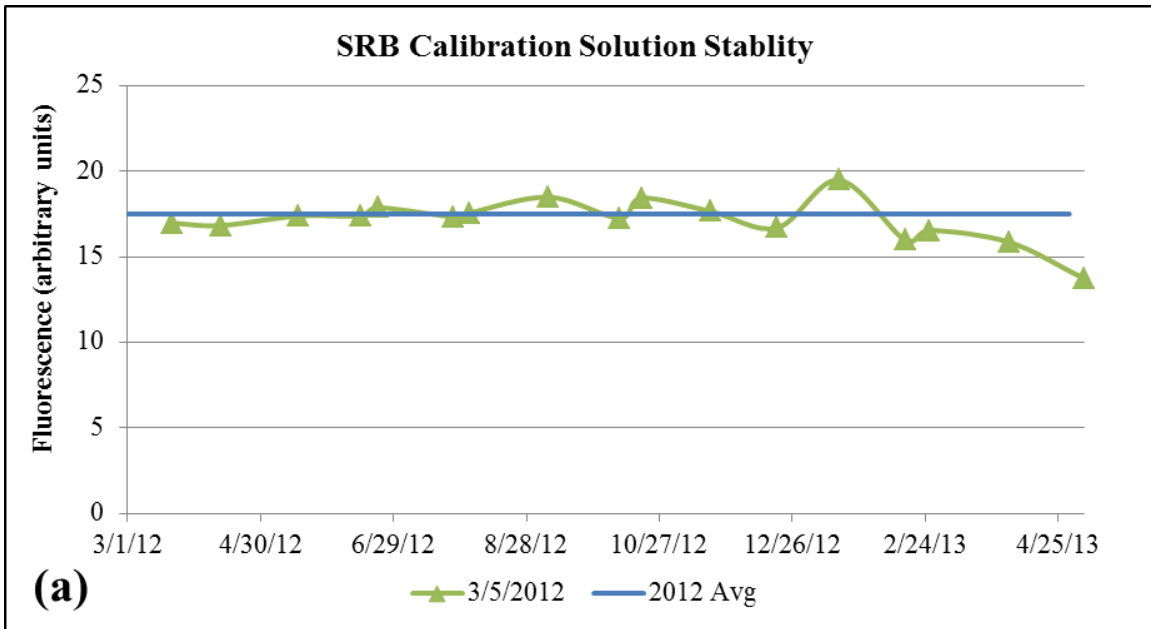


Figure 4-33: Time series graphs showing fluorescence intensity measurements and emission wavelength synchronous scans of the 1 ppb SRB calibration solution.

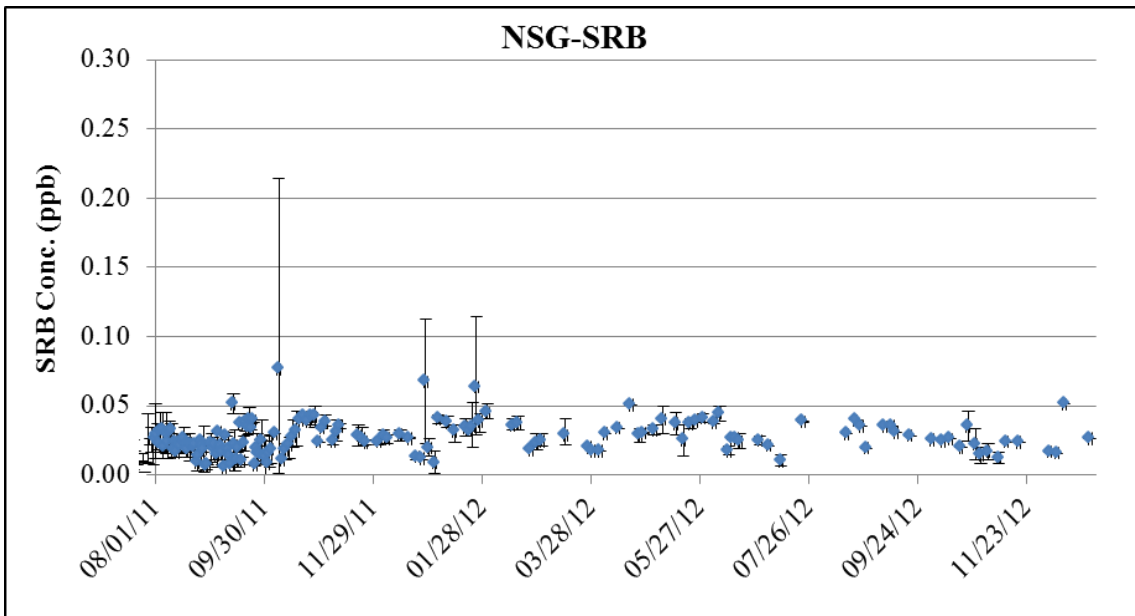


Figure 4-34: Fluorescence in the SRB wavelength measured at the NSG. Error bars indicate the maximum and minimum while the symbol indicates the average SRB fluorescence on the day the samples were collected.

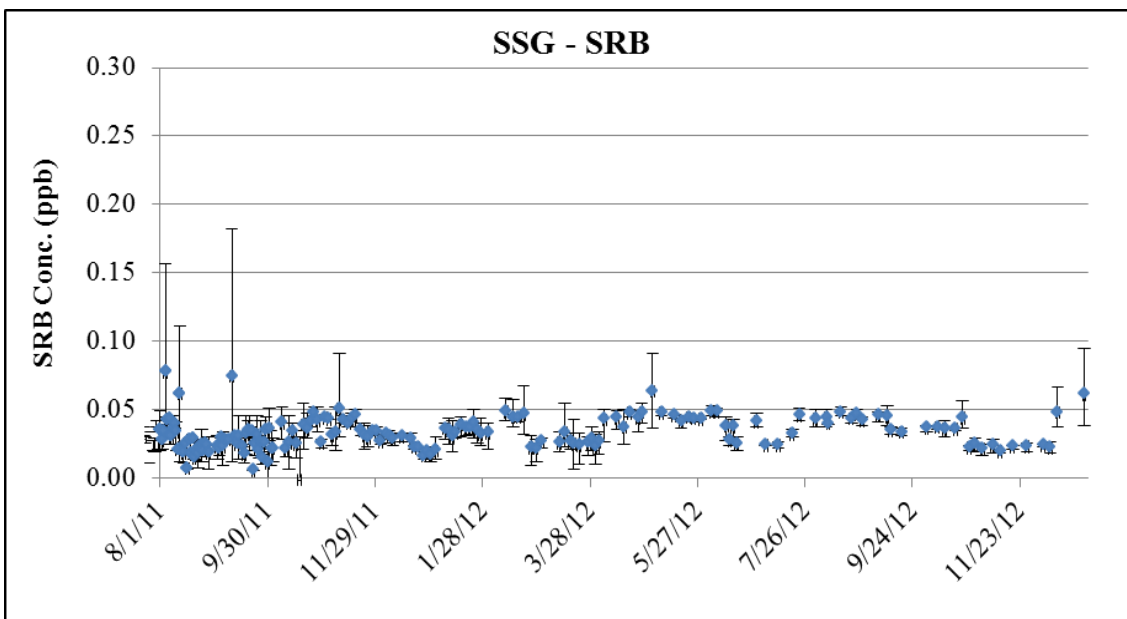


Figure 4-35: Fluorescence in the SRB wavelength for the SSG. Error bars indicate the maximum and minimum while the symbol indicates the average SRB fluorescence on the day the samples were collected.

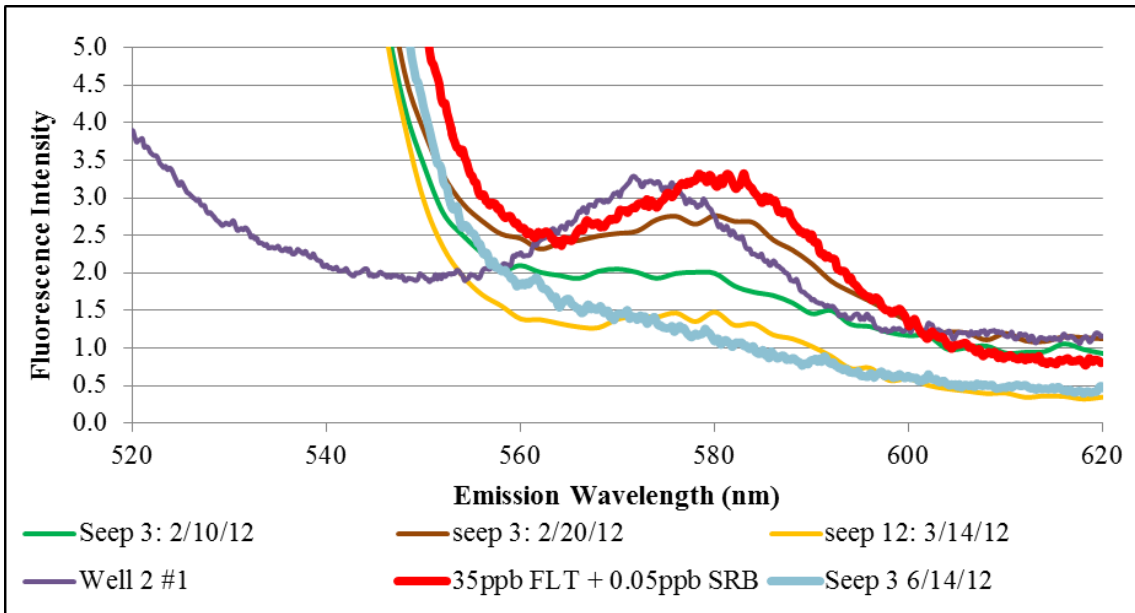


Figure 4-36: Synchronous scans of samples collected in February and March 2012 compared to solutions spiked with SRB.

The laboratory prepared sample (35 ppb FLT + 0.05ppb SRB) is a reference to which the field samples can be compared. The declining limb of the FLT peak is evident from about 550 to 560 nm. The SRB is shown as curve with a peak center at 580 nm. The sample “Seep 3 6/14/12” is shown as an example of a sample with no indication of SRB.

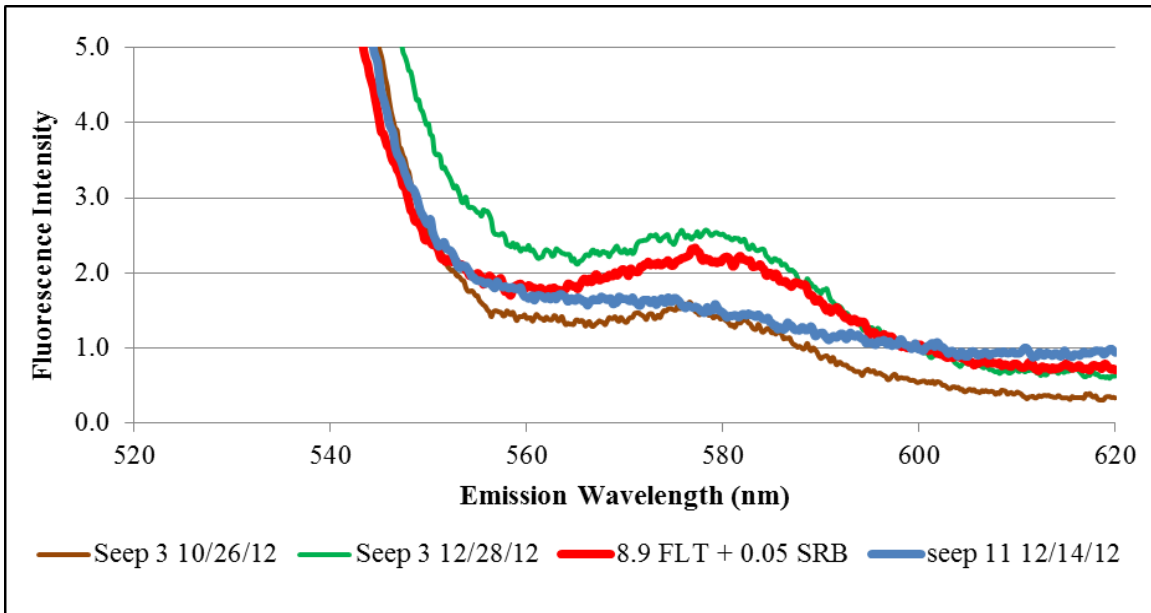


Figure 4-37: Synchronous scans of samples collected in October and December 2012 compared to solutions spiked with SRB.

The trace labeled “8.9 FLT + 0.05 SRB” is a laboratory prepared sample shown for reference. The trace labeled “Seep 11 12/14/12” is an example of a sample with no indication of SRB.

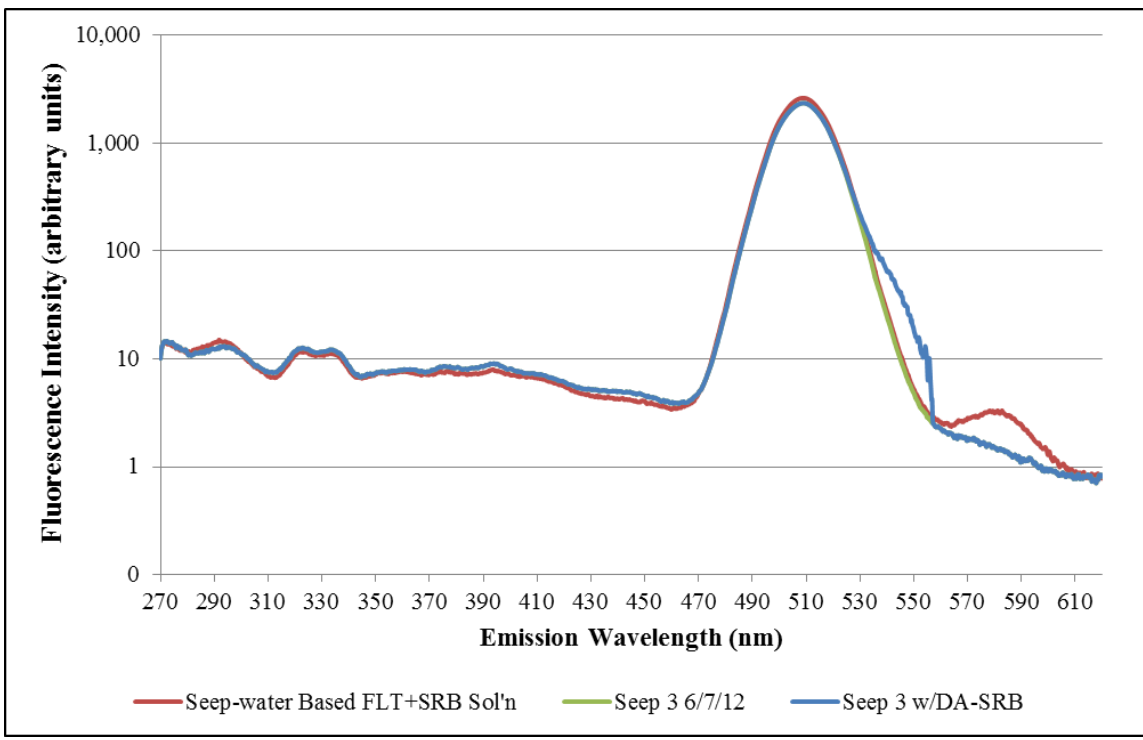


Figure 4-38: Graphed are three synchronous scans to show the spectra of fluorescein, SRB, and fluorescein plus a hypothetical DA-SRB trace.

The first trace (shown in red) is a laboratory-prepared sample containing about 35 ppb of fluorescein and about 0.1 ppb of SRB. The second trace (shown in green) is a scan of a sample collected from Seep 3 on June 7, 2012. The fluorescein concentration in this sample was 32 ppb, but there is no indication that this sample contains SRB. The AFHF indicated this sample contained 3.3 ppb of SRB. The third trace (shown in blue) is the emission spectra of what the Seep 3 sample might look like if it contained 3.3 ppb of DA-SRB. The degraded SRB results in an asymmetrical fluorescein fluorescence trace with a “bulge” on the descending limb.

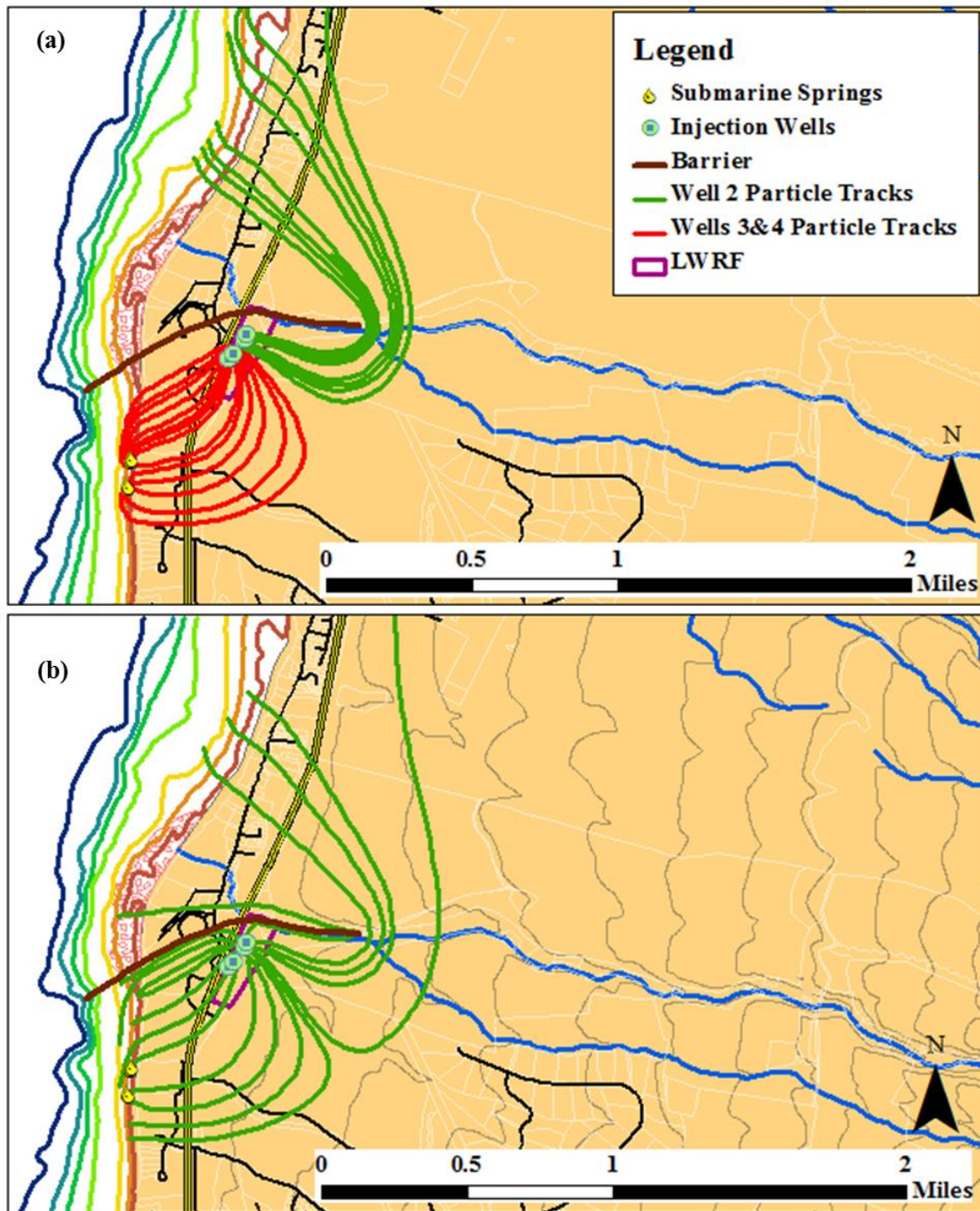


Figure 4-39: The results of the particle tracking MODPATH model that shows the possible groundwater pathways with injected wastewater.

Figure 4-38a shows the tracks that simulated particle take when the majority of the treated wastewater is injected into Wells 3 and 4. The particle tracks of the Well 2 injectate (shown in green) are displaced inland and to the north by the injectate from Wells 3 and 4 (shown in red). Figure 4-38b shows that when all of the treated wastewater is injected into Well 2, many of the particle tracks from Well 2 reach the submarine springs.

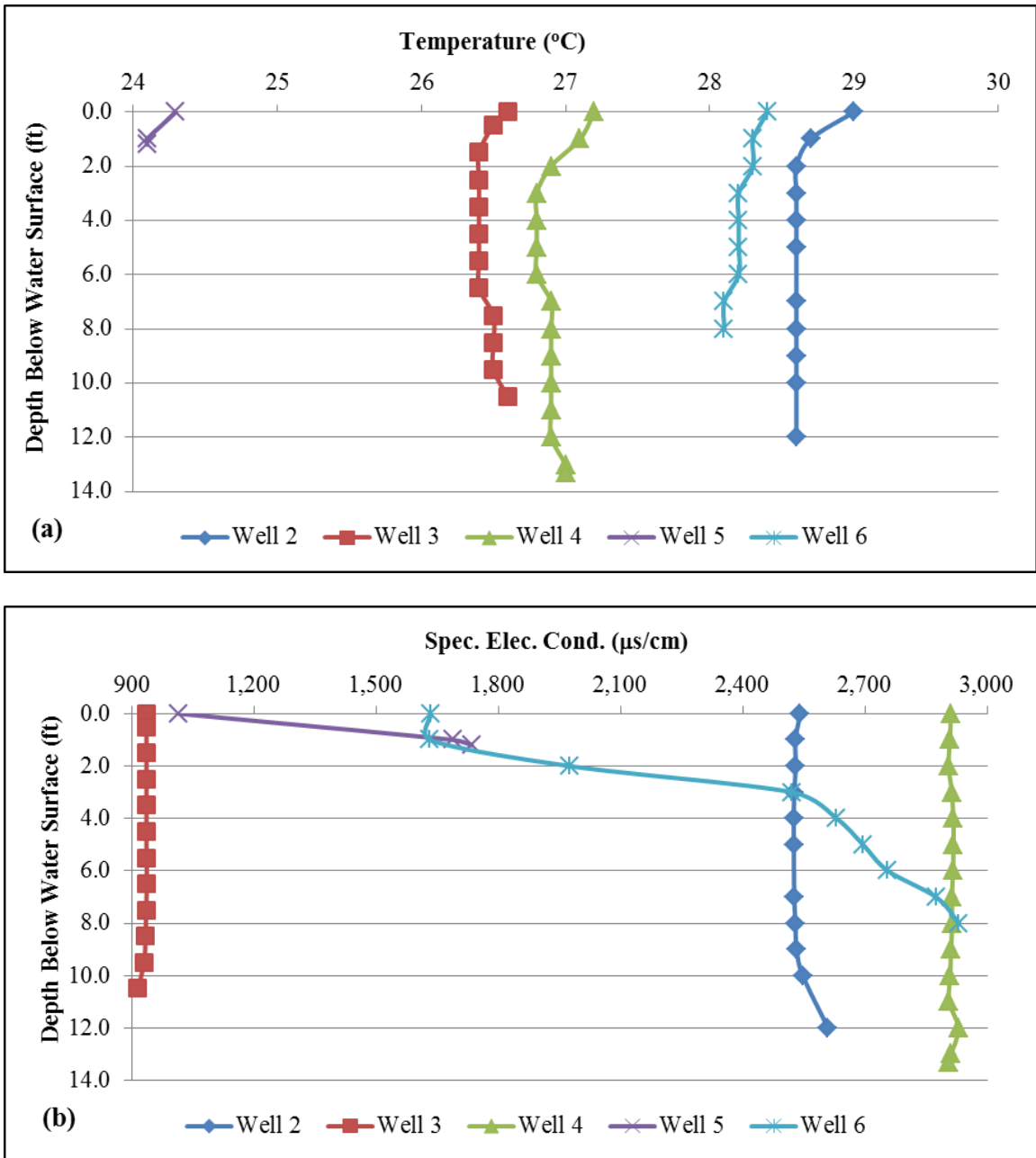


Figure 4-40: Temperature and specific electrical conductivity profiles for the SVO wells. The temperature profiles (a) show a warm layer of water at the surface of the water table in all wells. The SEC profiles (b) shows that there is a layer of fresher water at the surface of the water table of Well 5 and Well 6.

This page is intentionally left blank.

SECTION 5: TRACER TEST NUMERICAL MODELING

5.1 INTRODUCTION

Groundwater modeling was used by this study to aid in the design of the tracer test, interpret the dye tracer breakthrough curve (BTC), and assess processes that affect the fate and transport of the injected treated wastewater. In general, estimation of critical tracer test parameters is not an easy task. For the current study, the complexity of the problem is compounded by hydrogeology, where the tracer plume is affected by the density difference between freshwater and salt water and the fact that the point of monitoring is where this plume enters the marine environment. A numerical model is appropriate for a detailed interpretation of the fate and transport of the dissolved tracer utilized in this study.

The approach used for modeling the Lahaina Groundwater Water Tracer Study was three-fold. First, a basic model was developed to aid in the design of the tracer test, which was termed the Tracer Test Design Model (TTDM). The primary purpose of this model was to estimate the tracer dye dilution that would occur as it traveled from the injection wells to the submarine springs. The secondary purposes were to aid in the sampling plan by estimating the time of first dye arrival and the duration of the BTC. Once the dye started emerging from the submarine springs, the developing BTC was compared to the output of the TTDM. As differences were noted, the TTDM was modified to obtain an improved agreement between the model output and the tracer data. Finally, after the BTC was sufficiently developed, the model output was compared against the tracer data and a comprehensive revision of the model was undertaken. The final model was modified to match the BTC data. Different hydrogeological processes and features were then tested to determine which process might be affecting the tracer dye transport.

5.2 MODELING OBJECTIVES

The specific modeling objectives were to: (1) provide critical data needed to design the tracer test; (2) investigate the role of hydrologic features, such as barriers or preferential flow paths, on the dye transport; and (3) assess the impacts of aquifer processes, such as sorption and dispersion, on the temporal and spatial distribution of the tracer dye concentration. In contrast to analytical approaches, numerical solutions rely more on physically based equations that are more realistic if supported by adequate data. Hence, modeling the tracer test results can shed light on the aquifer and hydrologic conditions at the study site. One should recognize, however, that there is significant uncertainty regarding aquifer properties and chemical interactions in the aquifer. A major difficulty is related to the potential existence of preferential flow. Adopted modeling approaches are suitable for porous media

or if the media can be treated as an equivalent porous media. Models for discrete fractures are not readily available and their data requirements are not easy to satisfy. For this reason, we limit the modeling objectives to assessing the influence of a limited number of processes (dispersion, sorption, and advection) on the transport of the dye. Advection is the movement of the dissolved species due to the flow of groundwater, dispersion is the spreading of the dissolved species due to mechanical dispersion and molecular diffusion, and sorption is the partitioning of a dissolved species onto the aquifer matrix (Fetter, 1992).

This report describes the models developed this study, how these models were used to assess the monitoring results, and evaluates various site conceptual models and their limitations.

5.3 MODELING APPROACH

The models used in this study neglect density-dependent flow by only considering freshwater movement. Uniform density models have advantages including the ease of development and use, and the relatively limited data requirements. The saltwater interface used to specify the bottom boundary of the model was based on the density-dependent model developed by Gingerich (2008). Using this approach is reasonable considering that models indicated that, shortly after being injected, the buoyancy of the treated wastewater causes it to rise relative the surrounding saline water, placing it in the freshwater zone (Wheatcraft et al., 1976; Burnham et al., 1977; Hunt, 2007). Hence, the majority of the flow is restricted to the fresh water lens.

The Modular Finite Difference Groundwater Flow Model MODFLOW (Harbaugh et al., 2000), developed by the U.S. Geological Survey, is widely used software for simulating groundwater systems. In general, the applicability of MODFLOW for this site is limited due to its inability to simulate density-dependent flow. However, this model was used due to its relative ease of use and limited data requirement in comparison to a variable density model. In addition, as described above, the majority of flow of the treated wastewater transport occurs in the freshwater zone, which justifies the use of such an approach. To accomplish this, the centerline of the freshwater/seawater-mixing zone was taken as a no-flow boundary representing the bottom of the freshwater zone.

The groundwater flow solution computed by MODFLOW is used by transport models to simulate the movement of dissolved constituents in groundwater. The first such model used by this study was the USGS particle tracking model MODPATH (Pollock, 1994). The MODPATH model uses the groundwater flow solution from MODFLOW to track the movement of virtual particles from cell to cell in the finite difference grid, by only considering advection. The output is a visual track representing the path the virtual particles take from a point of origin to a point of termination. The point of termination can either be defined by an elapsed time designated by the modeler, or as a boundary or sink in the modeled area.

Results of the MODFLOW run were used as an input to the solute transport code Multi-Species Transport Model in Three Dimensions (MT3DMS) (Zheng and Wang, 1999; Zheng,

2006) to simulate the tracer test experiment. MT3DMS is a contaminant transport model that simulates the dissolved transport of multiple species. The code simulates the effect of advection, hydrodynamic dispersion retardation (slowing of the plume transport due to the dissolved species sorbing onto the aquifer matrix), and the role that hydraulic conductivity anisotropy play in the transport of the dissolved tracer dye.

To simplify the model setup, the Groundwater Modeling System (GMS) (www.aquaveo.com/GMS) graphical user interface was used. GMS is used to create a conceptual model directly or to extract data from Geographic Information System (GIS) maps that are read into GMS. Once the model simulation has been completed, the results can be converted to shapefiles or to a GIS raster for use in ArcGIS.

5.4 Tracer Test Design Model (TTDM)

The Tracer Test Design model was developed to aid in designing the tracer test. The objectives were to: (1) assess the expected dilution of the dye; (2) estimate the time of the first arrival of the tracer to the submarine springs; and (3) estimate the duration of the dye emergence at the submarine springs. Such information was critical for planning the dye addition procedures and developing the submarine spring monitoring plan.

5.4.1 Numerical Model

5.4.1.1 Model Grid

Computer calculations for the groundwater flow are performed using a matrix of cells, referred to as a grid, that contain the pertinent data. The TTDM grid consisted of 31,094 cells distributed among six layers. The bottom elevation of the first layer was set at -19.7 ft (-2 m) in reference to mean sea level (m msl). The bottom elevations of the remaining layers were evenly distributed between -19.7 m msl and the bottom of the model. The bottom elevation of the bottom layer was set to -39.4 ft msl (-12 m msl) at the western extent of this layer. The top layer of the model only extended to the shoreline. Layer 2 of the model extended approximately half way between the shoreline and the western extent of the model, where the total thickness of the four layers was 26.3 ft (8 m). The grid was refined in the area of the submarine springs. The cell size varies from 32.8 by 65.6 ft (10 by 20 m) near the submarine springs, to 328 by 328 ft (100 by 100 m) away from the study area.

5.4.1.2 Boundary Conditions

The modeled area was in the Kaanapali area of West Maui, Hawaii. Figure 5-1 is a map of the modeled area showing the extent of the top layer (layer 1) and the bottom layer (layer 6), as well as the major features such as the Lahaina Wastewater Reclamation Facility (LWRF) injection wells and the submarine springs. The map also illustrates the boundary conditions for layer 1. The model boundaries extend approximately 13,120 ft (3,400 m) inland from the shoreline, and 656 to 1,310 ft (200 to 400 m) seaward of the shoreline to about the 49 ft (15 m) bathymetric contour (Figure 5-1). Groundwater flow was modeled using a specified

flux and recharge rate as regional inputs, and a specified head at the coastal and submarine boundaries as a regional sink. The northern and southern boundaries of the model were approximately 6,560 and 13,120 ft (2,000 and 4,000 m) away from the LWRF, respectively. The eastern boundary was a specified flux boundary with 7.2 million gallons per day (mgd) (27,400 m³/d) of water entering the model. The eastern specified flux boundary represents inflow from the recharge areas in the interior highlands of the West Maui Volcano. This value was based on the recharge values for West Maui of Engott and Vana (2007) with the modifications described below. The northern and southern boundaries were no-flow boundaries that were roughly aligned parallel to the groundwater flow direction. The western boundary was a series of specified head arcs at the shoreline and nearshore ocean bottom based roughly on the bathymetric contours in the nearshore Kaanapali Area. The specified head value assigned to the submarine layers was the depth of the boundary arc multiplied by 0.025 to account for the greater density of seawater. The model's bottom boundary was at the mid-point of the freshwater/saltwater transition zone and was treated as a no-flow boundary.

5.4.1.3 Recharge

Flux into the top layer was modeled as a groundwater recharge of 29 inches per year (0.002 meters per day [m/d]) based on a USGS recharge study (Engott and Vana, 2007). Upon reviewing the model it was found that the proper value of recharge into the modeled area was only 14 in/yr (0.001 m/d) (Gingerich, 2008). This oversight was corrected in the final BTC interpretation model. The eastern boundary was a specified flux boundary with 7.2 mgd (27,400 m³/d) of water entering the model, representing inflow from the recharge areas in the interior highlands of the West Maui Volcano. The recharge was estimated as a fraction of the total recharge for the Honokowai Aquifer of 26.5 mgd, estimated by Engott and Vana (2009), based on the length of the coastline of this aquifer covered by the TTDM model. The total coastline length of the Honokowai Aquifer is 7.33 miles while that of the model is 5.0 miles. Based on the relative coastline lengths, 68% or 18 mgd of the Honokowai Aquifer recharge should enter the model at the top (ground surface) and eastern boundaries. Direct recharge accounts for 10.8 mgd, leaving 7.2 mgd to enter the model at the eastern boundary.

5.4.1.4 Hydrogeologic Parameters

The area covered by the conceptual model comprises three geologic units (see Section 1 for a more detailed description of the study area). The first unit is the Wailuku Basalts comprised of shield building stage lavas of the West Maui Volcano, which are generally thin-bedded lava flows. The majority of groundwater flow occurs at the interface between lava flows (interflow boundaries) that commonly consist of clinker zones giving this path a hydraulic conductivity similar to that of clean gravels. The next geologic unit is the sediments, which are comprised of a combination of alluvial material, shoreline deposits, and fossil and modern reef materials. The fine grains of the alluvial sediments and the lithified reef material give this unit a relatively low bulk hydraulic conductivity. However, preferential flow paths in sedimentary deposits can result in locally high hydraulic conductivity values, which were not accounted for in these models. The sediments occur along the coast and

extend inland. The third unit is the Lahaina Volcanics, which resulted from post-erosional volcanism and forms localized flows on top of the Wailuku Basalts. In the modeled area, the Lahaina Volcanics were represented by a single cone in the southwest section of the model and have no real impact on groundwater flow between the injection wells and the submarine springs.

Most of the hydraulic parameter values used in the TTDM were based on literature or obtained from LWRP operational data. Flows into or out from the modeled domain include the four LWRP injection wells, groundwater flow into the model from the upgradient area, and groundwater recharge. For simulations, an injection rate of 3 mgd (11,355 m³/d) at Injection Well 2 was used, which was the approximate average rate of total LWRP injection for late spring and early summer (County of Maui, 2011).

Numerical groundwater models need multiple hydraulic parameters to execute the groundwater flow computations. These include hydraulic conductivity¹, aquifer porosity², the flux of water at the model boundaries³, and the hydraulic gradient⁴. The values for these parameters were obtained from field experimentation, review of pertinent literature, or model calibration, which entails a series of trial and error simulations to find the most appropriate values.

The porosity of the aquifer is one of the major variables that determines the rate of solute (in this case tracer dye) transport. Nichols et al. (1996) list probable values for effective porosity (that porosity that contributes to groundwater flow) as varying between 0.05 and 0.10. Gingerich (2008) and Gingerich and Engott (2012) used 0.15 as the porosity value. A value of 0.10 was used for the TTDM model, which was within the range of these three studies. Table 5-1 lists the hydraulic parameters used by the TTDM to that of other studies.

There was no comprehensive calibration done for this model. The guiding philosophy was to use reasonable hydraulic parameter values to obtain a preliminary BTC. However, two major hydraulic parameters were adjusted so confidence could be placed in the model results. These were the hydraulic conductivity of the aquifer formations and the conductance assigned to the drains that were used to simulate the submarine springs.

Nichols et al. (1996) list the probable range of hydraulic conductivities for dike free basalts on Oahu as varying between 500 to 5,000 ft/d. Table 5-1 compares the values used by this model as compared to those used for previous studies (Gingerich, 2008; Gingerich and Engott, 2012; Whittier et al., 2004; and Whittier and El-Kadi, 2009). The value of the hydraulic conductivity chosen for the TTDM model was significantly greater than that used by the other models. It was estimated using a simplified trial and error method. The only site-specific data available to estimate the hydraulic conductivity of the Wailuku Basalts were capacity tests completed for the injection wells at the LWRP. The hydraulic

¹ The ability of the aquifer media to transmit water.

² The fraction of the aquifer volume that it voids.

³ Flux includes groundwater recharge and groundwater into and out of the model boundaries.

⁴ The slope of the water, which is needed for the transport model, and is computed by the groundwater model.

conductivity value of 2,900 ft/d used was higher than that used by previous models, but was chosen to get a reasonable match between the actual and simulated rise in the hydraulic head due to the injection of treated wastewater into Well 2. Capacity tests done by the County of Maui (2010) showed that the hydraulic head in Well 2 would increase 1.7 ft (0.5 m) for each 1 mgd of treated wastewater injected. The simulated injection rate was 3.0 mgd, which would result in an increase of 5.1 ft (1.5 m) for head within the well bore. However, MODFLOW computes an average hydraulic head for each cell, so the simulated increase in hydraulic head resulting from injection is expected to be much less than 5.1 ft. The hydraulic conductivity of the Wailuku Basalts was adjusted until the rise in hydraulic head within the cell where injection occurred was less than 3.3 ft (1 m). This required a 180% increase in hydraulic conductivity from that of the SWAP/OSDS model and a 140% increase from that used by Gingerich (2008) used for the USGS West Maui groundwater model. Many possible reasons could account for the difference in the modeled hydraulic conductivities. First, the SWAP/OSDS model and the USGS West Maui model were both regional in nature, while the TTDM was localized to the Kaanapali area. The hydraulic conductivity on a local scale can be much different from that on a regional scale. Also, the USGS West Maui model simulated variable density flow that accounted for the interaction between fresh and saline groundwater and dynamically adjusted the midpoint between the two. The TTDM and other models used in this study assigned a fixed depth to the midpoint between the fresh and saline groundwater and assigned a no-flow condition to this boundary.

The other hydraulic parameter that was adjusted to increase the accuracy of the TTDM model was the conductance of the drains used to simulate the submarine springs. The submarine springs act as leakage points with outflow controlled by drain conductance; an option that seems to be an appropriate representation. The conductance (a composite parameter describing the hydraulic conductivity and thickness of the media surrounding the spring) and bottom elevation of the drains representing the springs were adjusted so that a particle tracking simulation showed the dominant flow from the injection well going to the submarine springs. Figure 5-2 shows the pathways indicated by the simulated particle track from Well 2 to the ocean discharge points. The conductance of the submarine spring drains was incrementally increased until they captured a significant fraction of the inserted particles.

5.4.1.5 Tracer Test Design Model – Transport Model

As explained above, the transport model MT3DMS uses the groundwater flow solution from the flow model MODFLOW to simulate the transport of dissolved species in an aquifer. This model simulated the addition of FLT into Well 2. All injection in this preliminary model was into Well 2. Advection and dispersion were the only processes simulated to maintain simplicity and aid in the speed of model execution. The simulation was run for a total of 1,466 days, with no dye injected for the first 90 days. On day 91, a simulated concentration of 12,000 ppb dye was added for a period of 24 hours, which was the expected dye addition duration. There was no dye addition for the remaining 1,375 days of the model run. The simulated observation points were located at the North Seep Group (NSG) and at the South Seep Group (SSG).

5.4.2 Tracer Test Design Model Results

The first runs of this model were used in the design of the tracer field experiment to estimate the mass of dye needed for a successful test. Figure 5-3 shows the tracer test design model (TTDM) breakthrough curves for the NSG and the SSG, and the actual BTC measured at the NSG. The dye concentrations are shown as the ratio of the dye at the monitoring point to the average concentration of dye in the injection well. This model indicated that by the time the tracer plume reached the NSG monitoring point the dye concentration will have decreased to a concentration of about 0.8×10^{-3} of that added during injection. Thus, in the tracer test design, an over three orders of magnitude reduction was expected to occur. Additionally, the first arrival would be about 108 days, after which the dye concentration would be high enough to be discernible from the background fluorescence (assuming a reliable detection limit of 1 ppb). If the actual method detection limit of 0.02 ppb of FLT were used, elapsed time to first detection were would decrease to 70 days. The model indicated that only a small concentration of dye would be detected at the SSG, a result that proved to be inaccurate.

Table 5-2 compares the BTC simulated by the TTDM with the actual BTC measured at the NSG. No comparison was done for the SSG because the difference between the simulation and the actual BTC was so great. The first arrival time of the TTDM was two weeks shorter than the actual 84-day travel based on the method detection limit of 0.02 ppb. The TTDM peak concentration was a little less than one-half that of the actual BTC. At 263 days, the time to the peak concentration was about one and a half months shorter than that of the actual BTC. The agreement between the TTDM and actual BTC at the NSG was remarkably good for a predictive model. However, of greater importance is that the TTDM model enabled the tracer test plan to correctly identify the mass of dye needed for a successful tracer test and as well as the first arrival of the dye at the submarine springs. Based on the model's results, 360 lbs of FLT and 180 lbs of SRB were acquired, and, depending on the treated wastewater injection rate at the time of dye addition, these amounts of dye would produce BTC peak concentrations of 10 to 15 and 1 to 2 ppb, respectively. A greater amount of FLT was used because of the assessment that the reliable detection limit for FLT was significantly higher than for SRB. When the actual MDLs were determined, however, there was very little difference between the value for FLT and that for SRB (refer to Sections 4.2.1.3.3. and 4.3.2.1.2 for a detailed description of the MDLs).

5.5 Lahaina Groundwater Tracer Test Model

After the initial detection of the FLT dye, the results of the developing BTC were compared to those simulated and the model was modified to improve the agreement. Specifically, the TTDM conceptual model was modified to: (1) accurately reflect the addition of two dyes (FLT and SRB); (2) include the average injection rates into each well rather than injection into a single well; and (3) complete limited sensitivity analyses to assess what geologic configurations, features, and boundary conditions produced the best agreement between the simulated and actual BTCs.

The TTDM model was modified to distribute the treated wastewater injection between Wells 1 through 4 at a rate equal to the average value from July through October 2011, except on the day of SRB dye addition. On this day, the model accurately reflected the injection rates as they were on August 11, 2011 for the SRB tracer test initiation. The model was then run and the results compared to that of the developing BTC

5.5.1 Numerical Model

5.5.1.1 Model Grid

Minor adjustments were made to the TTDM grid. The primary adjustment was to use a uniform cell size of 164 x 164 ft (50 x 50 m). The total number of cells in the model grid was 80,640, distributed among 120 rows, 112 columns, and 6 layers. Only 47,553 cells were active because the remaining cells were located outside of the model boundaries. Figure 5-4 shows the model grid in a plan view (layer 1 only) and in cross-section. The elevation of the bottom of the grid was the elevation of the mid-point of the freshwater/saltwater transition as modeled by Gingerich (2008). The top of layer 2 (bottom of layer 1) was assigned a fixed elevation of -6.6 ft msl (-2.0 m msl). The other layer elevations were equally spaced between -6.6 ft msl and the bottom of the model. The western extent of the submarine layers was extended to accommodate the revised submarine boundaries.

5.5.1.2 Boundary Conditions

The extent of the Lahaina Groundwater Tracer model remained unchanged from the previous versions except the submarine boundaries. The submarine boundaries were extended to the west, and the depths were assigned to be consistent with the nearshore bathymetry. The western boundary of layers 2 through 6 were terminated at the designated depth contours of 6.6, 18.0, 29.5, 41.0, and 54.0 ft msl, respectively. The specified head assigned to these boundaries was the absolute value of the depth multiplied by 0.025 to account for the density of seawater relative to that of freshwater.

5.5.1.3 Recharge

As discussed in Section 5.4.1.1, the recharge assigned to the TTDM was higher than that in the Kaanapali area. The recharge was reduced from 29 in/yr to 14.5 in/yr better reflect that estimated by Engott and Vana (2007). However, the groundwater flux from the interior highlands had to be increased to keep the total amount of water entering the model accurate. The groundwater flux into the eastern boundary of the model was thus increased from 7.2 mgd to 8.8 mgd.

5.5.1.4 Hydrologic Parameters

The injection rate into the four injection wells was increased slightly from 3.0 to 3.2 mgd to reflect the average injection rate from July 2011 through June 2012. The TTDM model was modified to distribute the treated wastewater injection between Wells 1 through 4 at a rate

equal to the average value from July through October 2011, except on the day of SRB dye addition. On this day, the model accurately reflected the injection rates as they were on August 11, 2011 for the SRB tracer test initiation. The conductance and bottom elevation of the drains representing the NSG and SSG were iteratively modified until there was a suitable match between the simulated uptake in the drains and the discharge from the seep groups as estimated by the nearshore radon survey. These values were 2,500 m³/d and 6,300 m³/d for the NSG and SSG, respectively (Glenn et al., 2012). In the initial model runs, the hydraulic conductivity remained unchanged from the TTDM. In the final model runs this parameter was modified to agree with that of Gingerich and Engott (2012) with the exception of the alignment of the dominant anisotropy axis.

5.5.1.5 Transport Model

The TTDM model was modified to distribute the treated wastewater injection between Wells 1 through 4 at a rate equal to the average value from July through October 2011, except on the day of SRB dye addition. On this day, the model accurately reflected the injection rates as they were on August 11, 2011 for the SRB tracer test initiation. The model was then run and the results were compared to that of the developing BTC. Rather than simulating the transport of a single dye, both the FLT and SRB dye additions and transport were simulated. Table 5-3 lists the well injection rates, and the dates and concentrations of the dye addition.

5.5.2 Description of Scenarios

5.5.2.1 Effects of a Horizontal Flow Barrier

The transport of the tracer plume to the west and northwest directions, which is inconsistent with the physical data, became the next model deficiency to overcome. To address this problem, a horizontal flow barrier (HFB) was placed along the possible track of an ancestral Honokowai Stream as hypothesized by Hunt and Rosa (2009). Figure 5-6 shows the revised conceptual model. A horizontal flow barrier is a line type feature used to represent physical obstructions to groundwater flow, with a specified hydraulic characteristic expressed as the product of the hydraulic conductivity of the barrier divided by its width. A value of 0.0001 d⁻¹ was assigned to this barrier.

In the model the HFB represents the low hydraulic conductivity sediments or weathered basalts beneath the current and former channels of the Honokowai Stream (see discussion in Hunt and Rosa, 2009). An inspection of the shore bathymetry (Figure 5-6) shows evidence of a submerged stream channel that correlates well with the northern boundary of the TIR plume and is just north of the NSG. The evidence for a drowned stream valley is the eastward indentation of the 60 to 100 ft bathymetric contours. Figure 5-7 shows the geologic stratigraphy in the boreholes that were drilled for the LWRF injection wells. The alluvium extends to about 10 ft below sea level and well into the groundwater; within the paleostream channel the thickness of alluvial fill and the depth to weathered basalt will be much deeper than this. The existence of a valley-fill deep enough to block the flow of non-saline water to the north and to the west of the LWRF is thus a likely possibility.

5.5.2.2 Effects of Bathymetry

Another primary method used to investigate discrepancies between the simulated and actual BTC at the SSG was to modify the geometry of the nearshore geology and that of the marine boundaries. The particle track simulation shown in Figure 5-2 illustrates that the groundwater flows preferentially to the NSG, and no groundwater reaches the SSG. Upon closer inspection, the marine boundary of the first submarine layer (layer 2) juts to the shoreline (layer 1) near the NSG then juts back offshore near the SSG. The indentation of the layer 2 specified head boundary places it in closer proximity to the shoreline near the NSG than the rest of western boundary. The closer proximity of the specified boundary to the shoreline near the submarine springs may result in the simulated groundwater flow converging on this zone. This hypothesis was tested by modifying the layer 2 specified head boundary to place it adjacent to the shoreline near SSG, as is the case at the NSG.

The submarine layers of the model were modified to closely follow the nearshore bathymetry. The western boundaries of layers 2 through 6 were modified to coincide with the 6.6, 18.0, 29.5, 41.0, and 54.0 ft msl bathymetric contours, respectively. Figures 5-5 and 5-6 show the location of the submarine boundary for layers 2 through 6 and the geology used in layer 1.

5.5.2.3 Effects of a Preferential Flow Path

To further investigate hydrogeologic factors influencing the transport of the FLT, a sequence of simulations was performed using different preferential flow path (PFP) layer placement. Because significant improvement in the simulated SSG BTC occurred when the boundary condition geometry for layer 2 was modified, we adopted this as the base model for the PFP simulations. As with the modified boundary condition simulations, the goal of these simulations was to improve the agreement between the model and the SSG BTC. To accomplish this, a polygon was created that connected Injection Wells 3 and 4 to the SSG. Figure 5-8 shows the geology and boundary conditions for the PFP model runs. A hydraulic conductivity of 8,860 ft/d, three times that assigned to the Wailuku Basalts, was assigned to this polygon. A PFP polygon was assigned one at a time to layers 2 through 6 and a transport simulation was run for each case. Figure 5-8 shows the geometry of the PFP polygon for layer 2. In the simulations for the remaining layers, the PFP polygon was extended to the western boundary of the respective layer.

5.5.2.4 Effect of Porosity

Porosity is a major factor for the travel velocity of groundwater. A higher porosity results in a slower groundwater velocity. The TTDM simulations used a porosity of 0.10. The time of first arrival and peak concentration of the TTDM was early indicating that the porosity might have been set too low. A range of porosities from 0.10 to 0.30 were tested and compared to the first arrival and to the first peak of the measured BTCs.

5.5.2.5 Effect of Dispersivity

Dispersion changes a pulse addition of dye (near instantaneous on and off condition) to a peaked curve with ascending and declining limbs. The two primary causes of dispersion are the multiple pathways taken and various travel velocities of particles dissolved in groundwater (hydrodynamic dispersion) and the “spreading” of a plume due to a concentration gradient (molecular diffusion). As groundwater velocity increases, the role of hydrodynamic dispersion dominates over molecular diffusion, which can be safely ignored in many situations. The relative contribution of each type of dispersion is quantified by the Peclet Number, which is the ratio of hydrodynamic dispersion to molecular diffusion. The higher the Peclet Number, the less relevant molecular diffusion becomes. At Peclet Numbers greater than 6, hydrodynamic dispersion is considered to dominate over molecular diffusion (Fetter, 1992). The BTC interpretation model QTracer2 (Field, 2002) calculated Peclet Numbers of 12 and 20 for the NSG and SSG, respectively. The Peclet Numbers computed for the submarine springs by QTracer2 justifies ignoring molecular diffusion in the modeling for this project.

The groundwater flow and transport models were used to assess the role of dispersion in the transport of the dye. The primary emphasis was to match the characteristics of the NSG BTC up to and including the initial peak. Subsequent features of the BTC after the initial peak, such as a plateau or a long trailing edge, are likely the result of other flow pathways or processes. The actual parameter used to quantify dispersion is dispersivity.

5.5.2.6 Effects of Sorption

Analysis to this point has assumed that there are no interaction between the tracer dyes and the aquifer media. A truly conservative tracer will stay in solution and travel through the aquifer with no a physical or chemical reaction with the aquifer, i.e., without degrading or transforming to another species. Very few dissolved substances fit this description. SRB is the dye used in this study that is most likely to degrade (Käss, 1998). The evaluation of SRB degradation is discussed in Section 4.3.3.

Modeling was used to assess the sorption of FLT and SRB. Sorption occurs when a dissolved constituent attaches to the aquifer matrix. Sorption is generally thought of as a reversible process that is dependent on the sorption properties of the dissolved constituent, chemical properties of the aquifer matrix (organic carbon content and surface charge for example [Fetter, 1992; Schulz, 1998; Sabatini, 2000]), and the dissolved concentration of that constituent. In a tracer test, the dye may sorb onto the aquifer matrix during the ascending limb of the BTC, then desorb back into solution during the descending limb of the BTC. This process is referred to as equilibrium sorption if the exchange between the dissolved and sorbed phase is instantaneous and dependent on the dissolved concentration. The primary effect of this process is a slower transport velocity (Schulz, 1998). In the absence of a reference tracer with known sorption characteristics, it is difficult to assess sorption using a BTC because the primary difference will be slower travel time. Sabatini (2000) evaluated the sorption of FLT and SRB on limestone and sandstone. FLT does not sorb onto sandstone

and only slightly sorbs onto limestone. SRB was slightly sorbed onto sandstone, but had significant sorption onto limestone. Smart and Laidlaw (1977) tested the sorption of tracer dyes on various types of sediments and aquifer media using laboratory columns. They found that FLT experienced a small loss to sorption onto orthoquartzite, kaolinite, and limestone. SRB showed moderate sorption onto limestone and kaolinite that increased with the dissolved dye concentration.

A numerical model can be used to evaluate the possibility of sorption by comparing simulated BTCs with and without sorption. A simulation was run using the data from Sabatini (2000) to test the possible impact of sorption on the transport of the tracers used in this project. In this evaluation, Sabatini (2000) used Freundlich Sorption Isotherms to describe the relationship between the dissolved and the sorbed mass of dye. Freundlich Sorption Isotherms use an exponent to describe this relationship shown in the following equation (Fetter, 1992).

$$C_s = K_r * C_L^N \quad \text{Equation 5-1}$$

Where:

C_s = the sorbed concentration ($\mu\text{g}/\text{kg}$)

K_r = the sorption coefficient (L/kg)

C_L = the dissolved concentration ($\mu\text{g}/\text{L}$)

N = Freundlich exponent

Table 5-4 lists values used for K_r and N for each dye and aquifer material. GMS does not have the capability to assign the sorption characteristics directly to the aquifer materials. These parameters must be assigned cell by cell, or layer by layer. Due to the labor-intensive nature of entering the data into the individual cells, the layer option was used. The sorption values for limestone were assigned to layer 2 to represent the carbonate materials the dye plume would encounter when discharging from submarine springs. The sorption values for sandstone were assigned to the remaining layers to represent the lower sorption onto basalt. The model was run with the same hydraulic parameters and for the same duration as previous simulations.

5.5.2.7 Effects of Anisotropy

In many cases, for the sake of simplicity, the hydraulic conductivity is assumed to be uniform in a given aquifer medium, regardless of the direction of groundwater flow. Structures in the aquifer material such as an alignment of fractures in a preferred direction can result in a hydraulic conductivity value that is greater in one direction than another (Knochenmus and Robinson, 1996). During the early stages of model refinement, a hydraulic conductivity of 2,900 ft/d and an aquifer porosity of 0.19 were found to produce the best match between the simulated and measured BTC for the NSG. These values were significantly greater than the hydraulic conductivity and porosity used by Gingerich and Engott (2012) in the USGS groundwater model of the Lahaina District. They modeled the Wailuku Basalts as an anisotropic medium. In the Lahaina District Model, a longitudinal hydraulic conductivity of 1,800 ft/d was aligned roughly east-west was assigned to the Wailuku Basalts. For this

Formation, the transverse hydraulic conductivity of 590 ft/d was aligned roughly north-south, while the vertical hydraulic conductivity was 17 ft/d. The hydraulic conductivity anisotropy used by Gingerich and Engott (2012) and an anisotropy with the dominant and minor axes swapped were tested to evaluate the impact on the modeled BTC and the spatial extent of the FLT plume.

5.5.3 Model Results

The initial runs of the Lahaina Groundwater Tracer model were compared to those simulated with TTDM. The descriptions that follow detail the sequential results of the model modifications to better understand the impact of the FLT transport.

5.5.3.1 Effects of a Horizontal Flow Barrier (HFB)

Placing a HFB over the ancestral channel of the Honokowai Stream as hypothesized by Hunt and Rosa (2009) resulted in a significant increase in the simulated peak FLT concentration at the NSG. Overall, this was an improvement from the TTDM where the simulated FLT concentration was less than half of that measured. However, there was little improvement in the simulated BTC for the SSG. The HFB did accomplish the primary intended purpose by preventing the transport of the tracer dyes to the northwest and directly west to stretches along the shoreline that the $\delta^{15}\text{N}$ and TIR data indicated were not impacted by the treated wastewater plume. Figure 5-9 compares the actual BTC to that simulated by the Lahaina Groundwater Tracer model. The simulated NSG BTC arrives at the submarine springs about one and a half months prior to the actual arrival time. The peak concentration was about 1.5 times that of the actual concentration and occurred on March 29, 2012, two months prior to the actual peak that occurred on May 29, 2012. More problematic was the simulated FLT concentration at the SSG. The simulated first arrival on December 17, 2011 was about a month later than the actual first arrival at the SSG. The simulated peak concentration of 2.2 ppb was less than one-fifteenth of that of the actual peak concentration. In addition, the model predicted that the peak would occur at the SSG on June 5, 2013, which is more than a year after the actual peak occurred. Investigating the cause of the large discrepancy at the SSG became a subsequent task of the modeling.

5.5.3.2 Effects of Bathymetry

Modifying the western boundary of the submarine layers greatly improved the simulated BTC for the SSG. Figure 5-10 shows the BTC simulated by the model run after modifying the submarine boundaries. The modeled time of travel for the FLT to the SSG was closer with the simulated peak concentration occurring on May 24, 2012, compared to the actual peak, which occurred approximately a month earlier. The simulated peak FLT concentration was 14.5 ppb compared to the actual peak concentration of 34 ppb, which shows that the boundary modifications improved the model based on this criterion (Figure 5-9). Although the modeled BTC did not closely match the actual BTC, this simulation demonstrates the important role that nearshore bathymetry plays in the transport of the tracer dye, and thus the transport of the treated wastewater, to the submarine springs.

5.5.3.3 Effects of a Preferential Flow Path

Simulating PFPs resulted in significant improvement in agreement between the measured and simulated SSG BTC. However, this improvement came at the expense of the agreement between the measured and simulated NSG BTC. All layers were tested using a PFP, but placing the PFP in layer 2 produced the best results. The simulated SSG BTC with a PFP (Figure 5-11) was only about 5 ppb less than that measured, showing much better agreement than the simulation without the PFP (Figure 5-10). The agreement between the simulated and measured NSG BTC was much better when a PFP was used. The first arrival and peak concentration times were significantly earlier than that measured and the peak concentration was almost three times that measured. Placing the preferential flow polygon in the other layers produced similar results. Table 5-5 compares the actual FLT BTCs to that simulated by each preferential flow model scenario. Even using a porosity of 0.30, the first arrival time at both the NSG and SSG varies from a week to two months early. A higher porosity lowers the transport velocity of the groundwater due to the increase in the pore space available for the flow. The porosity used in these simulations was greater than the upper bound of 0.10 estimated by Nichols et al. (1996) and the value of 0.15 used by Gingerich and Engott (2012) in the Lahaina District Groundwater Model. Gingerich and Engott (2012) varied porosity to match the measured slope of the freshwater/saltwater transition zone in West Maui. Since Gingerich and Engott (2012) calibrated their porosity using physically measured data, that value is the best estimate available for the study site. As stated above, the primary goal of simulating PFPs was to capture the FLT concentration at the NSG relative to that at the SSG. In the model runs, the ratio of the peak NSG FLT concentration to that at the SSG varied from 2.2 to 4.7 with the average being 2.7. This is much greater than the actual value of 0.63. In addition, the use of a PFP increased the peak concentration at the NSG to more than twice the measured value even though this set of submarine springs was outside the PFP zone.

5.5.3.4 Effect of Dispersivity

Changes in dispersivity will change the slope of the leading edge of the BTC by altering the rate of rise and descent of the BTC limbs. Dispersivities of 32, 82, 164, and 246 ft were tested. Figure 5-12 shows the simulated BTCs for the NSG using the dispersivities tested. Table 5-6 lists the date of first arrival, and the date and magnitude of the peak concentration for both the NSG and SSG. A higher dispersivity resulted in an earlier date of first arrival, but lower peak concentration. The lower dispersivity values gave the best match between the simulated and measured data for the NSG. A dispersivity of 32 ft resulted in a close agreement with the measured peak concentration of 22.5 ppb, but the simulated arrival date was delayed and the ascending limb of the simulated BTC was too steep. A dispersivity of 82 ft provided good agreement with slope of the BTC ascending limb, but the peak concentration of 19.2 ppb was 17% less than that measured. The higher dispersivities of 164 and 246 ft resulted in first arrivals much earlier than that measured and ascending limb slopes much less steep than that measured. The highest value tested (246 ft) was very close to the value of 250 ft used by Gingerich and Engott (2012) in the Lahaina District model. Figure 5-

12 illustrates that using a value that high results in simulated BTC that differs significantly from that measured.

5.5.3.5 Effect of Porosity

Porosity affects the travel velocity and the peak concentration of the FLT plume. Porosities of 0.10, 0.15, 0.20, and 0.30 were tested using a model version with a dispersivity of 82 ft, an east-west hydraulic conductivity of 590 ft/d, and a north-south hydraulic conductivity of 1,770 ft/d. Figure 5-13 compares the results of these simulations to the measured BTC at the NSG while Table 5-6 lists the dates of first arrivals, and the dates and magnitude of the peak concentrations for the NSG and the SSG. A lower porosity results in an earlier arrival and a higher peak concentration. The date of first arrival when a porosity of 0.10 was used was 9/27/11, nearly two months before FLT was actually detected at the NSG. The simulated peak concentration was 27.4 ppb, 120% of that measured. When a porosity of 0.30 used, the simulated date of first arrival was 2/10/12 and the peak concentration was 9.7 ppb. These two simulated results were much different from that measured. In the case of simulation using the porosity of 0.30 the FLT would remain undetected until 2/10/12. A porosity of 0.15 used with a dispersivity of 82 ft produced the best agreement between the simulated and measured BTC at the NSG. The agreement between simulated and measured results at the SSG was only fair, regardless of the porosity and dispersivity used.

5.5.3.6 Effects of Sorption

Figure 5-14a shows the modeled FLT BTC when sorption is simulated. The peak concentration was highly attenuated compared to the measured BTC, and the peak of the SSG BTC is thus barely discernible on this figure. Sorption should delay the time when the BTC reaches the peak concentration. This did not appear to happen in this simulation. Figure 5-14b compares the modeled BTCs normalized to the maximum FLT concentration for the cases with and without sorption. In both scenarios, the peaks occur at nearly the same time. However, the trailing edge was much more pronounced. At the NSG, the times of first detection were November 13, 2011 and October 24, 2011 for the cases with and without sorption, respectively, showing a slight slowing of the BTC. The peak concentrations of the FLT BTC were severely attenuated and were followed by a very elongated trailing edge. The modeled SRB concentrations at the submarine springs were well below the MDL for this dye.

As stated above, a definitive evaluation of whether or not sorption is a factor is difficult without aid of another tracer with known sorption characteristics (preferably a conservative tracer). However, this study used groundwater transport modeling and reasonable sorption parameters for FLT and SRB to evaluate what effect sorption would have on the transport of these two dyes. This modeling indicated that a delay in the peak concentration would not occur, but that the peak concentration would be severely attenuated and followed by a very long trailing edge. However, the good agreement of the FLT first arrival and peak concentration between the simulations using a porosity of 0.15 and a dispersivity of 82 ft but no sorption and that of the measured BTC indicate that sorption is minimal with this dye.

Since no SRB was detected, the sorption effects on this dye cannot be adequately evaluated. Nevertheless, as Table 5-4 indicates, sorption likely has a greater impact on the transport of this dye likely making this process a contributing factor to the failure to detect SRB.

5.5.3.7 Effects of Anisotropy

An aquifer where the hydraulic conductivity is not equal in all directions can result in a transport direction for dissolved-constituents that differs from the direction of the hydraulic gradient. Rahn and Johnson (2002) incorporated anisotropy into a MODFLOW/MT3D model of a contaminated site in South Dakota. The direction of the hydraulic gradient was due east, but the ethylene dibromide plume tracked to the southeast of the source area. They used anisotropy with the dominant axis aligned with the foliation of the metamorphic rocks that formed the aquifer and obtained a good agreement between the measured and simulated contaminant plume. In the present study, the best match between the simulated and measured FLT BTCs when an isotropic hydraulic conductivity was simulated used a value of 2,900 ft/d and aquifer porosity of 0.19. The values of these parameters were significantly greater than the respective values used by Gingerich and Engott (2012) in the USGS groundwater model of the Lahaina District. Additionally, the modeled spatial extent of the FLT plume failed to extend south of the SSG as indicated by the field data. Gingerich and Engott (2012) modeled the Wailuku Basalts as an anisotropic aquifer. The longitudinal hydraulic conductivity of 1,800 ft/d was aligned roughly east-west. A transverse hydraulic conductivity of 590 ft/d was aligned roughly north-south, while a vertical hydraulic conductivity was 17 ft/d; the aquifer porosity was 0.15. Using these values with our model produced very poor agreement between the simulated and measured BTCs (Figure 5-15a). The simulated BTC for the NSG had a very low peak concentration of about 5.5 ppb that appeared in January 2013, and FLT in the simulated BTC for the SSG remained barely discernible.

The simulation described above showed that the anisotropy used by the Lahaina District Groundwater Model (Gingerich and Engott, 2012) was not suitable for the current study, and that the BTC needed for the present study is sensitive to changes in horizontal anisotropy. A simulation was run using the Lahaina District groundwater model hydraulic parameters, but with the dominant hydraulic conductivity axis aligned north-south, the opposite of the previous simulation. Figure 5-15b shows the results of this simulation. The agreement between the simulated and measured BTC at the NSG was similar to the model that utilized an isotropic aquifer, although there was some improvement in the agreement between the simulated and measured SSG BTC. The time of peak concentration was much closer than that of the model for the isotropic case. However, the simulated peak concentration was still only about 30% of that measured. At the SSG the ascending limb of the BTC was slightly less steep than that measured, resulting in a time of peak concentration that is offset by 51 days from the actual time compared to 91 days as simulated by the horizontally isotropic model. It is important to note that the peak concentration at the SSG occurred at the end of a one-month long plateau so an offset of 51 days in the anisotropic simulation places the modeled peak value just prior to the start of the plateau.

The anisotropic model version was thus selected as the base model for evaluating the remaining processes such as sorption and the trailing edge. This model version had the advantage of using the hydraulic parameter values of Gingerich and Engott (2012) with the major exception of the orientation of the hydraulic conductivity ellipse. In the Lahaina District groundwater model Gingerich and Engott (2012) aligned the dominant hydraulic conductivity axis east-west, while this study aligned the dominant hydraulic conductivity axis north-south. Another important criteria to consider when evaluating the model results is the simulated spatial extent of FLT plume. As described above, the simulated FLT plume did not extend south of the SSG when an isotropic hydraulic conductivity was used. As described in Section 4.2.6.2, FLT has been detected in field samples as far south as the southern TIR plume boundary, significantly south of the SSG. Figure 5-16a shows the simulated FLT plume 620 days after the addition of this dye using an isotropic model, a porosity of 0.15, a dispersivity of 82 ft, and an isotropic hydraulic conductivity of 2,900 ft/d. In this simulation, the strong conductance of the SSG captures the FLT and no dye extends south of the feature. Using the same values for porosity and dispersivity, but with an east-west hydraulic conductivity of 590 ft/d and a north-south hydraulic conductivity of 1,800 ft/d, a simulation was run to test the change in the spatial distribution of the FLT plume. Figure 5-16b shows the results of this simulation. The extent of the modeled FLT plume in this simulation extends southward to the southern TIR plume boundary, matching the observed occurrence of FLT in samples collected during the area surveys. The results of this simulation shows the importance of considering anisotropy when modeling solute transport in dipping lava flows; it further shows that the direction of dominant hydraulic conductivity is likely perpendicular to the dip of the lava flows.

5.5.3.8 Best Fit Model

The PFP simulations described in Section 5.5.3.3 failed to produce a SSG peak BTC concentration that was greater than that at the NSG, which is the case with the measured data. In the previous sets of PFP simulations, the peak concentration at the SSG was only about half that at the NSG, while the measured data shows that the peak concentration at the SSG was about 1.5 times that of the NSG. These results indicate that a PFP alone cannot account for the relative peak concentrations measured at the two groups of submarine springs. An additional simulation was thus performed using a PFP in layer 2 and anisotropic hydraulic conductivity in an attempt to obtain an improved agreement between the measured and modeled relative peak concentrations at the NSG and SSG. This simulation tested the hypothesis that horizontal anisotropy with major axis aligned north-south combined with a PFP could provide results that more closely reflected those measured. Figure 5-17a shows the configuration of the PFP in layer 2. A hydraulic conductivity of 11,500 ft/d was assigned to the PFP polygon that connects Injection Wells 3 and 4 to the SSG.

The combination of the PFP, dominant north-south anisotropy, and more southerly flow path significantly improved the simulated peak FLT concentration measured at the SSG relative to that at the NSG. Figure 5-17b shows that in this simulation, the peak concentration at the SSG is now just slightly below that at the NSG, although the simulated peak concentration at the SSG was about one-half of that measured with a peak concentration occurring about two

months before the actual peak. This simulation was not meant to show an actual configuration of a PFP, however, but to demonstrate that such a feature likely contributes to the high FLT concentration at the SSG relative to that at the NSG. There is very little information on the subsurface geology in the study area and any postulated PFP is purely conjecture. The results of this simulation nonetheless showed that using a dominant north-south anisotropy ellipse combined with a southerly track for a PFP could improve the agreement between the simulated and measured results.

5.5.3.9 Fate of SRB

Nearly all of the previous discussion has dealt with modeling the transport of FLT because there was measured FLT data with which to compare the model results. The reasonable agreement between the BTC-IM FLT simulations and the measured field data increases the confidence that this model can be used to investigate the causes for the non-detection of SRB. As the transport model MT3D-MS can simulate the simultaneous transport of multiple species, the transport of SRB was also simulated in all model runs of Lahaina Groundwater Tracer model.

When SRB was physically added to the treated wastewater stream, the injection setup was modified to increase the discharge into Well 2 (see section 4.3). The treated wastewater that would normally be injected into these two wells was diverted to Well 2. Upon completion of the SRB addition, the injection setup was returned to the normal configuration whereby the majority of the treated wastewater is discharged through Wells 3 and 4. Because Wells 3 and 4 are between Well 2 and the submarine springs, the possibility of their injectate interfering with the SRB plume was investigated using the model. The second injection scenario was modified by ceasing injection into Wells 3 and 4 after the SRB addition was complete. Figure 5-18 compares the simulated SRB BTC with injection as it actually occurred (i.e., with Wells 3 and 4 as the primary injection wells after SRB addition) to a scenario where Well 2 is the primary injection well and there was no injection into Wells 3 and 4. With injection into Wells 3 and 4, the BTC at the NSG is barely discernible. The maximum simulated concentration of 0.034 on August 21, 2012 is less than the MDL of 0.05 ppb. At the SSG, the concentration does rise above the MDL to a concentration of 0.12 ppb. The simulated current concentration was 0.07 ppb just slightly above the MDL. With no injection into Wells 3 and 4 after the SRB addition, the simulated BTC significantly exceeds the MDL. At the NSG, the simulated SRB concentration exceeds the MDL on December 30, 2011 and reaches a peak concentration of 2.2 ppb on May 24, 2012. At the SSG, the simulated SRB concentration exceeds the MDL on February 25, 2012 and reaches a peak of 1.4 ppb on September 15, 2012. Figure 5-19 shows two simulated SRB plumes 620 days after this dye was added to the treated wastewater stream. Figure 5-19a shows the results of the simulation where injection into Wells 3 and 4 resumed after the SRB was added, which is what actually occurred. Interference from the injection into Wells 3 and 4 diverts the SRB plume to the east-southeast and away from the submarine springs. Figure 5-19b shows the simulation results if Well 2 received all of the treated wastewater for injection after the addition of SRB. Under this injection scenario, the core of the SRB plume moves south and southwest resulting in a significantly higher concentration of this dye being discharged from the

submarine springs. Assumed correct, this shows that continued injection into Wells 3 and 4 after the SRB addition deflected the injectate from Well 2 and the SRB within it away from the submarine springs. The deflected pathway greatly reduced the SRB concentration at the springs and significantly delayed time of arrival, although this model result does not preclude other processes such as sorption, degradation, and other discharge points from also playing a role in the failure to detect SRB.

5.6 Conceptual Model of the Kaanapali Groundwater Flow and Transport System

This section describes the groundwater flow and transport for the Kaanapali study area as defined by the model boundaries describe above. Groundwater flow in the Kaanapali area is controlled by groundwater recharge from rainfall and from the central highlands entering the system from the east, and as treated wastewater injection into the wells at the LWRF.

The regional component of groundwater flow results from groundwater recharge creating a freshwater lens that floats on top of the underlying saltwater. This recharge is estimated to be approximately 18 mgd (Section 5.5.1.3). Groundwater that is not extracted by production wells or returned to the atmosphere as evapotranspiration will discharge into the ocean as submarine groundwater discharge. Being less dense, the fresh groundwater will float on top of the saline seawater. The interface between the two is located at a depth that is approximately 40 times the groundwater table elevation (Freeze and Cherry, 1979, page 375). The mixing of the two waters in the basal lens along the groundwater flow path results in a sloping transition rather than a sharp interface between fresh and saltwater. Because the modeling software used by this study does not consider the density differences of fresh and saltwater, only the flow of the non-saline water is considered in the numerical and conceptual models. To accommodate this approach the mid-point of the freshwater/saltwater transition zone is thus considered a no-flow boundary. The numerical model's ability to capture the major characteristics of the measured BTC shows that this approach is reasonable.

Concerning the injected treated wastewater, the screen and open intervals of the wells occur in the transition or saltwater zone, placing the injection in the saline zone and below the bottom boundary of the numerical models (Gingerich and Engott, 2012, see their Figure 27). However, due to its buoyancy, the injectate quickly rises up into the freshwater zone and its associated flow system (Hunt, 2007; Burnham et al., 1977; Wheatcraft et al., 1976; Tetra Tech, 1993). The injectate is then transported in the groundwater flow system to submarine groundwater discharge points.

Prior to this study, the best evidence showing that the injectate from the wells takes an oblique rather than direct path to the submarine discharge points are the $\delta^{15}\text{N}$ algal surveys of Dailer et al. (2010) and a coastal geochemical, temperature, and salinity survey done by Hunt and Rosa (2009). These studies showed that the nearshore waters southwest of the LWRF were enriched in ^{15}N , had abnormally high temperatures and that the non-saline water discharge contained wastewater indicator compounds. This phenomenon has been confirmed

in this report by the spatial distribution of FLT in the nearshore waters of the study area. The groundwater flow and transport modeling done by this study have identified four major controls on the pathway the injectate takes: (1) the density difference between saltwater and the non-saline treated wastewater (described above); (2) low hydraulic conductivity alluvium and weathered basalt associated with the current past channels of the Honokowai Stream; (3) the nearshore bathymetric gradient; and (4) the dominant north-south hydraulic conductivity of the basalt aquifer.

The low hydraulic conductivity alluvium and weathered basalt associated with current and past channels of the Honokowai Stream pose a barrier to the transport of the injectate to the north and probably to the west. The valley fill associated with stream channels is recognized as barrier to groundwater flow. In their delineations of aquifers for the State of Hawaii, Mink and Lau commonly used the axis of stream valleys as boundaries (Mink and Lau, 1987, 1992a, 1992b, 1993a, 1993b). Oki (2005) showed that the response to pumpage of the Pearl Harbor Aquifer on Oahu was sensitive to the depth of the valley fills beneath Waimalu Stream. He estimated that the depth of valley fills extended from about 100 to over 300 ft beneath the bottom of the stream channel. Rock borings in Kipapa Gulch, Oahu, showed that sediments or highly weathered basalt were present at depths greater than 50 ft beneath the streambed of Kipapa Stream (TEC, 2001). As described by Stearns and MacDonald (1942), the island of Maui has experienced repeated emergence and submergence cycles. After the shield building stage of the Wailuku Basalts ended, stream channels developed in West Maui. Thus, the current stream channels, including the Honokowai Stream, could have started forming in the early to mid-Pleistocene (0.13 to 1.8 million years ago). No later stage lava flows (Honolua or Lahaina Volcanics) are present in the Kaanapali area inland or in the vicinity of the LWRF or Honokowai Stream (Figure 1-4) that would have filled the stream valleys incised into the Wailuku basalts. Since that time, Maui has experienced emergence and submergence. During periods of emergence, stream channels will cut to beneath the current sea level and then be filled as submergence occurred. Stearns and Macdonald (1942) estimated that there have been at least three cycles of submergence and re-emergence since the cessation of major volcanic activity on West Maui. The submergence could have resulted in a shoreline 2,500 ft above the current shoreline. The emergence could have resulted in a shoreline 950 ft below the current sea level. This process occurred over a period of 1.8 million years, providing ample time for deep cut stream valleys to develop. The proximity of the submarine valley shown by the bathymetry in Figure 5-20 to the current Honokowai Stream strengthens the hypothesis of Hunt and Rosa (2009) and this study that stream valley fill and weathered basalt pose a barrier to the flow of the LWRF injectate to the north and west.

Modifying the model boundaries to more precisely follow the actual bathymetry changed the peak FLT concentration simulated at the SSG from less than 1 ppb to about 15 ppb. Even though the simulated SSG FLT concentration was about half of that measured, the improvement over the previous model version was substantial. Modifying the model to accurately reflect the nearshore bathymetry resulted in a bathymetric gradient that was steeper near the submarine springs. This moved the specified-head boundaries for the submarine layers closer to the shoreline, thereby reducing the width of sedimentary

formations between the basalt aquifer and submarine boundary. This slightly increases the effective hydraulic conductivity between the injection wells and submarine specified head relative to pathways to the north. Sensitivity model runs showed that it was the contrast between the greater width of sediments to north of the submarine springs and the reduced width at the submarine springs that had the greatest effect on the FLT time of arrival and peak concentration simulated at these springs. The preferential flow orifices of the submarine springs (as evidenced by the visible wisps of dye discharging from the SSG) combined with steeper nearshore bathymetric gradient play an important role determining the flow path of the FLT plume.

The controls on the FLT plume described were instrumental in obtaining a reasonable match between the simulated and measured BTCs. However, the spatial distribution of FLT simulated by the model fell short of the southern extent indicated by tracer sampling program, the algal $\delta^{15}\text{N}$ survey, and the TIR survey. To arrive at a reasonable agreement between modeled and measured plume extent, an anisotropy factor of 3 had to be combined with a direction of dominant hydraulic conductivity aligned north-south. This direction is perpendicular to the dip of the lava flows, and contradicts the prevailing notion that the direction of dominant hydraulic conductivity is always parallel to the dip of the lava flows. The major large-scale flow paths in basalt aquifers occur at the interflow boundaries where rubble at the top and bottom of the lava flows produce a continuous flow path with high porosity (Nichols et al., 1996). This would indicate that the dominant axis of hydraulic conductivity should be aligned parallel to dip of the lava flows. However, there is a difference between the plane of the dip of the lava flows and the near horizontal to slightly vertical direction of groundwater flow. In West Maui, the lava flows dip from 5 to 20 degrees with thicknesses ranging from 1 to 100 ft (Stearns and MacDonald, 1942). By contrast, the water table in the study area is nearly horizontal relative to the dip of the lava beds. In addition, near the coast, the thinning of the freshwater zone adds an upward vertical component to the groundwater flow. Figure 5-21 is a gridded representation of a basalt aquifer around the shoreline. The layers in this figure dip 8° and have an individual thickness of 66 ft (20 m). The blue line indicates the water table (upper line) and the midpoint of the freshwater/saltwater transition zone (bottom curved-line). A generalized groundwater flow path from the injection well to a coastal discharge point is shown by the green arrow. To get from the injection well to a submarine point of discharge, the groundwater must cross multiple layers of lava forcing the injected fluids out of preferential interflow pathway. This would reduce the effective hydraulic conductivity from the well to the coast pathway. By contrast, a southerly flow direction would allow the injectate to remain in the interflow boundaries for a much longer distance resulting in a higher effective hydraulic conductivity. The blocking nature of the deep valley fills to the north and the regional hydraulic gradient that is parallel to the dip of the lava flows will exert a westerly influence on the injectate plume resulting in the southwest oblique pathway that is observed. To test this hypothesis, the groundwater simulation described in Section 5.5.2.7 was run using the hydraulic parameters of the Lahaina District Groundwater Model, but with the major and minor anisotropy axes reversed so that the dominant axis as aligned north-south. Figure 5-22 shows the modeled FLT plume on April 2013 using isotropic hydraulic conductivity ellipse (Figure 5-22a) and an anisotropic hydraulic conductivity ellipse (Figure

5-22b) with the dominant axis aligned north-south. The plume extent for the isotopic model only extends as far south as the SSG. By contrast, the plume for the anisotropic model extends south to the southern TIR plume boundary. As described in Section 4.2.6.2, the southern extent of the FLT plume as measured by shoreline sampling agrees with the south TIR plume boundary indicating that the treated wastewater plume extends as far south as those two points.

The anisotropic model provided the best agreement between the simulated and measured data. However, the orientation of the hydraulic conductivity ellipse is opposite of what is commonly assumed (e.g., Gingerich and Engott, 2012; Oki, 2005; Nichols et al., 1996). In the cited examples, regional groundwater flow was assessed and the relationship between the dip of the lava bedding to the path lines of the groundwater flow from a point source were not considered. This study evaluated the travel of a plume from a point source (the injection wells) and was able to infer the extent of the plume from direct measurement of dye fluorescence, TIR imagery, and $\delta^{15}\text{N}$ data. The modeling showed that anisotropy with dominant axis aligned north-south was critical to matching the spatial extent of simulated plume to that measured. This study also indicates that factors other than the anisotropy influence the pathway taken by the treated wastewater (i.e., buried stream channels and nearshore bathymetry). Together, these factors combine to constrain plume travel in a southwest direction. For example, in the absence of the valley fills to the north and west, the plume would spread laterally north and south resulting in a broader distribution with a much lower peak concentration at the submarine discharge points.

5.7 The BTC Trailing Edge

Two major hypotheses exist to explain the trailing edge that is commonly observed in BTCs. In the first, it is possible that multiple travel paths of varying hydraulic characteristics generating varying travel velocities between the point of the tracer injection and the point where the samples are collected. Multiple BTCs resulting from the various transport velocities may appear as a single BTC with a long trailing edge and possibly a plateau near the peak (Schulz, 1998). The second major hypothesis is that the tracer diffuses into the aquifer matrix during the ascending limb of the BTC, and then diffuses back into the aquifer pore channels on the descending limb of the BTC (Maloszewski and Zuber, 1993). The diffusion process described is a concentration dependent interaction between the groundwater and the aquifer matrix similar to sorption.

As described in Section 5.5.3.6, sorption will tend to slow the velocity and decrease the peak concentration of the dissolved species as the groundwater flows through the aquifer. It is difficult to conclude that sorption is occurring using a single tracer. Although comparison between an ideal tracer BTC and the dyes used by this study cannot be made with the physically collected data, the model results do allow a comparison. Related to this discussion is that different aquifer materials have differing sorption characteristics whether from surface charges on the matrix or diffusion into micro-fractures. This will result in different transport velocities based on the pathway the plume takes in the matrix. For example, the upper portion of the plume may be in contact with carbonate sediments that have a higher sorption

coefficient (Sabatini, 2000), while the lower part of the plume would travel through the non-carbonate basalts. The NSG BTC has characteristics consistent with multiple BTCs being superimposed forming a plateau followed by a long trailing edge. The plateau could result in the merging of the FLT plume from differing pathways. Figure 5-23a, for example, shows a combination of three BTCs of differing hydraulic characteristics that together produce an apparent plateau and a long trailing edge. The first BTC is the result of model simulations using an anisotropy with the dominant axis aligned north-south and a porosity of 0.14. The second BTC was produced using an isotropic hydraulic conductivity and porosity of 0.20. The isotropic simulation could represent a lava flow of a very shallow dip and a high porosity. The third BTC (“sorpt”) simulated FLT transport with sorption reducing the peak concentration but significantly extending the declining limb. A line that envelopes the two simulations was created by tracing the maximum concentration of the three BTCs at each time step. This composite BTC produces an apparent plateau that extends from mid-January 2012 to about April 2012. This is followed by a long trailing edge that maintains the FLT above the MDL for the foreseeable future.

A three-peak composite BTC can also be developed from the various simulations produced for this study. Annotated on Figure 23b are three apparent peaks of the measured BTC. Figure 5-23b shows that a composite BTC simulated using three different porosities can also produce a BTC with three peaks. The time and magnitude of the peaks is, however, much different from those measured. Still, the composite line that envelopes these three simulated BTCs does bear some resemblance to the measured BTC, including the long trailing edge.

Not enough is known about the subsurface geology in the study area to constrain these models with certainty because there are no boreholes that penetrate the basalt aquifer, with the exception of those drilled for the injection wells. That is, the actual processes and site-specific characteristics of the aquifer in the Kaanapali area responsible for postulated multiple peaks, the plateau, and trailing edge, cannot be determined from the hydrogeologic data available. However, the simulations described in this section do show that multiple pathways of varying hydrogeologic characteristics can produce results similar to those observed. Similar techniques have been used by other studies with more robust geologic data to demonstrate that multiple pathway BTCs can account for the plateaus and multiple peaks observed in actual BTCs. For example, Käss (1998) and Schulz (1998), have used the superposition of multiple simulated BTCs to produce good agreement with the measured data. This study simulated BTCs with various flow velocities then combined them into a single BTC to account for the multiple peaks and a sloping plateau. In order to use the superposition to develop a composite BTC, more detail must be known about the travel paths than is available for this study. A trial and error effort could produce a combined set of BTCs that more closely match the measured data. However, such an effort would require calibration far in excess of the hydrogeologic data available.

The uncertainty regarding the cause of the long trailing edge of the BTCs occurring in this study has not been definitively resolved, however, the discussion above supports the hypotheses that trailing edge is a combination of the differing hydraulic characteristics of the broad section of the aquifer encountered by the tracer plume and by the differing magnitudes

of interaction between the aquifer and the plume (i.e., sorption in the carbonate fraction and no sorption in the non-carbonate fraction). Model simulations were not successful in adequately replicating the extended plateau and the trailing edge of the BTC. Nevertheless, good agreement between the simulated and measured ascending limb and the physical extent of the plume show that modeling has adequately captured the major factors affecting the dye transport and affecting the transport of the treated wastewater injected into Wells 3 and 4.

5.8 ASSUMPTIONS AND LIMITATIONS

Modeling results were based on a MODFLOW model that ignored the effects of density variations. The groundwater transport was simulated by using a no-flow boundary at a point equivalent to the mid-point of the freshwater seawater transition zone. Implicit is the assumption that the aquifer can be treated as an equivalent porous medium. In such a case, aquifer properties are averaged over a representative elementary volume (REV), preserving the true aquifer's behavior (Bear, 1979). The REV should be large enough to include the effects of solids and fractures (for consolidated material) or solids, fractures, and porous material (for unconsolidated material), but small enough to be treated as a point in mathematical terms. In this case, Darcy's law is valid and the resulting solutions for the hydraulic head or solute concentrations are also averaged over the REV. However, due to preferential flow, the BTCs for solute transport can still show multiple peaks, even though Darcy's law is still valid. Multiple peaks can be considered as fluctuations similar to those attributed to heterogeneities. In the case of large fractures, BTCs should display a fast first-arrival and steep ascending and descending limbs, which was not manifested in this current study.

Factors contributing to modeling uncertainty include estimating water flux rates for both seeps and for the diffuse sources. These estimates are essential for calculating the amount of tracer mass recovered and assessing the overall success of the tracer test. The lack of accurate accounting can imply the existence of discharge points not covered by monitoring activities. The potential presence of other discharge locations is supported by the lack of detection of SRB at the NSG and the SSG. The flux rates are also needed for model calibration and validation. However, identifying other discharge points farther from shore and in deeper water are beyond the capabilities of this study. Uncertainty also exists in the models themselves due to the assumptions innate in their mathematical formulation and the lack of accurate supporting data. Results can be non-unique depending on parameter choices.

Exact replication of the BTCs was not possible due to the limitations of the model, including the absence of variable density flow representation and lack of detailed geological information about the site. Lack of data about the study area between the injection and receiving points of the tracer is a major complication.

5.9 CONCLUSIONS

As a planning tool, the TTDM, with minimal calibration, was able to estimate the first arrival, time of peak concentration, and, of greatest importance, the expected dye dilution, which is used in estimating the correct amount of the dye to use in this work. Although submarine springs in the current study are evidence of preferential flow, it seems reasonable to treat the aquifer as an equivalent porous media. The calibration values of aquifer parameters are in acceptable ranges, as well as the good match with the first solute arrival, which further supports this conclusion. The submarine springs act as leakage points and were treated as drains in our simulations, with outflow controlled by drain conductance.

This portion of the study reached two primary conclusions regarding the oblique path that the FLT and thus the injectate from Wells 3 and 4 takes to the marine discharge points. First, the valley fill and highly weathered basalt associated with current and past channels of the Honokowai Stream block the flow of the buoyant wastewater plume to the north and west. Evidence to support this conclusion include the downed stream valley just north of the NSG, and the cycles of sea level change that have occurred since the Wailuku Basalt Formation were laid down. The second conclusion is that the dominant axis of hydraulic conductivity for groundwater flow in the Kaanapali region of West Maui is aligned north-south, perpendicular to the dip of the lava flows. The cause of the anisotropy is that the dip of lava flows is significantly steeper than the slope of the water table. For the groundwater to flow directly west, which is the shortest path to the ocean, the water would have to cross multiple lava flows. This would force the groundwater out of the interflow zones, with their high hydraulic conductivity, and into the less permeable cores of the lava flows. Combined with the northwestward blockage to flow by a filled ancestral stream channel in the subsurface, the pathway to the marine discharge points southwest of the LWRF becomes the path of least resistance.

Although the reason for the failure of this study to positively detect SRB has not been determined with complete certainty, the interference between the flow fields of the injection wells appears the most probable cause. Wells 3 and 4 lie directly between Well 2 and the identified submarine springs southwest of the LWRF. Wells 3 and 4 are the primary injection wells, receiving more than 80% of the treated wastewater. Modeling indicates this interference reduces the SRB concentration at the submarine springs more than an order of magnitude to concentrations just above the MDL for this dye. The core of the SRB plume is diverted to the southeast before it can make its way to submarine discharge points. The displacement significantly lengthens the travel path this dye takes, and increases its dispersion. Other processes such as sorption and degradation have an ample opportunity to further reduce the concentration due to the increased pathway length and transit time. To test the hydraulic connectivity between Well 2 and the nearshore, a second tracer test would need to be conducted with Well 2 as the primary injection well.

A long trailing edge on the declining limb of a BTC is a common phenomenon observed during tracer tests, and this tracer test was no exception. The NSG BTC has the most pronounced plateau and trailing edge. We believe that this BTC is actually a composite of

multiple BTCs with different transit times superimposed on each other. Although modeling could not adequately replicate the entire NSG BTC, it was shown that there is a wide range of probable transit times using reasonable aquifer hydraulic parameters.

Table 5-1. Hydraulic parameter values for the various geologic units used in the TTDM compared to that of other models.

	Horiz. Hyd. Conductivity (ft/d)	Vert. Hyd. Conductivity (ft/d)	Long. Dispersivity (ft)	Porosity (Unitless)
TDDM				
Wailuku Basalts	2,950	29.5	164	0.1
Sediments	9.8	6.6	164	0.2
Lahaina Volcanics	16.4	1.6	164	0.1
SWAP/OSDS*				
Wailuku Basalts	1,630	16	NA	0.05
Sediments	49	0.49	NA	0.05
Gingerich and Engott (2012)				
Wailuku Basalts	590 (Transverse) 1,800(Longitudinal)	17	250	0.15
Sediments	190	3.8	250	0.15
* Whittier et al. (2004) and Whittier and El-Kadi (in preparation)				

Table 5-2. A comparison of the TTDM results and the measured NSG BTC.

Parameter	Units	TTDM	NSG BTC
First Arrival	(d)	70	84
Dilution	(C_{max}/C_{inj})	7.60E-04	1.70E-03
Peak Conc.	(ppb)	9.2	22.5
Time to Peak Conc.	(d)	263	306
Conc. at 1376 days	(ppb)	0.2	0.2

Table 5-3. Well injection and dye concentrations for the BTC Evaluation Model.

Start	End	Well 1	Well 2	Well 3		Well 4		
		Injection Rate (mgd)	Injection Rate (mgd)	SRB Conc. (ppb)	Injection Rate (mgd)	FLT Conc. (ppb)	Injection Rate (mgd)	FLT Conc. (ppb)
4/29/11	7/28/11	0.2	0.4	0	1.3	0	1.1	0
7/28/11	7/29/11	0.2	0.4	0	1.3	12,800	1.1	12,800
7/29/11	8/11/11	0.2	0.4	2,500	1.3	0	1.1	0
8/11/11	8/12/11	0.0	2.1	0	1.5	0	1.5	0
8/12/11	5/5/15	0.2	0.4	0	1.3	0	1.1	0

Table 5-4. Coefficients from Sabatini (2000) used in the sorption simulation.

Aquifer Media	Dye	Kr (L/kg)	N
Limestone	FLT	6.1	0.92
Limestone	SRB	168	0.81
Sandstone	FLT	0	NA
Sandstone	SRB	0.99	0.83

Table 5-5. A summary of the simulated dates of first arrival and peak concentrations of the preferential flow simulations.

Model	NSG			SSG			NSG:SSG
	First Arrival	Date of Peak Conc.	Peak Conc. (ppb)	First Arrival	Date of Peak Conc.	Peak Conc. (ppb)	
Measured	10/22/11	5/29/12	22.5	11/14/11	4/24/12	35	0.63
PFP in Layer 2	10/14/11	3/12/12	57.3	11/13/11	5/24/12	24.5	2.34
PFP in Layer 3	10/5/11	3/12/12	56.2	10/24/11	5/24/12	21.8	2.58
PFP in Layer 3 Cond 500	9/11/11	1/12/12	65.2	9/11/11	1/26/12	13.8	4.72
PFP in Layer 3 Cond 5000	9/11/11	1/26/12	61.1	9/18/11	3/13/12	23	2.66
PFP in Layer 4	9/27/11	2/25/12	54	10/14/11	6/14/12	20.7	2.61
PFP in Layer 5	9/27/11	2/25/12	54	10/14/11	6/14/12	20.7	2.61
PFP in Layer 6	9/3/11	1/26/12	46.1	9/18/11	6/14/12	19.6	2.35

Table 5-6. Results of porosity and dispersivity sensitivity simulations.

Porosity	Dispersivity (ft)	First Arrival (Date)	Peak Concentration (Date)	(ppb)	First Arrival (Date)	Peak Concentration (Date)	(ppb)
0.10	82	09/27/11	12/30/11	27.4	10/24/11	02/25/12	16.5
0.20	82	11/24/11	05/05/12	14.7	01/12/12	08/21/12	8.7
0.30	82	02/10/12	10/11/12	9.7	05/05/12	04/17/13	5.8
0.15	32	12/05/11	03/12/12	23.1	01/12/12	06/14/12	12.9
<i>0.15*</i>	<i>82</i>	<i>11/03/11</i>	<i>03/12/12</i>	<i>19.2</i>	<i>12/05/11</i>	<i>06/14/12</i>	<i>11.3</i>
0.15	164	10/05/11	02/25/12	15.6	11/13/11	05/24/12	9.6
0.15	246	09/27/11	02/10/12	14.3	10/24/11	05/24/12	8.7
	Measured	10/22/11	05/29/12	22.5	11/14/11	04/24/12	35.4

Bold italics indicates base case values

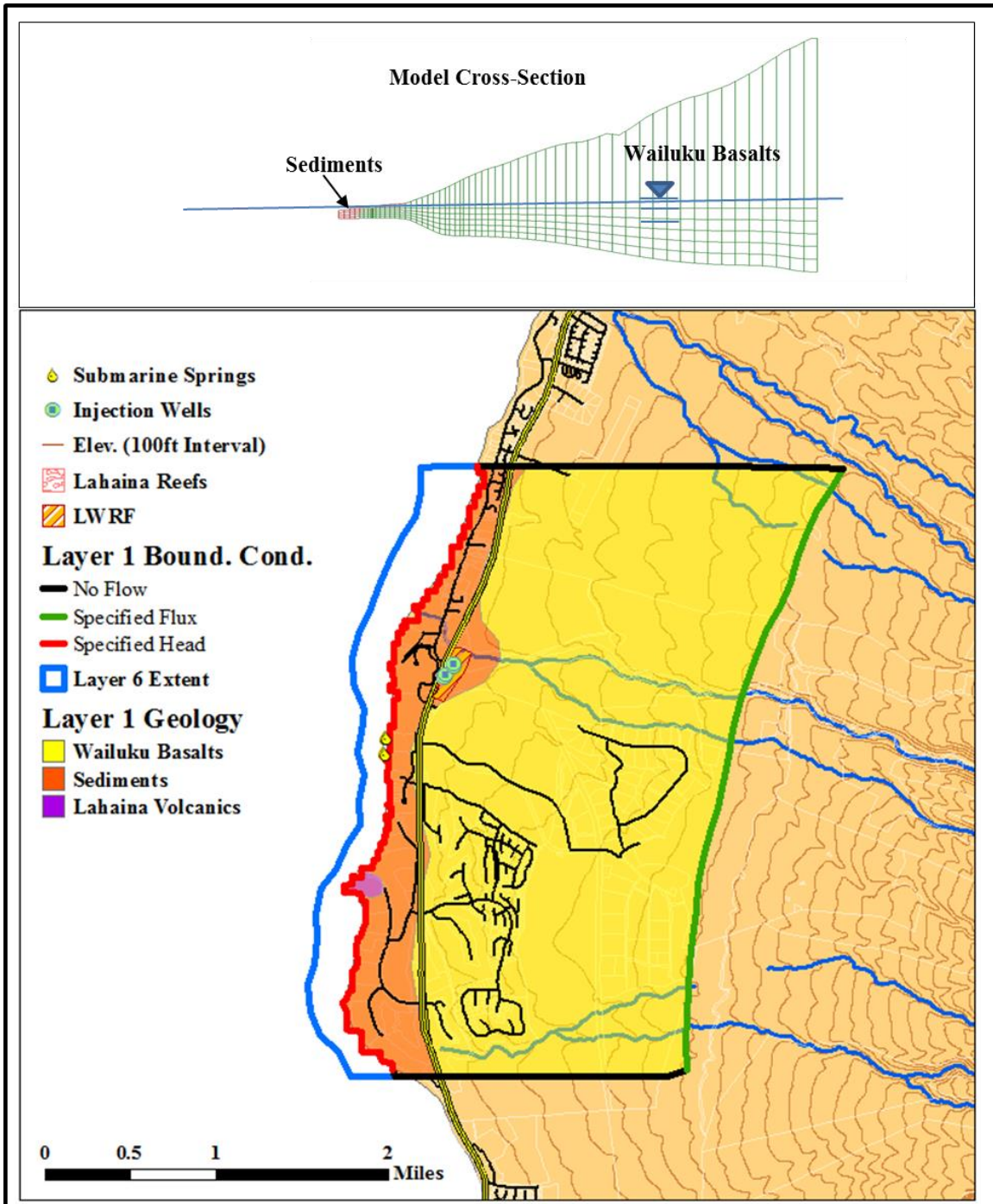


Figure 5-1: A plan view of the Tracer Test Design Model conceptual model and a cross section of the model grid.

The geology and boundaries conditions for layer 1 are shown in the map. The western boundary of this layer is the shoreline. The western boundary of the model is shown by extent of layer 6 that is approximately 1200 ft offshore at a simulated depth of about 34 ft. It also is a specified head boundary with an assigned head of 1.1 ft to reflect the greater density of seawater relative to freshwater.

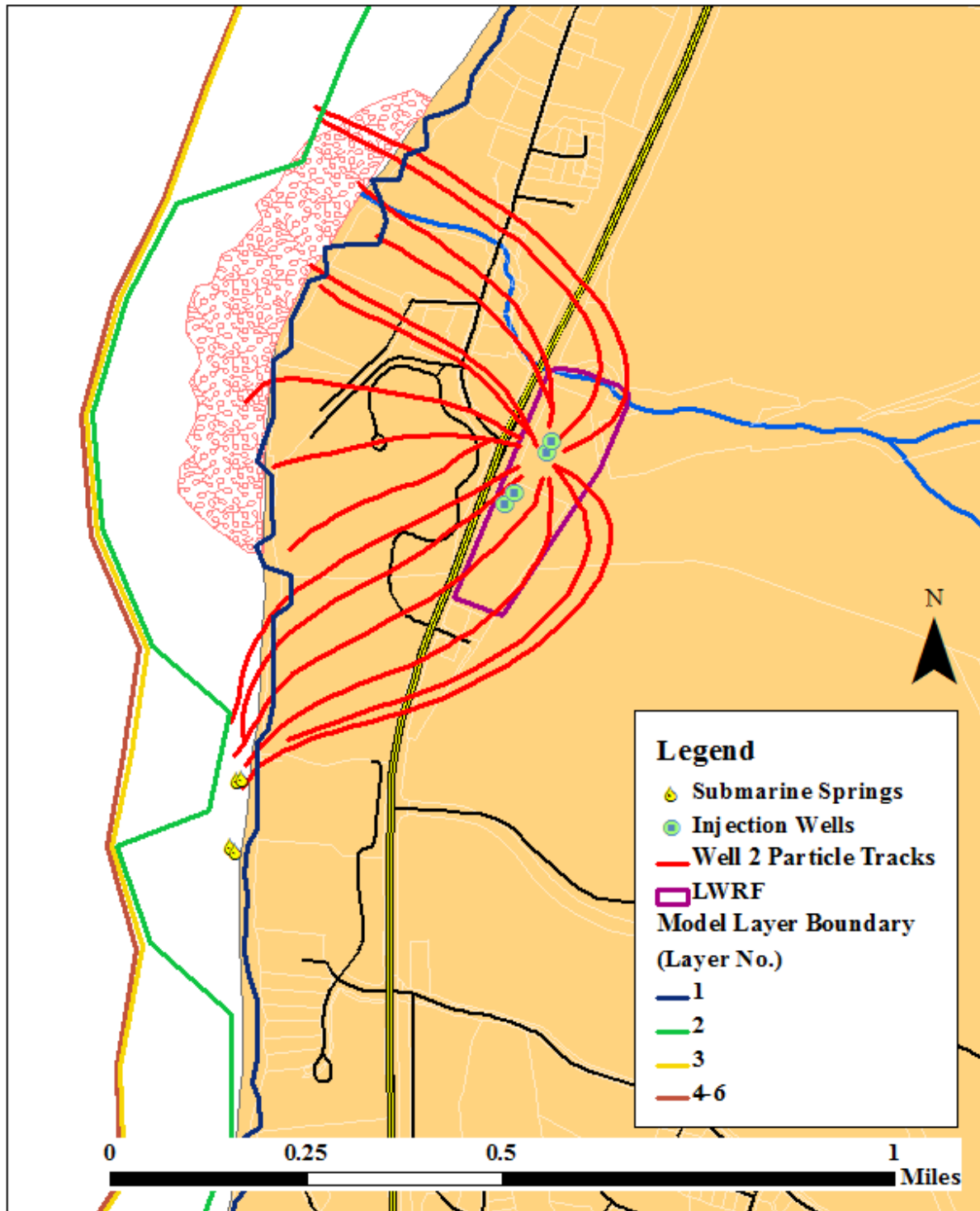


Figure 5-2: The results of the MODPATH particle track simulation used adjust the conductance of the springs. The conductance of the drains representing the submarine springs was increased until the drains started capturing the MODPATH particles.

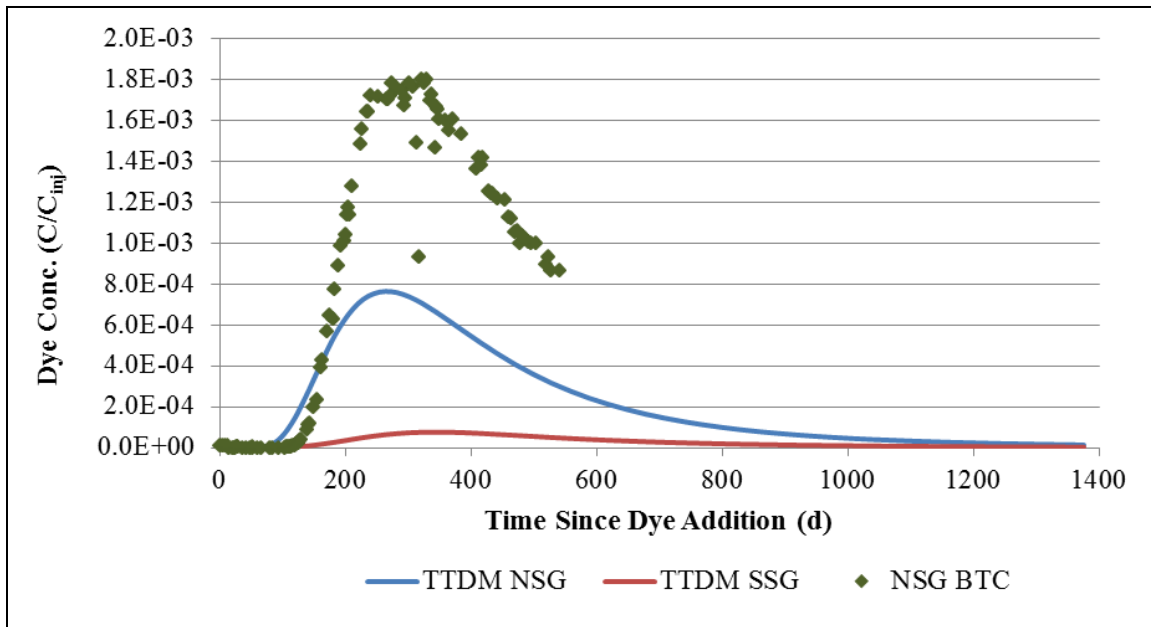


Figure 5-3: Results of the Tracer Test Design Model shown as the ratio of the submarine spring concentration to that at injection wells on the day of dye addition. The y-axis is the ratio of the FLT concentration at the submarine spring (C) to the FLT concentration in the injection wells (C_{inj}) at the time of dye addition. The measured data is shown as green diamonds, that simulated at the NSG is shown as a blue line (TTDM NSG) and that at the SSG as a red line (TTDM SSG).

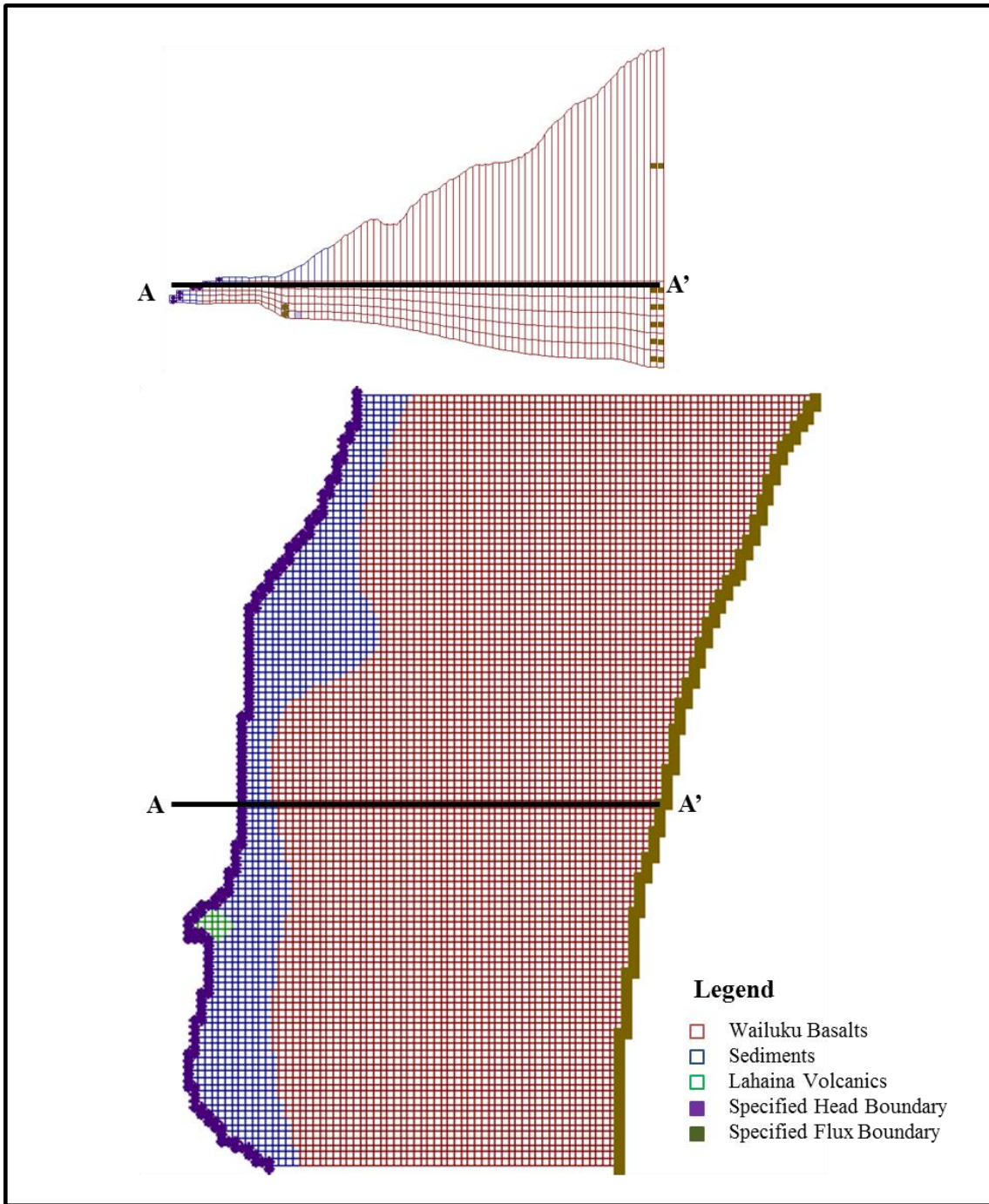


Figure 5-4: The numeric grid used for the Lahaina Groundwater Tracer Study model. The grid is shown in plan view and in cross-section. Only layer 1 is shown in plan view for simplicity. The cross section shows the east-west extent of the layers 2 through 6 in relation to that of layer 1.

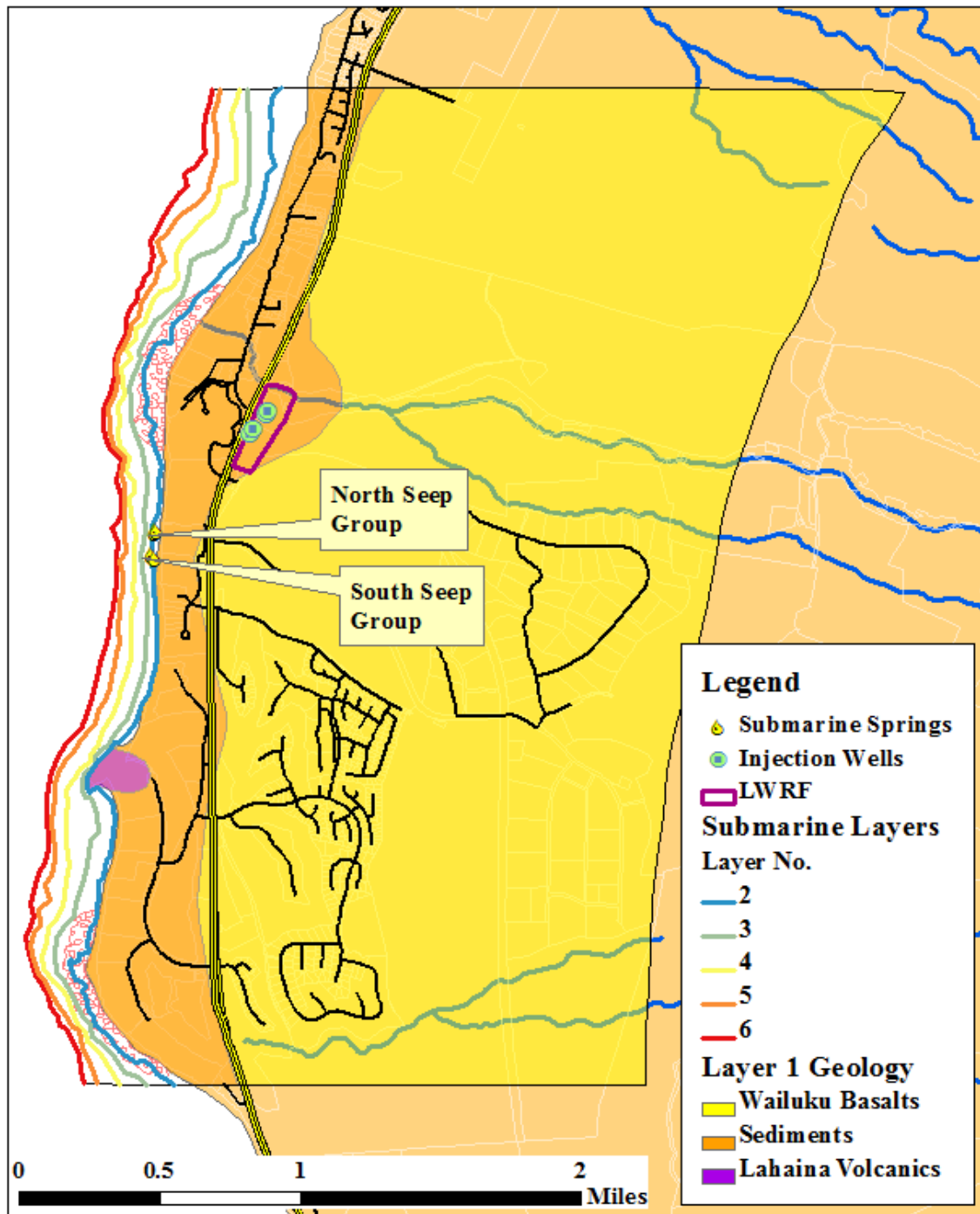


Figure 5-5: The conceptual model for the Lahaina Groundwater Study showing the extent of the submarine layers. Western boundaries of layers 2 through 6 followed the 6.6, 18, 29.5, 41, and 54 ft depth contours, respectively.

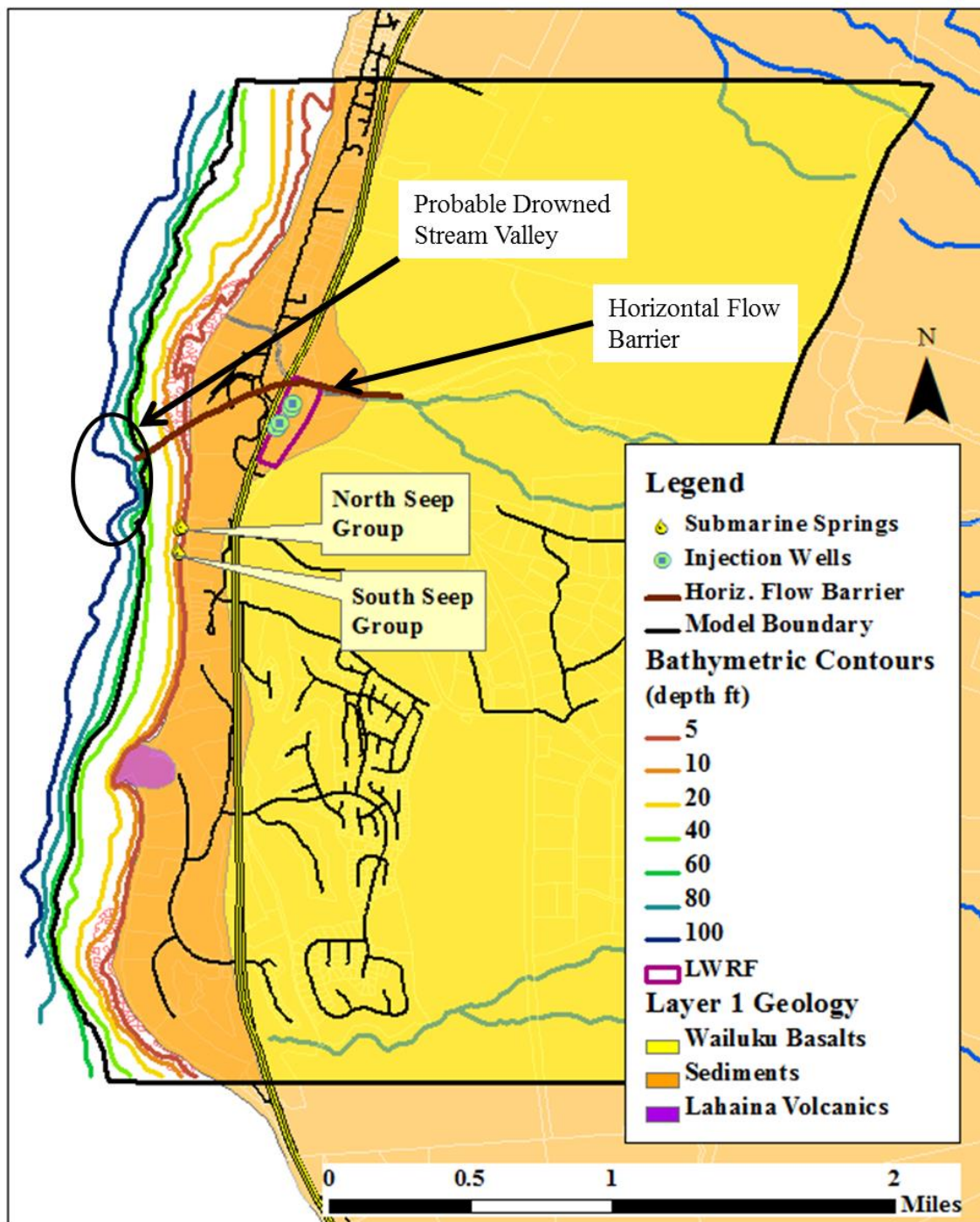


Figure 5-6: The Lahaina Groundwater Tracer Study conceptual model and the nearshore bathymetry.

Shown on this figure is the location of the horizontal flow barrier relative to that of the probable drowned stream valley.

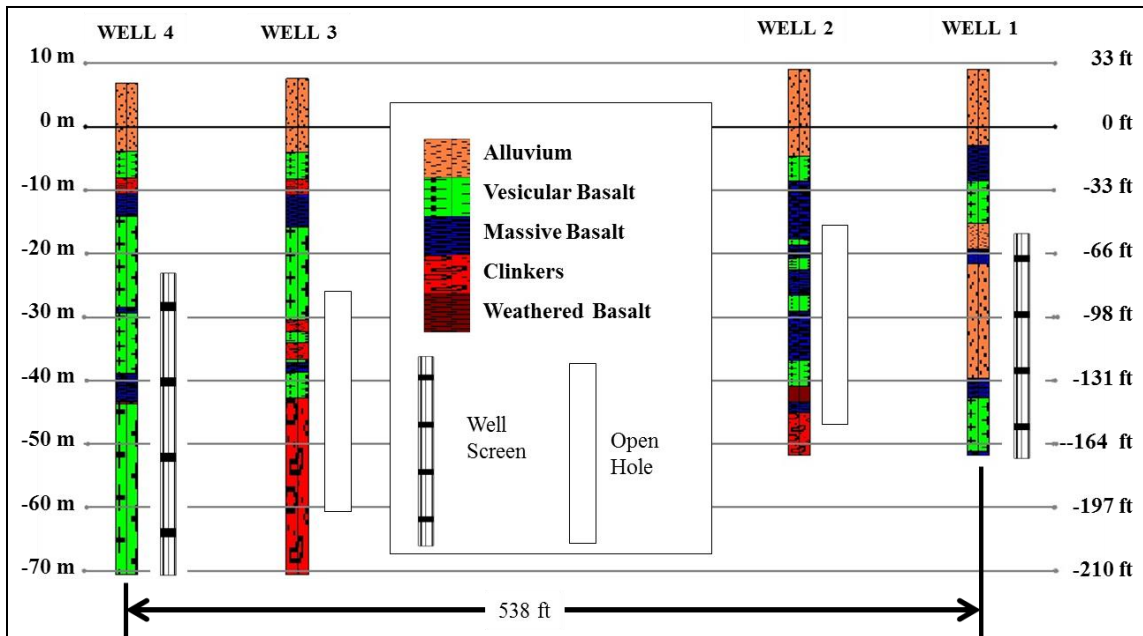


Figure 5-7: Borehole stratigraphy for the LWRF injection wells developed from the drillers' logs (County of Maui, 2004).

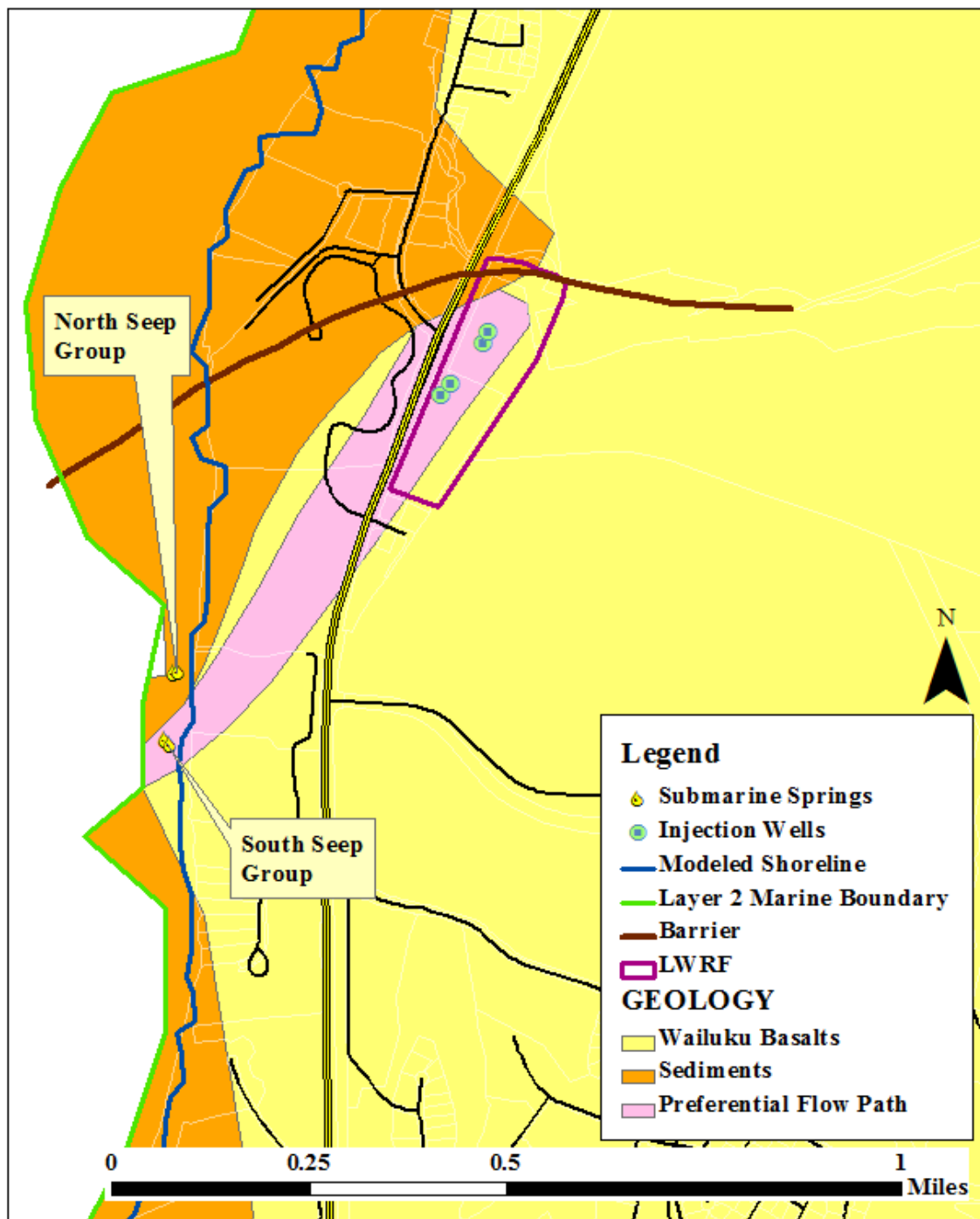


Figure 5-8: The conceptual model used in the PFP sensitivity simulations. This figure shows the PFP location in layer 2. In the sensitivity simulations a similar feature was simulated one at a time in layers 3 through 6.

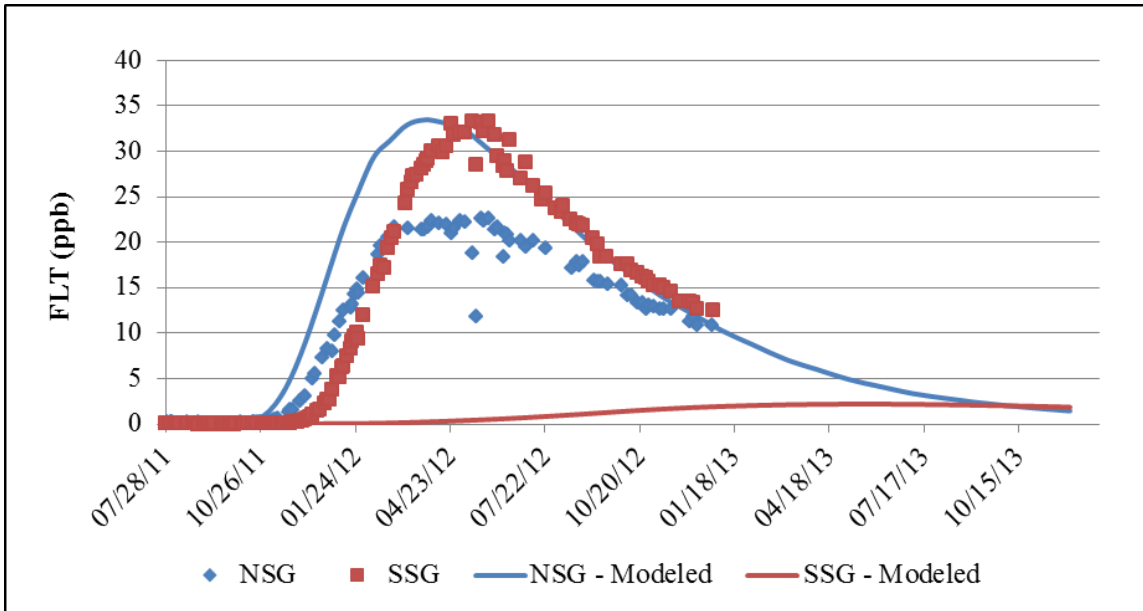


Figure 5-9: The measured BTCs compare the model results when a horizontal flow barrier was included in the model.

The NSG modeled BTC (blue line) shows good agreement with the measured (blue diamonds) when a horizontal flow barrier was added to the model. The BTC modeled for the SSG (red line) has a peak concentration that is over an order magnitude less than that measured (red squares) and arrives much later.

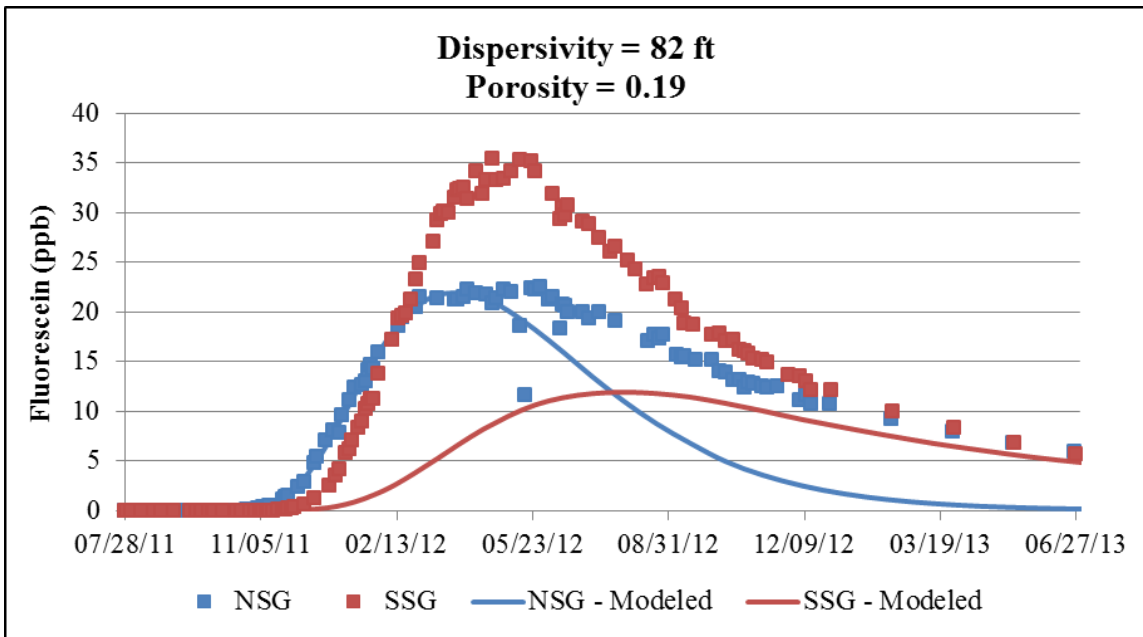


Figure 5-10: The measured and simulated BTCs after the model marine boundaries were modified.

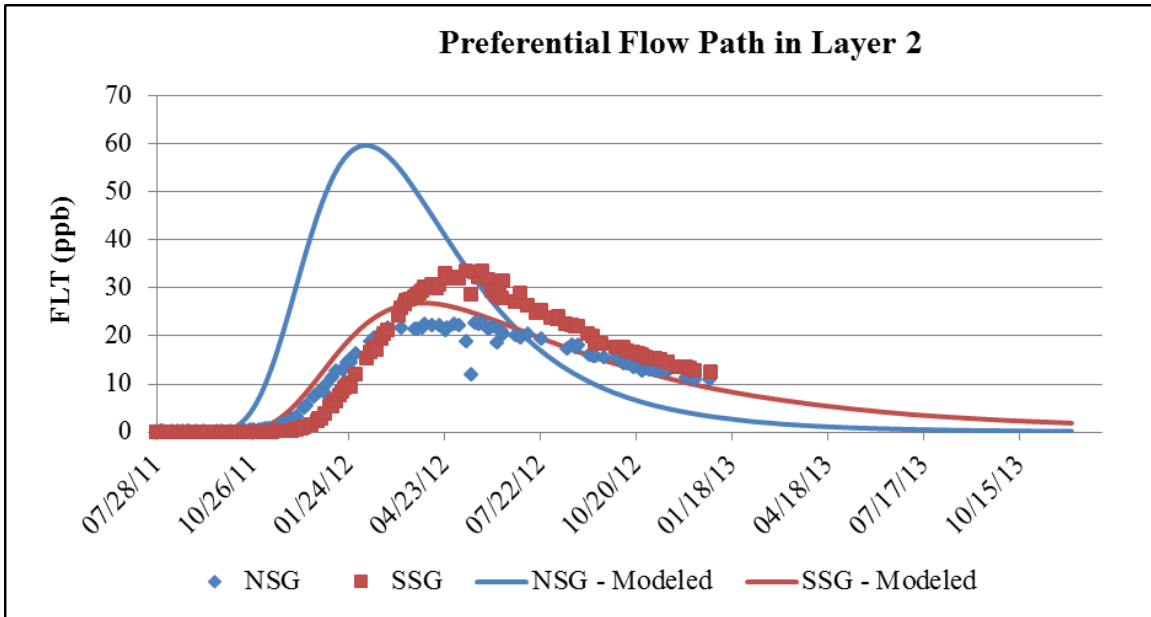


Figure 5-11: The modeled BTCs compared to that measured when a PFP was placed in layer 2.

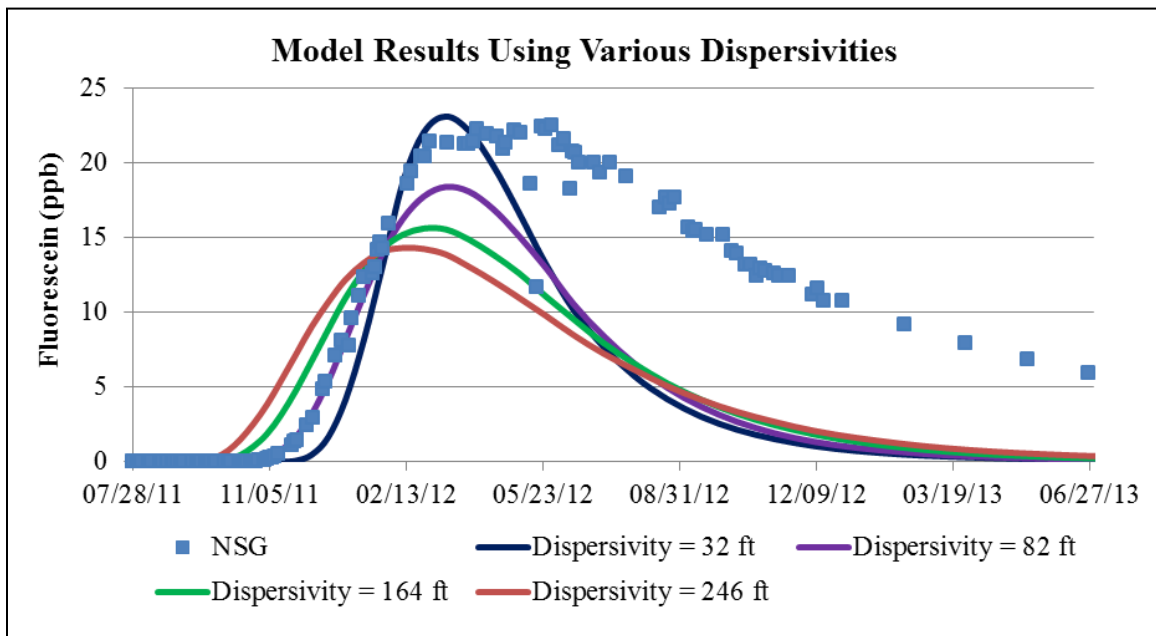


Figure 5-12: The results of the dispersivity sensitivity simulations compared to the BTC for the NSG.

Dispersivities tested were 32 ft (blue line), 82 ft (violet line), 164 ft (green line), and 246 ft (red line). A dispersivity of 82 ft consistently provided the best match between the simulated and measured BTCs.

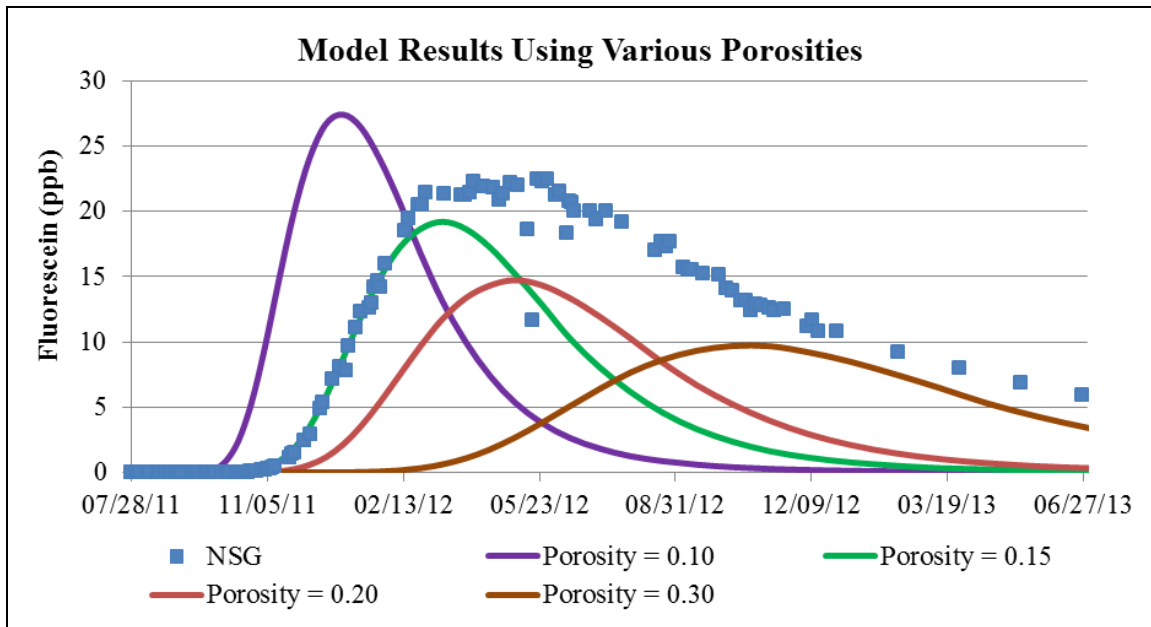


Figure 5-13: The results of the porosity sensitivity simulations compared to the BTC at the NSG.

The porosities tested were 0.10 (violet line), 0.15 (green line), 0.20 (red line), and 0.30 (brown line). A porosity of 0.15 provided the best match between the simulated and measured BTC.

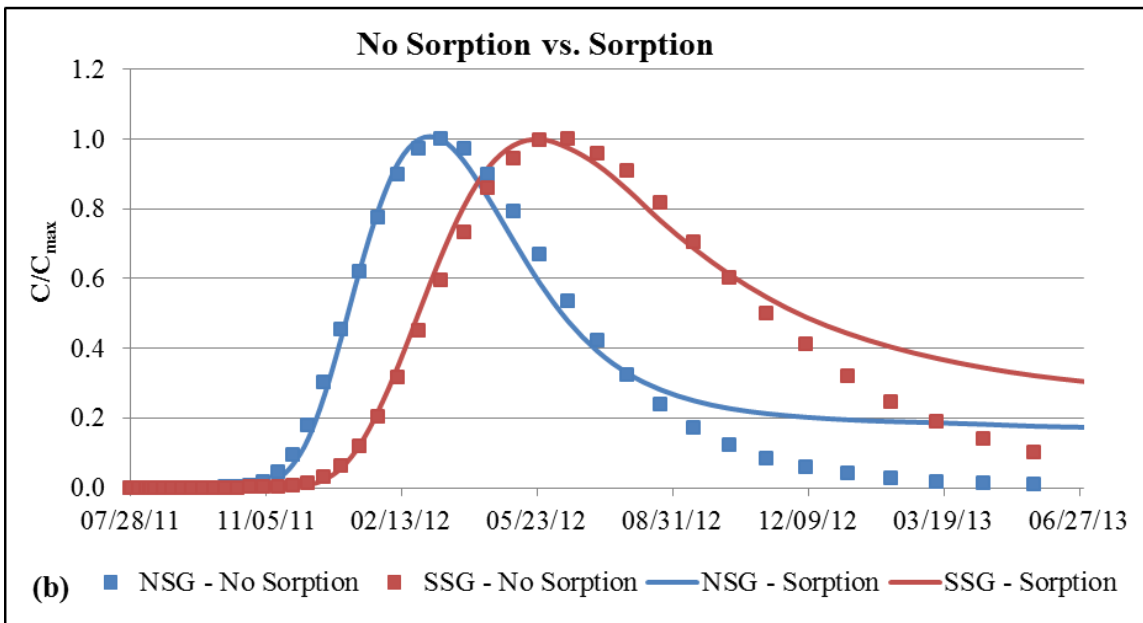
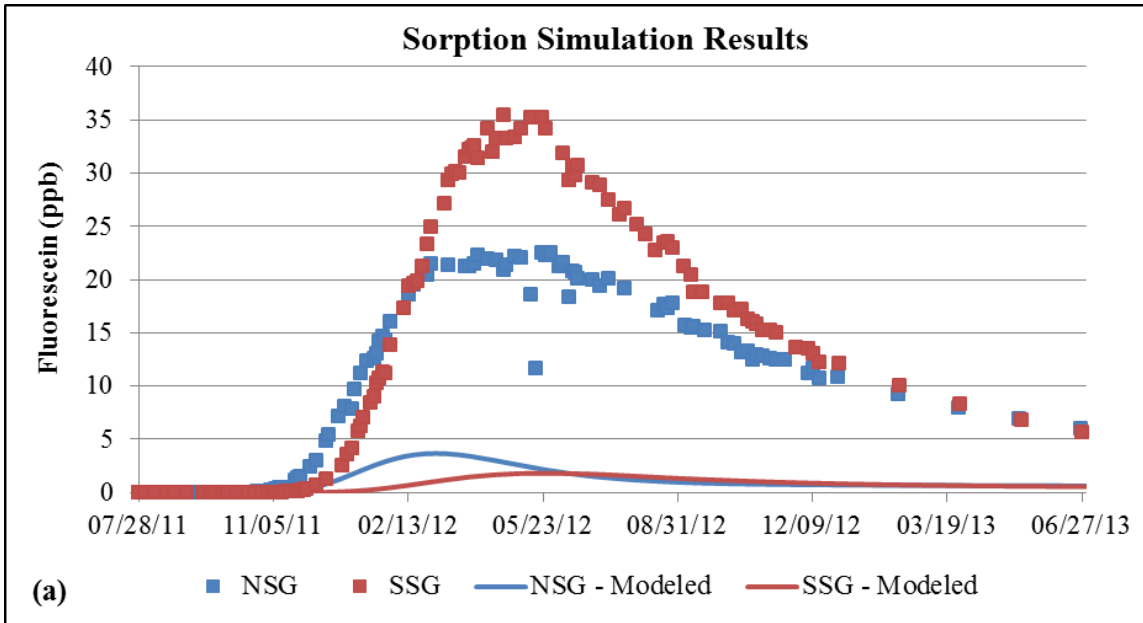


Figure 5-14: Modeled BTC when sorption of FLT was simulated. Figure 5-14a shows the measured and simulated BTCs when sorption was simulated.

Sorption of FLT on carbonate aquifer materials was simulated using the coefficients derived by Sabatini (2000) and assigning those coefficients to layer 2 (layer where the submarine springs were simulated). Figure 5-14b compares the simulation with no sorption (symbols) with that simulated using the sorption (line only) described above. The y-axis is the ratio of the temporal concentration (C) to the peak concentration (C_{max}).

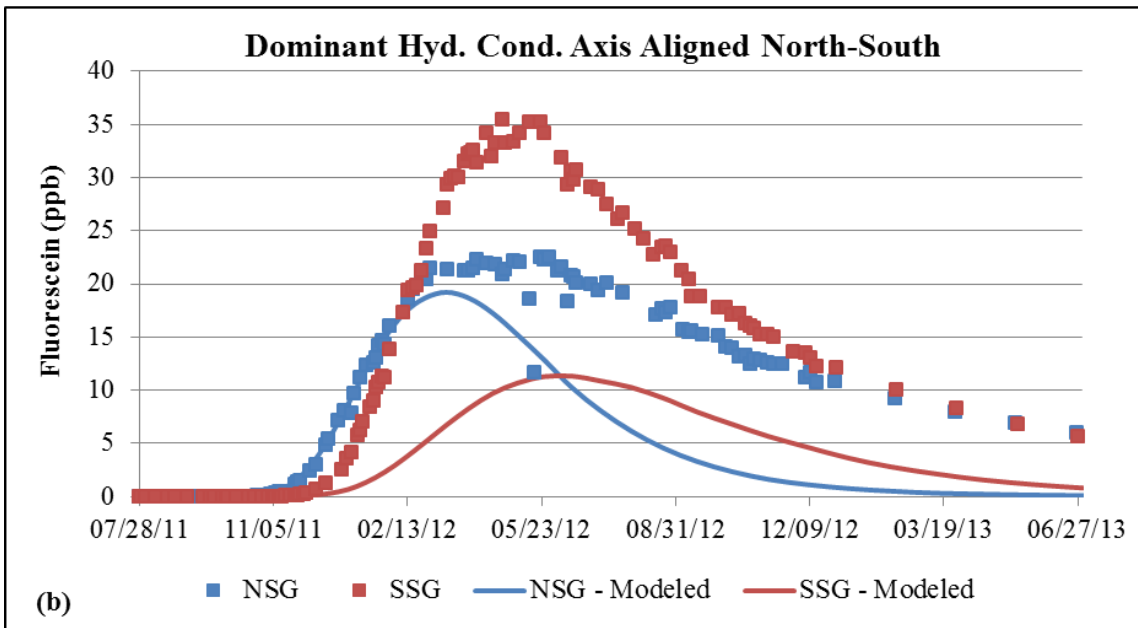
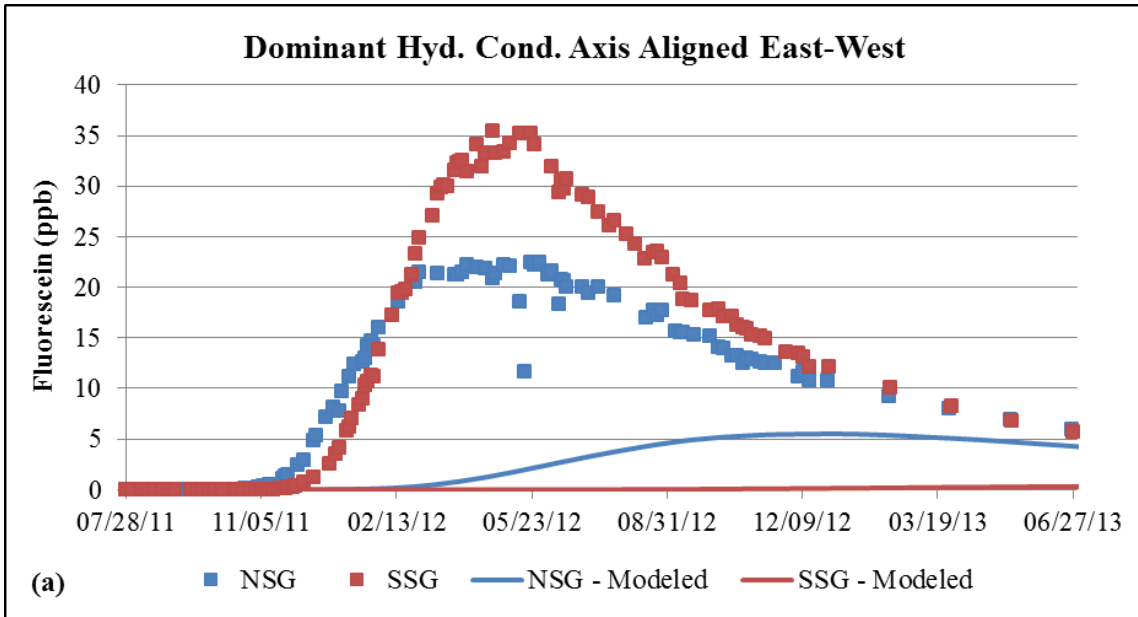


Figure 5-15: The simulated and measured BTCs with differing anisotropy ellipse alignments. When the dominant axis of the hydraulic conductivity is aligned east-west (Figure 15a), the simulated BTCs are severely attenuated. A much better agreement between the simulated and measure BTCs results when the dominant axis of hydraulic conductivity is aligned north-south.

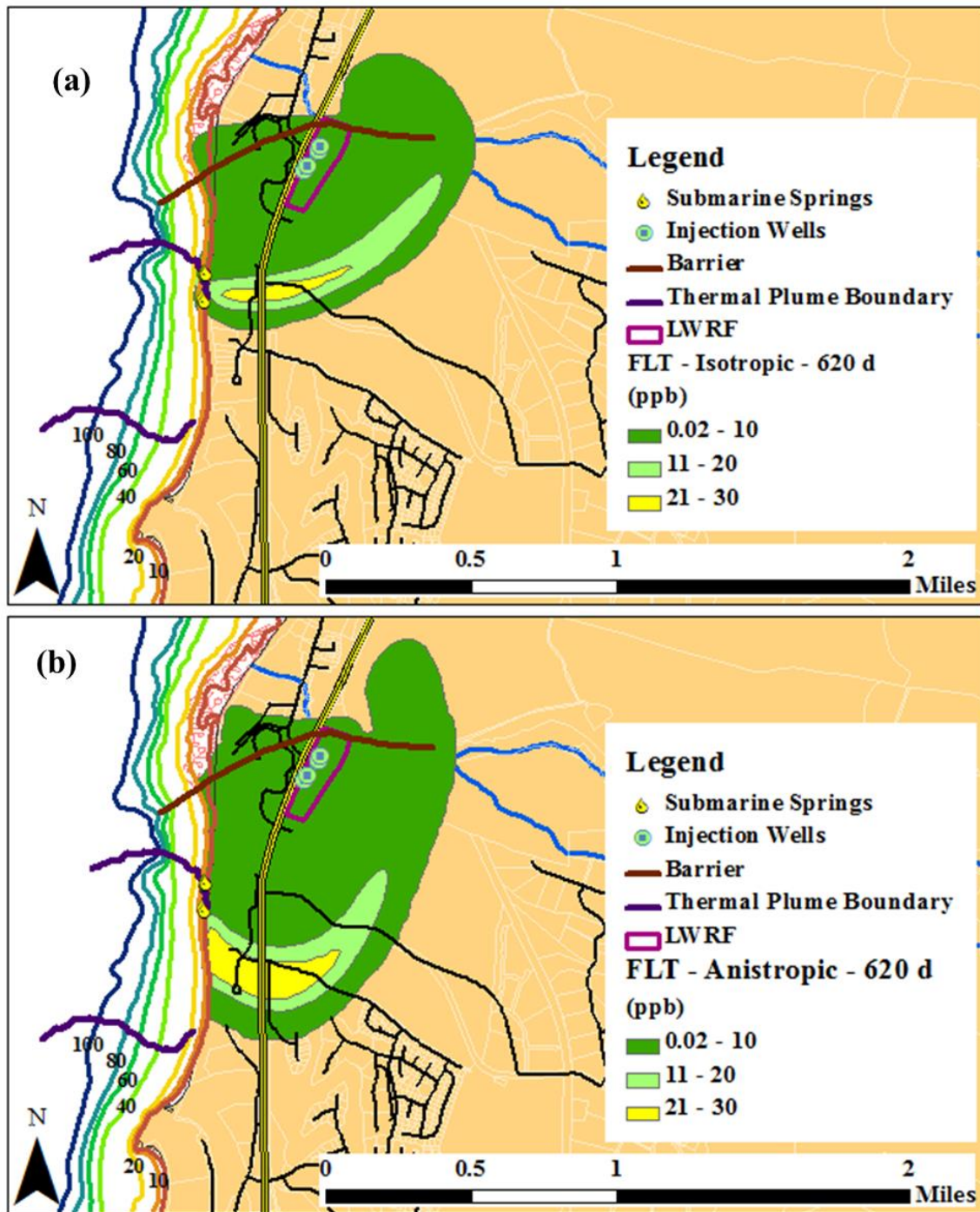


Figure 5-16: FLT plume simulated using and isotropic model (a) and an anisotropic model (b).

The model results show the simulated FLT plume 620 days after the dye addition. When isotropic hydraulic conductivity is simulated the plume only reaches the SSG. When the dominant hydraulic conductivity axis is aligned north-south, the plume reaches the southern TIR boundary.

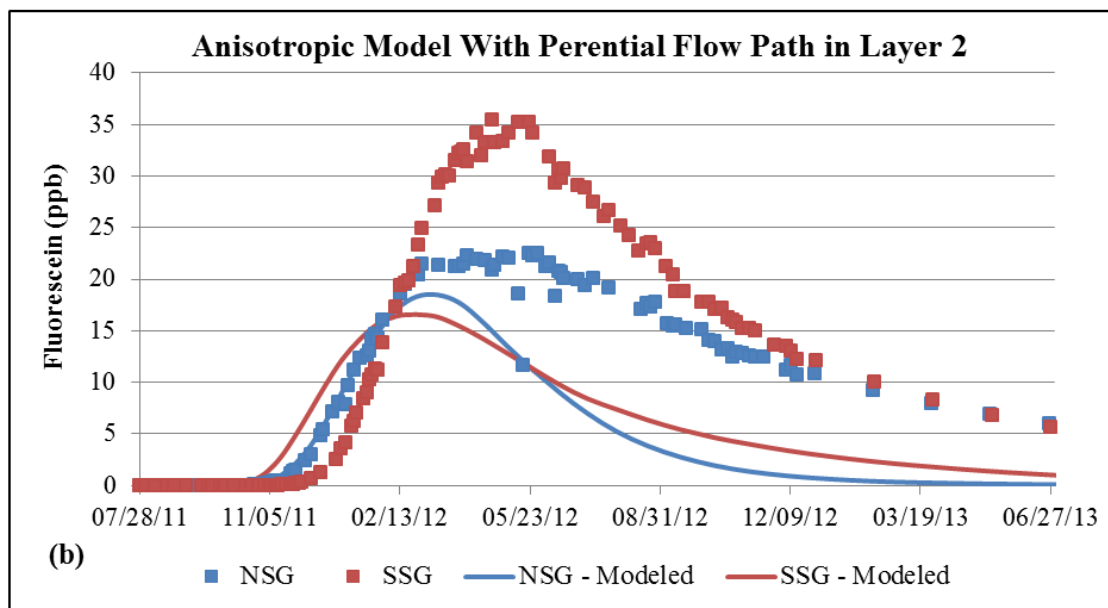
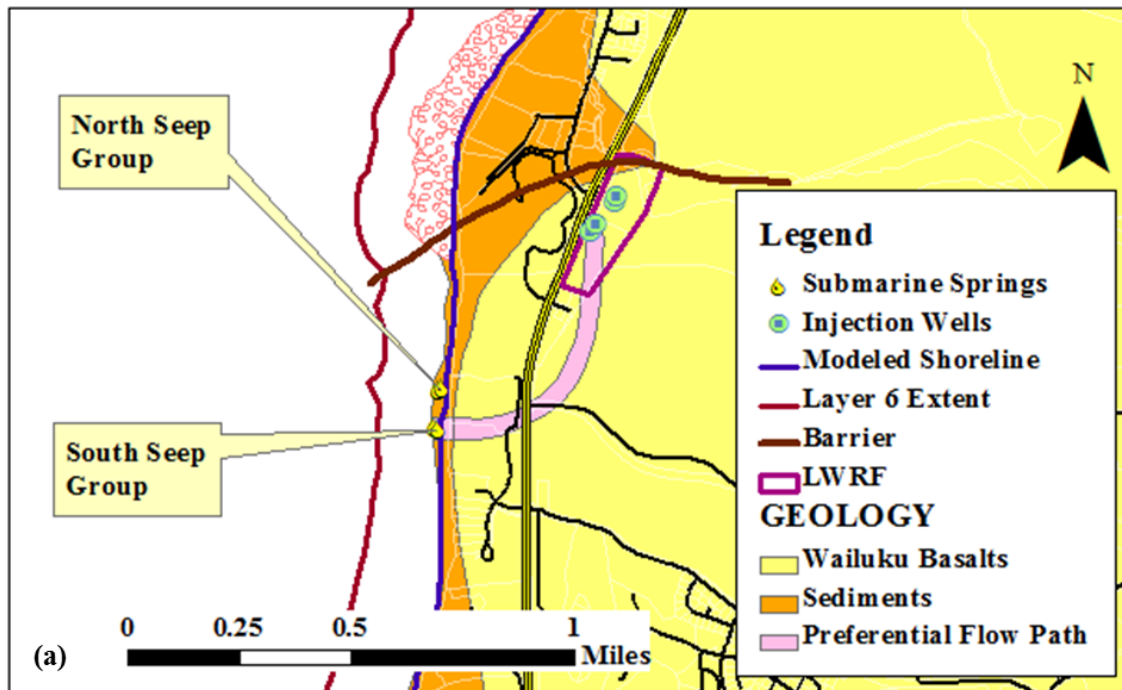


Figure 5-17: A map and modeled BTC when a PFP and anisotropy are simulated. The map (Figure 5-18a) shows the geometry of a preferential flow path between Injection Wells 3 and 4 and the SSG. The graph shows a significant improvement in the simulated SSG BTC relative to the NSG BTC. However, the peak concentration of the simulated SSG BTC is still only about half that measured.

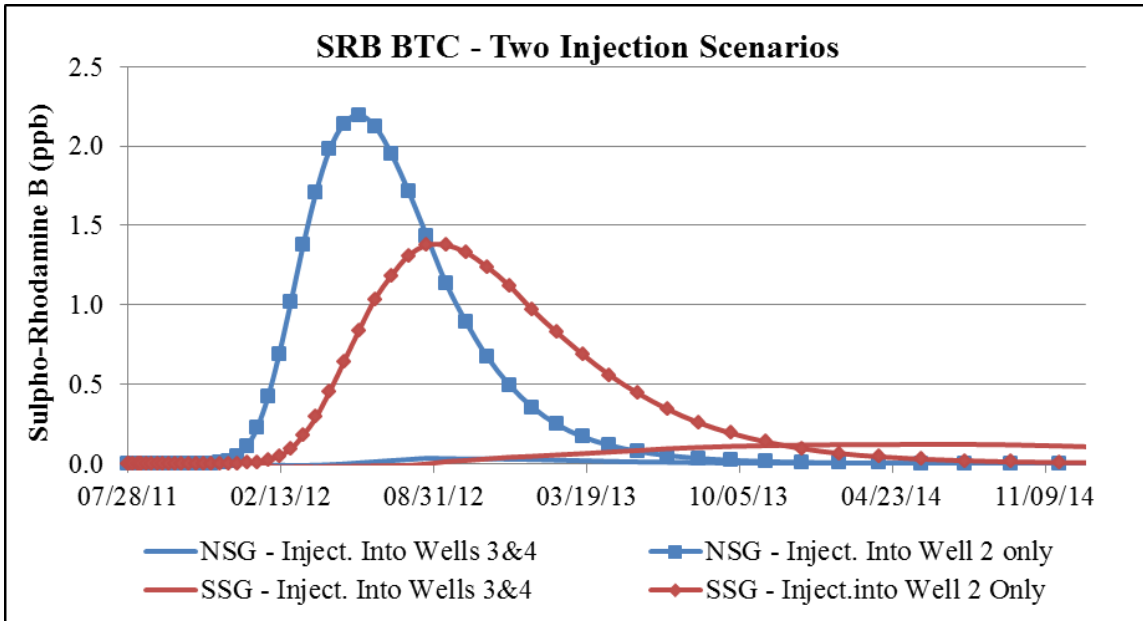


Figure 5-18: Simulated SRB BTCs under two different treated wastewater injection scenarios.

The first scenario (lines only) simulates treated wastewater injection continuing into Wells 3 and 4 after the addition of SRB. The second scenario (lines with symbols) shows the simulated BTCs if treated wastewater was injected into Well 2 only after the addition of SRB. Under the first scenario, the peak SRB concentration occurs at the SSG and is just above the MDL of 0.05 ppb. Under the second scenario, the peak SRB concentration occurs at the NSG and at both groups of submarine springs exceeds the MDL by an order of magnitude.

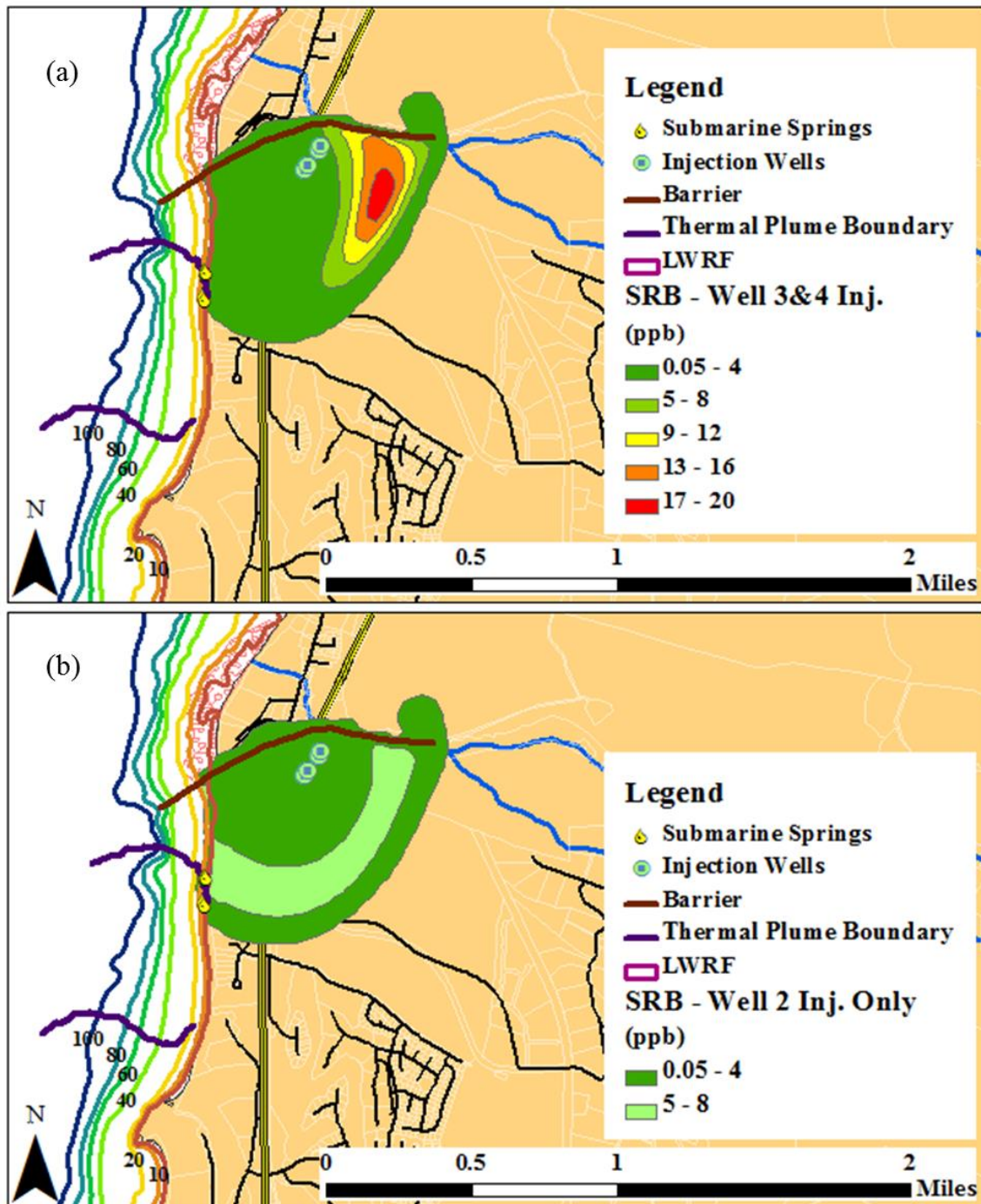


Figure 5-19: The SRB plume one year after dye addition under two different treated wastewater injection scenarios.

(a) Continuing injection into Wells 3 and 4 after the addition of SRB displaces the core of the plume to the southeast. The valley fill barrier to the north and west prevent plume for going in those directions. (b) The simulation done with injection into Well 2 only after SRB additions shows the core of the plume reaching the submarine springs.

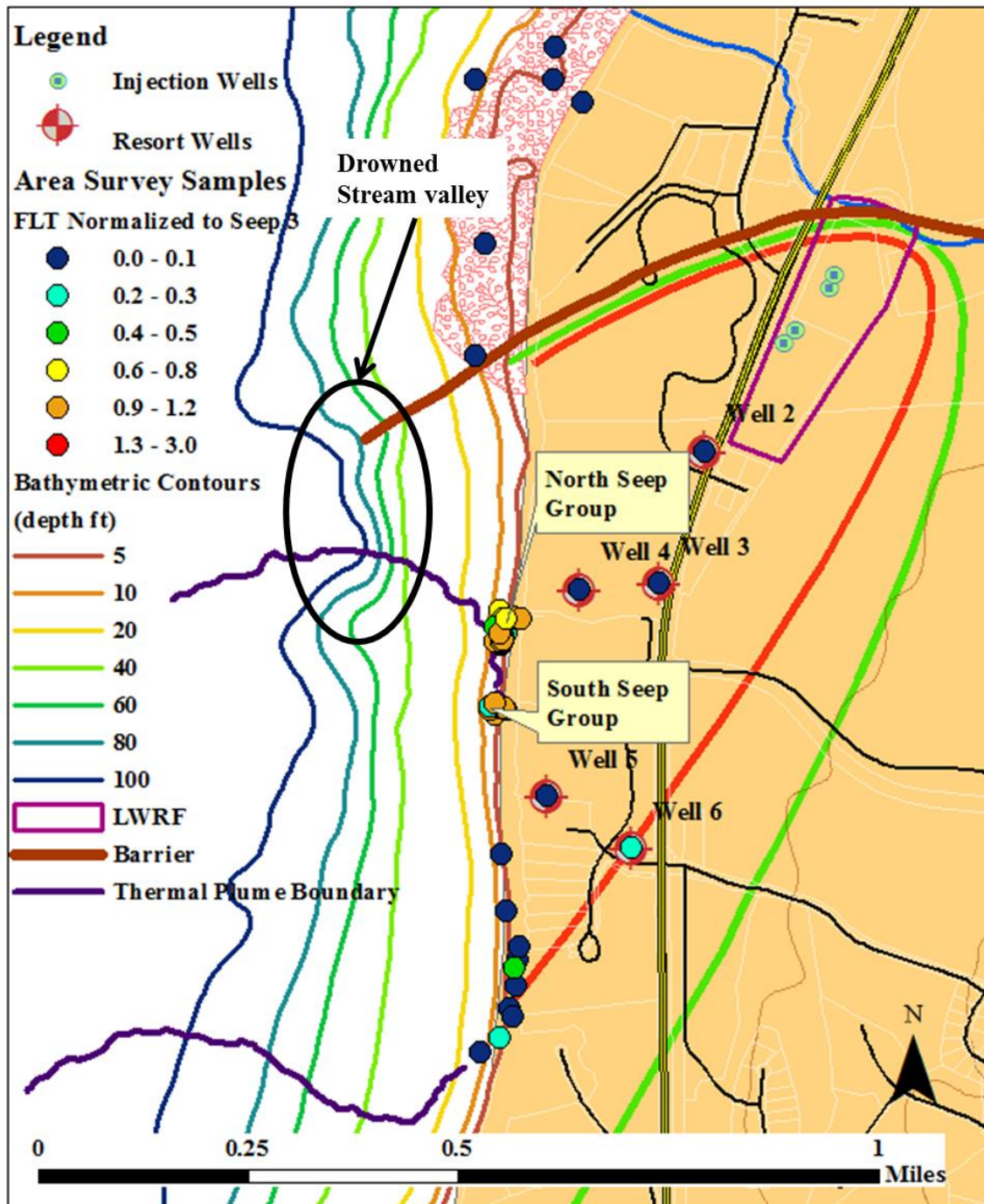


Figure 5-20: The study area showing the location of a probable drowned stream valley relative to the FLT plume.

The probable drowned stream valley (denoted by the ellipse) is indicated by an eastward indentation of the 60 to 100 ft bathymetric contours. The southern ridge of the drowned stream valley aligns with northern TIR plume boundary and the northern most sample collected that test positive for FLT.

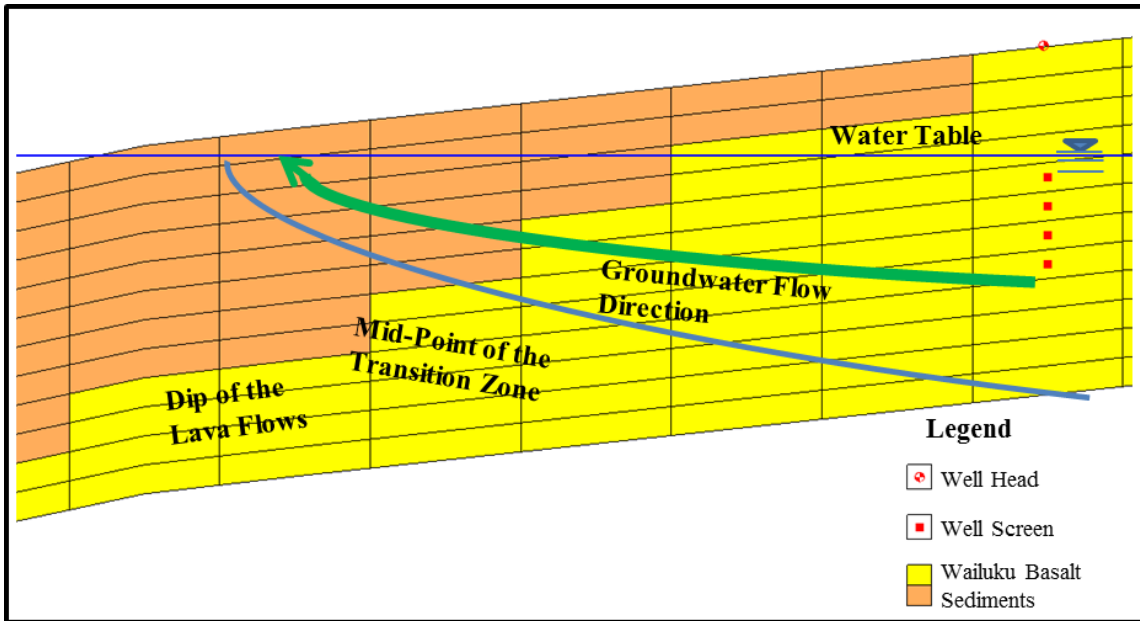


Figure 5-21: A cross-section of a coastal aquifer comparing the dip of the lava bedding to the generalized groundwater flow path.

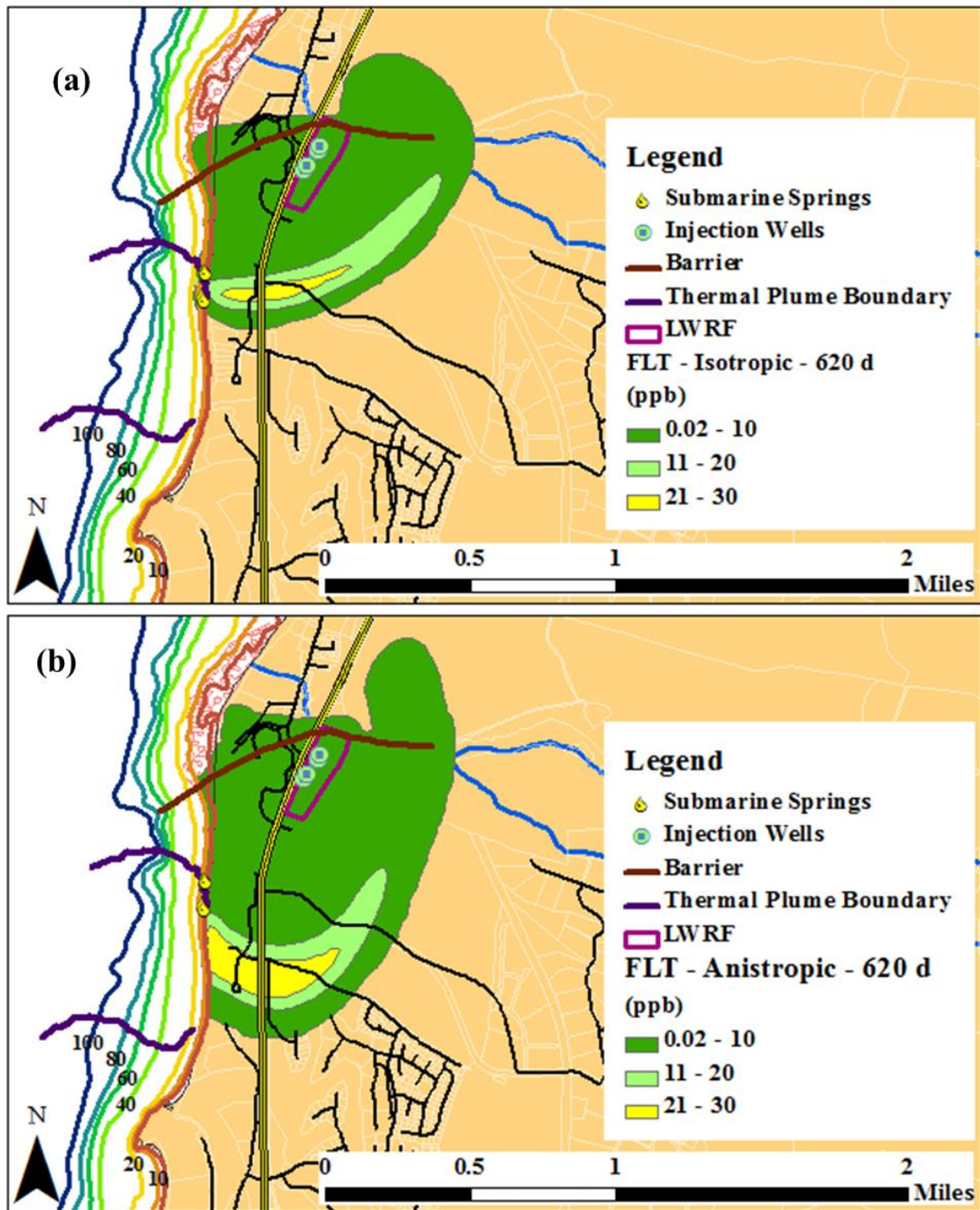


Figure 5-22: The simulated FLT plume 620 days after the dye addition using an isotropic model (a) and using an anisotropic model (b).

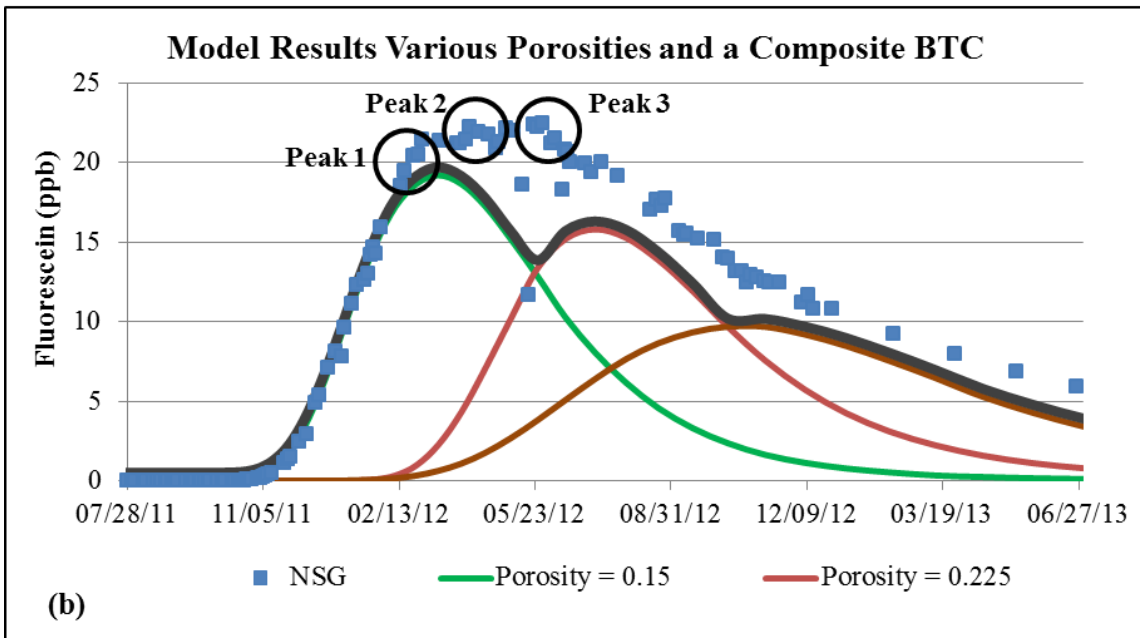
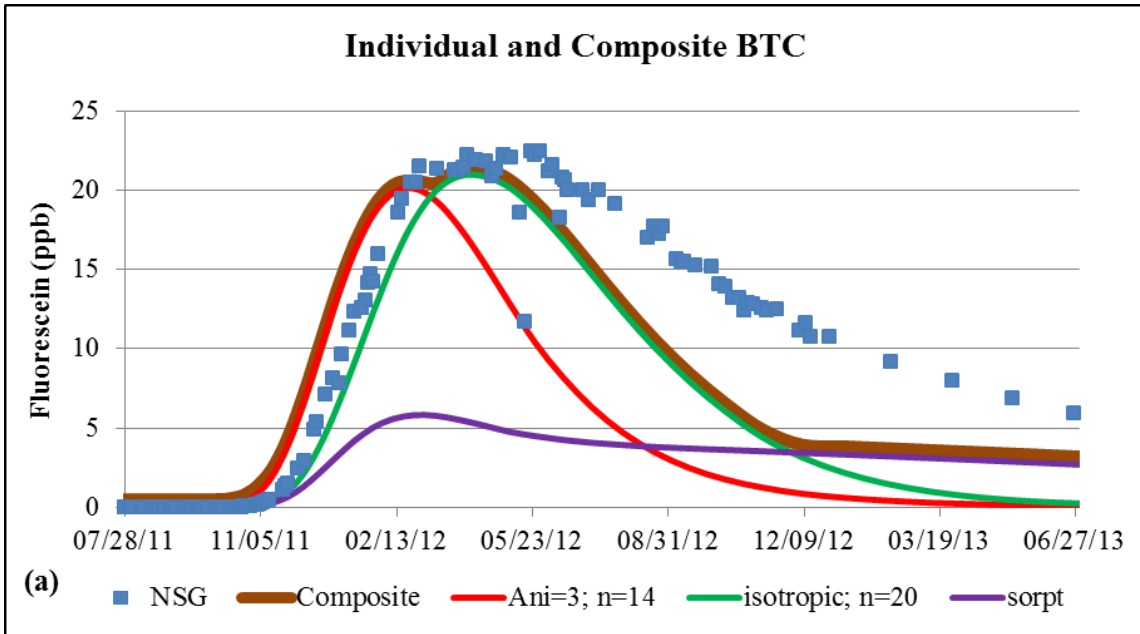


Figure 5-23: Simulated individual BTCs and composites showing a possible resulting BTC with multiple peaks and a plateau.

(a) Model results from isotopic and anisotropic simulations. A composite consisting of the maximum concentrations of the two BTCs show how different transport conditions could result in a combined BTC with a plateau. (b) Model results when three different porosities were simulated and a three peak composite BTC with a trailing edge similar to that measured.

SECTION 6: REFERENCES

- Appelo, C.A.J., and Potsma, D., 1993, *Geochemistry, Groundwater and Pollution*, Rotterdam, Brookfield, VT, A.A. Balkema, 536 p.
- Aley, T., 2002, *Groundwater Tracing Handbook—A Handbook Prepared for the Use of Clients and Colleagues of the Ozark Underground Laboratory*, Ozark Underground Laboratory, 35 p.
- Atkinson, S., Atkinson, M.J., and Tarrant, A.M., 2003, Estrogens from sewage in coastal marine environments, *Environ. Health Persp.*, 111, 531-535.
- Baker, A., Inverarity, R., Charlton, M., and Richmond, S., 2003, Detecting river pollution using fluorescence spectrophotometry: Case studies from the Ouseburn, NE England, *Environ. Pollut.*, 124, 57-70.
- Bear, J., 1979, *The Hydraulics of Groundwater*, McGraw-Hill, London, UK, 567 p.
- Berner, R.A. 1980, *Early Diagenesis: A Theoretical Approach*, Princeton University Press, 241p.
- Berner, E. K. and Berner, R. A., 1996, *Global Environment, Water, Air, and Geochemical Cycles*, Prentice-Hall, Upper Saddle, River, NJ.
- Bienfang, P., De Carlo, E.H., Christopher, S., DeFelice, S., and Moeller, P., 2009, Trace element concentrations in coastal Hawaiian waters, *Marine Chem.*, 113, 164-171.
- Bourke, R., 1996, Maui algae bloom studies-distribution and abundance, Oceanit Laboratories, Inc., Honolulu, HI.
- Brown, T.L., 2009, Fluorescence Characterization of Karst Aquifers in East Tennessee, M.S. thesis, Knoxville, University of Tennessee.
- Burnham, W.L., Larson, S.P., and Cooper, H.H., Jr., 1977, Distribution of injected wastewater in the saline lava aquifer, Wailuku-Kahului Wastewater treatment Facility, Kahului, Maui, Hawaii, U.S. Geological Survey Open-File Report 77-469, 58p.
- Burnett, W.C., and Dulaiova, H., 2003, Estimating the dynamics of groundwater input into the coastal zone via continuous radon-222 measurements, *J. Environ. Radioactiv.*, 69, 21-35.
- Burnett, W.C., Aggarwal, P.K., Aureli, A., Bokuniewicz, H., Cable, J.E., Charette, M.A., Kontar, E., Krupa, S., Kulkarni, K.M., Loveless, A., Moore, W.S., Oberdorfer, J.A., Oliveira, J., Ozyurt, N., Povinec, P., Privitera, A.M.G., Rajar, R., Ramessur, R.T., Scholten, J., Stieglitz, T., Taniguchi, M., and Turner, J.V., 2006, Quantifying submarine groundwater discharge in the coastal zone via multiple methods, *Sci. Total Environ.*, 367, 498p.
- Chua, L.H.C., Robertson, A.P., Yee, W.K., Shuy, E.B., Edmond, Y.M., Lo, T.T., and Tan, S.K., 2007, Use of Fluorescein as a Ground Water Tracer in Brackish Water Aquifers, *Ground Water*, v. 45(1), p. 85-88.
- County of Maui, 2004, Lahaina Wastewater Reclamation Facility U.I.C. Permit—Permit No. HI596001—Permit Renewal Application, Dated December 1, 2004.
- County of Maui, 2010, Lahaina Wastewater Reclamation Facility Underground Injection Control (UIC) Injection Well Status Report Number 30 - July 2010—Submitted to: State of Hawaii, Safe Drinking Water Branch.
- County of Maui, 2011, Injection Well Flows, 0411 to 0611, unpublished data.

- County of Maui, 2012-2013, Injection Well Flows, unpublished data.
- Dailer, M.L., Knox, R.S., Smith, J.E., Napier, M., and Smith, C.M., 2010, Using $\delta^{15}\text{N}$ values in algal tissue to map locations and potential sources of anthropogenic nutrient inputs on the island of Maui, Hawaii, USA, *Mar. Pollut. Bull.*, 60, 655-671.
- Dailer, M.L., Ramey, H.L., Saephan, S., and Smith, C.M., 2012, Algal $\delta^{15}\text{N}$ values detect a wastewater effluent plume in nearshore and offshore surface waters and three-dimensionally model the plume across a coral reef on Maui, Hawai'i, USA, *Mar. Pollut. Bull.*, 64, 207-213.
- Davis, S.N., Thompson, G.M., Bently, H.W., and Stiles, G., 1980, Groundwater tracers—A short review, *Ground Water*, 18, 14-23.
- Department of Business, Economic Development, and Tourism, 2010, 2010 Census—DBEDT Products (Highlights, Reports, Presentations and Tables), http://dbedt.hawaii.gov/census/Census_2010/cen2010all_rep/ accessed 5/15/2013.
- Dever, J.L., 1997, *The Geochemistry of Natural Waters*. Prentice Hall, 436 p.
- Dollar, S., and Andrews, C., 1997, Algal blooms off west Maui—assessing causal linkages between land and the coast ocean, Final Report for National Oceanic and Atmospheric Administration Coastal Ocean Program Office and University of Hawaii Sea Grant College Program, Honolulu, HI.
- Dollar, S.J., Atkinson, M., and Atkinson, S., 1999, Investigation the relationship between cesspool nutrients and abundance of *Hypnea musciformis* in West Maui, Hawaii, Report State of Hawaii Department of Health, Honolulu, Hawaii.
- Dulaiova, H., Camilli, R., P. B. Henderson, and M. A. Charette, 2010. Coupled radon, methane and nitrate sensors for large-scale assessment of groundwater discharge and non-point source pollution to coastal waters, *Journal of Environmental Radioactivity*, 101, 553-563, doi: 10.1016/j.jenvrad.2009.12.004.
- Ekern, P.C., and Chang, J.H., 1985, Pan evaporation: State of Hawai'i, 1894-1983, Hawai'i Department of Land and Natural Resources, Division of Water and Land Development, Report R74, Honolulu, HI, 172p.
- Engott, J.A., and Vana, T.T., 2007, Effects of agricultural land-use changes and rainfall on ground-water recharge in Central and West Maui, Hawaii, 1926-2004, U.S. Geological Survey Scientific Investigations Report 2007-5103, 56p.
- Fetter, C.W., 1992, *Contaminant Hydrogeology*, Macmillan Publishing Co, 458 p.
- Fetter, C.W., 1998, *Applied Hydrogeology*, Second Edition, Macmillan Publishing Co., 589 p.
- Field, M.S., Wilhelm, R.G., Quinlan, J.F., and Aley, T.J., 1995, An assessment of the potential adverse properties of fluorescent tracer dyes used for groundwater tracing, *Environ. Monitor. Assess.*, 38, 75-96.
- Field, M.S., 2002, The QTRACER2 Program for tracer-breakthrough curve analysis for tracer tests in karst and other hydrologic systems, EPA/600/R-02/001, U.S. Environmental Protection Agency.
- Flury, M., and Wai, N.N., 2003, Dyes as tracers for vadose zone hydrology, *Rev. Geophys.*, 41(1), 2-1-2-37.
- Freeze, R.A., and Cheery, I.A., 1979, *Groundwater*, Prentice-Hall, Inc., Englewood Cliffs, NJ, 604 p.

- Froelich, P. N., Klinkhammer, G. P., Bender, M. L., Luedtke, N., Heath, G. R., Cullen, D., Dauphin, P., Hammond, D., Hartman, B., and Maynard, V., 1979, Early oxidation of organic matter in pelagic sediments of the eastern equatorial Atlantic: suboxic diagenesis, *Geochim. Cosmochim. Acta*, 43, 1075-1090.
- Galapate, R.P., Baes, A.U., Ito, K., Mukai, T., Shoto, E., and Okada, M., 1998, Technical note: Detection of domestic wastes in Durose River using synchronous fluorescence spectroscopy, *Water Res.*, 32, 2232-2239.
- Giambelluca, T.W., Chen, Q., Frazier, A.G., Price, J.P., Chen, Y.-L., Chu, P.-S., Eischeid, J., and Delparte, D., 2011, *The Rainfall Atlas of Hawai'i*, <http://rainfall.geography.hawaii.edu>.
- Gingerich, S.B., 2008, Ground-water availability in the Wailuku area, Maui, Hawaii, U.S. Geological Survey Scientific Investigations Report 2008-5236, 95p.
- Gingerich, S.B., and Voss, C.I., 2005, Three-dimensional variable-density flow simulation of a coastal aquifer in southern Oahu, Hawaii, USA, *Hydrogeol. J.*, 13, 436-450.
- Gingerich, S. B., and Engott, J.A., 2012, Groundwater availability in the Lahaina District, West Maui, Hawaii, U.S. Geological Survey Scientific Investigations Report 2012-5010, 90 p.
- Glenn, C.R., Whittier, R.B., Dailer, M.L., Dulaiova, H., El-Kadi, A.I., Fackrell, J., Kelly, J.L., and Waters, C.A., 2012, Lahaina groundwater tracer study—Lahaina, Maui, Hawaii, Interim Report. Prepared from the State of Hawaii Department of Health, the U.S. Environmental Protection Agency, and the U.S. Army Engineer Research and Development Center. <http://www.epa.gov/region9/water/groundwater/uic-pdfs/lahaina02/lahaina-final-interim-report.pdf>.
- Green R.E., and Young, R.H., 1970. Herbicide and fertilizer in Hawaiian sugarcane soils in relation to subsurface water quality, Hawaiian Sugar Technologists.
- Guilbault, G.G. (Ed). 1990. *Practical Fluorescence*, Marcel Dekker, Inc. New York.
- Harbaugh, A.W., Banta, E.R., Hill, M.C., McDonald, M.G., 2000, MODFLOW-2000, the U.S. Geological Survey Modular Ground-Water Model—User guide to modularization concepts and the ground-water flow process.
- Harvey, R.W., 1997, Microorganisms as tracers in groundwater injection and recovery experiments: A review, *FEMS Microbiol. Rev.*, 20, 461-472.
- Hubaux, A., and Vos, C., 1970, Decision and detection limits for linear calibration curves, *Analyt. Chem.*, 42(8), 849-855.
- Hunt, C.D., Jr., 1996, Geohydrology of the Island of Oahu, Hawaii, U.S. Geological Survey Professional Paper 1412-B, 54p.
- Hunt, C.D., Jr., 2004, Ground-water quality and its relation to land use on Oahu, Hawaii, 2000-01, U.S. Geological Survey Water-Resources Investigations Report 03-4305.
- Hunt, C.D., Jr., 2007, Ground-water nutrient flux to coastal waters and numerical simulation of wastewater injection at Kihei, Maui, Hawaii: U.S. Geological Survey Scientific Investigations Report 2006-5283, 69 p.

- Hunt, C.D., Jr., and Rosa, S.N., 2009, A multitracer approach to detecting wastewater plumes from municipal injection wells in near shore marine waters at Kihei and Lahaina, Maui, Hawaii, U.S. Geological Survey Scientific Investigations Report 2009-5253, 166p.
- Izuka, S.K., and Gingerich, S.B., 1998, Estimation of the depth to the fresh-water/salt-water interface from vertical head gradients in wells in coastal and island aquifers: *Hydrogeology Journal*, v. 6, p. 365-373.
- Johnson, A. G., Glenn, C. R., Burnett, W. C., Peterson, R. N., and Lucey, P. G., 2008, Aerial infrared imaging reveals large nutrient-rich groundwater inputs to the ocean, *Geophysical Research Letters*, v. 35. DOI: 10.1029/2008GL034574.
- Karl, D.M., Bjorkman, K.M., Dore, J.E., Fujieki, L., Hebel, D.V., Houlihan, T., Letelier, R.M., and Tupas, L.M., 2001, Ecological nitrogen-to-phosphorus stoichiometry at station ALOHA, *Deep-Sea Res. II*, 48, 1529-1566.
- Kasnavia, T., Vu, D., and Sabatini, D.A., 1999, Fluorescent dye and media properties affection sorption and tracer selection, *Groundwater*, 47(3), 376-381.
- Käss, W., 1998, *Tracing Techniques in Geohydrology*, A.A. Balkema Publishers, Taylor and Francis, CRC, 581p.
- Kelly, J.L., Glenn, C.R., and Lucey, P.G., 2013, High-resolution aerial infrared mapping of groundwater discharge to the coastal zone, *Limnol. Oceanogr. Meth.*, 11, 262-277. DOI 10.4319/lom.2013.11.262.
- Kingscote Chemicals, 2010, Water Tracing Dyes FLT Yellow/Green Products— Technical Data Bulletin, downloaded from <http://www.brightdyes.com/technical/FLTGreen.html>.
- Knee, K.L., Street, J.H., Grossman, E.E., and Paytan, A., 2008, Submarine ground-water discharge and fate along the coast of Kaloko-Honokohau National Historical Park, Island of Hawai‘i, Part 2, Spatial and temporal variations in salinity, radium-isotope activity, and nutrient concentrations in coastal waters, December 2003–April 2006, USGS Scientific Investigations Report 2008–5128.
- Knochenmus, L.A., and Robinson, J.L., 1996, Descriptions of anisotropy and heterogeneity and their effect on ground-water flow and areas of contribution to public supply wells in a karst carbonate aquifer system, U.S. Geological Survey Water-Supply Paper 2475, 46p.
- Kwon, B.-D., Chung, H.-J., and Lee, H.-S., 1993, Physical properties of volcanic rocks in Chejudo, *J. Korean Earth Sci. Soc.*, 14(3), 348-357 (in Korean).
- Langenheim, V.A.M, and Clague, D.A., 1987, The Hawaiian Emperor volcanic chain, Part II, Stratigraphic framework of volcanic rocks of the Hawaiian Island, Chap. 1 of Decker, R.W., Wright, T.L., Stauffer, P.H. (eds.), *Volcanism in Hawaii*: U.S. Geological Survey Professional Paper 1350, vol. 1, p. 55-84.
- Lau, L.S., and Mink, J.F., 2006, *Hydrology of the Hawaiian Islands*, University of Hawai‘i Press, Honolulu, 274p.
- Laws, E.A., Brown, D., and Peace, C., 2004, Coastal water quality in the Kihei and Lahaina districts of the island of Maui, Hawaiian Islands. Impacts from physical habitat and groundwater seepage: implications for water quality standards, *Inter. J. Environ. Pollut.*, 22, 531-547.

- Levy, B.S., and Chamber, R.M., 1987, Bromide as a conservative tracer for soil-water studies, *Hydrol. Process.*, 1, 385-389.
- Limtiaco Consulting Group, 2005, Hawaii water reuse survey and report—Final, Prepared for State of Hawaii, Department of Land and Natural Resources, Commission on Water Resource Management, February 2005.
- MacDonald, G.A., Abbott, A.T., and Peterson, F.L., 1983, *Volcanoes in the Sea, the Geology of Hawaii*, 2nd Ed., University of Hawaii Press, Honolulu, 517p.
- Malcolm, R.L., Aiken, G.R., Thurman, E.M., and Avery, P.A., 1980, Hydrophilic organic solutes as tracers in groundwater recharge studies, in Baker, R.A. (ed.), *Contaminants and Sediments*, Butterworth-Heinemann, p. 71-88.
- Maloszewski, P., and Zuber, A., 1993, Tracer experiments in fractured rocks: Matrix diffusion and the validity of models, *Water Resour. Res.*, 29(8), 2723-2735.
- Meus, P., Käss, W., and Schnegg, P.A., 2006, Background and detection of fluorescent tracers in karst groundwater, International Congress ‘Ground Water in Mediterranean Countries, AQUAinMED, Malaga, Spain, April 24-28, 2006.
- Mink, J.F., and Lau, L.S., 1990a, Aquifer identification and classification for Oahu: Groundwater protection strategy for Hawaii, Water Resources Research Center Technical Report No. 179, University of Hawaii at Manoa.
- Mink, J.F., and Lau, L.S., 1990b, Aquifer identification and classification for Maui: Groundwater protection strategy for Hawaii, Water Resources Research Center Technical Report No. 185, University of Hawaii at Manoa.
- Mink, J.F., and Lau, L.S., 1992a, Aquifer identification and classification for Kauai: Groundwater protection strategy for Hawaii, Water Resources Research Center Technical Report No. 186, University of Hawaii at Manoa.
- Mink, J.F., and Lau, L.S., 1992b, Aquifer identification and classification for Molokai: Groundwater protection strategy for Hawaii, Water Resources Research Center Technical Report No. 187, University of Hawaii at Manoa.
- Mink, J.F., and Lau, L.S., 1993a, Aquifer identification and classification for Lanai: Groundwater protection strategy for Hawaii, Water Resources Research Center Technical Report No. 190, University of Hawaii at Manoa.
- Mink, J.F., and Lau, L.S., 1993b, Aquifer identification and classification for island of Hawaii: Groundwater protection strategy for Hawaii, Water Resources Research Center Technical Report No. 191, University of Hawaii at Manoa.
- Nichols, W.D., Shade, P.J., and Hunt, C.D., 1996, Summary of the Oahu, Hawaii, Regional aquifer-system analysis, U.S. Geological Survey Professional Paper 1412-A, 61p.
- Oberdorfer, J.A., 1983, Wastewater injection: Near-well processes and their relationship to clogging, Ph.D. Dissertation, University of Hawaii, Honolulu, HI. 194p (with appendices).
- Oberdorfer, J.A., and Peterson, F.L., 1982, Wastewater injection well problems, processes, and standards, Water Resources Research Center Technical Report No. 146, 131p.

- Oki, D.S., 2005, Numerical simulation of the effects of low-permeability valley-fill barriers and the redistribution of ground-water withdrawals in the Pearl Harbor Area, Oahu, Hawaii, U.S. Geological Survey Scientific Investigations Report 2005-5253, 111p.
- Olsen, L.D., and Tenbus, F.J., 2004, Design of a natural-gradient ground-water tracer test in freshwater tidal wetland, West Branch Canal Creek, Aberdeen Proving Ground, Maryland, U. S. Geological Survey Scientific Investigations Report 2004-5190.
- Petty, S., and Peterson, F.L., 1979, Hawaiian waste injection practices and problems, Water Resources Research Center Technical Report No. 123, 104p.
- Poiger, T., Field, J.A., Field, T.M., Siegest, H., and Giger, W., 1998, Behavior of fluorescent whitening agents during sewage treatment, *Water Res.*, 32(6), 1939-1947.
- Pollock, D.W., 1994, User's guide for MODPATH/MODPATH-PLOT, Version 3: A particle tracking post-processing package for MODFLOW, The U.S. Geological Survey finite difference ground-water flow model—Open-File Report 94-464. U.S. Geological Survey.
- Rahn, P.H., and Johnson, C.S., 2002, Effects of anisotropic transmissivity on a contaminant plume at Nemo, South Dakota, *Environ. Eng. Geosci.*, VIII(1), 11-18.
- Rotzoll, K., and El-Kadi, A.I., 2007, Estimating hydraulic conductivity from specific capacity for Hawaii aquifers, USA, *Hydrogeol. J.*, 16, 969-979.
- Sabatini, D.A., 2000, Sorption and intraparticle diffusion of fluorescent dyes with consolidated aquifer media, *Ground Water*, 38(5), 651-656.
- Scholl, M.A., Gingerich, S.B., Loope, L.L., Giambelluca, T.W., and Nullett, M.A., 2004, Quantifying the importance of fog drip to ecosystem hydrology and water resources in tropical montane cloud forests on East Maui, Hawaii, Venture Capital Project final report, July 2004.
- Schulz, H.D., 1998, Evaluation and interpretation of tracer tests, in Käss, W., *Tracing Techniques in Geohydrology*, A.A. Balkema Publishers, Taylor and Francis, CRC.
- Shade, P.J., 1996, Water budget for the Lahaina district, island of Maui, Hawaii, Water-Resources Investigations Report 96-4238, 27p.
- Shade, P.J., 1997, Water budget for the Iao area, Island of Maui, Hawaii, U.S. Geological Survey Water-Resources Investigations Report 97-4244, 29p.
- Shade, P.J., 1999, Water budget of East Maui, Hawaii, U.S. Geological Survey Water Resources Investigations Report 98-4159, 36p.
- Sherrod, D.R., Sinton, J.M., Watkins, S.E., and Brunt, K.M., 2007, Geologic map of the state of Hawaii, U.S. Geological Survey Open-File Report 2007-1089, with GIS database.
- Smart, P.L., and Laidlaw, I.M.S., 1977, An evaluation of some fluorescent dyes for water tracing, *Water Resour. Res.*, 13, 15-33.
- Smart, C.C., and Karunaratne, K.C., 2002, Characterization of fluorescence background in dye tracing, *Environ. Geol.*, 42, 492-498.

- Smith, C.M., and Smith, J.E., 2007, Algal blooms in north Kihei; an assessment of patterns and processes relating nutrient dynamics to algal abundance, Report to City and County of Maui, 65p.
- Smith, J.E., Runcie, J.W., and Smith, C.M., 2005, Characterization of a large-scale ephemeral bloom of the green alga *Cladophora sericea* on the coral reefs of West Maui, Hawaii, *Mar. Ecol. Prog. Ser.*, 302, 77-91.
- Soicher, A.J., and Peterson, F.L., 1997, Terrestrial nutrient and sediment fluxes to the coastal waters of west Maui, Hawaii, *Pac. Sci.*, 51, 221-232.
- Souza, W.R., 1981, Ground-water status report, Lahaina District, Maui, Hawaii, 1980, U.S. Geological Survey Open-File Report 81-549, 2 map sheets.
- Souza, W.R., and Voss, C.I., 1987, Analysis of an anisotropic coastal aquifer system using variable-density flow and solute transport simulation. *J. Hydrol.*, 92, 17-41.
- Stanley, N.D., Thompson, G.M., Bentley, H.W., and Stiles, G., 1980, Ground-water tracers—A short review, *Ground Water*, 18(1), 14-23.
- Stearns, H.T., and MacDonald, G.A., 1942, Geology and groundwater resources of the island of Maui, Hawaii, Hawaii (Territory) Division of Hydrography Bulletin, vol. 7, 344p.
- Stokes, T.R. and Griffiths, P., 2000, Working Paper 51—A preliminary discussion of karst inventory systems and principles (KISP) for British Columbia, British Columbia Ministry of Forest Research Program, 124 p.
- Storlazzi, C.D., and Field, M.E., 2008, Winds, waves, tides, and the resulting flow patterns and fluxes of water, sediment, and coral larvae off West Maui, Hawaii, U.S. Geological Survey Open File Report 2008-1215, 13p.
- Street, J.H., Knee, K.L., Grossman, E.E., and Paytan, A., 2008, Submarine groundwater discharge and nutrient addition to the coastal zone and coral reefs of leeward Hawaii, *Mar. Chem.*, 109, 355-376.
- Stuart, M., Dignan, C., and McClary, D., 2008, Evaluation of marine response tools: Subtidal containment and treatment system, prepared for MAF Biosecurity New Zealand, 45 p.
- Stumm, W., and Morgan, J. J., 1996, *Aquatic Chemistry*, Wiley, New York, 1022p.
- Sutton, D.J., Kabala, Z.J., Franciso, A., and Vasudevan, D., 2001, Limitations and potential of commercially available rhodamine WT as a groundwater tracer, *Water Resour. Res.*, 37(6), 1641-1656.
- Swarzenski, P.W., Storlazzi, C.D., Presto, M.K., Gibbs, A.E., Smith, C.G., Dimova, N.T., Dailer, M.L., and Logan, J.B., 2012, Nearshore morphology, benthic structure, hydrodynamics, and coastal groundwater discharge near Kahekili Beach Park, Maui, Hawaii, U.S. Geological Survey Open-File Report 2012-1166, 34p.
- TEC, 2001, Remedial investigation report—Remedial investigation for Waiakakalaua and Kipapa Fuel storage annexes at Hickam Petroleum, Oil, and Lubricants (POL) Pipeline and Facilities, Oahu, Hawaii, prepared for U.S. Air Force 15th Air Base Wing Environmental Restoration Program, 285p (with appendices).
- Tetra Tech, Inc., 1993, Preliminary assessment of possible anthropogenic nutrient sources in the Lahaina District of Maui—Final, prepared for USEPA Region 9, Hawaii Department of Health, and the County of Maui, July 1993, 116p (plus appendices).

- Tetra Tech, Inc., 1994, Effluent fate study, Lahaina wastewater reclamation facility, Maui, Hawaii, prepared for U.S. Environmental Protection Agency Region 9, 73p (plus appendices).
- Turner Designs, 1999, Model 10-AU-005-CE Fluorometer User's Manual.
- U.S.A., 2011, 40 CFR Appendix B to Part 136—Definition and procedure for the Determination of the Method Detection Limit – Revision 1.11. <http://ecfr.gpoaccess.gov/cgi/t/text/text-idx?c=ecfr&sid=8136cdb6d5784c413366cd1386e6a005&rgn=div9&view=text&node=40:22.0.1.1.0.1.7.2&idno=40>. Downloaded 5/10/2011.
- USEPA. 2011. 40 CFR Parts 144 through 147—UIC regulations, <http://ecfr.gpoaccess.gov/cgi/t/text/text-idx?c=ecfr&sid=a96a3a46e4fc893355a2f89e7d5c7a57&rgn=div5&view=text&node=40:22.0.1.1.6&idno=40>. Downloaded 4/11/2011
- Wagner, R.J., Boulger, R.W., Jr., Oblinger, C.J., and Smith, B.A., 2006, Guidelines and standard procedures for continuous water-quality monitors—Station operation, record computation, and data reporting, U.S. Geological Survey Techniques and Methods 1–D3, 51p + 8 attachments.
- West Maui Watershed Management Advisory Committee, 1977, West Maui Watershed Owner's Manual, 18p.
- Wheatcraft, S.W., 1976, Waste injection into the Hawaiian Ghyben-Herzberg Aquifer—a laboratory study using a sand-packed hydraulic model, Water Resources Research Center Technical Report No. 96, 69p (plus appendices).
- Whittier, R.B., Rotzoll, K., Dhal, S., El-Kadi, A.I., Ray, C., Chen, G. and Chang, D., 2004. Hawaii Source Water Assessment Report, Volume I, Approach Use for the Hawaii Source Water Assessments, Water Resources Research Center, University of Hawaii at Manoa
- Whittier, R.B. and El-Kadi, A.I., 2009, Human and environmental risk ranking of onsite sewage disposal systems, Final Draft, submitted to State of Hawaii, Department of Health, Safe Drinking Water Branch, Honolulu, Hawaii.
- Whittier, R.B. and El-Kadi, A.I., in preparation, Human and environmental risk ranking of onsite sewage disposal systems for the Hawaiian Islands of Kauai, Maui, Molokai, and Hawaii, prepared for the State of Hawaii, Department of Health, Honolulu, Hawaii.
- Wilson, R.D., and McKay, D.M., 1993, SF6 as a conservative tracer in saturated media with high intragranular porosity of high organic carbon content, *Ground Water*, 34, 241-249.
- Wisconsin Dept. of Natural Resources, 1996, Analytical Detection Limit Guidance & Laboratory Guide for Determining Method Detection Limits—PUBL-TS-056-96.
- Wood, P.J., and Dykes, A.P., 2002, The use of salt dilution gauging techniques: ecological considerations and insights, *Water Res.*, 36(7), 3054-3062.
- Zheng, C., and Wang, P., 1999, MT3DMS: A modular three-dimensional multispecies transport model for simulation of advection, dispersion, and chemical reactions of contaminants in groundwater systems; Documentation and user's guide, U.S. Army Corps of Engineers, Engineer Research and Development Center, 220p.

Zheng, C., 2006, MT3DMS v5.2—Supplemental user's guide, Dept. of Geological Sciences, University of Alabama, 46p.

This page is intentionally left blank.

**APPENDIX A: FIELD WATER QUALITY AND
FLUORESCENCE MEASUREMENTS OF
SUBMARINE SPRINGS AND CONTROL
LOCATIONS**

**APPENDIX FOR SECTION 2:
SUBMARINE SPRING AND MARINE CONTROL
LOCATION SAMPLING, WATER QUALITY, AND
FLUORESCENCE**

This page is intentionally left blank

Table A-1. Calibration of the handheld YSI for pH and specific conductivity.

Model: YSI Model 63 **Serial Number:** 07A1999 AA

Date	Time	Parameter (Spec. Cond. or pH)	Units	Exp. Date	Conc. or Stand.	Initial Reading	Corrected Reading	Operator's initials and remarks
7/7/2011	8:00 AM	7.00	pH	5/1/2012	pH 7.00	7.03	7.00	Temperature at 27.3°C
7/7/2011	8:00 AM	10.00	pH	3/1/2012	pH 10.00	9.99	9.99	
7/7/2011	8:00 AM	1000 µS/cm	µS/cm	5/3/2012	1000 µS/cm	1034.00	1043.00	
7/7/2011	8:00 AM	58,700 µS/cm	µS/cm	3/27/2012	58,700 µS/cm	60100.00	61500.00	
7/15/2011	8:00 AM	7.00	pH	5/1/2012	pH 7.00	7.16	7.00	Temperature at 28.3°C
7/15/2011	8:00 AM	10.00	pH	3/1/2012	pH 10.00	10.07	10.00	
7/15/2011	8:00 AM	1000 µS/cm	µS/cm	5/3/2012	1000 µS/cm	1024.00	NA	
7/15/2011	8:00 AM	58,700 µS/cm	µS/cm	3/27/2012	58,700 µS/cm	59000.00	NA	
7/31/2011	12:00 PM	7.00	pH	5/1/2012	pH 7.00	7.04	NA	
7/31/2011	12:00 PM	10.00	pH	3/1/2012	pH 10.00	10.02	NA	
8/8/2011	12:00 PM	7.00	pH	5/1/2012	pH 7.00	7.03	NA	
8/8/2011	12:00 PM	10.00	pH	3/1/2012	pH 10.00	10.01	NA	
8/18/2011	12:45 PM	7.00	pH	5/1/2012	pH 7.00	7.05	6.99	Temperature at 28.9°C
8/18/2011	12:45 PM	10.00	pH	3/1/2012	pH 10.00	9.96	10.02	
8/18/2011	12:45 PM	1000 µS/cm	µS/cm	5/3/2012	1000 µS/cm	1087.00	1086.00	
8/18/2011	12:45 PM	58,700 µS/cm	µS/cm	3/27/2012	58,700 µS/cm	63000.00	62700.00	
8/25/2011	8:15 AM	7.00	pH	5/1/2012	pH 7.00	7.14	6.99	Temperature at 25.7°C
8/25/2011	8:15 AM	10.00	pH	3/1/2012	pH 10.00	9.99	10.03	

Table A-1 Continued		Parameter (Spec. Cond. or pH)	Units	Exp. Date	Conc. or Stand.	Initial Reading	Corrected Reading	Operator's initials and remarks
Date	Time							
9/1/2011	8:00 AM	7.00	pH	5/1/2012	pH 7.00	7.03	NA	Temperature at 25.5°C
9/1/2011	8:00 AM	10.00	pH	3/1/2012	pH 10.00	10.01	NA	
9/8/2011	8:00 AM	7.00	pH	5/1/2012	pH 7.00	7.06	7.01	Temperature at 25.7°C
9/8/2011	8:00 AM	10.00	pH	3/1/2012	pH 10.00	9.95	9.99	
9/15/2011	8:00 AM	7.00	pH	5/1/2012	pH 7.00	7.02	NA	Temperature at 25.4°C
9/15/2011	8:00 AM	10.00	pH	3/1/2012	pH 10.00	10.03	NA	
9/15/2011	8:00 AM	1000 µS/cm	µS/cm	5/3/2012	1000 µS/cm	1091.00	NA	
9/15/2011	8:00 AM	58,700 µS/cm	µS/cm	3/27/2012	58,700 µS/cm	59300.00	NA	
9/22/2011	8:00 AM	7.00	pH	5/1/2012	pH 7.00	7.10	6.99	
9/22/2011	8:00 AM	10.00	pH	3/1/2012	pH 10.00	10.05	10.01	
9/29/2011	8:00 AM	7.00	pH	5/1/2012	pH 7.00	7.02	NA	
9/29/2011	8:00 AM	10.00	pH	3/1/2012	pH 10.00	10.01	NA	
10/6/2011	8:00 AM	7.00	pH	5/1/2012	pH 7.00	7.04	7.01	
10/6/2011	8:00 AM	10.00	pH	3/1/2012	pH 10.00	10.05	10.00	
10/13/2011	8:00 AM	7.00	pH	5/1/2012	pH 7.00	7.02	NA	
10/13/2011	8:00 AM	10.00	pH	3/1/2012	pH 10.00	10.01	NA	
10/20/2011	8:00 AM	7.00	pH	5/1/2012	pH 7.00	1.01	NA	Temperature at 25.6°C
10/20/2011	8:00 AM	10.00	pH	3/1/2012	pH 10.00	10.03	NA	
10/20/2011	8:00 AM	1000 µS/cm	µS/cm	5/3/2012	1000 µS/cm	1078.00	NA	
10/20/2011	8:00 AM	58,700 µS/cm	µS/cm	3/27/2012	58,700 µS/cm	58900.00	NA	
10/27/2011	8:00 AM	7.00	pH	5/1/2012	pH 7.00	7.05	7.01	

Table A-1 Continued								
Date	Time	Parameter (Spec. Cond. or pH)	Units	Exp. Date	Conc. or Stand.	Initial Reading	Corrected Reading	Operator's initials and remarks
10/27/2011	8:00 AM	10.00	pH	3/1/2012	pH 10.00	10.06	10.02	
11/3/2011	8:00 AM	7.00	pH	5/1/2012	pH 7.00	7.03	NA	
11/3/2011	8:00 AM	10.00	pH	3/1/2012	pH 10.00	10.04	NA	
11/10/2011	8:00 AM	7.00	pH	5/1/2012	pH 7.00	7.09	7.01	
11/10/2011	8:00 AM	10.00	pH	3/1/2012	pH 10.00	10.02	10.02	
11/17/2011	8:00 AM	7.00	pH	5/1/2012	pH 7.00	7.02	NA	
11/17/2011	8:00 AM	10.00	pH	3/1/2012	pH 10.00	10.01	NA	
11/28/2011	1:00 PM	7.00	pH	5/1/2012	pH 7.00	6.97	6.95	Temperature at 26.1°C
11/28/2011	1:00 PM	10.00	pH	3/1/2012	pH 10.00	10.03	10.03	
11/28/2011	1:00 PM	1000 µS/cm	µS/cm	5/3/2012	1000 µS/cm	1026.00	NA	
11/28/2011	1:00 PM	58,700 µS/cm	µS/cm	3/27/2012	58,700 µS/cm	59600.00	NA	
12/6/2011	8:00 AM	7.00	pH	5/1/2012	pH 7.00	7.02	NA	
12/6/2011	8:00 AM	10.00	pH	3/1/2012	pH 10.00	10.02	NA	
12/13/2011	8:00 AM	7.00	pH	5/1/2012	pH 7.00	7.01	NA	
12/13/2011	8:00 AM	10.00	pH	3/1/2012	pH 10.00	10.03	NA	
12/20/2011	8:00 PM	7.00	pH	5/1/2012	pH 7.00	6.99	7.01	
12/20/2011	8:00 PM	10.00	pH	3/1/2012	pH 10.00	10.04	10.02	
1/3/2012	8:00 PM	7.00	pH	5/1/2012	pH 7.00	7.02	NA	
1/3/2012	8:00 PM	10.00	pH	3/1/2012	pH 10.00	10.02	NA	
1/3/2012	8:00 PM	1000 µS/cm	µS/cm	5/3/2012	1000 µS/cm	1015	NA	Temperature at 27.6°C
1/3/2012	8:00 PM	58,700 µS/cm	µS/cm	3/27/2012	58,700 µS/cm	59800	NA	
1/10/2012	9:00 AM	7.00	pH	5/1/2012	pH 7.00	6.98	7.01	
1/10/2012	9:00 AM	10.00	pH	3/1/2012	pH 10.00	10.04	10.02	

Table A-1 Continued								
Date	Time	Parameter (Spec. Cond. or pH)	Units	Exp. Date	Conc. or Stand.	Initial Reading	Corrected Reading	Operator's initials and remarks
1/17/2012	9:00 AM	7.00	pH	5/1/2012	pH 7.00	6.99	NA	
1/17/2012	9:00 AM	10.00	pH	3/1/2012	pH 10.00	10.00	NA	
1/24/2012	8:00 PM	7.00	pH	5/1/2012	pH 7.00	7.02	7.04	Temperature at 24.4°C
1/24/2012	8:00 PM	10.00	pH	3/1/2012	pH 10.00	10.04	10.11	
1/30/2012	8:00 PM	7.00	pH	5/1/2012	pH 7.00	7.13	7.03	Temperature at 26.3°C
1/30/2012	8:00 PM	10.00	pH	3/1/2012	pH 10.00	10.15	10.06	
1/30/2012	8:00 PM	1000 µS/cm	µS/cm	5/3/2012	1000 µS/cm	1066	NA	
1/30/2012	8:00 PM	58,700 µS/cm	µS/cm	3/27/2012	58,700 µS/cm	59400	NA	
2/8/2012	8:00 PM	7.00	pH	5/1/2012	pH 7.00	7.02	NA	Temperature at 26.1°C
2/8/2012	8:00 PM	10.00	pH	3/1/2012	pH 10.00	10.01	NA	
2/14/2012	8:00 AM	7.00	pH	5/1/2012	pH 7.00	7.03	NA	Temperature at 26.1°C
2/14/2012	8:00 AM	10.00	pH	3/1/2012	pH 10.00	10.02	NA	
2/21/2012	9:00 AM	7.00	pH	5/1/2012	pH 7.00	7.02	NA	Temperature at 26.2°C
2/21/2012	9:00 AM	10.00	pH	3/1/2012	pH 10.00	10.03	NA	
2/28/2012	9:00 AM	7.00	pH	5/1/2012	pH 7.00	7.00	NA	Temperature at 25.9°C
2/28/2012	9:00 AM	10.00	pH	3/1/2012	pH 10.00	10.01	NA	
3/16/2012	9:00 AM	7.00	pH	7/6/2013	pH 7.00	7.09	6.99	Temperature at 25.8°C
3/16/2012	9:00 AM	10.00	pH	7/12/2013	pH 10.00	10.05	10.01	
3/29/2012	8:00 AM	7.00	pH	7/6/2013	pH 7.00	7.05	7.02	Temperature at 25.1°C
3/29/2012	8:00 AM	10.00	pH	7/12/2013	pH 10.00	10.09	10.00	
4/3/2012	7:30 PM	7.00	pH	7/6/2013	pH 7.00	6.37	6.89	Temperature at 28.9°C
4/3/2012	7:30 PM	10.00	pH	7/12/2013	pH 10.00	10.02	9.96	
4/15/2012	7:30 PM	7.00	pH	7/6/2013	pH 7.00	6.97	NA	Temperature at 28.3°C

Table A-1 Continued								
Date	Time	Parameter (Spec. Cond. or pH)	Units	Exp. Date	Conc. or Stand.	Initial Reading	Corrected Reading	Operator's initials and remarks
4/15/2012	7:30 PM	10.00	pH	7/12/2013	pH 10.00	10.03	NA	
5/1/2012	8:00 PM	7.00	pH	7/6/2013	pH 7.00	7.03	NA	Temperature at 26.1°C
5/1/2012	8:00 PM	10.00	pH	7/12/2013	pH 10.00	10.05	NA	
5/15/2012	9:00 AM	7.00	pH	7/6/2013	pH 7.00	7.03	6.86	Temperature at 24.9°C
5/15/2012	9:00 AM	10.00	pH	7/12/2013	pH 10.00	9.96	9.98	
6/8/2012	9:00 AM	7.00	pH	7/6/2013	pH 7.00	6.89	6.95	Temperature at 26.2°C
6/8/2012	9:00 AM	10.00	pH	7/12/2013	pH 10.00	9.86	10.02	
6/22/2012	9:30 AM	7.00	pH	7/6/2013	pH 7.00	6.86	7.01	Temperature at 25.1°C
6/22/2012	9:30 AM	10.00	pH	7/12/2013	pH 10.00	10.02	10.00	
7/1/2012	7:30 PM	7.00	pH	7/6/2013	pH 7.00	7.10	6.98	Temperature at 32.0°C
7/1/2012	7:30 PM	10.00	pH	7/12/2013	pH 10.00	9.84	10.00	
7/8/2012	6:00 PM	7.00	pH	7/6/2013	pH 7.00	6.98	NA	Temperature at 26.1°C
7/8/2012	6:00 PM	10.00	pH	7/12/2013	pH 10.00	10.01	NA	
7/16/2012	5:00 PM	7.00	pH	7/6/2013	pH 7.00	6.99	NA	Temperature at 27.1°C
7/16/2012	5:00 PM	10.00	pH	7/12/2013	pH 10.00	10.02	NA	
7/22/2012	6:10 PM	7.00	pH	7/6/2013	pH 7.00	6.99	NA	Temperature at 26.5°C
7/22/2012	6:10 PM	10.00	pH	7/12/2013	pH 10.00	10.01	NA	
8/3/2012	6:00 PM	7.00	pH	7/6/2013	pH 7.00	6.96	7.01	Temperature at 26.3°C
8/3/2012	6:00 PM	10.00	pH	7/12/2013	pH 10.00	10.03	10.02	
8/11/2012	6:00 PM	7.00	pH	7/6/2013	pH 7.00	6.99	NA	Temperature at 27.2°C
8/11/2012	6:00 PM	10.00	pH	7/12/2013	pH 10.00	10.01	NA	
8/18/2012	9:00 AM	7.00	pH	7/6/2013	pH 7.00	6.97	7.02	Temperature at 25.1°C
8/18/2012	9:00 AM	10.00	pH	7/12/2013	pH 10.00	10.04	10.02	

Table A-1 Continued		Parameter (Spec. Cond. or pH)	Units	Exp. Date	Conc. or Stand.	Initial Reading	Corrected Reading	Operator's initials and remarks
Date	Time							
8/23/2012	9:00 AM	7.00	pH	7/6/2013	pH 7.00	6.98	NA	Temperature at 24.9°C
8/23/2012	9:00 AM	10.00	pH	7/12/2013	pH 10.00	10.01	NA	
8/30/2012	9:00 AM	7.00	pH	7/6/2013	pH 7.00	6.99	NA	Temperature at 26.2°C
8/30/2012	9:00 AM	10.00	pH	7/12/2013	pH 10.00	10.02	NA	
9/3/2012	9:00 AM	7.00	pH	7/6/2013	pH 7.00	7.01	NA	Temperature at 25.2°C
9/3/2012	9:00 AM	10.00	pH	7/12/2013	pH 10.00	10.02	NA	
9/9/2012	6:00 PM	7.00	pH	7/6/2013	pH 7.00	6.96	7.01	Temperature at 26.3°C
9/9/2012	6:00 PM	10.00	pH	7/12/2013	pH 10.00	10.03	10.02	
9/11/2012	4:30 PM	7.00	pH	7/6/2013	pH 7.00	7.02	NA	Temperature at 28.8°C
9/11/2012	4:30 PM	10.00	pH	7/12/2013	pH 10.00	10.01	NA	
9/18/2012	8:00 AM	7.00	pH	7/6/2013	pH 7.00	7.01	NA	Temperature at 26.4°C
9/18/2012	8:00 AM	10.00	pH	7/12/2013	pH 10.00	10.02	NA	
9/27/2012	6:00 PM	7.00	pH	7/6/2013	pH 7.00	6.98	7.01	Temperature at 26.3°C
9/27/2012	6:00 PM	10.00	pH	7/12/2013	pH 10.00	10.00	10.02	
10/1/2012	6:00 PM	7.00	pH	7/6/2013	pH 7.00	6.99	NA	Temperature at 26.5°C
10/1/2012	6:00 PM	10.00	pH	7/12/2013	pH 10.00	9.99	NA	
10/9/2012	9:00 AM	7.00	pH	7/6/2013	pH 7.00	7.01	NA	Temperature at 27.1°C
10/9/2012	9:00 AM	10.00	pH	7/12/2013	pH 10.00	10.02	NA	
10/23/2012	9:00 AM	7.00	pH	7/6/2013	pH 7.00	6.97	7.01	Temperature at 27.2°C
10/23/2012	9:00 AM	10.00	pH	7/12/2013	pH 10.00	9.96	10.02	
10/29/2012	8:00 AM	7.00	pH	7/6/2013	pH 7.00	7.01	NA	Temperature at 26.5°C
10/29/2012	8:00 AM	10.00	pH	7/12/2013	pH 10.00	10.02	NA	
11/6/2012	9:00 AM	7.00	pH	7/6/2013	pH 7.00	7.01	NA	Temperature at 27.5°C

Table A-1 Continued								
Date	Time	Parameter (Spec. Cond. or pH)	Units	Exp. Date	Conc. or Stand.	Initial Reading	Corrected Reading	Operator's initials and remarks
11/6/2012	9:00 AM	10.00	pH	7/12/2013	pH 10.00	10.02	NA	
11/15/2012	9:00 AM	7.00	pH	7/6/2013	pH 7.00	6.98	7.01	Temperature at 27.2°C
11/15/2012	9:00 AM	10.00	pH	7/12/2013	pH 10.00	10.01	10.00	
11/26/2012	9:00 AM	7.00	pH	7/6/2013	pH 7.00	6.98	7.02	Temperature at 26.2°C
11/26/2012	9:00 AM	10.00	pH	7/12/2013	pH 10.00	9.98	10.01	
12/3/2012	9:00 AM	7.00	pH	7/6/2013	pH 7.00	7.01	NA	Temperature at 25.9°C
12/3/2012	9:00 AM	10.00	pH	7/12/2013	pH 10.00	10.02	NA	
12/13/2012	9:00 AM	7.00	pH	7/6/2013	pH 7.00			Temperature at 26.3°C
12/13/2012	9:00 AM	10.00	pH	7/12/2013	pH 10.00			
12/26/2012	9:00 AM	7.00	pH	7/6/2013	pH 7.00	6.97	7.03	Temperature at 26.1°C
12/26/2012	9:00 AM	10.00	pH	7/12/2013	pH 10.00	10.02	10.03	

Table A-2. Calibration record of the hand held fluorometer. Calibration Solutions: 100 ppb standards of Fluorescein and Rhodamine. NA = Not Applicable.

Model: Aquafluor

Serial Number: 801398

Date	Time	Conc. of Stand. (ppb)	Initial Reading (ppb)	Corrected Reading (ppb)	Fluorescein or Rhodamine
8/2/2011	9:30 PM	100	97.44	99.84	Fluorescein
8/2/2011	9:30 PM	100	86.13	100.1	Rhodamine
8/4/2011	2:15 PM	100	100.70	NA	Fluorescein
8/4/2011	2:15 PM	100	103.30	99.8	Rhodamine
8/8/2011	1:00 PM	100	101.20	NA	Fluorescein
8/8/2011	1:00 PM	100	103.70	99.91	Rhodamine
8/10/2011	9:05 PM	100	99.48	NA	Fluorescein
8/10/2011	9:05 PM	100	96.31	100.1	Rhodamine
8/14/2011	11:00 AM	100	101.90	99.66	Fluorescein
8/14/2011	11:00 AM	100	107.30	99.99	Rhodamine
8/15/2011	9:00 PM	100	98.58	99.72	Fluorescein
8/15/2011	9:00 PM	100	96.46	100.1	Rhodamine
8/16/2011	10:32 PM	100	100.60	NA	Fluorescein
8/16/2011	10:32 PM	100	99.45	NA	Rhodamine
8/22/2011	9:30 AM	100	101.40	99.95	Fluorescein
8/22/2011	9:30 AM	100	102.40	100	Rhodamine
8/27/2011	12:30 PM	100	98.74	99.97	Fluorescein
8/27/2011	12:30 PM	100	97.56	99.84	Rhodamine
8/28/2011	12:00 PM	100	99.77	NA	Fluorescein
8/28/2011	12:00 PM	100	99.51	NA	Rhodamine
8/29/2011	1:30 PM	100	100.20	NA	Fluorescein
8/29/2011	1:30 PM	100	100.10	NA	Rhodamine
8/29/2011	9:30 AM	100	101.60	99.93	Fluorescein
8/29/2011	9:30 AM	100	103.40	99.87	Rhodamine
9/13/2011	8:00 PM	100	98.88	99.97	Fluorescein
9/13/2011	8:00 PM	100	97.57	99.95	Rhodamine

Table A-2 Continued					
Date	Time	Conc. of Stand. (ppb)	Initial Reading (ppb)	Corrected Reading (ppb)	Fluorescein or Rhodamine
9/19/2011	8:00 PM	100	99.69	NA	Fluorescein
9/19/2011	8:00 PM	100	99.10	NA	Rhodamine
10/3/2011	1:30 PM	100	99.66	NA	Fluorescein
10/3/2011	1:30 PM	100	99.42	NA	Rhodamine
10/7/2011	10:00 AM	100	101.50	99.91	Fluorescein
10/7/2011	10:00 AM	100	105.50	99.7	Rhodamine
10/12/2011	8:00 PM	100	98.71	99.65	Fluorescein
10/12/2011	8:00 PM	100	96.62	99.99	Rhodamine
10/20/2011	8:00 PM	100	101.90	99.85	Fluorescein
10/20/2011	8:00 PM	100	102.70	99.88	Rhodamine
10/28/2011	1:00 PM	100	101.90	99.67	Fluorescein
10/28/2011	1:00 PM	100	105.60	100	Rhodamine
11/4/2011	10:00 AM	100	101.10	99.81	Fluorescein
11/4/2011	10:00 AM	100	104.50	99.97	Rhodamine
11/14/2011	1:00 PM	100	99.05	NA	Fluorescein
11/14/2011	1:00 PM	100	96.31	99.9	Rhodamine
11/18/2011	1:00 PM	100	99.26	NA	Fluorescein
11/18/2011	1:00 PM	100	101.50	100	Rhodamine
11/21/2011	7:00 PM	100	97.66	99.61	Fluorescein
11/21/2011	7:00 PM	100	92.77	99.99	Rhodamine
11/24/2011	12:00 PM	100	103.70	99.65	Fluorescein
11/24/2011	12:00 PM	100	118.10	99.82	Rhodamine
11/26/2011	12:00 PM	100	99.05	NA	Fluorescein
11/26/2011	12:00 PM	100	97.43	99.9	Rhodamine
12/2/2011	1:00 PM	100	98.82	99.81	Fluorescein
12/2/2011	1:00 PM	100	98.35	99.81	Rhodamine
12/11/2011	6:00 PM	100	100.30	NA	Fluorescein
12/11/2011	6:00 PM	100	103.50	99.95	Rhodamine
12/16/2011	8:00 PM	100	100.40	NA	Fluorescein
12/16/2011	8:00 PM	100	102.30	99.94	Rhodamine
1/13/2011	8:00 PM	100	86.09	99.69	Fluorescein

Table A-2 Continued					
Date	Time	Conc. of Stand. (ppb)	Initial Reading (ppb)	Corrected Reading (ppb)	Fluorescein or Rhodamine
1/13/2011	8:00 PM	100	94.45	99.92	Rhodamine
1/26/2012	8:00 PM	100	98.05	99.75	Fluorescein
1/26/2012	8:00 PM	100	99.29	NA	Rhodamine
1/27/2012	7:30 PM	100	99.79	NA	Fluorescein
1/27/2012	7:30 PM	100	100.60	NA	Rhodamine
2/10/2012	8:00 PM	100	97.48	99.9	Fluorescein
2/10/2012	8:00 PM	100	99.93	99.93	Rhodamine
2/17/2012	5:00 PM	100	100.10	NA	Fluorescein
2/17/2012	5:00 PM	100	103.40	99.8	Rhodamine
2/21/2012	9:00 AM	100	101.70	99.82	Fluorescein
2/21/2012	9:00 AM	100	102.80	99.78	Rhodamine
3/2/2012	1:00 PM	100	97.49	99.79	Fluorescein
3/2/2012	1:00 PM	100	94.69	99.85	Rhodamine
3/13/2012	8:00 PM	100	101.00	99.73	Fluorescein
3/13/2012	8:00 PM	100	103.40	99.97	Rhodamine
3/22/2012	7:00 PM	100	97.47	100.3	Fluorescein
3/22/2012	7:00 PM	100	98.12	99.83	Rhodamine
3/29/2012	7:00 PM	100	101.20	99.62	Fluorescein
3/29/2012	7:00 PM	100	103.50	99.85	Rhodamine
4/2/2012	5:30 PM	100	95.76	99.82	Fluorescein
4/2/2012	5:30 PM	100	88.10	99.8	Rhodamine
4/14/2012	11:00 AM	100	104.30	100.1	Fluorescein
4/14/2012	11:00 AM	100	117.60	100.3	Rhodamine
4/20/2012	5:00 PM	100	102.50	100.6	Fluorescein
4/20/2012	5:00 PM	100	108.80	99.59	Rhodamine
5/3/2012	5:00 PM	100	96.02	99.92	Fluorescein
5/3/2012	5:00 PM	100	95.79	100.1	Rhodamine
6/5/2012	11:00 AM	100	91.77	100.10	Fluorescein
6/5/2012	11:00 AM	100	91.59	99.83	Rhodamine
6/7/2012	7:00 PM	100	98.74	99.93	Fluorescein
6/7/2012	7:00 PM	100	100.30	NA	Rhodamine

Table A-2 Continued					
Date	Time	Conc. of Stand. (ppb)	Initial Reading (ppb)	Corrected Reading (ppb)	Fluorescein or Rhodamine
6/22/2012	11:00 AM	100	101.80	99.90	Fluorescein
6/22/2012	11:00 AM	100	100.00	NA	Rhodamine
7/6/2012	2:00 PM	100	99.42	NA	Fluorescein
7/6/2012	2:00 PM	100	97.98	99.00	Rhodamine
8/20/2012	1:00 PM	100	90.89	99.77	Fluorescein
8/20/2012	1:00 PM	100	72.49	99.79	Rhodamine
9/10/2012	4:30 PM	100	98.45	99.68	Fluorescein
9/10/2012	4:30 PM	100	97.80	99.79	Rhodamine
9/22/2012	9:00 AM	100	96.43	99.83	Fluorescein
9/22/2012	9:00 AM	100	93.18	99.81	Rhodamine
10/3/2012	10:30 AM	100	104.70	99.71	Fluorescein
10/3/2012	10:30 AM	100	115.40	99.78	Rhodamine
10/11/2012	10:00 AM	100	102.10	99.67	Fluorescein
10/11/2012	10:00 AM	100	108.90	99.97	Rhodamine
10/16/2012	9:00 AM	100	100.60	NA	Fluorescein
10/16/2012	9:00 AM	100	106.70	99.63	Rhodamine
10/23/2012	3:00 PM	100	98.76	99.74	Fluorescein
10/23/2012	3:00 PM	100	86.59	99.68	Rhodamine
11/13/2012	9:00 AM	100	100.30	NA	Fluorescein
11/13/2012	9:00 AM	100	111.10	99.79	Rhodamine
12/12/2012	9:00 AM	100	103.20	99.73	Fluorescein
12/12/2012	9:00 AM	100	115.20	99.67	Rhodamine
12/29/2012	4:00 PM	100	97.69	99.75	Fluorescein
12/29/2012	4:00 PM	100	94.09	99.80	Rhodamine

Table A-3. Water quality parameters collected from submarine spring samples in the South Seep Group (Seeps 3, 4, 5, and 11). Parameters were measured with a handheld YSI Model 63 and field fluorescence measurements of S-Rhodamine-B (SRB) and Fluorescein (FLT) with a handheld Aquafluor fluorometer model 8000-10 from 7/19/2011 to 12/29/2012. Missing fluorescence values are due to shipment of samples prior to analysis.

Location	Date	Time	Temp. (°C)	pH	Spec. Cond. (mS/cm)	Salinity	SRB (ppb)	FLT (ppb)
Seep 3	7/19/2011	10:15 AM	27.2	7.41	5.51	2.8	-0.174	-0.174
	7/20/2011	10:38 AM	27.1	7.36	5.45	2.8	0.725	0.109
	7/21/2011	9:05 AM	25.9	7.36	5.32	2.8	-0.235	0.321
	7/22/2011	10:42 AM	28.3	7.42	5.60	2.8	0.185	0.321
	7/23/2011	10:26 AM	27.8	7.50	6.48	3.3	0.115	0.105
	7/24/2011	10:10 AM	26.4	7.54	6.65	3.5	-0.111	0.012
	7/25/2011	10:47 AM	27.5	7.51	5.64	2.9	0.451	0.269
	7/26/2011	10:12 AM	26.4	7.44	5.45	2.8	0.717	0.077
	7/27/2011	10:55 AM	27.1	7.35	5.31	3.0	0.333	0.050
	7/28/2011	10:16 AM	27.6	7.38	5.50	2.8	-0.099	-0.154
	7/28/2011	4:34 PM	27.0	7.37	5.54	2.9	-0.015	-0.059
	7/29/2011	10:25 AM	26.6	7.40	5.31	2.8	0.302	0.107
	7/29/2011	4:29 PM	28.3	7.45	6.88	3.6	-0.044	0.056
	7/30/2011	11:38 AM	27.8	7.43	5.75	2.9	0.617	0.031
	7/30/2011	5:15 PM	26.8	7.44	5.63	2.9	0.565	-0.002
	7/31/2011	10:51 AM	27.5	7.46	5.49	2.8	0.545	0.031
	7/31/2011	4:52 PM	26.8	7.48	14.91	8.3	1.176	0.022
	8/1/2011	10:49 AM	27.8	7.46	5.51	2.8	0.863	0.224
	8/1/2011	4:21 PM	27.8	7.51	20.73	11.6	0.682	-0.056
	8/2/2011	9:04 AM	25.6	7.49	5.20	2.8	-0.223	-0.174
	8/2/2011	4:12 PM	26.8	7.42	5.41	2.8	0.649	-0.013
	8/3/2011	10:28 AM	30.7	7.30	5.56	2.7	0.414	-0.100
	8/3/2011	4:38 PM	28.6	7.35	5.53	2.8	0.138	0.000
	8/4/2011	11:17 AM	29.9	7.42	5.55	2.8	-0.400	-0.189
	8/4/2011	4:48 PM	27.5	7.47	5.40	2.8	-0.116	-0.097
	8/5/2011	11:07 AM	27.9	7.50	5.50	2.8	0.480	0.096
	8/5/2011	5:17 PM	26.7	7.49	5.41	2.8	-0.527	-0.132
	8/6/2011	9:37 AM	27.1	7.31	5.46	2.8	-0.327	0.052
	8/6/2011	4:01 PM	30.0	7.36	5.70	2.8	-0.303	0.016
	8/7/2011	10:03 AM	26.7	7.44	5.38	2.8	-0.269	-0.040
	8/7/2011	4:18 PM	28.1	7.40	5.52	2.8	-0.062	-0.048
	8/8/2011	10:15 AM	27.8	7.47	6.09	3.1	-0.204	-0.194
	8/8/2011	4:12 PM	29.4	7.44	5.66	2.8	0.512	-0.081
	8/9/2011	10:05 AM	28.2	7.52	5.58	2.8	0.868	-0.030
	8/9/2011	4:02 PM	28.8	7.45	5.63	2.8	0.271	0.121
	8/10/2011	12:29 PM	29.2	7.56	6.47	3.2	-0.040	-0.084

Table A-3 Cont. Location	Date	Time	Temp. (°C)	pH	Spec. Cond. (mS/cm)	Salinity	SRB (ppb)	FLT (ppb)
Seep 3 Cont.	8/10/2011	4:38 PM	28.3	7.60	5.60	2.8	0.076	-0.078
	8/11/2011	10:04 AM	27.9	7.76	5.53	2.8	-0.490	0.284
	8/11/2011	4:27 PM	28.9	7.64	6.75	3.4	-0.834	0.088
	8/12/2011	10:02 AM	26.6	7.64	5.31	2.8	0.359	0.227
	8/12/2011	4:21 PM	29.5	7.61	6.75	3.3	-0.300	0.183
	8/13/2011	9:55 AM	27.0	7.55	5.43	2.8	-0.311	0.351
	8/13/2011	4:02 PM	29.9	7.50	6.43	3.1	0.545	0.346
	8/14/2011	10:26 AM	27.6	7.58	5.50	2.8	0.571	0.296
	8/14/2011	4:23 PM	25.9	7.59	6.34	3.4	0.176	0.402
	8/15/2011	9:56 AM	25.9	7.55	5.29	2.8	0.250	0.201
	8/15/2011	4:08 PM	27.9	7.58	6.68	3.4	0.086	0.294
	8/16/2011	10:22 AM	27.8	7.59	5.52	2.8	-0.014	0.193
	8/16/2011	3:55 PM	28.3	7.55	5.85	2.5	1.065	0.211
	8/17/2011	11:15 AM	29.1	7.61	5.67	2.8	0.822	0.210
	8/17/2011	4:39 PM	28.4	7.58	6.76	3.4	-0.285	0.365
	8/18/2011	10:35 AM	29.9	7.53	5.73	2.8	0.074	0.177
	8/18/2011	4:41 PM	26.7	7.46	5.93	3.1	0.200	0.294
	8/19/2011	10:33 AM	30.1	7.54	6.02	3.0	0.209	0.282
	8/19/2011	4:43 PM	29.2	7.49	5.74	2.8	0.695	0.087
	8/20/2011	10:31 AM	29.5	7.56	6.14	3.0	0.155	0.034
	8/20/2011	4:32 PM	26.6	7.59	5.41	2.8	-0.236	0.228
	8/21/2011	10:34 AM	27.7	7.55	6.07	3.1	-0.151	0.118
	8/21/2011	4:41 PM	28.0	7.54	5.55	2.8	0.812	0.134
	8/22/2011	4:39 PM	29.1	7.53	8.17	4.2	0.636	0.314
	8/22/2011	10:01 AM	28.1	7.57	12.25	6.6	0.172	0.246
	8/23/2011	10:07 AM	30.0	7.54	13.31	6.9	-0.285	0.184
	8/23/2011	4:02 PM	28.2	7.44	7.99	4.1	0.203	0.086
	8/24/2011	11:20 AM	28.4	7.71	28.18	16.1	0.440	0.141
	8/24/2011	5:46 PM	28.0	7.56	5.56	2.9	0.188	0.067
	8/25/2011	10:55 AM	29.8	7.62	5.88	2.9	0.497	0.091
	8/25/2011	5:23 PM	27.6	7.71	5.59	2.9	0.230	0.093
	8/26/2011	10:15 AM	29.0	7.80	5.83	2.9	0.329	-0.035
	8/26/2011	4:24 PM	28.2	7.71	5.82	3.0	0.328	0.338
	8/27/2011	10:51 AM	28.8	7.49	5.72	2.9	0.349	0.092
	8/27/2011	5:29 PM	27.7	7.49	5.70	2.9	0.147	0.375
	8/28/2011	10:17 AM	28.6	7.57	5.65	2.8	0.155	0.033
	8/28/2011	4:36 PM	28.2	7.79	6.00	3.0	0.239	0.269
	8/29/2011	10:32 AM	28.0	7.32	5.64	2.9	0.230	0.326
	8/29/2011	4:37 PM	28.8	7.36	8.47	4.4	0.420	0.082
	8/30/2011	10:10 AM	28.4	7.45	6.19	3.1	0.791	0.185
9/2/2011	12:17 PM	32.2	7.64	5.86	2.7	-0.345	0.480	

Table A-3 Cont. Location	Date	Time	Temp. (°C)	pH	Spec. Cond. (mS/cm)	Salinity	SRB (ppb)	FLT (ppb)
Seep 3 Cont.	9/2/2011	5:00 PM	28.8	7.61	5.57	2.8	-0.606	0.160
	9/3/2011	10:35 AM	27.4	7.79	5.49	2.8	-0.424	0.501
	9/3/2011	4:47 PM	27.7	7.90	5.51	2.8	-0.320	0.302
	9/4/2011	4:48 PM	30.2	7.39	5.73	2.8	-0.175	0.364
	9/5/2011	10:18 AM	29.9	7.46	5.77	2.8	-0.248	0.303
	9/5/2011	4:41 PM	26.8	7.49	5.39	2.8	-0.340	0.387
	9/6/2011	10:04 AM	27.1	7.27	5.49	2.8	-0.415	0.182
	9/6/2011	4:30 PM	30.8	7.48	5.73	2.7	-0.471	0.310
	9/7/2011	10:02 AM	29.3	7.49	6.09	3.0	-0.383	0.264
	9/8/2011	10:09 AM	29.1	7.40	5.63	2.8	-0.741	0.339
	9/9/2011	11:23 AM	30.6	7.45	5.79	2.8	-0.694	0.184
	9/10/2011	11:36 AM	30.4	7.41	5.59	3.0	-0.666	0.219
	9/12/2011	12:39 PM	32.3	7.44	5.83	2.7	0.316	0.462
	9/13/2011	11:52 AM	33.3	7.55	6.05	2.8	-0.130	0.241
	9/14/2011	10:49 AM	32.1	7.53	7.02	3.3	-0.466	0.282
	9/15/2011	10:27 AM	33.2	7.77	6.19	2.8	0.289	0.253
	9/16/2011	12:20 PM	34.9	7.63	6.49	2.9	-0.291	0.147
	9/17/2011	3:37 PM	31.5	7.41	6.92	3.3	-0.384	0.345
	9/18/2011	12:19 PM	31.3	7.39	6.09	2.9	-0.836	0.223
	9/19/2011	11:20 AM	32.6	7.39	17.08	8.5	-0.584	0.199
	9/20/2011	10:30 AM	28.9	7.43	9.83	5.1	0.026	0.235
	9/21/2011	10:08 AM	30.6	7.37	7.49	3.6	-0.302	0.412
	9/22/2011	10:19 AM	29.4	7.94	6.54	3.3	-0.219	0.365
	9/23/2011	10:23 AM	31.1	7.49	6.81	3.2	-0.079	0.391
	9/24/2011	9:55 AM	30.3	7.56	6.58	3.2	0.624	0.324
	9/25/2011	11:24 AM	31.3	7.48	6.70	3.2	-0.308	0.395
	9/26/2011	11:39 AM	32.6	7.57	15.18	7.5	0.331	0.411
	9/27/2011	10:14 AM	30.8	7.46	5.71	2.7	-0.117	0.153
	9/28/2011	10:07 AM	29.2	7.40	5.56	2.8	-0.971	0.283
	9/29/2011	10:14 AM	29.0	7.41	5.56	2.8	-0.589	0.092
	9/30/2011	10:25 AM	30.3	7.43	5.64	2.7	-0.404	0.251
	10/1/2011	10:38 AM	32.9	7.75	5.95	2.7	0.272	0.116
	10/2/2011	1:13 PM	33.8	7.50	6.56	3.0	0.193	0.100
	10/3/2011	10:16 AM	28.4	7.48	5.66	2.9	0.072	0.131
	10/8/2011	5:12 PM	27.8	7.64	5.49	2.8	0.610	0.356
	10/10/2011	12:28 PM	33.6	7.59	6.84	2.8	-0.430	0.403
	10/12/2011	10:07 AM	29.5	7.56	5.53	2.7	-0.243	0.489
	10/14/2011	10:15 AM	30.5	7.55	5.56	2.7	0.338	0.297
	10/16/2011	10:06 AM	31.1	7.55	5.72	2.7	1.344	0.243
	10/18/2011	12:47 PM	31.9	7.60	5.98	2.8	0.547	0.202
10/20/2011	10:33 AM	29.9	7.63	5.71	2.8	1.019	0.207	

Table A-3 Cont. Location	Date	Time	Temp. (°C)	pH	Spec. Cond. (mS/cm)	Salinity	SRB (ppb)	FLT (ppb)
Seep 3 Cont.	10/22/2011	10:39 AM	30.9	7.67	5.72	2.7	0.176	0.167
	10/24/2011	10:18 AM	32.7	7.49	5.90	2.7	0.435	0.317
	10/26/2011	10:28 AM	31.0	7.50	5.82	2.8	-0.353	0.046
	10/28/2011	10:19 AM	27.7	7.62	5.56	2.8	0.658	0.101
	10/30/2011	12:27 PM	32.7	7.65	6.16	2.9	-0.460	0.271
	11/1/2011	12:26 PM	33.3	7.61	6.14	2.8	-0.150	0.283
	11/3/2011	10:21 AM	29.9	7.57	5.79	2.8	-0.257	0.413
	11/5/2011	2:29 PM	33.4	7.56	6.16	2.8	-0.334	0.239
	11/7/2011	10:10 AM	31.0	7.60	5.85	2.8	-0.177	0.523
	11/9/2011	10:54 AM	29.2	7.52	5.68	2.8	0.120	0.307
	11/11/2011	10:44 AM	27.2	7.62	5.51	2.8	-0.180	0.234
	11/14/2011	9:47 AM	29.2	7.22	5.59	2.8	0.418	0.581
	11/16/2011	10:39 AM	28.7	7.27	5.67	2.8	0.725	0.218
	11/18/2011	10:59 AM	28.1	7.36	5.68	2.9	0.723	0.426
	11/21/2011	10:42 AM	30.3	7.44	5.87	2.8	0.223	-0.102
	11/23/2011	10:25 AM	29.3	7.54	5.66	2.8	-0.117	0.127
	11/25/2011	10:47 AM	27.9	7.40	5.60	2.8	-0.170	0.200
	11/28/2011	10:35 AM	29.1	7.60	5.65	2.8	0.443	0.237
	11/30/2011	10:18 AM	27.6	7.45	5.48	2.8	0.285	0.351
	12/2/2011	10:21 AM	27.8	7.45	5.52	2.8	-0.038	0.392
	12/5/2011	10:35 AM	27.7	7.50	5.54	2.9	0.222	0.730
	12/7/2011	10:34 AM	29.0	7.50	5.59	2.8	0.579	0.653
	12/9/2011	10:15 AM	25.4	7.63	5.34	2.8	0.307	0.756
	12/12/2011	10:16 AM	24.6	7.65	5.59	3.0	0.137	1.010
	12/14/2011	10:10 AM	25.7	7.41	5.72	2.9	-0.173	1.237
	12/16/2011	10:16 AM	27.7	7.52	5.62	2.9	0.105	1.468
	12/19/2011	10:26 AM	26.7	7.47	5.65	2.9		
	12/21/2011	11:23 AM	28.3	7.43	5.88	3.0		
	12/23/2011	10:56 AM	24.2	7.63	5.42	3.0		
	12/26/2011	10:57 AM	27.3	7.39	5.66	2.9		
	12/28/2011	10:34 AM	27.7	7.52	6.03	3.1		
	12/30/2011	11:13 AM	28.9	7.65	7.33	3.7		
	1/2/2012	11:37 AM	29.1	7.68	14.89	8.0		
	1/7/2012	3:51 PM	28.5	7.55	5.88	3.0	1.145	5.392
	1/9/2012	12:34 PM	27.8	7.40	5.84	3.0	1.041	6.102
	1/11/2012	11:35 AM	24.9	7.44	5.38	2.9	0.997	6.739
	1/16/2012	2:04 PM	28.4	7.67	5.67	2.8		
	1/19/2012	10:52 AM	28.1	7.52	5.60	2.8	0.896	9.339
	1/21/2012	2:37 PM	28.7	7.52	6.58	3.3	1.080	10.19
	1/23/2012	12:15 PM	26.5	7.49	5.49	2.9	1.556	10.96
1/25/2012	12:38 PM	28.3	7.51	5.75	2.9	1.069	11.74	

Table A-3 Cont. Location	Date	Time	Temp. (°C)	pH	Spec. Cond. (mS/cm)	Salinity	SRB (ppb)	FLT (ppb)
Seep 3 Cont.	1/27/2012	1:26 PM	29.0	7.74	5.81	2.9	1.140	11.57
	1/31/2012	12:25 PM	27.4	7.60	5.66	2.9	1.332	13.98
	2/10/2012	12:56 PM	27.4	7.64	6.08	3.1	1.453	17.53
	2/14/2012	2:22 PM	28.7	7.58	5.97	3.0	1.771	19.87
	2/17/2012	12:32 PM	26.2	7.65	6.04	3.2	2.455	20.14
	2/20/2012	2:40 PM	29.6	7.59	6.83	3.4	1.759	20.98
	2/24/2012	12:05 PM	27.7	7.64	8.18	4.3	1.336	21.30
	2/27/2012	11:33 PM	28.2	7.66	7.29	3.8	1.677	23.10
	3/1/2012	12:34 PM	29.4	7.56	5.94	2.9	2.197	25.11
	3/11/2012	11:59 AM	29.9	7.65	6.26	3.0	2.551	28.16
	3/14/2012	11:05 AM	24.5	7.66	5.56	3.0		
	3/17/2012	10:24 AM	26.0	7.60	5.65	3.0	3.340	32.14
	3/19/2012	10:40 AM	27.4	7.61	5.87	3.0	3.074	32.81
	3/22/2012	10:50 AM	27.5	7.49	6.24	3.2	3.131	32.00
	3/27/2012	10:30 AM	25.5	7.55	5.73	3.1	2.571	33.77
	3/29/2012	11:19 AM	25.6	7.43	5.84	3.1	3.255	34.56
	3/31/2012	4:39 PM	27.4		5.96	3.1	3.897	35.22
	4/2/2012	11:14 AM	26.8		6.11	3.2	3.562	35.16
	4/5/2012	9:25 AM	25.1	7.35	5.72	3.1	2.788	35.95
	4/12/2012	9:34 AM	28.2	7.46	6.03	3.1	3.218	36.51
	4/16/2012	10:42 AM	29.7	7.51	6.14	3.0	2.620	34.33
	4/19/2012	12:18 PM	27.6	7.58	6.15	3.2	2.803	35.55
	4/24/2012	4:08 PM	26.9	7.65	8.27	4.4	3.369	37.27
	4/26/2012	11:40 AM	28.4	7.66	6.34	3.2	3.816	36.81
	5/2/2012	11:44 AM	28.7	7.52	6.61	3.3	4.525	37.20
	5/7/2012	10:51 AM	27.9	7.45	6.23	3.2	3.838	39.35
	5/14/2012	10:14 AM	27.0	7.60	8.35	4.5	3.736	39.51
	5/18/2012	2:24 PM	30.9	7.67	8.66	4.3	3.759	34.73
	5/22/2012	4:07 PM	27.9	7.54	9.94	5.3	4.294	37.80
	5/25/2012	3:45 PM	29.0	7.47	6.59	3.3	3.945	38.69
	6/4/2012	3:00 PM	28.2	7.73	19.95	11.1	3.462	31.93
	6/7/2012	1:20 PM	29.4	7.47	6.56	3.2	3.281	36.51
	6/12/2012	12:27 PM	32.2	7.50	6.95	3.3	3.056	34.33
	6/14/2012	3:37 PM	33.4	7.53	6.94	3.2	3.167	35.62
	6/16/2012	1:02 PM	32.3	7.38	7.09	3.4	3.472	34.66
	6/18/2012	11:00 AM	29.8	7.56	6.93	3.4	3.470	35.45
6/29/2012	1:23 PM	33.6	7.51	7.00	3.2	2.787	32.61	
7/4/2012	1:21 PM	29.6	7.59	6.61	3.3	3.024	31.53	
7/11/2012	2:35 PM	35.1	7.57	7.26	3.3			
7/19/2012	11:40 PM	33.3	7.60	7.11	3.3			
7/23/2012	10:50 AM	31.9	7.63	6.75	3.2	1.917	25.41	

Table A-3 Cont. Location	Date	Time	Temp. (°C)	pH	Spec. Cond. (mS/cm)	Salinity	SRB (ppb)	FLT (ppb)
Seep 3 Cont.	8/1/2012	10:35 AM	31.7	7.60	6.81	3.2	2.489	23.62
	8/7/2012	10:25 AM	33.6	7.50	7.12	3.3	2.123	22.88
	8/15/2012	11:32 AM	31.8	7.53	6.87	3.2	1.659	21.34
	8/21/2012	10:28 AM	31.4	7.42	6.76	3.2	3.488	22.08
	8/24/2012	12:33 PM	31.7	7.60	6.76	3.2	2.524	22.13
	8/27/2012	10:38 AM	29.7	7.52	6.60	3.3	2.794	21.98
	9/5/2012	10:46 AM	32.6	7.44	6.88	3.3	2.708	19.93
	9/10/2012	1:45 PM	33.3	7.59	7.07	3.3	2.079	19.52
	9/12/2012	10:33 AM	32.2	7.45	7.01	3.3	2.065	19.09
	9/18/2012	12:36 PM	32.3	7.40	6.82	3.2	2.368	18.97
	10/2/2012	12:17 PM	29.5	7.50	6.53	3.2	2.060	17.29
	10/8/2012	3:39 PM	29.9	7.44	6.55	3.2	1.433	17.43
	10/12/2012	11:54 PM	30.3	7.43	6.60	3.2	1.560	16.97
	10/18/2012	12:24 PM	28.6	7.52	6.49	3.3	0.847	16.75
	10/22/2012	10:56 AM	29.9	7.55	6.73	3.3	0.561	15.93
	10/26/2012	11:32 AM	29.5	7.51	6.63	3.3	1.251	16.23
	10/29/2012	12:00 PM	28.5	7.48	6.50	3.3	1.707	15.89
	11/2/2012	3:40 PM	30.6	7.57	8.94	4.4	1.315	14.47
	11/8/2012	12:44 PM	29.3	7.55	6.49	3.2	1.228	14.79
	11/12/2012	11:51 AM	27.9	7.49	6.32	3.3	0.958	14.65
11/27/2012	10:04 AM	27.0	7.57	6.30	3.3	1.138	13.56	
12/6/2012	11:47 AM	29.1	7.49	7.25	3.7	1.377	13.08	
12/10/2012	10:58 AM	28.8	7.50	6.28	3.2	1.133	13.03	
12/14/2012	1:01 PM	29.3	7.49	7.03	3.5	1.189	12.500	
12/29/2012	11:55 AM	27.7	7.40	7.35	3.8	1.764	11.720	
Seep 4	7/19/2011	10:25 AM	27.8	7.47	6.09	3.1	0.983	0.110
	7/20/2011	10:53 AM	27.9	7.50	6.16	3.1	0.709	0.375
	7/21/2011	9:15 AM	25.9	7.20	5.97	3.2	0.328	0.170
	7/22/2011	10:52 AM	27.6	7.35	6.27	3.2	-0.121	0.185
	7/23/2011	10:31 AM	27.1	7.47	6.10	3.2	0.022	0.232
	7/24/2011	10:20 AM	26.3	7.53	6.61	3.6	1.025	0.151
	7/25/2011	10:48 AM	26.5	7.54	8.45	4.5	-0.056	-0.171
	7/26/2011	10:26 AM	26.4	7.47	6.26	3.4	0.024	0.033
	7/27/2011	11:04 AM	26.7	7.48	6.05	3.2	-0.256	0.077
	7/28/2011	10:25 AM	27.0	7.47	6.16	3.2	0.330	0.100
	7/28/2011	5:01 PM	26.8	7.33	6.43	3.4	0.221	-0.193
	7/29/2011	10:34 AM	26.6	7.38	6.00	3.1	1.056	-0.054
	7/29/2011	4:36 PM	28.0	7.46	9.26	4.8	0.549	-0.052
	7/30/2011	11:44 AM	28.0	7.42	6.27	3.2	-0.291	-0.113
	7/30/2011	6:26 PM	27.0	7.43	7.42	3.9	-0.115	-0.107

Table A-3 Cont. Location	Date	Time	Temp. (°C)	pH	Spec. Cond. (mS/cm)	Salinity	SRB (ppb)	FLT (ppb)
Seep 4 Cont.	7/31/2011	11:01 AM	27.7	7.43	6.25	3.2	1.021	-0.060
	7/31/2011	5:08 PM	27.4	7.57	22.25	12.7	-0.114	0.091
	8/1/2011	10:49 AM	28.5	7.44	6.82	3.5	0.584	0.086
	8/1/2011	4:32 PM	27.8	7.49	8.24	4.3	0.914	-0.055
	8/2/2011	9:13 AM	26.3	7.48	5.80	3.1	0.474	0.064
	8/2/2011	4:20 PM	27.0	7.38	5.94	3.1	-0.007	0.022
	8/3/2011	10:38 AM	27.4	7.36	6.03	3.1	0.600	-0.126
	8/3/2011	4:48 PM	27.0	7.36	6.29	3.3	0.035	-0.190
	8/4/2011	11:23 AM	27.3	7.43	5.97	3.1	-0.102	0.199
	8/4/2011	4:55 PM	27.1	7.42	6.20	3.2	0.799	-0.073
	8/5/2011	11:15 AM	27.6	7.46	6.11	3.1	0.482	0.173
	8/5/2011	5:25 PM	26.4	7.55	5.94	3.1	-0.137	-0.092
	8/6/2011	9:49 AM	26.4	7.42	5.96	3.1	0.740	-0.012
	8/6/2011	4:10 PM	29.1	7.41	6.21	3.1	0.151	-0.031
	8/7/2011	10:13 AM	26.3	7.36	6.03	3.1	-0.384	-0.187
	8/7/2011	4:25 PM	27.4	7.41	6.07	3.1	-0.058	-0.144
	8/8/2011	10:25 AM	28.4	7.44	6.32	2.8	0.152	-0.043
	8/8/2011	4:22 PM	29.0	7.36	6.29	3.1	0.561	-0.129
	8/9/2011	10:18 AM	27.5	7.47	6.17	3.2	0.260	-0.095
	8/9/2011	4:10 PM	28.1	7.42	6.40	3.2	-0.034	-0.056
	8/10/2011	12:40 PM	28.3	7.58	7.77	4.0	-0.027	-0.156
	8/10/2011	4:48 PM	27.9	7.52	6.18	3.2	-0.459	-0.232
	8/11/2011	10:08 AM	27.4	7.67	6.06	3.1	0.733	0.104
	8/11/2011	4:33 PM	28.7	7.66	6.25	3.2	-0.212	0.402
	8/12/2011	10:09 AM	26.7	7.63	5.95	3.1	0.080	0.105
	8/12/2011	4:29 PM	28.9	7.51	8.62	4.4	0.094	0.155
	8/13/2011	10:07 AM	27.5	7.51	6.06	3.1	0.410	0.328
	8/13/2011	4:08 PM	28.2	7.47	9.36	4.9	-0.523	0.004
	8/14/2011	10:37 AM	27.2	7.46	6.02	3.1	0.576	0.358
	8/14/2011	4:30 PM	26.2	7.40	6.96	3.7	0.611	0.311
	8/15/2011	10:04 AM	25.9	7.46	5.88	3.1	0.334	0.185
	8/15/2011	4:16 PM	27.3	7.47	7.12	3.7	0.289	1.335
	8/16/2011	10:30 AM	28.0	7.51	6.07	3.1	0.612	0.330
	8/16/2011	4:03 PM	27.8	7.55	6.20	3.2	0.098	0.182
8/17/2011	11:27 AM	29.5	7.47	6.18	3.1	-0.049	0.317	
8/17/2011	4:47 PM	28.5	7.45	6.56	3.3	0.861	0.201	
8/18/2011	11:02 AM	29.1	7.50	6.23	3.1	-0.185	0.144	
8/18/2011	4:51 PM	27.5	7.37	6.06	3.1	-0.080	0.821	
8/19/2011	10:45 AM	29.0	7.52	6.19	3.1	-0.288	0.200	
8/19/2011	4:51 PM	28.9	7.52	6.16	3.1			
8/20/2011	10:40 AM	28.9	7.57	6.20	3.1	0.628	0.322	

Table A-3 Cont. Location	Date	Time	Temp. (°C)	pH	Spec. Cond. (mS/cm)	Salinity	SRB (ppb)	FLT (ppb)
Seep 4 Cont.	8/20/2011	4:39 PM	26.6	7.55	5.92	3.1	0.110	0.165
	8/21/2011	10:44 AM	27.7	7.48	6.05	3.1	0.232	0.191
	8/21/2011	4:55 PM	27.9	7.51	6.10	3.1	0.370	0.582
	8/22/2011	10:12 AM	27.7	7.51	9.62	5.4	0.020	0.304
	8/22/2011	4:48 PM	28.6	7.57	6.51	3.5	0.824	0.345
	8/23/2011	10:25 AM	28.0	7.66	8.49	4.4	-0.332	-0.019
	8/23/2011	4:08 PM	28.3	7.48	7.05	3.9	0.009	0.103
	8/24/2011	11:38 AM	27.5	7.58	9.25	4.9	-0.070	0.081
	8/24/2011	5:58 PM	27.6	7.50	6.06	3.1	-0.130	0.052
	8/25/2011	11:05 AM	27.7	7.63	6.99	3.6	0.477	0.100
	8/25/2011	5:35 PM	27.1	7.57	6.02	3.1	0.571	0.541
	8/26/2011	10:24 AM	27.6	7.55	6.93	3.6	0.330	0.162
	8/26/2011	4:33 PM	27.9	7.57	7.10	3.7	0.361	0.372
	8/27/2011	11:02 AM	28.5	7.65	6.33	3.2	0.773	0.029
	8/27/2011	5:41 PM	27.5	7.58	6.06	3.1	0.233	0.371
	8/28/2011	10:22 AM	28.1	7.57	6.13	3.1	0.030	0.038
	8/28/2011	4:44 PM	29.9	7.56	6.11	3.0	0.283	0.119
	8/29/2011	10:42 AM	28.4	7.59	6.21	3.1	0.045	0.095
	8/29/2011	4:41 PM	27.7	7.51	10.40	5.6	0.623	0.388
	9/2/2011	11:53 AM	32.4	7.60	7.63	3.6	0.401	0.151
	9/2/2011	5:14 PM	28.1	7.55	6.94	3.6	0.160	0.335
	9/3/2011	10:44 AM	26.9	7.74	6.25	3.3	-0.168	0.404
	9/4/2011	5:00 PM	29.7	7.47	6.30	3.1	-0.176	0.600
	9/5/2011	10:28 AM	31.0	7.46	7.71	3.8	-0.201	0.247
	9/5/2011	4:50 PM	26.8	7.48	5.99	3.1	-0.536	0.604
	9/6/2011	10:13 AM	28.1	7.35	6.55	3.0	-0.306	0.567
	9/6/2011	4:40 PM	31.0	7.50	6.25	3.0	-0.472	0.253
	9/7/2011	10:10 AM	29.9	7.49	6.83	3.4	-0.464	0.485
	9/8/2011	10:18 AM	29.1	7.47	7.38	3.7	-0.348	0.404
	9/9/2011	11:36 AM	29.4	7.47	9.28	4.7	-0.718	0.337
	9/10/2011	11:52 AM	30.9	7.50	10.99	5.5	-0.880	0.161
	9/12/2011	12:55 PM	29.2	7.48	8.41	4.3	-0.397	0.575
	9/13/2011	12:07 PM	32.9	7.55	10.55	5.0	-0.295	0.262
	9/14/2011	11:03 AM	31.9	7.51	6.91	3.3	0.312	0.122
	9/15/2011	10:45 AM	33.5	7.85	7.08	3.4	-0.590	0.091
	9/16/2011	12:31 PM	34.6	7.55	9.05	4.1	-0.273	0.388
	9/17/2011	3:50 PM	31.5	7.49	10.30	5.1	0.288	0.358
	9/18/2011	12:35 PM	33.9	7.48	7.17	3.3	0.209	0.163
	9/19/2011	11:36 AM	32.3	7.55	13.17	6.5	-0.590	0.070
	9/20/2011	10:41 AM	29.0	7.47	9.92	5.1	-0.414	0.167
	9/21/2011	10:18 AM	31.1	7.51	9.87	4.9	-0.724	0.188

Table A-3 Cont. Location	Date	Time	Temp. (°C)	pH	Spec. Cond. (mS/cm)	Salinity	SRB (ppb)	FLT (ppb)
Seep 4 Cont.	9/23/2011	10:34 AM	30.1	7.47	9.23	4.6	-0.129	0.297
	9/24/2011	10:05 AM	30.5	7.48	7.61	3.7	-0.326	0.262
	9/25/2011	11:40 AM	31.2	7.41	12.99	6.4	-0.496	0.227
	9/26/2011	11:53 AM	31.6	7.45	9.54	4.7	-0.027	0.445
	9/27/2011	10:25 AM	29.7	7.42	6.21	3.1	-0.183	0.076
	9/28/2011	10:18 AM	29.8	7.43	6.07	3.0		
	9/29/2011	10:31 AM	30.8	7.47	6.18	3.0	-0.842	0.251
	9/30/2011	10:36 AM	30.9	7.44	6.21	3.0	-0.505	0.135
	10/1/2011	10:51 AM	32.5	7.69	6.48	3.0	-0.164	-0.026
	10/2/2011	1:27 PM	32.1	7.40	6.44	3.0	0.645	-0.003
	10/3/2011	10:28 AM	31.4	7.43	6.74	3.2	-0.033	0.003
	10/8/2011	5:27 PM	27.2	7.40	5.71	3.1	-0.040	0.540
	10/10/2011	12:37 PM	32.7	7.47	6.51	3.0	-0.047	0.273
	10/12/2011	10:20 AM	30.4	7.46	6.05	2.9	-0.356	0.500
	10/14/2011	10:26 AM	31.0	7.43	6.36	3.0	0.576	0.190
	10/16/2011	10:19 AM	30.9	7.52	7.06	3.4	0.443	0.189
	10/18/2011	12:59 PM	32.2	7.47	6.56	3.1	0.460	0.328
	10/20/2011	10:44 AM	30.5	7.41	9.23	4.6	0.466	0.219
	10/22/2011	10:16 AM	31.9	7.57	6.89	3.3	0.174	0.236
	10/24/2011	10:29 AM	31.3	7.51	6.60	3.2	-0.334	0.130
	10/26/2011	10:39 AM	30.7	7.42	6.34	3.0	-0.106	0.307
	10/28/2011	10:30 AM	29.7	7.48	6.33	3.1	-0.059	0.169
	10/30/2011	12:55 PM	34.3	7.47	6.95	3.2	-0.245	0.285
	11/1/2011	12:37 PM	32.4	7.46	8.52	3.3	-0.598	0.225
	11/3/2011	10:35 AM	31.0	7.45	9.98	5.0	-0.115	0.298
	11/5/2011	2:58 PM	33.2	7.45	6.85	3.2	0.506	0.317
	11/7/2011	10:20 AM	31.9	7.49	6.37	3.0	-0.457	0.347
	11/9/2011	11:19 AM	30.7	7.43	6.32	3.0	0.008	0.319
	11/11/2011	10:55 AM	27.8	7.46	6.81	3.5	-0.339	0.271
	11/14/2011	9:58 AM	29.0	7.26	6.16	3.1	-0.064	0.517
	11/16/2011	10:57 AM	28.9	7.36	6.25	3.1	0.365	0.375
	11/18/2011	11:16 AM	27.5	7.32	6.14	3.2	0.313	0.443
	11/21/2011	10:53 AM	30.0	7.43	6.74	3.3	0.351	0.095
	11/23/2011	10:36 AM	29.0	7.45	6.75	3.4	0.028	0.197
	11/25/2011	10:57 AM	28.2	7.35	6.10	3.1	0.376	0.240
	11/28/2011	10:48 AM	28.7	7.37	7.38	3.7	0.836	0.082
	11/30/2011	10:29 AM	27.3	7.33	6.14	3.2	-0.043	0.044
	12/2/2011	10:34 AM	27.9	7.33	6.78	3.5	0.847	0.260
	12/5/2011	10:46 AM	27.7	7.33	6.11	3.1	0.255	0.476
	12/7/2011	10:45 AM	29.1	7.34	6.38	3.2	0.379	0.362
12/9/2011	10:25 AM	26.8	7.42	5.95	3.1	0.353	0.485	

Table A-3 Cont. Location	Date	Time	Temp. (°C)	pH	Spec. Cond. (mS/cm)	Salinity	SRB (ppb)	FLT (ppb)
Seep 4 Cont.	12/12/2011	10:29 AM	25.8	7.53	8.02	4.4	-0.282	0.897
	12/14/2011	10:22 AM	27.5	7.33	6.24	3.2	-0.011	0.877
	12/16/2011	10:25 AM	28.0	7.33	6.73	3.4	-0.048	1.143
	12/19/2011	10:37 AM	27.4	7.42	6.10	3.1		
	12/21/2011	11:38 AM	28.2	7.26	6.26	3.2		
	12/23/2011	11:06 AM	24.5	7.43	5.82	3.2		
	12/26/2011	11:17 AM	28.3	7.38	6.35	3.2		
	12/28/2011	10:53 AM	25.8	7.42	6.63	3.6		
	12/30/2011	11:33 AM	30.6	7.54	8.17	4.0		
	1/2/2012	11:50 AM	29.0	7.60	19.18	10.5		
	1/7/2012	4:05 PM	28.3	7.48	6.17	3.1	0.760	4.38
	1/9/2012	12:02 PM	28.3	7.32	6.72	3.5	1.058	4.87
	1/11/2012	11:48 AM	24.9	7.30	5.63	3.1	1.140	5.76
	1/13/2012	12:23 PM	25.8	7.45	6.07	3.2	1.297	6.23
	1/16/2012	2:16 PM	27.5	7.40	5.90	3.0		
	1/19/2012	11:18 AM	28.1	7.35	6.04	3.1	1.064	7.83
	1/21/2012	2:51 PM	28.5	7.34	5.99	3.0	1.216	8.99
	1/23/2012	1:26 PM	25.9	7.60	5.81	3.1	1.202	9.57
	1/25/2012	1:39 PM	28.6	7.39	6.14	3.1	1.643	10.03
	1/27/2012	1:49 PM	30.5	7.90	6.42	3.1	0.767	6.00
	1/31/2012	12:39 PM	27.9	7.48	6.11	3.1	1.122	11.62
	2/10/2012	1:16 PM	27.2	7.81	10.46	5.7	1.074	13.32
	2/14/2012	2:38 PM	27.5	7.67	12.30	6.7	1.423	13.70
	2/17/2012	12:47 PM	25.9	7.67	15.82	9.0	2.097	14.28
	2/20/2012	3:00 PM	28.6	7.67	24.16	13.6	0.540	10.83
	2/24/2012	12:20 PM	28.0	7.80	34.57	20.2	0.160	8.08
	2/27/2012	12:13 PM	29.6	7.88	37.70	21.6	0.138	7.46
	3/1/2012	12:50 PM	29.5	7.58	8.16	4.2	1.513	19.69
	3/11/2012	12:23 PM	29.5	7.74	15.40	8.2	2.371	19.53
	3/14/2012	11:17 AM	24.7	7.69	16.57	9.8		
	3/17/2012	10:47 AM	25.9	7.70	26.18	15.8	1.170	15.51
	3/19/2012	10:55 AM	26.9	7.86	36.94	22.5	1.072	10.08
	3/22/2012	11:08 AM	26.4	7.75	30.78	18.6	1.017	13.49
	3/27/2012	11:03 AM	26.5	7.75	28.87	17.3	0.400	14.81
	3/29/2012	11:36 AM	26.6	7.70	28.91	17.4	0.447	13.79
	3/31/2012	4:53 PM	26.3		28.67	17.3	2.033	15.23
	4/2/2012	11:33 AM	27.4		36.30	21.8	1.175	11.56
	4/5/2012	9:40 AM	25.7	7.70	28.56	17.3	1.565	15.79
	4/12/2012	9:50 AM	26.5	7.51	24.15	14.1	2.119	18.87
	4/16/2012	11:12 AM	28.2	7.67	29.52	17.1	1.021	15.82

Table A-3 Cont. Location	Date	Time	Temp. (°C)	pH	Spec. Cond. (mS/cm)	Salinity	SRB (ppb)	FLT (ppb)
Seep 5	7/19/2011	10:35 AM	26.7	7.54	5.29	3.1	0.667	0.159
	7/20/2011	11:03 AM	27.8	7.57	6.02	3.0	0.108	0.086
	7/21/2011	9:25 AM	25.5	7.35	5.78	3.1	0.227	0.312
	7/22/2011	11:03 AM	27.2	7.67	5.66	3.1	0.099	0.215
	7/23/2011	10:44 AM	27.1	7.52	5.88	3.0	-0.168	0.006
	7/24/2011	10:30 AM	26.2	7.55	5.79	3.1	-0.346	0.217
	7/25/2011	10:51 AM	27.2	7.56	5.91	3.1	0.423	0.165
	7/26/2011	10:22 AM	26.2	7.52	5.77	3.0	-0.044	-0.002
	7/27/2011	11:12 AM	26.6	7.53	5.81	3.0	0.055	-0.006
	7/28/2011	10:36 AM	27.6	7.47	5.97	3.1	-0.252	0.078
	7/28/2011	4:59 PM	26.4	7.33	5.78	3.0	-0.067	-0.062
	7/29/2011	10:40 AM	27.2	7.33	5.84	3.0	0.084	0.040
	7/29/2011	4:51 PM	27.8	7.46	5.98	3.1	0.779	0.102
	7/30/2011	11:53 AM	27.0	7.43	5.90	3.1	0.240	-0.021
	7/30/2011	5:33 PM	27.1	7.44	5.93	3.1	0.682	-0.039
	7/31/2011	11:09 AM	27.4	7.42	5.95	3.1	0.374	0.029
	7/31/2011	5:19 PM	26.6	7.46	6.52	3.4	0.856	0.068
	8/1/2011	4:40 PM	26.6	7.40	6.17	3.3	-0.110	-0.124
	8/2/2011	9:20 AM	26.0	7.49	5.71	3.0	0.113	-0.077
	8/2/2011	4:27 PM	27.3	7.40	5.90	3.0	-0.201	0.015
	8/3/2011	10:44 AM	28.0	7.41	5.94	3.0	-0.345	0.105
	8/3/2011	4:55 PM	26.5	7.32	5.85	3.1	0.546	-0.110
	8/4/2011	11:30 AM	27.5	7.44	5.62	3.0	0.077	-0.122
	8/4/2011	5:02 PM	28.1	7.46	5.64	3.0	0.453	0.062
	8/5/2011	11:21 AM	27.5	7.49	5.91	3.0	-0.415	-0.023
	8/5/2011	5:31 PM	26.4	7.48	5.76	3.0	0.567	-0.110
	8/6/2011	9:44 AM	26.4	7.42	5.83	3.1	0.269	-0.060
	8/6/2011	4:15 PM	28.8	7.41	6.09	3.0	0.076	0.003
	8/7/2011	10:25 AM	26.9	7.42	5.91	3.1	0.140	-0.123
	8/7/2011	4:33 PM	27.0	7.40	5.88	3.1	-0.121	0.062
	8/8/2011	10:32 AM	28.2	7.43	6.09	3.1	0.353	0.008
	8/8/2011	4:33 PM	28.9	7.40	6.10	3.1	-0.238	-0.213
	8/9/2011	10:25 AM	27.2	7.51	5.98	3.1	0.673	0.005
	8/9/2011	4:17 PM	27.9	7.46	6.03	3.1	0.729	0.164
	8/10/2011	1:00 PM	27.7	7.60	6.05	3.1	0.024	0.329
	8/10/2011	4:54 PM	27.5	7.53	6.00	3.1	-0.084	-0.095
	8/11/2011	10:13 AM	27.6	7.68	6.00	3.1	0.067	0.338
	8/11/2011	4:40 PM	28.4	7.74	6.07	3.1	-0.405	0.201
	8/12/2011	10:16 AM	27.1	7.65	5.90	3.1	-0.196	0.185
	8/12/2011	4:36 PM	28.4	7.62	6.09	3.1	-0.360	0.244
8/13/2011	10:15 AM	27.2	7.54	5.93	3.1	0.555	0.438	

Table A-3 Cont. Location	Date	Time	Temp. (°C)	pH	Spec. Cond. (mS/cm)	Salinity	SRB (ppb)	FLT (ppb)
Seep 5 Cont.	8/13/2011	4:16 PM	27.9	7.55	5.74	3.1	-0.180	0.315
	8/14/2011	10:45 AM	27.0	7.52	5.91	3.1	0.475	0.649
	8/14/2011	4:36 PM	26.1	7.40	5.86	3.1	0.194	0.404
	8/15/2011	10:11 AM	25.6	7.44	5.74	3.1	0.936	0.258
	8/15/2011	4:24 PM	27.1	7.48	5.96	3.1	0.284	0.275
	8/16/2011	10:37 AM	27.9	7.57	5.97	3.0	0.432	0.380
	8/16/2011	4:10 PM	27.3	7.57	5.96	3.1	-0.167	0.239
	8/17/2011	11:21 AM	28.8	7.48	6.07	3.0	0.064	0.202
	8/17/2011	4:54 PM	28.4	7.45	6.05	3.1	-0.132	0.152
	8/18/2011	10:54 AM	28.6	7.50	6.05	3.0	-0.175	0.226
	8/18/2011	5:01 PM	27.7	7.43	5.97	3.1	0.357	0.266
	8/19/2011	10:53 AM	28.4	7.56	6.03	3.1	0.634	0.178
	8/19/2011	4:59 PM	28.5	7.53	6.06	3.1	-0.026	0.058
	8/20/2011	10:46 AM	29.3	7.56	6.12	3.0	-0.102	0.608
	8/20/2011	4:46 PM	26.6	7.53	5.84	3.1	-0.007	0.439
	8/21/2011	10:51 AM	27.9	7.48	5.97	3.0	0.130	0.259
	8/21/2011	5:03 PM	27.4	7.53	5.93	3.1	0.402	0.306
	8/22/2011	10:21 AM	27.6	7.57	6.00	3.1	0.156	0.072
	8/22/2011	4:54 PM	28.6	7.63	6.07	3.1	0.015	0.352
	8/23/2011	10:32 AM	28.1	7.63	6.03	3.1	-0.031	0.024
	8/23/2011	4:14 PM	28.8	7.51	6.09	3.1	-0.223	0.399
	8/24/2011	11:46 AM	27.2	7.63	5.91	3.0	0.036	0.399
	8/24/2011	6:06 PM	27.4	7.53	5.94	3.1	0.737	0.186
	8/25/2011	11:15 AM	27.2	7.61	5.95	3.1	0.528	0.119
	8/25/2011	5:45 PM	26.8	7.58	5.90	3.1	1.180	0.155
	8/26/2011	10:32 AM	27.6	7.55	6.01	3.1	0.776	0.124
	8/26/2011	4:41 PM	27.6	7.58	6.04	3.1	1.173	0.048
	8/27/2011	11:11 AM	29.2	7.66	6.10	3.0	0.662	0.541
	8/27/2011	5:51 PM	27.0	7.58	5.90	3.0	0.365	0.141
	8/28/2011	10:30 AM	27.7	7.59	5.99	3.1	0.357	0.403
	8/28/2011	4:54 PM	27.8	7.63	6.01	3.1	0.200	0.090
	8/29/2011	10:51 AM	27.3	7.63	5.90	3.0	0.487	0.106
	8/29/2011	4:49 PM	28.0	7.53	6.09	3.1	0.231	0.195
	9/2/2011	12:07 PM	31.9	7.55	6.34	3.0	-0.412	0.148
	9/2/2011	5:27 PM	28.0	7.54	5.98	3.0	0.106	0.225
	9/3/2011	10:52 AM	27.0	7.70	5.85	3.0	-0.511	0.176
	9/4/2011	5:12 PM	29.6	7.48	6.19	3.1	0.189	0.393
	9/5/2011	10:37 AM	28.2	7.55	6.05	3.1	0.258	0.623
	9/5/2011	4:58 PM	26.6	7.47	5.81	3.0	-0.125	0.306
	9/6/2011	10:21 AM	28.5	7.48	6.08	3.1	0.053	0.536
9/6/2011	4:49 PM	30.2	7.51	6.19	3.0	0.112	0.572	

Table A-3 Cont. Location	Date	Time	Temp. (°C)	pH	Spec. Cond. (mS/cm)	Salinity	SRB (ppb)	FLT (ppb)
Seep 5 Cont.	9/7/2011	10:18 AM	29.7	7.48	6.18	3.0	-0.390	0.221
	9/8/2011	10:26 AM	29.4	7.49	6.16	3.1	-0.345	0.678
	9/9/2011	11:47 AM	29.8	7.50	6.22	3.0	-0.239	0.155
	9/10/2011	12:00 PM	30.8	7.51	6.40	3.1	-0.550	0.444
	9/12/2011	1:05 PM	30.8	7.46	6.31	3.0	-0.240	0.175
	9/13/2011	12:18 PM	33.5	7.56	10.43	5.0	-0.366	0.198
	9/14/2011	11:13 AM	31.9	7.49	6.91	3.3	-0.266	0.174
	9/15/2011	11:00 AM	33.4	7.85	6.99	3.2	-0.348	0.313
	9/16/2011	12:41 PM	34.9	7.50	9.01	4.1	-0.501	0.288
	9/17/2011	4:03 PM	31.2	7.49	11.04	5.5	-0.070	0.422
	9/18/2011	12:49 PM	34.1	7.50	7.06	3.2	-0.086	0.127
	9/19/2011	11:49 AM	32.2	7.53	12.59	6.2	-0.435	0.252
	9/20/2011	10:50 AM	29.2	7.50	7.00	3.5	0.061	0.283
	9/21/2011	10:27 AM	30.0	7.52	6.84	3.4	-0.652	0.384
	9/23/2011	10:43 AM	28.2	7.49	6.76	3.5	-0.383	0.214
	9/24/2011	9:45 AM	28.3	7.64	6.40	3.2	0.040	0.233
	9/25/2011	11:54 AM	31.9	7.43	9.64	4.7	-0.227	0.407
	9/26/2011	12:00 PM	32.1	7.51	7.43	3.6	-0.408	0.247
	9/27/2011	10:36 AM	31.0	7.44	6.19	3.0		
	9/28/2011	10:26 AM	30.8	7.42	6.23	3.0	-0.478	0.057
	9/29/2011	10:46 AM	30.8	7.43	6.18	3.0	-0.672	0.189
	9/30/2011	10:45 AM	29.7	7.44	6.08	3.0	-0.705	0.287
	10/1/2011	11:02 AM	33.4	7.64	6.59	3.0	-0.130	0.283
	10/2/2011	1:48 PM	32.9	7.42	6.52	3.0	0.274	0.052
	10/3/2011	10:38 AM	30.4	7.51	6.35	3.1	0.157	0.117
	10/10/2011	12:47 PM	33.1	7.49	6.53	3.0	-0.506	0.377
	10/12/2011	10:31 AM	30.5	7.51	6.08	2.9	0.330	0.269
	10/14/2011	10:36 AM	30.1	7.51	6.46	3.1	1.103	0.244
	10/16/2011	10:29 AM	31.4	7.49	6.85	3.0	0.647	0.213
	10/18/2011	1:11 PM	31.3	7.45	6.27	3.0	0.913	0.265
	10/20/2011	10:52 AM	31.4	7.49	6.26	3.0	0.693	0.191
	10/22/2011	10:26 AM	30.9	7.54	6.25	3.0	0.099	0.219
	10/24/2011	10:40 AM	29.8	7.49	6.19	3.0	-0.140	0.143
	10/26/2011	10:51 AM	30.8	7.44	6.33	3.1	-0.419	0.153
	10/28/2011	10:44 AM	27.9	7.47	6.02	3.1	-0.110	0.077
	10/30/2011	12:41 PM	34.0	7.47	6.79	3.1	0.430	0.429
	11/1/2011	12:49 PM	29.1	7.45	6.25	3.1	-0.208	0.349
	11/3/2011	10:49 AM	31.3	7.45	6.48	3.1	0.355	0.241
	11/5/2011	2:44 PM	32.8	7.49	6.66	3.1	-0.045	0.228
	11/7/2011	10:33 AM	32.0	7.50	6.43	3.0	-0.023	0.227
11/9/2011	11:33 AM	30.4	7.47	6.33	3.1	-0.124	0.374	

Table A-3 Cont. Location	Date	Time	Temp. (°C)	pH	Spec. Cond. (mS/cm)	Salinity	SRB (ppb)	FLT (ppb)
Seep 5 Cont.	11/11/2011	11:04 AM	28.1	7.52	6.12	3.1	0.413	0.375
	11/14/2011	10:08 AM	29.1	7.34	6.12	3.0	-0.334	0.206
	11/16/2011	11:09 AM	30.0	7.37	6.28	3.1	0.466	0.595
	11/16/2011	11:09 AM	30.0	7.37	6.28	3.1	0.932	0.363
	11/18/2011	11:29 AM	28.2	7.33	6.17	3.1	0.932	0.363
	11/21/2011	11:05 AM	30.8	7.46	6.39	3.1	0.370	-0.161
	11/23/2011	10:47 AM	29.8	7.45	6.25	3.1	-0.264	0.018
	11/25/2011	11:27 AM	28.2	7.36	6.11	3.1	-0.159	0.138
	11/28/2011	10:58 AM	29.8	7.39	6.23	3.1	0.043	0.180
	11/30/2011	10:40 AM	27.3	7.36	6.15	3.2	0.288	0.069
	12/2/2011	10:43 AM	27.1	7.33	6.50	3.4	1.048	0.345
	12/5/2011	11:03 AM	27.7	7.42	6.79	3.5	0.232	0.331
	12/7/2011	10:56 AM	29.2	7.36	8.28	4.2	-0.054	0.343
	12/9/2011	10:35 AM	27.8	7.41	7.02	3.7	-0.004	0.482
	12/12/2011	10:41 AM	25.8	7.49	6.80	3.7	0.678	0.675
	12/14/2011	10:32 AM	26.1	7.34	8.09	4.4	0.247	1.027
	12/16/2011	10:34 AM	28.3	7.33	7.42	3.8	0.473	0.852
	12/19/2011	10:46 AM	27.3	7.44	7.77	4.1		
	12/21/2011	11:48 AM	28.3	7.39	8.15	4.2		
	12/26/2011	11:08 AM	27.6	7.41	9.14	4.8		
	12/28/2011	10:45 AM	26.9	7.41	13.80	7.6		
	12/30/2011	11:24 AM	29.5	7.69	17.01	9.1		
	1/2/2012	12:05 PM	28.9	7.49	27.82	15.6		
	1/7/2012	4:15 PM	27.9	7.33	28.12	16.4	0.686	2.85
	1/9/2012	12:20 PM	29.1	7.65	32.31	18.4	0.898	1.766
	1/11/2012	12:00 PM	24.9	7.54	34.75	21.8	1.456	2.007
	1/13/2012	12:33 PM	28.0	7.50	31.39	18.3	0.907	2.88
	1/16/2012	2:28 PM	27.9	7.46	32.51	19.1		
	1/19/2012	11:31 AM	28.5	7.54	19.09	10.4	0.620	6.26
	1/21/2012	3:03 PM	27.8	7.53	23.17	13.2	0.672	6.08
	1/23/2012	1:36 PM	26.2	7.51	32.25	19.7	0.882	4.74
	1/25/2012	2:16 PM	28.1	7.35	29.88	17.3	0.970	5.19
	1/27/2012	2:24 PM	26.5	7.57	24.80	14.6	1.110	7.05
	1/31/2012	12:51 PM	27.4	7.90	30.70	18.1	0.660	5.52
	2/10/2012	1:30 PM	26.6	7.82	13.03	7.2	0.822	13.22
	2/14/2012	3:13 PM	28.7	7.62	13.88	7.4	1.631	13.90
	2/17/2012	1:00 PM	26.6	7.65	13.57	7.6	1.614	14.84
	2/20/2012	3:14 PM	28.6	7.72	10.52	5.5	0.896	13.52
	2/24/2012	12:36 PM	27.0	7.81	14.24	8.0	1.215	15.87
	2/27/2012	12:24 PM	27.6	7.68	15.12	8.3	0.922	17.18
3/1/2012	1:04 PM	29.0	7.58	19.08	10.3	1.260	16.02	

Table A-3 Cont. Location	Date	Time	Temp. (°C)	pH	Spec. Cond. (mS/cm)	Salinity	SRB (ppb)	FLT (ppb)
Seep 5 Cont.	3/11/2012	12:38 PM	29.3	7.72	11.47	6.0	2.576	23.13
	3/14/2012	11:30 AM	26.8	7.67	13.25	7.4		-0.65
	3/17/2012	10:57 AM	25.0	7.80	15.36	8.9	1.984	23.17
	3/19/2012	11:05 AM	26.7	7.74	19.75	11.4	2.247	20.93
	3/22/2012	11:20 AM	26.6	7.80	25.48	15.0	1.573	18.48
	3/27/2012	11:17 AM	26.7	7.51	18.34	10.4	1.149	23.18
	3/29/2012	11:49 AM	26.7	7.65	21.90	12.2	1.487	22.65
	4/2/2012	11:44 AM	27.0		21.49	12.4	2.276	23.01
	4/5/2012	9:52 AM	25.0	7.63	16.73	9.8	2.606	26.91
	4/12/2012	10:22 AM	26.2	7.45	15.05	8.5	2.375	27.24
	4/16/2012	11:25 AM	28.8	7.51	13.72	7.3	2.028	28.56
	4/19/2012	12:34 PM	27.5	7.63	16.07	8.9	1.941	25.85
	4/24/2012	4:21 PM	26.5	7.80	20.18	11.7	2.223	24.82
	4/26/2012	11:54 AM	28.9	7.59	16.22	8.8	2.420	28.10
	5/2/2012	12:01 PM	28.0	7.59	19.72	11.0	2.575	25.90
	5/7/2012	11:22 AM	28.3	7.63	16.52	9.0	3.197	28.85
	5/14/2012	10:40 AM	27.2	7.63	16.03	8.9	2.493	29.07
	5/25/2012	3:57 PM	27.6	7.50	19.91	11.3	3.540	28.03
	5/29/2012	3:13 PM	29.3	7.70	24.16	13.4	2.987	25.70
	6/4/2012	3:29 PM	28.0	7.70	14.33	7.8	2.690	27.26
	6/7/2012	1:35 PM	29.1	7.43	7.44	3.8	2.792	29.22
	6/12/2012	12:44 PM	31.3	7.45	7.92	3.8	2.605	30.35
	6/14/2012	3:54 PM	31.9	7.50	8.22	4.0	2.755	30.54
	6/16/2012	1:18 PM	30.3	7.30	8.43	4.2	2.528	30.52
	6/18/2012	11:51 AM	28.9	7.58	22.60	12.5	2.396	25.29
	6/29/2012	1:49 PM	32.4	7.41	9.46	4.5	2.098	27.16
	7/11/2012	2:50 PM	33.8	7.59	7.54	3.7		
	7/19/2012	11:55 AM	33.4	7.59	7.26	3.4		
	7/23/2012	11:23 AM	31.9	7.63	7.51	3.6	2.166	23.09
	8/1/2012	11:05 AM	29.7	7.57	7.31	3.6	1.929	21.91
	8/7/2012	10:40 AM	32.6	7.52	7.79	3.7	1.608	20.41
	8/15/2012	11:49 AM	30.3	7.51	7.53	3.7	1.814	20.31
	8/21/2012	11:00 AM	33.0	7.49	7.81	3.7	2.383	20.16
	8/24/2012	12:50 PM	32.2	7.55	11.01	5.4	2.703	18.62
	8/27/2012	11:00 AM	29.4	7.56	7.41	3.7	2.393	19.23
	9/5/2012	11:10 AM	32.5	7.48	7.97	3.7	2.736	18.47
	9/10/2012	2:05 PM	33.2	7.62	8.21	3.9	2.213	18.38
	9/12/2012	11:06 AM	33.4	7.42	7.94	3.7	2.358	17.89
	9/18/2012	1:10 PM	32.5	7.42	7.46	3.5	2.333	18.08
	10/2/2012	12:33 PM	28.7	7.56	7.15	3.7	1.727	17.94
10/8/2012	3:12 PM	29.1	7.47	7.44	3.7	0.928	16.33	

Table A-3 Cont. Location	Date	Time	Temp. (°C)	pH	Spec. Cond. (mS/cm)	Salinity	SRB (ppb)	FLT (ppb)
Seep 5 Cont.	10/12/2012	12:09 PM	29.3	7.52	8.25	4.2	1.822	15.82
	10/18/2012	12:43 PM	31.7	7.57	7.52	3.6	1.132	15.69
	10/22/2012	11:30 AM	29.3	7.59	8.00	4.0	1.186	15.73
	10/26/2012	11:45 AM	29.4	7.59	7.46	3.7	1.450	16.14
	10/29/2012	12:13 PM	28.4	7.52	7.24	3.7	1.897	15.81
	11/2/2012	3:54 PM	30.4	7.55	7.01	3.5	1.118	15.08
	11/8/2012	12:58 PM	29.2	7.58	7.20	3.6	0.950	15.06
	11/12/2012	12:09 PM	28.1	7.51	7.07	3.7	1.574	14.81
	11/19/2012	12:15 PM	29.8	7.57	7.31	3.6	1.262	14.63
	11/27/2012	10:46 AM	27.1	7.60	7.35	3.9	1.246	13.02
	12/6/2012	12:04 PM	28.8	7.48	7.05	3.6	1.473	13.19
	12/10/2012	11:25 AM	28.8	7.53	7.04	3.6	1.782	13.16
	12/14/2012	1:15 PM	29.5	7.51	7.91	4.0	1.432	12.83
12/29/2012	12:10 PM	28.9	7.51	8.14	4.2	1.944	12.12	
Seep 11	1/21/2012	3:14 PM	28.9	7.37	5.00	3.2	1.186	8.498
	1/23/2012	1:46 PM	26.3	7.44	5.93	3.1	1.511	9.375
	1/27/2012	2:13 PM	26.3	7.54	5.96	3.1	1.443	10.15
	2/14/2012	2:58 PM	28.1	7.67	6.37	3.3	1.832	16.89
	2/17/2012	1:14 PM	28.4	7.61	6.60	3.3	2.300	16.65
	2/20/2012	3:27 PM	25.9	7.67	7.03	3.8	2.163	18.62
	2/24/2012	12:53 PM	26.6	7.64	7.83	4.2	1.368	19.40
	2/27/2012	12:52 PM	28.4	7.66	6.39	3.2	1.000	20.27
	3/1/2012	1:17 PM	29.0	7.56	6.54	3.2	1.712	21.36
	3/11/2012	12:52 PM	28.8	7.60	6.36	3.2	1.987	24.80
	3/14/2012	11:42 AM	25.2	7.68	6.03	3.2		
	3/17/2012	10:36 AM	26.6	7.59	6.02	3.2	2.483	26.63
	3/19/2012	11:16 AM	26.6	7.62	6.35	3.3	2.460	27.81
	3/22/2012	11:30 AM	26.3	7.58	8.32	4.5	2.954	27.13
	3/27/2012	11:46 AM	26.6	7.58	6.30	3.3	2.374	28.28
	3/29/2012	12:03 PM	26.8	7.57	6.27	3.3	1.803	29.01
	3/31/2012	5:04 PM	26.1		6.84	3.4	3.062	30.24
	4/2/2012	11:55 AM	26.7		6.27	3.3	3.193	30.65
	4/5/2012	10:04 AM	25.6	7.48	6.08	3.3	3.025	31.23
	4/12/2012	10:37 AM	26.5	7.46	6.28	3.3	2.877	31.88
	4/16/2012	11:55 AM	28.9	7.50	6.56	3.3	2.402	32.61
	4/19/2012	12:46 PM	28.5	7.59	6.65	3.4	1.929	30.89
	4/24/2012	4:31 PM	27.1	7.48	6.48	3.4	2.976	33.84
4/26/2012	12:14 PM	28.3	7.55	6.68	3.4	3.419	33.31	
5/2/2012	12:14 PM	28.0	7.53	6.74	3.5	3.714	33.27	
5/7/2012	11:52 AM	29.1	7.50	6.88	3.4	3.130	34.73	

Table A-3 Cont. Location	Date	Time	Temp. (°C)	pH	Spec. Cond. (mS/cm)	Salinity	SRB (ppb)	FLT (ppb)
Seep 11 Cont.	5/18/2012	2:43 PM	30.9	7.65	7.21	3.5	2.800	29.08
	5/22/2012	4:20 PM	27.3	7.48	6.83	3.6	3.483	34.89
	5/25/2012	4:09 PM	27.4	7.48	6.87	3.6	3.063	34.03
	6/4/2012	3:12 PM	27.4	7.73	11.80	6.4	2.654	28.52
	6/7/2012	1:46 PM	28.6	7.40	6.93	3.5	3.517	32.24
	6/12/2012	12:56 PM	31.9	7.48	7.70	3.7	3.048	31.28
	6/14/2012	4:04 PM	32.4	7.48	7.36	3.5	2.680	32.19
	6/16/2012	1:30 PM	31.1	7.31	9.74	4.8	3.361	28.49
	6/29/2012	2:02 PM	32.6	7.40	7.40	3.5	2.362	29.96
	7/11/2012	3:02 PM	34.6	7.64	7.70	3.5		
	7/19/2012	12:08 PM	33.3	7.60	7.62	3.5		
	7/23/2012	11:51 AM	32.6	7.59	7.50	3.5		
	8/1/2012	11:31 AM	30.4	7.50	8.82	4.4		
	8/8/2012	12:47 PM	30.8	7.57	6.93	3.4	2.402	22.52
	8/15/2012	12:03 PM	30.1	7.50	7.13	3.5	1.583	20.89
	8/21/2012	11:30 AM	34.5	7.55	7.62	3.5	2.445	20.75
	8/24/2012	1:03 PM	32.5	7.56	11.10	5.4	2.272	19.61
	8/27/2012	11:13 AM	27.8	7.57	6.90	3.6	2.580	21.20
	9/5/2012	11:26 AM	30.3	7.46	7.18	3.5	3.059	19.49
	9/10/2012	2:21 PM	33.2	7.60	7.61	3.5	2.489	18.77
	9/12/2012	11:37 AM	33.3	7.47	7.79	3.6	2.497	18.35
	9/18/2012	1:20 PM	31.1	7.46	7.39	3.6	1.898	18.51
	10/2/2012	12:47 PM	28.6	7.52	6.79	3.4	1.734	17.39
	10/8/2012	3:24 PM	29.2	7.49	7.05	3.6	1.607	16.98
	10/22/2012	11:53 AM	29.4	7.57	7.26	3.7	1.270	15.72
	10/26/2012	11:58 AM	29.8	7.58	7.18	3.6	1.530	15.81
	10/29/2012	12:25 PM	29.3	7.50	6.97	3.5	1.514	15.31
	11/2/2012	4:10 PM	31.5	7.55	7.11	3.4	1.061	14.99
	11/8/2012	1:10 PM	29.8	7.57	6.84	3.4	1.238	15.13
	11/12/2012	12:21 PM	28.4	7.49	6.88	3.5	1.109	14.53
	11/19/2012	12:29 PM	29.1	7.54	6.87	3.5	1.169	14.35
	11/27/2012	11:28 AM	29.6	7.58	6.93	3.5	1.098	13.27
	12/6/2012	12:16 PM	29.4	7.47	6.81	3.4	0.970	13.01
	12/10/2012	11:48 AM	29.1	7.51	6.79	3.4		
12/14/2012	1:28 PM	28.9	7.52	7.34	3.7	1.498	12.87	
12/29/2012	12:24 PM	29.8	7.78	25.89	14.3	1.692	8.928	

Table A-4. North Seep Group (Seeps 1, 2, 6, 7, 8, 9, 10, 12, 13, 14, 15, 16, 17, 18, 19, 20, and 21) water quality parameters. Parameters were measured with a handheld YSI Model 63 and field fluorescence measurements of S-Rhodamine-B (SRB) and Fluorescein (FLT) analyzed with a handheld Aquafluor fluorometer model 8000-10 from 7/19/2011 to 12/28/2012. Missing fluorescence values are due to shipment of samples prior to analysis in the field.

Location	Date	Time	Temp. (°C)	pH	Spec. Cond. (mS/cm)	Salinity	SRB (ppb)	FLT (ppb)
Seep 1	7/19/2011	9:34 AM	28.3	7.48	7.83	4.0	-0.252	0.187
	7/20/2011	10:11 AM	26.4	7.46	7.69	4.1	0.592	0.308
	7/21/2011	8:42 AM	25.9	7.47	7.52	4.1	0.173	0.425
	7/22/2011	10:14 AM	28.2	7.37	7.80	4.0	0.569	0.206
	7/23/2011	9:37 AM	26.7	7.47	7.68	4.1	0.566	0.036
	7/24/2011	9:33 AM	29.9	7.41	8.15	4.1	-0.078	-0.094
	7/25/2011	10:00 AM	28.4	7.45	8.06	4.2	0.277	0.179
	7/26/2011	9:37 AM	28.1	7.35	8.06	4.2	0.228	0.052
	7/27/2011	10:23 AM	26.7	7.53	8.02	4.3	0.018	-0.252
	7/28/2011	9:44 AM	28.8	7.37	8.40	4.3	0.843	0.188
	7/28/2011	4:16 PM	28.3	7.33	7.68	3.9	0.752	-0.053
	7/29/2011	9:51 AM	26.8	7.27	8.13	4.3	0.062	-0.040
	7/29/2011	4:02 PM	27.9	7.41	7.69	4.0	-0.213	0.000
	7/30/2011	10:55 AM	27.1	7.38	8.14	4.3	0.188	0.023
	7/30/2011	4:37 PM	26.7	7.38	7.34	4.0	0.194	-0.073
	7/31/2011	10:08 AM	29.7	7.39	8.65	4.4	-0.219	-0.122
	7/31/2011	4:27 PM	28.1	7.38	8.15	4.2	0.077	0.145
	8/1/2011	10:10 AM	27.4	7.39	8.05	4.2	0.607	-0.004
	8/1/2011	3:53 PM	27.5	7.37	7.77	4.1	0.263	-0.009
	8/2/2011	8:39 AM	25.3	7.42	7.37	4.0	0.179	-0.102
	8/2/2011	3:43 PM	27.5	7.30	7.79	4.1	0.580	0.158
	8/3/2011	9:52 AM	28.1	7.31	7.82	4.1	-0.200	-0.207
	8/3/2011	4:04 PM	29.2	7.35	8.07	4.1	-0.023	-0.115
	8/4/2011	10:52 AM	29.2	7.38	7.90	4.0	0.212	-0.035
	8/4/2011	4:19 PM	29.3	7.35	7.41	4.1	0.463	-0.049
	8/5/2011	10:30 AM	27.3	7.41	7.51	4.0	-0.097	-0.089
	8/5/2011	4:48 PM	29.9	7.59	8.12	4.1	0.237	-0.097
	8/6/2011	9:10 AM	26.8	7.36	7.82	4.2	-0.022	-0.154
	8/6/2011	3:38 PM	31.3	7.36	8.25	4.0	-0.636	-0.129
	8/7/2011	9:30 AM	26.0	7.51	7.78	4.2	0.334	-0.039
	8/7/2011	3:52 PM	28.5	7.31	7.84	4.0	0.012	0.037
	8/8/2011	9:35 AM	27.6	7.39	8.14	4.3	-0.100	-0.044
	8/8/2011	3:43 PM	30.2	7.39	8.05	4.0	-0.127	-0.015
	8/9/2011	9:38 AM	27.0	7.45	8.10	4.3	0.354	-0.097
	8/9/2011	3:35 PM	29.4	7.45	7.97	4.0	-0.020	-0.030

Table A-4 Cont. Location	Date	Time	Temp. (°C)	pH	Spec. Cond. (mS/cm)	Salinity	SRB (ppb)	FLT (ppb)
Seep 1 Cont.	8/10/2011	11:27 AM	29.1	7.70	8.25	4.3	0.763	0.047
	8/10/2011	4:15 PM	31.8	7.60	8.25	4.0	-0.080	-0.087
	8/11/2011	9:34 AM	28.8	7.60	8.38	4.3	0.432	0.261
	8/11/2011	4:02 PM	31.2	7.71	8.16	4.0	0.503	0.432
	8/12/2011	9:34 AM	28.1	7.65	7.79	4.3	-0.374	0.149
	8/12/2011	3:54 PM	32.0	7.63	8.50	4.1	-0.676	0.065
	8/13/2011	9:32 AM	28.4	7.49	8.36	4.3	0.077	0.141
	8/13/2011	3:35 PM	29.6	7.51	8.26	4.2	0.324	0.282
	8/14/2011	9:56 AM	27.2	7.46	8.13	4.3	0.901	0.440
	8/14/2011	3:49 PM	28.9	7.49	8.12	4.1	0.386	0.360
	8/15/2011	12:39 AM	25.2	7.62	7.64	4.2	0.500	0.307
	8/15/2011	9:20 AM	27.1	7.54	7.98	4.2	0.254	0.278
	8/15/2011	3:33 PM	30.7	7.42	8.47	4.2	0.157	0.313
	8/16/2011	9:55 AM	28.5	7.46	8.12	4.2	0.783	0.328
	8/16/2011	3:25 PM	30.1	7.50	8.37	4.2	0.479	0.308
	8/17/2011	10:23 AM	28.2	7.50	8.06	4.2	0.511	0.281
	8/17/2011	4:11 PM	30.9	7.41	8.39	4.1	0.024	0.510
	8/18/2011	12:50 AM	24.8	7.54	7.57	4.2	0.297	0.271
	8/18/2011	9:23 AM	29.2	7.54	8.03	4.1	0.161	0.237
	8/18/2011	3:51 PM	31.9	7.44	8.47	4.1	0.007	0.210
	8/19/2011	9:51 AM	30.3	7.56	8.19	4.1	-0.045	0.169
	8/19/2011	4:11 PM	29.8	7.46	8.13	4.1	0.018	0.692
	8/20/2011	10:07 AM	27.8	7.48	7.79	4.1	0.130	0.133
	8/20/2011	4:12 PM	27.1	7.46	7.71	4.1	0.095	0.523
	8/21/2011	10:03 AM	27.5	7.44	8.17	4.3	0.120	0.017
	8/21/2011	4:09 PM	28.6	7.48	7.95	4.1	0.273	0.825
	8/22/2011	9:38 AM	27.3	7.48	7.96	4.2	0.801	0.085
	8/22/2011	4:18 PM	31.1	7.54	8.24	4.0	0.804	0.004
	8/23/2011	9:43 AM	27.1	7.45	7.90	4.2	-0.667	0.111
	8/23/2011	3:43 PM	28.1	7.41	7.72	4.0	0.024	0.213
	8/24/2011	10:38 AM	27.2	7.49	8.01	4.2	-0.227	0.063
	8/24/2011	5:01 PM	29.4	7.51	7.32	4.0	-0.120	0.308
	8/25/2011	10:08 AM	29.3	7.54	8.39	4.3	0.413	0.552
	8/25/2011	4:44 PM	28.0	7.50	7.74	4.0	0.339	0.271
	8/26/2011	9:45 AM	27.7	7.52	8.29	4.3	0.523	0.119
	8/26/2011	3:54 PM	29.7	7.53	7.94	4.0	1.171	0.116
	8/27/2011	9:38 AM	29.8	7.52	8.46	4.3	0.353	0.285
	8/27/2011	4:12 PM	30.8	7.44	8.10	4.0	0.786	0.090
	8/28/2011	9:36 AM	28.7	7.41	8.37	4.3	0.894	0.084
	8/28/2011	3:54 PM	31.2	7.76	8.31	4.1	0.013	0.065

Table A-4 Cont. Location	Date	Time	Temp. (°C)	pH	Spec. Cond. (mS/cm)	Salinity	SRB (ppb)	FLT (ppb)
Seep 1 Cont.	8/29/2011	9:57 AM	27.5	7.56	8.05	4.2	0.175	0.069
	8/29/2011	4:12 PM	29.1	7.47	7.97	4.0	0.490	0.137
	8/30/2011	9:39 AM	29.1	7.49	7.52	4.1	0.049	0.210
	9/1/2011	10:31 AM	30.2	7.50	8.19	4.1	-0.399	0.286
	9/1/2011	4:23 PM	29.9	7.45	8.12	4.1	-0.227	0.186
	9/2/2011	10:35 AM	29.2	7.46	7.92	4.0	-0.662	0.159
	9/2/2011	4:06 PM	31.8	7.57	8.47	4.2	-0.473	0.416
	9/3/2011	10:04 AM	27.4	7.60	7.72	4.0	-0.481	0.421
	9/3/2011	4:18 PM	29.0	7.56	8.04	4.1	-0.490	0.361
	9/4/2011	3:52 PM	32.8	7.42	8.53	4.0	-0.741	0.257
	9/5/2011	9:55 AM	29.8	7.45	8.28	4.2	-0.241	0.318
	9/5/2011	4:14 PM	28.0	7.43	7.75	4.0	-0.554	0.249
	9/6/2011	9:39 AM	27.0	7.47	7.95	4.2	-0.201	0.221
	9/6/2011	3:50 PM	30.8	7.27	8.18	4.0	-0.608	0.225
	9/7/2011	9:19 AM	29.0	7.28	8.26	4.2	0.180	0.337
	9/8/2011	9:29 AM	29.5	7.31	8.29	4.2	0.300	0.359
	9/9/2011	10:19 AM	31.2	7.33	8.66	4.2	-0.334	0.286
	9/10/2011	10:20 AM	28.5	7.20	8.84	4.6	-0.478	0.312
	9/11/2011	10:35 AM	31.3	7.46	8.96	4.4	-0.145	0.282
	9/12/2011	11:38 AM	30.8	7.42	10.16	5.1	-0.473	0.444
	9/13/2011	10:36 AM	33.1	7.34	8.98	4.2	0.102	0.316
	9/14/2011	9:42 AM	29.8	7.39	8.50	4.3	-0.259	0.178
	9/15/2011	9:22 AM	30.8	7.41	8.54	4.2	-0.388	0.393
	9/16/2011	11:16 AM	33.4	7.41	9.80	4.6	-0.463	0.212
	9/17/2011	2:23 PM	33.7	7.30	12.39	5.9	0.073	0.208
	9/18/2011	10:58 AM	34.3	7.26	14.80	6.7	-0.596	0.216
	9/19/2011	10:02 AM	30.5	7.40	14.29	7.3	-0.476	0.240
	9/20/2011	9:58 AM	31.5	7.51	10.49	5.2	-0.721	0.184
	9/21/2011	9:39 AM	29.5	7.48	10.22	5.2	-0.529	0.299
	9/22/2011	9:27 AM	25.0	7.18	9.54	5.3	-0.100	0.275
	9/23/2011	9:58 AM	30.0	7.43	9.48	4.8	-0.180	0.494
	9/24/2011	9:18 AM	30.3	7.45	11.35	5.8	-0.054	0.223
	9/25/2011	10:20 AM	32.4	7.44	7.64	4.1	-0.195	0.232
	9/26/2011	10:05 AM	30.8	7.45	10.27	5.1	0.303	0.476
9/27/2011	9:44 AM	29.6	7.44	8.19	4.1	-0.793	0.152	
9/28/2011	9:44 AM	29.5	7.42	8.11	4.1	-0.861	0.026	
9/29/2011	9:46 AM	27.5	7.41	7.73	4.0	-0.034	0.143	
9/30/2011	9:49 AM	29.5	7.46	8.21	4.1	-0.663	0.154	
10/1/2011	10:04 AM	30.9	7.48	8.28	4.1	-0.041	-0.086	
10/2/2011	12:15 PM	34.4	7.41	8.65	4.0	0.044	-0.093	

Table A-4 Cont. Location	Date	Time	Temp. (°C)	pH	Spec. Cond. (mS/cm)	Salinity	SRB (ppb)	FLT (ppb)
Seep 1 Cont.	10/3/2011	9:50 AM	27.3	7.43	7.77	4.1	0.243	0.017
	10/4/2011	9:22 AM	27.8	7.50	8.04	4.2	0.299	0.018
	10/8/2011	4:20 PM	28.9	7.40	8.02	4.1	-0.080	0.360
	10/10/2011	12:05 PM	33.3	7.44	8.62	4.0	-0.416	0.376
	10/12/2011	9:29 AM	29.4	7.43	7.94	4.0	0.715	0.361
	10/14/2011	9:27 AM	29.1	7.37	7.99	4.1	0.335	0.253
	10/16/2011	9:27 AM	28.0	7.41	8.28	4.3	0.514	0.244
	10/18/2011	11:43 AM	33.1	7.47	8.83	4.1	0.388	0.067
	10/20/2011	9:29 AM	28.2	7.38	8.02	4.2	0.426	0.325
	10/22/2011	9:34 AM	29.6	7.43	8.04	4.0	-0.037	0.158
	10/24/2011	9:31 AM	29.6	7.46	8.23	4.1	-0.100	0.212
	10/26/2011	9:30 AM	28.4	7.55	8.00	4.1	0.304	0.284
	10/28/2011	9:35 AM	27.1	7.43	7.62	4.0	0.571	0.251
	10/30/11	11:32 AM	33.0	7.43	8.48	4.0	-0.053	0.552
	11/1/2011	11:29 AM	32.3	7.53	8.42	4.1	-0.238	0.248
	11/3/2011	9:46 AM	29.6	7.41	8.22	4.1	-0.087	0.455
	11/5/2011	1:34 PM	29.2	7.46	8.09	4.1	0.109	0.465
11/9/2011	10:11 AM	28.6	7.48	8.11	4.2	-0.316	0.764	
11/11/2011	10:05 AM	27.1	7.48	8.09	4.3	-0.050	0.620	
Seep 2	7/20/2011	12:16 PM	29.1	7.35	7.91	4.0	-0.038	-0.279
	7/21/2011	8:38 AM	25.1	7.43	7.41	4.1	-0.099	-0.280
	7/22/2011	10:20 AM	28.6	7.39	8.01	4.1	0.580	0.145
	7/23/2011	9:45 AM	26.5	7.46	7.66	4.1	-0.152	0.135
	7/25/2011	10:08 AM	27.6	7.50	7.97	4.0	0.529	-0.095
	7/26/2011	9:45 AM	27.6	7.44	8.09	4.2	0.788	0.094
	7/27/2011	10:33 AM	26.6	7.47	8.01	4.3	0.147	0.045
	7/28/2011	9:53 AM	28.6	7.39	8.25	4.3	1.049	-0.110
	7/28/2011	4:25 PM	27.5	7.13	7.45	3.9	0.172	0.052
	7/29/2011	10:00 AM	26.8	7.35	8.06	4.3	0.877	0.081
	7/29/2011	4:09 PM	27.5	7.38	7.46	3.9	0.173	0.119
	7/30/2011	11:04 AM	26.9	7.39	8.11	4.3	-0.242	-0.007
	7/30/2011	4:44 PM	27.9	7.33	7.49	3.8	0.252	0.070
	7/31/2011	10:14 AM	30.0	7.41	8.53	4.3	0.165	0.016
	7/31/2011	4:20 PM	28.3	7.34	7.04	4.0	0.839	0.121
	8/1/2011	3:59 AM	28.5	7.39	8.13	4.2	0.114	0.149
	8/1/2011	9:56 AM	26.9	7.31	7.60	4.0	0.702	0.079
	8/2/2011	8:46 AM	25.6	7.42	7.48	4.1	0.159	-0.027
	8/2/2011	3:49 PM	27.8	7.35	7.89	4.1	-0.293	-0.137
	8/3/2011	12:13 AM	24.3	7.23	7.38	4.1	0.179	-0.016

Table A-4 Cont. Location	Date	Time	Temp. (°C)	pH	Spec. Cond. (mS/cm)	Salinity	SRB (ppb)	FLT (ppb)
Seep 2 Cont.	8/3/2011	9:45 AM	28.3	7.13	8.36	4.4	-0.049	0.017
	8/3/2011	4:11 PM	29.2	7.37	8.13	4.1	-0.315	-0.211
	8/4/2011	10:41 AM	31.4	7.28	7.92	3.9	0.411	-0.128
	8/4/2011	4:12 PM	29.3	7.25	7.91	4.1	-0.164	-0.053
	8/5/2011	12:37 AM	24.9	7.37	7.49	4.1	0.392	-0.030
	8/5/2011	10:46 AM	27.3	7.41	7.62	4.0	-0.380	-0.205
	8/5/2011	4:58 PM	29.8	7.64	8.32	4.2	-0.221	-0.035
	8/6/2011	12:58 AM	24.0	7.23	7.53	4.2	-0.253	-0.074
	8/6/2011	9:00 AM	27.0	7.30	7.95	4.2	-0.437	-0.059
	8/6/2011	3:46 PM	30.8	7.27	8.28	4.1	0.173	-0.044
	8/7/2011	3:15 AM	24.9	7.34	7.68	4.3	-0.293	-0.276
	8/7/2011	9:20 AM	26.0	7.32	7.79	4.3	-0.590	-0.132
	8/7/2011	4:01 PM	28.2	7.33	7.94	4.1	0.552	-0.101
	8/7/2011	11:25 PM	25.2	7.28	7.59	4.2	-0.339	-0.217
	8/8/2011	9:27 AM	26.7	7.36	8.10	4.3	0.282	-0.151
	8/8/2011	3:48 PM	30.2	7.41	7.41	4.0	0.138	0.085
	8/9/2011	12:08 AM	26.5	7.42	7.64	4.1	0.368	0.024
	8/9/2011	9:30 AM	27.1	7.44	8.24	4.4	0.377	0.119
	8/9/2011	3:45 PM	29.4	7.45	7.92	4.0	-0.334	0.121
	8/10/2011	12:00 AM	25.2	7.75	7.58	4.2	0.455	-0.026
	8/10/2011	11:18 AM	30.5	7.65	8.64	4.3	0.265	0.102
	8/10/2011	4:19 PM	30.5	7.59	8.07	4.0	0.094	0.115
	8/11/2011	12:26 AM	25.6	7.67	7.58	4.2	0.468	-0.004
	8/11/2011	9:26 AM	29.2	7.56	7.87	4.3	0.031	0.238
	8/11/2011	4:09 PM	30.6	7.67	7.95	3.9	-0.264	0.094
	8/12/2011	12:25 AM	24.5	7.68	7.59	4.2	-0.208	0.047
	8/12/2011	9:27 AM	27.8	7.65	7.72	4.3	0.169	0.005
	8/13/2011	12:28 AM	25.2	7.58	7.67	4.2	0.067	0.267
	8/13/2011	9:25 AM	28.4	7.54	8.31	4.3	0.060	0.293
	8/13/2011	3:45 PM	29.7	7.37	8.22	4.1	-0.261	0.082
	8/14/2011	12:23 AM	24.7	7.56	7.64	4.2	0.867	0.457
	8/14/2011	9:40 AM	28.1	7.43	8.03	4.2	0.790	0.406
	8/14/2011	3:54 PM	28.1	7.43	8.03	4.2	0.147	0.296
	8/15/2011	9:27 AM	26.9	7.53	7.95	4.2	0.439	0.329
	8/15/2011	3:39 PM	29.5	7.49	8.31	4.2	-0.129	0.310
	8/16/2011	10:08 AM	28.0	7.50	8.08	4.2	0.065	0.233
	8/16/2011	3:16 PM	30.1	7.48	8.42	4.2	0.194	0.210
	8/17/2011	10:32 AM	28.9	7.54	8.24	4.2	-0.075	0.135
	8/17/2011	4:03 PM	31.3	7.47	8.53	4.2	-0.320	0.210
	8/18/2011	9:38 AM	29.3	7.49	8.07	4.1	0.097	0.163

Table A-4 Cont. Location	Date	Time	Temp. (°C)	pH	Spec. Cond. (mS/cm)	Salinity	SRB (ppb)	FLT (ppb)
Seep 2 Cont.	8/18/2011	3:41 PM	32.1	7.54	8.63	4.1	-0.027	0.265
	8/19/2011	9:34 AM	29.3	7.65	8.00	4.1	0.154	0.325
	8/19/2011	4:03 PM	29.8	7.49	8.14	4.1	0.098	0.128
	8/20/2011	10:02 AM	28.8	7.46	7.97	4.1	0.181	0.100
	8/20/2011	4:05 PM	27.4	7.47	7.80	4.1	0.214	0.628
	8/21/2011	9:53 AM	26.5	7.44	7.70	4.1	-0.296	0.055
	8/21/2011	4:03 PM	28.5	7.47	7.98	4.1	0.213	0.471
	8/22/2011	9:31 AM	28.5	7.48	8.11	4.2	0.064	0.394
	8/22/2011	4:11 PM	31.1	7.57	8.32	4.1	-0.241	0.197
	8/24/2011	5:10 PM	29.3	7.55	7.96	4.0	0.268	0.108
	8/25/2011	9:58 AM	29.6	7.47	8.49	4.3	-0.120	0.538
	8/25/2011	4:34 PM	28.5	7.51	7.78	4.0	0.496	0.219
	8/26/2011	9:38 AM	27.7	7.50	8.29	4.3	0.446	-0.005
	8/26/2011	3:47 PM	30.6	7.49	7.94	3.9	0.213	0.181
	8/27/2011	9:48 AM	29.1	7.49	8.40	4.3	0.309	0.033
	8/27/2011	4:23 PM	29.4	7.59	7.83	3.9	0.452	0.175
	8/28/2011	9:45 AM	28.3	7.52	8.20	4.2	-0.231	0.106
	8/28/2011	4:02 PM	30.9	7.58	8.12	4.0	0.182	0.178
	8/29/2011	9:49 AM	27.3	7.47	7.97	4.2	0.068	0.094
	8/29/2011	4:05 PM	28.6	7.46	7.76	4.0	0.085	0.063
	8/30/2011	9:33 AM	28.7	7.49	7.95	4.1	0.116	0.489
	9/1/2011	10:49 AM	29.6	7.59	8.11	4.1	-0.355	0.369
	9/1/2011	4:13 PM	30.3	7.51	8.33	4.2	-0.315	0.194
	9/2/2011	10:23 AM	28.9	7.44	8.00	4.1	-0.435	0.156
	9/2/2011	3:55 PM	31.2	7.75	8.74	4.3	-0.311	0.388
	9/3/2011	9:56 AM	27.9	7.65	7.98	4.2	0.155	0.579
	9/3/2011	4:09 PM	29.5	7.56	8.18	4.1	-0.608	0.335
	9/4/2011	3:40 PM	33.8	7.55	8.79	4.1	-0.538	0.282
	9/5/2011	9:46 AM	29.6	7.48	8.41	4.2	-0.318	0.145
	9/5/2011	4:05 PM	28.3	7.46	7.91	4.1	-0.235	0.207
	9/6/2011	9:32 AM	27.0	7.47	8.25	4.4	-0.283	0.599
	9/6/2011	3:59 PM	31.5	7.48	8.46	4.1	-0.046	0.575
	9/7/2011	9:27 AM	29.0	7.47	8.39	4.3	-0.337	0.595
	9/8/2011	9:38 AM	29.6	7.48	8.38	4.2	-0.689	0.137
	9/9/2011	10:30 AM	32.1	7.54	9.26	4.4	-0.193	0.488
	9/10/2011	10:32 AM	27.4	7.48	9.28	4.9	-0.374	0.286
9/11/2011	10:20 AM	29.0	7.35	11.94	6.2	-0.342	0.491	
9/12/2011	11:26 AM	31.4	7.31	10.85	5.4	-0.184	0.458	
9/13/2011	10:50 AM	33.7	7.49	9.20	4.3	-0.052	0.303	
9/14/2011	9:55 AM	30.2	7.52	9.17	4.6	-0.269	0.211	

Table A-4 Cont. Location	Date	Time	Temp. (°C)	pH	Spec. Cond. (mS/cm)	Salinity	SRB (ppb)	FLT (ppb)
Seep 2 Cont.	9/15/2011	9:34 AM	31.2	7.49	8.73	4.3	-0.068	0.394
	9/16/2011	11:27 AM	33.6	7.48	9.00	4.2	-0.224	0.243
	9/17/2011	2:38 PM	33.9	7.52	12.72	6.1	-0.341	0.342
	9/18/2011	11:13 AM	34.5	7.51	14.58	7.0	-0.399	0.112
	9/19/2011	10:18 AM	29.9	7.51	13.06	6.8	-0.548	0.185
	9/20/2011	9:49 AM	31.2	7.45	13.24	6.7	-0.433	0.291
	9/21/2011	9:30 AM	27.7	7.44	11.27	6.0	0.318	0.254
	9/22/2011	9:36 AM	26.2	7.51	17.36	9.9	-0.261	0.202
	9/23/2011	9:39 AM	29.3	7.19	10.98	5.7	0.603	0.138
	9/24/2011	9:09 AM	29.7	7.46	12.23	6.3	0.226	0.184
	9/25/2011	10:02 AM	33.6	7.39	9.59	4.5	-0.307	0.284
	9/26/2011	10:18 AM	31.4	7.52	10.48	5.2	0.160	0.124
	9/27/2011	9:35 AM	28.7	7.47	8.23	4.2	-1.185	0.127
	9/28/2011	9:35 AM	29.5	7.44	8.08	4.1	-0.684	0.227
	9/29/2011	9:34 AM	27.4	7.45	7.88	4.1	-0.039	0.419
	9/30/2011	9:39 AM	29.0	7.47	8.22	4.2	-0.566	0.258
	10/1/2011	9:55 AM	30.0	7.51	8.58	4.3	0.231	-0.012
	10/2/2011	12:27 PM	34.9	7.48	8.88	4.1	0.197	0.182
	10/3/2011	9:40 AM	28.1	7.46	8.74	4.6	0.632	0.300
	10/4/2011	9:34 AM	28.6	7.49	8.60	4.4	0.630	-0.029
	10/8/2011	4:30 PM	28.7	7.46	7.90	4.0	-0.164	0.419
	10/10/2011	11:57 AM	33.9	7.46	8.72	4.0	-0.203	0.359
	10/12/2011	9:38 AM	30.2	7.49	8.00	4.0	-0.131	0.419
	10/14/2011	9:34 AM	29.9	7.48	8.09	4.1	0.178	0.148
	10/16/2011	9:36 AM	27.9	7.50	8.39	4.4	0.558	0.223
	10/18/2011	11:58 AM	34.3	7.52	9.44	4.4	0.483	0.174
	10/20/2011	9:40 AM	28.2	7.51	8.04	4.2	1.172	0.173
	10/22/2011	9:41 AM	30.2	7.50	8.09	4.0	-0.107	0.046
	10/24/2011	9:41 AM	30.2	7.51	8.13	4.1	-0.211	0.264
	10/26/2011	9:40 AM	28.4	7.50	7.92	4.1	-0.233	0.209
	10/28/2011	9:45 AM	27.3	7.47	7.68	4.0	0.508	0.181
	10/30/11	11:44 AM	34.1	7.50	8.66	4.0	-0.302	0.346
11/1/11	11:42 AM	33.5	7.51	8.52	4.0	-0.341	0.500	
11/3/11	9:39 AM	29.4	7.50	7.99	4.0	-0.121	0.447	
11/5/2011	1:22 PM	30.1	7.49	8.13	4.1	0.109	0.543	
11/7/2011	9:41 AM	26.5	7.43	7.53	4.1	0.649	0.558	
11/9/2011	9:58 AM	28.3	7.51	8.12	4.2	0.537	0.583	
Seep 6	7/19/2011	9:25 AM	27.8	7.36	7.91	4.1	-0.322	0.041
	7/20/2011	9:59 AM	27.0	7.21	7.78	4.1	0.046	-0.116

Table A-4 Cont. Location	Date	Time	Temp. (°C)	pH	Spec. Cond. (mS/cm)	Salinity	SRB (ppb)	FLT (ppb)
Seep 6 Cont.	7/21/2011	8:25 AM	25.0	7.20	7.00	3.8	0.730	0.044
	7/22/2011	10:03 AM	27.9	7.31	7.71	4.0	0.224	-0.053
	7/23/2011	9:57 AM	27.1	7.40	7.72	4.1	0.070	-0.161
	7/24/2011	9:48 AM	27.8	7.43	7.99	4.2	0.939	-0.062
	7/25/2011	10:16 AM	26.0	7.46	7.72	4.2	0.018	-0.165
	7/26/2011	9:55 AM	27.3	7.40	8.02	4.2	0.152	-0.227
	7/28/2011	9:32 AM	27.9	7.29	7.67	4.2	0.237	0.113
	7/28/2011	4:07 PM	29.5	7.23	7.78	3.9	0.670	0.045
	7/29/2011	1:27 AM	23.8	7.25	7.20	4.1	-0.203	0.073
	7/29/2011	9:43 AM	27.1	7.22	7.97	4.2	0.002	0.020
	7/29/2011	3:55 PM	28.6	7.29	7.76	4.0	0.344	-0.120
	7/30/2011	12:35 AM	24.5	7.28	7.35	4.1	-0.080	-0.020
	7/30/2011	4:24 PM	27.0	7.34	8.10	4.3	0.760	-0.080
	7/31/2011	10:00 AM	27.6	7.38	7.73	4.0	0.140	-0.025
	7/30/2011	11:09 AM	23.9	7.37	7.34	4.1	0.716	-0.021
	7/31/2011	4:10 PM	29.5	7.37	8.52	4.3	-0.243	-0.042
	7/31/2011	12:42 AM	29.0	7.30	8.09	4.1	0.811	-0.021
	8/1/2011	10:04 AM	27.3	7.34	7.97	4.2	0.141	-0.072
	8/1/2011	3:47 PM	29.4	7.32	8.10	4.1	-0.139	-0.234
	8/2/2011	8:29 AM	25.5	7.35	7.43	4.1	-0.341	-0.039
	8/2/2011	3:35 PM	29.4	7.30	8.14	4.1	0.015	-0.113
	8/3/2011	9:58 AM	28.3	7.33	7.96	4.1	0.424	-0.019
	8/3/2011	3:55 PM	30.4	7.21	8.26	4.1	-0.109	-0.123
	8/4/2011	10:56 AM	29.5	7.32	8.12	4.1	-0.174	-0.030
	8/4/2011	4:25 PM	28.3	7.40	8.13	4.0	-0.434	-0.137
	8/5/2011	10:31 AM	27.5	7.27	7.71	4.1	0.653	-0.023
	8/5/2011	4:37 PM	30.6	7.59	7.43	4.1	-0.214	-0.071
	8/6/2011	9:20 AM	27.0	7.36	7.87	4.2	-0.343	-0.225
	8/6/2011	3:30 PM	32.1	7.23	8.47	4.1	0.309	0.115
	8/7/2011	9:40 AM	26.1	7.31	7.85	4.2	0.316	-0.065
	8/7/2011	3:43 PM	29.1	7.30	7.91	4.0	-0.353	-0.020
	8/8/2011	9:42 AM	27.6	7.35	8.22	4.3	-0.021	-0.146
	8/8/2011	3:34 PM	31.6	7.33	8.31	4.0	-0.137	-0.086
	8/9/2011	9:48 AM	27.3	7.38	8.21	4.3	0.691	0.017
	8/9/2011	3:30 PM	29.8	7.42	8.10	4.1	0.650	-0.068
	8/10/2011	11:30 AM	29.3	7.69	8.47	4.3	0.480	-0.043
	8/10/2011	4:05 PM	31.9	7.60	8.29	4.0	0.634	-0.229
	8/11/2011	9:37 AM	29.3	7.58	8.49	4.3	-0.055	0.302
	8/11/2011	3:55 PM	31.4	7.63	8.12	3.9	-0.647	0.119
	8/12/2011	9:41 AM	28.1	7.71	8.26	4.3	-0.360	0.270

Table A-4 Cont. Location	Date	Time	Temp. (°C)	pH	Spec. Cond. (mS/cm)	Salinity	SRB (ppb)	FLT (ppb)
Seep 6 Cont.	8/12/2011	3:37 PM	33.0	7.70	8.53	4.0	0.273	0.126
	8/13/2011	9:40 AM	27.3	7.49	8.15	4.3	-0.405	0.181
	8/13/2011	3:23 PM	30.6	7.47	8.51	4.2	-0.795	0.084
	8/14/2011	4:01 PM	28.0	7.34	8.03	4.2	1.301	0.306
	8/15/2011	9:34 AM	27.0	7.54	7.98	4.2	0.776	0.371
	8/15/2011	3:47 PM	29.5	7.43	8.32	4.2	-0.026	0.398
	8/16/2011	2:39 AM	24.3	7.45	7.59	4.2	0.441	0.386
	8/16/2011	9:47 AM	28.6	7.47	8.18	4.2	-0.063	0.301
	8/16/2011	3:33 PM	30.0	7.55	8.32	4.2	0.056	0.217
	8/17/2011	12:25 AM	24.7	7.54	7.60	4.2	0.824	0.239
	8/17/2011	10:08 AM	28.9	7.51	8.04	4.1	-0.090	0.094
	8/18/2011	9:55 AM	30.0	7.46	8.13	4.1	0.148	0.339
	8/18/2011	4:00 PM	31.6	7.41	8.51	4.1	0.286	0.197
	8/19/2011	9:43 AM	29.2	7.44	8.01	4.1	0.400	0.286
	8/19/2011	3:56 PM	30.7	7.34	8.23	4.0	-0.408	0.012
	8/20/2011	9:54 AM	29.4	7.41	8.04	4.0	0.062	0.506
	8/20/2011	3:57 PM	28.1	7.61	7.87	4.1	-0.063	0.405
	8/21/2011	9:49 AM	26.5	7.47	7.80	4.2	0.704	0.225
	8/21/2011	4:16 PM	28.3	7.94	7.48	4.1	0.604	0.145
	8/22/2011	9:25 AM	29.0	7.40	8.20	4.2	0.138	0.160
	8/22/2011	4:04 PM	31.0	7.73	8.32	4.1	-0.137	0.116
	8/23/2011	9:35 AM	28.2	7.21	8.19	4.2	-0.005	0.174
	8/23/2011	3:36 PM	28.8	7.38	7.82	4.0	0.513	0.068
	8/24/2011	10:26 AM	27.6	7.23	8.22	4.3	0.060	0.217
	8/24/2011	4:50 PM	29.5	7.45	7.94	4.0	-0.134	0.443
	8/25/2011	10:18 AM	28.9	7.51	8.34	4.3	0.141	0.007
	8/25/2011	4:25 PM	28.8	7.53	7.89	4.0	0.420	0.243
	8/26/2011	9:30 AM	29.0	7.50	8.73	4.4	0.806	0.169
	8/26/2011	3:38 PM	30.4	7.72	8.01	4.0	0.339	0.109
	8/27/2011	9:57 AM	29.1	7.65	8.40	4.3	0.648	0.108
	8/27/2011	4:32 PM	29.9	7.57	7.95	4.0	0.669	0.280
	8/28/2011	9:52 AM	28.5	7.51	8.26	4.3	0.331	0.191
	8/28/2011	4:08 PM	30.7	7.56	8.19	4.0	0.179	0.514
	8/29/2011	9:39 AM	28.2	7.28	8.02	4.1	0.089	0.021
	8/29/2011	3:55 PM	29.4	7.22	7.97	4.0	0.351	0.197
	8/30/2011	9:24 AM	29.4	7.18	7.77	3.9	0.552	0.482
	9/1/2011	11:00 AM	30.9	7.70	9.67	4.8	-0.162	0.372
	9/1/2011	4:33 PM	31.9	7.50	8.69	4.2	0.082	0.280
	9/2/2011	10:46 AM	30.5	7.55	8.26	4.1	-0.268	0.147
	9/2/2011	4:16 PM	32.5	7.57	10.67	5.1	-0.191	0.182

Table A-4 Cont. Location	Date	Time	Temp. (°C)	pH	Spec. Cond. (mS/cm)	Salinity	SRB (ppb)	FLT (ppb)
Seep 6 Cont.	9/3/2011	9:45 AM	27.4	7.67	7.86	4.1	0.048	0.149
	9/3/2011	3:59 PM	30.0	7.55	8.27	4.1	0.081	0.399
	9/4/2011	4:05 PM	34.2	7.42	9.88	4.6	0.189	0.436
	9/5/2011	9:32 AM	31.1	7.42	8.54	4.2	-0.476	0.284
	9/5/2011	3:57 PM	29.1	7.33	7.96	4.0	0.376	0.145
	9/6/2011	9:24 AM	26.8	7.33	7.97	4.2	-0.275	0.232
	9/6/2011	4:07 PM	32.0	7.43	8.40	4.0	0.107	0.351
	9/7/2011	9:36 AM	29.0	7.42	8.26	4.2	-0.294	0.360
	9/8/2011	9:46 AM	29.5	7.43	8.29	4.2	-0.742	0.816
	9/9/2011	10:40 AM	34.8	7.43	9.18	4.2	-0.011	0.463
	9/10/2011	10:42 AM	30.1	7.40	7.79	4.3	-0.739	0.167
	9/11/2011	10:48 AM	32.5	7.37	8.98	4.3	0.217	0.209
	9/12/2011	12:00 PM	30.9	7.36	8.66	4.3	0.576	0.389
	9/13/2011	11:02 AM	33.3	7.40	8.99	4.2	-0.482	0.341
	9/14/2011	10:05 AM	31.3	7.39	8.16	4.2	-0.217	0.347
	9/15/2011	9:46 AM	32.0	7.41	8.69	4.2	-0.323	0.254
	9/16/2011	11:37 AM	33.7	7.42	8.92	4.2	-0.548	0.379
	9/17/2011	2:48 PM	32.2	7.46	11.58	5.7	-0.429	0.588
	9/18/2011	11:25 AM	35.9	7.50	10.23	5.7	0.006	0.251
	9/19/2011	10:32 AM	30.2	7.50	13.54	7.0	-0.418	0.499
	9/20/2011	9:40 AM	30.3	7.06	8.68	4.3	-0.415	0.510
	9/21/2011	9:21 AM	28.2	7.34	9.49	5.0	-0.600	0.224
	9/22/2011	9:48 AM	28.7	7.52	12.31	6.5	-0.150	0.396
	9/23/2011	9:50 AM	29.9	7.42	9.18	4.6	0.115	0.487
	9/24/2011	8:57 AM	30.0	7.31	9.65	4.8	0.154	0.232
	9/25/2011	10:33 AM	33.3	7.41	9.71	5.4	-0.152	0.126
	9/26/2011	10:36 AM	31.9	7.47	12.01	5.9	-0.576	0.221
	9/27/2011	9:25 AM	29.7	6.90	9.15	4.6	-1.226	0.141
	9/28/2011	9:26 AM	29.9	7.20	8.06	4.0	-0.546	0.163
	9/29/2011	9:21 AM	27.4	7.21	7.72	4.0	-0.729	0.340
	9/30/2011	9:28 AM	28.9	7.23	8.07	4.1	0.092	0.174
	10/1/2011	9:45 AM	29.8	7.44	8.47	4.2	0.265	0.041
	10/2/2011	12:03 PM	33.5	7.27	8.53	4.0	0.194	0.057
	10/3/2011	9:30 AM	27.6	7.25	7.71	4.0	0.486	-0.041
	10/4/2011	9:47 AM	29.1	7.47	8.10	4.1	0.586	-0.024
	10/6/2011	12:18 PM	30.5	7.32	8.39	4.1	0.626	0.472
10/8/2011	4:09 PM	29.5	7.35	8.02	4.0	-0.366	0.473	
10/10/2011	11:49 AM	34.2	7.30	8.69	4.0	0.295	0.328	
10/12/2011	9:20 AM	28.7	7.46	7.95	4.1	0.011	0.559	
10/14/2011	9:47 AM	28.0	7.44	7.96	4.1	0.376	0.338	

Table A-4 Cont. Location	Date	Time	Temp. (°C)	pH	Spec. Cond. (mS/cm)	Salinity	SRB (ppb)	FLT (ppb)
Seep 6 Cont.	10/16/2011	9:46 AM	28.1	7.43	8.27	4.3	0.489	0.161
	10/18/2011	11:32 AM	32.6	7.30	9.00	4.3	0.146	0.157
	10/20/2011	9:53 AM	28.8	7.42	8.11	4.1	0.222	0.236
	10/22/2011	9:51 AM	30.8	7.46	8.12	4.0	0.232	0.234
	10/24/2011	9:51 AM	29.2	7.43	8.08	4.1	0.418	0.217
	10/26/2011	9:58 AM	28.4	7.42	7.93	4.1	-0.114	0.264
	10/28/2011	9:25 AM	27.0	7.41	7.58	4.0	-0.165	0.293
	10/30/2011	11:18 AM	32.2	7.35	8.29	4.0	-0.085	0.506
	11/1/2011	11:52 AM	31.9	7.42	8.49	4.1	0.137	0.383
	11/3/2011	9:53 AM	29.7	7.39	8.20	4.1	0.228	0.456
	11/5/2011	1:07 PM	30.4	7.35	8.26	4.1	-0.225	0.626
	11/7/2011	9:31 AM	26.1	7.64	7.60	4.1	0.000	0.559
	11/9/2011	9:39 AM	29.3	7.30	8.18	4.1	-0.108	0.670
	11/11/2011	9:54 AM	25.4	7.32	7.92	4.3	-0.405	0.634
	11/16/2011	9:49 AM	27.7	7.42	7.59	3.9	0.167	0.974
	11/18/2011	10:02 AM	29.8	7.70	9.43	4.8	0.596	0.718
	11/21/2011	9:37 AM	28.3	7.24	8.03	4.2	0.909	1.007
11/23/2011	9:34 AM	27.4	7.27	7.60	4.0	0.533	1.183	
Seep 7	11/16/2011	9:10 AM	27.9	7.29	7.83	4.1	0.116	0.988
	11/18/2011	9:45 AM	27.4	7.28	7.76	4.1	0.951	1.387
	11/21/2011	9:49 AM	28.5	7.34	7.71	4.0	0.171	0.991
	11/23/2011	9:57 AM	27.2	7.45	7.61	4.0	-0.164	1.160
	11/25/2011	10:08 AM	28.0	7.40	8.01	4.2	0.499	1.389
	11/28/2011	9:41 AM	24.9	7.42	11.46	6.5	0.302	1.583
	11/30/2011	10:39 AM	26.0	7.46	7.50	4.0	0.391	1.920
	12/2/2011	9:44 AM	26.1	7.45	7.72	4.2	0.595	2.175
	12/5/2011	10:03 AM	29.6	7.43	7.98	4.0	1.429	2.727
	12/9/2011	9:39 AM	23.9	7.47	7.24	4.1	0.352	3.355
	12/12/2011	9:32 AM	25.1	7.43	7.29	3.9	0.319	3.969
	12/14/2011	9:25 AM	27.7	7.26	7.67	4.0	0.067	4.663
	12/19/2011	9:58 AM	27.3	7.35	7.60	4.0		
	12/21/2011	10:18 AM	26.4	7.44	7.64	4.1		
	12/23/2011	10:10 AM	22.4	7.80	7.83	4.6		
	12/26/2011	10:14 AM	27.0	7.57	7.76	4.1		
	12/28/2011	10:06 AM	29.5	7.42	8.19	4.1		
	12/30/2011	10:21 AM	27.7	7.57	8.44	4.4		
	1/2/2012	10:18 AM	28.4	7.54	15.08	8.2		
	1/4/2012	2:48 PM	29.3	7.59	8.35	4.2	0.91	9.088
1/7/2012	2:46 PM	29.1	7.46	8.26	4.2	1.28	10.23	

Table A-4 Cont. Location	Date	Time	Temp. (°C)	pH	Spec. Cond. (mS/cm)	Salinity	SRB (ppb)	FLT (ppb)
Seep 7 Cont.	1/9/2012	11:11 AM	28.1	7.32	7.80	4.0	1.26	6.102
	1/11/2012	10:55 AM	25.6	7.48	7.46	4.0	1.22	11.57
	1/13/2012	11:25 AM	27.7	7.44	7.95	4.1	1.43	11.75
	1/16/2012	1:04 PM	29.0	7.44	8.05	4.1		
	1/19/2012	10:12 AM	26.0	7.52	7.97	4.3	1.110	12.73
	1/21/2012	4:00 PM	29.9	7.55	8.38	4.2	1.892	13.40
	1/23/2012	11:30 AM	28.9	7.50	8.09	4.1	2.179	13.97
	1/25/2012	9:43 AM	25.9	7.58	7.55	4.1	1.672	15.05
	1/27/2012	12:20 PM	29.8	7.81	8.32	4.1	2.339	14.30
	1/31/2012	11:13 AM	28.5	7.47	8.00	4.1	1.481	15.18
	2/10/2012	12:06 AM	27.7	7.54	8.15	4.3	1.352	16.91
	2/14/2012	1:17 PM	30.3	7.45	8.48	4.2	1.583	18.57
	2/17/2012	11:20 AM	26.9	7.56	7.97	4.2	2.219	19.58
	2/20/2012	1:46 PM	28.4	7.66	8.15	4.3	1.812	20.23
	2/24/2012	11:03 AM	28.7	7.50	8.21	4.2	1.524	19.41
	2/27/2012	10:05 AM	26.3	7.62	7.83	4.2	1.667	21.07
3/1/2012	11:29 AM	26.4	7.67	7.99	4.3	1.222	21.44	
Seep 8	11/16/2011	9:35 AM	27.4	7.45	9.43	5.0	0.267	1.029
	11/23/2011	9:45 AM	26.4	7.26	7.79	4.2	-0.197	1.372
	11/25/2011	10:18 AM	28.3	7.20	8.39	4.3	0.060	1.448
	11/28/2011	9:53 AM	26.2	7.90	10.66	5.9	0.745	1.235
	11/30/2011	10:49 AM	26.9	7.29	7.61	4.0	0.395	2.147
	12/2/2011	9:54 AM	26.5	7.29	7.74	4.1	0.392	2.519
	12/5/2011	9:51 AM	29.3	7.26	8.04	4.1	0.318	2.885
	12/7/2011	9:54 AM	26.3	7.30	7.76	4.2	0.638	2.548
	12/9/2011	9:49 AM	24.8	7.34	7.47	4.1	0.421	3.738
	12/12/2011	9:52 AM	25.2	7.39	7.53	4.1	-0.046	4.244
	12/14/2011	9:44 AM	26.1	7.24	7.67	4.1	-0.022	4.769
	12/16/2011	9:50 AM	28.8	7.28	7.91	4.0	0.211	4.993
	12/19/2011	9:47 AM	26.9	7.32	7.76	4.1		
	12/21/2011	10:43 AM	26.3	7.09	7.85	4.2		
	12/23/2011	10:34 AM	25.6	7.30	7.81	4.2		
	12/26/2011	10:35 AM	28.0	7.29	8.24	4.3		
	12/28/2011	10:15 AM	30.0	7.30	8.61	4.3		
	12/30/2011	10:45 AM	28.9	7.33	8.99	4.6		
	1/2/2012	10:50 AM	28.8	7.85	37.88	22.0		
	1/4/2012	3:17 PM	28.6	7.42	8.51	4.4	1.01	10.17
1/7/2012	3:08 PM	28.5	7.39	8.36	4.3	1.26	10.90	
1/9/2012	10:36 AM	29.0	7.37	8.15	4.2	1.85	11.62	

Table A-4 Cont. Location	Date	Time	Temp. (°C)	pH	Spec. Cond. (mS/cm)	Salinity	SRB (ppb)	FLT (ppb)
Seep 8 Cont.	1/11/2012	10:33 AM	24.7	7.49	7.67	4.2	1.66	12.75
	1/13/2012	11:02 AM	26.5	7.16	7.85	4.2	1.69	12.82
	1/16/2012	12:47 PM	31.0	7.33	8.41	4.1		
Seep 9								
Seep 9	11/30/2011	9:27 AM	26.5	7.36	7.52	4.0	0.653	1.868
	12/2/2011	9:30 AM	25.8	7.31	7.67	4.2	0.818	2.063
	12/5/2011	9:39 AM	28.6	7.34	7.93	4.0	0.132	2.635
	12/7/2011	9:44 AM	27.4	7.39	7.52	3.9	0.431	2.750
	12/9/2011	9:28 AM	26.7	7.36	7.36	3.9	1.123	3.239
	12/12/2011	9:41 AM	24.8	7.47	7.21	4.0	-0.194	3.909
	12/14/2011	9:35 AM	27.7	7.30	7.66	4.0	0.371	4.623
	12/16/2011	9:37 AM	29.3	7.38	7.69	3.9	0.261	4.693
	12/19/2011	10:06 AM	26.8	7.35	7.64	4.1		
	12/21/2011	10:31 AM	26.2	6.75	7.59	4.0		
	12/23/2011	10:21 AM	23.3	7.32	7.26	4.1		
	12/26/2011	10:24 AM	27.4	7.37	7.75	4.0		
	12/28/2011	9:57 AM	28.1	7.31	7.90	4.1		
	12/30/2011	10:36 AM	28.0	7.42	8.22	4.2		
	1/2/2012	10:36 AM	28.5	7.67	24.95	14.0		
	1/4/2012	3:03 PM	29.5	7.63	10.12	5.2	0.98	8.646
	1/7/2012	2:58 PM	28.7	7.49	14.62	7.9	1.60	8.682
	1/9/2012	10:56 AM	28.8	7.31	8.14	4.2	0.99	10.20
	1/11/2012	10:45 AM	24.7	7.45	7.91	4.4	1.32	11.03
	1/13/2012	11:15 AM	26.2	7.52	28.10	16.8	0.87	6.834
	1/16/2012	1:16 PM	29.4	7.80	31.57	17.9		
1/19/2012	9:58 AM	26.0	7.65	9.59	5.3	1.319	11.94	
1/21/2012	4:13 PM	30.5	7.75	42.91	24.6	1.131	8.478	
1/23/2012	11:19 AM	28.6	7.65	42.77	25.3	0.487	4.683	
Seep 10								
Seep 10	1/21/2012	4:26 PM	29.0	7.75	9.73	5.0	1.450	12.53
	1/23/2012	11:03 AM	29.5	7.56	9.73	5.0	1.297	13.59
	1/25/2012	10:30 AM	27.7	7.38	8.25	4.3	2.073	14.45
	1/27/2012	12:34 PM	29.2	7.66	11.85	6.2	1.407	13.25
	1/31/2012	11:29 AM	27.6	7.52	8.53	4.4	1.493	15.99
	2/10/2012	11:30 AM	28.5	7.76	9.80	5.1	1.293	16.99
	2/14/2012	12:47 PM	29.5	7.26	8.37	4.2	1.723	18.45
	2/17/2012	11:05 AM	27.2	7.63	8.00	4.3	2.075	19.81
	2/20/2012	1:12 PM	28.4	7.66	8.31	4.3	1.473	20.50
	2/24/2012	10:51 AM	28.4	7.62	7.99	4.1	1.244	19.66
	2/27/2012	9:37 AM	26.7	7.67	9.65	5.2	1.088	18.69

Table A-4 Cont. Location	Date	Time	Temp. (°C)	pH	Spec. Cond. (mS/cm)	Salinity	SRB (ppb)	FLT (ppb)
Seep 10 Cont.	3/1/2012	11:18 AM	26.5	7.68	7.97	4.3	1.474	20.82
	6/29/2012	12:16 PM	34.6	7.31	8.35	4.6	1.458	20.36
	7/4/2012	12:34 PM	31.6	7.70	9.54	4.7	1.829	20.11
Seep 12	1/25/2012	11:24 AM	29.1	7.36	8.49	4.3	1.667	14.96
	1/27/2012	12:05 PM	29.6	7.78	8.44	4.3	1.219	14.67
	1/31/2012	11:41 AM	29.4	7.62	8.26	4.2	1.188	16.17
	2/10/2012	11:47 AM	27.5	7.63	8.23	4.4	0.833	17.42
	2/14/2012	1:02 PM	29.5	7.43	8.41	4.3	1.956	18.79
	2/17/2012	11:31 AM	27.4	7.61	8.03	4.2	1.983	19.39
	2/20/2012	1:25 PM	28.7	7.68	9.55	4.9	1.506	20.11
	2/24/2012	11:16 AM	27.5	7.56	8.07	4.2	1.356	20.69
	2/27/2012	10:32 AM	26.9	7.56	8.20	4.4	1.178	21.07
	3/1/2012	11:40 AM	28.6	7.60	9.28	4.8	1.166	21.12
	3/14/2012	10:21 AM	26.7	7.73	7.88	4.2		
	3/17/2012	9:36 AM	26.6	7.61	7.90	4.2	2.032	21.46
	3/19/2012	10:12 AM	29.0	7.67	8.13	4.1	2.017	22.35
Seep 13	3/14/2012	9:53 AM	26.0	7.71	7.69	4.2		
	3/17/2012	9:12 AM	29.7	7.69	8.74	4.4	2.320	21.67
	3/19/2012	9:46 AM	28.2	7.67	8.10	4.2	2.113	22.71
Seep 14	3/14/2012	10:11 AM	24.7	7.72	7.67	4.2		
	3/17/2012	9:23 AM	27.8	7.62	8.05	4.2	1.753	21.36
	3/19/2012	9:57 AM	28.7	7.66	8.02	4.1	2.036	22.67
Seep 15	3/27/2012	9:09 AM	25.6	7.63	8.68	4.8	0.982	21.34
	3/29/2012	10:28 AM	28.1	7.53	8.17	4.2	1.526	21.34
	4/2/2012	10:19 AM	27.1		16.54	9.3	2.393	18.51
	4/5/2012	8:27 AM	24.6	7.47	15.83	9.3	2.148	18.75
	4/12/2012	11:30 AM	31.1	7.48	8.45	4.2	1.769	22.14
	4/16/2012	9:09 AM	26.5	7.45	7.86	4.2	1.895	22.84
	4/19/2012	11:32 AM	31.6	7.61	8.79	4.3	1.524	21.77
	4/24/2012	3:25 PM	29.9	7.71	8.57	4.3	1.988	21.46
	4/26/2012	10:40 AM	30.3	7.72	8.46	4.2	1.959	21.81
	5/2/2012	9:42 AM	29.5	7.58	8.59	4.3	2.378	22.95
	5/7/2012	9:51 AM	29.8	7.59	8.56	4.3	2.392	23.63
	5/14/2012	9:22 AM	29.9	7.60	8.82	4.4	2.420	17.67
	5/18/2012	1:29 PM	34.8	7.75	10.20	4.7	0.811	8.22
5/22/2012	3:16 PM	33.2	7.44	9.56	4.5	2.048	24.17	

Table A-4 Cont. Location	Date	Time	Temp. (°C)	pH	Spec. Cond. (mS/cm)	Salinity	SRB (ppb)	FLT (ppb)
Seep 15 Cont.	5/25/2012	3:06 PM	34.2	7.55	9.58	4.4	2.196	24.05
	5/29/2012	2:18 PM	32.6	7.68	9.21	4.4	2.153	24.20
	6/4/2012	2:14 PM	33.7	7.61	9.88	4.7	2.448	22.47
	6/7/2012	12:30 PM	30.3	7.69	9.07	4.5	2.427	22.80
	6/12/2012	11:27 AM	34.9	7.40	9.79	4.5	1.740	18.70
	6/14/2012	2:43 PM	31.3	7.60	8.96	4.4	2.099	23.21
	6/16/2012	11:59 AM	31.0	7.48	9.32	4.6	2.108	22.49
	6/18/2012	9:43 AM	29.0	7.70	8.95	4.6	2.629	22.37
Seep 16	4/24/2012	3:11 PM	30.6	7.69	8.95	4.5	2.279	21.15
	4/26/2012	10:53 AM	30.4	7.71	8.79	4.4	2.108	22.33
	5/2/2012	9:32 AM	29.4	7.50	8.81	4.5	2.694	22.82
	5/7/2012	9:13 AM	27.1	7.59	8.57	4.6	2.409	23.79
	5/14/2012	9:02 AM	28.1	7.57	8.57	4.5	2.398	24.90
	5/18/2012	1:07 PM	34.8	7.68	9.79	4.5	1.960	20.72
	5/22/2012	3:06 PM	32.8	7.38	9.65	4.6	2.876	24.18
	5/25/2012	2:55 PM	34.6	7.48	9.86	4.6	2.541	24.11
	5/29/2012	2:32 PM	32.3	7.52	9.19	4.4	2.492	24.53
	6/4/2012	2:02 PM	33.3	7.62	10.05	4.8	2.036	22.63
	6/7/2012	12:19 PM	30.5	7.62	9.39	4.6	2.071	22.63
	6/12/2012	11:44 AM	34.7	7.39	9.74	4.5	2.567	22.66
	6/14/2012	2:27 PM	33.5	7.62	9.73	4.6	2.182	22.71
	6/16/2012	12:12 PM	32.2	7.46	9.47	4.6	2.259	23.25
	6/18/2012	9:07 AM	28.6	7.80	21.60	12.0	1.712	16.46
Seep 17	6/29/2012	12:38 PM	34.6	7.83	28.57	14.5	0.965	15.56
	7/11/2012	1:53 PM	35.0	7.63	26.60	13.3		
	7/23/2012	9:39 AM	29.0	7.53	12.33	6.5	2.060	16.67
Seep 18	7/11/2012	1:40 PM	33.4	7.52	9.79	4.6		
	7/23/2012	9:03 AM	28.9	7.59	9.08	4.7	1.376	17.63
	8/1/2012	9:20 AM	31.0	7.65	9.56	4.7	1.285	16.04
Seep 19	8/8/2012	1:54 PM	33.8	7.70	9.68	4.5	1.278	16.44
	8/16/2012	9:43 AM	31.2	7.73	9.64	4.8	1.174	15.40
	8/21/2012	9:09 AM	29.3	7.67	8.89	4.5	1.899	16.52
	8/24/2012	11:36 AM	32.2	7.64	8.99	4.3	1.797	16.32
	8/27/2012	9:11 AM	25.4	7.67	8.51	4.7	1.840	16.53
	9/6/2012	9:39 AM	33.1	7.70	9.43	4.5	1.657	14.52
	9/10/2012	12:51 PM	34.9	7.63	10.54	4.9	2.016	14.66

Table A-4 Cont. Location	Date	Time	Temp. (°C)	pH	Spec. Cond. (mS/cm)	Salinity	SRB (ppb)	FLT (ppb)
Seep 19	9/12/2012	9:01 AM	26.1	7.49	8.33	4.5	1.786	15.26
Seep 20	9/20/2012	11:44 AM	32.1	7.61	9.29	4.5	1.398	14.52
	10/2/2012	11:30 AM	29.7	7.63	9.60	4.9	1.545	13.84
	10/8/2012	2:08 PM	31.3	7.70	12.36	6.0	0.847	12.73
	10/12/2012	11:05 AM	30.6	7.72	21.35	11.3	1.434	10.21
	10/18/2012	11:19 AM	32.3	7.80	29.80	15.9	0.463	7.93
	10/22/2012	9:40 AM	28.2	7.61	13.64	7.3	0.315	11.13
	10/26/2012	10:42 AM	30.6	7.82	28.01	15.2	0.540	8.42
	10/29/2012	11:14 AM	31.6	7.75	26.35	14.0	0.512	8.79
	11/2/2012	2:51 PM	30.3	7.71	24.55	13.3	0.651	8.78
	11/8/2012	11:56 AM	30.1	7.74	23.57	12.9	0.547	8.48
	11/12/2012	11:09 AM	30.6	7.59	9.08	4.5	1.016	11.58
	11/19/2012	11:26 AM	30.0	7.60	9.53	4.8	1.937	11.56
	12/6/2012	10:50 AM	28.3	7.76	20.63	11.5	0.769	8.35
	12/10/2012	9:26 AM	25.7	7.73	17.40	10.1		
	12/14/2012	12:16 PM	29.3	7.63	12.75	6.7	1.010	9.79
	12/28/2012	12:59 PM	28.8	7.72	21.11	11.7	1.159	8.32
Seep 21	10/22/2012	9:09 AM	27.3	7.57	13.69	7.5	0.553	11.69
	10/26/2012	10:26 AM	30.5	7.63	9.27	4.7	0.960	11.97
	10/29/2012	11:02 AM	30.5	7.63	10.18	5.1	1.054	12.40
	11/2/2012	2:40 PM	30.6	7.55	9.64	4.8	0.825	12.16
	11/8/2012	11:43 AM	29.9	7.70	13.61	7.1	0.832	11.43

Table A-5. Water quality parameters collected from control locations (Honokowai Beach Park, Wahikuli Wayside Beach Park, and Olowalu). Parameters were measured with a handheld YSI Model 63 and field fluorescence measurements of S-Rhodamine-B (SRB) and Fluorescein (FLT) with a handheld Aquafluor fluorometer model 8000-10 from 8/5/2011 to 5/29/2012.

Location	Date	Time	Temp. (°C)	pH	Spec. Cond. (mS/cm)	Salinity	SRB (ppb)	FLT (ppb)
Honokowai Beach Park	8/5/2011	5:54 PM	26.4	8.13	54.60	35.1	-0.021	-0.192
	8/12/2011	5:26 PM	27.3	8.15	56.10	35.4	-0.064	0.046
	8/22/2011	3:25 PM	27.8	8.25	56.10	35.0	-0.227	0.145
	9/2/2011	2:00 PM	28.2	8.27	57.00	35.5	-0.606	0.068
	9/15/2011	12:00 PM	29.3	8.06	55.50	33.2	-0.731	-0.112
	9/26/2011	1:30 PM	28.8	8.00	56.80	34.7	-0.172	0.105
	10/14/2011	1:47 PM	28.3	8.10	56.40	34.4	0.118	0.048
	10/22/2011	1:00 PM	29.2	8.13	58.00	35.7	-0.238	-0.021
	11/14/2011	11:15 AM	27.1	7.90	52.10	32.7	-0.131	0.360
	11/25/2011	12:07 PM	27.2	8.06	51.40	32.3	-0.047	-0.227
	12/9/2011	12:05 PM	28.6	7.96	50.70	30.6	0.186	-0.127
	1/13/2012	3:15 PM	27.1	8.00	55.70	35.4	0.45	-0.655
	1/27/2012	4:34 PM	26.9	8.05	55.50	35.5	0.257	-0.543
	2/10/2012	3:34 PM	27.4	8.15	55.60	35.0	-0.501	-0.607
	2/17/2012	3:04 PM	27.2	8.06	51.30	32.1	0.271	-0.696
	2/24/2012	3:02 PM	27.6	8.10	56.80	35.7	0.263	-0.669
	3/1/2012	3:05 PM	30.3	7.98	51.00	29.9	-0.634	-0.685
	3/11/2012	2:30 PM	26.1	8.12	53.40	34.5	0.420	-0.179
	3/22/2012	3:00 PM	25.1	7.99	47.30	31.3	0.242	-0.612
	3/27/2012	2:30 PM	26.5	8.03	53.60	34.4	-0.708	-0.613
	4/5/2012	11:55 AM	25.4	7.95	52.80	34.5	-0.183	-0.835
	4/12/2012	2:18 PM	28.8	8.01	56.20	34.4	-0.231	-0.707
	4/19/2012	2:53 PM	26.3	8.02	52.90	33.9	-0.112	-0.799
5/2/2012	2:28 PM	26.8	7.99	54.00	34.1	0.339	-0.870	
5/18/2012	4:18 PM	25.6	7.98	53.60	33.0	0.445	-0.429	
5/29/2012	5:00 PM	27.6	8.02	48.77	30.1	0.148	-0.674	
Wahikuli Wayside Beach Park	8/5/2011	6:20 PM	25.9	8.16	55.10	35.8	-0.635	-0.635
	8/12/2011	5:50 PM	27.2	8.16	57.40	36.4	0.273	0.134
	8/22/2011	5:45 PM	27.8	8.00	56.40	34.8	-0.292	-0.047
	9/2/2011	1:30 PM	29.7	8.02	56.60	33.6	-0.339	0.247
	9/15/2011	12:00 PM	27.8	8.00	56.20	35.1	-0.747	0.106
	9/26/2011	2:00 PM	27.4	7.99	57.70	36.2	-0.190	0.221
	10/14/2011	2:13 PM	28.2	8.13	56.80	35.2	0.951	0.122
	10/22/2011	1:10 PM	27.9	8.15	57.40	36.1	0.071	-0.125
	11/14/2011	11:34 AM	26	7.89	54.40	35.2	0.548	0.000
	11/25/2011	12:26 PM	25.6	8.05	53.10	34.5	0.046	-0.161
12/9/2011	12:20 PM	25.3	8.03	52.30	34.5	-0.107	-0.270	

Table A-5 Continued Location	Date	Time	Temp. (°C)	pH	Spec. Cond. (mS/cm)	Salinity	SRB (ppb)	FLT (ppb)
	1/13/2012	3:30 PM	26.0	8.01	54.00	35.2	0.74	-0.70
	1/27/2012	4:51 PM	26.0	8.04	53.60	34.7	0.569	-0.486
	2/10/2012	3:50 PM	25.8	8.13	52.60	34.0	-0.894	-0.628
	2/17/2012	3:20 PM	24.9	8.10	54.00	35.4	0.005	-0.643
	2/24/2012	3:36 PM	27.5	8.08	55.00	34.4	-0.367	-0.187
	3/1/2012	3:28 PM	26.2	8.10	53.20	33.8	-0.466	-0.492
	3/11/2012	3:00 PM	26.0	8.10	53.50	34.1	-0.095	-0.501
	3/22/2012	3:30 PM	24.9	8.06	50.40	33.8	0.565	-0.843
	3/27/2012	2:48 PM	26.5	8.10	53.30	34.0	-1.244	-0.820
	4/5/2012	12:13 PM	25.2	8.04	52.80	34.4	-0.026	-0.851
	4/12/2012	2:37 PM	27.2	7.97	52.20	32.7	0.039	-0.772
	4/19/2012	3:13 PM	25.6	7.99	55.40	36.4	-0.820	-0.909
	5/2/2012	2:51 PM	25.7	7.98	55.00	35.7	0.192	-0.908
	5/18/2012	4:45 PM	26.9	8.00	55.90	35.7	0.199	-0.264
	5/29/2012	5:15 PM	25.7	7.99	53.80	35.4	0.785	-0.385
Olowalu	12/2/2011	8:00 AM	28.8	7.92	56.60	34.7	-0.173	-0.093
	12/9/2011	1:00 PM	24.8	8.03	54.70	36.3	0.252	-0.182
	1/13/2012	4:00 PM	27.6	7.99	48.14	29.5	0.48	-0.489
	1/27/2012	5:24 PM	28.4	8.03	54.50	33.5	0.648	-0.553
	2/10/2012	4:30 PM	25.3	8.11	53.00	34.6	-0.221	-0.585
	2/17/2012	4:00 PM	25.4	8.09	54.00	35.0	0.393	-0.269
	2/24/2012	4:19 PM	28.9	8.08	57.60	35.3	-0.784	-0.667
	3/1/2012	4:20 PM	30.0	8.12	55.90	33.4	-0.159	-0.888
	3/11/2012	3:35 PM	29.6	8.08	57.90	35.2	-0.057	-0.315
	3/22/2012	4:15 PM	26.0	8.05	58.30	36.3	0.138	-0.761
	3/27/2012	4:00 PM	29.9	8.13	57.10	34.1	-0.976	-0.737
	4/5/2012	1:06 PM	28.8	7.99	56.50	34.6	0.465	-0.435
	4/12/2012	3:51 PM	31.5	7.95	57.30	33.3	0.141	-0.779
	4/20/2012	12:02 PM	29.5	7.98	55.00	33.1	-0.535	-0.839
	5/2/2012	3:42 PM	26.4	7.95	55.80	35.8	0.892	-0.567
	5/19/2012	11:46 AM	29.9	7.99	55.50	33.1	0.823	-0.351

Table A-6. Submarine Spring, Shoreline Survey, and SVO Well Sampling Results. Survey area, coordinates, collection method, submarine spring (seep) measurements and area, Fluorescein (FLT) and S-Rhodamine-B (SRB) concentrations, specific conductivity, substrate, and additional observations are provided here (arranged by date) for the submarine spring survey as well as additional coastal and well water samples. Also provided here is the adjusted FLT concentrations based on the specific conductivity of the water sample. Seep locations used for tracer dye monitoring are italicized. Survey area abbreviations are as follows: Honokowai Point (HP), Honua Kai (HK), Kahekili Reef (KR), South of Kahekili Reef (S. KR), and the Westin Resort (WR). NA = not applicable; ----- = no data.

Sample Name	Survey Area	Sampling Date	Analysis Date	Latitude	Longitude	Collection Method	Seep Length (cm)	Seep Width (cm)	Seep Area (cm ²)	FLT	SRB	Spec. Cond.	Adj. FLT	Substrate	Additional Observations
31	HP	7/9/12	08/24/12	N20.95005	W156.69180	Grab	No Visible Seep		NA	0.06	0.00	50,030	0.72	Basalt	Shimmery water
24	HP	7/9/12	08/24/12	N20.94952	W156.69329	Grab	No Visible Seep		NA	0.06	0.02	52,110	1.69	Basalt	Shimmery water
28	HK	7/9/12	08/24/12	N20.94754	W156.69361	Grab	No Visible Seep		NA	0.06	0.02	50,790	0.83	Surface Water	Shimmery water
6	HK	7/9/12	08/24/12	N20.93861	W156.69319	Grab	No Visible Seep		NA	0.06	0.02	50,800	0.92	Surface Water	Shimmery water
8	NSG KR	7/10/12		N20.94035	W156.69297	Syringe	5.2	2.0	10.4	5.04	-----	37,820	15.0	Dead Coral	
11	NSG KR	7/10/12	08/24/12	N20.94032	W156.69296	Syringe	24.0	9.0	216.0	3.40	0.02	42,830	14.9	Dead Coral	
48	NSG KR	7/10/12	08/24/12	N20.93610	W156.69302	Grab	-----	-----	-----	0.07	0.03	50,530	0.88	Sand	Diffuse discharge
12	NSG KR	7/12/12	08/03/12	N20.93976	W156.69294	Syringe	4.0	1.0	4.0	5.31	0.01	49,652	64.6	Dead Coral	
13	NSG KR	7/12/12	08/24/12	N20.93976	W156.69294	Syringe	3.0	4.0	12.0	4.86	0.01	42,900	21.5	Dead Coral	

Table A-6 Cont.	Survey Area	Sampling Date	Analysis Date	Latitude	Longitude	Collection Method	Seep Length (cm)	Seep Width (cm)	Seep Area (cm²)	FLT	SRB	Spec. Cond.	Adj. FLT	Substrate	Additional Observations
16	NSG KR	7/12/12	08/24/12	N20.93976	W156.69294	Syringe	4.0	1.0	4.0	9.98	0.03	35,050	25.3	Basalt / Sand	
20	NSG KR	7/12/12	08/24/12	N20.93976	W156.69294	Syringe	1.5	1.0	1.5	4.92	0.03	42,020	20.1	Basalt	
23	NSG KR	7/12/12	07/25/12	N20.93976	W156.69294	Syringe	6.0	1.0	6.0	1.99	-----	48,800	19.8	Basalt	
25	NSG KR	7/12/12	07/25/12	N20.93976	W156.69294	Syringe	1.0	1.0	1.0	7.69	-----	39,500	25.7	Dead Coral	
27	NSG KR	7/12/12	08/24/12	N20.93976	W156.69294	Syringe	5.2	0.5	2.6	7.17	0.03	39,480	24.0	Basalt / Sand	
37	NSG KR	7/12/12	08/24/12	N20.93976	W156.69294	Syringe	11.0	1.5	16.5	6.14	0.02	39,590	20.7	Basalt	
42	NSG KR	7/12/12	08/24/12	N20.93976	W156.69294	Syringe	6.2	3.2	19.8	3.32	0.03	-----	2.90	Dead Coral	
43	NSG KR	7/12/12	08/24/12	N20.93976	W156.69294	Syringe	4.2	2.5	10.5	4.94	0.04	42,940	21.9	Dead Coral	
47	NSG KR	7/12/12	08/24/12	N20.93976	W156.69294	Syringe	8.1	0.5	4.1	8.42	0.04	37,570	24.8	Basalt / Sand	
49	NSG KR	7/12/12	08/24/12	N20.93976	W156.69294	Syringe	2.0	1.0	2.0	12.1	0.03	27,210	21.6	Dead Coral / Sand	
40	NSG KR	7/12/12	08/24/12	N20.93973	W156.69294	Syringe	2.0	3.0	6.0	0.54	0.02	49,550	6.25	Dead Coral	
3	NSG KR	7/12/12	08/24/12	N20.93976	W156.69297	Syringe	1.0	2.0	2.0	13.4	0.05	28,600	25.2	Dead Coral	
5	NSG KR	7/12/12	08/24/12	N20.93976	W156.69297	Syringe	0.5	0.5	0.3	2.21	0.03	46,920	15.7	Sand	

Table A-6 Cont.	Survey Area	Sampling Date	Analysis Date	Latitude	Longitude	Collection Method	Seep Length (cm)	Seep Width (cm)	Seep Area (cm²)	FLT	SRB	Spec. Cond.	Adj. FLT	Substrate	Additional Observations
9	NSG KR	7/12/12	08/03/12	N20.93976	W156.69297	Syringe	4.0	5.0	20.0	3.94	0.02	45,247	22.3	Dead Coral	Green tint
10	NSG KR	7/12/12	08/03/12	N20.93976	W156.69297	Syringe	3.0	6.0	18.0	1.72	0.01	48,455	15.9	Dead Coral	
14	NSG KR	7/12/12	08/24/12	N20.93976	W156.69297	Syringe	2.0	2.0	4.0	3.26	0.03	45,720	19.6	Dead Coral	
15	NSG KR	7/12/12	07/25/12	N20.93976	W156.69297	Syringe	1.0	1.0	1.0	1.94	-----	49,150	20.8	Sand	
18	NSG KR	7/12/12	07/25/12	N20.93976	W156.69297	Syringe	1.0	0.5	0.5	5.36	-----	43,600	25.3	Sand	
21	NSG KR	7/12/12	08/24/12	N20.93976	W156.69297	Syringe	4.0	5.0	20.0	2.64	0.01		2.31	Dead Coral	
22	NSG KR	7/12/12	08/24/12	N20.93976	W156.69297	Syringe	7.0	4.0	28.0	3.64	0.02	44,990	20.0	Dead Coral	
32	NSG KR	7/12/12	08/24/12	N20.93976	W156.69297	Syringe	1.0	2.0	2.0	9.20	0.04	35,530	24.0	Dead Coral	
34	NSG KR	7/12/12	08/24/12	N20.93976	W156.69297	Syringe	1.0	1.0	1.0	6.50	0.03	40,240	23.0	Sand	
39	NSG KR	7/12/12	08/24/12	N20.93976	W156.69297	Syringe	3.0	3.0	9.0	3.24	0.02	46,800	22.6	Dead Coral	
41	NSG KR	7/12/12	08/24/12	N20.93976	W156.69297	Syringe	2.0	2.0	4.0	7.86	0.03	36,360	21.5	Dead Coral	
44	NSG KR	7/12/12	07/25/12	N20.93976	W156.69297	Syringe	4.0	2.0	8.0	9.01	-----	37,300	26.1	Dead Coral	
46	NSG KR	7/12/12	08/24/12	N20.93976	W156.69297	Syringe	3.0	2.0	6.0	2.93	0.04	46,140	18.6	Dead Coral	

Table A-6 Cont.	Survey Area	Sampling Date	Analysis Date	Latitude	Longitude	Collection Method	Seep Length (cm)	Seep Width (cm)	Seep Area (cm²)	FLT	SRB	Spec. Cond.	Adj. FLT	Substrate	Additional Observations
35	NSG KR	7/12/12	08/24/12	N20.93981	W156.69296	Syringe	3.0	8.0	24.0	2.73	0.02	46,760	18.9	Dead Coral	Green tint
74	NSG KR	7/12/12	08/24/12	N20.93979	W156.69295	Syringe	1.0	1.0	1.0	6.22	0.04	41,980	25.3	Basalt / Sand	
NA	NSG KR	7/12/12	----	N20.93979	W156.69295	----	2.0	1.0	2.0	----	----	----	----	Dead Coral	
NA	NSG KR	7/12/12	----	N20.93979	W156.69295	----	2.0	3.0	6.0	----	----	----	----	Dead Coral	
NA	NSG KR	7/12/12	----	N20.93979	W156.69295	----	3.0	0.5	1.5	----	----	----	----	Dead Coral	
NA	NSG KR	7/12/12	----	N20.93979	W156.69295	----	4.0	1.0	4.0	----	----	----	----	Dead Coral	
71	NSG KR	7/12/12	08/24/12	N20.93979	W156.69293	Syringe	2.0	2.0	4.0	1.54	0.02	48,670	14.9	Sand	Sand volcano
NA	NSG KR	7/12/12	----	N20.93979	W156.69293	----	1.0	1.0	1.0	----	----	----	----	Dead Coral	
NA	NSG KR	7/12/12	----	N20.93979	W156.69293	----	2.0	1.5	3.0	----	----	----	----	Basalt / Sand	
NA	NSG KR	7/12/12	----	N20.93979	W156.69293	----	2.0	1.0	2.0	----	----	----	----	Dead Coral	
NA	NSG KR	7/12/12	----	N20.93979	W156.69293	----	4.0	1.5	6.0	----	----	----	----	Dead Coral	
69	NSG KR	7/12/12	08/24/12	N20.93981	W156.69301	Syringe	4.0	4.0	16.0	6.16	0.03	41,890	24.8	Dead Coral	Green tint
53	NSG KR	7/12/12	08/24/12	N20.93979	W156.69301	Syringe	2.5	1.5	3.8	5.28	0.05	38,470	16.4	Dead Coral	Green tint

Table A-6 Cont.	Survey Area	Sampling Date	Analysis Date	Latitude	Longitude	Collection Method	Seep Length (cm)	Seep Width (cm)	Seep Area (cm²)	FLT	SRB	Spec. Cond.	Adj. FLT	Substrate	Additional Observations
NA	NSG KR	7/12/12	----	N20.93979	W156.69301	----	2.0	0.5	1.0	----	----	----	----	Dead Coral	
NA	NSG KR	7/12/12	----	N20.93979	W156.69301	----	3.0	1.0	3.0	----	----	----	----	Dead Coral	
72	NSG KR	7/12/12	08/24/12	N20.93981	W156.69293	Syringe	11.0	0.5	5.5	4.18	0.02	44,640	22.1	Basalt / Sand	
NA	NSG KR	7/12/12	----	N20.93981	W156.69293	----	4.0	0.5	2.0	----	----	----	----	Dead Coral	
64	NSG KR	7/12/12	08/24/12	N20.93983	W156.69299	Syringe	4.0	2.0	8.0	4.61	0.02	43,540	21.7	Dead Coral	
NA	NSG KR	7/12/12	----	N20.93983	W156.69299	----	5.0	1.0	5.0	----	----	----	----	Dead Coral	
38	NSG KR	7/12/12	07/25/12	N20.93982	W156.69297	Syringe	2.0	2.0	4.0	17.7	----	20,630	25.2	Dead Coral	
NA	NSG KR	7/12/12	----	N20.93982	W156.69297	----	1.0	1.0	1.0	----	----	----	----	Dead Coral	
NA	NSG KR	7/12/12	----	N20.93982	W156.69297	----	2.0	1.0	2.0	----	----	----	----	Dead Coral	
NA	NSG KR	7/12/12	----	N20.93982	W156.69297	----	2.5	1.0	2.5	----	----	----	----	Dead Coral	
NA	NSG KR	7/12/12	----	N20.93982	W156.69297	----	3.0	2.0	6.0	----	----	----	----	Dead Coral	
NA	NSG KR	7/12/12	----	N20.93982	W156.69297	----	4.0	0.5	2.0	----	----	----	----	Dead Coral	
70	NSG KR	7/12/12	08/24/12	N20.93984	W156.69299	Syringe	8.0	6.0	48.0	3.34	0.02	45,910	20.6	Dead Coral	Green tint

Table A-6 Cont.	Survey Area	Sampling Date	Analysis Date	Latitude	Longitude	Collection Method	Seep Length (cm)	Seep Width (cm)	Seep Area (cm²)	FLT	SRB	Spec. Cond.	Adj. FLT	Substrate	Additional Observations
58	NSG KR	7/12/12	08/24/12	N20.93985	W156.69295	Syringe	2.0	2.0	4.0	1.56	0.03	49,050	16.3	Dead Coral	
NA	NSG KR	7/12/12	----	N20.93985	W156.69295	----	1.0	1.0	1.0	----	----	----	----	Dead Coral	
NA	NSG KR	7/12/12	----	N20.93985	W156.69295	----	1.0	1.0	1.0	----	----	----	----	Dead Coral	
NA	NSG KR	7/12/12	----	N20.93985	W156.69295	----	3.0	1.0	3.0	----	----	----	----	Dead Coral	
56	NSG KR	7/12/12	08/24/12	N20.93982	W156.69294	Syringe	8.0	0.5	4.0	7.10	0.03	39,460	23.7	Basalt / Sand	
NA	NSG KR	7/12/12	----	N20.93982	W156.69294	----	1.0	1.0	1.0	----	----	----	----	Basalt / Sand	
NA	NSG KR	7/12/12	----	N20.93982	W156.69294	----	1.0	1.0	1.0	----	----	----	----	Basalt / Sand	
NA	NSG KR	7/12/12	----	N20.93982	W156.69294	----	1.0	1.0	1.0	----	----	----	----	Basalt / Sand	
NA	NSG KR	7/12/12	----	N20.93982	W156.69294	----	5.0	0.5	2.5	----	----	----	----	Basalt / Sand	
52	NSG KR	7/12/12	08/24/12	N20.93987	W156.69296	Syringe	4.0	2.0	8.0	2.97	0.03	46,350	19.4	Dead Coral	
NA	NSG KR	7/12/12	----	N20.93987	W156.69296	----	4.0	2.0	8.0	----	----	----	----	Dead Coral	
NA	NSG KR	7/12/12	----	N20.93987	W156.69296	----	4.0	2.0	8.0	----	----	----	----	Dead Coral	
NA	NSG KR	7/12/12	----	N20.93987	W156.69296	----	5.0	3.0	15.0	----	----	----	----	Dead Coral	

Table A-6 Cont.	Survey Area	Sampling Date	Analysis Date	Latitude	Longitude	Collection Method	Seep Length (cm)	Seep Width (cm)	Seep Area (cm²)	FLT	SRB	Spec. Cond.	Adj. FLT	Substrate	Additional Observations
NA	NSG KR	7/12/12	----	N20.93987	W156.69296	----	9.0	6.0	54.0	----	----	----	----	Dead Coral	
54	NSG KR	7/12/12	08/24/12	N20.93988	W156.69302	Syringe	16.0	13.0	208.0	2.27	0.02	48,560	21.5	Dead Coral	Green tint
NA	NSG KR	7/12/12	----	N20.93988	W156.69302	----	1.0	1.0	1.0	----	----	----	----	Dead Coral	
NA	NSG KR	7/12/12	----	N20.93988	W156.69302	----	2.0	1.5	3.0	----	----	----	----	Dead Coral	
57	NSG KR	7/12/12	08/24/12	N20.93984	W156.69293	Syringe	10.0	0.5	5.0	4.59	0.04	43,650	21.8	Basalt / Sand	
NA	NSG KR	7/12/12	----	N20.93984	W156.69293	----	7.0	1.0	7.0	----	----	----	----	Basalt / Sand	
63	NSG KR	7/12/12	08/24/12	N20.93988	W156.69301	Syringe	2.0	4.0	8.0	4.31	0.03	44,140	21.5	Dead Coral	
NA	NSG KR	7/12/12	----	N20.93988	W156.69301	----	1.0	0.5	0.5	----	----	----	----	Dead Coral	
36	NSG KR	7/12/12	08/24/12	N20.93986	W156.69296	Syringe	7.0	2.0	14.0	3.10	0.02	46,200	19.9	Dead Coral	
61	NSG KR	7/12/12	08/24/12	N20.93992	W156.69300	Syringe	1.5	4.0	6.0	4.53	0.03	44,480	23.5	Dead Coral	Green tint
NA	NSG KR	7/12/12	----	N20.93992	W156.69300	----	2.0	1.0	2.0	----	----	----	----	Dead Coral	
NA	NSG KR	7/12/12	----	N20.93992	W156.69300	----	2.0	1.0	2.0	----	----	----	----	Dead Coral	
NA	NSG KR	7/12/12	----	N20.93992	W156.69300	----	2.0	1.0	2.0	----	----	----	----	Dead Coral	

Table A-6 Cont.	Survey Area	Sampling Date	Analysis Date	Latitude	Longitude	Collection Method	Seep Length (cm)	Seep Width (cm)	Seep Area (cm²)	FLT	SRB	Spec. Cond.	Adj. FLT	Substrate	Additional Observations
19	NSG KR	7/12/12	07/25/12	N20.93988	W156.69295	Syringe	3.5	1.0	3.5	2.52	-----	48,400	23.1	Dead Coral	
51	NSG KR	7/12/12	08/24/12	N20.93991	W156.69296	Syringe	4.0	4.0	16.0	3.41	0.03	45,650	20.3	Dead Coral	
55	NSG KR	7/12/12	08/24/12	N20.93990	W156.69293	Syringe	2.5	2.0	5.0	14.3	0.04		12.5	Dead Coral	Green tint
68	NSG KR	7/13/12	08/24/12	N20.93989	W156.69296	Syringe	7.0	7.0	49.0	1.64	0.02	48,800	16.3	Dead Coral	
NA	NSG KR	7/13/12	-----	N20.93989	W156.69296	-----	3.0	5.0	15.0	-----	-----	-----	-----	Dead Coral	
85	NSG KR	7/13/12	07/25/12	N20.93987	W156.69292	Syringe	5.0	4.0	20.0	6.19	-----	41,920	25.0	Dead Coral	
NA	NSG KR	7/13/12	-----	N20.93987	W156.69292	-----	3.0	2.0	6.0	-----	-----	-----	-----	Dead Coral	
NA	NSG KR	7/13/12	-----	N20.93987	W156.69292	-----	6.0	2.0	12.0	-----	-----	-----	-----	Sand	
NA	NSG KR	7/13/12	-----	N20.93987	W156.69292	-----	6.0	2.0	12.0	-----	-----	-----	-----	Dead Coral / Sand	
84	NSG KR	7/13/12	08/24/12	N20.93990	W156.69293	Syringe	1.0	0.5	0.5	6.06	0.03	40,703	22.2	Dead Coral	
NA	NSG KR	7/13/12	-----	N20.93990	W156.69293	-----	1.0	0.5	0.5	-----	-----	-----	-----	Dead Coral	
NA	NSG KR	7/13/12	-----	N20.93990	W156.69293	-----	2.0	0.5	1.0	-----	-----	-----	-----	Basalt / Sand	
NA	NSG KR	7/13/12	-----	N20.93990	W156.69293	-----	2.5	1.0	2.5	-----	-----	-----	-----	Dead Coral	

Table A-6 Cont.	Survey Area	Sampling Date	Analysis Date	Latitude	Longitude	Collection Method	Seep Length (cm)	Seep Width (cm)	Seep Area (cm²)	FLT	SRB	Spec. Cond.	Adj. FLT	Substrate	Additional Observations
NA	NSG KR	7/13/12	----	N20.93990	W156.69293	----	4.0	0.5	2.0	----	----	----	----	Basalt / Sand	
NA	NSG KR	7/13/12	----	N20.93990	W156.69293	----	7.0	1.0	7.0	----	----	----	----	Dead Coral	
83	NSG KR	7/13/12	07/25/12	N20.93991	W156.69297	Syringe	1.0	1.0	1.0	5.47	----	43,400	25.4	Dead Coral	
NA	NSG KR	7/13/12	----	N20.93991	W156.69297	----	1.0	1.0	1.0	----	----	----	----	Dead Coral	
NA	NSG KR	7/13/12	----	N20.93991	W156.69297	----	1.0	1.0	1.0	----	----	----	----	Dead Coral	
NA	NSG KR	7/13/12	----	N20.93991	W156.69297	----	2.0	1.0	2.0	----	----	----	----	Dead Coral	
NA	NSG KR	7/13/12	----	N20.93991	W156.69297	----	2.0	2.0	4.0	----	----	----	----	Dead Coral	
80	NSG KR	7/13/12	08/24/12	N20.93992	W156.69300	Syringe	11.0	4.0	44.0	5.34	0.03	42,900	23.6	Dead Coral	
NA	NSG KR	7/13/12	----	N20.93992	W156.69300	----	0.5	0.5	0.3	----	----	----	----	Dead Coral	
NA	NSG KR	7/13/12	----	N20.93992	W156.69300	----	1.0	0.5	0.5	----	----	----	----	Dead Coral	
NA	NSG KR	7/13/12	----	N20.93992	W156.69300	----	1.0	1.0	1.0	----	----	----	----	Dead Coral	
NA	NSG KR	7/13/12	----	N20.93992	W156.69300	----	1.0	1.0	1.0	----	----	----	----	Dead Coral	
NA	NSG KR	7/13/12	----	N20.93992	W156.69300	----	2.0	1.0	2.0	----	----	----	----	Dead Coral	

Table A-6 Cont.	Survey Area	Sampling Date	Analysis Date	Latitude	Longitude	Collection Method	Seep Length (cm)	Seep Width (cm)	Seep Area (cm²)	FLT	SRB	Spec. Cond.	Adj. FLT	Substrate	Additional Observations
NA	NSG KR	7/13/12	----	N20.93992	W156.69300	----	3.0	1.0	3.0	----	----	----	----	Dead Coral	
60	NSG KR	7/13/12	08/24/12	N20.93994	W156.69287	Grab	2.0	1.5	3.0	0.17	0.03	50,810	2.82	Basalt / Sand	Diffuse discharge
NA	NSG KR	7/13/12	----	N20.93994	W156.69287	----	9.0	0.5	4.5	----	----	----	----	Basalt / Sand	Diffuse discharge
76	NSG KR	7/13/12	08/24/12	N20.94013	W156.69290	Syringe	5.0	4.0	20.0	10.6	0.04	30,800	21.9	Basalt / Sand	
NA	NSG KR	7/13/12	----	N20.94013	W156.69290	----	2.0	1.0	2.0	----	----	----	----	Basalt / Sand	
NA	NSG KR	7/13/12	----	N20.94013	W156.69290	----	5.0	0.5	2.5	----	----	----	----	Basalt / Sand	
NA	NSG KR	7/13/12	----	N20.94013	W156.69290	----	7.0	0.5	3.5	----	----	----	----	Basalt / Sand	
2	NSG KR	7/13/12	08/24/12	N20.94017	W156.69292	Syringe	3.0	1.0	3.0	2.64	0.02	46,570	17.8	Sand	Sand volcano
66	NSG KR	7/13/12	08/24/12	N20.94017	W156.69292	Syringe	6.0	3.0	18.0	2.12	0.02	47,590	16.7	Basalt	
75	NSG KR	7/13/12	08/24/12	N20.94017	W156.69292	Syringe	9.0	4.0	36.0	2.84	0.03	45,990	17.7	Basalt	
65	NSG KR	7/13/12	08/24/12	N20.94012	W156.69287	Syringe	3.0	3.0	9.0	20.5	0.05	8,670	21.4	Basalt / Sand	
86	NSG KR	7/13/12	08/24/12	N20.94012	W156.69287	Syringe	2.0	2.0	4.0	14.7	0.04	21,650	21.6	Basalt / Sand	
NA	NSG KR	7/13/12	----	N20.94012	W156.69287	----	0.5	0.5	0.3	----	----	----	----	Basalt / Sand	

Table A-6 Cont.	Survey Area	Sampling Date	Analysis Date	Latitude	Longitude	Collection Method	Seep Length (cm)	Seep Width (cm)	Seep Area (cm²)	FLT	SRB	Spec. Cond.	Adj. FLT	Substrate	Additional Observations
NA	NSG KR	7/13/12	----	N20.94012	W156.69287	----	0.5	0.5	0.3	----	----	----	----	Basalt / Sand	
NA	NSG KR	7/13/12	----	N20.94012	W156.69287	----	1.0	0.5	0.5	----	----	----	----	Basalt / Sand	
NA	NSG KR	7/13/12	----	N20.94012	W156.69287	----	1.0	0.5	0.5	----	----	----	----	Basalt / Sand	
NA	NSG KR	7/13/12	----	N20.94012	W156.69287	----	3.0	1.0	3.0	----	----	----	----	Basalt / Sand	
79	NSG KR	7/13/12	08/24/12	N20.94015	W156.69288	Syringe	0.5	0.5	0.3	15.0	0.04	20,260	21.2	Basalt	
NA	NSG KR	7/13/12	----	N20.94015	W156.69288	----	0.2	0.2	0.04	----	----	----	----	Basalt	
NA	NSG KR	7/13/12	----	N20.94015	W156.69288	----	0.5	0.5	0.3	----	----	----	----	Basalt	
NA	NSG KR	7/13/12	----	N20.94015	W156.69288	----	1.0	1.0	1.0	----	----	----	----	Basalt	
59	NSG KR	7/13/12	08/24/12	N20.94016	W156.69288	Syringe	2.0	2.0	4.0	2.25	0.03	47,340	17.1	Sand	Sand volcano
33	NSG KR	7/13/12	08/24/12	N20.94019	W156.69282	Syringe	7.0	2.5	17.5	19.8	0.05	7,910	20.4	Basalt / Sand	
45 <i>Seep 18</i>	NSG KR	7/13/12	08/24/12	N20.94019	W156.69282	Syringe	9.0	2.0	18.0	17.9	0.06	8,160	18.5	Basalt / Sand	
77	NSG KR	7/13/12	08/24/12	N20.94019	W156.69282	Syringe	6.0	9.0	54.0	5.93	0.03		5.19	Sand	Sand volcano
81 <i>Seep 17</i>	NSG KR	7/13/12	08/24/12	N20.94019	W156.69282	Syringe	5.0	4.0	20.0	5.44	0.03	40,710	19.9	Sand	Sand volcano
NA	NSG KR	7/13/12	----	N20.94019	W156.69282	----	2.0	0.5	1.0	----	----	----	----	Basalt / Sand	

Table A-6 Cont.	Survey Area	Sampling Date	Analysis Date	Latitude	Longitude	Collection Method	Seep Length (cm)	Seep Width (cm)	Seep Area (cm²)	FLT	SRB	Spec. Cond.	Adj. FLT	Substrate	Additional Observations
NA	NSG KR	7/13/12	----	N20.94019	W156.69282	----	2.0	1.0	2.0	----	----	----	----	Sand	Sand volcano
NA	NSG KR	7/13/12	----	N20.94019	W156.69282	----	4.0	3.0	12.0	----	----	----	----	Sand	Sand volcano
NA	NSG KR	7/13/12	----	N20.94019	W156.69282	----	6.0	1.0	6.0	----	----	----	----	Basalt / Sand	
4	NSG KR	7/13/12	08/24/12	N20.94017	W156.69284	Syringe	0.5	0.5	0.3	1.40	0.02	48,790	13.8	Basalt	
62	NSG KR	7/13/12	08/24/12	N20.94017	W156.69284	Syringe	2.0	1.5	3.0	3.92	0.03	43,740	18.8	Basalt	
73	NSG KR	7/13/12	08/24/12	N20.94017	W156.69284	Syringe	3.0	2.0	6.0	4.36	0.03	43,000	19.4	Basalt	
NA	NSG KR	7/13/12	----	N20.94017	W156.69284	----	0.2	0.2	0.04	----	----	----	----	Basalt	
NA	NSG KR	7/13/12	----	N20.94017	W156.69284	----	0.5	0.5	0.3	----	----	----	----	Basalt	
NA	NSG KR	7/13/12	----	N20.94017	W156.69284	----	0.5	0.5	0.3	----	----	----	----	Basalt	
NA	NSG KR	7/13/12	----	N20.94017	W156.69284	----	0.5	0.5	0.3	----	----	----	----	Sand	Sand volcano
NA	NSG KR	7/13/12	----	N20.94017	W156.69284	----	0.5	0.5	0.3	----	----	----	----	Sand	
NA	NSG KR	7/13/12	----	N20.94017	W156.69284	----	2.0	1.0	2.0	----	----	----	----	Sand	
NA	NSG KR	7/13/12	----	N20.94017	W156.69284	----	2.0	2.0	4.0	----	----	----	----	Sand	
NA	NSG KR	7/13/12	----	N20.94017	W156.69284	----	2.0	1.0	2.0	----	----	----	----	Sand	

Table A-6 Cont.	Survey Area	Sampling Date	Analysis Date	Latitude	Longitude	Collection Method	Seep Length (cm)	Seep Width (cm)	Seep Area (cm²)	FLT	SRB	Spec. Cond.	Adj. FLT	Substrate	Additional Observations
NA	NSG KR	7/13/12	----	N20.94017	W156.69284	----	2.0	0.5	1.0	----	----	----	----	Basalt	
NA	NSG KR	7/13/12	----	N20.94017	W156.69284	----	3.0	1.0	3.0	----	----	----	----	Basalt	
NA	NSG KR	7/13/12	----	N20.94017	W156.69284	----	4.0	1.0	4.0	----	----	----	----	Sand	
NA	NSG KR	7/13/12	----	N20.94017	W156.69284	----	5.0	2.0	10.0	----	----	----	----	Basalt	
17	NSG KR	7/13/12	08/24/12	N20.94017	W156.69283	Syringe	1.0	1.0	1.0	7.02	0.03	37,530	20.6	Sand	Sand volcano
67	NSG KR	7/13/12	08/24/12	N20.94017	W156.69283	Syringe	4.0	3.0	12.0	3.83	0.03	43,850	18.6	Sand	Sand volcano
78	NSG KR	7/13/12	08/24/12	N20.94017	W156.69283	Syringe	5.0	5.0	25.0	5.15	0.03	41,390	19.9	Basalt	
82	NSG KR	7/13/12	08/24/12	N20.94017	W156.69283	Syringe	3.0	3.0	9.0	9.18	0.03	32,970	20.9	Sand	Sand volcano
NA	NSG KR	7/13/12	----	N20.94017	W156.69283	----	3.0	1.0	3.0	----	----	----	----	Sand	Sand volcano
NA	NSG KR	7/13/12	----	N20.94017	W156.69283	----	3.0	1.0	3.0	----	----	----	----	Dead Coral / Sand	
NA	NSG KR	7/13/12	----	N20.94017	W156.69283	----	3.0	1.0	3.0	----	----	----	----	Dead Coral / Sand	
NA	NSG KR	7/13/12	----	N20.94017	W156.69283	----	4.0	1.0	4.0	----	----	----	----	Sand	Sand volcano
NA	NSG KR	7/13/12	----	N20.94017	W156.69283	----	8.0	2.0	16.0	----	----	----	----	Dead Coral	

Table A-6 Cont.	Survey Area	Sampling Date	Analysis Date	Latitude	Longitude	Collection Method	Seep Length (cm)	Seep Width (cm)	Seep Area (cm²)	FLT	SRB	Spec. Cond.	Adj. FLT	Substrate	Additional Observations
91	NSG KR	7/19/12	07/25/12	N20.94017	W156.69283	Syringe	-----	-----	-----	0.59	-----	51,279	12.2	Surface Water	NSG Control
7	SSG KR	7/13/12	07/25/12	N20.93852	W156.69309	Syringe	4.0	1.0	4.0	2.79	-----	48,300	25.1	Basalt / Sand	
NA	SSG KR	7/13/12	-----	N20.93852	W156.69309	-----	8.0	0.5	4.0	-----	-----	-----	-----	Basal / Sand	Diffuse discharge
26	SSG KR	7/13/12	08/24/12	N20.93861	W156.69318	Syringe	3.0	1.0	3.0	21.0	0.05	13,490	24.6	Dead Coral	Green tint
29 <i>Seep 5</i>	SSG KR	7/13/12	08/24/12	N20.93861	W156.69318	Syringe	8.0	4.0	32.0	15.7	0.05	25,660	26.4	Dead Coral	Green tint
50	SSG KR	7/13/12	08/24/12	N20.93861	W156.69318	Syringe	10.5	6.0	63.0	22.3	0.06	9,540	23.8	Dead Coral	Green tint
90	SSG KR	7/13/12	08/03/12	N20.93861	W156.69318	Syringe	2.0	3.5	7.0	19.9	0.04	16,590	25.3	Dead Coral	
92	SSG KR	7/13/12	08/03/12	N20.93861	W156.69318	Syringe	6.0	2.0	12.0	14.5	0.03	28,477	27.2	Dead Coral	Green tint
93	SSG KR	7/13/12	08/03/12	N20.93861	W156.69318	Syringe	4.0	1.0	4.0	10.7	0.03	35,450	27.8	Dead Coral	Green tint
99	SSG KR	7/13/12	07/25/12	N20.93861	W156.69318	Syringe	3.5	1.0	3.5	11.0	-----	35,247	28.2	Dead Coral	Green tint
102	SSG KR	7/13/12	08/03/12	N20.93861	W156.69318	Syringe	3.0	1.0	3.0	14.9	0.03	28,529	28.0	Dead Coral	Green tint
103	SSG KR	7/13/12		N20.93861	W156.69318	Syringe	4.0	4.0	16.0					Dead Coral	Green tint
107	SSG KR	7/13/12	08/03/12	N20.93861	W156.69318	Syringe	6.0	2.0	12.0	4.93	0.01	44,240	24.9	Dead Coral	

Table A-6 Cont.	Survey Area	Sampling Date	Analysis Date	Latitude	Longitude	Collection Method	Seep Length (cm)	Seep Width (cm)	Seep Area (cm²)	FLT	SRB	Spec. Cond.	Adj. FLT	Substrate	Additional Observations
110 <i>Seep 4</i>	SSG KR	7/13/12	08/03/12	N20.93861	W156.69318	Syringe	13.0	7.0	91.0	9.86	0.03	35,710	26.0	Dead Coral	Green tint
112	SSG KR	7/13/12	07/25/12	N20.93861	W156.69318	Syringe	3.5	4.0	14.0	7.36	-----	40,604	26.7	Dead Coral	
115	SSG KR	7/13/12	08/03/12	N20.93861	W156.69318	Syringe	6.0	3.5	21.0	17.0	0.04	22,050	25.3	Dead Coral	
117	SSG KR	7/13/12	07/25/12	N20.93861	W156.69318	Syringe	7.0	3.0	21.0	17.3	-----	23,357	26.9	Dead Coral	Green tint
118	SSG KR	7/13/12	08/03/12	N20.93861	W156.69318	Syringe	9.0	10.0	90.0	16.1	0.04	23,900	25.5	Dead Coral	Green tint
119	SSG KR	7/13/12	08/03/12	N20.93861	W156.69318	Syringe	7.0	4.0	28.0	3.48	0.02	46,650	23.8	Dead Coral	
NA	SSG KR	7/13/12	-----	N20.93861	W156.69318	-----	0.2	0.2	0.04	-----	-----	-----	-----	Dead Coral	
NA	SSG KR	7/13/12	-----	N20.93861	W156.69318	-----	1.0	1.0	1.0	-----	-----	-----	-----	Dead Coral	
NA	SSG KR	7/13/12	-----	N20.93861	W156.69318	-----	1.0	1.0	1.0	-----	-----	-----	-----	Dead Coral	
NA	SSG KR	7/13/12	-----	N20.93861	W156.69318	-----	1.0	1.0	1.0	-----	-----	-----	-----	Dead Coral	
NA	SSG KR	7/13/12	-----	N20.93861	W156.69318	-----	1.0	1.0	1.0	-----	-----	-----	-----	Dead Coral	

Table A-6 Cont.	Survey Area	Sampling Date	Analysis Date	Latitude	Longitude	Collection Method	Seep Length (cm)	Seep Width (cm)	Seep Area (cm²)	FLT	SRB	Spec. Cond.	Adj. FLT	Substrate	Additional Observations
NA	SSG KR	7/13/12	----	N20.93861	W156.69318	----	1.0	1.0	1.0	----	----	----	----	Dead Coral	
NA	SSG KR	7/13/12	----	N20.93861	W156.69318	----	1.0	1.0	1.0	----	----	----	----	Dead Coral	
NA	SSG KR	7/13/12	----	N20.93861	W156.69318	----	1.0	1.0	1.0	----	----	----	----	Dead Coral	
NA	SSG KR	7/13/12	----	N20.93861	W156.69318	----	1.0	1.0	1.0	----	----	----	----	Dead Coral	
NA	SSG KR	7/13/12	----	N20.93861	W156.69318	----	1.0	1.0	1.0	----	----	----	----	Dead Coral	
NA	SSG KR	7/13/12	----	N20.93861	W156.69318	----	1.0	1.0	1.0	----	----	----	----	Dead Coral	
NA	SSG KR	7/13/12	----	N20.93861	W156.69318	----	1.0	1.0	1.0	----	----	----	----	Dead Coral	
NA	SSG KR	7/13/12	----	N20.93861	W156.69318	----	1.0	1.0	1.0	----	----	----	----	Dead Coral	
NA	SSG KR	7/13/12	----	N20.93861	W156.69318	----	1.0	1.0	1.0	----	----	----	----	Dead Coral	
NA	SSG KR	7/13/12	----	N20.93861	W156.69318	----	1.0	1.0	1.0	----	----	----	----	Dead Coral	
NA	SSG KR	7/13/12	----	N20.93861	W156.69318	----	1.5	1.0	1.5	----	----	----	----	Dead Coral	
NA	SSG KR	7/13/12	----	N20.93861	W156.69318	----	1.5	1.0	1.5	----	----	----	----	Dead Coral	

Table A-6 Cont.	Survey Area	Sampling Date	Analysis Date	Latitude	Longitude	Collection Method	Seep Length (cm)	Seep Width (cm)	Seep Area (cm²)	FLT	SRB	Spec. Cond.	Adj. FLT	Substrate	Additional Observations
NA	SSG KR	7/13/12	----	N20.93861	W156.69318	----	1.5	1.0	1.5	----	----	----	----	Dead Coral	
NA	SSG KR	7/13/12	----	N20.93861	W156.69318	----	1.5	0.5	0.8	----	----	----	----	Dead Coral	
NA	SSG KR	7/13/12	----	N20.93861	W156.69318	----	2.0	1.0	2.0	----	----	----	----	Dead Coral	
NA	SSG KR	7/13/12	----	N20.93861	W156.69318	----	2.5	5.0	12.5	----	----	----	----	Dead Coral	
NA	SSG KR	7/13/12	----	N20.93861	W156.69318	----	2.5	2.5	6.3	----	----	----	----	Dead Coral	
NA	SSG KR	7/13/12	----	N20.93861	W156.69318	----	3.0	1.0	3.0	----	----	----	----	Dead Coral	
NA	SSG KR	7/13/12	----	N20.93861	W156.69318	----	3.0	1.0	3.0	----	----	----	----	Dead Coral	
NA	SSG KR	7/13/12	----	N20.93861	W156.69318	----	3.0	1.0	3.0	----	----	----	----	Dead Coral	
NA	SSG KR	7/13/12	----	N20.93861	W156.69318	----	4.0	1.5	6.0	----	----	----	----	Dead Coral	
NA	SSG KR	7/13/12	----	N20.93861	W156.69318	----	4.5	1.0	4.5	----	----	----	----	Dead Coral	
NA	SSG KR	7/13/12	----	N20.93861	W156.69318	----	5.0	1.0	5.0	----	----	----	----	Dead Coral	
NA	SSG KR	7/13/12	----	N20.93861	W156.69318	----	6.0	3.0	18.0	----	----	----	----	Dead Coral	
NA	SSG KR	7/13/12	----	N20.93861	W156.69318	----	9.0	1.5	13.5	----	----	----	----	Dead Coral	

Table A-6 Cont.	Survey Area	Sampling Date	Analysis Date	Latitude	Longitude	Collection Method	Seep Length (cm)	Seep Width (cm)	Seep Area (cm²)	FLT	SRB	Spec. Cond.	Adj. FLT	Substrate	Additional Observations
NA	SSG KR	7/13/12	----	N20.93861	W156.69318	----	12.0	2.0	24.0	----	----	----	----	Dead Coral	
105	SSG KR	7/13/12	08/03/12	N20.93861	W156.69319	Syringe	10.0	1.0	10.0	9.73	0.03	36,620	27.0	Dead Coral	Green tint
114	SSG KR	7/13/12	07/25/12	N20.93861	W156.69319	Syringe	5.0	3.0	15.0	24.2	----	10,727	26.5	Dead Coral	Green tint
NA	SSG KR	7/13/12	----	N20.93861	W156.69319	----	0.5	1.0	0.5	----	----	----	----	Dead Coral	
NA	SSG KR	7/13/12	----	N20.93861	W156.69319	----	0.5	2.0	1.0	----	----	----	----	Dead Coral	
NA	SSG KR	7/13/12	----	N20.93861	W156.69319	----	0.5	1.0	0.5	----	----	----	----	Dead Coral	
NA	SSG KR	7/13/12	----	N20.93861	W156.69319	----	1.0	1.0	1.0	----	----	----	----	Dead Coral	
NA	SSG KR	7/13/12	----	N20.93861	W156.69319	----	1.0	1.0	1.0	----	----	----	----	Dead Coral	
NA	SSG KR	7/13/12	----	N20.93861	W156.69319	----	2.0	1.0	2.0	----	----	----	----	Dead Coral	
NA	SSG KR	7/13/12	----	N20.93861	W156.69319	----	0.5	1.0	0.5	----	----	----	----	Dead Coral	
NA	SSG KR	7/13/12	----	N20.93861	W156.69319	----	1.0	1.0	1.0	----	----	----	----	Dead Coral	
NA	SSG KR	7/13/12	----	N20.93861	W156.69319	----	1.0	0.5	0.5	----	----	----	----	Dead Coral	
NA	SSG KR	7/13/12	----	N20.93861	W156.69319	----	1.5	1.0	1.5	----	----	----	----	Dead Coral	

Table A-6 Cont.	Survey Area	Sampling Date	Analysis Date	Latitude	Longitude	Collection Method	Seep Length (cm)	Seep Width (cm)	Seep Area (cm²)	FLT	SRB	Spec. Cond.	Adj. FLT	Substrate	Additional Observations
NA	SSG KR	7/13/12	----	N20.93861	W156.69319	----	1.5	1.5	2.3	----	----	----	----	Dead Coral	
NA	SSG KR	7/13/12	----	N20.93861	W156.69319	----	2.0	1.0	2.0	----	----	----	----	Dead Coral	
NA	SSG KR	7/13/12	----	N20.93861	W156.69319	----	2.0	1.0	2.0	----	----	----	----	Dead Coral	
NA	SSG KR	7/13/12	----	N20.93861	W156.69319	----	2.0	1.0	2.0	----	----	----	----	Dead Coral	
NA	SSG KR	7/13/12	----	N20.93861	W156.69319	----	2.0	2.0	4.0	----	----	----	----	Dead Coral	
NA	SSG KR	7/13/12	----	N20.93861	W156.69319	----	2.0	0.5	1.0	----	----	----	----	Dead Coral	
NA	SSG KR	7/13/12	----	N20.93861	W156.69319	----	2.0	2.0	4.0	----	----	----	----	Dead Coral	
NA	SSG KR	7/13/12	----	N20.93861	W156.69319	----	2.0	2.0	4.0	----	----	----	----	Dead Coral	
NA	SSG KR	7/13/12	----	N20.93861	W156.69319	----	2.5	2.0	5.0	----	----	----	----	Dead Coral	
NA	SSG KR	7/13/12	----	N20.93861	W156.69319	----	3.0	2.0	6.0	----	----	----	----	Dead Coral	
NA	SSG KR	7/13/12	----	N20.93861	W156.69319	----	3.0	2.0	6.0	----	----	----	----	Dead Coral	
NA	SSG KR	7/13/12	----	N20.93861	W156.69319	----	4.0	1.0	4.0	----	----	----	----	Dead Coral	
NA	SSG KR	7/13/12	----	N20.93861	W156.69319	----	6.0	6.0	36.0	----	----	----	----	Dead Coral	

Table A-6 Cont.	Survey Area	Sampling Date	Analysis Date	Latitude	Longitude	Collection Method	Seep Length (cm)	Seep Width (cm)	Seep Area (cm²)	FLT	SRB	Spec. Cond.	Adj. FLT	Substrate	Additional Observations
NA	SSG KR	7/13/12	----	N20.93861	W156.69319	----	6.0	0.5	3.0	----	----	----	----	Dead Coral	
104	SSG KR	7/13/12	07/25/12	N20.93866	W156.69318	Syringe	1.0	0.5	0.5	18.5	----	22,850	28.3	Dead Coral	Green tint
NA	SSG KR	7/13/12	----	N20.93866	W156.69318	----	0.2	0.2	0.04	----	----	----	----	Dead Coral	
NA	SSG KR	7/13/12	----	N20.93866	W156.69318	----	0.5	0.5	0.3	----	----	----	----	Dead Coral	
NA	SSG KR	7/13/12	----	N20.93866	W156.69318	----	1.0	1.0	1.0	----	----	----	----	Dead Coral	
NA	SSG KR	7/13/12	----	N20.93866	W156.69318	----	1.0	1.0	1.0	----	----	----	----	Dead Coral	
NA	SSG KR	7/13/12	----	N20.93866	W156.69318	----	1.0	1.0	1.0	----	----	----	----	Dead Coral	
NA	SSG KR	7/13/12	----	N20.93866	W156.69318	----	2.0	1.0	2.0	----	----	----	----	Dead Coral	
NA	SSG KR	7/13/12	----	N20.93866	W156.69318	----	3.0	2.0	6.0	----	----	----	----	Dead Coral	
NA	SSG KR	7/13/12	----	N20.93866	W156.69318	----	5.0	1.0	5.0	----	----	----	----	Dead Coral	
133	SSG KR	7/19/12	07/25/12	N20.93866	W156.69318	Syringe	----	----	----	0.08	----	52,309	2.87	Surface Water	SSG Control
100	SSG KR	7/13/12	07/25/12	N20.93865	W156.69303	Syringe	0.5	0.5	0.3	4.80	----	45,609	28.5	Sand	
NA	SSG KR	7/13/12	----	N20.93865	W156.69303	----	1.0	1.0	1.0	----	----	----	----	Dead Coral	

Table A-6 Cont.	Survey Area	Sampling Date	Analysis Date	Latitude	Longitude	Collection Method	Seep Length (cm)	Seep Width (cm)	Seep Area (cm²)	FLT	SRB	Spec. Cond.	Adj. FLT	Substrate	Additional Observations
NA	SSG KR	7/13/12	----	N20.93865	W156.69303	----	5.0	1.0	5.0	----	----	----	----	Dead Coral	
97	SSG KR	7/13/12	07/25/12	N20.93866	W156.69315	Syringe	10.0	2.0	20.0	6.10	----	43,769	29.4	Dead Coral / Basalt	
<i>101 Seep 3</i>	<i>SSG KR</i>	<i>7/13/12</i>	<i>08/03/12</i>	<i>N20.93866</i>	<i>W156.69315</i>	<i>Syringe</i>	<i>15.0</i>	<i>5.0</i>	<i>75.0</i>	<i>18.9</i>	<i>0.06</i>	<i>22,875</i>	<i>28.9</i>	<i>Dead Coral / Basalt</i>	<i>Green tint</i>
120	SSG KR	7/13/12	08/03/12	N20.93866	W156.69315	Syringe	1.0	1.0	1.0	23.1	0.04	16,040	28.9	Dead Coral / Basalt	Green tint
NA	SSG KR	7/13/12	----	N20.93866	W156.69315	----	2.0	2.0	4.0	----	----	----	----	Dead Coral / Basalt	
NA	SSG KR	7/13/12	----	N20.93866	W156.69315	----	3.0	1.0	3.0	----	----	----	----	Dead Coral / Basalt	
NA	SSG KR	7/13/12	----	N20.93866	W156.69315	----	5.0	7.0	35.0	----	----	----	----	Dead Coral / Basalt	
113	SSG KR	7/16/12	07/25/12	N20.93866	W156.69310	Syringe	2.0	1.0	2.0	10.6	----	35,813	28.1	Dead Coral	
NA	SSG KR	7/16/12	----	N20.93866	W156.69310	----	1.0	0.5	0.5	----	----	----	----	Dead Coral	
NA	SSG KR	7/16/12	----	N20.93866	W156.69310	----	1.0	0.5	0.5	----	----	----	----	Dead Coral	

Table A-6 Cont.	Survey Area	Sampling Date	Analysis Date	Latitude	Longitude	Collection Method	Seep Length (cm)	Seep Width (cm)	Seep Area (cm²)	FLT	SRB	Spec. Cond.	Adj. FLT	Substrate	Additional Observations
NA	SSG KR	7/16/12	----	N20.93866	W156.69310	----	2.0	0.5	1.0	----	----	----	----	Dead Coral	
125	SSG KR	7/16/12	08/03/12	N20.93867	W156.69312	Syringe	4.0	0.5	2.0	9.38	0.04	35,462	24.4	Dead Coral	
NA	SSG KR	7/16/12	----	N20.93867	W156.69312	----	1.0	0.5	0.5	----	----	----	----	Dead Coral	
NA	SSG KR	7/16/12	----	N20.93867	W156.69312	----	2.0	0.5	1.0	----	----	----	----	Dead Coral	
NA	SSG KR	7/16/12	----	N20.93867	W156.69312	----	2.0	0.5	1.0	----	----	----	----	Dead Coral	
NA	SSG KR	7/16/12	----	N20.93867	W156.69312	----	2.0	0.5	1.0	----	----	----	----	Dead Coral	
NA	SSG KR	7/16/12	----	N20.93867	W156.69312	----	2.0	0.5	1.0	----	----	----	----	Dead Coral	
NA	SSG KR	7/16/12	----	N20.93867	W156.69312	----	2.0	0.5	1.0	----	----	----	----	Dead Coral	
NA	SSG KR	7/16/12	----	N20.93867	W156.69312	----	2.0	0.5	1.0	----	----	----	----	Dead Coral	
109	HP	7/17/12	08/03/12	N20.94949	W156.69185	Grab	No visible seep		NA	0.07	0.01	48,680	0.58	Dead Coral	Shimmery water
134	S. KR	7/17/12	08/03/12	N20.93512	W156.69294	Grab	4.0	1.0	4.0	0.09	0.02	48,393	0.77	Basalt / Sand	Diffuse discharge
NA	S. KR	7/17/12	----	N20.93512	W156.69294	----	0.5	0.5	0.3	----	----	----	----	Basalt / Sand	
126	HP	7/18/12	08/03/12	N20.94669	W156.69313	Grab	No visible seep		NA	0.06	0.02	51,577	1.24	Sand	Shimmery water

Table A-6 Cont.	Survey Area	Sampling Date	Analysis Date	Latitude	Longitude	Collection Method	Seep Length (cm)	Seep Width (cm)	Seep Area (cm²)	FLT	SRB	Spec. Cond.	Adj. FLT	Substrate	Additional Observations
132	N. BR	7/18/12	08/03/12	N20.93269	W156.69345	Grab	No visible seep		NA	0.07	0.03	51,263	1.26	Sand	Diffuse discharge
128	NSG KR	7/16/12	07/25/12	N20.94003	W156.69307	Syringe	2.0	2.0	4.0	1.65	-----	45,484	9.60	Dead Coral	
NA	NSG KR	7/16/12	-----	N20.94003	W156.69307	-----	1.0	0.5	0.5	-----	-----	-----	-----	Dead Coral	
NA	NSG KR	7/16/12	-----	N20.94003	W156.69307	-----	1.0	1.0	1.0	-----	-----	-----	-----	Dead Coral	
NA	NSG KR	7/16/12	-----	N20.94003	W156.69307	-----	1.0	1.0	1.0	-----	-----	-----	-----	Dead Coral	
NA	NSG KR	7/16/12	-----	N20.94003	W156.69307	-----	2.0	1.0	2.0	-----	-----	-----	-----	Dead Coral	
NA	NSG KR	7/16/12	-----	N20.94003	W156.69307	-----	2.0	1.0	2.0	-----	-----	-----	-----	Dead Coral	
NA	NSG KR	7/16/12	-----	N20.94003	W156.69307	-----	2.0	0.5	1.0	-----	-----	-----	-----	Dead Coral	
NA	NSG KR	7/16/12	-----	N20.94003	W156.69307	-----	5.0	0.5	2.5	-----	-----	-----	-----	Dead Coral	
89	NSG KR	7/16/12	07/25/12	N20.93978	W156.69307	Syringe	3.0	1.0	3.0	3.42	-----	46,670	23.4	Sand	Sand volcano
106	NSG KR	7/16/12	07/25/12	N20.93978	W156.69307	Syringe	2.5	2.5	6.3	2.31	-----	48,762	22.8	Dead Coral	Green tint
NA	NSG KR	7/16/12	-----	N20.93978	W156.69307	-----	0.5	0.5	0.3	-----	-----	-----	-----	Sand	
NA	NSG KR	7/16/12	-----	N20.93978	W156.69307	-----	1.0	1.0	1.0	-----	-----	-----	-----	Sand	Sand volcano

Table A-6 Cont.	Survey Area	Sampling Date	Analysis Date	Latitude	Longitude	Collection Method	Seep Length (cm)	Seep Width (cm)	Seep Area (cm²)	FLT	SRB	Spec. Cond.	Adj. FLT	Substrate	Additional Observations
NA	NSG KR	7/16/12	----	N20.93978	W156.69307	----	1.0	1.0	1.0	----	----	----	----	Sand	
NA	NSG KR	7/16/12	----	N20.93978	W156.69307	----	2.0	1.5	3.0	----	----	----	----	Dead Coral	
NA	NSG KR	7/16/12	----	N20.93978	W156.69307	----	2.0	1.0	2.0	----	----	----	----	Dead Coral	
NA	NSG KR	7/16/12	----	N20.93978	W156.69307	----	2.0	2.0	4.0	----	----	----	----	Dead Coral	
NA	NSG KR	7/16/12	----	N20.93978	W156.69307	----	2.0	1.0	2.0	----	----	----	----	Sand	
NA	NSG KR	7/16/12	----	N20.93978	W156.69307	----	3.0	1.0	3.0	----	----	----	----	Sand	Sand volcano
NA	NSG KR	7/16/12	----	N20.93978	W156.69307	----	3.0	1.0	3.0	----	----	----	----	Sand	Sand volcano
Well 2	WR	7/31/12	08/03/12	N20.94303	W156.68915	Bailer	----	----	----	0.04	----	2,538	0.04	NA	
Well 3	WR	7/31/12	08/04/12	N20.94076	W156.69003	Bailer	----	----	----	0.09	----	932	0.09	NA	
Well 4	WR	7/31/12	08/05/12	N20.94068	W156.69149	Bailer	----	----	----	0.09	----	2,912	0.09	NA	
Well 5	WR	7/31/12	08/06/12	N20.93710	W156.69215	Bailer	----	----	----	0.12	----	1,480	0.12	NA	
Well 6	WR	7/31/12	08/07/12	N20.93618	W156.69061	Pump	----	----	----	4.59	----	2,405	4.59	NA	
Sand sample 1	S. KR	11/2/12	11/17/12	N20.93402	W156.6928	Piez	----	----	----	0.01	0.00	52,300	- 0.04	Sand	
Sand sample 2	S. KR	12/20/12	01/12/13	N20.93427	W156.69273	Piez	----	----	----	0.08	0.03	19,520	0.10	Sand	

Table A-6 Cont.	Survey Area	Sampling Date	Analysis Date	Latitude	Longitude	Collection Method	Seep Length (cm)	Seep Width (cm)	Seep Area (cm²)	FLT	SRB	Spec. Cond.	Adj. FLT	Substrate	Additional Observations
Sand sample 3	S. KR	12/20/12	01/12/13	N20.93384	W156.69277	Piez	----	----	----	0.04	0.03	49,360	0.36	Sand	
Sand sample 4	S. KR	12/20/12	01/12/13	N20.93344	W156.69289	Piez	----	----	----	0.02	0.05	51,940	0.42	Sand	
Sand sample 5	S. KR	12/20/12	01/12/13	N20.93294	W156.69308	Piez	----	----	----	0.07	0.04	52,425	2.40	Sand	
Sand sample 6	S. KR	12/21/12	01/12/13	N20.93451	W156.69271	Piez	----	----	----	0.06	0.03	36,560	0.14	Sand	
Sand sample 7	S. KR	12/21/12	01/12/13	N20.93384	W156.69277	Piez	----	----	----	0.05	0.02	25,800	0.08	Sand	
Sand sample 8	S. KR	12/21/12	01/12/13	N20.93331	W156.69284	Piez	----	----	----	0.02	0.02	52,390	0.38	Sand	
Sand sample 9	S. KR	12/21/12	01/12/13	N20.93415	W156.69279	Piez	----	----	----	0.94	0.07	45,970	5.77	Sand	
Sand sample 10	HP	12/29/12	01/12/13	N20.94910	W156.69131	Piez	----	----	----	0.03	0.02	44,030	0.09	Sand	
Syringe sample 1	SSG KR	12/29/12	01/12/13	N20.93978	W156.69295	Syringe	----	----	----	1.44	0.02	46,760	9.94	Dead Coral / Basalt	Seep 11

Table A-6 Cont.	Survey Area	Sampling Date	Analysis Date	Latitude	Longitude	Collection Method	Seep Length (cm)	Seep Width (cm)	Seep Area (cm)	FLT	SRB	Spec. Cond.	Adj. FLT	Substrate	Additional Observations
Syringe sample 2	SSG KR	12/29/12	01/12/13	N20.93981	W156.69291	Syringe	----	----	----	1.40	0.02	47,250	10.4	Dead Coral / Basalt	Seep 3
Syringe sample 3	NSG KR	12/29/12	01/12/13	N20.93992	W156.69299	Syringe	----	----	----	1.29	0.02	47,900	10.7	Dead Coral / Basalt	
Syringe sample 4	NSG KR	12/29/12	01/12/13	N20.94017	W156.69286	Syringe	----	----	----	0.95	0.02	48,890	9.5	Sand / Basalt	Seep 20
Syringe sample 5	SSG KR	12/29/12	01/12/13	N20.93871	W156.69309	Syringe	----	----	----	1.71	0.01	46,380	11.2	Dead Coral / Basalt	Seep 4
NSG sand sample 1	KR	1/8/13	01/12/13	N20.94020	W156.69274	Piez	----	----	----	9.62	0.04	8,617	10.0	Sand	Nearshore of Seep 7
NSG sand sample 2	KR	1/8/13	01/12/13	N20.94018	W156.69258	Piez	----	----	----	9.41	0.04	9,311	10.0	Sand	Nearshore of Seep 20
SSG sand sample 1	KR	1/8/13	01/12/13	N20.93860	W156.69289	Piez	----	----	----	3.08	0.02	42,380	12.9	Sand	Nearshore of Seep 3
SSG sand sample 2	KR	1/8/13	01/12/13	N20.93863	W156.69292	Piez	----	----	----	4.91	0.05	36,440	13.5	Sand	Nearshore of Seeps 4, 5, & 11

**APPENDIX B: PROCEDURES FOR ESTABLISHING
THE METHOD DETECTION LIMIT**

**APPENDIX FOR SECTION 4:
FLUORESCENT DYE GROUNDWATER TRACER STUDY**

This page is intentionally left blank.

[Home Page](#) > [Executive Branch](#) > [Code of Federal Regulations](#) > [Electronic Code of Federal Regulations](#)



e-CFR Data is current as of June 1, 2011

Title 40: Protection of Environment

[PART 136—GUIDELINES ESTABLISHING TEST PROCEDURES FOR THE ANALYSIS OF POLLUTANTS](#)

[Browse Previous](#) | [Browse Next](#)

Appendix B to Part 136—Definition and Procedure for the Determination of the Method Detection Limit—Revision 1.11

Definition

The method detection limit (MDL) is defined as the minimum concentration of a substance that can be measured and reported with 99% confidence that the analyte concentration is greater than zero and is determined from analysis of a sample in a given matrix containing the analyte.

Scope and Application

This procedure is designed for applicability to a wide variety of sample types ranging from reagent (blank) water containing analyte to wastewater containing analyte. The MDL for an analytical procedure may vary as a function of sample type. The procedure requires a complete, specific, and well defined analytical method. It is essential that all sample processing steps of the analytical method be included in the determination of the method detection limit.

The MDL obtained by this procedure is used to judge the significance of a single measurement of a future sample.

The MDL procedure was designed for applicability to a broad variety of physical and chemical methods. To accomplish this, the procedure was made device- or instrument-independent.

Procedure

1. Make an estimate of the detection limit using one of the following:

- (a) The concentration value that corresponds to an instrument signal/noise in the range of 2.5 to 5.
- (b) The concentration equivalent of three times the standard deviation of replicate instrumental measurements of the analyte in reagent water.
- (c) That region of the standard curve where there is a significant change in sensitivity, *i.e.*, a break in the slope of the standard curve.
- (d) Instrumental limitations.

It is recognized that the experience of the analyst is important to this process. However, the analyst must include the above considerations in the initial estimate of the detection limit.

2. Prepare reagent (blank) water that is as free of analyte as possible. Reagent or interference free

water is defined as a water sample in which analyte and interferent concentrations are not detected at the method detection limit of each analyte of interest. Interferences are defined as systematic errors in the measured analytical signal of an established procedure caused by the presence of interfering species (interferent). The interferent concentration is presupposed to be normally distributed in representative samples of a given matrix.

3. (a) If the MDL is to be determined in reagent (blank) water, prepare a laboratory standard (analyte in reagent water) at a concentration which is at least equal to or in the same concentration range as the estimated method detection limit. (Recommend between 1 and 5 times the estimated method detection limit.) Proceed to Step 4.

(b) If the MDL is to be determined in another sample matrix, analyze the sample. If the measured level of the analyte is in the recommended range of one to five times the estimated detection limit, proceed to Step 4.

If the measured level of analyte is less than the estimated detection limit, add a known amount of analyte to bring the level of analyte between one and five times the estimated detection limit.

If the measured level of analyte is greater than five times the estimated detection limit, there are two options.

(1) Obtain another sample with a lower level of analyte in the same matrix if possible.

(2) The sample may be used as is for determining the method detection limit if the analyte level does not exceed 10 times the MDL of the analyte in reagent water. The variance of the analytical method changes as the analyte concentration increases from the MDL, hence the MDL determined under these circumstances may not truly reflect method variance at lower analyte concentrations.

4. (a) Take a minimum of seven aliquots of the sample to be used to calculate the method detection limit and process each through the entire analytical method. Make all computations according to the defined method with final results in the method reporting units. If a blank measurement is required to calculate the measured level of analyte, obtain a separate blank measurement for each sample aliquot analyzed. The average blank measurement is subtracted from the respective sample measurements.

(b) It may be economically and technically desirable to evaluate the estimated method detection limit before proceeding with 4a. This will: (1) Prevent repeating this entire procedure when the costs of analyses are high and (2) insure that the procedure is being conducted at the correct concentration. It is quite possible that an inflated MDL will be calculated from data obtained at many times the real MDL even though the level of analyte is less than five times the calculated method detection limit. To insure that the estimate of the method detection limit is a good estimate, it is necessary to determine that a lower concentration of analyte will not result in a significantly lower method detection limit. Take two aliquots of the sample to be used to calculate the method detection limit and process each through the entire method, including blank measurements as described above in 4a. Evaluate these data:

(1) If these measurements indicate the sample is in desirable range for determination of the MDL, take five additional aliquots and proceed. Use all seven measurements for calculation of the MDL.

(2) If these measurements indicate the sample is not in correct range, reestimate the MDL, obtain new sample as in 3 and repeat either 4a or 4b.

5. Calculate the variance (S^2) and standard deviation (S) of the replicate measurements, as follows:

$$S^2 = \frac{1}{n-1} \left[\sum_{i=1}^n x_i^2 - \frac{\left(\sum_{i=1}^n X_i \right)^2}{n} \right] \quad S = (S^2)^{\frac{1}{2}}$$

where:

X_i ; $i=1$ to n , are the analytical results in the final method reporting units obtained from the n sample

aliquots and Σ refers to the sum of the X values from $i=1$ to n .

6. (a) Compute the MDL as follows:

$$\text{MDL} = t(n-1, 1-\alpha=0.99) (S)$$

where:

MDL = the method detection limit

$t(n-1, 1-\alpha=.99)$ = the students' t value appropriate for a 99% confidence level and a standard deviation estimate with $n-1$ degrees of freedom. See Table.

S = standard deviation of the replicate analyses.

(b) The 95% confidence interval estimates for the MDL derived in 6a are computed according to the following equations derived from percentiles of the chi square over degrees of freedom distribution (χ^2/df).

$$\text{LCL} = 0.64 \text{ MDL}$$

$$\text{UCL} = 2.20 \text{ MDL}$$

where: LCL and UCL are the lower and upper 95% confidence limits respectively based on seven aliquots.

7. Optional iterative procedure to verify the reasonableness of the estimate of the MDL and subsequent MDL determinations.

(a) If this is the initial attempt to compute MDL based on the estimate of MDL formulated in Step 1, take the MDL as calculated in Step 6, spike the matrix at this calculated MDL and proceed through the procedure starting with Step 4.

(b) If this is the second or later iteration of the MDL calculation, use S^2 from the current MDL calculation and S^2 from the previous MDL calculation to compute the F-ratio. The F-ratio is calculated by substituting the larger S^2 into the numerator S^2_A and the other into the denominator S^2_B . The computed F-ratio is then compared with the F-ratio found in the table which is 3.05 as follows: if $S^2_A/S^2_B < 3.05$, then compute the pooled standard deviation by the following equation:

$$S_{\text{pooled}} = \left[\frac{6S_A^2 + 6S_B^2}{12} \right]^{1/2}$$

if $S^2_A/S^2_B > 3.05$, respoke at the most recent calculated MDL and process the samples through the procedure starting with Step 4. If the most recent calculated MDL does not permit qualitative identification when samples are spiked at that level, report the MDL as a concentration between the current and previous MDL which permits qualitative identification.

(c) Use the S_{pooled} as calculated in 7b to compute The final MDL according to the following equation:

$$\text{MDL} = 2.681 (S_{\text{pooled}})$$

where 2.681 is equal to $t(12, 1-\alpha=.99)$.

(d) The 95% confidence limits for MDL derived in 7c are computed according to the following equations derived from percentiles of the chi squared over degrees of freedom distribution.

$$\text{LCL} = 0.72 \text{ MDL}$$

UCL=1.65 MDL

where LCL and UCL are the lower and upper 95% confidence limits respectively based on 14 aliquots.

Tables of Students' t Values at the 99 Percent Confidence Level

Number of replicates	Degrees of freedom (n-1)	$t_{cn-1,.99}$
7	6	3.143
8	7	2.998
9	8	2.896
10	9	2.821
11	10	2.764
16	15	2.602
21	20	2.528
26	25	2.485
31	30	2.457
61	60	2.390
00	00	2.326

Reporting

The analytical method used must be specifically identified by number or title and the MDL for each analyte expressed in the appropriate method reporting units. If the analytical method permits options which affect the method detection limit, these conditions must be specified with the MDL value. The sample matrix used to determine the MDL must also be identified with MDL value. Report the mean analyte level with the MDL and indicate if the MDL procedure was iterated. If a laboratory standard or a sample that contained a known amount analyte was used for this determination, also report the mean recovery.

If the level of analyte in the sample was below the determined MDL or exceeds 10 times the MDL of the analyte in reagent water, do not report a value for the MDL.

[49 FR 43430, Oct. 26, 1984; 50 FR 694, 696, Jan. 4, 1985, as amended at 51 FR 23703, June 30, 1986]

[Browse Previous](#) | [Browse Next](#)

For questions or comments regarding e-CFR editorial content, features, or design, email ecfr@nara.gov.

For questions concerning e-CFR programming and delivery issues, email webteam@gpo.gov.

[Section 508 / Accessibility](#)

Decision and Detection Limits for Linear Calibration Curves

André Hubaux¹ and Gilbert Vos²

C.C.R. Euratom, 21020 Ispra (Va), Italy

For linear calibration curves, two kinds of lower limits may be connected to the notion of confidence limits—a decision limit, the lowest signal that can be distinguished from the background and a detection limit, the content under which, *a priori*, any sample may erroneously be taken for the blank. From a few algebraical and computational developments, several practical rules are deduced to lower these limits. The influence of the precision of the analytical method, the number of standards, the range of their contents, the various modes of their repartition, and the replication of measurements on the unknown sample are studied from a statistical point of view.

EXTERNAL STANDARDS are of very common use in analytical practice. In many methods, *e.g.*, as in X-ray spectrochemical analysis, the analyst used a linear calibration curve obtained from measurements made on these standards, to estimate the concentration of the unknown. Obviously the sensitivity of his method may be enhanced by a judicious choice of standards, but the quantitative estimate of this enhancement is not straightforward. The various definitions of the detection limits found in the literature, although having different advantages do not explicitly include this influence.

Linning and Mandel (1) have presented a very interesting discussion on the determination of the precision of an analytical method involving a calibration curve. They emphasize that, because there is always some scatter in the calibration data, the precision of analysis for an unknown will be poorer than indicated from several repeat determinations on the same sample. Various authors have proposed an objective way to calculate the detection limit of an analytical determination. They suggest that a signal higher than the standard deviation of the background multiplied by a conventionally chosen factor (usually 3), should be considered as characteristic of a detectable amount of the element to be analyzed. Kaiser, in several papers (2-4) develops this concept at length and proposes to work at the confidence level of 99.86%, which corresponds to a value of 3 for the factor.

B. Altshuler and B. Pasternak (5) have connected the notion of detection limits with the statistical concepts of the errors of the first and second kind; these concepts will be also used in the present text. A review of the published definitions of the limits for qualitative detection and quantitative determination has been done by L. A. Currie (6), who proposes to introduce three specific levels: *A decision limit* to which corresponds a *critical level* L_c , the net signal level (instrument response) above which an observed signal may be recognized reliably enough to be detected; at this limit, one may decide whether or not the result of an analysis indicates presence; *A detection limit*, L_D , the "true" net signal level which may be *a priori* ex-

pected to lead to detection; this is the limit at which a given analytical procedure may be relied upon to lead to detection; and *A determination limit*, L_Q , the level at which the measurement precision will be satisfactory for quantitative determination.

We will show how estimates of the decision and detection limits may be introduced by considering the confidence limits of the linear calibration curve. The dependence of these limits upon the standards will thereby be made explicit.

DECISION AND DETECTION LIMITS—A NEW APPROACH

In the analytical methods of interest here, the response signals of a certain number of standards are measured and a straight line (the regression line) is passed through the representative points. This line is an estimate of the true calibration line. It may be predicted that any new standard will give a signal falling in the neighborhood of this obtained line. At this point two questions may arise:

Above which level are the signals significantly different from the background?

Above which concentration is a confusion with the null concentration unlikely?

To seek an answer, let us scrutinize what the expression "in the neighborhood of" really implies. The representative point of a measured signal does not fall exactly on the line for two independent reasons: the drawn calibration line does not exactly coincide with the true calibration line but is only an estimate (this estimate is based on a limited number of standards); and for a given content, the corresponding response signal does not assume a fixed value but is randomly distributed around a mean value, and this distribution is not exactly known. In order to make precise the combined effects of these two uncertainties, one due to the insufficiency of our information, and the other to a lack of perfect reproductivity inherent to the method, four basic hypotheses are necessary.

First, the standards are supposed to be independent. Practically, this means that they should be prepared separately, *i.e.*, in such a way that they will differ in their preparation, as much from each other as from the samples to be analyzed. This condition is not so easily met as seems at first sight.

Second, the variance of the error distribution of the signals around their expectation is supposed to remain constant. Practically, this means that the scatter of the signals does not depend on the contents, in the studied range of these contents.

Third, the contents of the standards are supposed to be accurately known.

Fourth, it is assumed that the observed signals have a gaussian distribution around their expectation. Although this hypothesis is very widely accepted, it is not certain that it is always correct. On the contrary, K. Behrends (7) has shown that the error distribution definitely is not gaussian in a number of cases. But, although another type of distribution would yield somewhat different numerical results than those presented here, it would probably not significantly modify the main conclusions.

(7) K. Behrends, *Z. Anal. Chem.*, **235**, 391 (1967).

¹ C.E.T.I.S.

² Analytical Chemistry Section.

(1) F. J. Linning and J. Mandel, *ANAL. CHEM.*, **36** (13), 25A (1964).

(2) H. Kaiser, *Z. Anal. Chem.*, **149**, 46 (1956).

(3) *Ibid.*, **209**, 1 (1965).

(4) *Ibid.*, **216**, 80 (1966).

(5) B. Altshuler and B. Pasternak, *Health Phys.*, **9**, 293 (1963).

(6) L. A. Currie, *ANAL. CHEM.*, **40**, 586 (1968).

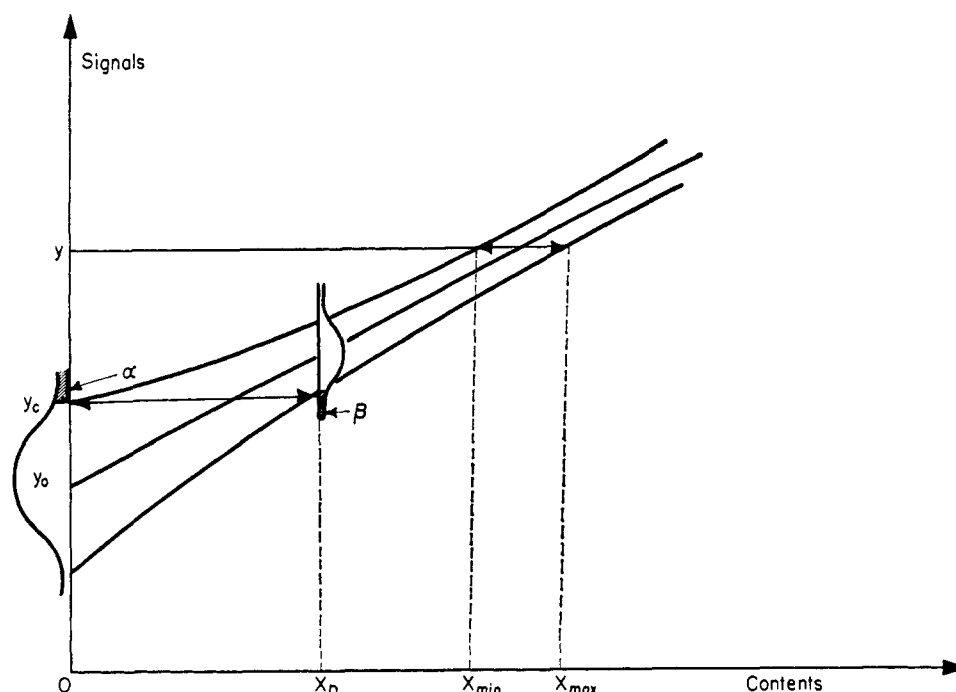


Figure 1. The linear calibration line, with its upper and lower confidence limits. y_c is the decision limit and x_D the detection limit, as explained in text

Starting from these hypotheses, formulas can be established from which several conclusions may be deduced, as will be shown in the next paragraphs. The considerations upon which the reasoning will be based are as follows:

On either side of the regression line, two confidence limits may be drawn, with an *a priori* chosen level of confidence, which we will note as $1-\alpha-\beta$, α and β having prefixed small values, of the order of a few percent (see Figure 1). The regression line and its two confidence limits represent a graphic synthesis of our knowledge about the relationship between content and signal. With it we may predict that an as yet unexplored content will yield a signal falling inside the confidence band. We will do this prediction with $1-\alpha-\beta$ probability; if we did a series of such predictions and then made the measurements, we would observe that, in the long run, we would be right $1-\alpha-\beta$ of the time; α % of the points would fall above the higher limit, and β % under the lower limit. The width of the confidence band depends on: the dispersion of signals for a given content, the knowledge we have of that dispersion and the degree of uncertainty about the true position of the calibration line.

The confidence limits, then, do not represent the dispersion of signals but our capacity to predict likely values for signals, taking into account the actual knowledge we possess of the case.

The confidence band may also be used in reverse; for a measured value y of the signal on a sample of unknown content (see Figure 1) we may predict the range of this content. The intersection of a horizontal line through y with the two confidence limits will define this range $x_{max}-x_{min}$, again with $1-\alpha-\beta$ probability. This, incidentally, is a valid method to estimate confidence limits of contents corresponding to a given signal. In particular, for a measured signal equal to y_c (see Figure 1), the lower limit of content is zero. Signals equal to or lower than y_c have a non-negligible probability to be due to a sample with a nul concentration, and hence we cannot distinguish, with such signals, whether or not the sought element is really present or not.

y_c is then the lowest measurable signal: if we are not ready to take a risk greater than α % to state that the element is present when it is absent (*i.e.*, to take a wrong decision more than α % of the time) we must decide that any signal under y_c must be disregarded. It is then clear that y_c corresponds to L_c as defined by L. A. Currie. More exactly, y_c is the estimate of L_c which may be obtained with the knowledge at hand. y_c could also be called the reading threshold, an expression proposed by H. Kaiser in an article published while the present paper was in press [H. Kaiser, *ANAL. CHEM.*, **42** (4), 26A (1970)].

Hence, a measurement being made, we decide whether the sample may be a blank or not. (The blank being a sample which is identical, in principle, to the samples of interest, except that the substance sought is absent, or in such minute quantity that it will give signals not higher than the background). Before making any measurement, on the other hand, we can state that the lowest content we may distinguish from zero is x_D , the abscissa corresponding to y_c on the lower confidence limit. Indeed, with the knowledge in our possession, when we measure an unknown with a content lower than x_D , we run a risk higher than β to obtain a signal lower than y_c , and hence to state that it is a blank. x_D is then our estimate of the "limit of guarantee for purity," as defined by Kaiser (3) which in turn is equivalent to the "minimum detectable true activity" of Altshuler and Pasternak (5) and to the "detection limit" of Currie (6).

It is perhaps not useless to remark that y_c and x_D have not a fixed value. For a given method and a given number of standards they will vary because, first α and β may be chosen at will, according to the acceptable levels of risk one is ready to run to derive false conclusions, and second, by making a second series of standards, identical to the actual series, we would obtain signals differing at random from the actual signals. The regression line and the confidence limits we would then draw would not exactly coincide with the actual lines, and y_c and x_D would be somewhat different. In other words, y_c and x_D are random variables and estimates only.

But this is the normal situation whenever randomness is an integral part of the phenomenon.

By way of summary, two sensitivity limits are proposed here: a signal level y_c and a content x_D . These notions are very similar to the lower limits of detection for radioactivity counters proposed by B. Altshuler and B. Pasternak (5). The first limit concerns signals and will lead to an *a posteriori* decision, *i.e.*, a decision taken after the signal is measured; the second limit is relative to contents and is inherent to the method; it specifies *a priori* the content which will be safely detected without confusion with blanks. It will be seen that y_c and x_D are directly connected with the statistical notions of the "errors of the first and the second kind," respectively. [A good introduction to these classical notions will be found in (5)]. As the direct relationship between these limits and the confidence limits is now established, it is clear that the problem is equivalent to the study of the influence of the standards on the confidence limits: to lower y_c and x_D , the confidence limits must be brought nearer to the regression line.

MATHEMATICAL DEVELOPMENTS

Notations. The following notations have already been introduced: α, β, y_c, x_D . We will also use:

Y_0 = estimate of the expectation of the response signal for a blank ($x = 0$) (y_0 is the intersection of the calibration line with the axis of ordinates)

y_D = signal corresponding to x_D on the calibration line

x_C = abscissa corresponding to y_c on the calibration line

N = number of standards

x_i = concentration of the element of interest in the i th standard ($i = 1, N$)

Σ = the summation sign; stands for $\sum_{i=1}^N$

\bar{x} = mean; $\bar{x} = \Sigma x_i / N$

x_1 = lowest concentration within the series of standards

x_N = highest concentration within the series of standards

K = number of standards equal to x_1 in the "three values" repartition of the contents of the standards

λ_i = dimensionless factor; $\lambda_i = \frac{x_i - x_1}{x_N - x_1}$ (1)

λ_D = value of λ_i corresponding to x_D ; $\lambda_D = \frac{x_D - x_1}{x_N - x_1}$ (2)

γ = exponent of the parabolic repartition (Eq 24)

y_i = the observed intensity of a characteristic line of the element of interest measured for the i th standard

\bar{y} = mean; $\bar{y} = \Sigma y_i / N$

b = angular coefficient of the regression line, whose equation is:

$$Y = \bar{y} + b(x - \bar{x}) \quad (3)$$

with

$$b = \frac{\Sigma(x_i - \bar{x})(y_i - \bar{y})}{\Sigma(x_i - \bar{x})^2} \quad (4)$$

by the least squares method

Y_i = calculated signal corresponding to x_i

$$Y_i = \bar{y} + b(x_i - \bar{x}) \quad (5)$$

s^2 = the estimate of the residual variance

$$s^2 = \Sigma(y_i - Y_i)^2 / (N - 2); \quad (6)$$

s is the estimate of the residual standard deviation

t = Student's t corresponding to $N - 2$ degrees of freedom and $(1 - \alpha)$ or $(1 - \beta)$ confidence level

$$R = \text{range ratio of the standards } R = (x_N - x_1) / x_1 \quad (7)$$

P = factor of s in Equation 16

$$P = t_{1-\alpha} \sqrt{1 + \frac{1}{N} + \frac{\bar{x}^2}{\Sigma(x_i - \bar{x})^2}} \quad (8)$$

P_{III} = third term under the radical in the preceding equation

$$P_{III} = \frac{\bar{x}^2}{\Sigma(x_i - \bar{x})^2} \quad (9)$$

Q = factor of s in Equation 18

$$Q = t_{1-\beta} \sqrt{1 + \frac{1}{N} + \frac{(x_D - \bar{x})^2}{\Sigma(x_i - \bar{x})^2}} \quad (10)$$

Q_{III} = third term under the radical in the preceding equation

$$Q_{III} = \frac{(x_D - \bar{x})^2}{\Sigma(x_i - \bar{x})^2} \quad (11)$$

n = number of replicates on each unknown sample.

Equations of y_c and y_D . The equations of the upper and lower curves of Figure 1 (*i.e.*, the confidence limits) are derived [see (8) for instance] by considering that any value y corresponding to a given value of x has a gaussian distribution around its calculated value Y . The confidence limits at any point x are then expressed by

$$y = \bar{y} + b(x - \bar{x}) \pm t \sqrt{V[y]} \quad (12)$$

t corresponding to a probability of $1 - \alpha$ for the upper limit and $1 - \beta$ for the lower limit. The variance of y , $V[y]$, is the sum of the variance of Y plus the residual variance

$$V(y) = V[\bar{y} + b(x - \bar{x})] + \sigma^2 \quad (13)$$

with

$$V[\bar{y}] = \frac{\sigma^2}{N}, \quad V[b] = \frac{\sigma^2}{\Sigma(x_i - \bar{x})^2} \quad (14)$$

The residual variance σ^2 may be replaced by its estimate s^2 and Equation 12 becomes

$$y = \bar{y} + b(x - \bar{x}) \pm st \sqrt{1 + \frac{1}{N} + \frac{(x - \bar{x})^2}{\Sigma(x_i - \bar{x})^2}} \quad (15)$$

In particular, for $x = 0$, the upper limit will be

$$y_c = \bar{y} - b\bar{x} + st_{1-\alpha} \sqrt{1 + \frac{1}{N} + \frac{\bar{x}^2}{\Sigma(x_i - \bar{x})^2}} \quad (16)$$

y_c may be considered as the sum of two terms:

$$y_c = Y_0 + P \cdot s \quad (17)$$

with Y_0 and P as defined in the list hereabove. We have no possibility to reduce Y_0 , the intersection of the calibration line with the axis of ordinates. But we may reduce P and s and hence enhance the decision limit.

For the detection limit, it will be convenient to consider y_D , the ordinate of x_D on the regression line. Developments as in

(8) K. A. Brownlee, "Statistical Theory and Methodology in Science and Engineering," John Wiley & Sons, Inc., New York, N. Y., 1960.

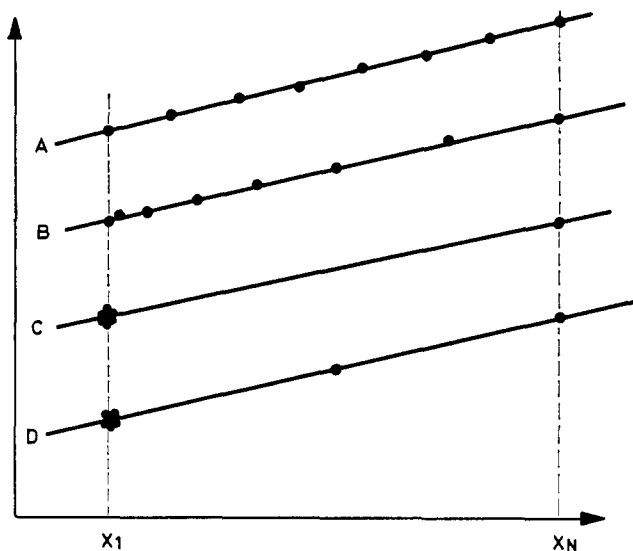


Figure 2. Four types of repartition of the standards

- A. Equidistant or linear
- B. Parabolic
- C. In two values
- D. In three values

the preceding paragraph will yield

$$y_D = y_C + st_{1-\beta} \sqrt{1 + \frac{1}{N} + \frac{(x_D - \bar{x})^2}{\sum(x_i - \bar{x})^2}} \quad (18)$$

and a decrease of y_C will generally bring about a decrease of y_D . y_D may be considered as the sum of three terms

$$y_D = Y_0 + P_s + Q_s \quad (19)$$

and the problem is thus concerned with the reduction of P and Q .

Computation of P. It will prove useful to express the x 's as functions of R , λ_i , and x_1

$$x_i = (1 + \lambda_i R)x_1 \quad (20)$$

where R represents the "range ratio" of the contents of the standards (Equation 7) and where the λ_i 's are dimensionless factors which depend on the repartition of the standards. Let us observe that

$$0 \leq \lambda_i \leq 1, \lambda_1 = 0, \lambda_N = 1 \quad (21)$$

It will readily be seen that the third term of P , P_{III} , does not depend on the scale of the x 's, but may be expressed as a function of the range ratio and the λ_i 's only:

$$\frac{\bar{x}^2}{\sum(x_i - \bar{x})^2} = \frac{\left(\bar{\lambda} + \frac{1}{R}\right)^2}{\sum(\lambda_i - \bar{\lambda})^2} \quad (22)$$

hence

$$P = t \sqrt{1 + \frac{1}{N} + \frac{\left(\bar{\lambda} + \frac{1}{R}\right)^2}{\sum(\lambda_i - \bar{\lambda})^2}} \quad (23)$$

P may thus be expressed as a function of R , for given values of N and several combinations of the λ_i 's. When one may prepare the standards at will, he has, theoretically, an infinity of possible ways of distributing the λ 's. In practice, however, these modes of repartition are rather limited. We have here selected four types; the first two are of very common use; the

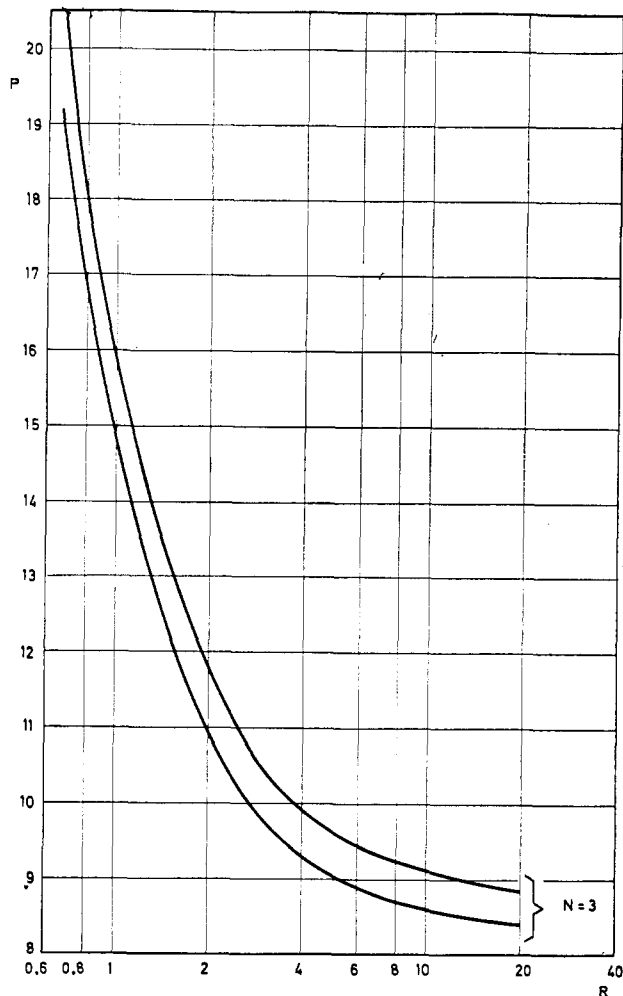


Figure 3. Influence of range (R) on the decision limit, in the case of three standards, with $\alpha = 5\%$; P is in ordinates

Upper curve, linear repartition; lower curve, parabolic repartition with $\gamma = 2$

last two have been introduced for reasons which will be clear later on.

A) the repartition may be linear—*i.e.*, the x 's are equidistant (see Figure 2A);

B) the distribution may be parabolic, its general expression being

$$\lambda_i = \left(\frac{i-1}{N-1}\right)^\gamma \quad (24)$$

each λ_i corresponding to one x_i by formula 1. In practice, γ is around 2 or 3. An example would be:

10, 12, 18, 29, 43, 61, 85, 110 ppm;

here $\gamma = 2$, $N = 8$, $x_1 = 10$, $x_N = 110$, $R = 10$; this distribution corresponds to line B in Figure 2;

C) a repartition of theoretical importance is one where a certain number of standards all have the smallest permissible content (*i.e.*, equal to x_1) and the others the highest permissible content x_N . This is line C of Figure 2.

D) Finally, we have also studied the disposition

K standards at x_1
 1 standard at $(x_1 + x_N)/2$
 $N - K - 1$ standards at x_N

This repartition is represented at Figure 2D. We will call it the "three values repartition."

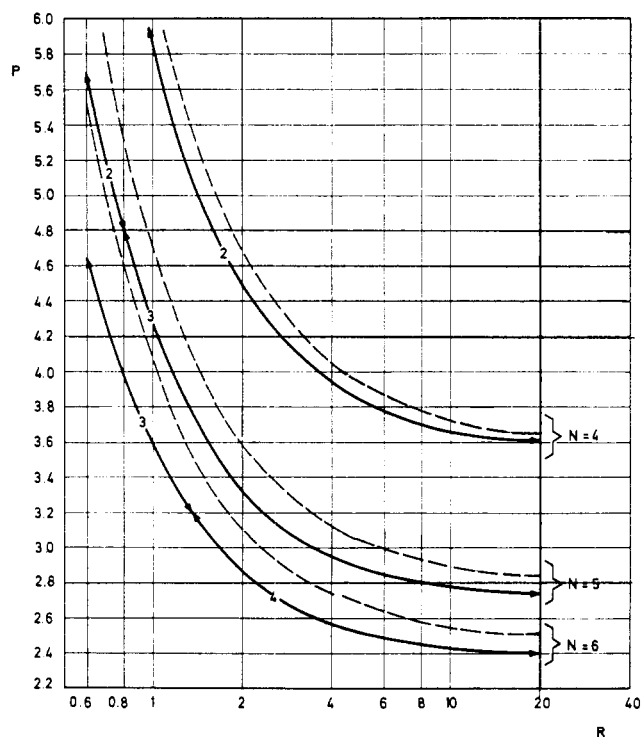


Figure 4. Influence of range R on decision limit, four to six standards, $\alpha = 5\%$. P is in ordinates. For each N , the upper curve corresponds to the parabolic repartition with $\gamma = 2$, and the lower curve to the three values repartition, with the values of K written on the curve

Values of P as a function of R have been computed for these four types of repartition and for different values of N . The computations have been done with the program TABFUN (9) on the IBM 360/65 of the CETIS at Ispra (Italy). The principal results are presented in Figure 3 for $N = 3$ and in Figures 4 and 5 for $N = 4$ to 10. For the three graphs, R is in abscissae and P in ordinates. In Figure 3, the upper curve corresponds to the linear repartition, and the lower curve to the parabolic repartition with $\gamma = 2$. In Figures 4 and 5, the three values repartition is represented by plain curves. The values of K which give the smallest P are written on these curves, the field of validity being limited by arrows. Thus, for $N = 10$, $R = 3$, it is seen on Figure 5 that K must be equal to 7. Except for R inferior to 4, an unusual occurrence, K is equal to $N - 2$. The parabolic repartition with $\gamma = 2$ is represented on the same graphs as dotted lines. For the sake of clarity, the curves corresponding to the linear repartition have not been included in graphs 4 and 5. Had they been represented, the parabolic curves would have been roughly at mid-distance between them and the three values curves.

Estimation of Q . Q_{III} contains x_D and hence, unlike P , Q may not be expressed as a function of t , R , N , and the λ 's. But, on the other hand, if we could make \bar{x} equal to x_D , Q_{III} would vanish. In practice, as x_D is known only after the standards are measured, it is not possible to realize a complete equality, but a fair approximation will be sufficient. It is thus to be recommended that the contents of the standards be chosen in such a way that \bar{x} will fall in the neighborhood of the region where x_D will most probably be.

Contrary to x_C , which is obtained after few computations, the algebraic expression for x_D is really cumbersome [see (8),

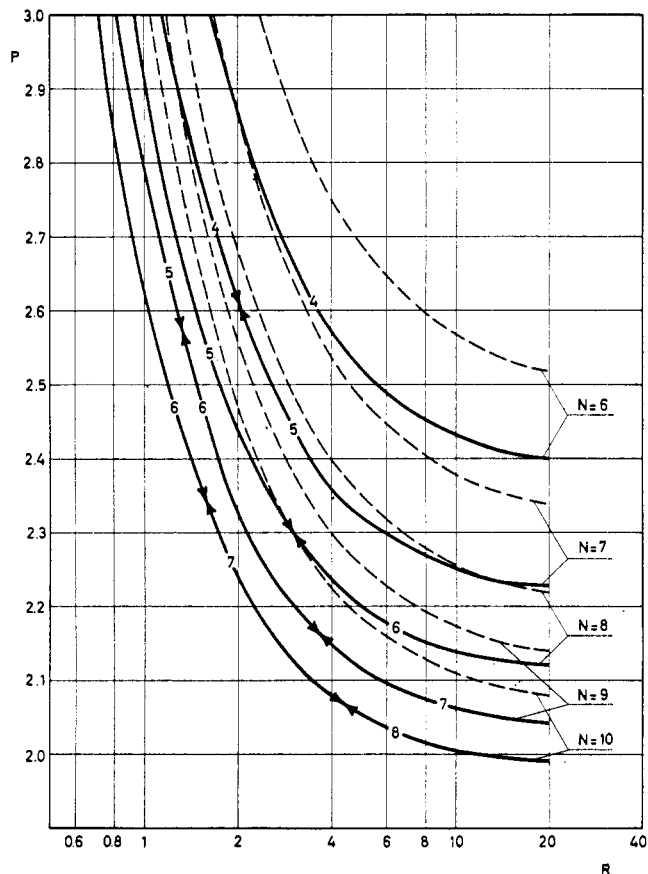


Figure 5. Same as Figure 4, for six to ten standards

§ 11.5]. A graphical solution will be quicker: compute L_C by Equation 16, possibly using the graphs of Figures 3 to 5, compute three or four points of the lower confidence limit by Equation 15 using the minus sign, and draw the line through the points with a French curve. The intersection of this line with $y = L_C$ has x_D as its abscissa. Let us observe that

$$x_C > x_D - x_C \geq \left(s t_{1-\beta} \sqrt{1 + \frac{1}{N}} \right) / b \quad (25)$$

the equality on the right being carried out when $x_D = \bar{x}$. When that condition is fulfilled,

$$Q = t_{1-\beta} \sqrt{1 + \frac{1}{N}} \quad (26)$$

This expression may be used as an estimate of Q in analytical practice.

WAYS TO IMPROVE DECISION AND DETECTION LIMITS

Enhancing the sensitivity of an analytical method can be obtained by improving the precision of the method (s); increasing the number of standards (N); increasing the range of the contents of these standards (R); optimizing the repartition of these standards within this range (the λ_i 's and \bar{x}); and performing replicate measurements on the unknown sample (n).

Precision. The residual standard deviation s is a good measure of the goodness of fit of the observed signals of the standards, or, in other words, of the precision of the method. It is clear from Equations 17 and 19 that there is a direct relationship between precision and sensitivity: improving the precision will lower the limits y_C and x_D .

(9) A. Hubaux and M. Lecloux, Tabulation de Fonctions, CEEA Report EUR 2987.f (1966).

Number of Standards. The influence of N is, of course, important, see Figures 3 to 5, especially between 3 and 6. This is due to the fact that t , $1/N$, and $\Sigma(x_i - \bar{x})^2$ all depend on N . Obviously, as results from Equation 18, the influence of N on y_D will be important also. Although the equation cannot be computed in a general way, it may be said, in first approximation, that Q will diminish in the same proportion as P , when N increases.

Range of Contents of Standards. The influence on P of the range ratio R is expressed in Equation 23 and illustrated by Figures 3 to 5. P is very sensitive to small values of the range ratio, say under 10. From 10 to 20, on the other hand, P goes down only a few percent. Above 20, the gain becomes completely negligible. This consideration may be of use in a number of cases: if the lowest possible standard is at 10 ppm, there is no gain in sensitivity by preparing standards with more than 200 ppm. On the other hand, if we have at our disposal only standards between 80 and 120 ppm ($R = 0.5$) we should expect a really poor sensitivity, unless s is very small, that is unless all the observed signals fall neatly on the regression line. Let us note that, when a "blank" is available, x_1 will be very small (it will never be exactly equal to zero) and the range ratio will take a very high value. For all practical purposes, the right extremity of the graphs ($R = 20$) may be used in this case.

The influence of R on Q is not so readily computed. It may be said however, that this influence will be small as long as \bar{x} remains in the neighborhood of x_D , and nil when the two coincide.

Modes of Repartition of Standards. Very often, N is fixed by economical considerations, various conditions determine the value of x_1 and x_N , and s is made as small as practically possible by a careful preparation of the standards and a good checking of the measurements. When N , R , and s are fixed, however, one still has the liberty to distribute the λ_i 's in the manner best suited for his purposes. Generally, two aims are pursued: first, to check the linearity of the content/signal relation, and second, to lower the sensitivity limit as much as possible. There is no strategy which optimizes both aims: to obtain a maximum of information on the linearity, the x 's should be as far as possible from each other, or, in other words, they should be equidistant (see Figure 2A). On the other hand, the best disposition which we have found after some computations to enhance the sensitivity is to have a certain number of standards with the smallest admissible content (*i.e.*, equal to x_1) and the other standards with the maximum permissible content x_N (see Figure 2C). When the range ratio is greater than 4 or 5, there should be $N - 1$ standards equal to x_1 , and only one equal to x_N . The diminution of P , by adopting the second scheme instead of the first, may be as high as 30% when the range ratio is small and remains of the order of 10 to 15% when this ratio tends to infinity. But unfortunately, this disposition is impossible to adopt in practice because there would not be any control on linearity and because any error on the standard at x_N would be impossible to assess.

As an alternative, we have studied what appears to be the best substitute, the three values distribution, as illustrated at Figure 2D, where there is a check on linearity and on the absence of gross errors. The values of P obtained from Equation 23 with this disposition are plotted as plain curves on Figures 4 and 5. As a comparison, the values of P corresponding to the parabolic distribution with $\gamma = 2$ are given as dotted curves. Computations have shown that this parabolic distribution yields a lower P than the equidistant distribution

(2.25 instead of 2.42 with $N = 8$, $R = 10$). But on the other hand, this P is still notably higher than the corresponding P of the three values disposition: 2.13. With the parabolic repartition, this value of 2.13 is not even reached by the use of 9 standards ($P = 2.17$). Thus, with the three values disposition, we may gain the effect on sensitivity of more than one standard. When the range ratio is smaller and N bigger, the gain is still more important: 8 standards with the three values disposition will give a sensitivity as good (for $R = 3$ or less) as 10 standards distributed parabolically: a gain of two standards!

With the three values repartition, \bar{x} is low and, hence, more likely to fall near x_D , thus contributing also to reduce Q . More specifically, it may be shown that, if we take the three values mode with $K = N - 2$, the third term of Q is equal to

$$Q_{III} = \frac{\left(\lambda_D - \frac{1.5}{N}\right)^2}{1.25 - \frac{2.25}{N}} \quad (27)$$

(the developments are straightforward and too long to be given here). From this equation it will be clear that if λ_D is not too far from $1.5/N$, Q_{III} will be conspicuously smaller than unity; hence, the exact coincidence of \bar{x} and x_D is not required.

Replication on the Unknown. By making n replicates on the unknown sample, the residual variance is divided by n and P must be replaced by P_n , with

$$P_n = t \sqrt{\frac{1}{n} + \frac{1}{N} + \frac{\bar{x}^2}{\Sigma(x_i - \bar{x})^2}} \quad (28)$$

It should be emphasized that this equation applies to replicates which may really be considered as "independent" from each other. It is readily seen that

$$P_n^2 = P^2 - \left(1 - \frac{1}{n}\right)t^2 \quad (29)$$

and hence that replication may conspicuously improve the sensitivity. Let us also remark that the influence of replications will have somewhat more effect when P diminishes. For instance, with $N = 4$ and $\alpha = 5\%$, t is 2.92; if P is equal to 3.7, four replications ($n = 4$) will yield $P_4 = 2.7$, a gain of 27%. With $N = 10$, $t_{0.5\%} = 1.86$; if $P = 2.0$, $n = 4$ will yield $P_{10} = 1.19$, a gain of 40%.

Likewise, Q must be replaced by Q_n , and in symmetry with Equation 29, we have

$$Q_n^2 = Q^2 - \left(1 - \frac{1}{n}\right)t^2 \quad (30)$$

Hence, the effect of replication on y_D will be about the same as the effect on y_C .

A further advantage of replication is that it will yield estimates of the residual variance. It will then be possible to test whether this variance remains constant, as supposed in the present developments; if it does, a better estimate of this variance may be obtained and thus a t with more degrees of freedom may be used, and this smaller t will also contribute to diminish y_C and x_D .

CONCLUSIONS

The definition of the decision and detection limits is here attached to the concept of confidence limits. This presents the advantage that the influence of the standards on the sensi-

tivity may be quantitatively estimated. The most important conclusions are:

A direct relationship exists between the precision of the method and its sensitivity.

There is, as expected, an important gain in sensitivity when increasing the number of standards from 3 to 6. Above 10 standards, the gain is of the order of 2 to 1% on P and Q for one additional standard.

The range ratio should be higher than 10, a condition which is easily met in most cases. But there is no need that it be higher than 20.

When blanks may be added to the series of standards, Figures 3 to 5 may also be used, the results for $R = \infty$ being practically equal to those of $R = 20$.

Where it is important to have a limit of detection as low as possible, it may be of advantage to distribute the standards into three groups of contents only: K standards with the lowest possible content, $N - K - 1$ standards with the highest possible content and one at midway between. The value of K may be read on Figures 4 and 5, where it is seen that when R is greater than 4, $K = N - 2$. This distribution in three values will allow a gain which may be of one or even two standards, when used instead of the more common equidistant or parabolic distributions.

The mean content of the standards, \bar{x} , should fall in the neighborhood of the presupposed value of x_D , a requirement which will be easier to meet with the three values repartition.

Replicate measurements on the unknown samples conspicuously improve the decision and detection limits; this improvement may be computed by Equations 29 and 30.

ILLUSTRATIONS

Case 1. In order to be accepted, an organic material should have a chlorine content inferior to 3.5 ppm. The

material is to be analyzed by X-ray fluorescence and the lowest possible content for reliable standards (x_1) is 1 ppm Cl. As has been shown, the range of the standards, R , should be around 20, hence $x_N = 21$ ppm. α and β are both chosen as 5%. Six standards are prepared and measured, with contents distributed in the three-values mode, yielding as equation of the regression line $y = 2286 + 54.4 x$ (x in ppm, y in counts, for a counting time of 100 seconds) with a standard deviation of 40.0 counts. From Figure 5, $P = 2.39$, hence $y_C = 2382$ and $x_C = 1.77$ ppm. Graphical estimate of x_D yields 3.2 ppm. This value is too high, but duplicates on the unknown will give $P_2 = 1.89$, $Q_2 = 2.08$, and hence $x_D = 2.51$ ppm.

Case 2. Only three standards of a particular impurity in an alloy are available. The contents are 89, 91, and 144 ppm. Hence $\bar{x} = 108$ and $R = 0.62$, a low value indeed! Careful analysis of the three standards gives a regression line with equation: $y = 64690 + 45.2 x$ counts (100 sec counting time) and residual standard deviation of 400 counts. $t_{95\%}$ for 1 degree of freedom = 6.314. Hence $P = 17.1$ by Equation 8, from which $x_C = 151$ ppm! It may only be concluded that this poor series of standards is really inappropriate. The addition of one standard at 400 ppm (supposing linearity remains) would yield $R = 3.5$, hence $P = 4.0$ and $x_C = 35$ ppm. The decision limit may be lowered by adding to the series a standard with a higher content.

ACKNOWLEDGMENT

We express thanks to our colleagues, L. Farese, F. Girardi, and J. Larisse, for fruitful discussions on various aspects of the concepts exposed here.

RECEIVED for review May 21, 1969. Accepted February 24, 1970.

Computer Evaluation of Continuously Scanned Mass Spectra of Gas Chromatographic Effluents

Ronald A. Hites¹ and K. Biemann

Department of Chemistry, Massachusetts Institute of Technology, Cambridge, Mass. 02139

Efficient utilization of the vast amount of data produced by a continuously scanning mass spectrometer coupled to a gas chromatograph required the development of novel data processing techniques. One of the most useful is the display of the change in abundance of certain ions during the gas chromatogram (called "mass chromatogram"). This technique permits detection of the presence or absence of homologous series of compounds as well as specific substances of known or predictable mass spectra. The selection of the m/e values to be plotted can be based on a knowledge of the chemical system under investigation or can be supported by an evaluation of the data itself. Applications of these approaches to geochemical and biomedical problems are discussed.

THE DESIRABILITY of obtaining mass spectral information on practically all components of a complex mixture led to the design of a gas chromatograph-mass spectrometer system which uses a computer to continuously and automatically record mass spectra of the gas chromatographic effluent (1).

¹ NIH predoctoral fellow 1966-68.

(1) R. A. Hites and K. Biemann, *ANAL. CHEM.*, **40**, 1217 (1968).

The need to efficiently utilize the resulting data at a speed comparable to that at which they are acquired made it necessary to develop entirely new approaches to this problem. One approach was the computerized searching of reference mass spectra files (2-4). These techniques relieve the chemist from a great deal of routine work but, because of the limited number of spectra in the reference file (*ca.* 7500 are now available), search results sometimes do not indicate a definite compound. Frequently, the suggestions of such a library search, even though not conclusive, aid in the manual identification of the spectra (2-4). In the course of using these library search techniques for an extended time, several other approaches were developed for certain problems presented by

(2) R. A. Hites and K. Biemann in "Advances in Mass Spectrometry," Vol. 4, E. Kendrick, Ed., The Institute of Petroleum, London, 1968, p 37; presented at the International Mass Spectrometry Conference, Berlin, September 1967.

(3) R. A. Hites, Ph.D. Thesis, Massachusetts Institute of Technology, Cambridge, Mass., 1968.

(4) R. A. Hites, H. S. Hertz, and K. Biemann, Massachusetts Institute of Technology, Cambridge, Mass., unpublished work, 1969.

This page is intentionally left blank.

**APPENDIX C: DYE CONCENTRATIONS:
LABORATORY RESULTS**

**APPENDIX FOR SECTION 4:
FLUORESCENT DYE GROUNDWATER TRACER STUDY**

This page is intentionally left blank.

Table C-1. The fluorescent dye analytical results for the North Seep Group

Location	Date	Time	Salinity	FLT Analysis	FLT	FLT Conc. Adj	SRB Analysis	SRB
				Date	Conc.	for Salinity	Date	Conc.
					(ppb)	(ppb)		(ppb)
seep 1	7/5/11	12:23		2/8/12	0.10	0.10	8/24/11	0.03
seep 1	7/6/11	13:15					8/24/11	0.02
seep 1	7/7/11	9:44					8/24/11	0.03
seep 1	7/9/11	9:47					8/31/11	0.04
seep 1	7/10/11	9:58					8/31/11	0.06
seep 1	7/11/11	8:42					9/23/11	0.02
seep 1	7/11/11	10:20		2/8/12	0.09	0.09	12/30/11	0.03
seep 1	7/11/11	10:20					11/23/11	0.04
seep 1	7/12/11	11:32					8/31/11	0.05
seep 1	7/13/11	9:29					8/31/11	0.04
seep 1	7/14/11	9:33					8/24/11	0.02
seep 1	7/15/11	9:47					8/24/11	0.03
seep 1	7/16/11	10:03					8/31/11	0.04
seep 1	7/17/11	9:29		2/8/12	0.09	0.09	8/24/11	0.03
seep 1	07/19/11	9:34	4.0					
seep 1	07/25/11	10:00	4.2	2/8/12	0.11	0.00		
seep 1	07/27/11	10:23	4.3					
seep 1	07/28/11	9:44	4.3				09/23/11	0.06
seep 1	07/28/11	16:16	3.9				9/9/11	0.03
seep 1	07/29/11	9:51	4.3	2/8/12	0.11	0.00	9/9/11	0.03
seep 1	07/29/11	9:51	4.3	2/8/12	0.11	0.00	9/23/11	0.01
seep 1	07/29/11	16:02	4.0	2/8/12	0.11	0.00	9/9/11	0.03
seep 1	07/29/11	16:02	4.0	2/8/12	0.11	0.00	9/23/11	0.01
seep 1	07/30/11	10:55	4.3				9/23/11	0.02

Table C-1. The fluorescent dye analytical results for the North Seep Group (Continued)

Location	Date	Time	Salinity	FLT Analysis	FLT	FLT Conc. Adj	SRB Analysis	SRB
				Date	Conc.	for Salinity	Date	Conc.
					(ppb)	(ppb)		(ppb)
seep 1	07/30/11	16:37	4.0				9/23/11	0.02
seep 1	07/31/11	10:08	4.4				9/9/11	0.04
seep 1	07/31/11	10:08	4.4				9/23/11	0.02
seep 1	07/31/11	16:27	4.2				9/9/11	0.04
seep 1	07/31/11	16:27	4.2				9/23/11	0.02
seep 1	08/01/11	10:10	4.2	2/8/12	0.13	0.02	9/23/11	0.02
seep 1	08/01/11	10:10	4.2	2/8/12	0.13	0.02	9/23/11	0.01
seep 1	08/01/11	15:53	4.1	2/8/12	0.13	0.02	9/23/11	0.02
seep 1	08/01/11	15:53	4.1	2/8/12	0.13	0.02	9/23/11	0.01
seep 1	08/02/11	8:39	4.0				9/9/11	0.03
seep 1	08/02/11	15:43	4.1				9/9/11	0.03
seep 1	08/03/11	9:52	4.1				9/9/11	0.04
seep 1	08/03/11	9:52	4.1				9/23/11	0.01
seep 1	08/03/11	16:04	4.1				9/9/11	0.04
seep 1	08/03/11	16:04	4.1				9/23/11	0.01
seep 1	08/04/11	10:52	4.0				9/23/11	0.05
seep 1	08/04/11	10:52	4.0				9/9/11	0.04
seep 1	08/04/11	16:19	4.1				9/23/11	0.05
seep 1	08/04/11	16:19	4.1				9/9/11	0.04
seep 1	08/05/11	10:30	4.0				9/9/11	0.04
seep 1	08/05/11	16:48	4.1				9/9/11	0.04
seep 1	08/08/11	9:35	4.3				9/9/11	0.03
seep 1	08/08/11	9:35	4.3				9/23/11	0.01
seep 1	08/08/11	15:43	4.0				9/9/11	0.03

Table C-1. The fluorescent dye analytical results for the North Seep Group (Continued)

Location	Date	Time	Salinity	FLT Analysis	FLT	FLT Conc. Adj	SRB Analysis	SRB
				Date	Conc.	for Salinity	Date	Conc.
					(ppb)	(ppb)		(ppb)
seep 1	08/08/11	15:43	4.0				9/23/11	0.01
seep 1	08/09/11	9:38	4.3				9/23/11	0.02
seep 1	08/09/11	15:35	4.0				9/23/11	0.02
seep 1	08/10/11	11:27	4.3				9/9/11	0.04
seep 1	08/10/11	11:27	4.3				9/9/11	0.04
seep 1	08/10/11	16:15	4.0				9/9/11	0.04
seep 1	08/10/11	16:15	4.0				9/9/11	0.04
seep 1	08/11/11	9:34	4.3				9/23/11	0.01
seep 1	08/11/11	16:02	4.0				9/23/11	0.01
seep 1	08/13/11	9:32	4.3				9/23/11	0.01
seep 1	08/13/11	15:35	4.2				9/23/11	0.01
seep 1	08/14/11	9:56	4.3				10/14/11	0.03
seep 1	08/14/11	15:49	4.1				10/14/11	0.03
seep 1	08/15/11	0:39	4.2				9/23/11	0.02
seep 1	08/15/11	9:20	4.2				9/23/11	0.02
seep 1	08/15/11	15:33	4.2				9/23/11	0.02
seep 1	08/17/11	10:23	4.2				9/23/11	0.02
seep 1	08/17/11	16:11	4.1				9/23/11	0.02
seep 1	08/18/11	0:50	4.2				9/23/11	0.02
seep 1	08/18/11	9:23	4.1				9/23/11	0.02
seep 1	08/18/11	15:51	4.1				9/23/11	0.02
seep 1	08/19/11	9:51	4.1	2/8/12	0.09	-0.02	9/23/11	0.01
seep 1	08/19/11	9:51	4.1	2/8/12	0.09	-0.02	9/23/11	0.04
seep 1	08/19/11	16:11	4.1	2/8/12	0.09	-0.02	9/23/11	0.01

Table C-1. The fluorescent dye analytical results for the North Seep Group (Continued)

Location	Date	Time	Salinity	FLT Analysis	FLT	FLT Conc. Adj	SRB Analysis	SRB
				Date	Conc.	for Salinity	Date	Conc.
					(ppb)	(ppb)		(ppb)
seep 1	08/19/11	16:11	4.1	2/8/12	0.09	-0.02	9/23/11	0.04
seep 1	08/20/11	10:07	4.1				9/23/11	0.01
seep 1	08/20/11	16:12	4.1				9/23/11	0.01
seep 1	08/21/11	10:03	4.3				9/23/11	0.02
seep 1	08/21/11	10:03	4.3				11/4/11	0.02
seep 1	08/21/11	16:09	4.1				9/23/11	0.02
seep 1	08/21/11	16:09	4.1				11/4/11	0.02
seep 1	08/22/11	9:38	4.2				9/23/11	0.02
seep 1	08/22/11	16:18	4.0				9/23/11	0.02
seep 1	08/27/11	9:38	4.3	2/8/12	0.11	0.00	9/23/11	0.02
seep 1	08/27/11	16:12	4.0	2/8/12	0.11	0.00	9/23/11	0.02
seep 1	08/28/11	9:36	4.3				11/23/11	0.04
seep 1	08/28/11	15:54	4.1				11/23/11	0.04
seep 1	09/01/11	10:31	4.1	2/8/12	0.11	0.00	11/23/11	0.03
seep 1	09/01/11	16:23	4.1	2/8/12	0.11	0.00	11/23/11	0.03
seep 1	09/02/11	10:35	4.0				11/23/11	0.03
seep 1	09/02/11	16:06	4.2				11/23/11	0.03
seep 1	09/04/11	15:52	4.0				11/23/11	0.02
seep 1	09/06/11	9:39	4.2				11/23/11	0.03
seep 1	09/06/11	15:50	4.0				11/23/11	0.03
seep 1	09/07/11	9:19	4.2				11/23/11	0.03
seep 1	09/11/11	10:35	4.4				11/23/11	0.03
seep 1	09/13/11	10:36	4.2	2/8/12	0.11	0.00	11/23/11	0.06
seep 1	09/14/11	9:42	4.3	2/10/11	0.11	0.00	2/14/12	0.03

Table C-1. The fluorescent dye analytical results for the North Seep Group (Continued)

Location	Date	Time	Salinity	FLT Analysis	FLT	FLT Conc. Adj	SRB Analysis	SRB
				Date	Conc.	for Salinity	Date	Conc.
					(ppb)	(ppb)		(ppb)
seep 1	09/16/11	11:16	4.6				11/23/11	0.02
seep 1	09/17/11	14:23	5.9				11/23/11	0.04
seep 1	09/21/11	9:39	5.2	2/8/12	0.11	0.00	11/23/11	0.04
seep 1	09/22/11	9:27	5.3				11/23/11	0.04
seep 1	09/23/11	9:58	4.8				11/23/11	0.04
seep 1	09/24/11	9:18	5.8				11/23/11	0.04
seep 1	09/25/11	10:20	4.1				11/4/11	0.01
seep 1	09/26/11	10:05	5.1	2/8/12	0.10	-0.01	11/4/11	0.01
seep 1	09/27/11	9:44	4.1	2/8/12	0.11	0.00	11/4/11	0.02
seep 1	09/28/11	9:44	4.1				11/4/11	0.01
seep 1	09/29/11	9:46	4.0				11/23/11	0.03
seep 1	09/29/11	9:46	4.0				11/4/11	0.01
seep 1	09/30/11	9:49	4.1				11/4/11	0.01
seep 1	10/01/11	10:04	4.1				11/4/11	0.00
seep 1	10/02/11	12:15	4.0				11/4/11	0.01
seep 1	10/03/11	9:50	4.1				11/23/11	0.03
seep 1	10/04/11	9:22	4.2				11/4/11	0.01
seep 1	10/08/11	16:20	4.1	2/8/12	0.10	-0.01	11/4/11	0.00
seep 1	10/10/11	12:05	4.0				11/4/11	0.01
seep 1	10/12/11	9:29	4.0				11/4/11	0.02
seep 1	10/14/11	9:27	4.1	4/11/12	0.10	-0.01	4/12/12	0.01
seep 1	10/16/11	9:27	4.3				11/23/11	0.02
seep 1	10/18/11	11:43	4.1	2/8/12	0.12	0.01	11/23/11	0.02
seep 1	10/20/11	9:29	4.2	2/20/12	0.13	0.02	11/23/11	0.04

Table C-1. The fluorescent dye analytical results for the North Seep Group (Continued)

Location	Date	Time	Salinity	FLT Analysis	FLT	FLT Conc. Adj	SRB Analysis	SRB
				Date	Conc.	for Salinity	Date	Conc.
					(ppb)	(ppb)		(ppb)
seep 1	10/20/11	9:29	4.2	2/7/12	0.13	0.02	11/23/11	0.04
seep 1	10/20/11	9:29	4.2	1/30/12	0.13	0.03	11/23/11	0.04
seep 1	10/22/11	9:34	4.0	2/20/12	0.14	0.03	11/23/11	0.05
seep 1	10/24/11	9:31	4.1	2/20/12	0.16	0.05	11/23/11	0.04
seep 1	10/26/11	9:30	4.1	2/7/12	0.17	0.07	11/23/11	0.05
seep 1	10/26/11	9:30	4.1	2/20/12	0.17	0.06	11/23/11	0.05
seep 1	10/28/11	9:35	4.0	2/20/12	0.21	0.10	11/23/11	0.04
seep 1	10/30/11	11:32	4.0				12/30/11	0.02
seep 1	11/01/11	11:29	4.1				11/23/11	0.03
seep 1	11/01/11	11:29	4.1				11/23/11	0.04
seep 1	11/03/11	9:46	4.1	2/7/12	0.30	0.20	11/23/11	0.04
seep 1	11/09/11	10:11	4.2	1/27/12	0.53	0.43	11/23/11	0.03
seep 1	11/11/11	10:05	4.3	2/7/12	0.58	0.49	11/23/11	0.04
seep 2	07/05/11	0:03		2/8/12	0.11	0.11	8/31/11	0.04
seep 2	07/06/11	12:38					8/31/11	0.02
seep 2	07/07/11	10:03					8/31/11	0.03
seep 2	07/08/11	9:24					8/31/11	0.04
seep 2	07/08/11	9:49					8/31/11	0.02
seep 2	07/08/11	9:49					8/31/11	0.03
seep 2	07/09/11	10:20					8/31/11	0.04
seep 2	07/10/11	10:20		2/8/12	0.10	0.10	8/31/11	0.05
seep 2	07/11/11	10:44					8/31/11	0.04
seep 2	07/12/11	9:47					8/31/11	0.04
seep 2	07/13/11	9:44		2/8/12	0.10	0.10	8/31/11	0.04

Table C-1. The fluorescent dye analytical results for the North Seep Group (Continued)

Location	Date	Time	Salinity	FLT Analysis	FLT	FLT Conc. Adj	SRB Analysis	SRB
				Date	Conc.	for Salinity	Date	Conc.
					(ppb)	(ppb)		(ppb)
seep 2	07/14/11	9:52					8/31/11	0.07
seep 2	07/15/11	10:00					8/31/11	0.04
seep 2	07/16/11	10:20					8/24/11	0.03
seep 2	07/17/11	9:49		2/8/12	0.08	0.08	8/24/11	0.03
seep 2	07/20/11	12:16	4.0				10/4/11	0.00
seep 2	07/21/11	8:38	4.1				10/4/11	0.01
seep 2	07/22/11	10:20	4.1				10/4/11	0.01
seep 2	07/23/11	9:45	4.1				10/4/11	0.01
seep 2	07/25/11	10:08	4.0				10/4/11	0.01
seep 2	07/26/11	9:45	4.2				10/4/11	0.00
seep 2	07/27/11	10:33	4.3				10/4/11	0.01
seep 2	07/28/11	9:53	4.3	2/8/12	0.11	0.00	10/4/11	0.01
seep 2	07/28/11	9:53	4.3	2/8/12	0.11	0.00	10/4/11	0.01
seep 2	07/28/11	9:53	4.3	2/8/12	0.11	0.00	10/4/11	0.01
seep 2	07/28/11	16:25	3.9	2/8/12	0.11	0.00	10/4/11	0.01
seep 2	07/28/11	16:25	3.9	2/8/12	0.11	0.00	10/4/11	0.01
seep 2	07/28/11	16:25	3.9	2/8/12	0.11	0.00	10/4/11	0.01
seep 2	07/29/11	10:00	4.3				10/4/11	0.01
seep 2	07/29/11	10:00	4.3				9/9/11	0.04
seep 2	07/29/11	16:09	3.9				10/4/11	0.01
seep 2	07/29/11	16:09	3.9				9/9/11	0.04
seep 2	07/30/11	11:04	4.3				10/4/11	0.01
seep 2	07/30/11	11:04	4.3				12/30/11	0.04
seep 2	07/30/11	11:04	4.3				9/23/11	0.01

Table C-1. The fluorescent dye analytical results for the North Seep Group (Continued)

Location	Date	Time	Salinity	FLT Analysis	FLT	FLT Conc. Adj	SRB Analysis	SRB
				Date	Conc.	for Salinity	Date	Conc.
					(ppb)	(ppb)		(ppb)
seep 2	07/30/11	16:44	3.8				10/4/11	0.01
seep 2	07/30/11	16:44	3.8				12/30/11	0.04
seep 2	07/30/11	16:44	3.8				9/23/11	0.01
seep 2	07/31/11	10:14	4.3				10/4/11	0.01
seep 2	07/31/11	10:14	4.3				10/4/11	0.00
seep 2	07/31/11	16:20	4.0				10/4/11	0.01
seep 2	07/31/11	16:20	4.0				10/4/11	0.00
seep 2	08/01/11	3:59	4.2				10/4/11	0.01
seep 2	08/01/11	3:59	4.2				10/4/11	0.01
seep 2	08/01/11	9:56	4.0				10/4/11	0.01
seep 2	08/01/11	9:56	4.0				10/4/11	0.01
seep 2	08/02/11	8:46	4.1				9/9/11	0.04
seep 2	08/02/11	8:46	4.1				10/4/11	0.01
seep 2	08/02/11	15:49	4.1				9/9/11	0.04
seep 2	08/02/11	15:49	4.1				10/4/11	0.01
seep 2	08/03/11	0:13	4.1	2/8/12	0.12	0.01	10/4/11	0.00
seep 2	08/03/11	0:13	4.1	2/8/12	0.12	0.01	10/4/11	0.02
seep 2	08/03/11	0:13	4.1	2/8/12	0.12	0.01	10/14/11	0.02
seep 2	08/03/11	0:13	4.1	2/8/12	0.12	0.01	12/30/11	0.03
seep 2	08/03/11	0:13	4.1	2/8/12	0.12	0.01	10/14/11	0.02
seep 2	08/03/11	9:45	4.4	2/8/12	0.12	0.01	10/4/11	0.00
seep 2	08/03/11	9:45	4.4	2/8/12	0.12	0.01	10/4/11	0.02
seep 2	08/03/11	9:45	4.4	2/8/12	0.12	0.01	10/14/11	0.02
seep 2	08/03/11	9:45	4.4	2/8/12	0.12	0.01	12/30/11	0.03

Table C-1. The fluorescent dye analytical results for the North Seep Group (Continued)

Location	Date	Time	Salinity	FLT Analysis	FLT	FLT Conc. Adj	SRB Analysis	SRB
				Date	Conc.	for Salinity	Date	Conc.
					(ppb)	(ppb)		(ppb)
seep 2	08/03/11	9:45	4.4	2/8/12	0.12	0.01	10/14/11	0.02
seep 2	08/03/11	16:11	4.1	2/8/12	0.12	0.01	10/4/11	0.00
seep 2	08/03/11	16:11	4.1	2/8/12	0.12	0.01	10/4/11	0.02
seep 2	08/03/11	16:11	4.1	2/8/12	0.12	0.01	10/14/11	0.02
seep 2	08/03/11	16:11	4.1	2/8/12	0.12	0.01	12/30/11	0.03
seep 2	08/03/11	16:11	4.1	2/8/12	0.12	0.01	10/14/11	0.02
seep 2	08/04/11	10:41	3.9				10/4/11	0.02
seep 2	08/04/11	16:12	4.1				10/4/11	0.02
seep 2	08/05/11	0:37	4.1				10/4/11	0.01
seep 2	08/05/11	0:37	4.1				10/4/11	0.01
seep 2	08/05/11	10:46	4.0				10/4/11	0.01
seep 2	08/05/11	10:46	4.0				10/4/11	0.01
seep 2	08/05/11	16:58	4.2				10/4/11	0.01
seep 2	08/05/11	16:58	4.2				10/4/11	0.01
seep 2	08/06/11	0:58	4.2				10/4/11	0.01
seep 2	08/06/11	0:58	4.2				12/30/11	0.03
seep 2	08/06/11	0:58	4.2				10/4/11	0.02
seep 2	08/06/11	9:00	4.2				10/4/11	0.01
seep 2	08/06/11	9:00	4.2				12/30/11	0.03
seep 2	08/06/11	9:00	4.2				10/4/11	0.02
seep 2	08/06/11	15:46	4.1				10/4/11	0.01
seep 2	08/06/11	15:46	4.1				12/30/11	0.03
seep 2	08/06/11	15:46	4.1				10/4/11	0.02
seep 2	08/07/11	3:15	4.3				10/4/11	0.02

Table C-1. The fluorescent dye analytical results for the North Seep Group (Continued)

Location	Date	Time	Salinity	FLT Analysis Date	FLT	FLT Conc. Adj	SRB Analysis	SRB
					Conc.	for Salinity	Date	Conc.
					(ppb)	(ppb)		
seep 2	08/07/11	3:15	4.3				10/4/11	0.01
seep 2	08/07/11	3:15	4.3				10/4/11	0.02
seep 2	08/07/11	3:15	4.3				10/4/11	0.01
seep 2	08/07/11	9:20	4.3				10/4/11	0.02
seep 2	08/07/11	9:20	4.3				10/4/11	0.01
seep 2	08/07/11	9:20	4.3				10/4/11	0.02
seep 2	08/07/11	9:20	4.3				10/4/11	0.01
seep 2	08/07/11	16:01	4.1				10/4/11	0.02
seep 2	08/07/11	16:01	4.1				10/4/11	0.01
seep 2	08/07/11	16:01	4.1				10/4/11	0.02
seep 2	08/07/11	16:01	4.1				10/4/11	0.01
seep 2	08/07/11	23:25	4.2				10/4/11	0.02
seep 2	08/07/11	23:25	4.2				10/4/11	0.01
seep 2	08/07/11	23:25	4.2				10/4/11	0.02
seep 2	08/07/11	23:25	4.2				10/4/11	0.01
seep 2	08/08/11	9:27	4.3				10/4/11	0.00
seep 2	08/08/11	9:27	4.3				9/23/11	0.02
seep 2	08/08/11	15:48	4.0				10/4/11	0.00
seep 2	08/08/11	15:48	4.0				9/23/11	0.02
seep 2	08/09/11	0:08	4.1				9/9/11	0.04
seep 2	08/09/11	0:08	4.1				9/9/11	0.04
seep 2	08/09/11	0:08	4.1				9/9/11	0.03
seep 2	08/09/11	0:08	4.1				9/9/11	0.03
seep 2	08/09/11	9:30	4.4				9/9/11	0.04

Table C-1. The fluorescent dye analytical results for the North Seep Group (Continued)

Location	Date	Time	Salinity	FLT Analysis	FLT	FLT Conc. Adj	SRB Analysis	SRB
				Date	Conc.	for Salinity	Date	Conc.
				(ppb)		(ppb)		(ppb)
seep 2	08/09/11	9:30	4.4				9/9/11	0.04
seep 2	08/09/11	9:30	4.4				9/9/11	0.03
seep 2	08/09/11	9:30	4.4				9/9/11	0.03
seep 2	08/09/11	15:45	4.0				9/9/11	0.04
seep 2	08/09/11	15:45	4.0				9/9/11	0.04
seep 2	08/09/11	15:45	4.0				9/9/11	0.03
seep 2	08/09/11	15:45	4.0				9/9/11	0.03
seep 2	08/10/11	0:00	4.2				9/9/11	0.03
seep 2	08/10/11	11:18	4.3				9/9/11	0.03
seep 2	08/10/11	16:19	4.0				9/9/11	0.03
seep 2	08/11/11	0:26	4.2	2/8/12	0.11	0.00	11/4/11	0.03
seep 2	08/11/11	0:26	4.2	2/8/12	0.11	0.00	10/4/11	0.01
seep 2	08/11/11	0:26	4.2	2/8/12	0.11	0.00	10/4/11	0.00
seep 2	08/11/11	0:26	4.2	2/8/12	0.11	0.00	9/9/11	0.03
seep 2	08/11/11	9:26	4.3	2/8/12	0.11	0.00	11/4/11	0.03
seep 2	08/11/11	9:26	4.3	2/8/12	0.11	0.00	10/4/11	0.01
seep 2	08/11/11	9:26	4.3	2/8/12	0.11	0.00	10/4/11	0.00
seep 2	08/11/11	9:26	4.3	2/8/12	0.11	0.00	9/9/11	0.03
seep 2	08/11/11	16:09	3.9	2/8/12	0.11	0.00	11/4/11	0.03
seep 2	08/11/11	16:09	3.9	2/8/12	0.11	0.00	10/4/11	0.01
seep 2	08/11/11	16:09	3.9	2/8/12	0.11	0.00	10/4/11	0.00
seep 2	08/11/11	16:09	3.9	2/8/12	0.11	0.00	9/9/11	0.03
seep 2	08/12/11	0:25	4.2				11/4/11	0.03
seep 2	08/12/11	0:25	4.2				11/4/11	0.02

Table C-1. The fluorescent dye analytical results for the North Seep Group (Continued)

Location	Date	Time	Salinity	FLT Analysis Date	FLT	FLT Conc. Adj	SRB Analysis Date	SRB
					Conc.	for Salinity		Conc.
					(ppb)	(ppb)		
seep 2	08/12/11	0:25	4.2				10/14/11	0.02
seep 2	08/12/11	0:25	4.2				12/30/11	0.03
seep 2	08/12/11	9:27	4.3				11/4/11	0.03
seep 2	08/12/11	9:27	4.3				11/4/11	0.02
seep 2	08/12/11	9:27	4.3				10/14/11	0.02
seep 2	08/12/11	9:27	4.3				12/30/11	0.03
seep 2	08/12/11	16:01	4.0				11/4/11	0.03
seep 2	08/12/11	16:01	4.0				11/4/11	0.02
seep 2	08/12/11	16:01	4.0				10/14/11	0.02
seep 2	08/12/11	16:01	4.0				12/30/11	0.03
seep 2	08/13/11	0:28	4.2				10/14/11	0.02
seep 2	08/13/11	0:28	4.2				10/14/11	0.02
seep 2	08/13/11	9:25	4.3				10/14/11	0.02
seep 2	08/13/11	9:25	4.3				10/14/11	0.02
seep 2	08/13/11	15:45	4.1				10/14/11	0.02
seep 2	08/13/11	15:45	4.1				10/14/11	0.02
seep 2	08/14/11	0:23	4.2				11/4/11	0.02
seep 2	08/14/11	0:23	4.2				10/4/11	0.01
seep 2	08/14/11	9:40	4.2				11/4/11	0.02
seep 2	08/14/11	9:40	4.2				10/4/11	0.01
seep 2	08/14/11	15:54	4.2				11/4/11	0.02
seep 2	08/14/11	15:54	4.2				10/4/11	0.01
seep 2	08/15/11	9:27	4.2				11/4/11	0.03
seep 2	08/15/11	9:27	4.2				11/4/11	0.03

Table C-1. The fluorescent dye analytical results for the North Seep Group (Continued)

Location	Date	Time	Salinity	FLT Analysis	FLT	FLT Conc. Adj	SRB Analysis	SRB
				Date	Conc.	for Salinity	Date	Conc.
					(ppb)	(ppb)		(ppb)
seep 2	08/15/11	15:39	4.2				11/4/11	0.03
seep 2	08/15/11	15:39	4.2				11/4/11	0.03
seep 2	08/16/11	10:08	4.2				10/4/11	0.00
seep 2	08/16/11	10:08	4.2				11/4/11	0.04
seep 2	08/16/11	15:16	4.2				10/4/11	0.00
seep 2	08/16/11	15:16	4.2				11/4/11	0.04
seep 2	08/17/11	10:32	4.2	2/8/12	0.11	0.00	10/14/11	0.02
seep 2	08/17/11	10:32	4.2	2/8/12	0.11	0.00	11/23/11	0.05
seep 2	08/17/11	16:03	4.2	2/8/12	0.11	0.00	10/14/11	0.02
seep 2	08/17/11	16:03	4.2	2/8/12	0.11	0.00	11/23/11	0.05
seep 2	08/18/11	9:38	4.1				10/4/11	0.01
seep 2	08/18/11	9:38	4.1				11/4/11	0.02
seep 2	08/18/11	15:41	4.1				10/4/11	0.01
seep 2	08/18/11	15:41	4.1				11/4/11	0.02
seep 2	08/19/11	9:34	4.1				10/4/11	0.00
seep 2	08/19/11	9:34	4.1				11/4/11	0.02
seep 2	08/19/11	16:03	4.1				10/4/11	0.00
seep 2	08/19/11	16:03	4.1				11/4/11	0.02
seep 2	08/20/11	10:02	4.1				10/4/11	0.01
seep 2	08/20/11	10:02	4.1				11/23/11	0.05
seep 2	08/20/11	16:05	4.1				10/4/11	0.01
seep 2	08/20/11	16:05	4.1				11/23/11	0.05
seep 2	08/21/11	9:53	4.1				11/4/11	0.02
seep 2	08/21/11	9:53	4.1				11/4/11	0.02

Table C-1. The fluorescent dye analytical results for the North Seep Group (Continued)

Location	Date	Time	Salinity	FLT Analysis	FLT	FLT Conc. Adj	SRB Analysis	SRB
				Date	Conc.	for Salinity	Date	Conc.
					(ppb)	(ppb)		(ppb)
seep 2	08/21/11	16:03	4.1				11/4/11	0.02
seep 2	08/21/11	16:03	4.1				11/4/11	0.02
seep 2	08/22/11	9:31	4.2	2/8/12	0.11	0.00	11/4/11	0.03
seep 2	08/22/11	9:31	4.2	2/8/12	0.11	0.00	10/4/11	0.01
seep 2	08/22/11	16:11	4.1	2/8/12	0.11	0.00	11/4/11	0.03
seep 2	08/22/11	16:11	4.1	2/8/12	0.11	0.00	10/4/11	0.01
seep 2	08/24/11	17:10	4.0				11/4/11	0.01
seep 2	08/25/11	9:58	4.3				10/4/11	0.00
seep 2	08/25/11	9:58	4.3				11/4/11	0.03
seep 2	08/25/11	16:34	4.0				10/4/11	0.00
seep 2	08/25/11	16:34	4.0				11/4/11	0.03
seep 2	08/26/11	9:38	4.3	2/8/12	0.11	0.00	11/4/11	0.02
seep 2	08/26/11	15:47	3.9	2/8/12	0.11	0.00	11/4/11	0.02
seep 2	08/27/11	9:48	4.3				11/4/11	0.03
seep 2	08/27/11	9:48	4.3				11/4/11	0.02
seep 2	08/27/11	16:23	3.9				11/4/11	0.03
seep 2	08/27/11	16:23	3.9				11/4/11	0.02
seep 2	08/28/11	9:45	4.2				10/4/11	0.00
seep 2	08/28/11	9:45	4.2				10/4/11	0.00
seep 2	08/28/11	16:02	4.0				10/4/11	0.00
seep 2	08/28/11	16:02	4.0				10/4/11	0.00
seep 2	08/29/11	9:49	4.2				10/4/11	0.01
seep 2	08/29/11	9:49	4.2				10/4/11	0.01
seep 2	08/29/11	16:05	4.0				10/4/11	0.01

Table C-1. The fluorescent dye analytical results for the North Seep Group (Continued)

Location	Date	Time	Salinity	FLT Analysis	FLT	FLT Conc. Adj	SRB Analysis	SRB
				Date	Conc.	for Salinity	Date	Conc.
					(ppb)	(ppb)		(ppb)
seep 2	08/29/11	16:05	4.0				10/4/11	0.01
seep 2	08/30/11	9:33	4.1	2/8/12	0.11	0.00	10/4/11	0.01
seep 2	09/01/11	10:49	4.1				11/4/11	0.03
seep 2	09/01/11	10:49	4.1				11/4/11	0.03
seep 2	09/01/11	16:13	4.2				11/4/11	0.03
seep 2	09/01/11	16:13	4.2				11/4/11	0.03
seep 2	09/02/11	10:23	4.1				10/14/11	0.02
seep 2	09/02/11	15:55	4.3				10/14/11	0.02
seep 2	09/03/11	9:56	4.2	2/8/12	0.11	0.00	11/4/11	0.02
seep 2	09/03/11	9:56	4.2	2/8/12	0.11	0.00	11/23/11	0.03
seep 2	09/03/11	16:09	4.1	2/8/12	0.11	0.00	11/4/11	0.02
seep 2	09/03/11	16:09	4.1	2/8/12	0.11	0.00	11/23/11	0.03
seep 2	09/04/11	15:40	4.1				11/4/11	0.02
seep 2	09/05/11	9:46	4.2				11/4/11	0.03
seep 2	09/05/11	16:05	4.1				11/4/11	0.03
seep 2	09/07/11	9:27	4.3				10/4/11	0.01
seep 2	09/10/11	10:32	4.9	2/8/12	0.11	0.00	10/4/11	0.01
seep 2	09/11/11	10:20	6.2				10/4/11	0.01
seep 2	09/14/11	9:55	4.6				10/4/11	0.00
seep 2	09/15/11	9:34	4.3				10/4/11	0.01
seep 2	09/18/11	11:13	7.0				10/4/11	0.01
seep 2	09/18/11	11:13	7.0				10/4/11	0.00
seep 2	09/19/11	10:18	6.8				11/23/11	0.03
seep 2	09/20/11	9:49	6.7	2/10/11	0.10	-0.01	2/14/12	0.03

Table C-1. The fluorescent dye analytical results for the North Seep Group (Continued)

Location	Date	Time	Salinity	FLT Analysis	FLT	FLT Conc. Adj	SRB Analysis	SRB
				Date	Conc.	for Salinity	Date	Conc.
					(ppb)	(ppb)		(ppb)
seep 2	09/21/11	9:30	6.0	2/8/12	0.11	0.00	11/23/11	0.03
seep 2	09/22/11	9:36	9.9				11/23/11	0.05
seep 2	09/23/11	9:39	5.7				11/23/11	0.03
seep 2	09/24/11	9:09	6.3				11/23/11	0.04
seep 2	09/26/11	10:18	5.2				11/4/11	0.02
seep 2	09/27/11	9:35	4.2				11/4/11	0.01
seep 2	09/28/11	9:35	4.1				11/4/11	0.03
seep 2	09/29/11	9:34	4.1				11/23/11	0.04
seep 2	09/30/11	9:39	4.2				11/4/11	0.02
seep 2	10/01/11	9:55	4.3				11/4/11	0.01
seep 2	10/03/11	9:40	4.6	2/8/12	0.11	0.00	11/4/11	0.01
seep 2	10/04/11	9:34	4.4				11/4/11	0.02
seep 2	10/08/11	16:30	4.0				11/4/11	0.21
seep 2	10/12/11	9:38	4.0				11/4/11	0.02
seep 2	10/14/11	9:34	4.1	2/8/12	0.11	0.00	11/23/11	0.03
seep 2	10/16/11	9:36	4.4				11/23/11	0.02
seep 2	10/18/11	11:58	4.4	2/8/12	0.11	0.00	11/23/11	0.03
seep 2	10/20/11	9:40	4.2	2/20/12	0.12	0.02	11/23/11	0.04
seep 2	10/20/11	9:40	4.2	2/7/12	0.13	0.02	11/23/11	0.04
seep 2	10/22/11	9:41	4.0	2/20/12	0.13	0.02	11/23/11	0.04
seep 2	10/22/11	9:41	4.0	2/7/12	0.13	0.02	11/23/11	0.04
seep 2	10/24/11	9:41	4.1	2/20/12	0.15	0.04	11/23/11	0.04
seep 2	10/26/11	9:40	4.1	2/7/12	0.17	0.06	11/23/11	0.05
seep 2	10/26/11	9:40	4.1	2/20/12	0.17	0.06	11/23/11	0.05

Table C-1. The fluorescent dye analytical results for the North Seep Group (Continued)

Location	Date	Time	Salinity	FLT Analysis	FLT	FLT Conc. Adj	SRB Analysis	SRB
				Date	Conc.	for Salinity	Date	Conc.
					(ppb)	(ppb)		(ppb)
seep 2	10/28/11	9:45	4.0	2/20/12	0.19	0.08	11/23/11	0.03
seep 2	11/03/11	9:39	4.0				11/23/11	0.04
seep 2	11/05/11	13:22	4.1	1/30/12	0.35	0.25		
seep 2	11/07/11	9:41	4.1	2/7/12	0.42	0.32	11/23/11	0.02
seep 2	11/09/11	9:58	4.2	2/7/12	0.49	0.39	11/23/11	0.02
seep 6	07/19/11	9:25	4.1				9/23/11	0.02
seep 6	07/20/11	9:59	4.1	2/9/11	0.11	0.00	11/4/11	0.03
seep 6	07/21/11	8:25	3.8	2/9/11	0.11	0.00	9/23/11	0.02
seep 6	07/25/11	10:16	4.2				9/23/11	0.02
seep 6	07/28/11	9:32	4.2	2/9/11	0.11	0.00	9/23/11	0.02
seep 6	07/28/11	16:07	3.9	2/9/11	0.11	0.00	9/23/11	0.02
seep 6	07/29/11	1:27	4.1				9/9/11	0.04
seep 6	07/29/11	1:27	4.1				10/14/11	0.02
seep 6	07/29/11	9:43	4.2				9/9/11	0.04
seep 6	07/29/11	9:43	4.2				10/14/11	0.02
seep 6	07/29/11	15:55	4.0				9/9/11	0.04
seep 6	07/29/11	15:55	4.0				10/14/11	0.02
seep 6	07/30/11	0:35	4.1				9/23/11	0.02
seep 6	07/30/11	0:35	4.1				11/4/11	0.03
seep 6	07/30/11	0:35	4.1				8/31/11	0.04
seep 6	07/30/11	0:35	4.1				8/31/11	0.05
seep 6	07/30/11	16:24	4.3				9/23/11	0.02
seep 6	07/30/11	16:24	4.3				11/4/11	0.03
seep 6	07/30/11	16:24	4.3				8/31/11	0.04

Table C-1. The fluorescent dye analytical results for the North Seep Group (Continued)

Location	Date	Time	Salinity	FLT Analysis	FLT	FLT Conc. Adj	SRB Analysis	SRB
				Date	Conc.	for Salinity	Date	Conc.
					(ppb)	(ppb)		(ppb)
seep 6	07/30/11	16:24	4.3				8/31/11	0.05
seep 6	07/31/11	10:00	4.0				12/30/11	0.03
seep 6	07/31/11	10:00	4.0				9/23/11	0.02
seep 6	07/31/11	10:00	4.0				10/14/11	0.02
seep 6	07/31/11	10:00	4.0				9/23/11	0.02
seep 6	07/30/11	11:09	4.1				9/23/11	0.02
seep 6	07/30/11	11:09	4.1				11/4/11	0.03
seep 6	07/30/11	11:09	4.1				8/31/11	0.04
seep 6	07/30/11	11:09	4.1				8/31/11	0.05
seep 6	07/31/11	16:10	4.3				12/30/11	0.03
seep 6	07/31/11	16:10	4.3				9/23/11	0.02
seep 6	07/31/11	16:10	4.3				10/14/11	0.02
seep 6	07/31/11	16:10	4.3				9/23/11	0.02
seep 6	07/31/11	0:42	4.1				12/30/11	0.03
seep 6	07/31/11	0:42	4.1				9/23/11	0.02
seep 6	07/31/11	0:42	4.1				10/14/11	0.02
seep 6	07/31/11	0:42	4.1				9/23/11	0.02
seep 6	08/01/11	10:04	4.2				8/31/11	0.05
seep 6	08/01/11	10:04	4.2				9/9/11	0.05
seep 6	08/01/11	15:47	4.1				8/31/11	0.05
seep 6	08/01/11	15:47	4.1				9/9/11	0.05
seep 6	08/02/11	8:29	4.1	2/9/11	0.12	0.01	9/9/11	0.05
seep 6	08/02/11	8:29	4.1	2/9/11	0.12	0.01	9/23/11	0.03
seep 6	08/02/11	15:35	4.1	2/9/11	0.12	0.01	9/9/11	0.05

Table C-1. The fluorescent dye analytical results for the North Seep Group (Continued)

Location	Date	Time	Salinity	FLT Analysis	FLT	FLT Conc. Adj	SRB Analysis	SRB
				Date	Conc.	for Salinity	Date	Conc.
					(ppb)	(ppb)		(ppb)
seep 6	08/02/11	15:35	4.1	2/9/11	0.12	0.01	9/23/11	0.03
seep 6	08/03/11	9:58	4.1				12/30/11	0.03
seep 6	08/03/11	9:58	4.1				10/14/11	0.03
seep 6	08/03/11	9:58	4.1				9/23/11	0.03
seep 6	08/03/11	15:55	4.1				12/30/11	0.03
seep 6	08/03/11	15:55	4.1				10/14/11	0.03
seep 6	08/03/11	15:55	4.1				9/23/11	0.03
seep 6	08/04/11	10:56	4.1				9/23/11	0.03
seep 6	08/04/11	10:56	4.1				9/9/11	0.04
seep 6	08/04/11	16:25	4.0				9/23/11	0.03
seep 6	08/04/11	16:25	4.0				9/9/11	0.04
seep 6	08/05/11	10:31	4.1				9/9/11	0.04
seep 6	08/05/11	16:37	4.1				9/9/11	0.04
seep 6	08/06/11	9:20	4.2				9/23/11	0.02
seep 6	08/06/11	15:30	4.1				9/23/11	0.02
seep 6	08/07/11	9:40	4.2				8/31/11	0.05
seep 6	08/07/11	9:40	4.2				9/9/11	0.04
seep 6	08/07/11	15:43	4.0				8/31/11	0.05
seep 6	08/07/11	15:43	4.0				9/9/11	0.04
seep 6	08/08/11	9:42	4.3				9/9/11	0.05
seep 6	08/08/11	9:42	4.3				9/23/11	0.02
seep 6	08/08/11	15:34	4.0				9/9/11	0.05
seep 6	08/08/11	15:34	4.0				9/23/11	0.02
seep 6	08/09/11	9:48	4.3	2/9/11	0.11	0.00	9/9/11	0.04

Table C-1. The fluorescent dye analytical results for the North Seep Group (Continued)

Location	Date	Time	Salinity	FLT Analysis	FLT	FLT Conc. Adj	SRB Analysis	SRB
				Date	Conc.	for Salinity	Date	Conc.
					(ppb)	(ppb)		(ppb)
seep 6	08/09/11	9:48	4.3	2/9/11	0.11	0.00	9/9/11	0.03
seep 6	08/09/11	15:30	4.1	2/9/11	0.11	0.00	9/9/11	0.04
seep 6	08/09/11	15:30	4.1	2/9/11	0.11	0.00	9/9/11	0.03
seep 6	08/10/11	11:30	4.3				9/9/11	0.04
seep 6	08/10/11	11:30	4.3				9/23/11	0.03
seep 6	08/10/11	11:30	4.3				9/9/11	0.02
seep 6	08/10/11	16:05	4.0				9/9/11	0.04
seep 6	08/10/11	16:05	4.0				9/23/11	0.03
seep 6	08/10/11	16:05	4.0				9/9/11	0.02
seep 6	08/11/11	9:37	4.3	2/9/11	0.12	0.01	9/23/11	0.02
seep 6	08/11/11	15:55	3.9	2/9/11	0.12	0.01	9/23/11	0.02
seep 6	08/12/11	9:41	4.3				9/23/11	0.02
seep 6	08/12/11	15:37	4.0				9/23/11	0.02
seep 6	08/14/11	16:01	4.2				9/23/11	0.02
seep 6	08/15/11	9:34	4.2				9/23/11	0.02
seep 6	08/15/11	15:47	4.2				9/23/11	0.02
seep 6	08/16/11	2:39	4.2				12/14/11	0.03
seep 6	08/16/11	2:39	4.2				9/23/11	0.03
seep 6	08/16/11	9:47	4.2				12/14/11	0.03
seep 6	08/16/11	9:47	4.2				9/23/11	0.03
seep 6	08/16/11	15:33	4.2				12/14/11	0.03
seep 6	08/16/11	15:33	4.2				9/23/11	0.03
seep 6	08/18/11	9:55	4.1				9/23/11	0.03
seep 6	08/18/11	16:00	4.1				9/23/11	0.03

Table C-1. The fluorescent dye analytical results for the North Seep Group (Continued)

Location	Date	Time	Salinity	FLT Analysis	FLT	FLT Conc. Adj	SRB Analysis	SRB
				Date	Conc.	for Salinity	Date	Conc.
					(ppb)	(ppb)		(ppb)
seep 6	08/20/11	9:54	4.0				9/23/11	0.03
seep 6	08/20/11	15:57	4.1				9/23/11	0.03
seep 6	08/21/11	9:49	4.2				9/23/11	0.02
seep 6	08/21/11	16:16	4.1				9/23/11	0.02
seep 6	08/22/11	9:25	4.2	2/9/11	0.12	0.01	9/23/11	0.02
seep 6	08/22/11	16:04	4.1	2/9/11	0.12	0.01	9/23/11	0.02
seep 6	08/23/11	9:35	4.2				12/14/11	0.02
seep 6	08/23/11	15:36	4.0				12/14/11	0.02
seep 6	08/24/11	10:26	4.3				10/4/11	0.00
seep 6	08/24/11	16:50	4.0				10/4/11	0.00
seep 6	08/26/11	9:30	4.4				12/5/11	0.02
seep 6	08/26/11	15:38	4.0				12/5/11	0.02
seep 6	08/29/11	9:39	4.1				10/4/11	0.00
seep 6	08/29/11	15:55	4.0				10/4/11	0.00
seep 6	09/01/11	11:00	4.8				10/4/11	0.01
seep 6	09/01/11	16:33	4.2				10/4/11	0.01
seep 6	09/02/11	10:46	4.1	2/9/11	0.11	0.00	12/5/11	0.01
seep 6	09/02/11	10:46	4.1	2/9/11	0.11	0.00	10/4/11	0.01
seep 6	09/02/11	16:16	5.1	2/9/11	0.11	0.00	12/5/11	0.01
seep 6	09/02/11	16:16	5.1	2/9/11	0.11	0.00	10/4/11	0.01
seep 6	09/04/11	16:05	4.6				10/4/11	0.01
seep 6	09/06/11	9:24	4.2				10/4/11	0.01
seep 6	09/06/11	16:07	4.0				10/4/11	0.01
seep 6	09/08/11	9:46	4.2				10/4/11	0.01

Table C-1. The fluorescent dye analytical results for the North Seep Group (Continued)

Location	Date	Time	Salinity	FLT Analysis	FLT	FLT Conc. Adj	SRB Analysis	SRB
				Date	Conc.	for Salinity	Date	Conc.
					(ppb)	(ppb)		(ppb)
seep 6	09/09/11	10:40	4.2				11/4/11	0.03
seep 6	09/10/11	10:42	4.3	2/10/11	0.11	0.00	2/14/12	0.03
seep 6	09/11/11	10:48	4.3				10/4/11	0.01
seep 6	09/12/11	12:00	4.3				10/4/11	0.01
seep 6	09/13/11	11:02	4.2				11/23/11	0.04
seep 6	09/14/11	10:05	4.2	2/9/11	0.11	0.00	11/23/11	0.03
seep 6	09/15/11	9:46	4.2				10/4/11	0.01
seep 6	09/15/11	9:46	4.2				12/5/11	0.02
seep 6	09/16/11	11:37	4.2	2/9/11	0.11	0.00	12/5/11	0.02
seep 6	09/18/11	11:25	5.7				10/4/11	0.01
seep 6	09/19/11	10:32	7.0				11/23/11	0.02
seep 6	09/20/11	9:40	4.3				11/23/11	0.04
seep 6	09/21/11	9:21	5.0				11/23/11	0.03
seep 6	09/22/11	9:48	6.5				11/23/11	0.03
seep 6	09/23/11	9:50	4.6	2/9/11	0.11	0.00	11/23/11	0.03
seep 6	09/24/11	8:57	4.8				11/23/11	0.04
seep 6	09/25/11	10:33	5.4				11/4/11	0.01
seep 6	09/26/11	10:36	5.9				11/23/11	0.03
seep 6	09/27/11	9:25	4.6				11/4/11	0.02
seep 6	09/28/11	9:26	4.0				11/4/11	0.01
seep 6	09/29/11	9:21	4.0				11/4/11	0.01
seep 6	09/30/11	9:28	4.1				11/4/11	0.02
seep 6	10/01/11	9:45	4.2				11/23/11	0.02
seep 6	10/02/11	12:03	4.0				11/4/11	0.01

Table C-1. The fluorescent dye analytical results for the North Seep Group (Continued)

Location	Date	Time	Salinity	FLT Analysis	FLT	FLT Conc. Adj	SRB Analysis	SRB
				Date	Conc.	for Salinity	Date	Conc.
					(ppb)	(ppb)		(ppb)
seep 6	10/02/11	12:03	4.0				11/4/11	0.01
seep 6	10/03/11	9:30	4.0				11/4/11	0.01
seep 6	10/04/11	9:47	4.1				11/23/11	0.03
seep 6	10/06/11	12:18	4.1	2/9/11	0.11	0.00	11/4/11	0.03
seep 6	10/08/11	16:09	4.0				11/4/11	0.01
seep 6	10/12/11	9:20	4.1				11/4/11	0.01
seep 6	10/14/11	9:47	4.1	2/9/11	0.11	0.00	11/23/11	0.03
seep 6	10/16/11	9:46	4.3	2/9/11	0.11	0.00	11/23/11	0.04
seep 6	10/18/11	11:32	4.3	2/10/11	0.11	0.00	11/23/11	0.05
seep 6	10/20/11	9:53	4.1	2/20/12	0.13	0.02	11/23/11	0.04
seep 6	10/20/11	9:53	4.1	2/9/11	0.13	0.02	11/23/11	0.04
seep 6	10/22/11	9:51	4.0	2/20/12	0.14	0.03	11/23/11	0.04
seep 6	10/22/11	9:51	4.0	2/7/12	0.14	0.03	11/23/11	0.04
seep 6	10/24/11	9:51	4.1	2/20/12	0.15	0.05		
seep 6	10/26/11	9:58	4.1				11/23/11	0.04
seep 6	10/28/11	9:25	4.0	1/30/12	0.20	0.09	11/23/11	0.05
seep 6	11/01/11	11:52	4.1	1/27/12	0.24	0.14	11/23/11	0.03
seep 6	11/03/11	9:53	4.1	2/9/11	0.29	0.18	11/23/11	0.04
seep 6	11/05/11	13:07	4.1	1/27/12	0.35	0.24		
seep 6	11/07/11	9:31	4.1	2/9/11	0.40	0.30	11/23/11	0.03
seep 6	11/09/11	9:39	4.1	2/7/12	0.47	0.37	11/23/11	0.04
seep 6	11/09/11	9:39	4.1	1/30/12	0.48	0.38	11/23/11	0.04
seep 6	11/11/11	9:54	4.3				11/23/11	0.03
seep 6	11/16/11	9:49	3.9	1/27/12	0.89	0.80	11/23/11	0.04

Table C-1. The fluorescent dye analytical results for the North Seep Group (Continued)

Location	Date	Time	Salinity	FLT Analysis	FLT	FLT Conc. Adj	SRB Analysis	SRB
				Date	Conc.	for Salinity	Date	Conc.
					(ppb)	(ppb)		(ppb)
seep 6	11/16/11	9:49	3.9	1/30/12	0.18	0.07	11/23/11	0.04
seep 6	11/18/11	10:02	4.8	2/9/11	0.94	0.88	11/23/11	0.03
seep 6	11/18/11	10:02	4.8	2/7/12	0.53	0.45	11/23/11	0.03
seep 6	11/21/11	9:37	4.2	1/27/12	1.18	1.10	12/5/11	0.02
seep 6	11/23/11	9:34	4.0	1/27/12	1.37	1.29	12/5/11	0.03
Seep 7	11/16/11	9:10	4.1				11/23/11	0.04
Seep 7	11/18/11	9:45	4.1				11/23/11	0.04
Seep 7	11/21/11	9:49	4.0				12/14/11	0.04
Seep 7	11/23/11	9:57	4.0	1/27/12	1.43	1.36	12/5/11	0.02
Seep 7	11/25/11	10:08	4.2	1/27/12	1.54	1.48	12/5/11	0.03
Seep 7	11/28/11	9:41	6.5	1/30/12	1.77	1.86	12/5/11	0.03
Seep 7	11/28/11	9:41	6.5	2/7/12	1.76	1.85	12/5/11	0.03
Seep 7	11/30/11	10:39	4.0	1/27/12	2.27	2.22	12/5/11	0.02
Seep 7	12/02/11	9:44	4.2	1/30/12	2.39	2.36	12/5/11	0.02
Seep 7	12/05/11	10:03	4.0				12/30/11	0.02
Seep 7	12/07/11	9:33	3.9	1/30/12	3.15	3.12	1/20/12	0.03
Seep 7	12/09/11	9:39	4.1	2/7/12	3.70	3.71	12/30/11	0.03
Seep 7	12/14/11	9:25	4.0	2/7/12	4.85	4.88	12/30/11	0.02
Seep 7	12/19/11	9:58	4.0				12/30/11	0.03
Seep 7	12/21/11	10:18	4.1				1/11/12	0.01
Seep 7	12/23/11	10:10	4.6	2/7/12	6.82	7.04	1/11/12	0.01
Seep 7	12/26/11	10:14	4.1				1/11/12	0.01
Seep 7	12/28/11	10:06	4.1	2/7/12	7.80	7.93	1/11/12	0.02
Seep 7	12/30/11	10:21	4.4				1/11/12	0.03

Table C-1. The fluorescent dye analytical results for the North Seep Group (Continued)

Location	Date	Time	Salinity	FLT Analysis	FLT	FLT Conc. Adj	SRB Analysis	SRB
				Date	Conc.	for Salinity	Date	Conc.
					(ppb)	(ppb)		(ppb)
Seep 7	01/02/12	10:18	8.2				1/11/12	0.02
Seep 7	01/04/12	14:48	4.2	2/10/11	9.25	9.47	2/14/12	0.04
Seep 7	01/07/12	14:46	4.2	1/27/12	10.08	10.33	1/20/12	0.04
Seep 7	01/09/12	11:11	4.0	1/27/12	10.59	10.78	1/20/12	0.04
Seep 7	01/11/12	10:55	4.0	1/27/12	11.50	11.72	1/20/12	0.09
Seep 7	01/13/12	11:25	4.1	1/27/12	11.80	12.07	1/20/12	0.04
Seep 7	01/16/12	13:04	4.1	1/27/12	12.11	12.39	1/20/12	0.04
Seep 7	01/19/12	10:12	4.3	2/10/11	12.51	12.89	2/14/12	0.04
Seep 7	01/21/12	16:00	4.2	2/10/11	13.31	13.68	2/14/12	0.03
Seep 7	01/23/12	11:30	4.1	2/10/11	13.92	14.25	2/14/12	0.03
Seep 7	01/25/12	9:43	4.1	2/20/12	14.66	15.02	3/7/12	0.05
Seep 7	01/27/12	12:20	4.1	2/10/11	13.82	14.15	2/14/12	0.03
Seep 7	01/31/12	11:13	4.1	2/10/11	15.02	15.40	2/14/12	0.04
Seep 7	02/10/12	0:06	4.3	3/5/12	16.45	16.98	3/7/12	0.04
Seep 7	02/14/12	13:17	4.2	3/5/12	17.78	18.30	3/7/12	0.03
Seep 7	02/17/12	11:20	4.2	3/5/12	19.01	19.58	3/7/12	0.04
Seep 7	02/20/12	13:46	4.3	3/5/12	19.93	20.60	3/7/12	0.04
Seep 7	02/24/12	11:03	4.2	3/24/12	19.65	20.24	3/21/12	0.02
Seep 7	02/27/12	10:05	4.2				3/21/12	0.03
Seep 7	03/01/12	11:29	4.3	3/18/12	21.50	22.23	3/21/12	0.02
Seep 8	11/16/11	9:35	5.0				11/23/11	0.04
Seep 8	11/23/11	9:45	4.2	1/27/12	1.60	1.54	12/5/11	0.02
Seep 8	11/25/11	10:18	4.3				12/5/11	0.02
Seep 8	11/28/11	9:53	5.9	1/27/12	1.65	1.69	12/5/11	0.03

Table C-1. The fluorescent dye analytical results for the North Seep Group (Continued)

Location	Date	Time	Salinity	FLT Analysis	FLT	FLT Conc. Adj	SRB Analysis	SRB
				Date	Conc.	for Salinity	Date	Conc.
					(ppb)	(ppb)		(ppb)
Seep 8	11/30/11	10:49	4.0	2/7/12	2.53	2.49	12/5/11	0.02
Seep 8	12/02/11	9:54	4.1	1/27/12	2.74	2.71	12/5/11	0.02
Seep 8	12/05/11	9:51	4.1				12/30/11	0.03
Seep 8	12/07/11	9:54	4.2	1/27/12	2.78	2.76	1/20/12	0.02
Seep 8	12/09/11	9:49	4.1	2/7/12	3.91	3.93	12/30/11	0.03
Seep 8	12/14/11	9:44	4.1				12/30/11	0.03
Seep 8	12/16/11	9:50	4.0	2/7/12	5.32	5.37		
Seep 8	12/19/11	9:47	4.1				12/30/11	0.03
Seep 8	12/21/11	10:43	4.2				1/11/12	0.02
Seep 8	12/23/11	10:34	4.2	2/7/12	7.13	7.27	1/11/12	0.01
Seep 8	12/26/11	10:35	4.3				1/11/12	0.01
Seep 8	12/28/11	10:15	4.3	2/7/12	8.39	8.60	1/11/12	0.11
Seep 8	12/30/11	10:45	4.6				1/11/12	0.02
Seep 8	01/02/12	10:50	22.0				1/11/12	0.00
Seep 8	01/04/12	15:17	4.4	2/10/11	10.40	10.73	2/14/12	0.04
Seep 8	01/07/12	15:08	4.3	2/7/12	11.35	11.67	1/20/12	0.04
Seep 8	01/07/12	15:08	4.3	1/27/12	11.40	11.73	1/20/12	0.04
Seep 8	01/09/12	10:36	4.2	1/27/12	11.80	12.11	1/20/12	0.04
Seep 8	01/11/12	10:33	4.2	1/27/12	12.82	13.16	1/20/12	0.04
Seep 8	01/11/12	10:33	4.2	1/27/12	12.82	13.16	1/20/12	0.03
Seep 8	01/13/12	11:02	4.2	1/27/12	12.92	13.26	1/20/12	0.04
Seep 8	01/16/12	12:47	4.1	1/27/12	13.73	14.06	1/20/12	0.05
Seep 8	01/16/12	12:47	4.1	1/27/12	13.63	13.95	1/20/12	0.05
Seep 9	11/30/11	9:27	4.0	2/7/12	2.17	2.12	12/5/11	0.03

Table C-1. The fluorescent dye analytical results for the North Seep Group (Continued)

Location	Date	Time	Salinity	FLT Analysis	FLT	FLT Conc. Adj	SRB Analysis	SRB
				Date	Conc.	for Salinity	Date	Conc.
					(ppb)	(ppb)		(ppb)
Seep 9	11/30/11	9:27	4.0	1/30/12	2.17	2.12	12/5/11	0.03
Seep 9	12/02/11	9:30	4.2	1/30/12	2.40	2.37	12/5/11	0.03
Seep 9	12/07/11	9:44	3.9	1/27/12	3.08	3.05	1/20/12	0.03
Seep 9	12/09/11	9:28	3.9	2/7/12	3.54	3.52	12/30/11	0.03
Seep 9	12/09/11	9:28	3.9	2/7/12	3.54	3.52	12/30/11	0.03
Seep 9	12/14/11	9:35	4.0	2/7/12	4.82	4.85	12/30/11	0.03
Seep 9	12/19/11	10:06	4.1				12/30/11	0.03
Seep 9	12/21/11	10:31	4.0	2/7/12	5.98	6.04	1/11/12	-0.01
Seep 9	12/21/11	10:31	4.0	2/7/12	5.98	6.04	1/11/12	0.02
Seep 9	12/23/11	10:21	4.1				1/11/12	0.01
Seep 9	12/26/11	10:24	4.0				1/11/12	0.01
Seep 9	12/28/11	9:57	4.1	2/7/12	7.83	7.97		
Seep 9	12/30/11	10:36	4.2				1/11/12	0.01
Seep 9	01/02/12	10:36	14.0	2/7/12	5.25	7.81	1/11/12	0.01
Seep 9	01/04/12	15:03	5.2	2/10/11	8.68	9.17	2/14/12	0.04
Seep 9	01/07/12	14:58	7.9	1/27/12	9.00	10.46	1/20/12	0.03
Seep 9	01/09/12	10:56	4.2	1/27/12	10.59	10.85	1/20/12	0.03
Seep 9	01/11/12	10:45	4.4	2/10/11	11.00	11.36	2/14/12	0.04
Seep 9	01/13/12	11:15	16.8	1/27/12	6.95	11.99	1/20/12	0.02
Seep 9	01/16/12	13:16	17.9	1/27/12	6.99	12.84	1/20/12	0.03
Seep 9	01/19/12	9:58	5.3	2/10/11	11.71	12.46	2/14/12	0.03
Seep 9	01/21/12	16:13	15.0	2/20/12	8.31	13.08		
Seep 9	01/23/12	11:19	25.3	2/10/11	4.56	14.63	2/14/12	0.02
Seep 10	01/21/12	16:26	5.0	2/20/12	12.02	12.67	3/7/12	0.03

Table C-1. The fluorescent dye analytical results for the North Seep Group (Continued)

Location	Date	Time	Salinity	FLT Analysis	FLT	FLT Conc. Adj	SRB Analysis	SRB
				Date	Conc.	for Salinity	Date	Conc.
					(ppb)	(ppb)		(ppb)
Seep 10	01/23/12	11:03	5.0	2/10/11	13.21	13.93	2/14/12	0.05
Seep 10	01/25/12	10:30	4.3	2/20/12	13.94	14.37	3/7/12	0.03
Seep 10	01/27/12	12:34	6.2	2/10/11	12.81	14.07	2/14/12	0.04
Seep 10	01/31/12	11:29	4.4	2/10/11	15.93	16.49	2/14/12	0.05
Seep 10	02/10/12	11:30	5.1	3/5/12	16.14	17.10	3/7/12	0.04
Seep 10	02/14/12	12:47	4.2	3/5/12	18.09	18.62	3/7/12	0.03
Seep 10	02/17/12	11:05	4.3	3/5/12	18.60	19.21	3/7/12	0.03
Seep 10	02/20/12	13:12	4.3	3/5/12	19.73	20.39	3/7/12	0.04
Seep 10	02/24/12	10:51	4.1	3/24/12	19.76	20.28	3/21/12	0.02
Seep 10	02/27/12	9:37	5.2	3/24/12	18.63	19.83	3/21/12	0.02
Seep 10	03/01/12	11:18	4.3	3/18/12	20.27	20.95	3/21/12	0.03
Seep 10	06/29/12	12:16	4.6	7/20/12	18.31	19.10	7/26/12	0.03
Seep 10	07/04/12	12:34	4.7	7/20/12	18.51	19.37	7/26/12	0.02
Seep 12	01/25/12	11:24	4.3	2/10/11	14.52	14.97	2/14/12	0.11
Seep 12	01/27/12	12:05	4.3	2/10/11	14.22	14.66	2/14/12	0.04
Seep 12	01/31/12	11:41	4.2	2/10/11	16.13	16.59	2/14/12	0.04
Seep 12	02/10/12	11:47	4.4	3/5/12	16.65	17.25	3/7/12	0.04
Seep 12	02/10/12	11:47	4.4	3/5/12	16.76	17.35	3/7/12	0.04
Seep 12	02/14/12	13:02	4.3	3/5/12	18.40	19.00	3/7/12	0.04
Seep 12	02/17/12	11:31	4.2	3/5/12	19.22	19.79	3/7/12	0.04
Seep 12	02/20/12	13:25	4.9	3/5/12	19.63	20.68	3/7/12	0.04
Seep 12	02/20/12	13:25	4.9	3/5/12	19.63	20.68	3/7/12	0.06
Seep 12	02/20/12	13:25	4.9	3/5/12	20.04	21.12	3/7/12	0.04
Seep 12	02/20/12	13:25	4.9	3/5/12	20.04	21.12	3/7/12	0.06

Table C-1. The fluorescent dye analytical results for the North Seep Group (Continued)

Location	Date	Time	Salinity	FLT Analysis	FLT	FLT Conc. Adj	SRB Analysis	SRB
				Date	Conc.	for Salinity	Date	Conc.
					(ppb)	(ppb)		(ppb)
Seep 12	02/24/12	11:16	4.2	3/24/12	20.47	21.09	3/21/12	0.02
Seep 12	02/27/12	10:32	4.4	3/24/12	20.98	21.76	3/21/12	0.02
Seep 12	03/01/12	11:40	4.8	3/18/12	20.68	21.73	3/21/12	0.02
Seep 12	03/14/12	10:21	4.2	3/18/12	20.68	21.31	3/21/12	0.04
Seep 12	03/17/12	9:36	4.2	4/11/12	21.01	21.65	4/12/12	0.02
Seep 12	03/19/12	10:12	4.1	4/11/12	21.51	22.10	4/12/12	0.02
Seep 13	03/14/12	9:53	4.2	3/18/12	20.89	21.52	3/21/12	0.02
Seep 13	03/17/12	9:12	4.4	4/11/12	20.61	21.37	4/12/12	0.02
Seep 13	03/19/12	9:46	4.2	4/11/12	21.81	22.48	4/12/12	0.02
Seep 14	03/14/12	10:11	4.2				3/21/12	0.02
Seep 14	03/17/12	9:23	4.2	4/11/12	20.41	21.03	4/12/12	0.02
Seep 14	03/17/12	9:23	4.2	4/11/12	20.41	21.03	4/12/12	0.02
Seep 14	03/19/12	9:57	4.1	4/11/12	21.51	22.10	4/12/12	0.02
Seep 14	03/19/12	9:57	4.1	4/11/12	21.51	22.10	4/12/12	0.02
Seep 15	03/27/12	9:09	4.8	4/11/12	20.21	21.23	4/12/12	0.02
Seep 15	03/29/12	10:28	4.2	4/11/12	20.61	21.23	4/12/12	0.02
Seep 15	04/02/12	10:19	9.3	4/11/12	17.40	21.46	4/12/12	0.02
Seep 15	04/05/12	8:27	9.3	5/11/12	18.03	22.24	5/17/12	0.03
Seep 15	04/12/12	11:30	4.2	5/11/12	21.30	21.94	5/17/12	0.03
Seep 15	04/16/12	9:09	4.2	5/11/12	21.81	22.47	10/9/12	0.04
Seep 15	04/16/12	9:09	4.2	5/11/12	21.81	22.47	5/17/12	0.04
Seep 15	04/19/12	11:32	4.3	5/11/12	21.09	21.80	5/17/12	0.05
Seep 15	04/24/12	15:25	4.3	5/11/12	20.17	20.85	5/17/12	0.03
Seep 15	04/26/12	10:40	4.2	5/11/12	20.38	20.99	5/17/12	0.03

Table C-1. The fluorescent dye analytical results for the North Seep Group (Continued)

Location	Date	Time	Salinity	FLT Analysis	FLT	FLT Conc. Adj	SRB Analysis	SRB
				Date	Conc.	for Salinity	Date	Conc.
					(ppb)	(ppb)		(ppb)
Seep 15	05/02/12	9:42	4.3	5/11/12	21.40	22.12	5/17/12	0.03
Seep 15	05/07/12	9:51	4.3	6/14/12	21.15	21.86	6/22/12	0.03
Seep 15	05/14/12	9:22	4.4	6/14/12	15.72	16.28	6/22/12	0.03
Seep 15	05/18/12	13:29	4.7	6/14/12	7.54	7.82	6/22/12	0.01
Seep 15	05/22/12	15:16	4.5	6/14/12	21.35	22.21	6/22/12	0.03
Seep 15	05/25/12	15:06	4.4	6/15/12	21.31	22.10	6/22/12	0.04
Seep 15	05/29/12	14:18	4.4	6/15/12	21.61	22.41	6/22/12	0.04
Seep 15	06/04/12	14:14	4.7	6/15/12	20.20	21.15	6/22/12	0.04
Seep 15	06/07/12	12:30	4.5	6/15/12	20.70	21.54	6/22/12	0.05
Seep 15	06/12/12	11:27	4.5	7/20/12	16.40	17.04	7/26/12	0.01
Seep 15	06/14/12	14:43	4.4	7/20/12	20.02	20.75	7/26/12	0.03
Seep 15	06/16/12	11:59	4.6	7/20/12	19.72	20.57	7/26/12	0.03
Seep 15	06/18/12	9:43	4.6	7/20/12	19.62	20.47	7/26/12	0.03
Seep 16	04/24/12	15:11	4.5	5/11/12	20.17	20.98	5/17/12	0.02
Seep 16	04/26/12	10:53	4.4	5/11/12	21.19	21.98	5/17/12	0.03
Seep 16	05/02/12	9:32	4.5	5/11/12	21.50	22.37	5/17/12	0.04
Seep 16	05/07/12	9:13	4.6	6/15/12	21.41	22.35	6/22/12	0.05
Seep 16	05/14/12	9:02	4.5	6/15/12	22.32	23.22	6/22/12	0.04
Seep 16	05/18/12	13:07	4.5	6/15/12	18.59	19.32	6/22/12	0.04
Seep 16	05/22/12	15:06	4.6	6/15/12	21.91	22.88	6/22/12	0.04
Seep 16	05/25/12	14:55	4.6	6/15/12	21.61	22.56	6/22/12	0.04
Seep 16	05/29/12	14:32	4.4	6/15/12	21.81	22.62	6/22/12	0.04
Seep 16	06/04/12	14:02	4.8	6/15/12	20.30	21.33	6/22/12	0.04
Seep 16	06/07/12	12:19	4.6	6/15/12	20.70	21.61	6/22/12	0.04

Table C-1. The fluorescent dye analytical results for the North Seep Group (Continued)

Location	Date	Time	Salinity	FLT Analysis	FLT	FLT Conc. Adj	SRB Analysis	SRB
				Date	Conc.	for Salinity	Date	Conc.
					(ppb)	(ppb)		(ppb)
Seep 16	06/12/12	11:44	4.5	7/20/12	20.02	20.82	7/26/12	0.02
Seep 16	06/14/12	14:27	4.6	7/20/12	20.02	20.89	7/26/12	0.03
Seep 16	06/16/12	12:12	4.6	7/20/12	19.92	20.78	7/26/12	0.03
Seep 16	06/18/12	9:07	12.0	7/20/12	14.40	19.82	7/26/12	0.02
Seep 17	06/29/12	12:38	14.5	7/20/12	14.10	21.76	7/26/12	0.02
Seep 17	07/11/12	13:53	13.3	7/25/12	13.71	19.99	7/26/12	0.01
Seep 17	07/23/12	9:39	6.5	10/3/12	17.13	19.05	10/9/12	0.04
Seep 18	07/11/12	13:40	4.6	7/25/12	19.29	20.13	7/26/12	0.01
Seep 18	07/23/12	9:03	4.7	10/3/12	18.45	19.30	10/9/12	0.04
Seep 18	08/01/12	9:20	4.7	8/3/12	17.06	17.85	8/2/12	0.04
Seep 18	08/01/12	9:20	4.7	8/3/12	17.06	17.85	10/9/12	0.04
Seep 18	08/01/12	9:20	4.7	10/3/12	17.03	17.81	8/2/12	0.04
Seep 18	08/01/12	9:20	4.7	10/3/12	17.03	17.81	10/9/12	0.04
Seep 19	08/08/12	13:54	4.5	10/3/12	17.54	18.23	10/9/12	0.04
Seep 19	08/08/12	13:54	4.5	10/3/12	17.13	17.80	10/9/12	0.04
Seep 19	08/16/12	9:43	4.8	10/3/12	16.22	17.02	10/9/12	0.03
Seep 19	08/21/12	9:09	4.5	10/3/12	17.03	17.70	10/9/12	0.04
Seep 19	08/24/12	11:36	4.3	10/3/12	16.73	17.27	10/9/12	0.04
Seep 19	08/27/12	9:11	4.7	10/3/12	16.93	17.71	10/9/12	0.02
Seep 19	09/06/12	9:39	4.5	10/3/12	15.11	15.69	10/9/12	0.03
Seep 19	09/10/12	12:51	4.9	10/3/12	14.70	15.47	10/9/12	0.04
Seep 19	09/12/12	9:01	4.5	10/12/12	14.96	15.53	10/19/12	0.03
Seep 20	09/20/12	11:44	4.5	10/12/12	14.66	15.22	10/19/12	0.03
Seep 20	10/02/12	11:30	4.9	10/12/12	13.95	14.67	10/19/12	0.03

Table C-1. The fluorescent dye analytical results for the North Seep Group (Continued)

Location	Date	Time	Salinity	FLT Analysis	FLT	FLT Conc. Adj	SRB Analysis	SRB
				Date	Conc.	for Salinity	Date	Conc.
					(ppb)	(ppb)		(ppb)
Seep 20	10/02/12	11:30	4.9	10/12/12	14.86	15.63	10/19/12	0.03
Seep 20	10/08/12	14:08	6.0	11/2/2012	12.91	14.07	11/2/12	0.02
Seep 20	10/12/12	11:05	11.3	11/2/2012	10.47	13.95	11/2/12	0.03
Seep 20	10/18/12	11:19	15.9	11/2/2012	8.00	13.18	11/2/12	0.02
Seep 20	10/22/12	9:40	7.3	11/2/2012	11.99	13.69	11/2/12	0.05
Seep 20	10/26/12	10:42	15.2	11/17/2012	8.41	13.37	11/19/12	0.01
Seep 20	10/29/12	11:14	14.0	11/17/2012	8.58	12.87	11/19/12	0.01
Seep 20	11/02/12	14:51	13.3	11/17/2012	8.78	12.75	11/19/12	0.01
Seep 20	11/08/12	11:56	12.9	11/17/2012	8.70	12.40	11/19/12	0.01
Seep 20	11/12/12	11:09	4.5	11/17/2012	12.01	12.44	11/19/12	0.02
Seep 20	11/19/12	11:26	4.8	12/14/2012	11.92	12.47	12/19/12	0.02
Seep 20	12/06/12	10:50	11.5	12/14/2012	8.34	11.17	12/19/12	0.02
Seep 20	12/10/12	9:26	10.1	12/14/2012	9.20	11.64	12/19/12	0.02
Seep 20	12/14/12	12:16	6.7	1/12/2013	9.67	10.77	1/16/13	0.05
Seep 20	12/28/12	12:59	11.7	1/12/2013	7.99	10.78	1/16/13	0.03
Seep 21	10/22/12	9:09	7.5	11/2/12	11.28	12.96	11/2/12	0.02
Seep 21	10/26/12	10:26	4.7	11/17/12	11.50	11.99	11/19/12	0.03
Seep 21	10/29/12	11:02	5.1	11/17/12	12.31	13.02	11/19/12	0.02
Seep 21	11/02/12	14:40	4.8	11/17/12	12.31	12.89	11/19/12	0.02
Seep 21	11/08/12	11:43	7.1	11/17/12	11.40	12.91	11/19/12	0.02

Table C-2. The fluorescent dye analytical results for the South Seep Group

Location	Date	Time	Salinity	FLT Analysis		FLT Conc. Adj		SRB Analysis	
				Date	FLT Conc.	for Salinity	Date	SRB Conc.	
						(ppb)	(ppb)		
						(ppb)	(ppb)		
seep 3	07/19/11	10:15	2.8					10/14/11	0.01
seep 3	07/23/11	10:26	3.3	2/8/12	0.12	0.01		11/4/11	0.04
seep 3	07/24/11	10:10	3.5					11/4/11	0.03
seep 3	07/24/11	10:10	3.5					12/30/11	0.03
seep 3	07/24/11	10:10	3.5					11/4/11	0.03
seep 3	07/26/11	10:12	2.8					10/14/11	0.01
seep 3	07/28/11	10:16	2.8	2/8/12	0.13	0.02		12/30/11	0.03
seep 3	07/28/11	10:16	2.8	2/8/12	0.13	0.02		10/14/11	0.03
seep 3	07/28/11	10:16	2.8	2/8/12	0.13	0.02		9/9/11	0.04
seep 3	07/28/11	16:34	2.9	2/8/12	0.13	0.02		12/30/11	0.03
seep 3	07/28/11	16:34	2.9	2/8/12	0.13	0.02		10/14/11	0.03
seep 3	07/28/11	16:34	2.9	2/8/12	0.13	0.02		9/9/11	0.04
seep 3	07/29/11	10:25	2.8					8/31/11	0.03
seep 3	07/29/11	16:29	3.6					8/31/11	0.03
seep 3	07/30/11	11:38	2.9					11/23/11	0.04
seep 3	07/30/11	11:38	2.9					8/31/11	0.05
seep 3	07/30/11	17:15	2.9					11/23/11	0.04
seep 3	07/30/11	17:15	2.9					8/31/11	0.05
seep 3	07/31/11	10:51	2.8					12/30/11	0.03
seep 3	07/31/11	10:51	2.8					9/23/11	0.02
seep 3	07/31/11	10:51	2.8					10/14/11	0.01
seep 3	07/31/11	16:52	8.3					12/30/11	0.03
seep 3	07/31/11	16:52	8.3					9/23/11	0.02

Table C-2. The fluorescent dye analytical results for the South Seep Group (Continued)

Location	Date	Time	Salinity	FLT Analysis	FLT	FLT Conc. Adj	SRB Analysis	SRB
				Date	Conc.	for Salinity	Date	Conc.
					(ppb)	(ppb)		(ppb)
seep 3	07/31/11	16:52	8.3				10/14/11	0.01
seep 3	08/02/11	9:04	2.8	2/8/12	0.12	0.01	9/23/11	0.02
seep 3	08/02/11	9:04	2.8	2/8/12	0.12	0.01	9/9/11	0.03
seep 3	08/02/11	16:12	2.8	2/8/12	0.12	0.01	9/23/11	0.02
seep 3	08/02/11	16:12	2.8	2/8/12	0.12	0.01	9/9/11	0.03
seep 3	08/04/11	11:17	2.8				9/9/11	0.04
seep 3	08/04/11	11:17	2.8				10/14/11	0.02
seep 3	08/04/11	16:48	2.8				9/9/11	0.04
seep 3	08/04/11	16:48	2.8				10/14/11	0.02
seep 3	08/05/11	11:07	2.8				9/9/11	0.04
seep 3	08/05/11	11:07	2.8				8/31/11	0.05
seep 3	08/05/11	17:17	2.8				9/9/11	0.04
seep 3	08/05/11	17:17	2.8				8/31/11	0.05
seep 3	08/07/11	10:03	2.8				12/30/11	0.04
seep 3	08/07/11	10:03	2.8				11/4/11	0.04
seep 3	08/07/11	16:18	2.8				12/30/11	0.04
seep 3	08/07/11	16:18	2.8				11/4/11	0.04
seep 3	08/08/11	10:15	3.1				9/9/11	0.03
seep 3	08/08/11	10:15	3.1				9/9/11	0.04
seep 3	08/08/11	16:12	2.8				9/9/11	0.03
seep 3	08/08/11	16:12	2.8				9/9/11	0.04
seep 3	08/09/11	10:05	2.8	2/8/12	0.12	0.01	9/9/11	0.04
seep 3	08/09/11	10:05	2.8	2/8/12	0.12	0.01	9/9/11	0.05
seep 3	08/09/11	10:05	2.8	2/8/12	0.12	0.01	9/9/11	0.04

Table C-2. The fluorescent dye analytical results for the South Seep Group (Continued)

Location	Date	Time	Salinity	FLT Analysis	FLT	FLT Conc. Adj	SRB Analysis	SRB
				Date	Conc.	for Salinity	Date	Conc.
					(ppb)	(ppb)		(ppb)
seep 3	08/09/11	10:05	2.8	2/8/12	0.12	0.01	11/4/11	0.03
seep 3	08/09/11	10:05	2.8	2/8/12	0.12	0.01	9/9/11	0.04
seep 3	08/09/11	10:05	2.8	2/8/12	0.12	0.01	9/9/11	0.05
seep 3	08/09/11	10:05	2.8	2/8/12	0.12	0.01	9/9/11	0.04
seep 3	08/09/11	10:05	2.8	2/8/12	0.12	0.01	11/4/11	0.03
seep 3	08/09/11	16:02	2.8	2/8/12	0.12	0.01	9/9/11	0.04
seep 3	08/09/11	16:02	2.8	2/8/12	0.12	0.01	9/9/11	0.05
seep 3	08/09/11	16:02	2.8	2/8/12	0.12	0.01	9/9/11	0.04
seep 3	08/09/11	16:02	2.8	2/8/12	0.12	0.01	11/4/11	0.03
seep 3	08/09/11	16:02	2.8	2/8/12	0.12	0.01	9/9/11	0.04
seep 3	08/09/11	16:02	2.8	2/8/12	0.12	0.01	9/9/11	0.05
seep 3	08/09/11	16:02	2.8	2/8/12	0.12	0.01	9/9/11	0.04
seep 3	08/09/11	16:02	2.8	2/8/12	0.12	0.01	11/4/11	0.03
seep 3	08/10/11	12:29	3.2				9/9/11	0.04
seep 3	08/10/11	12:29	3.2				9/9/11	0.04
seep 3	08/10/11	16:38	2.8				9/9/11	0.04
seep 3	08/10/11	16:38	2.8				9/9/11	0.04
seep 3	08/11/11	10:04	2.8				11/4/11	0.02
seep 3	08/11/11	16:27	3.4				11/4/11	0.02
seep 3	08/12/11	10:02	2.8				10/14/11	0.01
seep 3	08/12/11	10:02	2.8				10/14/11	0.01
seep 3	08/12/11	16:21	3.3				10/14/11	0.01
seep 3	08/12/11	16:21	3.3				10/14/11	0.01
seep 3	08/14/11	10:26	2.8				10/14/11	0.01

Table C-2. The fluorescent dye analytical results for the South Seep Group (Continued)

Location	Date	Time	Salinity	FLT Analysis	FLT	FLT Conc. Adj	SRB Analysis	SRB
				Date	Conc.	for Salinity	Date	Conc.
					(ppb)	(ppb)		(ppb)
seep 3	08/14/11	16:23	3.4				10/14/11	0.01
seep 3	08/18/11	10:35	2.8	2/8/12	0.11	0.00	10/14/11	0.02
seep 3	08/18/11	16:41	3.1	2/8/12	0.11	0.00	10/14/11	0.02
seep 3	08/20/11	10:31	3.0				10/14/11	0.01
seep 3	08/20/11	16:32	2.8				10/14/11	0.01
seep 3	08/21/11	10:34	3.1				10/14/11	0.02
seep 3	08/21/11	16:41	2.8				10/14/11	0.02
seep 3	08/24/11	11:20	16.1	2/8/12	0.12	0.02	10/14/11	0.01
seep 3	08/24/11	17:46	2.9	2/8/12	0.12	0.01	10/14/11	0.01
seep 3	08/27/11	10:51	2.9				10/14/11	0.02
seep 3	08/27/11	17:29	2.9				10/14/11	0.02
seep 3	09/02/11	12:17	2.7	2/8/12	0.12	0.01	10/14/11	0.01
seep 3	09/02/11	17:00	2.8	2/8/12	0.12	0.01	10/14/11	0.01
seep 3	09/05/11	10:18	2.8				10/14/11	0.01
seep 3	09/05/11	16:41	2.8				10/14/11	0.01
seep 3	09/10/11	11:36	3.0				10/14/11	0.01
seep 3	09/14/11	10:49	3.3	2/10/11	0.11	0.00		
seep 3	09/17/11	15:37	3.3				10/14/11	0.01
seep 3	09/18/11	12:19	2.9				11/4/11	0.02
seep 3	09/19/11	11:20	8.5	2/8/12	0.09	0.00	11/23/11	0.04
seep 3	09/20/11	10:30	5.1				11/23/11	0.05
seep 3	09/21/11	10:08	3.6				11/23/11	0.03
seep 3	09/22/11	10:19	3.3	2/8/12	0.12	0.01	11/4/11	0.01
seep 3	09/24/11	9:55	3.2				11/4/11	0.02

Table C-2. The fluorescent dye analytical results for the South Seep Group (Continued)

Location	Date	Time	Salinity	FLT Analysis	FLT	FLT Conc. Adj	SRB Analysis	SRB
				Date	Conc.	for Salinity	Date	Conc.
					(ppb)	(ppb)		(ppb)
seep 3	09/25/11	11:24	3.2				11/4/11	0.01
seep 3	09/26/11	11:39	7.5				11/4/11	0.01
seep 3	09/27/11	10:14	2.7				11/4/11	0.02
seep 3	09/28/11	10:07	2.8	2/8/12	0.12	0.01	11/4/11	0.03
seep 3	09/29/11	10:14	2.8				11/4/11	0.03
seep 3	09/30/11	10:25	2.7				11/4/11	0.02
seep 3	10/01/11	10:38	2.7	2/8/12	0.11	0.00	11/4/11	0.03
seep 3	10/02/11	13:13	3.0	2/8/12	0.11	0.00	11/4/11	0.01
seep 3	10/03/11	10:16	2.9				11/4/11	0.03
seep 3	10/08/11	17:12	2.8	2/8/12	0.12	0.01	11/4/11	0.03
seep 3	10/10/11	12:28	2.8				11/4/11	0.03
seep 3	10/12/11	10:07	2.7				11/23/11	0.05
seep 3	10/14/11	10:15	2.7				11/23/11	0.04
seep 3	10/16/11	10:06	2.7				11/23/11	0.02
seep 3	10/18/11	12:47	2.8	2/8/12	0.11	0.00	11/23/11	0.02
seep 3	10/20/11	10:33	2.8				11/23/11	0.04
seep 3	10/22/11	10:39	2.7	2/8/12	0.12	0.01	11/23/11	0.05
seep 3	10/24/11	10:18	2.7				11/23/11	0.04
seep 3	10/24/11	10:18	2.7				5/17/12	0.03
seep 3	10/26/11	10:28	2.8				11/23/11	0.04
seep 3	10/28/11	10:19	2.8	2/7/12	0.12	0.01	11/23/11	0.05
seep 3	10/28/11	10:19	2.8	2/7/12	0.12	0.01	5/17/12	0.03
seep 3	10/30/11	12:27	2.9				12/30/11	0.03
seep 3	11/01/11	12:26	2.8	2/7/12	0.12	0.01	11/23/11	0.05

Table C-2. The fluorescent dye analytical results for the South Seep Group (Continued)

Location	Date	Time	Salinity	FLT Analysis	FLT	FLT Conc. Adj	SRB Analysis	SRB
				Date	Conc.	for Salinity	Date	Conc.
					(ppb)	(ppb)		(ppb)
seep 3	09/25/11	11:24	3.2				11/4/11	0.01
seep 3	09/26/11	11:39	7.5				11/4/11	0.01
seep 3	09/27/11	10:14	2.7				11/4/11	0.02
seep 3	09/28/11	10:07	2.8	2/8/12	0.12	0.01	11/4/11	0.03
seep 3	09/29/11	10:14	2.8				11/4/11	0.03
seep 3	09/30/11	10:25	2.7				11/4/11	0.02
seep 3	10/01/11	10:38	2.7	2/8/12	0.11	0.00	11/4/11	0.03
seep 3	10/02/11	13:13	3.0	2/8/12	0.11	0.00	11/4/11	0.01
seep 3	10/03/11	10:16	2.9				11/4/11	0.03
seep 3	10/08/11	17:12	2.8	2/8/12	0.12	0.01	11/4/11	0.03
seep 3	10/10/11	12:28	2.8				11/4/11	0.03
seep 3	10/12/11	10:07	2.7				11/23/11	0.05
seep 3	10/14/11	10:15	2.7				11/23/11	0.04
seep 3	10/16/11	10:06	2.7				11/23/11	0.02
seep 3	10/18/11	12:47	2.8	2/8/12	0.11	0.00	11/23/11	0.02
seep 3	10/20/11	10:33	2.8				11/23/11	0.04
seep 3	10/22/11	10:39	2.7	2/8/12	0.12	0.01	11/23/11	0.05
seep 3	10/24/11	10:18	2.7				11/23/11	0.04
seep 3	10/24/11	10:18	2.7				5/17/12	0.03
seep 3	10/26/11	10:28	2.8				11/23/11	0.04
seep 3	10/28/11	10:19	2.8	2/7/12	0.12	0.01	11/23/11	0.05
seep 3	10/28/11	10:19	2.8	2/7/12	0.12	0.01	5/17/12	0.03
seep 3	10/30/11	12:27	2.9				12/30/11	0.03
seep 3	11/01/11	12:26	2.8	2/7/12	0.12	0.01	11/23/11	0.05

Table C-2. The fluorescent dye analytical results for the South Seep Group (Continued)

Location	Date	Time	Salinity	FLT Analysis	FLT	FLT Conc. Adj	SRB Analysis	SRB
				Date	Conc.	for Salinity	Date	Conc.
					(ppb)	(ppb)		(ppb)
seep 3	11/03/11	10:21	2.8				11/23/11	0.04
seep 3	11/05/11	14:29	2.8	1/30/12	0.13	0.02	1/20/12	0.03
seep 3	11/07/11	10:10	2.8	2/7/12	0.13	0.02	11/23/11	0.02
seep 3	11/07/11	10:10	2.8	2/7/12	0.13	0.02	5/17/12	0.04
seep 3	11/09/11	10:54	2.8	2/20/12	0.13	0.02	11/23/11	0.03
seep 3	11/11/11	10:44	2.8	2/20/12	0.13	0.02	11/23/11	0.04
seep 3	11/14/11	9:47	2.8	2/7/12	0.15	0.04	11/23/11	0.04
seep 3	11/14/11	9:47	2.8	2/7/12	0.15	0.04	5/17/12	0.03
seep 3	11/14/11	9:47	2.8	1/30/12	0.15	0.04	11/23/11	0.04
seep 3	11/14/11	9:47	2.8	1/30/12	0.15	0.04	5/17/12	0.03
seep 3	11/16/11	10:39	2.8				11/23/11	0.04
seep 3	11/16/11	10:39	2.8				5/17/12	0.03
seep 3	11/18/11	10:59	2.9	1/30/12	0.19	0.08	11/23/11	0.05
seep 3	11/21/11	10:42	2.8	2/7/12	0.21	0.10	12/5/11	0.03
seep 3	11/23/11	10:25	2.8	1/27/12	0.25	0.14	12/5/11	0.03
seep 3	11/25/11	10:47	2.8	1/30/12	0.30	0.19	12/5/11	0.03
seep 3	11/25/11	10:47	2.8	1/30/12	0.30	0.19	5/17/12	0.03
seep 3	11/28/11	10:35	2.8	1/27/12	0.37	0.26	12/5/11	0.04
seep 3	11/30/11	10:18	2.8	1/27/12	0.44	0.33	12/5/11	0.03
seep 3	12/02/11	10:21	2.8				12/5/11	0.03
seep 3	12/07/11	10:34	2.8	2/7/12	0.76	0.65		
seep 3	12/09/11	10:15	2.8				12/30/11	0.03
seep 3	12/14/11	10:10	2.9	2/7/12	1.34	1.23	12/30/11	0.03
seep 3	12/19/11	10:26	2.9				12/30/11	0.03

Table C-2. The fluorescent dye analytical results for the South Seep Group (Continued)

Location	Date	Time	Salinity	FLT Analysis	FLT	FLT Conc. Adj	SRB Analysis	SRB
				Date	Conc.	for Salinity	Date	Conc.
					(ppb)	(ppb)		(ppb)
seep 3	12/21/11	11:23	3.0				1/11/12	0.02
seep 3	12/26/11	10:57	2.9	2/7/12	2.63	2.52	1/11/12	0.02
seep 3	12/28/11	10:34	3.1				1/11/12	0.02
seep 3	12/28/11	10:34	3.1				1/11/12	0.01
seep 3	12/30/11	11:13	3.7	2/7/12	3.55	3.51	1/11/12	0.02
seep 3	01/02/12	11:37	8.0	2/7/12	3.62	4.15	1/11/12	0.02
seep 3	01/07/12	15:51	3.0	1/27/12	5.87	5.76	1/20/12	0.04
seep 3	01/09/12	12:34	3.0	1/27/12	6.34	6.23		
seep 3	01/11/12	11:35	2.9	1/27/12	7.16	7.05	1/20/12	0.04
Seep 3	01/16/12	14:04	2.8	1/27/12	8.48	8.37	1/20/12	0.04
Seep 3	01/19/12	10:52	2.8	2/10/11	9.13	9.02	2/14/12	0.04
Seep 3	01/19/12	10:52	2.8	2/10/11	9.13	9.02	1/20/12	0.04
Seep 3	01/21/12	14:37	3.3	2/20/12	10.30	10.25	3/7/12	0.04
Seep 3	01/23/12	12:15	2.9	2/10/11	10.80	10.69	2/14/12	0.05
Seep 3	01/25/12	12:38	2.9	2/20/12	11.41	11.30	3/7/12	0.04
Seep 3	01/27/12	13:26	2.9	2/10/11	11.30	11.19	2/14/12	0.03
Seep 3	01/31/12	12:25	2.9	2/10/11	13.92	13.81	2/14/12	0.04
Seep 3	02/10/12	12:56	3.1	3/5/12	17.37	17.26	3/7/12	0.06
Seep 3	02/14/12	14:22	3.0	3/5/12	19.52	19.41	3/7/12	0.04
Seep 3	02/17/12	12:32	3.2	3/5/12	19.63	19.58	3/7/12	0.05
Seep 3	02/20/12	14:40	3.4	3/5/12	19.73	19.81	3/7/12	0.07
Seep 3	02/20/12	14:40	3.4	3/24/12	18.63	18.70	3/7/12	0.07
Seep 3	02/24/12	12:05	4.3	3/24/12	20.57	21.26	3/21/12	0.03
Seep 3	02/27/12	23:33	3.8	3/24/12	22.92	23.32	3/21/12	0.02

Table C-2. The fluorescent dye analytical results for the South Seep Group (Continued)

Location	Date	Time	Salinity	FLT Analysis	FLT	FLT Conc. Adj	SRB Analysis	SRB
				Date	Conc.	for Salinity	Date	Conc.
					(ppb)	(ppb)		(ppb)
Seep 3	03/01/12	12:34	2.9	3/18/12	24.98	24.87	3/21/12	0.03
Seep 3	03/01/12	12:34	2.9	3/18/12	24.98	24.87	12/19/12	0.03
Seep 3	03/11/12	11:59	3.0	3/24/12	27.21	27.10	3/21/12	0.03
Seep 3	03/14/12	11:05	3.0	3/18/12	29.37	29.26	3/21/12	0.03
Seep 3	03/17/12	10:24	3.0	4/11/12	29.94	29.83	4/12/12	0.03
Seep 3	03/19/12	10:40	3.0	4/11/12	30.24	30.13	4/12/12	0.02
Seep 3	03/22/12	10:50	3.2	4/11/12	30.04	30.03	4/12/12	0.03
Seep 3	03/27/12	10:30	3.1	4/11/12	31.65	31.54	4/12/12	0.03
Seep 3	03/29/12	11:19	3.1	4/11/12	32.35	32.24	4/12/12	0.04
Seep 3	03/31/12	16:39	3.1	4/11/12	32.45	32.34	4/12/12	0.03
Seep 3	04/02/12	11:14	3.2	4/11/12	32.55	32.54	4/12/12	0.03
Seep 3	04/05/12	9:25	3.1	5/11/12	31.51	31.40	5/17/12	0.04
Seep 3	04/12/12	9:34	3.1	5/11/12	34.27	34.16	5/17/12	0.05
Seep 3	04/16/12	10:42	3.0	5/11/12	32.02	31.91	5/17/12	0.05
Seep 3	04/19/12	12:18	3.2	5/11/12	33.25	33.24	5/17/12	0.05
Seep 3	04/24/12	16:08	4.4	5/11/12	34.07	35.40	5/17/12	0.05
Seep 3	04/26/12	11:40	3.2	5/11/12	33.25	33.24	5/17/12	0.05
Seep 3	05/02/12	11:44	3.3	5/11/12	33.25	33.35	5/17/12	0.06
Seep 3	05/07/12	10:51	3.2	6/14/12	34.21	34.21	6/22/12	0.05
Seep 3	05/14/12	10:14	4.5	6/14/12	33.81	35.25	6/22/12	0.04
Seep 3	05/18/12	14:24	4.3	6/14/12	29.99	31.05	6/22/12	0.05
Seep 3	05/22/12	16:07	5.3	6/14/12	32.91	35.23	6/22/12	0.04
Seep 3	05/25/12	15:45	3.3	6/14/12	34.01	34.12	6/22/12	0.04
Seep 3	06/04/12	15:00	11.1	6/14/12	28.49	37.87	6/22/12	0.05

Table C-2. The fluorescent dye analytical results for the South Seep Group (Continued)

Location	Date	Time	Salinity	FLT Analysis	FLT	FLT Conc. Adj	SRB Analysis	SRB
				Date	Conc.	for Salinity	Date	Conc.
					(ppb)	(ppb)		(ppb)
Seep 3	06/07/12	13:20	3.2	6/14/12	31.90	31.89	6/22/12	0.05
Seep 3	06/12/12	12:27	3.3	7/20/12	29.25	29.32	7/26/12	0.05
Seep 3	06/14/12	15:37	3.2	7/20/12	30.55	30.54	7/26/12	0.02
Seep 3	06/16/12	13:02	3.4	7/20/12	29.55	29.72	7/26/12	0.04
Seep 3	06/18/12	11:00	3.4	7/20/12	30.55	30.73	7/26/12	0.03
Seep 3	06/29/12	13:23	3.2	7/20/12	29.15	29.13	7/26/12	0.05
Seep 3	07/04/12	13:21	3.3	7/20/12	28.75	28.82	7/26/12	0.02
Seep 3	07/11/12	14:35	3.3	7/25/12	27.37	27.43	7/26/12	0.02
Seep 3	07/19/12	23:40	3.3	7/25/12	26.02	26.07	7/26/12	0.03
Seep 3	07/23/12	10:50	3.2	10/3/12	26.64	26.61	10/9/12	0.04
Seep 3	08/01/12	10:35	3.2	8/3/12	14.91	14.85	10/9/12	0.05
Seep 3	08/01/12	10:35	3.2	8/3/12	14.91	14.85	8/2/12	0.03
Seep 3	08/01/12	10:35	3.2	10/3/12	25.22	25.19	10/9/12	0.05
Seep 3	08/01/12	10:35	3.2	10/3/12	25.22	25.19	8/2/12	0.03
Seep 3	08/07/12	10:25	3.3	10/3/12	24.21	24.25	10/9/12	0.05
Seep 3	08/15/12	11:32	3.2	10/3/12	22.79	22.75	10/9/12	0.05
Seep 3	08/21/12	10:28	3.2	10/3/12	23.40	23.36	10/9/12	0.04
Seep 3	08/24/12	12:33	3.2	10/3/12	23.60	23.57	10/9/12	0.05
Seep 3	08/27/12	10:38	3.3	10/3/12	22.89	22.93	10/9/12	0.04
Seep 3	09/05/12	10:46	3.3	10/3/12	21.18	21.20	10/9/12	0.05
Seep 3	09/10/12	13:45	3.3	10/3/12	20.37	20.38	10/9/12	0.04
Seep 3	09/12/12	10:33	3.3	10/12/12	18.79	18.80	10/19/12	0.04
Seep 3	09/18/12	12:36	3.2	10/12/12	18.79	18.74	10/19/12	0.04
Seep 3	10/02/12	12:17	3.2	10/12/12	17.79	17.73	10/19/12	0.04

Table C-2. The fluorescent dye analytical results for the South Seep Group (Continued)

Location	Date	Time	Salinity	FLT Analysis	FLT	FLT Conc. Adj	SRB Analysis	SRB
				Date	Conc.	for Salinity	Date	Conc.
					(ppb)	(ppb)		(ppb)
Seep 3	10/02/12	12:17	3.2	10/12/12	17.79	17.73	10/19/12	0.04
Seep 3	10/02/12	12:17	3.2	10/12/12	17.79	17.73	10/19/12	0.04
Seep 3	10/02/12	12:17	3.2	10/12/12	17.79	17.73	10/19/12	0.04
Seep 3	10/08/12	15:39	3.2	11/2/12	17.87	17.81	11/2/12	0.04
Seep 3	10/12/12	23:54	3.2	11/2/12	17.16	17.10	11/2/12	0.04
Seep 3	10/12/12	23:54	3.2	11/2/12	16.86	16.80	11/2/12	0.04
Seep 3	10/18/12	12:24	3.3	11/2/12	17.16	17.16	11/2/12	0.03
Seep 3	10/22/12	10:56	3.3	11/2/12	16.25	16.24	11/2/12	0.06
Seep 3	10/26/12	11:32	3.3	11/17/12	16.06	16.05	11/19/12	0.02
Seep 3	10/29/12	12:00	3.3	11/17/12	15.86	15.85	11/19/12	0.02
Seep 3	11/02/12	15:40	4.4	11/17/12	14.75	15.26	11/19/12	0.02
Seep 3	11/08/12	12:44	3.2	11/17/12	15.25	15.19	11/19/12	0.03
Seep 3	11/12/12	11:51	3.3	11/17/12	14.95	14.93	11/19/12	0.02
Seep 3	11/27/12	10:04	3.3	12/14/12	13.66	13.63	12/19/12	0.02
Seep 3	12/06/12	11:47	3.7	12/14/12	13.35	13.49	12/19/12	0.02
Seep 3	12/10/12	10:58	3.2	12/14/12	13.15	13.08	12/19/12	0.02
Seep 3	12/14/12	13:01	3.5	1/12/13	12.13	12.17	1/16/13	0.04
Seep 3	12/29/12	11:55	3.8	1/12/13	11.92	12.08	1/16/13	0.10
seep 4	07/23/11	10:31	3.2				11/4/11	0.03
seep 4	07/24/11	10:20	3.6				11/4/11	0.03
seep 4	07/25/11	10:48	4.5	2/9/11	0.11	0.00		
seep 4	07/25/11	10:48	4.5	2/9/11	0.11	0.00	11/4/11	0.01
seep 4	07/27/11	11:04	3.2				9/9/11	0.03
seep 4	07/29/11	10:34	3.1				9/23/11	0.02

Table C-2. The fluorescent dye analytical results for the South Seep Group (Continued)

Location	Date	Time	Salinity	FLT Analysis	FLT	FLT Conc. Adj	SRB Analysis	SRB
				Date	Conc.	for Salinity	Date	Conc.
					(ppb)	(ppb)		(ppb)
seep 4	07/29/11	10:34	3.1				10/14/11	0.02
seep 4	07/29/11	16:36	4.8				9/23/11	0.02
seep 4	07/29/11	16:36	4.8				10/14/11	0.02
seep 4	07/30/11	11:44	3.2				9/9/11	0.04
seep 4	07/30/11	18:26	3.9				9/9/11	0.04
seep 4	07/31/11	11:01	3.2	2/9/11	0.12	0.01	9/23/11	0.02
seep 4	07/31/11	11:01	3.2	2/9/11	0.12	0.01	9/9/11	0.05
seep 4	07/31/11	17:08	12.7	2/9/11	0.12	0.01	9/23/11	0.02
seep 4	07/31/11	17:08	12.7	2/9/11	0.12	0.01	9/9/11	0.05
seep 4	08/01/11	10:49	3.5				12/30/11	0.02
seep 4	08/01/11	10:49	3.5				11/4/11	0.02
seep 4	08/01/11	16:32	4.3				12/30/11	0.02
seep 4	08/01/11	16:32	4.3				11/4/11	0.02
seep 4	08/02/11	9:13	3.1				9/9/11	0.04
seep 4	08/02/11	16:20	3.1				9/9/11	0.04
seep 4	08/03/11	10:38	3.1				11/4/11	0.03
seep 4	08/03/11	16:48	3.3				11/4/11	0.03
seep 4	08/04/11	11:23	3.1				11/4/11	0.04
seep 4	08/04/11	11:23	3.1				9/9/11	0.04
seep 4	08/04/11	16:55	3.2				11/4/11	0.04
seep 4	08/04/11	16:55	3.2				9/9/11	0.04
seep 4	08/06/11	9:49	3.1	2/9/11	0.14	0.03	9/9/11	0.04
seep 4	08/06/11	9:49	3.1	2/9/11	0.14	0.03	9/9/11	0.06
seep 4	08/06/11	16:10	3.1	2/9/11	0.14	0.03	9/9/11	0.04

Table C-2. The fluorescent dye analytical results for the South Seep Group (Continued)

Location	Date	Time	Salinity	FLT Analysis	FLT	FLT Conc. Adj	SRB Analysis	SRB
				Date	Conc.	for Salinity	Date	Conc.
					(ppb)	(ppb)		(ppb)
seep 4	08/06/11	16:10	3.1	2/9/11	0.14	0.03	9/9/11	0.06
seep 4	08/08/11	10:25	2.8				10/14/11	0.03
seep 4	08/08/11	10:25	2.8				9/23/11	0.02
seep 4	08/08/11	16:22	3.1				10/14/11	0.03
seep 4	08/08/11	16:22	3.1				9/23/11	0.02
seep 4	08/09/11	10:18	3.2				9/9/11	0.04
seep 4	08/09/11	10:18	3.2				9/9/11	0.04
seep 4	08/09/11	16:10	3.2				9/9/11	0.04
seep 4	08/09/11	16:10	3.2				9/9/11	0.04
seep 4	08/10/11	12:40	4.0	2/9/11	0.12	0.01	9/23/11	0.02
seep 4	08/10/11	12:40	4.0	2/9/11	0.12	0.01	9/9/11	0.04
seep 4	08/10/11	16:48	3.2	2/9/11	0.12	0.01	9/23/11	0.02
seep 4	08/10/11	16:48	3.2	2/9/11	0.12	0.01	9/9/11	0.04
seep 4	08/14/11	10:37	3.1				10/14/11	0.02
seep 4	08/14/11	16:30	3.7				10/14/11	0.02
seep 4	08/16/11	10:30	3.1				10/14/11	0.01
seep 4	08/16/11	16:03	3.2				10/14/11	0.01
seep 4	08/20/11	10:40	3.1				10/14/11	0.02
seep 4	08/20/11	16:39	3.1				10/14/11	0.02
seep 4	08/21/11	10:44	3.1				12/30/11	0.01
seep 4	08/21/11	16:55	3.1				12/30/11	0.01
seep 4	08/22/11	10:12	5.4				10/14/11	0.01
seep 4	08/22/11	16:48	3.5				10/14/11	0.01
seep 4	08/25/11	11:05	3.6				10/14/11	0.02

Table C-2. The fluorescent dye analytical results for the South Seep Group (Continued)

Location	Date	Time	Salinity	FLT Analysis		SRB Analysis		
				Date	FLT Conc. (ppb)	FLT Conc. Adj for Salinity (ppb)	Date	SRB Conc. (ppb)
seep 4	08/25/11	17:35	3.1				10/14/11	0.02
seep 4	08/26/11	10:24	3.6				12/14/11	0.02
seep 4	08/26/11	16:33	3.7				12/14/11	0.02
seep 4	08/28/11	10:22	3.1	2/9/11	0.01	0.00	10/14/11	0.01
seep 4	08/28/11	16:44	3.0	2/9/11	0.01	0.00	10/14/11	0.01
seep 4	09/03/11	10:44	3.3				10/14/11	0.02
seep 4	09/05/11	10:28	3.8				12/14/11	0.03
seep 4	09/05/11	16:50	3.1				12/14/11	0.03
seep 4	09/06/11	10:13	3.0	2/9/11	0.12	0.01	12/5/11	0.03
seep 4	09/06/11	10:13	3.0	2/9/11	0.12	0.01	10/14/11	0.02
seep 4	09/06/11	16:40	3.0	2/9/11	0.12	0.01	12/5/11	0.03
seep 4	09/06/11	16:40	3.0	2/9/11	0.12	0.01	10/14/11	0.02
seep 4	09/10/11	11:52	5.5	2/10/11	0.07	0.00	2/14/12	0.18
seep 4	09/14/11	11:03	3.3				10/14/11	0.01
seep 4	09/16/11	12:31	4.1				12/14/11	0.02
seep 4	09/17/11	15:50	5.1				10/14/11	0.02
seep 4	09/18/11	12:35	3.3	2/9/11	0.11	0.00	11/23/11	0.05
seep 4	09/19/11	11:36	6.5	2/9/11	0.10	0.00	11/23/11	0.03
seep 4	09/20/11	10:41	5.1	2/9/11	0.11	0.00	11/23/11	0.02
seep 4	09/23/11	10:34	4.6				11/4/11	0.02
seep 4	09/24/11	10:05	3.7				11/23/11	0.05
seep 4	09/25/11	11:40	6.4				11/23/11	0.03
seep 4	09/26/11	11:53	4.7				11/23/11	0.04
seep 4	09/27/11	10:25	3.1				11/4/11	0.01

Table C-2. The fluorescent dye analytical results for the South Seep Group (Continued)

Location	Date	Time	Salinity	FLT Analysis	FLT	FLT Conc. Adj	SRB Analysis	SRB
				Date	Conc.	for Salinity	Date	Conc.
					(ppb)	(ppb)		(ppb)
seep 4	09/28/11	10:18	3.0	2/9/11	0.12	0.01	11/4/11	0.02
seep 4	09/29/11	10:31	3.0				11/23/11	0.05
seep 4	09/30/11	10:36	3.0				11/4/11	0.02
seep 4	10/01/11	10:51	3.0				11/23/11	0.03
seep 4	10/02/11	13:27	3.0				11/4/11	0.03
seep 4	10/03/11	10:28	3.2				11/4/11	0.01
seep 4	10/08/11	17:27	3.1	2/9/11	0.12	0.01	11/23/11	0.05
seep 4	10/10/11	12:37	3.0	2/9/11	0.11	0.00	11/4/11	0.02
seep 4	10/12/11	10:20	2.9				11/4/11	0.02
seep 4	10/14/11	10:26	3.0	2/9/11	0.11	0.00	11/23/11	0.03
seep 4	10/16/11	10:19	3.4				11/23/11	0.02
seep 4	10/18/11	12:59	3.1	2/9/11	0.11	0.00	11/23/11	-0.05
seep 4	10/20/11	10:44	4.6				11/23/11	0.06
seep 4	10/20/11	10:44	4.6				5/17/12	0.04
seep 4	10/22/11	10:16	3.3				5/17/12	0.03
seep 4	10/22/11	10:16	3.3				11/23/11	0.04
seep 4	10/24/11	10:29	3.2				11/23/11	0.04
seep 4	10/26/11	10:39	3.0				11/23/11	0.05
seep 4	10/28/11	10:30	3.1	2/7/12	0.11	0.00	11/23/11	0.04
seep 4	10/30/11	12:55	3.2				12/30/11	0.02
seep 4	11/01/11	12:37	3.3				11/23/11	0.04
seep 4	11/03/11	10:35	5.0				11/23/11	0.04
seep 4	11/05/11	14:58	3.2	2/7/12	0.12	0.01	11/23/11	0.02
seep 4	11/07/11	10:20	3.0	2/20/12	0.12	0.01	11/23/11	0.03

Table C-2. The fluorescent dye analytical results for the South Seep Group (Continued)

Location	Date	Time	Salinity	FLT Analysis	FLT	FLT Conc. Adj	SRB Analysis	SRB
				Date	Conc.	for Salinity	Date	Conc.
					(ppb)	(ppb)		(ppb)
seep 4	11/09/11	11:19	3.0	2/20/12	0.12	0.01	11/23/11	0.03
seep 4	11/11/11	10:55	3.5	2/20/12	0.13	0.02	11/23/11	0.04
seep 4	11/11/11	10:55	3.5	1/27/12	0.13	0.02	11/23/11	0.04
seep 4	11/14/11	9:58	3.1	1/30/12	0.14	0.03	11/23/11	0.04
seep 4	11/14/11	9:58	3.1	2/7/12	0.14	0.03	11/23/11	0.04
seep 4	11/16/11	10:57	3.1				11/23/11	0.04
seep 4	11/16/11	10:57	3.1				5/17/12	0.03
seep 4	11/18/11	11:16	3.2	1/27/12	0.17	0.06	11/23/11	0.04
seep 4	11/21/11	10:53	3.3	1/30/12	0.19	0.08	1/20/12	0.03
seep 4	11/23/11	10:36	3.4	1/30/12	0.21	0.10	12/5/11	0.02
seep 4	11/25/11	10:57	3.1	2/7/12	0.25	0.14	12/5/11	0.02
seep 4	11/28/11	10:48	3.7	1/30/12	0.29	0.19	12/5/11	0.03
seep 4	11/28/11	10:48	3.7	1/30/12	0.29	0.19	5/17/12	0.03
seep 4	11/28/11	10:48	3.7	1/30/12	0.25	0.14	12/5/11	0.03
seep 4	11/28/11	10:48	3.7	1/30/12	0.25	0.14	5/17/12	0.03
seep 4	11/30/11	10:29	3.2	1/27/12	0.33	0.22	12/5/11	0.03
seep 4	12/02/11	10:34	3.5	1/27/12	0.38	0.27	12/5/11	0.03
seep 4	12/07/11	10:45	3.2	1/27/12	0.60	0.49	1/20/12	0.04
seep 4	12/07/11	10:45	3.2	1/27/12	0.60	0.49	5/17/12	0.04
seep 4	12/09/11	10:25	3.1	2/7/12	0.70	0.59	12/30/11	0.03
seep 4	12/14/11	10:22	3.2	2/7/12	1.00	0.89	12/30/11	0.03
seep 4	12/19/11	10:37	3.1	2/7/12	1.53	1.42	12/30/11	0.03
seep 4	12/21/11	11:38	3.2	2/7/12	1.66	1.56	1/11/12	0.02
seep 4	12/23/11	11:06	3.2				1/11/12	0.02

Table C-2. The fluorescent dye analytical results for the South Seep Group (Continued)

Location	Date	Time	Salinity	FLT Analysis	FLT	FLT Conc. Adj	SRB Analysis	SRB
				Date	Conc.	for Salinity	Date	Conc.
					(ppb)	(ppb)		(ppb)
seep 4	12/26/11	11:17	3.2				1/11/12	0.01
seep 4	12/28/11	10:53	3.6	2/7/12	2.71	2.64	1/11/12	0.02
seep 4	12/30/11	11:33	4.0				1/11/12	0.01
seep 4	01/02/12	11:50	10.5	2/7/12	3.09	3.87	1/11/12	0.03
seep 4	01/07/12	16:05	3.1	1/27/12	4.78	4.67	1/20/12	0.04
seep 4	01/09/12	12:02	3.5	1/27/12	5.19	5.14	1/20/12	0.04
seep 4	01/11/12	11:48	3.1	1/27/12	6.03	5.92	1/20/12	0.03
seep 4	01/13/12	12:23	3.2	1/27/12	6.80	6.71	1/20/12	0.04
Seep 4	01/16/12	14:16	3.0	1/27/12	7.48	7.37	1/20/12	0.05
Seep 4	01/16/12	14:16	3.0	1/27/12	7.48	7.37	1/20/12	0.04
Seep 4	01/16/12	14:16	3.0	1/27/12	7.50	7.39	1/20/12	0.05
Seep 4	01/16/12	14:16	3.0	1/27/12	7.50	7.39	1/20/12	0.04
Seep 4	01/19/12	11:18	3.1	2/10/11	7.93	7.82	2/14/12	0.04
Seep 4	01/21/12	14:51	3.0	2/10/11	8.83	8.72	2/14/12	0.03
Seep 4	01/23/12	13:26	3.1	2/10/11	9.72	9.61	2/14/12	0.04
Seep 4	01/25/12	13:39	3.1	2/20/12	10.09	9.98	3/7/12	0.04
Seep 4	01/27/12	13:49	3.1	2/10/11	6.20	6.09	2/14/12	0.02
Seep 4	01/31/12	12:39	3.1	2/10/11	11.81	11.70	2/14/12	0.04
Seep 4	02/10/12	13:16	5.7	3/5/12	12.66	13.66	3/7/12	0.04
Seep 4	02/14/12	14:38	6.7	3/5/12	13.17	14.72	3/7/12	0.06
Seep 4	02/17/12	12:47	9.0	3/5/12	13.99	17.03	3/7/12	0.04
Seep 4	02/20/12	15:00	13.6	3/5/12	10.81	15.95	3/7/12	0.04
Seep 4	02/24/12	12:20	20.2	3/24/12	8.27	17.58	3/21/12	0.01
Seep 4	02/27/12	12:13	21.6	3/24/12	7.76	18.20	3/21/12	0.01

Table C-2. The fluorescent dye analytical results for the South Seep Group (Continued)

Location	Date	Time	Salinity	FLT Analysis	FLT	FLT Conc. Adj	SRB Analysis	SRB
				Date	Conc.	for Salinity	Date	Conc.
					(ppb)	(ppb)		(ppb)
Seep 4	03/01/12	12:50	4.2	3/18/12	17.31	17.81	3/21/12	0.02
Seep 4	03/11/12	12:23	8.2	3/24/12	18.63	22.05	3/21/12	0.02
Seep 4	03/14/12	11:17	9.8	3/18/12	18.33	23.07	3/21/12	0.02
Seep 4	03/17/12	10:47	15.8	4/11/12	14.59	24.06	4/12/12	0.02
Seep 4	03/19/12	10:55	22.5	4/11/12	9.98	25.18	4/12/12	0.01
Seep 4	03/22/12	11:08	18.6	4/11/12	12.89	24.85	4/12/12	0.01
Seep 4	03/27/12	11:03	17.3	4/11/12	14.09	25.20	4/12/12	0.02
Seep 4	03/29/12	11:36	17.4	4/11/12	13.19	23.70	4/12/12	0.02
Seep 4	03/31/12	16:53	17.3	4/11/12	14.19	25.38	4/12/12	0.01
Seep 4	04/02/12	11:33	21.8	4/11/12	10.88	26.03	4/12/12	0.02
Seep 4	04/05/12	9:40	17.3	5/11/12	14.96	26.77	5/17/12	0.03
Seep 4	04/12/12	9:50	14.1	5/11/12	18.13	27.50	5/17/12	0.04
Seep 4	04/16/12	11:12	17.1	5/11/12	15.17	26.83	5/17/12	0.02
Seep 4	04/16/12	11:12	17.1	5/11/12	15.17	26.83	5/17/12	0.05
seep 5	07/19/11	10:35	3.1				11/4/11	0.03
seep 5	07/20/11	11:03	3.0				11/4/11	0.03
seep 5	07/24/11	10:30	3.1				11/4/11	0.03
seep 5	07/27/11	11:12	3.0	2/9/11	0.12	0.01		
seep 5	07/28/11	10:36	3.1				9/23/11	0.02
seep 5	07/28/11	16:59	3.0				9/23/11	0.02
seep 5	07/29/11	10:40	3.0				12/5/11	0.03
seep 5	07/29/11	10:40	3.0				9/9/11	0.05
seep 5	07/29/11	16:51	3.1				12/5/11	0.03
seep 5	07/29/11	16:51	3.1				9/9/11	0.05

Table C-2. The fluorescent dye analytical results for the South Seep Group (Continued)

Location	Date	Time	Salinity	FLT Analysis	FLT	FLT Conc. Adj	SRB Analysis	SRB
				Date	Conc.	for Salinity	Date	Conc.
					(ppb)	(ppb)		(ppb)
seep 5	07/30/11	11:53	3.1				9/9/11	0.04
seep 5	07/30/11	17:33	3.1				9/9/11	0.04
seep 5	07/31/11	11:09	3.1	2/9/11	0.12	0.01	11/4/11	0.02
seep 5	07/31/11	17:19	3.4	2/9/11	0.12	0.01	11/4/11	0.02
seep 5	08/01/11	16:40	3.3				9/9/11	0.05
seep 5	08/02/11	9:20	3.0				9/23/11	0.02
seep 5	08/02/11	16:27	3.0				9/23/11	0.02
seep 5	08/04/11	11:30	3.0				11/4/11	0.16
seep 5	08/04/11	17:02	3.0				11/4/11	0.16
seep 5	08/05/11	11:21	3.0	2/9/11	0.12	0.01	9/9/11	0.04
seep 5	08/05/11	11:21	3.0	2/9/11	0.12	0.01	12/5/11	0.02
seep 5	08/05/11	17:31	3.0	2/9/11	0.12	0.01	9/9/11	0.04
seep 5	08/05/11	17:31	3.0	2/9/11	0.12	0.01	12/5/11	0.02
seep 5	08/06/11	9:44	3.1				9/9/11	0.04
seep 5	08/06/11	16:15	3.0				9/9/11	0.04
seep 5	08/07/11	10:25	3.1				12/14/11	0.03
seep 5	08/07/11	16:33	3.1				12/14/11	0.03
seep 5	08/08/11	10:32	3.1				9/9/11	0.05
seep 5	08/08/11	16:33	3.1				9/9/11	0.05
seep 5	08/09/11	10:25	3.1				9/9/11	0.04
seep 5	08/09/11	10:25	3.1				9/9/11	0.03
seep 5	08/09/11	16:17	3.1				9/9/11	0.04
seep 5	08/09/11	16:17	3.1				9/9/11	0.03
seep 5	08/10/11	13:00	3.1				9/9/11	0.04

Table C-2. The fluorescent dye analytical results for the South Seep Group (Continued)

Location	Date	Time	Salinity	FLT Analysis	FLT	FLT Conc. Adj	SRB Analysis	SRB
				Date	Conc.	for Salinity	Date	Conc.
					(ppb)	(ppb)		(ppb)
seep 5	08/10/11	13:00	3.1				9/9/11	0.05
seep 5	08/10/11	16:54	3.1				9/9/11	0.04
seep 5	08/10/11	16:54	3.1				9/9/11	0.05
seep 5	08/12/11	10:16	3.1				12/14/11	0.11
seep 5	08/12/11	16:36	3.1				12/14/11	0.11
seep 5	08/14/11	10:45	3.1				11/4/11	0.03
seep 5	08/14/11	16:36	3.1				11/4/11	0.03
seep 5	08/15/11	10:11	3.1				12/5/11	0.03
seep 5	08/15/11	16:24	3.1				12/5/11	0.03
seep 5	08/17/11	11:21	3.0	2/9/11	0.11	0.00	11/4/11	0.03
seep 5	08/17/11	16:54	3.1	2/9/11	0.11	0.00	11/4/11	0.03
seep 5	08/19/11	10:53	3.1				12/5/11	0.03
seep 5	08/19/11	16:59	3.1				12/5/11	0.03
seep 5	08/21/11	10:51	3.0				12/5/11	0.03
seep 5	08/21/11	17:03	3.1				12/5/11	0.03
seep 5	08/22/11	10:21	3.1				12/14/11	0.03
seep 5	08/22/11	16:54	3.1				12/14/11	0.03
seep 5	08/23/11	10:32	3.1	2/9/11	0.12	0.01	11/4/11	0.02
seep 5	08/23/11	16:14	3.1	2/9/11	0.12	0.01	11/4/11	0.02
seep 5	08/24/11	11:46	3.0				12/14/11	0.04
seep 5	08/24/11	18:06	3.1				12/14/11	0.04
seep 5	08/25/11	11:15	3.1				12/5/11	0.02
seep 5	08/25/11	17:45	3.1				12/5/11	0.02
seep 5	08/26/11	10:32	3.1	2/9/11	0.12	0.01	11/4/11	0.03

Table C-2. The fluorescent dye analytical results for the South Seep Group (Continued)

Location	Date	Time	Salinity	FLT Analysis	FLT	FLT Conc. Adj	SRB Analysis	SRB
				Date	Conc.	for Salinity	Date	Conc.
					(ppb)	(ppb)		(ppb)
seep 5	08/26/11	16:41	3.1	2/9/11	0.12	0.01	11/4/11	0.03
seep 5	08/28/11	10:30	3.1				12/5/11	0.03
seep 5	08/28/11	16:54	3.1				12/5/11	0.03
seep 5	09/02/11	12:07	3.0				12/5/11	0.03
seep 5	09/02/11	17:27	3.0				12/5/11	0.03
seep 5	09/03/11	10:52	3.0				12/5/11	0.03
seep 5	09/04/11	17:12	3.1	2/9/11	0.12	0.01	12/5/11	0.03
seep 5	09/05/11	10:37	3.1				11/4/11	0.03
seep 5	09/05/11	16:58	3.0				11/4/11	0.03
seep 5	09/06/11	10:21	3.1				12/14/11	0.03
seep 5	09/06/11	16:49	3.0				12/14/11	0.03
seep 5	09/08/11	10:26	3.1				12/14/11	0.03
seep 5	09/10/11	12:00	3.1				11/4/11	0.03
seep 5	09/12/11	13:05	3.0	2/9/11	0.12	0.01	11/4/11	0.03
seep 5	09/13/11	12:18	5.0				12/14/11	0.03
seep 5	09/14/11	11:13	3.3	2/10/11	0.11	0.00	2/14/12	0.05
seep 5	09/17/11	16:03	5.5				11/23/11	0.03
seep 5	09/19/11	11:49	6.2	2/9/11	0.10	0.00	11/23/11	0.03
seep 5	09/20/11	10:50	3.5				11/23/11	0.04
seep 5	09/21/11	10:27	3.4				11/23/11	0.04
seep 5	09/23/11	10:43	3.5				11/23/11	0.03
seep 5	09/24/11	9:45	3.2				11/23/11	0.03
seep 5	09/25/11	11:54	4.7				11/4/11	0.02
seep 5	09/26/11	12:00	3.6	2/9/11	0.11	0.00	11/4/11	0.02

Table C-2. The fluorescent dye analytical results for the South Seep Group (Continued)

Location	Date	Time	Salinity	FLT Analysis	FLT	FLT Conc. Adj	SRB Analysis	SRB
				Date	Conc.	for Salinity	Date	Conc.
					(ppb)	(ppb)		(ppb)
seep 5	09/27/11	10:36	3.0				11/4/11	0.02
seep 5	09/28/11	10:26	3.0				11/4/11	0.03
seep 5	09/29/11	10:46	3.0				11/4/11	0.03
seep 5	09/30/11	10:45	3.0				11/4/11	-0.01
seep 5	10/01/11	11:02	3.0	2/9/11	0.11	0.00	11/23/11	0.05
seep 5	10/02/11	13:48	3.0				11/4/11	0.02
seep 5	10/03/11	10:38	3.1				11/4/11	0.02
seep 5	10/10/11	12:47	3.0				11/4/11	0.02
seep 5	10/12/11	10:31	2.9				11/4/11	0.01
seep 5	10/14/11	10:36	3.1	2/9/11	0.12	0.01	11/23/11	0.04
seep 5	10/16/11	10:29	3.0				11/23/11	0.04
seep 5	10/18/11	13:11	3.0				11/23/11	0.03
seep 5	10/20/11	10:52	3.0				11/23/11	0.02
seep 5	10/22/11	10:26	3.0	2/9/11	0.11	0.00	11/23/11	0.03
seep 5	10/24/11	10:40	3.0				11/23/11	0.04
seep 5	10/26/11	10:51	3.1				11/23/11	0.05
seep 5	10/28/11	10:44	3.1	2/9/11	0.12	0.01	11/23/11	0.03
seep 5	10/30/11	12:41	3.1	2/7/12	0.11	0.00	12/30/11	0.03
seep 5	11/01/11	12:49	3.1				11/23/11	0.04
seep 5	11/03/11	10:49	3.1	2/7/12	0.12	0.01	11/23/11	0.04
seep 5	11/05/11	14:44	3.1	1/27/12	0.12	0.01	11/23/11	0.04
seep 5	11/05/11	14:44	3.1	1/27/12	0.12	0.01	11/23/11	0.05
seep 5	11/07/11	10:33	3.0	1/27/12	0.13	0.02	11/23/11	0.05
seep 5	11/09/11	11:33	3.1	1/30/12	0.13	0.02	11/23/11	0.09

Table C-2. The fluorescent dye analytical results for the South Seep Group (Continued)

Location	Date	Time	Salinity	FLT Analysis	FLT	FLT Conc. Adj	SRB Analysis	SRB
				Date	Conc.	for Salinity	Date	Conc.
					(ppb)	(ppb)		(ppb)
seep 5	11/09/11	11:33	3.1	2/7/12	0.13	0.02	11/23/11	0.09
seep 5	11/11/11	11:04	3.1	1/30/12	0.14	0.03	11/23/11	0.05
seep 5	11/14/11	10:08	3.0	1/27/12	0.15	0.04	11/23/11	0.04
seep 5	11/16/11	11:09	3.1	1/30/12	0.15	0.04	11/23/11	0.05
seep 5	11/16/11	11:09	3.1	2/7/12	0.16	0.05	11/23/11	0.05
seep 5	11/16/11	11:09	3.1	1/30/12	0.15	0.04	11/23/11	0.05
seep 5	11/16/11	11:09	3.1	2/7/12	0.16	0.05	11/23/11	0.05
seep 5	11/18/11	11:29	3.1	1/30/12	0.17	0.06	11/23/11	0.05
seep 5	11/21/11	11:05	3.1	1/30/12	0.21	0.10	12/14/11	0.04
seep 5	11/23/11	10:47	3.1	1/27/12	0.22	0.11	12/5/11	0.04
seep 5	11/23/11	10:47	3.1	1/27/12	0.21	0.10	12/5/11	0.04
seep 5	11/25/11	11:27	3.1	1/27/12	0.25	0.14	12/5/11	0.04
seep 5	11/28/11	10:58	3.1	1/30/12	0.29	0.18	12/5/11	0.03
seep 5	11/30/11	10:40	3.2	1/30/12	0.35	0.24	12/5/11	0.04
seep 5	11/30/11	10:40	3.2	2/7/12	0.35	0.24	12/5/11	0.04
seep 5	12/02/11	10:43	3.4	1/30/12	0.42	0.31	12/5/11	0.03
seep 5	12/05/11	11:03	3.5	2/7/12	0.50	0.40	12/30/11	0.03
seep 5	12/05/11	11:03	3.5	2/7/12	0.50	0.40	12/30/11	0.03
seep 5	12/07/11	10:56	4.2	1/27/12	0.58	0.48	1/20/12	0.03
seep 5	12/09/11	10:35	3.7				12/30/11	0.02
seep 5	12/12/11	10:41	3.7	2/7/12	0.85	0.75		
seep 5	12/14/11	10:32	4.4				12/30/11	0.03
seep 5	12/19/11	10:46	4.1	2/9/11	1.41	1.34	12/30/11	0.03
seep 5	12/21/11	11:48	4.2				1/11/12	0.02

Table C-2. The fluorescent dye analytical results for the South Seep Group (Continued)

Location	Date	Time	Salinity	FLT Analysis	FLT	FLT Conc. Adj	SRB Analysis	SRB
				Date	Conc.	for Salinity	Date	Conc.
					(ppb)	(ppb)		(ppb)
seep 5	12/26/11	11:08	4.8	2/7/12	2.03	2.02	1/11/12	0.02
seep 5	12/28/11	10:45	7.6				1/11/12	0.02
seep 5	12/30/11	11:24	9.1	6/29/12	1.51	1.73	1/11/12	0.02
seep 5	01/02/12	12:05	15.6	2/7/12	2.11	3.28	1/11/12	0.01
seep 5	01/07/12	16:15	16.4	1/27/12	3.33	5.52	1/20/12	0.03
seep 5	01/09/12	12:20	18.4	1/27/12	2.29	4.19	1/20/12	0.03
seep 5	01/11/12	12:00	21.8	1/27/12	2.47	5.71	1/20/12	0.02
Seep 5	01/13/12	12:33	18.3	1/27/12	3.32	6.14	1/20/12	0.03
Seep 5	01/16/12	14:28	19.1	1/27/12	3.51	6.81	1/20/12	0.03
Seep 5	01/19/12	11:31	10.4	2/10/12	6.19	7.88	2/14/12	0.03
Seep 5	01/21/12	15:03	13.2	2/10/12	6.14	8.82	2/14/12	0.04
Seep 5	01/23/12	13:36	19.7	2/10/12	4.57	9.30	2/14/12	0.03
Seep 5	01/25/12	14:16	17.3	2/20/12	5.09	8.97	3/7/12	0.03
Seep 5	01/27/12	14:24	14.6	2/10/12	7.01	10.79	2/14/12	0.03
Seep 5	01/31/12	12:51	18.1	2/10/12	5.68	10.52	2/14/12	0.02
Seep 5	02/10/12	13:30	7.2	3/5/12	12.76	14.51	3/7/12	0.04
Seep 5	02/14/12	15:13	7.4	3/5/12	13.37	15.33	3/7/12	0.04
Seep 5	02/17/12	13:00	7.6	3/5/12	14.40	16.64	3/7/12	0.04
Seep 5	02/20/12	15:14	5.5	3/5/12	13.17	14.12	3/7/12	0.03
Seep 5	02/24/12	12:36	8.0	3/24/12	15.98	18.75	3/21/12	0.02
Seep 5	02/27/12	12:24	8.3	3/24/12	17.00	20.18	3/21/12	0.03
Seep 5	03/01/12	13:04	10.3	3/18/12	16.08	20.63	3/21/12	0.02
Seep 5	03/11/12	12:38	6.0	3/24/12	22.31	24.42	3/21/12	0.02
Seep 5	03/14/12	11:30	7.4	3/18/12	22.11	25.43	3/21/12	0.02

Table C-2. The fluorescent dye analytical results for the South Seep Group (Continued)

Location	Date	Time	Salinity	FLT Analysis	FLT	FLT Conc. Adj	SRB Analysis	SRB
				Date	Conc.	for Salinity	Date	Conc.
					(ppb)	(ppb)		(ppb)
Seep 5	03/17/12	10:57	8.9	4/11/12	22.02	26.77	4/12/12	0.03
Seep 5	03/17/12	10:57	8.9	4/11/12	21.92	26.65	4/12/12	0.03
Seep 5	03/19/12	11:05	11.4	4/11/12	20.01	26.90	4/12/12	0.03
Seep 5	03/22/12	11:20	15.0	4/11/12	17.40	27.58	4/12/12	0.02
Seep 5	03/27/12	11:17	10.4	4/11/12	22.02	28.41	4/12/12	0.03
Seep 5	03/29/12	11:49	12.2	4/11/12	21.61	30.09	4/12/12	0.03
Seep 5	04/02/12	11:44	12.4	4/11/12	21.21	29.79	4/12/12	0.02
Seep 5	04/05/12	9:52	9.8	5/11/12	25.28	31.86	5/17/12	0.05
Seep 5	04/12/12	10:22	8.5	5/11/12	25.79	30.92	5/17/12	0.05
Seep 5	04/19/12	12:34	8.9	5/11/12	24.57	29.89	5/17/12	0.04
Seep 5	04/24/12	16:21	11.7	5/11/12	23.65	32.22	5/17/12	0.03
Seep 5	04/26/12	11:54	8.8	5/11/12	26.30	31.89	5/17/12	0.04
Seep 5	05/02/12	12:01	11.0	5/11/12	24.36	32.23	5/17/12	0.04
Seep 5	05/07/12	11:22	9.0	6/14/12	25.67	31.36	6/22/12	0.05
Seep 5	05/14/12	10:40	8.9	6/14/12	25.77	31.36	6/22/12	0.05
Seep 5	05/25/12	15:57	11.3	6/14/12	24.87	33.32	6/22/12	0.04
Seep 5	05/25/12	15:57	11.3	6/14/12	24.87	33.32	11/2/12	0.04
Seep 5	05/29/12	15:13	13.4	6/14/12	22.66	33.30	6/22/12	0.04
Seep 5	06/04/12	15:29	7.8	6/14/12	24.67	28.80	6/22/12	0.05
Seep 5	06/04/12	15:29	7.8	6/14/12	24.67	28.80	7/26/12	0.04
Seep 5	06/04/12	15:29	7.8	7/20/12	24.63	28.76	6/22/12	0.05
Seep 5	06/04/12	15:29	7.8	7/20/12	24.63	28.76	7/26/12	0.04
Seep 5	06/07/12	13:35	3.8	6/14/12	26.48	26.96	6/22/12	0.05
Seep 5	06/12/12	12:44	3.8	7/20/12	26.74	27.23	7/26/12	0.04

Table C-2. The fluorescent dye analytical results for the South Seep Group (Continued)

Location	Date	Time	Salinity	FLT Analysis	FLT	FLT Conc. Adj	SRB Analysis	SRB
				Date	Conc.	for Salinity	Date	Conc.
					(ppb)	(ppb)		(ppb)
Seep 5	06/14/12	15:54	4.0	7/20/12	26.84	27.51	7/26/12	0.03
Seep 5	06/16/12	13:18	4.2	7/20/12	26.54	27.37	7/26/12	0.03
Seep 5	06/18/12	11:51	12.5	7/20/12	22.53	31.78	7/26/12	0.02
Seep 5	06/29/12	13:49	4.5	7/20/12	24.23	25.23	7/26/12	0.04
Seep 5	07/11/12	14:50	3.7	7/25/12	24.57	24.93	7/26/12	0.02
Seep 5	07/19/12	11:55	3.4	7/25/12	23.43	23.55	7/26/12	0.03
Seep 5	07/23/12	11:23	3.6	10/3/12	24.21	24.48	10/9/12	0.05
Seep 5	08/01/12	11:05	3.6	10/3/12	23.60	23.87	10/9/12	0.04
Seep 5	08/01/12	11:05	3.6	10/3/12	23.60	23.87	8/2/12	0.03
Seep 5	08/01/12	11:05	3.6	8/3/12	22.39	22.64	10/9/12	0.04
Seep 5	08/01/12	11:05	3.6	8/3/12	22.39	22.64	8/2/12	0.03
Seep 5	08/07/12	10:40	3.7	10/3/12	22.09	22.40	10/9/12	0.04
Seep 5	08/15/12	11:49	3.7	10/3/12	21.78	22.09	10/9/12	0.05
Seep 5	08/21/12	11:00	3.7	10/3/12	20.97	21.26	10/9/12	0.04
Seep 5	08/24/12	12:50	5.4	10/3/12	19.25	20.63	10/9/12	0.05
Seep 5	08/27/12	11:00	3.7	10/3/12	20.47	20.75	10/9/12	0.04
Seep 5	09/05/12	11:10	3.7	10/3/12	19.36	19.61	10/9/12	0.04
Seep 5	09/10/12	14:05	3.9	10/3/12	18.95	19.33	10/9/12	0.05
Seep 5	09/12/12	11:06	3.7	10/12/12	17.58	17.81	10/19/12	0.03
Seep 5	09/18/12	13:10	3.5	10/12/12	17.68	17.80	10/19/12	0.03
Seep 5	10/02/12	12:33	3.7	10/12/12	17.18	17.40	10/19/12	0.04
Seep 5	10/08/12	15:12	3.7	11/2/12	16.96	17.17	11/2/12	0.04
Seep 5	10/12/12	12:09	4.2	11/2/12	16.15	16.61	11/2/12	0.03
Seep 5	10/18/12	12:43	3.6	11/2/12	15.84	15.98	11/2/12	0.04

Table C-2. The fluorescent dye analytical results for the South Seep Group (Continued)

Location	Date	Time	Salinity	FLT Analysis	FLT	FLT Conc. Adj	SRB Analysis	SRB
				Date	Conc.	for Salinity	Date	Conc.
					(ppb)	(ppb)		(ppb)
Seep 5	10/22/12	11:30	4.0	11/2/12	15.94	16.29	11/2/12	0.04
Seep 5	10/26/12	11:45	3.7				11/19/12	0.02
Seep 5	10/29/12	12:13	3.7				11/19/12	0.03
Seep 5	11/02/12	15:54	3.5				11/19/12	0.03
Seep 5	11/02/12	15:54	3.5				11/19/12	0.02
Seep 5	11/08/12	12:58	3.6				11/19/12	0.03
Seep 5	11/12/12	12:09	3.7				11/19/12	0.02
Seep 5	11/19/12	12:15	3.6	12/14/12	14.48	14.59	12/19/12	0.02
Seep 5	11/27/12	10:46	3.9	12/14/12	13.25	13.48	12/19/12	0.02
Seep 5	12/06/12	12:04	3.6	12/14/12	13.55	13.66	12/19/12	0.02
Seep 5	12/10/12	11:25	3.6	12/14/12	13.45	13.56	12/19/12	0.03
Seep 5	12/14/12	13:15	4.0	1/12/13	12.64	12.89	1/16/13	0.07
Seep 5	12/29/12	12:10	4.2	1/12/13	11.92	12.24	1/16/13	0.04
Seep 11	01/21/12	15:14	3.2	2/20/12	8.50	8.42	3/7/12	0.04
Seep 11	01/23/12	13:46	3.1	2/10/11	9.30	9.19	2/14/12	0.05
Seep 11	01/27/12	14:13	3.1				2/14/12	0.04
Seep 11	02/14/12	14:58	3.3	3/5/12	16.45	16.44	3/7/12	0.04
Seep 11	02/17/12	13:14	3.3	3/5/12	16.65	16.65	3/7/12	0.05
Seep 11	02/20/12	15:27	3.8	3/5/12	18.40	18.70	3/7/12	0.04
Seep 11	02/24/12	12:53	4.2	3/24/12	19.45	20.03	3/21/12	0.03
Seep 11	02/27/12	12:52	3.2	3/24/12	20.16	20.12	3/21/12	0.02
Seep 11	03/01/12	13:17	3.2	3/18/12	21.09	21.05	3/21/12	0.03
Seep 11	03/11/12	12:52	3.2	3/24/12	23.74	23.70	3/21/12	0.03
Seep 11	03/14/12	11:42	3.2	3/18/12	25.39	25.36	3/21/12	0.05

Table C-2. The fluorescent dye analytical results for the South Seep Group (Continued)

Location	Date	Time	Salinity	FLT Analysis	FLT	FLT Conc. Adj	SRB Analysis	SRB
				Date	Conc.	for Salinity	Date	Conc.
					(ppb)	(ppb)		(ppb)
Seep 11	03/14/12	11:42	3.2	3/18/12	25.39	25.36	11/2/12	0.04
Seep 11	03/17/12	10:36	3.2	4/11/12	25.63	25.60	4/12/12	0.02
Seep 11	03/19/12	11:16	3.3	4/11/12	26.53	26.59	4/12/12	0.04
Seep 11	03/22/12	11:30	4.5	4/11/12	26.23	27.32	4/12/12	0.03
Seep 11	03/27/12	11:46	3.3	4/11/12	26.93	26.99	4/12/12	0.03
Seep 11	03/29/12	12:03	3.3	4/11/12	27.93	28.00	4/12/12	0.02
Seep 11	03/31/12	17:04	3.4	4/11/12	28.84	29.00	4/12/12	0.03
Seep 11	04/02/12	11:55	3.3	4/11/12	28.44	28.50	4/12/12	0.03
Seep 11	04/05/12	10:04	3.3	5/11/12	29.88	29.96	5/17/12	0.05
Seep 11	04/12/12	10:37	3.3	5/11/12	29.78	29.85	5/17/12	0.04
Seep 11	04/16/12	11:55	3.3	5/11/12	30.70	30.78	5/17/12	0.04
Seep 11	04/19/12	12:46	3.4	5/11/12	28.35	28.50	5/17/12	0.05
Seep 11	04/24/12	16:31	3.4	5/11/12	31.00	31.19	5/17/12	0.05
Seep 11	04/26/12	12:14	3.4	5/11/12	29.98	30.15	6/22/12	0.05
Seep 11	04/26/12	12:14	3.4	5/11/12	29.98	30.15	5/17/12	0.05
Seep 11	05/02/12	12:14	3.5	5/11/12	30.39	30.66	5/17/12	0.09
Seep 11	05/07/12	11:52	3.4	6/14/12	30.19	30.37	6/22/12	0.05
Seep 11	05/18/12	14:43	3.5	6/14/12	25.77	25.99	6/22/12	0.04
Seep 11	05/22/12	16:20	3.6	6/14/12	30.60	30.97	6/22/12	0.05
Seep 11	05/25/12	16:09	3.6	6/14/12	28.69	29.03	6/22/12	0.04
Seep 11	06/04/12	15:12	6.4	6/15/12	25.74	28.59	6/22/12	0.05
Seep 11	06/07/12	13:46	3.5	7/20/12	29.25	29.51	6/22/12	0.04
Seep 11	06/07/12	13:46	3.5	7/20/12	29.25	29.51	7/26/12	0.04
Seep 11	06/07/12	13:46	3.5	6/14/12	28.99	29.24	6/22/12	0.04

Table C-2. The fluorescent dye analytical results for the South Seep Group (Continued)

Location	Date	Time	Salinity	FLT Analysis	FLT	FLT Conc. Adj	SRB Analysis	SRB
				Date	Conc.	for Salinity	Date	Conc.
					(ppb)	(ppb)		(ppb)
Seep 11	06/07/12	13:46	3.5	6/14/12	28.99	29.24	7/26/12	0.04
Seep 11	06/12/12	12:56	3.7	7/20/12	27.94	28.37	7/26/12	0.03
Seep 11	06/14/12	16:04	3.5	7/20/12	28.45	28.70	7/26/12	0.03
Seep 11	06/16/12	13:30	4.8	7/20/12	25.03	26.33	7/26/12	0.04
Seep 11	06/29/12	14:02	3.5	7/20/12	26.54	26.77	7/26/12	0.04
Seep 11	07/11/12	15:02	3.5	7/25/12	26.02	26.24	7/26/12	0.03
Seep 11	07/19/12	12:08	3.5	7/25/12	24.37	24.56	7/26/12	0.04
Seep 11	07/23/12	11:51	3.5	10/3/12	24.61	24.81	10/9/12	0.04
Seep 11	08/01/12	11:31	4.4	10/3/12	21.28	22.07	10/9/12	0.04
Seep 11	08/01/12	11:31	4.4	10/3/12	21.28	22.07	8/2/12	0.04
Seep 11	08/01/12	11:31	4.4	8/3/12	23.73	24.62	10/9/12	0.04
Seep 11	08/01/12	11:31	4.4	8/3/12	23.73	24.62	8/2/12	0.04
Seep 11	08/08/12	12:47	3.4	10/3/12	23.91	24.02	10/9/12	0.04
Seep 11	08/15/12	12:03	3.5	10/3/12	22.59	22.77	10/9/12	0.05
Seep 11	08/21/12	11:30	3.5	10/3/12	21.58	21.74	10/9/12	0.05
Seep 11	08/24/12	13:03	5.4	10/3/12	20.27	21.72	10/9/12	0.04
Seep 11	08/27/12	11:13	3.6	10/3/12	21.48	21.71	10/9/12	0.05
Seep 11	09/05/12	11:26	3.5	10/3/12	20.37	20.51	10/9/12	0.05
Seep 11	09/10/12	14:21	3.5	10/3/12	19.46	19.59	10/9/12	0.04
Seep 11	09/12/12	11:37	3.6	10/12/12	18.19	18.37	10/19/12	0.03
Seep 11	09/18/12	13:20	3.6	10/12/12	18.39	18.57	10/19/12	0.03
Seep 11	10/02/12	12:47	3.4	10/12/12	17.38	17.44	10/19/12	0.03
Seep 11	10/02/12	12:47	3.4	10/12/12	17.38	17.44	10/19/12	0.03
Seep 11	10/02/12	12:47	3.4	10/12/12	17.48	17.54	10/19/12	0.03

Table C-2. The fluorescent dye analytical results for the South Seep Group (Continued)

Location	Date	Time	Salinity	FLT Analysis	FLT	FLT Conc. Adj	SRB Analysis	SRB
				Date	Conc.	for Salinity	Date	Conc.
					(ppb)	(ppb)		(ppb)
Seep 11	10/02/12	12:47	3.4	10/12/12	17.48	17.54	10/19/12	0.03
Seep 11	10/08/12	15:24	3.6	11/2/12	17.36	17.53	11/2/12	0.04
Seep 11	10/22/12	11:53	3.7	11/2/12	16.05	16.24	11/2/12	0.04
Seep 11	10/26/12	11:58	3.6	11/17/12	15.96	16.10	11/19/12	0.02
Seep 11	10/29/12	12:25	3.5	11/17/12	15.35	15.44	11/19/12	0.03
Seep 11	11/02/12	16:10	3.4	11/17/12	15.15	15.18	11/19/12	0.02
Seep 11	11/02/12	16:10	3.4	11/17/12	15.15	15.18	11/19/12	0.02
Seep 11	11/08/12	13:10	3.4	11/17/12	15.15	15.18	11/19/12	0.02
Seep 11	11/12/12	12:21	3.5	11/17/12	15.05	15.13	11/19/12	0.02
Seep 11	11/19/12	12:29	3.5	12/14/12	14.48	14.55	12/19/12	0.02
Seep 11	11/27/12	11:28	3.5	12/14/12	13.35	13.41	12/19/12	0.03
Seep 11	12/06/12	12:16	3.4	12/14/12	13.35	13.37	12/19/12	0.02
Seep 11	12/10/12	11:48	3.4	12/14/12	13.15	13.16	12/19/12	0.02
Seep 11	12/14/12	13:28	3.7	1/12/13	12.74	12.88	1/16/13	0.04
Seep 11	12/29/12	12:24	14.3	1/12/13	8.56	13.02	1/16/13	0.05

**APPENDIX D: STARWOOD VACATIONS OWNERSHIP
RESORTS (SVO) MONITORING WELL DATA**

This page is intentionally left blank.

Table D-1. Field, water quality measurements, and tracer dye concentrations for the 7/1/12 SVO well sampling

Well	Date	Time	Depth to Water (ft btoc)	Total Well Depth (ft btoc)	Temp (°C)	SEC (µs/cm)	pH	FLT (ppb)	SRB (ppb)	Comments
Well 2	7/31/12	14:20	16.31	22.83	31.08	2,527	7.52	0.15	0.09	Tracer Sample 1
		14:55						0.04	0.06	Tracer Sample 2
Well 3	7/31/12	15:45	9.97	21.00	27.03	970	7.54	0.07	0.02	Tracer Sample 1
		16:05						0.09	0.01	Tracer Sample 2
Well 4	7/31/12	16:50	7.71	21.30	27.04	2,892	7.81	0.09	0.03	Tracer Sample 1
		17:10						0.09	0.03	Tracer Sample 2
Well 5	7/31/12	12:28	13.94	17.20	28.64	726	6.89	0.20	0.04	Tracer Sample 1
		12:30						0.12	0.03	Tracer Sample 2
Well 6	7/31/12	13:02	23.65	32.00	28.32	2,841	6.85	0.46	0.07	Tracer Sample 1
		13:40						4.59	0.03	Tracer Sample 2

SEC - specific electrical conductivity

ft btoc - feet below top of casing

µs/cm - micro-siemens per centimeter at 25 °C

°C - degrees centigrade

Table D-2. Field, water quality measurements, and tracer dye concentrations for the 4/29/13 SVO well sampling

Well	Time	Depth to Water (ft btoc)	Purge Volume (gal.)	Temp (°C)	SEC (µs/cm)	pH	ORP (mv)	FLT (ppb)	SRB (ppb)	Comments	
Well 2	14:52	16.43	0					0.33	0.06	Tracer Sample 1	
			1	29.2	2,474	7.49	89.0				
			2	28.6	2,443	7.56	88.2				
				3	28.5	2,414	7.55	88.0			
				4	28.6	2,392	7.50	84.1			
				5	28.5	2,396	7.53	88.5			water slightly turbid and reddish brown
	15:15		6	28.6	2,391	7.53	89.2	0.25	0.04	Sample nutrients for HDOH analysis, tracer sample 2	
Well 3	13:00	10.31	0					0.87	0.01	Tracer sample 1	
			1	26.4	893	7.48	153				
			2	26.6	881	7.53	153				
			3	26.5	879	7.56	152				
			4	26.5	882	7.52	151			color - reddish brown	
				5	26.6	883	7.52	151			
	13:25		6	26.6	902	7.45	151	0.03	0.01	Sample nutrients for HDOH analysis, tracer sample 2	

Table D-2 (continued). Field, water quality measurements, and tracer dye concentrations for the 4/29/13 SVO well sampling

Well	Time	Depth to Water (ft btoc)	Purge Volume (gal.)	Temp (°C)	SEC (µs/cm)	pH	ORP (mv)	FLT (ppb)	SRB (ppb)	Comments
Well 4	14:00	8.03	0					0.34	0.02	Tracer Sample 1
			1	28.4	2,911	7.54	91.0			
			2	27.3	2,921	7.59	56.0			
			3	27.2	2,933	7.65	26.9			
			4	27.3	2,936	7.70	8.5			
	14:15		5	27.2	2,926	7.69	-5.8	0.58	0.03	Sample nutrients for HDOH analysis, tracer sample 2
Well 6	15:45	23.88	0					0.52	0.02	Tracer Sample 1
			1	28.4	2,571	6.85	135			
			2	27.9	2,674	6.92	126			
			3	27.9	2,692	6.93	127			
			4	27.0	2,688	6.93	131			
			5	27.9	2,691	6.95	129			
			6	27.9	2,690	6.98	130	0.24	0.02	Sample nutrients for HDOH analysis, tracer sample 2
Well 7	12:05									Duplicate of SVO Well 6

ft btoc - feet below top of casing

µs/cm - micro-siemens per centimeter at 25 °C

°C - degrees centigrade

Table D-3. Field, water quality measurements, and tracer dye concentrations for the 6/6/13 SVO well sampling

Well	Time	Depth to Water (ft btoc)	Purge Volume (gal.)	Temp (°C)	SEC (µs/cm)	pH	ORP (mv)	FLT (ppb)	SRB (ppb)	Comments
Well 2	11:38	16.22	0					0.37	0.05	Tracer sample 1
			1		2,533	7.47	37.4			
			2	28.6	2,521	7.5	39.3			
			3	28.4	2,478	7.44	43.3			
			4	28.5	2,470	7.43	42.9			
			5	28.3	2,462	7.43	46.1			
	12:10		6	28.3	2,442	7.41	49.3	0.27	0.06	Sample nutrients for HDOH analysis, tracer sample 2
12:28		12	29.1	2,435	7.49	55.1	0.25	0.09	Sample nutrients for UH analysis, tracer sample 3	
Well 3	10:05	10.36	0					0.03	0.01	Tracer sample 1
			1	26.6	901	7.42	-1.3			
			2	26.4	903	7.43	1.4			
			3	26.5	912	7.43	9.3			
			4	26.4	904	7.47	8.2			
			5	26.6	900	7.45	12.9			
	10:50		6	26.6	902	7.45	15.1	0.04	0.05	Sample nutrients for HDOH analysis, tracer sample 2
11:01		12	27	904	7.43	21.2	0.04	0.02	Sample nutrients for UH analysis, tracer sample 3	

Table D-3 (continued). Field, water quality measurements, and tracer dye concentrations for the 6/6/13 SVO well sampling

Well	Time	Depth to Water (ft btoc)	Purge Volume (gal.)	Temp (°C)	SEC (µs/cm)	pH	ORP (mv)	FLT (ppb)	SRB (ppb)	Comments
Well 4	9:20	7.53	0					0.11	0.03	Tracer Sample 1
			1	27	2,903	7.55	72.3			
			2	27.1	2,907	7.64	17.6			
			3	26.9	2,940	7.69	-9.6			
			4	26.8	2,945	7.71	-33.3			
	9:46	6	26.9	2,947	7.72	-45.1				
	9:46		6	26.9	2,945	7.72	-53.5	0.56	-0.03	Sample nutrients for HDOH analysis, tracer sample 2
	10:00		12	27.2	2,936	7.71	-58.4	0.46	0	Sample nutrients for UH analysis, tracer sample 3
Well 6	12:59	23.56	0					0.3	0.06	Tracer Sample 1
			1	28.4	26	7.07	74.2			
			2	28.1	2,705	6.89	77.1			
			3	28.1	2,731	6.84	79.7			
			4	28	2,743	6.82	80.5			
	13:15	6	28	2,742	6.84	81.2				
	13:15		6	28	2,742	6.84	83.7	0.18	0.07	Sample nutrients for HDOH analysis, tracer sample 2
	13:30		12	28.3	2,780	6.87	82.2	0.16	0.03	Sample nutrients for UH analysis, tracer sample 3
Well 7	12:05									Duplicate of SVO Well 2

ft btoc - feet below top of casing; µs/cm - micro-Siemens per centimeter at 25 °C; °C - degrees centigrade

This page is intentionally left blank.

**APPENDIX E: FINAL REPORT REVIEW
COMMENTS AND UNIVERSITY OF HAWAII
RESPONSES AND CORRECTIONS**

This page is intentionally left blank.

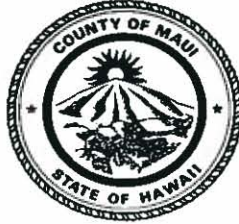
**APPENDIX E-1: Final Report review comments from the County of
Maui**

This page is intentionally left blank.

ALAN M. ARAKAWA
Mayor

KYLE K. GINOZA, P.E.
Director

MICHAEL M. MIYAMOTO
Deputy Director



TRACY TAKAMINE, P.E.
Solid Waste Division

ERIC NAKAGAWA, P.E.
Wastewater Reclamation Division

**COUNTY OF MAUI
DEPARTMENT OF
ENVIRONMENTAL MANAGEMENT**

2200 MAIN STREET, SUITE 100
WAILUKU, MAUI, HAWAII 96793

June 10, 2013

Mr. Craig R. Glenn, Professor
Department of Geology and Geophysics
University of Hawaii
School of Ocean and Earth Science and Technology
1680 East West Rd POST 701
Honolulu, HI 96822

Dear Professor Glenn;

**SUBJECT: DRAFT REPORT: FINAL LAHAINA GROUNDWATER TRACER STUDY
COUNTY OF MAUI COMMENTS**

Thank you for the opportunity to review the subject report. Below is a compilation of comments received from various parties within the County that we will hope will be included in the final version of the report. We have underlined or crossed out suggested changes to the text and have made comments in parentheses with a bold font:

1. General: This is one of the longest and most detailed executive summaries we have ever seen. Seems like it might be a good idea to move the report index ahead of it so we can find things like the acronym table, and understand the layout of the entire 450+ page report.
2. Pg. i "(1) Fluorescein tracer dye added to LWRF injection Wells 3 and 4 arrived at coastal submarine spring sites with a minimal travel time of 84 days and with an average time of 454(?) days; a second dye, Sulpho-Rhodamine-B added to LWRF injection Well 2, had yet to be confirmed. no confirmed detections. **(Should tell the whole story of travel time and it would follow that either you found the second dye or you didn't during the study period. You actually say it correctly on pg. 40 of the study why not in the summary?)**
3. Pg. i "(3) Waters discharging the fluorescein dye from the submarine springs are warm and brackish, and have a temperature >28°C, and an average salinity of 4.5 and a pH of 7.5. These differed from the effluent characteristics which were Temperature 27.8°, salinity 1.1 and a pH of 6.85". **(great facts but what do they mean without any comparisons)**
4. Pg. i "(4) Geochemical mixing analyses indicate that the submarine spring waters are predominately (XX%) LWRF treated wastewater which while in transit to the submarine springs undergo oxic, suboxic and likely anoxic microbial degradation reactions that consume dissolved oxygen, dissolved nitrate, and organic matter." **(without the percentage predominately could be 51% to 99.9% and could be misleading)**

5. Pg. i "(5) The N concentration of the submarine springs is reduced compared to LWRP treated wastewater, while the P concentration is enriched. Averaged N and P concentrations collected from the submarine springs were ca. 1,100 µg/L and 425 µg/L, respectively." Average values from the injected effluent are XXXX and XXX, respectively. **(again, great facts but what do they mean without any comparisons)**
6. Pg. ii "(1) Fluorescein tracer dye added to LWRP injection Wells 3 and 4 arrived at coastal submarine spring sites with a minimum travel time of 84 days; the peak breakthrough curve (BTC) occurred 9 and 10 months after the fluorescein dye addition at the north and south groups of submarine springs, respectively; and the average travel time to both monitoring locations is ~~in excess of one year~~ approximately 450 days. Dye continues to be detected at the publication of this report over 2 years after it was introduced. **(again the whole story adds perspective for some one who only reads this summary)**
7. Pg. iii "(4) ~~The primary~~ A possible cause for the non-detection of Sulpho-Rhodamine B is the displacement of the injectate plume containing this dye away from a direct travel path from Injection Well 2 to the submarine springs by the greater injection volume into Wells 3 and 4. This interference may further dilutes the Sulpho-Rhodamine B plume prior to reaching the submarine springs. In addition, secondary processes, such as dye degradation and sorption, may also decrease the concentration to less than detectable levels." **(Where is the physical proof that this is true? Isn't this the best guess cause for the data collected and the models that were developed)**
8. Pg. x "...SSG and NSG represent the largest sources of DON, DIP and DOP per meter coastline amongst other all identified sources..." **(1. In reviewing Table 3-6, this statement is somewhat misleading because it fails to mention that other sources provide a significantly larger total nutrient input when not quantified as per meter of coastline 2. There is a range for the seep groups whereas measurement for the limited number of other locations appears to be a single sample. Seems this should be qualified. 3. It should be mentioned that land runoff could also be a significant. 4. Lots of acronyms in this section, too bad you need to find the acronym page when we haven't even gotten to an index yet.)**
9. Pg. xv and Pg. 99 in Section 4 "As shown, the following three sets of mixing end members were used in geochemical/stable isotope source water partitioning analysis: (1) $\delta^{18}\text{O}$ and Cl, (2) $\delta^{18}\text{O}$ and Cl, and (3) $\delta^2\text{H}$ and Cl ." **($\delta^{18}\text{O}$ and Cl is repeated twice - one should be $\delta^{18}\text{O}$ and $\delta^2\text{H}$. Also, the fact that there were data outliers call into question the significance of the mixing model, however, there were no statistics performed on this mixing data so a conclusion can not be made.)**
10. Pg. xxvii Figure ES-1. Western Maui land-use map. **Wasn't the area just north of Honokowai Steam used for sugarcane prior to pineapple?**
11. Pg. xlvi "Figure ES-15: ...Continuing injection into Wells 3 and 4 after the addition of SRB may displaces the core of the plume to the southeast. **(This statement and Figure 5.19 are conjecture. Four possible scenarios for the non detection of the SRB, but there is no reason/explanation/proof for this answer being chosen as the most probable. Seems unlikely that water with the same characteristics flowing at such low velocities won't mix and instead displaces one another.)**

12. Pg. 1 “Each of these five primary objectives are addressed in(?) Sections 2 through 5 of this Final Report.”
13. Pg. 4 “The effluent that ~~is subjected~~ undergoes disinfection using ultraviolet radiation is sold as R-1 grade reuse water for irrigation and other approved uses (construction dust control etc.).”
14. Pg. 4 “In the mid-1990s Maui County upgraded the plant to produce R-1 water to be used as a resource and in part to address concerns about possible contributions to seasonal benthic algal blooms that were proliferating along the coast.”
15. Pg. 4 “After primary settling to remove a majority of the suspended solids, the LWRF effluent undergoes secondary treatment.” There is no primary clarification at the Lahaina WWRF. It is also stated “The treatment for the water not sold as irrigation water is subjected to tertiary treatment and fully disinfected to the R-2 standard” **(The tertiary treatment is the BNR removal, sand filtration and disinfection mentioned previously. All effluent undergoes this process. This statement is confusing and seems to indicate that injection water is subject to additional tertiary treatment)**
16. Pg. 5 “This infrastructure may be beneficial to the expansion of reuse in the Kaanapali area and the emerging diversified agriculture in West Maui.”
17. Pg. 5 “During With warmer, dryer months no more than 3.0 mgd is expected to be injected underground as current reuse has typically reached 1.8 mgd in these periods..”
18. Pg. 5 Section 1.3 **(Note that the County also operates its injection wells under Permit No. UM-1357 which expired on 3/28/2009 and is also operating under a extension to that permit currently thru 8/28/2013. It is expected that it will be extended until 8/28/2014 sometime in July or August.)**
19. Pg. 36 “The effect of salinity on the fluorescence values of FLT in the submarine spring water is quite substantial” **(Isn't this more of a relationship or correlation rather than an effect since you say it is due to the mixing of ocean water?)**
20. Pg. 37 “The fluorescence data collected in the field has not been corrected for the salinity.” **(Can it be corrected? Should it be corrected? Isn't the value just a field condition that changes with the actual SGD due to seasons (wet/dry), tides etc.?)**
21. Pg. 39 “Olowalu is located ~13 km south of the main study area and currently has no known major land-based pollution impacts due to the minimal development and the termination of sugarcane operations in the late 1990's.” **(as a point of information there is a landfill just north of Oluwalu, now a transfer station, that is no longer active. It could possibly have effects on SGD in the area)**
22. Pg. 40 “The July 2013 submarine spring survey covered 20.8 km or 12.9 miles of the study area from Honokowai Point to Black Rock over 86 transects.” **(Misleading. The total length of the transect may be 12.9 miles but it only covered about 1.3 miles of shoreline.)**
23. Pg. 72 “Depending on land-use, organic matter content, geology, etc. nutrients may be removed (dilution and geochemical cycling) and/or added (fertilizer use, cesspools or septic systems)”

24. Section 3, **It is assumed all seeps have the same discharge rate as seep 4. This does not seem like a plausible assumption. In section 4 it says that seep 4 showed the lowest and most variable dye concentration. Therefore one of the other seeps would have made a better representative sample. Also, data was only over a short portion of the year (over a 33 day period) and even during this time there was great variability. One would expect to see seasonal and weather related variability. Based on the limited data and significant variability the calculated groundwater fluxes are not very meaningful.**

25. Pg. 135 Figure 4-4: A line diagram of the LWRF showing the FLT dye addition points. **(This figure does not clearly show the injection points. Presumes we know that injection wells were used)**

Please contact me ((808) 270-7427 or scott.rollins@maui.co.hi.us) should you have any questions or need clarification.

Sincerely,



Scott R. Rollins, CE-VI
Wastewater Reclamation Division

sr(comments tracer may 2013.doc)

xc: Nancy Rumrill, EPA

Comments From and Replies To the County of Maui

June 10, 2013

Mr. Craig R. Glenn, Professor
Department of Geology and Geophysics
University of Hawaii
School of Ocean and Earth Science and Technology
1680 East West Rd POST 701
Honolulu, HI 96822

Dear Professor Glenn;

**SUBJECT: DRAFT REPORT: FINAL LAHAINA GROUNDWATER TRACER STUDY
COUNTY OF MAUI COMMENTS**

Thank you for the opportunity to review the subject report. Below is a compilation of comments received from various parties within the County that we will hope will be included in the final version of the report. **We have underlined or crossed out suggested changes to the text and have made comments in parentheses with a bold font:**

1. General: This is one of the longest and most detailed executive summaries we have ever seen. Seems like it might be a good idea to move the report index ahead of it so we can find things like the acronym table, and understand the layout of the entire 450+ page report.

Good idea. We did that.

2. Pg. i "(1) Fluorescein tracer dye added to LWRP injection Wells 3 and 4 arrived at coastal submarine spring sites with a minimal travel time of 84 days and with an average time of 454(?) days; a second dye, Sulpho-Rhodamine-B added to LWRP injection Well 2, had yet to be confirmed. no confirmed detections. **(Should tell the whole story of travel time and it would follow that either you found the second dye or you didn't during the study period. You actually say it correctly on pg. 40 of the study why not in the summary?)**

Thank you. We have modified the bullet to state that there was no confirmed detection of Sulpho-Rhodamine B and that the average time for Fluorescein was about 450 days.

3. Pg. I "(3) Waters discharging the fluorescein dye from the submarine springs are warm and brackish, and have a temperature >28°C, and an average salinity of 4.5 and a pH of 7.5. These differed from the effluent characteristics which were Temperature 27.8°, salinity 1.1 and a pH of 6.85°. **(great facts but what do they mean without any comparisons)**

We believe this bullet is appropriate as written. Being a mixture of groundwater and seawater, submarine groundwater discharge takes on the characteristics of both. In any event, in that this bullet is part of a larger set of observations, there is much presented through the Executive Summary to compare it with.

4. Pg. I “(4) Geochemical mixing analyses indicate that the submarine spring waters are predominately (XX%) LWRF treated wastewater which while in transit to the submarine springs undergo oxic, suboxic and likely anoxic microbial degradation reactions that consume dissolved oxygen, dissolved nitrate, and organic matter.” **(without the percentage predominately could be 51% to 99.9% and could be misleading)**

Bullet 4 (page i) pertains to relative redox and diagenetic state of the vent water and we believe adding statements about our different estimates of the proportion of effluent in those waters is not appropriate here.

5. Pg. I “(5) The N concentration of the submarine springs is reduced compared to LWRF treated wastewater, while the P concentration is enriched. Averaged N and P Concentrations collected from the submarine springs were ca. 1,100 /lg/l and 425 /lg/l, respectively.” Average values from the injected effluent are XXXX and XXX. Respectively. **(again, great facts but what do they mean without any comparisons)**

We agree, and deleted the actual numbers, especially since this is dealt with in the summary of the Executive Summary geochemistry discussions that follow.

6. Pg. ii “(1) Fluorescein tracer dye added to LWRF injection Wells 3 and 4 arrived at coastal submarine spring sites with a minimum travel time of 84 days; the peak breakthrough curve (BTC) occurred 9 and 10 months after the fluorescein dye addition at the north and south groups of submarine springs, respectively; and the average travel time to both monitoring locations is in excess of one year approximately 450 days. Dye continues to be detected at the publication of this report over 2 years after it was introduced.” **(again the whole story adds perspective for some one who only reads this summary)**

We believe this bullet is appropriate as written.

7. Pg. iii “(4) ~~The primary~~ A possible cause for the non-detection of Sulpho-Rhodamine B is the displacement of the injectate plume containing this dye away from a direct travel path from Injection Well 2 to the submarine springs by the greater injection volume into Wells 3 and 4. This interference may further dilutes the Sulpho-Rhodamine B plume prior to reaching the submarine springs. In addition, secondary processes, such as dye degradation and sorption, may also decrease the concentration to less than detectable levels.” **(Where is the physical proof that this is true? Isn't this the best guess cause for the data collected and the models that were developed)**

We strongly dispute the contention that no evidence was provided to support our conclusion regarding the failure to conclusively detect Sulpho-Rhodamine B. We refer you to Figure 6-1 of Mink, 1976, Guam WRRRC Tech Report #1 (and provided at the end of these replies). This figure shows that streamlines from injection wells do not cross or mix with groundwater flow streamlines from upgradient of the injection well. This is counter to COM's contention in Comment 11. Also, since the injection into Wells 3 and 4 is significantly greater than that into Well 2 the velocities would be much higher. The evidence is the model that uses sound and well-documented fluid flow principles to compute groundwater flow paths and velocities. Because injection was continued into Wells 3 and 4 after Sulpho-Rhodamine B was added, the hydraulic connection between Injection Well 2 and the submarine springs remains inconclusive.

8. Pg. x " SSG and NSG represent the largest sources of DON, DIP and DOP per meter coastline amongst other all identified sources " **(1. In reviewing Table 3-6, this statement is somewhat misleading because it fails to mention that other sources provide a significantly larger total nutrient input when not quantified as per meter of coastline 2. There is a range for the seep groups whereas measurement for the limited number of other locations appears to be a single sample. Seems this should be qualified. 3. It should be mentioned that land runoff could also be a significant. 4. Lots of acronyms in this section, too bad you need to find the acronym page when we haven't even gotten to an index yet.)**

To address notes 1., 3., 4. we edited the text on the Draft Report page x as follows:

"We found that groundwater discharge is responsible for significant nutrient fluxes to the coastal ocean. Fluxes of dissolved inorganic and organic nitrogen (DIN and DON) are the largest at Hanakao'o Beach (DIN: 2.9 kmol/d or 41,440 g/d of N and DON: 1.7 kmol/d or 23,700 g/d of N. Second largest DIN flux along this coastline is from Honokowai (1.9 kmol/d or 27,500 g/d of N) and DON flux at SSG (up to 650 mol/d or 9,500 g/d of N). At Hanakao'o and Honokowai groundwater discharges along 1,200 m and 300 m length, while at the seep clusters the discharge locations are only 50-100 m long. SSG and NSG alone represent the largest sources of DON, dissolved inorganic and organic phosphorus (DIP and DOP) per meter coastline amongst all identified sources. The two seep groups are responsible for fluxes of 100-218 mol/d or 1,400-3,053 g/d of N as DIN, 120-910 mol/d or 1,670-12,750 g of N as DON, 99-116 mol/d or 3,070-3,600 g/d of P as DIP, and 16 mol/d or 480 g/d of P as DOP. These inputs impact coastal water quality and result in elevated nutrient concentrations. At SSG and NSG coastal seawater DIN ranges are 0.38-0.81 μM or 5.3-11.3 $\mu\text{g/L}$ of N as opposed to offshore levels of $<0.1 \mu\text{M}$ or $<1.4 \mu\text{g/L}$, DON ranges are 4.8-12.7 μM or 67-178 $\mu\text{g/L}$ of N as opposed to 4.5-6 μM or 63-84 $\mu\text{g/L}$ of N offshore, DIP ranges 0.16-0.44 μM or 5.0-13.6 $\mu\text{g/L}$ of P in comparison to $<0.1 \mu\text{M}$ or $<3.0 \mu\text{g/L}$ of P offshore, and the DOP concentration range of 0.21-0.27 μM or 6.5-8.4 $\mu\text{g/L}$ of P is comparable to offshore levels (Karl et al., 2001). SSG and NSG are not the only location with elevated nutrients, however. For comparison, Hanakao'o Beach coastal ocean DIN concentrations (7.7 μM or 108 $\mu\text{g/L}$ of N) are 10-times and DIP levels (0.84 μM or 26 $\mu\text{g/L}$ of P) are 2-times higher than at the seep clusters. In comparison to other studied locations along the coastline, SSG and NSG seep sites had the lowest observed TN:TP and DIN:DIP ratios in groundwater (2-8 and 1-2) and also in coastal ocean water (15-20 and 2)." and

"We note that earlier studies identified surface runoff as an important coastal nutrient source (TetraTech, 1993), this current study did not quantify these inputs."

9. Pg. xv and Pg. 99 in Section 4 "As shown, the following three sets of mixing end members were used in geochemical/stable isotope source water partitioning analysis: (1) $\delta^{18}\text{O}$ and Cl, (2) $\delta^{18}\text{O}$ and Cl, and (3) $\delta^2\text{H}$ and Cl. **$\delta^{18}\text{O}$ and Cl is repeated twice -one should be $\delta^{18}\text{O}$ and $\delta^2\text{H}$. Also, the fact that there were data outliers call into question the significance of the mixing model, however, there were no statistics performed on this mixing data so a conclusion can not be made.)**

Thank you. The typographical errors have been corrected. The issues regarding mixing model data outliers were addressed in section 6.4.2.3 of the Interim Report.

10. Pg. xxvii Figure ES-I. Western Maui land-use map. **Wasn't the area just north of Honokowai Steam used for sugarcane prior to pineapple?**

This is correct. The shift in cultivation from sugar to pineapple in this area occurred in the mid 1980s. It can be considered as both former sugar cane land and former pineapple land.

11. Pg. xlvi "Figure ES-15: ... Continuing injection into Wells 3 and 4 after the addition of SRB may displaces the core of the plume to the southeast. **(This statement and Figure 5.19 are conjecture. Four possible scenarios for the non detection of the SRB, but there is no reason/explanation/proof for this answer being chosen as the most probable. Seems unlikely that water with the same characteristics flowing at such low velocities won't mix and instead displaces one another.)**

We refer you to our response to comment 7.

12. Pg. 1 "Each of these five primary objectives are addressed in(?) Sections 2 through 5 of this Final Report."

Thank you, we have made that change in Section 1.1.

13. Pg. 4 "The effluent that is ~~subjected~~ undergoes disinfection using ultraviolet radiation is sold as R-1 grade reuse water for irrigation and other approved uses (construction dust control etc.)."

Thank you, we have made those changes in Section 1.3.

14. Pg. 4 "In the mid-1990s Maui County upgraded the plant to produce R-1 water to be used as a resource and in part to address concerns about possible contributions to seasonal benthic algal blooms that were proliferating along the coast."

Thank you, we have made that change in Section 1.3.

15. Pg 4 "After primary settling to remove a majority of the suspended solids, the LWRFWWRF. It is also stated "The treatment for the water not sold as irrigation water is subjected to tertiary treatment and fully disinfected to the R-2 standard" **(The tertiary treatment is the BNR removal. sand filtration and disinfection mentioned previously. All effluent undergoes this process. This**

statement is confusing and seems to indicate that injection water is subject to additional tertiary treatment)

Thank you, we deleted the sentence " The treatment for the water not sold as irrigation water is subjected to tertiary treatment and fully disinfected to the R-2 standard " to make the appropriate improvements to our description of the LWRF.

16. Pg. 5 "This infrastructure may be beneficial to the expansion of reuse in the Kaanapali area and the emerging diversified agriculture in West Maui."

Thank you, we made that change.

17. Pg. 5 "During with warmer, dryer months no more than 3.0 mgd is expected to be injected underground as current reuse has typically reached 1.8 mgd in these periods .. "

Thank you, we made that change.

18. Pg. 5 Section 1.3 (Note that the County also operates its injection wells under Permit No. UM-1357 which expired on 3/28/2009 and is also operating under a extension to that permit currently thru 8/28/2013. It is expected that it will be extended until 8/28/2014 sometime in July or August.)

Thank you, we added that information.

19. Pg. 36 "The effect of salinity on the fluorescence values of FL T in the submarine spring water is quite substantial" (Isn't this more of a relationship or correlation rather than an effect since you say it is due to the mixing of ocean water?)

We have modified that statement to make the meaning more clear.

20. Pg. 37 "The fluorescence data collected in the field has not been corrected for the salinity." (Can it be corrected? Should it be corrected? Isn't the value just a field condition that changes with the actual SGD due to seasons (wet/dry), tides etc.?)

We modified the sentence to make it more clear.

21. Pg. 39 "Olowalu is located -13 km south of the main study area and currently has no known major land-based pollution impacts due to the minimal development and the termination of sugarcane operations in the late 1990's." (as a point of information there is a landfill just north of Oluwalu, now a transfer station, that is no longer active. It could possibly have effects on SGD in the area)

Thank you, that is an interesting observation, but it has no bearing on this report since no chemistry samples were taken in that area. The only samples collected in the Olowalu area were background samples for fluorescent dye analysis.

22. Pg. 40 "The July 2013 submarine spring survey covered 20.8 km or 12.9 miles of the study area from Honokowai Point to Black Rock over 86 transects." **(Misleading. The total length of the transect may be 12.9 miles but it only covered about 1.3 miles of shoreline.)**

We thank you for this comment, however, the sentence reads "a survey team consisting of two scuba divers completed a total of 86 transects of various lengths (from the shortest 47 m or 153 ft. to the longest 536 m or 1760 ft.) from Honokowai Point to Black Rock, covering a total of 20.8 km (12.9 miles). " which explains that 12.9 miles were covered over 86 transects of various lengths.

23. Pg. 72 "Depending on land use, organic matter content, geology, etc. nutrients may be removed (dilution and geochemical cycling) and/or added (e.g. fertilizer use, cesspools or septic systems)"

Thank you, this correction has been made.

24. Section 3, **It is assumed all seeps have the same discharge rate as seep 4. This does not seem like a plausible assumption. In section 4 it says that seep 4 showed the lowest and most variable dye concentration. Therefore one of the other seeps would have made a better representative sample. Also, data was only over a short portion of the year (over a 33 day period) and even during this time there was great variability. One would expect to see seasonal and weather related variability. Based on the limited data and significant variability the calculated groundwater fluxes are not very meaningful.**

In the text we indicated that the estimates are based on very crude assumptions, which were listed on page 70. Seep 4 was the best candidate for flow measurements because despite its variable FLT and salinity it consistently provided the strongest discharge, which was already close to detection limits of the instrument. Because of this, we believe that no other seep would have provided better results.

On page 70 it is stated that we observed as much as 100% change in discharge rates between the deployments. This is simply the nature of SGD and these numbers provide the best possible estimates for our study period.

25. Pg. 135 Figure 4-4: A line diagram of the LWRF showing the FLT dye addition points. **(This figure does not clearly show the injection points. Presumes we know that injection wells were used)**

Thank you, we made the appropriate changes to line diagram figures.

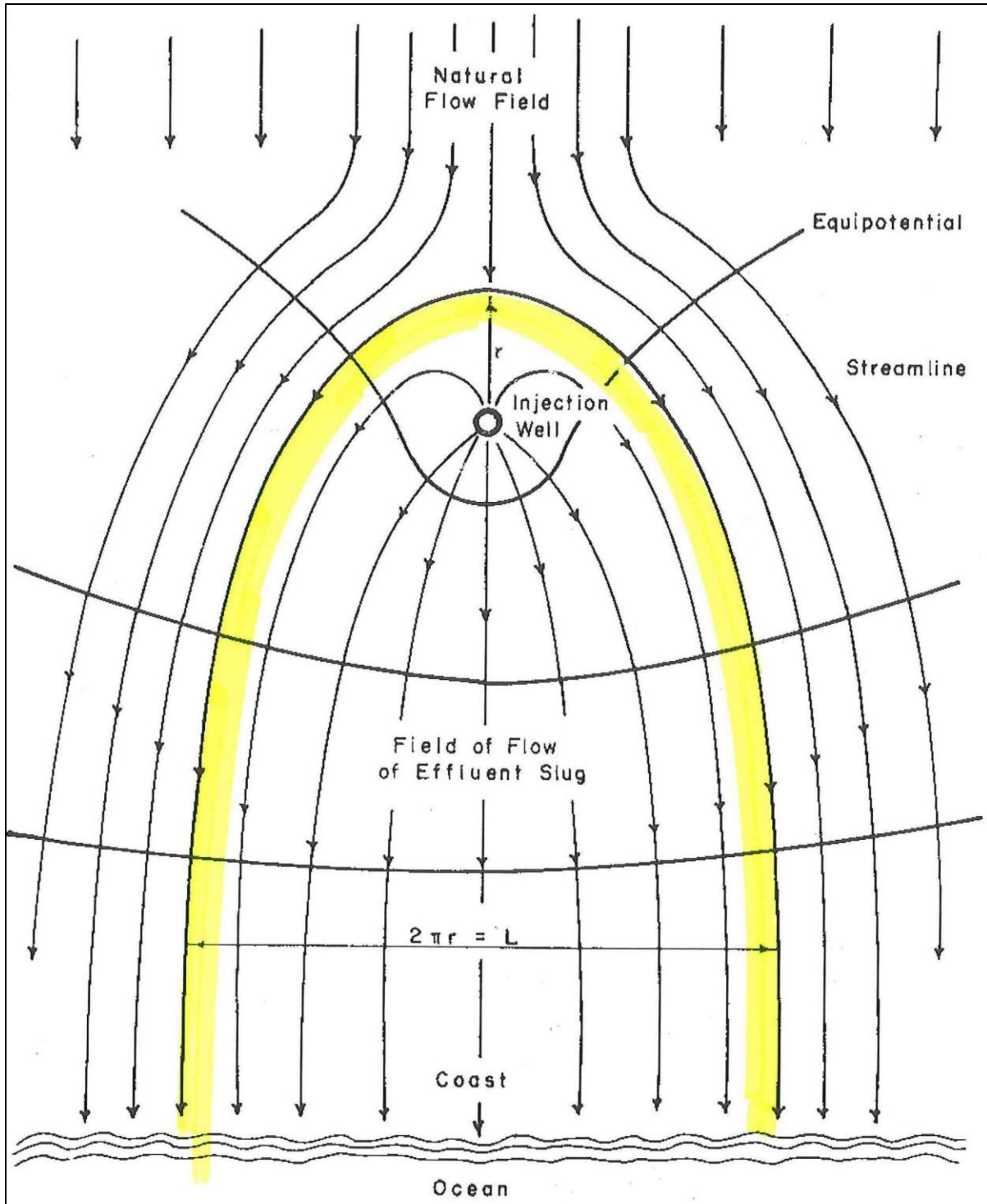


FIGURE 6-1

STEADY STATE FLOW FIELD OF AN EFFLUENT SLUG DERIVED FROM A FULLY PENETRATING INJECTION WELL RECEIVING A CONSTANT CONTINUOUS INPUT.

This page is intentionally left blank.

**APPENDIX E-2: Final Report review comments from the USEPA
Region IX**

This page is intentionally left blank.

**United States Environmental Protection Agency, Region IX (EPA) Comments
On the Lahaina Groundwater Tracer Study Draft Final Report (June 2013)
June 10, 2013**

Please consider the following comments on the Lahaina Groundwater Tracer Study Draft Final Report (June 2013).

General Comments.

1. The Lahaina Groundwater Tracer Study Draft Final Report (June 2013) (the “report”) is informative and interesting to read. Great job in summarizing a tremendous amount of information in a relatively concise manner and efficiently building upon the findings from the interim report.
2. The report provides important and useful information on the fate of effluent from injection wells and on Submarine Groundwater Discharge (SGD) in West Maui. We now know that Lahaina’s effluent discharges 3-25 m from shore in two fairly discrete areas off the Marriott and that it takes 3 months to under a year for most of the plume to reach the ocean. This is very different from the historical thinking that wells discharged far off shore in deep water over large areas. However, I do find the report to be overly long, repetitive, and sometimes inconsistent. I understand that it is organized according to the work of different investigators, but findings should be better integrated in the executive summary and throughout the report.
3. The report does need some proof reading. Please proof read the report and make corrections. Although most aspects detected by a proof reader maybe relatively insignificant, such as minor spelling mistakes (e.g., Mues near the end of page 90 should be Meus), others aspects are more critical (e.g., Tables 3-2 and 3-3 on page 88 and Tables 3-9 and 3-10 on page 91 should be Tables 4-2, 4-3, 4-9, and 4-10, respectively) and need to be corrected.

Executive Summary.

4. The Executive Summary should contain a summary paragraph describing the fate of the LWRF effluent. It appears that different tools result in slightly different (but related) answers to the questions of where does the effluent go, how much of the effluent emerges at the seep groups, and how much of the seep discharge is effluent versus groundwater. See below.

Page (P.) ii (6). Does this mean that 75% of the SGD at N and S seeps and surrounding seeps is LWRF effluent? Does it mean that 75% of the LWRF effluent emerges at these seeps?

P. iii (3). Does this mean that 64% of the effluent emerges at the N and S seeps and adjacent areas? Explain how this relates to (6) on P. ii.

P. xii and xv. How does the estimate from conservative tracers compare? Ave. 62% of SGD from springs is effluent?
5. How does interim finding, P. ii, (6) “...average total discharge from the submarine springs and the surrounding diffuse flow was about 2.76 mgd. The freshwater component of that flow was

about 2.25 mgd (8,500 m³/d), or about 75% of the LWRF total average daily injection rate (~3.0 mgd; 11,350 m³/d)” relate to the findings summarized in Table ES-8, specifically the percent effluent (68%) in the submarine spring discharge? Do the findings in Table ES-8 represent a refinement of the interim findings?

6. P. i-iii. It is confusing to summarize key results from Interim Report and then separately for the final report. Did any of the interim conclusions change with the latest information (see comment above)? It would be clearer to summarize key findings in total.
7. The draft final report appears to state findings about the cause of the elevated temperature of seep water, and the cause of the green coloration at seeps more conclusively than in the interim report. Thank you for addressing this issue. There was quite a bit of public interest in both of these observations, and the Executive Summary should state final conclusions based on all of the data.
8. P. ii. Please define “travel time,” in the Executive Summary. I think most people view travel time as the time between injection and the first detection at the seeps; however, it appears, based on page ii, that travel time for this study means the entire time of detection from first detection through the peak and until it drops below the MDL. Please define the term, so that it is not misinterpreted by the public.
9. P. iv. Please provide a better description of Lahaina’s wastewater treatment system. “Tertiary treatment” is not well-defined, as it can mean any advanced treatment on top of secondary treatment. Please specify the type of filtration.
10. P. vii. The top sentences are very unclear. Please clarify what is meant by the sentences: “Field data indicated an apparent increase in SRB fluorescence. Subsequent testing showed this was actually a response of the SRB channel the strong FLT fluorescence in the samples being analyzed.” Please refer the reader to where it is explained in the report.
11. P. vii. Please provide a better description of what “shimmering waters” means.
12. P. vii, Paragraph 2 and P. x, Paragraph 1. The characteristics of the seep field should be highlighted as a major finding. These two sections should be combined into a clear description of the location and size of the seep field. It is interesting that the seeps are diffuse, with a few discharging at higher rates, yet all cluster in two relatively small areas along a segment of coastline that basically coincides with the beachfront of the Marriott timeshare. How far offshore do the seeps extend? The P. vii paragraph (also section 2.3.4) gives the area covered by seeps, but does not fully describe the size of the seep field. It is not clear if the P. x paragraph accounts for the 289 seeps described on P. vii. In the past, the fate of the wastewater injected on Maui was thought to seep into the ocean offshore in deep water over a large area. This report shows differently.
13. P. ix. The estimated SGD rates at seeps, Honokowai and Hanakao’o are based on radon. To what extent does local mixing of seawater influence these flux estimates?
14. P. x, Paragraph 2, final sentence. Please clarify the details of what data values are being compared between the Hanakao Beach DIP and those at the seeps (e.g., flux in mol/d, concentration in micromol, etc).

15. P. x, Paragraph 2. Please report nutrient concentrations and species in terms that are relevant to Hawaii Department of Health (DOH) and comparable to Hawaii's water quality standards. We recognize that scientists use μM and DON/DIN etc, but this report is funded by and intended for use by DOH and EPA. Please provide data in a form that can be used by us. It is alright to show nutrient data both as μM and as $\mu\text{g/L}$.
16. P. x, Paragraph 2. Please consider an addition to the Executive Summary regarding the finding of the very low N:P ratios at the SSG and NSG when compared with the other sites (page 73, table 3-5, 3-6, 3-7).
17. P. xi-xii (2). The enrichment of phosphorus concentrations post-injection is likely an artifact of the small number of effluent samples taken in this study. The Executive Summary should make note that this observation may not be an accurate conclusion based on the limited number of effluent samples. Note there is a large range in your P concentrations for the effluent (170-700 $\mu\text{g/L}$). EPA averaged Maui County's monthly effluent data (from legally required reporting which was subject to QA requirements) for the period July 2011-June 2012 and obtained an average P concentration of 520 $\mu\text{g P/L}$ (range 110-1600 $\mu\text{g P/L}$). The variability in the P concentration found in the effluent calls into question the conclusion that the submarine seep concentration of P appears enriched relative to the LWRF wastewater effluent. P. xiii (4) same comment applies.
18. P. xiii (3). Please consider providing more detail on the Wahikuli area. The Wahikuli area is unsewered and a cluster of over 270 homes use cesspools (not septic) for sewage disposal. However, the dot for Wahikuli in Figure 2-2 (p. 46) is makai of Villages of Leali'i, which is a newer development and connected to the sewer system. The area immediately adjacent to the dot to the south is the unsewered housing area.
19. P. xv-xvi, for the Sulpho-Rhodamine B (SRB) Tracer Test. There is a statement in the first paragraph on page xv that says "there has been no confirmed detection of the SRB dye in the nearshore marine waters." However, the first paragraph on page xvi presents the possibility that SRB may have been detected, as demonstrated by the detection of fluorescence characteristics that are "indicative of trace concentrations of this dye." And further along in that same paragraph, the detection is considered a "possible" SRB detection. Please consider revision of these statements to be more consistent.
20. P. xv-xv,i SRB. This section starts by stating the purpose is to determine if well 2 discharges at the same seeps as Wells 3 and 4. What, if anything, can be concluded relative to this question? Does the study confirm or suggest a separate flow path for well 2? It is suggested to combine P. xvi, paragraph 2 SRB explanations with the top of P. vii regarding apparent SRB detection. If you were to do a new tracer study for well 2, where would you look to find the dye?
21. P. xxvii, Table ES-8. Please consider adding a heading regarding the method (tracer dye) used for the top half of the table similar to that used in the bottom half (e.g., Geochemical Estimations...).
22. P. xl, Figure ES-13. Should the term 'drowned stream valley' be used rather than 'downed stream valley' when referring to Honokowai ancient stream channel and associated alluvium?

Section 2.

23. P. 36, Section 2.3.1, line 2. Is “oceanic” is the right word here as it implies open ocean not influenced by land? Please consider using “coastal water”.

Section 3.

24. Section 3.3.2, Paragraph 3. This is confusing in the context of other information about the seeps. Please provide some clarification. What are the implications of assuming that all seeps discharge at same velocity as seep 4? What kind of error does this introduce? Does this calculation take into account the total 289 seeps or only sampled seeps? It certainly appears that the 289 seeps do not all discharge at the same velocity. What is meant by “ >90% of groundwater discharge is via diffuse seepage”? Does this mean 10% is from the sampled seeps and 90% from the 200+ seeps that cluster around the sampled seeps? Or does it mean that 90% emerges at areas away from the N and S seep fields? How does this relate to the percent of effluent that emerges at the sampled seeps and adjacent seep fields?
25. Section 3.3.3, Paragraph 1. Please reference a map of the wells here showing their names and locations. It is hard to follow this section without knowing where the named wells are located and the historical land use.
26. Section 3.3.3, Paragraph 2. The assumption that N and P are conservative along the flow path to the coastal zone is in conflict with other observations in the report that higher elevation wells have lower N than wells under former agricultural fields. Land use is widely demonstrated to influence N concentrations in Hawaii’s groundwater. Also Petersen reported the highest nitrate concentrations in West Maui coastal wells compared to those upgradient.
27. Section 3.3.3, Paragraph 3. Where are the referenced N15 data presented? For discussion, Hanakao’o is directly down gradient of a portion of Kaanapali golf course, which uses recycled wastewater for irrigation. There does not appear to be cesspools or septic systems upgradient of Hanakao’o.
28. Section 3.3.3, P. 73, Paragraph 1. As already mentioned in a previous comment, please express nutrients in species and units that are used by DOH and consistent with the water quality standards.
29. Table 3-5 and 3-6. The legends are confusing. Please clarify the information in the tables. The table legend should distinguish which sites are seeps, springs, and groundwater wells. Do the footnotes refer to wells? Is there a map that shows locations of the wells? Are any of these sites really springs? Table 3-5 legend states that June and September data are averaged, except for NSG and SSG where June and September averages are listed separately, but only one set of numbers is shown for NSG and SSG.
30. P. 73, 1st paragraph, 2nd sentence. “For a lower-limit estimate, nutrient fluxes for Honokowai and Hanakao reported in Table 3-6....” The placement of this sentence in this paragraph with no further information might confuse the reader. Please consider if it would be more appropriately placed prior to the final sentence of this paragraph, where the lower-limit scenario is outlined.

31. P. 73, 1st paragraph, 2nd sentence. Please provide more explanation about the use of a lower-limit estimate per Tetra Tech 1993. Is use of the lower-limit estimate more or less appropriate given the Honokowai and Hanakoo nutrient fluxes are based upon upgradient well data? Would the use of the lower-limit estimate modify the conclusions of the final sentence on Page 74 regarding the Hanakoo Beach coastal DIN and DIP levels?
32. Section 3.4, P. 74, last paragraph. Please highlight as a key finding that NSG and SSG represent the largest sources of DON, DIP, and DOP per meter of coastline.... It would be useful to know how long a coastline is involved (only a couple of meters at the seeps)? Please also present nutrient concentrations as ug/L. Same for Table 3.7. Please provide where the "offshore sites" referred to in this paragraph are located In the final sentences, elaborate on why ambient coastal concentrations are higher at Hanakao'o (i.e., less mixing, less nutrient uptake, greater flux) than coastal water at NSG/SSG.
33. Nutrient fluxes. The N and S seeps are distinct from other groundwater discharge sites studied in West Maui in the magnitude of both DON, DOP and DIP fluxes/sq m, and the low TN:TP and DIN:DIP ratios. These nutrient results are significant findings that should be highlighted in the Executive Summary with the consolidated description of the seep characteristics. The N:P ratios show that seeps are enriched in Phosphorus relative to nitrogen, when compared to other SGD sites (and to the Redfield ratio 16:1) which is a possible explanation for the history of algal blooms at Kahekili area. (From a preventative perspective, P may be managed in wastewater simply by shifting to low P detergents for laundry and dishes.)
34. Figure 3-6. It would be helpful to show the names of the wells on this figure and the nutrient units. Also, it appears that N and P values are shown for the shallow hotel wells makai of the treatment plant. Are these data available in a table somewhere in the report? At one point, there was mention of resampling these wells at greater depth. Is that data available?
35. P. 265, Table A-6. There does not appear to be any SVO well sampling results in the table (no survey area = SVO). Please clarify.

Comments From and Replies To the USEPA Region IX

United States Environmental Protection Agency, Region IX (EPA) Comments On the Lahaina Groundwater Tracer Study Draft Final Report (June 2013) June 10, 2013

Please consider the following comments on the Lahaina Groundwater Tracer Study Draft Final Report (June 2013).

General Comments.

1. The Lahaina Groundwater Tracer Study Draft Final Report (June 2013) (the “report”) is informative and interesting to read. Great job in summarizing a tremendous amount of information in a relatively concise manner and efficiently building upon the findings from the interim report.
2. The report provides important and useful information on the fate of effluent from injection wells and on Submarine Groundwater Discharge (SGD) in West Maui. We now know that Lahaina’s effluent discharges 3-25 m from shore in two fairly discrete areas off the Marriott and that it takes 3 months to under a year for most of the plume to reach the ocean. This is very different from the historical thinking that wells discharged far off shore in deep water over large areas. However, I do find the report to be overly long, repetitive, and sometimes inconsistent. I understand that it is organized according to the work of different investigators, but findings should be better integrated in the executive summary and throughout the report.

While it is true that the peak of the breakthrough curve occurred less than a year after the dye injection, it is untrue that it takes less than a year for most of the plume to reach the ocean. The mean transit time defined as the center of mass of the plume is well in excess of a year. In addition the effluent is emerging in front of the Westin not the Marriott.

3. The report does need some proof reading. Please proof read the report and make corrections. Although most aspects detected by a proof reader maybe relatively insignificant, such as minor spelling mistakes (e.g., Mues near the end of page 90 should be Meus), others aspects are more critical (e.g., Tables 3-2 and 3-3 on page 88 and Tables 3-9 and 3-10 on page 91 should be Tables 4-2, 4-3, 4-9, and 4-10, respectively) and need to be corrected.

We appreciate you pointing out the editing errors. We have corrected those errors and have reviewed the entire report for other errors.

Executive Summary.

4. The Executive Summary should contain a summary paragraph describing the fate of the LWRF effluent. It appears that different tools result in slightly different (but related) answers to the questions of where does the effluent go, how much of the effluent emerges at the seep groups, and how much of the seep discharge is effluent versus groundwater. See below.

In response to Comment 4 and 6: We have significantly altered the Overview of the Executive Summary in accord with this comment and those below. Whereas the draft version of the Final

Report Overview had two lists of principal findings (5 stemming from the Interim Report; 6 stemming from the Final Report; 11 total) the revision now has all bulleted finding combined into a succinct list of 16 total for all phases of the completed project. To compliment this list and in response to a comment below we have also added a summary paragraph at the bullet list's end, attempting to slightly gear it in more layman-friendly terms.

Re: Questions relating to the fate of the effluent: please see replies below.

Page (P.) ii (6). Does this mean that 75% of the SGD at N and S seeps and surrounding seeps is LWRF effluent? Does it mean that 75% of the LWRF effluent emerges at these seeps?

The answer to both of these questions is no. Although the measurement of submarine groundwater discharge (SGD) by radon mass balance measures can be used to calculate the amount of total (saline and fresh) SGD, as well as the amount of fresh SGD (using salinity), it cannot be used by itself to differentiate the fraction of effluent that may be a component of the water. In the draft, we were stating the June and September averaged total (fresh + marine = 2.76 mgd) SGD and fresh water (2.25 mgd) from the submarine springs and their surrounding diffuse flow, and simply comparing those results to an average LWRF total (fresh) daily injection rate (~3.0 mgd). Based on this injection rate, the SGD freshwater fraction is mathematically equivalent (only!) to 75% of the LWRF total average daily injection. However, given that the LWRF is not the only source of fresh groundwater to the coast, this is not the same as saying that 75% of the LWRF effluent emerges at these seeps.

In the revised Final Report Executive Summary we have thus eliminated the confusing 75% fresh water comparison, and therefore restated the conclusion in the new bullet number 11 (shown here), which is the same as that reported in the Interim Report's SGD summary Section 5.5 based on radon mass balance modeling from the radon time series measurements:

New Bullet (11): "As based on radon mass balance measurements, average total (fresh + saline) discharge from the submarine springs and the surrounding diffuse flow was about 2.19-3.33 million gallons per day (mgd) (8,300-12,600 m³/d). The freshwater component of that flow was about 1.61-2.88 mgd (6,100-10,900 m³/d), or about 73-87% of the total SGD."

So, again, the above is only discussing saline and fresh SGD, and not the percent of effluent that is delivered to the coast. To estimate the percentage of the total SGD that is effluent, one must use properties that are unique to that effluent. For this study, we accomplished this by using the amount of dye recovered as a function of the break through curves, and augmented that to the degree possible with stable isotopes and geochemistry.

P. iii (3). Does this mean that 64% of the effluent emerges at the N and S seeps and adjacent areas? Explain how this relates to (6) on P. ii.

Yes, that is correct (P. iii(3) is now shown as bullet (12) in the revised Executive Summary Overview). We have estimated that once the tracer dye break through curve has reached completion, that 64 percent of dye injected into Wells 3 and 4 will have been fully discharged at the submarine spring areas. Thus, as viewed at steady state, it is also our conclusion based on

these calculations that 64 percent of the treated wastewater injected into these wells currently discharges from the submarine spring areas.

P. ii(6) lists averages from time-series June -Sep, while Table ES-8 the June-Sep survey results. The detailed results were explained on page ix. Please also see our reply to 5. below.

P. xii and xv. How does the estimate from conservative tracers compare? Ave. 62% of SGD from springs is effluent?

We are not sure what is being asked for by this comment.

5. How does interim finding, P. ii, (6) “...average total discharge from the submarine springs and the surrounding diffuse flow was about 2.76 mgd. The freshwater component of that flow was about 2.25 mgd (8,500 m³/d), or about 75% of the LWRF total average daily injection rate (~3.0 mgd; 11,350 m³/d)” relate to the findings summarized in Table ES-8, specifically the percent effluent (68%) in the submarine spring discharge? Do the findings in Table ES-8 represent a refinement of the interim findings?

The results presented in Table E-8 do indeed present an update on the findings in the Interim Report. The total SGD reported in Final Report Table ES-8 (8,800 m³/d) is the total of rates determined for South and North Seep Group areas previously reported in Table 5-5 of the Interim Report, which is based on the areas of high Rn bound by the surface rectangles reported there, and as shown in revised Final Report Figures ES-4 and ES-8. Table ES-8 adds to the previous knowledge in showing that at the time of dye Break Through Curve completion, 64% of the FLT dye-traced-effluent will have been recovered at the spring areas, so at steady state, 64% of the total LWTF Well 3+4 injection rate of 9340 m³/d is released within the spring area, which is 5,978 m³/d (Table ES-8). To determine the proportion of FLT dye-traced-effluent discharge that is a component of the Total SGD rate, we divide 5978/8800 = 68%. One point of doing this calculation (with respect to total SGD) is to compare the tracer-dye result with that made on the basis of the stable isotope/geochemical ternary component analysis, which was calculated quite independently (with its own uncertainties), and yielded a mean submarine spring effluent discharge proportion of 62%, which we think is reasonable agreement.

6. P. i-iii. It is confusing to summarize key results from Interim Report and then separately for the final report. Did any of the interim conclusions change with the latest information (see comment above)? It would be clearer to summarize key findings in total.

We see no contradictions between the two reports. Our purpose of separating the results into the two parts in the draft of the executive summary was to make it easy for a reader now or later to know which set of results came from the Interim Report versus the Final Report. Nonetheless, we understand the desire to have one set of results so we have combined these together, as requested. Please also see Reply Comment 1.

7. The draft final report appears to state findings about the cause of the elevated temperature of seep water, and the cause of the green coloration at seeps more conclusively than in the Interim report. Thank you for addressing this issue. There was quite a bit of public interest in both of these observations, and the Executive Summary should state final conclusions based on all of the data.

We endeavor to state claims about causes and effects to the extent that all the available data will allow.

8. P. ii. Please define “travel time,” in the Executive Summary. I think most people view travel time as the time between injection and the first detection at the seeps; however, it appears, based on page ii, that travel time for this study means the entire time of detection from first detection through the peak and until it drops below the MDL. Please define the term, so that it is not misinterpreted by the public.

We apologize for the confusion. We substituted the more concise terms “time to first arrival” and “mean transit time” for the ambiguous “travel time.”

9. P. iv. Please provide a better description of Lahaina’s wastewater treatment system. “Tertiary treatment” is not well-defined, as it can mean any advanced treatment on top of secondary treatment. Please specify the type of filtration.

Thank you, we have added more detail in the Executive Summary describing the wastewater treatment at the LWRF.

10. P. vii. The top sentences are very unclear. Please clarify what is meant by the sentences: “Field data indicated an apparent increase in SRB fluorescence. Subsequent testing showed this was actually a response of the SRB channel the strong FLT fluorescence in the samples being analyzed.” Please refer the reader to where it is explained in the report.

We have modified those sentences to be more concise. The meaning we were trying to convey was that the fluorescence as read on the AquaFluor Handheld Fluorometer showed an increasing trend in SRB concentrations. Upon further testing it was determined that the strong fluorescence of FLT was affecting the Rhodamine channel of the field fluorometer and no SRB was present.

11. P. vii. Please provide a better description of what “shimmering waters” means.

This is an excellent point as most laypersons may not know what this means. Shown within the context, we defined shimmering water in the Executive Summary as well as in Section 2 as follows:

"The locations of all submarine springs and any other areas that showed evidence of submarine groundwater discharge, such as by the presence of shimmering waters (a varying refraction of light as seen when fresh and salt or warm and cold water mix; sometimes referred to as “schlieren”), were mapped." We encourage the EPA to help disseminate the use of the term schliern within the context of groundwater mixing in the ocean.

12. P. vii, Paragraph 2 and P. x, Paragraph 1. The characteristics of the seep field should be highlighted as a major finding. These two sections should be combined into a clear description of the location and size of the seep field. It is interesting that the seeps are diffuse, with a few discharging at higher rates, yet all cluster in two relatively small areas along a segment of coastline that basically coincides with the beachfront of the Marriott timeshare. How far offshore do the seeps extend? The P. vii paragraph (also section 2.3.4) gives the area covered by seeps, but does not fully describe the size of the seep field. It is not clear if the P. x paragraph accounts for the 289 seeps described on P. vii. In

the past, the fate of the wastewater injected on Maui was thought to seep into the ocean offshore in deep water over a large area. This report shows differently.

We have added to the executive summary and Section 2 that the furthest seep found offshore was 109 ft or 33 m offshore. The “seep field” is best described in Section 3, where fluxes are calculated for the north and south seep groups. To the Executive Summary and the paragraph on page x that in total, all submarine springs mapped within the mapped within the South Seep Group (106 seeps) were contained within an area of 500 m², and all submarine springs mapped within the North Seep Group (183 seeps) were contained within an area of 1,800 m³. We have also added a new Figure ES-4 in the revised Final Report that compares the exact delineation of the SSG and NSG and mapped by our scuba efforts and compare these to the polygons used in the Rn flux calculations (please compare with the Figure ES-8 in the revised Final Report).

13. P. ix. The estimated SGD rates at seeps, Honokowai and Hanakao’o are based on radon. To what extent does local mixing of seawater influence these flux estimates?

The radon models applied here and described in the Interim Report correct for coastal mixing which is estimated based on negative radon fluxes and tidal exchange in the time series model (see Burnett and Dulaiova 2003) and from estimates of coastal water residence times in the radon survey model (Dulaiova et al., 2010). We included the following “The model accounted for radon evasion to the atmosphere, inputs by diffusion and from offshore ocean, in-situ production from dissolved ²²⁶Ra, losses by coastal mixing and tidal exchange (Burnett and Dulaiova, 2003).”

14. P. x, Paragraph 2, final sentence. Please clarify the details of what data values are being compared between the Hanakao Beach DIP and those at the seeps (e.g., flux in mol/d, concentration in micromol, etc).

We edited the sentence to read: For comparison, Hanakao’o Beach coastal ocean DIN concentrations (7.7 μM or 108 μg/L of N) are 10-times and DIP levels (0.84 μM or 26 μg/L of P) are 2-times higher than at the seep clusters.

15. P. x, Paragraph 2. Please report nutrient concentrations and species in terms that are relevant to Hawaii Department of Health (DOH) and comparable to Hawaii’s water quality standards. We recognize that scientists use uM and DON/DIN etc, but this report is funded by and intended for use by DOH and EPA. Please provide data in a form that can be used by us. It is alright to show nutrient data both as uM and as ug/L.

We added mgd and ug/L to all listed values and have redrafted Figure 3-6 accordingly.

16. P. x, Paragraph 2. Please consider an addition to the Executive Summary regarding the finding of the very low N:P ratios at the SSG and NSG when compared with the other sites (page 73, table 3-5, 3-6, 3-7).

We added the following: In comparison to other studied locations along the coastline, SSG and NSG seep sites had the lowest observed TN:TP and DIN:DIP ratios in groundwater (2-8 and 1-2) and also in coastal ocean water (15-20 and 2).

17. P. xi-xii (2). The enrichment of phosphorus concentrations post-injection is likely an artifact of the small number of effluent samples taken in this study. The Executive Summary should make note that this observation may not be an accurate conclusion based on the limited number of effluent samples. Note there is a large range in your P concentrations for the effluent (170-700 ug/L). EPA averaged Maui County's monthly effluent data (from legally required reporting which was subject to QA requirements) for the period July 2011-June 2012 and obtained an average P concentration of 520 ug P/L (range 110-1600ug P/L). The variability in the P concentration found in the effluent calls into question the conclusion that the submarine seep concentration of P appears enriched relative to the LWRF wastewater effluent. P. xiii (4) same comment applies.

The TP concentrations cited for treated wastewater samples on page xii are incorrect and have been corrected. The actual numbers can be found in Tables ES-2 and ES-3 (June = 206 ug/L, September = 177 ug/L). Our conclusions were based on the data collected by us and previously published in the literature. The data we had available suggested that both phosphate and total P were present in significantly higher concentrations in unmixed submarine spring samples relative to treated wastewater samples. See section 6.4.3.1 of the interim report for more discussion on this topic. We were not provided with Maui County's P data for the effluent and thus were not able to use it in our evaluation of the system.

18. P. xiii (3). Please consider providing more detail on the Wahikuli area. The Wahikuli area is unsewered and a cluster of over 270 homes use cesspools (not septic) for sewage disposal. However, the dot for Wahikuli in Figure 2-2 (p. 46) is makai of Villages of Leali'i, which is a newer development and connected to the sewer system. The area immediately adjacent to the dot to the south is the unsewered housing area.

This section was modified to more accurately reflect land use in the Wahikuli area. Figure 2-2 (and ES-3) shows a control point for dye tracer sampling. Geochemical sample locations are shown on figure 6-2 and 6-3 of the interim report.

19. P. xv-xvi, for the Sulpho-Rhodamine B (SRB) Tracer Test. There is a statement in the first paragraph on page xv that says "there has been no confirmed detection of the SRB dye in the nearshore marine waters." However, the first paragraph on page xvi presents the possibility that SRB may have been detected, as demonstrated by the detection of fluorescence characteristics that are "indicative of trace concentrations of this dye." And further along in that same paragraph, the detection is considered a "possible" SRB detection. Please consider revision of these statements to be more consistent.

Thank you. We revised the discussions of Sulpho-Rhodamine B to be more consistent about the possibility of the detection of this dye.

20. P. xv-xv,i SRB. This section starts by stating the purpose is to determine if well 2 discharges at the same seeps as Wells 3 and 4. What, if anything, can be concluded relative to this question? Does the study confirm or suggest a separate flow path for well 2? It is suggested to combine P. xvi, paragraph 2 SRB explanations with the top of P. vii regarding apparent SRB detection. If you were to do a new tracer study for well 2, where would you look to find the dye?

Due to the interference from the Wells 3 and 4 flow field with that of Well 2, and the failure to detect Sulpho-Rhodamine B, no conclusions can be made regarding the possible marine

discharge points of injectate from Well 2. With no injection into Wells 3 and 4 it is entirely possible that the injectate from Well 2 could discharge at the submarine springs monitored by this study, but with available evidence there is no way to conclude whether or not this true. The detection of SRB was evaluated as "possible," which is a lower threshold than apparent. As the report states, a second tracer study with injection into Well 2-only would be needed to investigate the hydraulic connection between this well and the nearshore environment. If such a test was done, the nearshore zone that is monitored should be expanded beyond the NSG and SSG to include the entire span of coastline with elevated $\delta^{15}N$ and sea surface temperature as indicated in the aerial thermal infrared (TIR) survey. In addition, points further offshore should be surveyed with particular attention paid to the areas there the Tetra Tech survey found the fluorescence anomalies.

21. P. xxvii, Table ES-8. Please consider adding a heading regarding the method (tracer dye) used for the top half of the table similar to that used in the bottom half (e.g., Geochemical Estimations...).

Thank you for that observation, we have made the appropriate changes.

22. P. xl, Figure ES-13. Should the term 'drowned stream valley' be used rather than 'downed stream valley' when referring to Honokowai ancient stream channel and associated alluvium?

We have made that correction.

Section 2.

23. P. 36, Section 2.3.1, line 2. Is "oceanic" is the right word here as it implies open ocean not influenced by land? Please consider using "coastal water".

"Oceanic" has been replaced with "coastal water" in Section 2.3.1 and 2.3.2.

Section 3.

24. Section 3.3.2, Paragraph 3. This is confusing in the context of other information about the seeps. Please provide some clarification. What are the implications of assuming that all seeps discharge at same velocity as seep 4? What kind of error does this introduce?

We clarified this in the text as:

"Based on seep vent area measurements Seep 4 represents 11% of the sum of seep areas in SSG (838.8 cm²) and 3% of the sum of seep areas in SSG and NSG together (3,265 cm²) as shown on Figures 2-1 and 2-15. Besides their identification by divers we delineate the two seep clusters based on the radon plume identified during the radon survey performed in June and September 2011. SSG consists of 106 seeps plus any diffuse seepage in a 70x100 m² area identified as an isolated radon plume in the surface water and NSG consists of 183 seeps plus any diffuse seepage contributing to the 53x60 m² large surface radon plume. For a rough estimate of total discharge from the vents we assumed that all seeps within SSG and NSG discharge water at the same vertical velocity as Seep 4. This neglects the fact that vents may have higher or lower vertical water velocities depending on their size, or location with respect to the groundwater plume. The uncertainty introduced by this assumption cannot be quantified as no other seep

discharge was investigated in a systematic manner. By multiplying total seep areas with the above-derived vertical fluxes, we thus arrive at a total vent discharge of 21-86 m³/d and 83-336 m³/d for SSG (106 seeps) and SSG+NSG (289 seeps), respectively (Table 3-3). Average (June and September 2011) radon mass-balance derived total groundwater fluxes were 7,550 m³/d at SSG (106 seeps plus any diffuse seepage in a 70x100 m² area identified as an isolated radon plume in the surface water) and 2,950 m³/d at NSG (183 seeps plus any diffuse seepage in a 53x60 m² area)."

Does this calculation take into account the total 289 seeps or only sampled seeps? It certainly appears that the 289 seeps do not all discharge at the same velocity.

Please, see above.

What is meant by ">90% of groundwater discharge is via diffuse seepage"? Does this mean 10% is from the sampled seeps and 90% from the 200+ seeps that cluster around the sampled seeps? Or does it mean that 90% emerges at areas away from the N and S seep fields? How does this relate to the percent of effluent that emerges at the sampled seeps and adjacent seep fields?

We added the following for clarification:

"These results indicate that total SGD via seeps is only 0.5-1% at the SSG and 2-8% at the NSG of total water discharge and that >90% of groundwater discharge is via diffuse seepage within the 70x100 m² area of SSG and 53x60 m² area of NSG (Table 3-4)."

25. Section 3.3.3, Paragraph 1. Please reference a map of the wells here showing their names and locations. It is hard to follow this section without knowing where the named wells are located and the historical land use.

We included references to figures with maps of wells and land use in the text:

"We sampled 3 wells upstream of Honokowai, which were located 4 km from the coastline (Kaanapali P-4, P-5, P-6; see Glenn et al. 2012: Tables 6-3 and 6-4 and Figure 6-2) and one well (Hahakea 2) 2 km upstream of Hanakao'o Beach. These wells captured nutrient signatures from agricultural activities from pineapple (Kaanapali P-4, P-5, P-6) and sugarcane (Hahakea 2) cultivation and had relatively elevated nutrient levels (see Glenn et al. 2012: Figure 6-1, Tables 6-3 and 6-4)."

26. Section 3.3.3, Paragraph 2. The assumption that N and P are conservative along the flow path to the coastal zone is in conflict with other observations in the report that higher elevation wells have lower N than wells under former agricultural fields. Land use is widely demonstrated to influence N concentrations in Hawaii's groundwater. Also Petersen reported the highest nitrate concentrations in West Maui coastal wells compared to those upgradient.

Unfortunately, data from only these wells were available for our specific locations for calculations of nutrient fluxes. In the next paragraph we acknowledge that additions of nutrients are very well possible along groundwater flow paths down gradient from these wells.

27. Section 3.3.3, Paragraph 3. Where are the referenced N15 data presented? For discussion, Hanakao'o is directly down gradient of a portion of Kaanapali golf course, which uses recycled wastewater for irrigation. There does not appear to be cesspools or septic systems upgradient of Hanakao'o.

We included:

"Our study (Glenn et al., 2012) showed significant denitrification in groundwaters exiting SSG and NSG seeps based on a very heavy $\delta^{15}\text{N}$ signature (see Glenn et al., 2012: Figure 6-22). But denitrification was only evaluated at these two locations and these findings cannot be expanded to Honokowai and Hanakao'o. Coastal $\delta^{15}\text{N}$ values in the Hanakao'o area were enriched high enough to suggest that denitrification (possibly fueled by input of organic C and NO_3^- from irrigation with recycled waste water) is occurring in groundwater entering the ocean as SGD (see Glenn et al., 2012: Table 6-12)."

28. Section 3.3.3, P. 73, Paragraph 1. As already mentioned in a previous comment, please express nutrients in species and units that are used by DOH and consistent with the water quality standards.

We have listed all All units in ug/L, mgd, g/m/d.

29. Table 3-5 and 3-6. The legends are confusing. Please clarify the information in the tables. The table legend should distinguish which sites are seeps, springs, and groundwater wells. Do the footnotes refer to wells? Is there a map that shows locations of the wells? Are any of these sites really springs? Table 3-5 legend states that June and September data are averaged, except for NSG and SSG where June and September averages are listed separately, but only one set of numbers is shown for NSG and SSG.

We edited the legends to clarify the sources and nutrient values.

30. P. 73, 1st paragraph, 2nd sentence. "For a lower-limit estimate, nutrient fluxes for Honokowai and Hanakao'o reported in Table 3-6..." The placement of this sentence in this paragraph with no further information might confuse the reader. Please consider if it would be more appropriately placed prior to the final sentence of this paragraph, where the lower-limit scenario is outlined.

We moved this sentence as suggested.

31. P. 73, 1st paragraph, 2nd sentence. Please provide more explanation about the use of a lower limit estimate per Tetra Tech 1993. Is use of the lower-limit estimate more or less appropriate given the Honokowai and Hanakoo nutrient fluxes are based upon upgradient well data? Would the use of the lower-limit estimate modify the conclusions of the final sentence on Page 74 regarding the Hanakao'o Beach coastal DIN and DIP levels?

We edited the text: "For a lower-limit estimate, nutrient fluxes for Honokowai and Hanakao'o reported in Table 3-6 can be divided by 4 (Tetra Tech, 1993). This estimate is based on a hydrological model and only assumed dilution of the nutrient content by ambient groundwater. No biogeochemical transformations and additions of nutrients near the coastal areas were assumed. Under the lower-limit scenario of 4-fold nutrient dilution at Hanakao'o and Honokowai Beaches, DIN flux at SSG and NSG is comparable to other locations and DIP fluxes are significantly higher than at any other location."

32. Section 3.4, P. 74, last paragraph. Please highlight as a key finding that NSG and SSG represent the largest sources of DON, DIP, and DOP per meter of coastline.... It would be useful to know how long a coastline is involved (only a couple of meters at the seeps)?

Thank you for this comment and suggestion. We have addressed it extensively in the new paragraph added to the end of the Section 3.4 summary.

32. (continued). Please also present nutrient concentrations as ug/L. Same for Table 3.7.

Units have been converted and included in the text as well as separate tables.

32. (continued). Please provide where the “offshore sites” referred to in this paragraph are located in the final sentences,

We edited the text to read: “...offshore levels (ambient oligotrophic surface ocean at Station Aloha, data from Karl et al., 2001)...”

32. (continued). elaborate on why ambient coastal concentrations are higher at Hanakao’o (i.e., less mixing, less nutrient uptake, greater flux) than coastal water at NSG/SSG.

We added: “For comparison, Hanakao’o Beach coastal ocean DIN concentrations (7.7 μM or 108 μg/L of N) are 10-times and DIP levels (0.84 μM or 26 μg/L of P) are 2-times higher than at the seep clusters. These elevated nutrient levels may be a result of less intense coastal mixing, lower biotic nutrient uptake and/or as a result of larger nutrient fluxes.”

33. Nutrient fluxes. The N and S seeps are distinct from other groundwater discharge sites studied in West Maui in the magnitude of both DON, DOP and DIP fluxes/sq m, and the low TN:TP and DIN:DIP ratios. These nutrient results are significant findings that should be highlighted in the Executive Summary with the consolidated description of the seep characteristics. The N:P ratios show that seeps are enriched in Phosphorus relative to nitrogen, when compared to other SGD sites (and to the Redfield ratio 16:1) which is a possible explanation for the history of algal blooms at Kahekili area. (From a preventative perspective, P may be managed in wastewater simply by shifting to low P detergents for laundry and dishes.)

We included: “The SSG and NSG seeps are distinct from other groundwater discharge sites studied in West Maui in the magnitude of DON, DOP and DIP fluxes per meter shoreline, and their low TN:TP and DIN:DIP ratios. The N:P ratios show that the seeps are enriched in P relative to N, when compared to other SGD sites (and to the Redfield ratio of 16:1).”

34. Figure 3-6. It would be helpful to show the names of the wells on this figure and the nutrient units. Also, it appears that N and P values are shown for the shallow hotel wells makai of the treatment plant. Are these data available in a table somewhere in the report? At one point, there was mention of resampling these wells at greater depth. Is that data available?

The figure has been edited and data from all additional sampled wells are included in Table 4-24.

35. P. 265, Table A-6. There does not appear to be any SVO well sampling results in the table (no survey area = SVO). Please clarify

Due to the late execution of MOD 4 we had not yet received all of the results of SVO well sampling, but we have now provided the results and they are provided in both Section 4 and in an Appendix of the Final Report. Section 4 has also been now been considerably revised to include a discussion of these wells and the data we have obtained from them.

This page is intentionally left blank.

**APPENDIX E-3: Final Report review comments from the Hawaii
Department of Health**

This page is intentionally left blank.

Lahaina Tracer Study Project (ASO Log No. 11-047)
Comments (Hawaii Dept. of Health, Safe Drinking Water Branch)
June 10, 2013

The Monitoring Section of the Safe Drinking Water Branch has reviewed the Draft Lahaina Tracer Study Report and have the following comments:

The report is complete, well written, and meets all of the requirements of the Planning Assistance Agreement. The tracer study was well planned and executed. We do however, have some comments and suggestions to enhance the Final Report.

- (1) There are detailed QA data presented for FLT but none for SRB. We suggest adding tables similar to 4-4 through 4-7 for SRB.
- (2) Reference is made to evaluating sample degradation using periodic fluorescence measurements the of the calibration standards. No results for these measurements were found in the report. We suggest adding the data to the report to support the contention that no sample degradation is occurring.
- (3) We suggest the use of kg/d for the nutrient flux.
- (4) Task 8 of MOD 4 specifies monthly sampling of the SVO resort wells. We know that this has been done but no results were reported. We suggest adding the SVO resort well sample results as an appendix to this report.
- (5) One of the conclusions of the tracer study was that the failure to detect the Rhodamine was interference between flow fields of Wells 3 and 4, and that of Well 2 where the Rhodamine was added. Was any consideration given during the tracer test design to diverting all treated wastewater injection into Well 2 only after the Rhodamine was added? The high injection capacity of Well 2 seems to indicate that this was a viable option.
- (6) The Hawaii Rural Water Association assisted during both dye injections. We do not see any acknowledge of the assistance of this organization listed in the report. We suggest acknowledging their contribution and particularly that of Erin Vander Zee who assisted until the last dye was added during both events.

Comments From and Replies To the Hawaii Department of Health, Safe Water Drinking Branch

Lahaina Tracer Study Project (ASO Log No. 11-047)
Comments (Hawaii Dept. of Health, Safe Drinking Water Branch)
June 10, 2013

The Monitoring Section of the Safe Drinking Water Branch has reviewed the Draft Lahaina Tracer Study Report and have the following comments:

The report is complete, well written, and meets all of the requirements of the Planning Assistance Agreement. The tracer study was well planned and executed. We do however, have some comments and suggestions to enhance the Final Report.

- (1) There are detailed QA data presented for FLT but none for SRB. We suggest adding tables similar to 4-4 through 4-7 for SRB.

Thank you, we added the SRB QA tables to the report.

- (2) Reference is made to evaluating sample degradation using periodic fluorescence measurements of the calibration standards. No results for these measurements were found in the report. We suggest adding the data to the report to support the contention that no sample degradation is occurring.

We have that data and added it to the report.

- (3) We suggest the use of kg/d for the nutrient flux.

We have listed all Al units in ug/L, mgd, g/m/d.

- (4) Task 8 of MOD 4 specifies monthly sampling of the SVO resort wells. We know that this has been done but no results were reported. We suggest adding the SVO resort well sample results as an appendix to this report.

Due to the late execution of MOD 4 we had not yet received all of the results of SVO well sampling, but we have now provided the results and they are provided in both Section 4 and in an Appendix of the Final Report. Section 4 has also been now been considerably revised to include a discussion of these wells and the data we have obtained from them.

- (5) One of the conclusions of the tracer study was that the failure to detect the Rhodamine was interference between the flow fields of Wells 3 and 4, and that of Well 2 where the Rhodamine was added. Was any consideration given during the tracer test design to diverting all treated wastewater injection into Well 2 only after the Rhodamine was

added? The high injection capacity of Well 2 seems to indicate that this was a viable option.

Yes, diverting all treated wastewater injection into Well 2 for two weeks following the addition of SRB was initially proposed. However, during a conference call on August 3, 2011 between the UH, the EPA, Maui County, and HDOH it was decided that a prolonged deviation from the normal distribution of wastewater injection at the LWRF may complicate the geochemical interpretations and adversely affect the FLT tracer test results. Thus the SRB tracer test procedures were modified to return the wastewater injection distribution to the standard arrangement where Wells 3 and 4 receive the majority of the injectate after the addition of SRB was completed.

- (6) The Hawaii Rural Water Association assisted during both dye injections. We do not see any acknowledge of the assistance of this organization listed in the report. We suggest acknowledging their contribution and particularly that of Erin Vander Zee who assisted until the last dye was added during both events.

Thank you very much. That was an oversight our part. We have corrected this and acknowledged the valuable contributions of the Hawaii Rural Water Association.